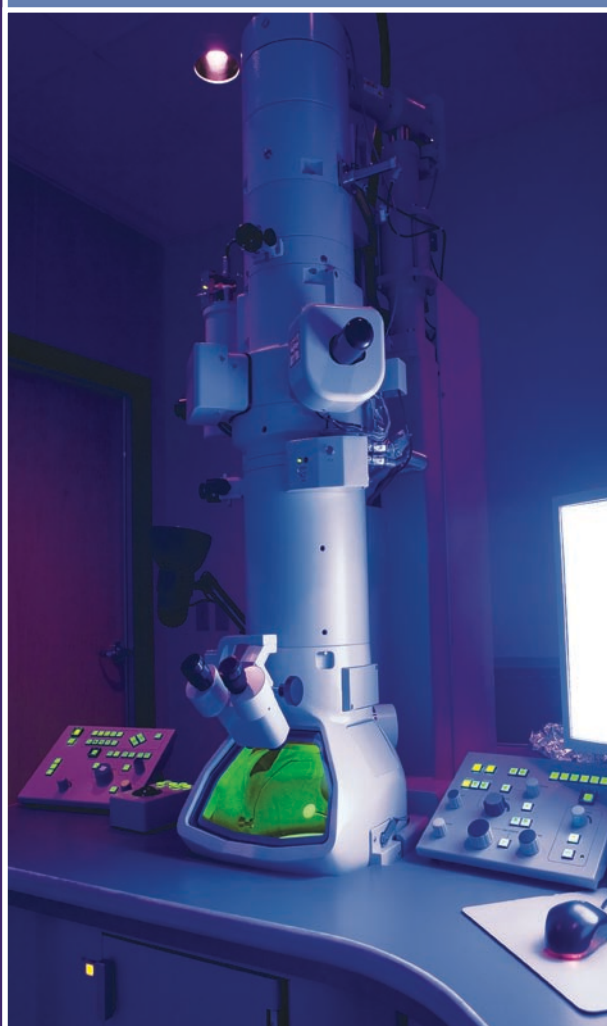# Characterisation of Polymers

Volume **1**

T.R. Crompton

Characterisation of Polymers

Volume 1

T.R. Crompton

Contents

Preface

This book is intended to be a complete compendium of the types of methodology that have evolved for the determination of the chemical composition of polymers. The structure and microstructure of polymers, copolymers and rubbers are dealt with in Volume 2. More detailed aspects, such as sequencing of monomer units in copolymers, end-group analysis, tacticity and stereochemcial determinations, will be dealt with in this subsequent volume.

Chapters 1 to 3 provide a discussion of the methodology used for the determination of metals, non-metals and organic functional groups, respectively. Metals in polymers usually originate as catalyst remnants, adventitious impurities or processing chemicals, a full knowledge of which can provide useful information on the manufacturing process and source. A wide variety of techniques are now used for the determination of metals in polymers. These can be broadly divided into two groups: destructive and non-destructive techniques. The latter includes X-ray fluorescence spectroscopy and neutron activation analysis.

Similarly, non-metals in polymers can originate either as low levels due to processing chemicals, or at major levels originating in monomers of, for example, vinyl chloride, acrylonitrile or hexfluoropropylene. In Chapter 2, both classical methods of analysis and automated instrumental methods for the determination of non-metals, are discussed.

Chapter 3 covers a discussion of recent work on the determination of the various types of organic functional groups that can occur in polymers. In many instances, detailed analytical methods, many previously unpublished, are described in a series of Appendices to Chapters 1 to 3.

Knowledge of the ratio in which different monomer units occur in copolymers is the next step, and methodology for determining this is discussed in Chapter 4. Recent work is reviewed on the application of pyrolysis-gas chromatography-mass spectrometry and other techniques such as nuclear magnetic resonance spectroscopy and infrared spectroscopy.

Chapters 5 and 6 discuss the techniques available for composition determination of homopolymers and copolymers, respectively. Chapters 7 to 10 discuss other

recent modern techniques such as X-ray photoelectron spectroscopy, atomic force microscopy, microthermal analysis and scanning electron microscopy and energy dispersive analysis using X-rays.

Frequently, it is necessary to utilise several different techniques to obtain full compositional information, and this is discussed in Chapter 9.

This book gives an up-to-date and thorough exposition of the state-of-the-art theories and availability of instrumentation needed to effect chemical and physical analysis of polymers. This is supported by approximately 1200 references. The book should be of great interest to all those engaged in the subject in industry, university research establishments and general education. The book is intended for all staff who are concerned with the elucidation of polymer structure and with the provision of suitable instrumentation in polymer research laboratories including work planners, chemists, engineers, chemical engineers and those concerned with the implementation of specifications and process control.

T. Roy Crompton

May 2008

1 Determination of Metals

Different techniques have evolved for trace metal analysis of polymers. Generally speaking, the techniques come under two broad headings:

- *Destructive techniques*: these are techniques in which the sample is decomposed by a reagent and then the concentration of the element in the aqueous extract is determined by a physical technique such as atomic absorption spectrometry (AAS; Section 1.1.1), graphite furnace atomic absorption spectrometry (GFAAS; Section 1.1.2), atom trapping atomic absorption spectrometry (Section 1.1.3) cold vapour atomic absorption spectrometry (Section 1.1.4), Zeeman atomic absorption spectrometry (ZAAS; Section 1.1.5), inductively coupled plasma atomic emission spectrometry (ICP-AES; Sections 1.1.6 to 1.1.8), visible spectrometry (Section 1.1.13), or polarographic or anodic scanning voltammetric techniques (Section 1.1.14).

- *Non-destructive techniques*: these include techniques such as X-ray fluorescence (XRF; Section 1.2.1) and neutron activation analysis (NAA; Section 1.2.2.), in which the sample is not destroyed during analysis.

1.1 Destructive Techniques

1.1.1 Atomic Absorption Spectrometry

1.1.1.1 Theory

Since shortly after its inception in 1955, AAS has been the standard tool employed by analysts for the determination of trace levels of metals. In this technique a fine spray of the analyte is passed into a suitable flame, frequently oxygen–acetylene or nitrous oxide–acetylene, which converts the elements to an atomic vapour. Through this vapour is passed radiation at the correct wavelength to excite the ground state atoms to the first excited electronic level. The amount of radiation absorbed can then be measured and directly related to the atom concentration: a hollow cathode lamp is used to emit light with the characteristic narrow line spectrum of the analyte element. The detection system consists of a monochromator (to reject other lines produced by the lamp and background flame radiation) and a photomultiplier. Another key

feature of the technique involves modulation of the source radiation, so that it can be detected against the strong flame and sample emission radiation.

This technique can determine a particular element with little interference from other elements. It does, however, have two major limitations. One of these is that the technique does not have the highest sensitivity. The other is that only one element at a time can be determined. This has reduced the extent to which it is currently used.

1.1.1.2 Instrumentation

Increasingly, due to their superior intrinsic sensitivity, the AAS currently available are capable of implementing the graphite furnace techniques. Available suppliers of this equipment are listed in Appendix 1.

Figures 1.1(a) and (b) show the optics of a single-beam flame spectrometer (Perkin Elmer 2280) and a double-beam instrument (Perkin Elmer 2380).
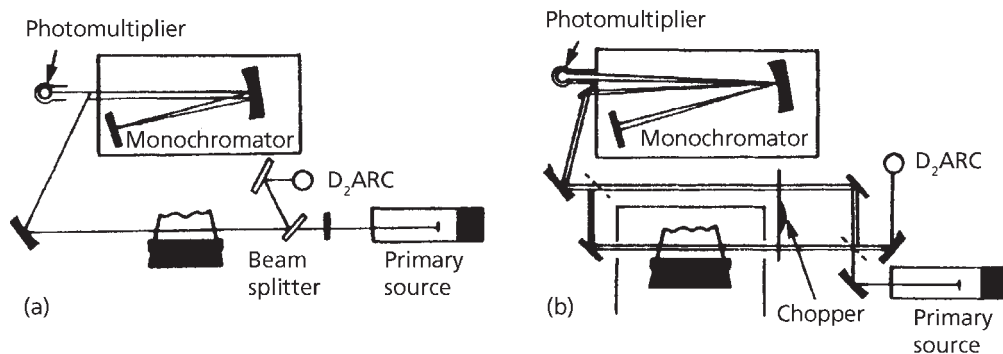
Figure 1.1(a) Optics Perkin Elmer Model 2280 single beam atomic absorption spectrometer; **(b)** Optics Perkin Elmer 2380 double beam atomic absorption spectrometer. (*Source: Author's own files*)

1.1.2 Graphite Furnace Atomic Absorption Spectrometry

1.1.2.1 Theory

The GFAAS technique, first developed in 1961 by L'vov, is an attempt to improve the detection limits achievable. In this technique, instead of being sprayed as a fine mist

into the flame, a measured portion of the sample is injected into an electrically heated graphite boat or tube, allowing a larger volume of sample to be handled. Furthermore, by placing the sample on a small platform inside the furnace tube, atomisation is delayed until the surrounding gas within the tube has heated sufficiently to minimise vapour phase interferences, which would otherwise occur in a cooler gas atmosphere.

The sample is heated to a temperature slightly above 100 °C to remove free water, then to a temperature of several hundred degrees centigrade to remove water of fusion and other volatiles. Finally, the sample is heated to a temperature near to 1000 °C to atomise it and the signals produced are measured by the instrument.

The problem of background absorption in this technique is solved by using a broad-band source, usually a deuterium arc or a hollow cathode lamp, to measure the background independently and subsequently to subtract it from the combined atomic and background signal produced by the analyte hollow cathode lamp. By interspersing the modulation of the hollow cathode lamp and 'background corrector' sources, the measurements are performed apparently simultaneously.

Graphite furnace techniques are approximately one order of magnitude more sensitive than direct injection techniques. Thus lead can be determined down to 50 µg/l by direct atomic absorption spectrometry and down to 5 µg/l using the graphite furnace modification of the technique.

Ritter and co-workers [1] conducted interlaboratory testing of polymers for the determination of cadmium, chromium and lead. They found that even when contaminant concentrations were identical the determination of heavy metals in plastics was strongly dependent on the polymer matrix.

An example of the application of atomic absorption spectrometry to the determination of heavy metals in polymers is given in Method 1.1 at the end of this chapter.

1.1.3 Atom Trapping Technique

The sensitivity difference between direct flame and furnace atomisation has been bridged via the general method of atom trapping as proposed by Watling [2]. A silica tube is suspended in the air–acetylene flame. This increases the residence time of the atoms within the tube and therefore within the measurement system. Further devices, such as water-cooled systems that trap the atom population on cool surfaces and then subsequently release them by temporarily halting the coolant flow, are sometimes employed. The application of atom-trapping atomic absorption spectrometry to the determination of lead and cadmium has been discussed by Hallam and Thompson [3].

1.1.4 Vapour Generation Atomic Absorption Spectrometry

1.1.4.1 Theory

In the past certain elements, for example, antimony, arsenic, bismuth, germanium, lead, mercury, selenium, tellurium, and tin, were difficult to measure by direct AAS [4–10].

A novel technique of atomisation, known as vapour generation via generation of the metal hydride, has been evolved which has increased the sensitivity and specificity enormously for these elements [6–8, 10]. In these methods the hydride generator is linked to an atomic absorption spectrometer (flame graphite furnace) or inductively coupled plasma optical emission spectrometer (ICP-OES) or an inductively coupled plasma mass spectrometer (IPC-MS). Typical detection limits achievable by these techniques range from 3 μg/l (arsenic) to 0.09 μg/l (selenium).

This technique makes use of the property that these elements form covalent, gaseous hydrides that are not stable at high temperatures. Antimony, arsenic, bismuth, selenium, tellurium, and tin (and to a lesser degree, germanium and lead) are volatilised by the addition of a reducing agent like sodium tetrahydroborate(III) to an acidified solution. Mercury is reduced by stannous chloride to the atomic form in a similar manner.

1.1.4.2 Instrumentation

Automating the sodium tetrahydroborate system based on continuous flow principles represents the most reliable approach in the design of commercial instrumentation. Thompson and co-workers [11] described a simple system for multi-element analysis using an inductively coupled plasma (ICP) spectrometer, based on the sodium tetrahydroborate approach. PS Analytical Ltd developed a reliable and robust commercial analytical hydride generator system, along similar lines, but using different pumping principles from those discussed by Thompson and co-workers [11].

A further major advantage of this range of instruments is that different chemical procedures can be operated in the instrument with little, if any, modification. Thus, in addition to using sodium tetrahydroborate as a reductant, stannous chloride can be used for the determination of mercury at very low levels.

The main advantage of hydride generation atomic absorption spectrometry for the determination of antimony, arsenic, selenium, and so on, is its superior sensitivity.

More recently, PS Analytical Ltd have introduced the PSA 10.003 and the Merlin Plus continuous flow vapour generation atomic absorption and atomic fluorescence spectrometers [12–14]. These facilitate the determination of very low concentrations

(ppt) of mercury, arsenic, and selenium in solution, enabling amounts down to 10–20 ppm of these elements to be determined in polymer digests.

1.1.5 Zeeman Atomic Absorption Spectrometry

1.1.5.1 Theory

The Zeeman technique, though difficult to establish, has an intrinsic sensitivity perhaps five times greater than that of the graphite furnace technique, e.g., 1 μg/l detection limit for lead.

The Zeeman effect is exhibited when the intensity of an atomic spectral line, emission or absorption, is reduced when the atoms responsible are subjected to a magnetic field, nearby lines arising instead (**Figure 1.2**). This makes a powerful tool for the correction of background attenuation caused by molecules or particles that do not normally show such an effect. The technique is to subtract from a 'field-off' measurement the average of 'field-on' measurements made just beforehand and just afterwards. The simultaneous, highly resolved graphic display of the analyte and the background signals on a video screen provides a means of reliable monitoring of the determination and simplifies method development.

The stabilised temperature platform furnace eliminates chemical interferences to such an extent that in most cases personnel- and cost-intensive sample preparation steps, such as solvent extractions, as well as the time-consuming method of additions, are no longer required.
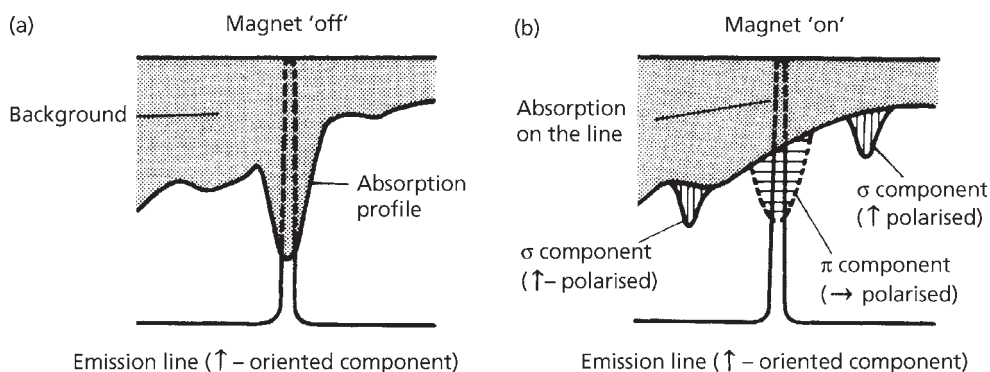
Figure 1.2 Zeeman patterns: (a) analyte signal plus background; (b) background only. (*Source: Author's own files*)

The advantages of Zeeman background correction are:

- Correction over the complete wavelength range.

- Correction for structural background.

- Correction for spectral interferences.

- Correction for high background absorptions.

- Single-element light source with no possibility of misalignment.

1.1.5.2 Instrumentation

The instrumentation for ZAAS is given in **Table 1.1**.

Figure 1.2 illustrates the operating principle of the Zeeman 5000 system. For Zeeman operation, the source lamps are pulsed at 100 Hz (120 Hz) while the current to the magnet is modulated at 50 Hz (60 Hz). When the field is off, both analyte and background absorptions are measured at the unshifted resonance line. This measurement directly compares with a 'conventional' atom and absorption measurement without background correction. However, when the field is on, only the background is measured since the σ absorption line profiles are shifted away from the emission line while the static polariser, constructed from synthetic crystalline quartz, rejects the signal from the π components. Background correction is achieved by subtraction of the field-on signal from the field-off signal. With this principle of operation, background absorption of up to 2 absorbance units can be corrected most accurately, even when the background shows a fine structure.

In assessing overall performance with a Zeeman effect instrument, the subject of analytical range must also be considered. For most normal class transitions, σ components will be completely separated at sufficiently high magnetic fields. Consequently, the analytical curves will generally be similar to those obtained by standard AAS. However, for certain anomalous transitions some overlap may occur. In these cases, curvature will be greater and may be so severe as to produce double-valued analytical curves. **Figure 1.3**, which shows calibration curves for copper, illustrates the reason for this behaviour. The Zeeman pattern for copper (324.8 nm) is particularly complex due to the presence of hyperfine structure. The dashed lines represent the separate field-off and field-on absorbance measurements. As sample concentration increases, field-off absorbance begins to saturate as in standard atomic absorption spectrometry. The σ absorbance measured with the field-on saturates at higher concentrations because of the greater separation from the emission line. When the increase in σ absorbance exceeds the incremental change in the field-off absorbance, the analytical curve (shown as the solid line) rolls over back towards the concentration axis. This behaviour can be observed

Table 1.1 Available Zeeman atomic absorption spectrometers

Supplier	Model	Microprocessor	Type	Hydride and mercury attachment	Autosampler
Perkin-Elmer	Zeeman 3030	Yes (method storage on floppy disk)	Integral flame/ graphite furnace	-	Yes
	Zeeman 5000	Yes, with programmer	Fully automated integral flame/ graphite furnace double-beam operation roll-over protection	Yes	Yes
Varian	SpectrA A30/40	Yes, method storage on floppy disk	Automated analysis of up to 12 elements; roll-over protection	-	Yes
	SpectrA A300/400	Yes, total system control and colour graphics; 90 methods stored on floppy disk	Automated analysis of up to 12 elements; roll-over protection	-	Yes

Source: Author's own files
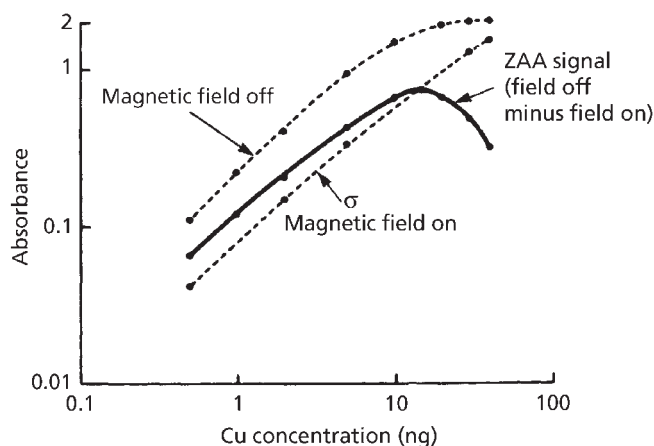
Figure 1.3 Copper calibration curves (324.8 nm) measured with the Zeeman 5000. (*Source: Author's own files*)

with all Zeeman designs regardless of how the magnet is positioned or operated. The existence of roll-over does introduce the possibility of ambiguous results, particularly when peak area is being measured.

1.1.6 Inductively Coupled Plasma Atomic Emission Spectrometry

1.1.6.1 Theory

An inductively coupled plasma is formed by coupling the energy from a radio frequency (1–3 kW or 27–50 MHz) magnetic field to free electrons in a suitable gas. The magnetic field is produced by a two- or three-turn water-cooled coil and the electrons are accelerated in circular paths around the magnetic field lines that run axially through the coil. The initial electron 'seeding' is produced by a spark discharge, but once the electrons reach the ionisation potential of the support gas further ionisation occurs and a stable plasma is formed.

The neutral particles are heated indirectly by collisions with the charged particles upon which the field acts. Macroscopically the process is equivalent to heating a conductor by a radio-frequency field, the resistance to eddy current flow producing Joule heating. The field does not penetrate the conductor uniformly and therefore the largest current flow is at the periphery of the plasma. This is the so-called 'skin' effect and coupled with a suitable gas-flow geometry it produces an annular, or doughnut-shaped, plasma. Electrically, the coil and plasma form a transformer

with the plasma acting as a one-turn coil of finite resistance.

If mass spectrometric determination of the analyte is to be incorporated, then the source must also be an efficient producer of ions.

Greenfield and co-workers [15] were the first to recognise the analytical potential of the annular ICP.

Wendt and Fassel [16] reported early experiments with a 'tear-drop'-shaped inductively coupled plasma but later described the medium power, 1–3 kW, 18 mm annular plasma now favoured in modern analytical instruments [17].

The current generation of ICP emission spectrometers provides limits of detection in the range 0.1–500 µg/l of metal in solution, a substantial degree of freedom from interferences, and a capability for simultaneous multi-element determination facilitated by a directly proportional response between the signal and the concentration of the analyte over a range of approximately five orders of magnitude.

The most common method of introducing liquid samples into the ICP is by using pneumatic nebulisation [18], in which the liquid is dispensed into a fine aerosol by the action of a high-velocity gas stream. The fine gas jets and liquid capillaries used in ICP nebulisers may cause inconsistent operation and even blockage when solutions containing high levels of dissolved solids, or particulate matter, are used. Such problems have led to the development of new types of nebuliser, the most successful being based on a principle originally described by Babington. In these types, the liquid is pumped from a wide-bore tube and then to the nebulising orifice by a V-shaped groove [19] or by the divergent wall of an over-expanded nozzle [20]. Such devices handle most liquids and even slurries without difficulty.

Two basic approaches are used for introducing samples into the plasma. The first involves indirect vaporisation of the sample in an electrothermal vaporiser, e.g., a carbon rod or tube furnace or heated metal filament as commonly used in AAS [21–23]. The second involves inserting the sample into the base of the ICP on a carbon rod or metal filament support [24, 25].

Table 1.2 compares the detection limits claimed for AAS and the graphite furnace and ICP variants.

Table 1.2 Guide to analytical values for IL spectrometers (IL 157/357/457/451/551/951/Video 11/12/22/S11/S12 Atomic Absorption Spectrophotometers® and IL Plasma-100/-200/-300 ICP Emission Spectrometers)

Element	Wavelength (nm)		AA Lamp current (mA)	Flame AA		Furnace AA (IL755 CTF Atomiser)			ICP
	AA	ICP		Sensitivity[2] (µg/l)	Detection limit (µg/l)	Sensitivity[2]	(µg/l)	Detection limit (µg/l)	Detection limit (µg/l)
Aluminium (Al)[1]	309.3	396.15	8	400	25	4.0	0.04	0.01	10
Antimony (Sb)	217.6	206.83	10	200	40	8.0	0.08	0.08	40
Arsenic (As)	193.7	193.70	8	400	1403	12	0.12	0.08	30
Barium (Ba)[1]	553.5	455.40	10	150	12	4.0	0.04	0.04	0.5
Beryllium (Be)[1]	234.9	313.04	8	10	1	1.0	0.01	0.003	0.1
Bismuth (Bi)	223.1	223.06	6	200	30	4.0	0.04	0.01	35
Boron (B)[1]	249.7	249.77	15	9,000	700	-	-	-	3
Cadmium (Cd)	228.8	214.44	3	10	1	0.2	0.002	0.0002	1.5
Calcium (Ca)	422.7	393.37	7	50	2	1.0	0.01	0.01	0.2
Calcium[1]	422.7	-	7	10	1	-	-	-	-
Carbon (C)	-	193.09	-	-	-	-	-	-	40
Cerium (Ce)	-	413.77	-	-	-	-	-	-	40
Caesium (Cs)	852.1	455.53	10	150	20	-	-	-	-
Chromium (Cr)	357.9	205.55	6	40	3	4.0	0.04	0.004	3
Cobalt (Co)	240.7	238.89	8	50	4	8.0	0.08	0.008	3
Copper (Cu)	324.7	324.75	5	30	1.8	4.0	0.04	0.005	1
Dysprosium (Dy)[1]	421.2	353.17	8	600	60	-	-	-	4
Erbium (Er)1	400.8	337.27	8	400	40	50	0.5	0.3	3

Table 1.2 Continued

Element	Wavelength (nm)		AA Lamp current (mA)	Flame AA		Furnace AA (IL755 CTF Atomiser)			ICP
	AA	ICP		Sensitivity[2] (µg/l)	Detection limit (µg/l)	Sensitivity[2]	(µg/l)	Detection limit (µg/l)	Detection limit (µg/l)
Europium (Eu)	-	381.97	-	-	-	-	-	-	2
Gadolinium (Gd)[1]	368.4	342.25	9	13,000	2,000	1,600	16	8	4
Gallium (Ga)	287.4	294.36	5	400	50	5.2	0.05	0.01	15
Germanium (Ge)[1]	265.1	209.43	5	800	50	40	0.4	0.1	20
Gold (Au)	242.8	242.80	5	100	6	5.0	0.05	0.01	10
Holmium (Hf)[1]	307.3	339.98	10	14,000	2,000	-	-	-	5
Halmium (Ho)[1]	410.4	345.60	12	660	60	90	0.9	0.7	1
Indium (In)	303.9	325.61	5	180	30	11	0.11	0.02	15
Iridium (Ir)[1]	208.8	224.27	15	1,500	500	170	1.7	0.5	8
Iron (Fe)	248.3	238.20	8	40	5	3.0	0.03	0.01	2
Lanthanum (La)[1]	550.1	333.75	10	22,000	2,000	58	0.58	0.5	2
Lead (Pb)	217.0	220.35	5	100	9	4.0	0.04	0.007	25
Lithium (Li)	670.8	670.78	8	16	1	4.0	0.04	0.01	25
Lutetium (Lu)	-	261.54	-	-	-	-	-	-	0.2
Magnesium (Mg)	285.2	279.55	3	3	0.3	0.07	0.0007	0.0002	0.1
Manganese (Mn)	279.5	257.61	5	20	1.8	1.0	0.01	0.0005	1
Mercury (Hg)	253.7	253.65	3	2,500	140	40	0.4	0.2	12
Molybdenum (Mo)[1]	313.3	202.03	6	200	25	12	0.12	0.03	4
Neodymium (Nd)[1]	492.5	401.23	10	5,000	700	-	-	-	8

Table 1.2 Continued

Element	Wavelength (nm)		AA Lamp current (mA)	Flame AA		Furnace AA (IL755 CTF Atomiser)			ICP
	AA	ICP		Sensitivity[2] (µg/l)	Detection limit (µg/l)	Sensitivity[2]	(µg/l)	Detection limit (µg/l)	Detection limit (µg/l)
Nickel (Ni)	232.0	221.65	10	60	5	20	0.2	0.05	4
Niobium (Nb)[1]	334.9	309.42	15	12,000	2,000	-	-	-	6
Osmium (Os)[1]	290.9	225.59	15	1,000	90	270	2.7	2	0.6
Palladium (Pd)	247.6	340.46	5	140	20	13	0.13	0.05	13
Phosphorus (P)	213.6	213.62	8	125,000	30,000	4,900	49	20	16
Platinum (Pt)	265.9	214.42	10	1,000	50	80	0.8	0.2	16
Potassium (K)	766.5	766.49	7	10	1	0.4	0.004	0.004	305
Praseodymium (Pr)[1]	495.1	390.84	15	20,000	2,000	-	-	-	20
Rhenium (Re)	346.1	221.43	15	8,000	800	1,000	10	10	6
Rhodium (Rh)	343.5	343.49	5	200	2	20	0.20	0.1	8
Rubidium (Rb)	780.0	-	10	30	2	-	-	-	-
Ruthenium (Ru)	349.9	240.27	10	800	400	-	-	-	8
Samarium (Sm)[1]	429.7	359.26	10	3,000	500	-	-	-	8
Scandium (Sc)[1]	391.2	361.38	10	100	20	-	-	-	0.5
Selenium (Se)	196.0	196.03	12	300	803	8.0	0.08	0.05	30
Silicon (Si)[1]	251.6	251.61	12	800	60	60	0.60	0.6	6
Silver (Ag)	328.1	328.07	3	30	1.2	0.5	0.005	0.001	3
Sodium (Na)	589.0	589.59	8	3	0.4	0.4	0.004	0.004	7
Strontium (Sr)	460.7	407.77	12	80	6	1.8	0.018	0.01	0.2

Table 1.2 Continued

Element	Wavelength (nm)		AA Lamp current (mA)	Flame AA		Furnace AA (IL755 CTF Atomiser)			ICP
	AA	ICP		Sensitivity[2] (µg/l)	Detection limit (µg/l)	Sensitivity[2]	(µg/l)	Detection limit (µg/l)	Detection limit (µg/l)
Tantalum (Ta)[1]	271.5	240.06	15	10,000	800	-	-	-	13
Tellurium (Te)	214.3	214.28	7	200	30	7.0	0.07	0.03	20
Terbium (Tb)[1]	432.7	350.92	8	3,300	1,000	-	-	-	3
Thallium (Tl)	276.8	276.79	8	100	30	4.0	0.04	0.01	27
Thorium (Th)	-	283.73	-	-	-	-	-	-	8
Thulium (Tm)	-	313.13	-	-	-	-	-	-	0.9
Tin (Sn)[1]	235.5	189.99	6	1,200	90	7.0	0.07	0.03	30
Titanium (Ti)[1]	364.3	334.94	8	900	60	50	0.50	0.3	1
Tungsten (W)[1]	255.1	207.91	15	5,000	500	-	-	-	14
Uranium (U)[1]	358.5	263.55	15	100,000	7,000	3,100	31	30	70
Vanadium (V)[1]	318.5	309.31	8	600	25	40	0.40	0.1	3
Ytterbium (Yb)	398.8	328.94	5	80	-	1.3	0.01	0.01	1
Yttrium (Y)[1]	410.2	371.03	6	1,800	200	1,300	13	10	0.7
Zinc (Zn)	213.9	213.86	3	8	1.23	0.3	0.003	0.001	2
Zirconium (Zr)[1]	360.1	343.82	10	10,000	2,000	-	-	-	2

[1] *Nitrous oxide/acetylene flame (AA)*
[2] *Sensitivity is concentration (or mass) yielding 1% absorption (0.0044 absorbance units)*
[3] *With background correction*
©*1985 Allied Analytical Sytems 7/85 5K*

15

1.1.6.2 Instrumentation

There are two main types of ICP spectrometer systems. The first is the monochromator system for sequential scanning, which consists of a high-speed, high-resolution scanning monochromator viewing one element wavelength at a time. Typical layouts are shown in **Figure 1.4**. **Figure 1.4(a)** shows a one-channel air path double monochromator design with a pre-monochromator for order sorting and stray light rejection, and a main monochromator to provide resolution of up to 0.02 nm. The air path design is capable of measuring wavelengths in the range 190–900 nm. The wide wavelength range enables measurements to be performed in the ultraviolet (UV), visible, and near-infrared regions of the spectrum (allowing determinations of elements from arsenic at 193.70 nm to caesium at 852.1 nm).

A second design (**Figure 1.4(b)**) is a vacuum monochromator design allowing measurements in the 160–500 nm wavelength range. The exceptionally low wavelength range gives the capability of determining trace levels of non-metals such as bromine at 163.34 nm as well as metals at low UV wavelengths, such as the extremely sensitive aluminium emission line at 167.08 nm. Elements such as boron, phosphorus or sulfur can be routinely determined using interference-free emission lines.
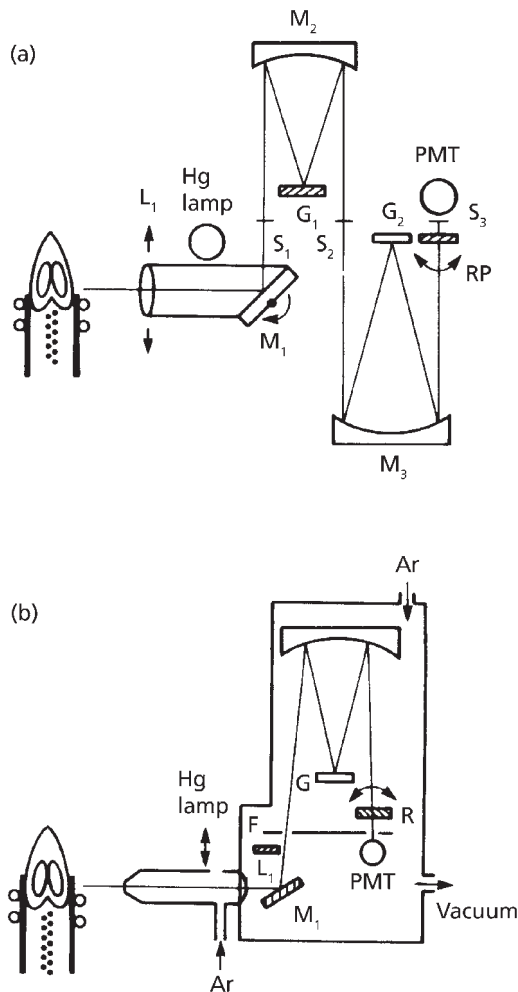
Figure 1.4 (a) A double monochromator consisting of an air-path monochromator with a pre-monochromator for order sorting and stray light rejection to determine elements in the 190-900 nm range; (b) the vacuum UV monochromator - an evacuated and argon-purged monochromator to routinely determine elements in the 160 to 500 µm range.
(*Source: Author's own files*)

The sequential instrument, equipped with either or both monochromators facilitates the sequential determination of up to 63 elements in turn, at a speed as fast as 18 elements per minute in a single sample. Having completed the analysis of the first sample, usually in less than a minute, it proceeds to the second sample, and so on.

The second main type of system is the polychromator system for simultaneous scanning. The polychromator systems scan many wavelengths simultaneously, i.e., several elements are determined simultaneously at higher speeds than are possible with monochromator systems. It then moves on to the next sample. A typical system is shown in **Figure 1.5**.
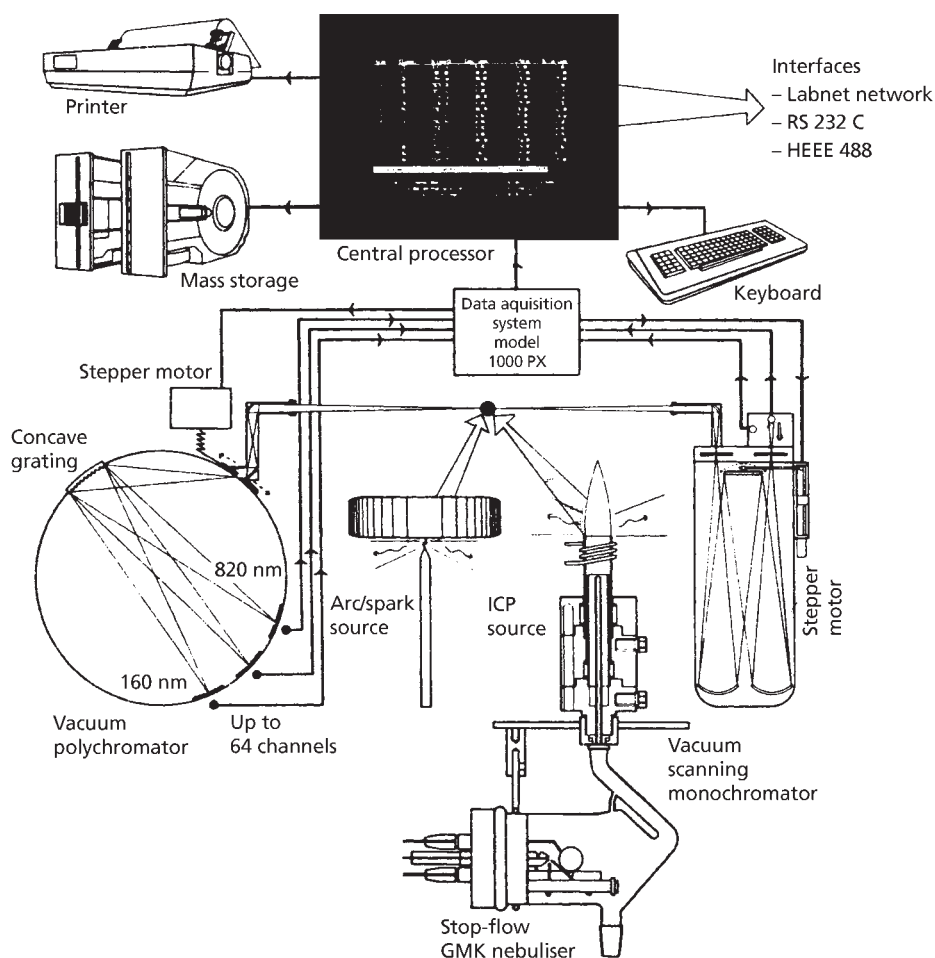
Figure 1.5 Polychromator system for inductively coupled plasma atomic emission spectrometer. (*Source: Author's own files*)

It is possible to obtain instruments that are equipped for both sequential and simultaneous scanning, such as the Labtam 8410.

1.1.6.3 Applications

Briseno and co-workers [26] quantified inorganic dopants in polypyrrole films by a combination of electrochemistry and ICP-AES.

1.1.7 Hybrid Inductively Coupled Plasma Techniques

1.1.7.1 Chromatography–Inductively Coupled Plasma

Direct introduction of a sample into an ICP produces information only on the total element content. It is now recognised that information on the form of the element present, or trace element speciation, is important in a variety of applications. One way of obtaining quantitative measurement of trace element speciation is to couple the separation power of chromatography to the ICP as a detector. Since the majority of interesting trace metal speciation problems concern either nonvolatile or thermally unstable species, high-performance liquid chromatography (HPLC) becomes the separation method of choice. The use of HPLC as the separation technique requires the introduction of a liquid sample into the ICP with the attendant sample introduction problem.

1.1.7.2 Flow Injection with Inductively Coupled Plasma

In conventional ICP-OES, a steady-state signal is obtained when a solution of an element is nebulised into the plasma. In flow injection [27] a carrier stream of solvent is fed continuously through a 1 mm id tube to the nebuliser using a peristaltic pump, and into this stream is injected, by means of a sampling valve, a discrete volume of a solution of the element of interest. When the sample volume injected is suitably small a transient signal is obtained (as opposed to a steady-state signal which is obtained with larger sample volumes) and it is this transient signal that is measured. Very little sample dispersion occurs under these conditions; the procedure is very reproducible; and sample rates of 180 samples per hour are feasible.

1.1.7.3 Inductively Coupled Plasma with Atomic Fluorescence Spectrometry

Atomic fluorescence is the process of radiational activation followed by radiational deactivation, unlike atomic emission which depends on the collisional excitation of

the spectral transition. For this, the ICP is used to produce a population of atoms in the ground state and a light source is required to provide excitation of the spectral transitions. Whereas a multitude of spectral lines from all the accompanying elements are emitted by the atomic emission process, the fluorescence spectrum is relatively simple, being confined principally to the resonance lines of the element used in the excitation source.

The ICP is a highly effective line source with a low background continuum. It is optically thin – it obeys Beer's law – and therefore exhibits little self-absorption. It is also a very good atomiser and the long tail flame issuing from the plasma has such a range of temperatures that conditions favourable to the production of atoms in the ground state for most elements are attainable. It is therefore possible to use two plasmas in one system: a source plasma to supply the radiation to activate the ground state atoms and another to activate the atomiser. This atomic fluorescence (AFS) mode of detection is relatively free from spectral interference, the main drawback of ICP-OES.

Good results have been obtained using a high-power (6 kW) ICP as a source and a low-power (<1 kW) plasma as an atomiser.

1.1.8 Inductively Coupled Plasma Optical Emission Spectrometry–Mass Spectrometry

1.1.8.1 Theory

ICP-MS combines the established ICP to break the sample into a stream of positively charged ions which are subsequently analysed on the basis of their mass. ICP-MS does not depend on indirect measurements of the physical properties of the sample. The elemental concentrations are measured directly – individual atoms are counted giving the key attribute of high sensitivity. The technique has the additional benefit of unambiguous spectra and the ability to directly measure different isotopes of the same element.

The sample under investigation is introduced, most typically in solution, into the inductively coupled plasma at atmospheric pressure and a temperature of approximately 6,000 K. The sample components are rapidly dissociated and ionised and the resulting atomic ions are introduced via a carefully designed interface into a high-performance quadrupole mass spectrometer at high vacuum.

A horizontally mounted ICP torch forms the basis of the ion source. Sample introduction is via a conventional nebuliser optimised for general-purpose solution analysis and suitable for use with both aqueous and organic solvents.

Nebulised samples enter the central channel of the plasma as a finely dispersed mist which is rapidly vaporised; dissociation is virtually complete during passage through the plasma core with most elements fully ionised.

Ions are extracted from the plasma through a water-cooled sampling aperture and a molecular beam is formed in the first vacuum stage and passes into the high-vacuum stage of the quadrupole mass analyser.

In an ICP-MS system a compact quadrupole mass analyser selects ions on the basis of their mass-to-charge ratio, m/z. The quadrupole is a simple compact form of mass analyser which relies on a time-dependent electric field to filter the ions according to their mass-to-charge ratio. Ions are transmitted sequentially in order of their m/z with constant resolution, across the entire mass range.

1.1.8.2 Instrumentation

Several manufacturers, including VG Isotopes and Perkin Elmer, supply equipment for ICP-MS.

The Perkin Elmer Elan 500 instrument is designed for routine and rapid multi-element quantitative determinations of trace and ultra-trace elements and isotopes. The Elan 500 can determine nearly all of the elements in the periodic table with exceptional sensitivity.

The entire Elan 500 Plasmalok system is designed for simplicity of operation. A typical daily start-up sequence from the standby mode includes turning on the plasma and changing to the operating mode. After a brief warm-up period for the plasma, routine sample analysis can begin.

VG Isotopes Ltd, is also a manufacturer of ICP-MS. The special features of their VG Plasmaquad PQ2 includes a multi-channel analyser which ensures rapid data acquisition over the whole mass range. The multi-channel analyser facilities include 4096 channels, 300 m facility for spectral analysis, user-definable number of measurements per peak in peak jumping mode, and the ability to monitor data as they are acquired. A multi-channel analyser is imperative for acquiring short-lived signals from accessories such as flow injection, electrothermal vaporisation, laser ablation, and so on, or for fast multi-element survey scans (typically 1 minute).

A variant of the Plasmaquad PQ2 is the Plasmaquad PQ2 plus instrument. This latter instrument has improved detector technology which incorporates a multimode system that can measure higher concentrations of elements without compromising the inherent sensitivity of the instrument. This extended dynamic range system (**Table 1.3**) produces

Table 1.3 Dynamic ranges of various techniques	
Graphite furnace AAS	0.1 µg/l to 1 µg/l
Plasmaquad PQ2	0.1 µg/l to 10 µg/l
Inductively coupled plasma - atomic absorption spectrometry	10.0 µg/l to 1000 µg/l
Plasmaquad PQ2 plus	0.1 µg/l to 1000 µg/l
Source: Author's own files	

an improvement in the effective linear dynamic range to eight orders of magnitude. Hence, traces at the microgram per litre level can be measured in the same analytical sequence as major constituents.

This technique has been applied to the analysis of aqueous digests of polymers containing up to 2% solids.

1.1.8.3 Applications

Dobney and co-workers [28] have used laser ablation ICP-MS to determine various metals in polyolefins.

1.1.9 Pre-concentration Atomic Absorption Spectrometry Techniques

Detection limits can be improved still further in the case of all three techniques mentioned previously by the use of a pre-concentration technique [29]. One such technique that has found great favour involves converting the metals to an organic chelate by reaction of a larger volume of sample with a relatively small volume of an organic solvent solution, commonly of diethyldithiocarbamates or ammonium pyrrolidone diethiocarbamates. The chelate dissolves in the organic phase and is then back-extracted into a small volume of aqueous acid for analysis by the techniques mentioned previously. If 0.5–1 litre of sample is originally taken and 20 ml of acid extract finally produced then concentration factors of 25–50 are thereby achieved with consequent lowering of detection limits. Needless to say, this additional step in the analysis considerably increases analysis time and necessitates extremely careful control of experimental conditions.

Microscale solvent extractions involving the extraction of 2.5 ml sample with 0.5 ml of an organic solvent solution of a chelate give detection limits for lead and cadmium by the Zeeman graphite furnace atomic absorption spectrometry method of 0.6 and

0.02 μg/l, respectively. This is equivalent to determining 1.2 ppm cadmium in polymers (assuming the digest of 10 mg of polymer is made up to 20 ml).

1.1.10 Microprocessors

In recent years the dominating influence on the design and performance of AAS is that of the microprocessor. Even the cheapest instruments are expected to provide autosampling systems for both flame and furnace use and therefore a means of recording the data produced.

1.1.11 Autosamplers

Gilson and PS Analytical supply autosamplers suitable for automation of AAS and ICP. The Gilson autosampler can house up to 300 samples and is capable of operation 24 hours per day. PS Analytical supply 20- and 80-position autosamplers.

For many applications such as hydride analysis, conventional multi-element analysis, and repetitive analysis for major element quantification, conventional autosamplers are not sufficiently sophisticated. The PS Analytical 20.020 twenty-position autosampler has been specifically developed to fill this void. It is easily interfaced to computer systems via a transistor-transistor logic (TTL) interface.

1.1.12 Applications: Atomic Absorption Spectrometric Determination of Metals

1.1.12.1 Catalyst Remnants and Other Impurities

Two types of catalysts used in polymer manufacture are metallic compounds, such as aluminium alkyls, and titanium halides used in low-pressure polyolefin manufacture. As the presence of residual catalysts can have important effects on polymer properties it is important to be able to determine trace elements which reflect the presence of these substances.

1.1.12.2 Elemental Analysis of Polymers

Elements occurring in polymers and copolymers can be divided into three categories:

1. Elements that are a constituent part of the monomers used in polymer manufacture, such as nitrogen in acrylonitrile used in the manufacture of, for example, acrylonitrile–butadiene–styrene terpolymers.

2. Elements that occur in substances deliberately included in polymer formulations, for example, zinc stearate.

3. Elements that occur as adventitious impurities in polymers. For example, during the manufacture of polyethylene (PE) by the low-pressure process, polymerisation catalysts such as titanium halides and organo-aluminium compounds are used, and the final polymer would be expected to, and indeed does, contain traces of aluminium, titanium, and chlorine residues.

The classic destructive techniques are generally based on one of three possible approaches to the analysis: (i) dry ashing of the polymer with or without an ashing aid, followed by acid digestion of the residue, or alternatively acid digestion of the polymer without prior ashing, (ii) fusion of the polymer with an inorganic compound to effect solution of the elements, and (iii) bomb or oxygen flask digestion techniques.

Another method for avoiding losses of metals during ashing is the low-temperature controlled decomposition technique using active oxygen. This method has been studied in connection with the determination of trace metals in polyvinyl chloride (PVC), polypropylene (PP), and polyethylene terephthalate [30].

1.1.12.3 Trace Metals in Polymers

Sources of trace metals in polymers are neutralising chemicals added to the final stages of manufacture to eliminate the effects of acidic catalyst remnants on polymer processing properties (e.g., hygroscopicity due to residual chloride ion). A case in point is high-density polyethylene (HDPE) and PP produced by the aluminium alkyl–titanium halide route which is treated with sodium hydroxide in the final stages of manufacture.

A technique that involves combustion of the polymer under controlled conditions in a platinum crucible, followed by dissolution of the residual ash in a suitable aqueous reagent prior to final analysis by spectrophotometry, is of limited value. A quite complicated and lengthy ashing programme is necessary in this technique to avoid losses of alkali metal during ignition: 0–1 hour from start: heat to 200 °C; 1–2 hours from start: hold at 200 °C; 3–5 hours from start: heat to 450 °C; 5–8 hours from start: hold at 450 °C.

After ignition the residue is dissolved in warm nitric acid and made up to a standard volume prior to evaluation by flame photometry or AAS. Alternatively, the polymer is ashed overnight at 500 °C with sulfur and a magnesium salt of a long-chain fatty acid (Magnesium AC dope, Shell Chemical Co. Ltd), and the ash mixed with twice its weight of carbon powder containing 0.1% palladium prior to emission spectrographic evaluation of the sodium/palladium 330.3/276.31 line pair.

Table 1.4 The effects of modification of ashing procedure on the flame photometric determination of sodium in polyethylenes					
Sodium by flame photometry (ppm)					
Sample	By neutron activation	By emission spectrography	Original (ashed between 650 °C and 800 °C)	Dope ash at 500 °C	Direct ash at 500 °C
1	99, 96, 99	95	60, 76, 55	100	75
2	256, 247, 259	258, 259	160, 178, 271	225	208
3	343, 321, 339	339, 287	250, 312	282	265
4	213, 210, 212	218, 212	140, 196	210	191
5	194, 189, 192	209, 198	80, 158, 229	196	169
6	186, 191, 198	191, 191	96, 173	193	173
Source: Author's own files					

The results in **Table 1.4** clearly show that flame photometry following dope ashing at 500 °C gives a quantitative recovery of sodium relative to results obtained by a non-destructive method of analysis, i.e., NAA. Direct ashing without the magnesium ashing aid at 500 °C causes losses of 10% or more of the sodium, while direct ashing at 800 °C causes even greater losses.

Dry ashing in platinum has been found to give reasonably good results in the determination of low concentrations of vanadium in an ethylene–propylene copolymer. An amount of 10 g of polymer is ashed in platinum by charring on a hot plate followed by heating over a Meker burner. Dilute nitric acid is added to the residue and any residue in the crucible dissolved by fusion with potassium persulfate. The vanadium is determined spectrophotometrically by the 3,3′-diaminobenzene method [31]. **Table 1.5** compares the results obtained by this method with those obtained by NAA, which in this case can be considered to be an accurate reference method. Good agreement is obtained between the two methods for samples containing vanadium.

It has been shown [32, 33] in studies using a radioactive copper isotope that, when organic materials containing copper are ashed in silica crucibles, losses of up to some 10% of the copper will occur due to retention in the silica; this could not be removed by acid washing. Virtually no retention of copper in the silica crucible occurred, however, when copper was ashed under the same conditions in the absence of added organic matter. This was attributed to reduction of copper to the metal by organic matter present, followed by partial diffusion of the copper metal into the crucible wall. Distinctly higher copper determinations are obtained for polyolefins by the procedure involving the use

Table 1.5 Results for Vanadium (ppm) by two different methods		
Sample	Dry ashing	Neutron activation
A	10.2	9.9 ± 0.2
B	14.0	14.1 ± 0.1
C	14.6	15.6 ± 0.3
D	0.5	0.14 ± 0.01
E	13.0	14.8 ± 0.2
F	0.9	0.27 ± 0.01
G	15.2	18.8 ± 0.3
H	18.2	17.9 ± 0.3
Source: Author's own files		

of a magnesium oxide ashing aid than are obtained without an ashing aid, or by the use of a molten potassium bisulfate fusion technique to take up the polymer ash.

Henn [34] has reported on a flameless atomic absorption technique with solid sampling for determining trace amounts of chromium, copper and iron in polymers such as polyacrylamide, with a detection limit of approximately 0.01 ppm.

AAS is a useful technique for the determination of traces of metals in polymers. Generally, the polymer is ashed at a maximum temperature of 450 °C: 0.1 hour from start: heat to 200 °C; 1–3 hours from start: hold at 200 °C; 3–5 hours from start: heat to 450 °C; 5–8 hours from start: hold at 450 °C. The ash is digested with warm nitric acid prior to spectrometric analysis. The detection limits for metals in polymers achievable by this procedure are given in **Table 1.6**.

Certain elements (such as arsenic, antimony, mercury, selenium, and tin) can, after producing the soluble digest of the polymer, be converted to gaseous metallic hydrides by reaction of the digest with reagents such as stannous chloride or sodium borohydide:

$$As_2O_3 + 3SnCl_2 + 6HCl = 2AsH_3 + 3H_2O + 3SnCl_4$$

$$NaBH_4 + 2H_2O = NaBO_2 + 4H_2$$

$$6H_2 + As_2O_3 = 2AsH_3 + 3H_2O$$
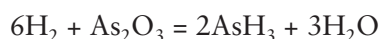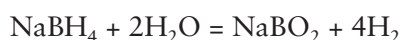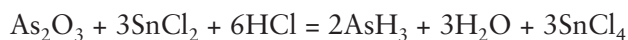
These hydrides can be determined by AAS. To illustrate, let us consider a method developed for the determination of trace amounts of arsenic in acrylic fibres containing antimony oxide fire-retardant additive [35]. The arsenic occurs as an impurity in the antimony oxide additive and, as such, its concentration must be controlled at a low level.

Table 1.6 Analytical conditions. Metals in polymers					
Element	Wavelength (nm)	Band pass	Operating range (in polymer) (ppm)	Detection limit (in polymer) (ppm)	Concentration of standard solution (ug/l)
Iron	248.3	0.3	5	0.57	500
Manganese	279.5	0.5	1.25	0.03	250
Chromium	357.9	0.5	2.5	0.03	500
Cadmium	228.8	1.0	0.5	0.015	50
Copper	324.7	1.0	1.25	0.045	250
Lead	217.0	1.0	5	0.15	1250
Nickel	232.0	0.15	2.5	0.07	500
Zinc	213.9	1.0	0.5	0.015	125
Reprinted from L. Henn, Analytica Chimica Acta, 1974, 73, 273, with permission from Elsevier.					

In this method (see Method 1.2 at the end of this chapter) a weighed amount of sample is digested with concentrated nitric and perchloric acids until the sample is completely dissolved. Pentavalent arsenic in the sample is then reduced to trivalent arsenic by the addition of titanium trichloride dissolved in concentrated hydrochloric acid:

$$As^{5+} + 2Ti^{3+} = As^{3+} + 2Ti^{4+}$$
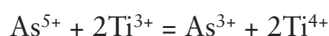
The trivalent arsenic is then separated from antimony by extraction with benzene, leaving antimony in the acid layer. The trivalent arsenic is then extracted with water from the benzene phase. This solution is then extracted with a mixture of hydrochloric acid, potassium iodide, and stannous chloride to convert trivalent arsenic to arsine (AsH_3), which is swept into the AAS. Arsenic is then determined at the 193.7 nm absorption line. Recoveries of between 96 and 104% are obtained by this procedure in the 0.5–1.0 µg arsenic range, with a detection limit of 0.04 ppm.

The results for the arsenic obtained with various acrylic fibre samples containing antimony oxide are given in **Table 1.7** (see Method 1.2). Antimony, present as the trioxide, has been accurately determined in a concentrated hydrochloric acid extract of PP powder [36].

Table 1.7 Results for the determination of arsenic in acrylic fibres containing antimony oxide				
Sample no.	Supplier	Content of Sb_2O_5* (%)	No. of determinations	Arsenic content (ppm)
1	A	5.1	4	50 ± 1
2	A	5.1	3	84 ± 4
3	A	4.5	2	94 ± 7
4	A	4.6	5	10.3 ± 0.5
5	A	5.0	5	4.1 ± 0.2
6	B	3.0 (Sb_2O_3)	3	45 ± 0
7	C	-	2	180 ± 11
8	C	-	4	103 ± 6
9	D	2.4 (Sb_2O_3)	2	8.5 ± 0.5
10	E	1.0 (Sb_2O_3)	4	3.2 ± 0.1
11	-	Sb_2O_5 50 mg + acrylic fibre (no Sb) 1 g	2	0.47 ± 0.03
12	-	Sb_2O_5 50 mg + acrylic fibre (no Sb) 1 g	1	0.08
* Even when antimony(III) was present in acrylic fibres (samples 6, 9 and 10), antimony(III) was easily and completely oxidised to antimony(V) by the wet digestion with a mixture of nitric, perchloric and sulfuric acids. Hence, arsenic in acrylic fibres containing antimony(III) oxide could be determined as well as that in acrylic fibre samples containing antimony(V) oxide by this method. Reprinted from T. Korenaga, Analyst, 1981, 106, 40, with permission from the Royal Society of Chemistry [35]				

1.1.12.4 Pressure Dissolution of Polymers

Pressure dissolution and digestion bombs have been used to dissolve polymers for which wet digestion is unsuitable. In this technique the sample is placed in a pressure dissolution vessel with a suitable mixture of acids and the combination of temperature and pressure effects dissolution of the sample. This technique is particularly useful for the analysis of volatile elements that may be lost in an open digestion.

1.1.12.5 Microwave Dissolution of Polymers

More recently, microwave ovens have been used for polymer dissolution. The sample is sealed in a Teflon bottle, or a specially designed microwave digestion vessel, with a mixture of suitable acids. The high-frequency microwave temperature (~100–250 °C) and increased pressure have a role to play in the success of this technique. An added advantage is the significant reduction in sample dissolution time [37, 38].

1.1.12.6 Equipment for Sample Digestions

Pressure Dissolution Acid Digestion Bombs. Inorganic and organic materials can be dissolved rapidly in Parr acid digestion bombs with Teflon liners and using strong mineral acids, usually nitric and/or *aqua regia* and, occasionally, hydrofluoric acid. Perchloric acid must not be used in these bombs due to the risk of explosion.

For nitric acid 200 °C (80 °C over the atmospheric boiling point) and 0.7 MPa can be achieved in 12 minutes and for hydrochloric acid 153 °C (43 °C over the atmospheric boiling point) and 0.7 MPa can be obtained in 5 minutes. The aggressive digestion action produced at the higher temperatures and pressures generated in these bombs results in remarkably short digestion times, with many materials requiring less than one minute to obtain a complete dissolution; considerably quicker than open-tube wet ashing or acid digestion procedures. Several manufacturers supply microwave ovens and digestion bombs (Parr Instruments, CEM Corporation, Prolabo).

Oxygen Combustion Bombs. Combustion with oxygen in a sealed Parr bomb has been accepted for many years as a standard method for converting solid combustible samples into soluble forms for chemical analysis. It is a reliable method whose effectiveness stems from its ability to treat samples quickly and conveniently within a closed system without losing any of the sample or its combustion products. Sulfur-containing polymers are converted to soluble forms and absorbed in a small amount of water placed in the bomb. Halogen-containing polymers are converted to hydrochloric acid or chlorides. Any mineral constituents remain as ash but other elements, such as arsenic, boron, mercury, nitrogen and phosphorus, and all of the halogens, are recovered with the bomb washings. In recent years the list of applications has been expanded to include metals such as beryllium, cadmium, chromium, copper, iron, lead, manganese, nickel, vanadium and zinc by using a quartz liner to eliminate interference from trace amounts of heavy metals leached from the bomb walls and electrodes [39–41].

Once the sample is in solution in the acid and the digest made up to a standard volume, the determination of metals is completed by standard procedures such as AAS, ICP-OES, or any of the techniques listed in Sections 1.1.1–1.1.8.

1.1.12.7 Techniques for Sample Digestion

Table 1.8 shows results obtained for the digestion in closed vessels of 1 g samples digested (a) in 20 ml of 1:1 nitric acid:water and (b) in 5 ml of concentrated nitric acid and 3 ml of 30% hydrogen peroxide. In the former, at a power input of 450 W, the temperature and pressure rose to 180 °C and 0.7 MPa. At that point, microwave power was reduced to maintain the temperature and pressure at those values for an additional 50 minutes. In the latter case, 1 g samples were open-vessel digested in 1:1 nitric acid: water for 10 minutes at 180 W. After cooling to room temperature, 5 ml of concentrated nitric acid and 3 ml of 30% hydrogen peroxide were added to each. The vessels were then sealed and power was applied for 15 minutes at 180 W followed by 15 minutes at 300 W. As can be seen, the temperature rose to 115 °C after the first 15 minutes and to 152 °C at 0.3 MPa after the final 15 minutes of heating. With both reagent systems element recoveries are in good agreement with the values obtained using a hot plate total sample digestion technique, which typically requires 4–6 hours.

Flame and GFAAS techniques have adequate sensitivity for the determination of metals in polymer samples. In this technique up to 1 g of dry sample is digested in a microwave oven for a few minutes with 5 ml of *aqua regia* in a small polytetrafluoroethylene-lined bomb, and then the bomb washings are transferred to a 50 ml volumetric flask prior to analysis by flame AAS. Detection limits (mg/kg) achieved by this technique

Table 1.8 Solid sample microwave digested in HNO_3:H_2O (1:1)			
Element	(a) in 1:1 HNO_3:H_2O	(b) in 5:3 HNO_3:H_2O_2	Certified value (%)
	Amount recovered (%)	Amount recovered (%)	
As	0.0060, 0.0060	0.0075, 0.0070	0.0066
Cd	0.0012, 0.0012	0.0011, 0.0012	0.0012 ± 0.00015
Cr	3.00, 2.98	3.04, 2.96	2.96 ± 0.28
Cu	0.0122, 0.0113	0.0118, 0.0119	0.0109 ± 0.0019
Mg	0.72, 0.72	0.70, 0.70	0.74 ± 0.02
Mn	0.0790, 0.0780	0.0720, 0.0725	0.0785 ± 0.0097
Ni	0.0050, 0.0050	0.0044, 0.0044	0.00458 ± 0.00029
Pb	0.0736, 0.0737	0.0736, 0.0733	0.0714 ± 0.0028
Se	0.0001, 0.0001	0.0001, 0.0001	(0.00015)
Zn	0.170, 0.168	0.160, 0.160	0.172 ± 0.017
Source: Author's own files			

were: 0.25 (cadmium, zinc); 0.5 (chromium, manganese); 1 (copper, nickel, iron); and 2.5 (lead). Application of this technique gave recoveries ranging between 85% (cadmium) and 101% (lead, nickel, iron) with an overall recovery of 95%.

1.1.13 Visible and UV Spectroscopy

The theory of visible and UV spectroscopy is discussed in an HMSO publication [42].

Visible spectrophotometers are commonly used for the estimation of colour in a sample or for the estimation of coloured products produced by reacting a colourless component of the sample with a reagent.

Visible spectrophotometry still finds extensive use in the determination of some anions such as chloride, phosphate and sulfate formed by the decomposition of chlorine, phosphorus and sulfur in polymers. An extensive modern application of visible spectrophotometry is in the determination of organic substances, including non-ionic detergents, in polymer extracts. An example is the determination of vanadium in ethylene-propylene rubber (see Method 1.3 at the end of this chapter).

Some commercially available instruments, in addition to visible spectrophotometry, can also perform measurements in the UV and near-infrared regions of the spectrum.

1.1.14 Polarography and Voltammetry

A large proportion of trace metal analysis carried out in polymer laboratories is based on the techniques of AAS and ICP-AES. Both of these methods give estimates of the total concentration of metal present and do not distinguish between different valency states of the same metal. For example, they would not distinguish between arsenic and antimony in the tri- or pentavalent states present in water extracts of polymers. Polarographic techniques can make such distinctions and, as discussed in Chapter 7, can be used to determine electroreducible organic materials such as antioxidants and monomers in polymers.

1.1.14.1 Instrumentation

Three basic techniques of polarography are of interest. The basic principles of these are outlined below.

Universal: differential pulse (DPN, DPI, DPR). In this technique a voltage pulse is superimposed on the voltage ramp during the last 40 ms of controlled drop growth

with a standard dropping mercury electrode – the drop surface is then constant. The pulse amplitude can be pre-selected. The current is measured by integration over a 20 ms period immediately before the start of the pulse and again for 20 ms as the pulse nears completion. The difference between the two current integrals ($l_2 - l_1$) is recorded and this gives a peak-shaped curve. If the pulse amplitude is increased, the peak current value is raised and the peak is broadened at the same time.

Classic: direct current (DCT). In this direct current method integration is performed over the last 20 ms of controlled drop growth (Tast procedure). During this time, the drop surface is constant in the case of a dropping mercury electrode. The resulting polarogram is step-shaped. Compared with classic DC polarography according to Heyrovsky, i.e., with a free-dropping mercury electrode, the DCT method offers great advantages: considerably shorter analysis times, no disturbance due to current oscillations, simpler evaluation, and larger diffusion-controlled limiting current.

Rapid: square wave (SQW). Five square-wave oscillations of frequency around 125 Hz are superimposed on the voltage ramp during the last 40 ms of controlled drop growth – with a dropping mercury electrode the drop surface is then constant. The oscillation amplitude can be pre-selected. Measurements are performed in the second, third, and fourth square-wave oscillation; the current is integrated over 2 ms at the end of the first and the end of the second half of each oscillation. The three differences of the six integrals ($l_1 - l_2$, $l_3 - l_4$, $l_5 - l_6$) are averaged arithmetically and recorded as one current value. The resulting polarogram is peak-shaped.

1.1.14.2 Applications

Polarography is an excellent method for trace and ultra-trace analysis of inorganic and organic substances and compounds. The basic process of electron transfer at an electrode is a fundamental electrochemical principle, and for this very reason polarography can be used over a wide range of applications.

After previous enrichment at a ranging mercury drop electrode, metals can be determined using differential pulse-stripping voltammetry. Detection limits are of the order of 0.05 µg/l.

Mal'kova and co-workers [43] described an AC polarographic method for the determination of cadmium, zinc, and barium stearates or laurates in PVC. The samples are prepared for analysis by being ashed in a muffle furnace at 500 °C, a solution of the ash in hydrochloric acid being made molar in lithium chloride and adjusted to pH 4.0 ± 0.2. The solution obtained is de-aerated by the passage of argon and the polarogram is recorded. Cadmium, zinc, and barium give sharp peaks at –0.65, –1.01, and –1.90 V, respectively, against the mercury-pool anode.

1.1.15 Ion Chromatography

When it is necessary to determine several metals in a polymer then application of ion chromatography [44] has several advantages over AAS, ICP-AES, and polarography. These include specificity, freedom from interference, speed of analysis, and sensitivity. It is, of course, necessary to digest the polymer using suitable reagent systems to produce an aqueous solution of the ions to be determined. Ion chromatography can complement atomic absorption and plasma methods as a back-up technique.

At the heart of the ion chromatography system is an analytical column containing an ion exchange column on which various anions and/or cations are separated before being detected and quantified by various detection techniques such as spectrophotometry, AAS (metals), or conductivity (anions).

Ion chromatography is not restricted to the separate analysis of only anions or only cations. With the proper selection of the eluant and separator columns the technique can be used for the simultaneous analysis of both anions and cations.

The principles of ion chromatography are discussed in an HMSO publication [45].

1.1.15.1 Instrumentation

Numerous manufacturers now supply instrumentation for ion chromatography. However, Dionex are still the leaders in the field; they have been responsible for many of the innovations introduced into this technique and are continuing to make such developments.

Some of the features of the Dionex series 4000i ion chromatograph instruments are discussed next.

Chromatography Module

- Up to six automated valves made of chemically inert, metal-free material eliminate corrosion and metal contamination.

- Liquid flow path is completely compatible with all HPLC solvents.

- Electronic valve switching, multi-dimensional, coupled chromatography, or multi-mode operation.

- Automated sample clean-up or pre-concentration.

- Environmentally isolates up to four separator columns and two suppressers for optimal results.

- Manual or remote control with Dionex Autoion 300 or Autoion 100 automation accessories.

- Individual column temperature control from ambient to 100 °C (optional).

Dionex Ion-Pac Columns

- Polymer ion exchange columns are packed with new pellicular resins for anion or cation exchange applications.

- New 4 µm polymer ion exchange columns have maximum efficiency and minimum operating pressure for high-performance ion and liquid chromatography applications.

- New ion exclusion columns with bifunctional cation exchange sites offer more selectivity for organic acid separations.

- Neutral polymer resins have high surface area for reversed phase ion pair and ion suppression applications without pH restriction.

- 5 and 10 µm silica columns are optimised for ion pair, ion suppression and reversed phase applications.

Micromembrane Suppressor

The micromembrane suppressor makes it possible to detect non-UV-absorbing compounds such as inorganic anions and cations, surfactants, fatty acids, and amines in ion exchange and ion pair chromatography.

Two variants of this exist: the anionic (AMMS) and the cationic (CMMS) suppressor. The micromembrane suppressor consists of a low dead volume eluent flow path through alternating layers of high-capacity ion exchange screens and ultra-thin ion exchange membranes. Ion exchange sites in each screen provide a site-to-site pathway for eluent ions to transfer to the membrane for maximum chemical suppression.

Dionex anion and cation micromembrane suppressors transform eluent ions into less conducting species without affecting sample ions under analysis. This improves conductivity detection, sensitivity, specificity, and baseline stability. It also dramatically increases the dynamic range of the system for inorganic and organic ion

chromatography. The high ion exchange capacity of the micromembrane suppressor permits changes in eluent composition by orders of magnitude, making gradient ion chromatography possible.

In addition, because of the increased detection specificity, preparation is dramatically reduced, making it possible to analyse most samples after simple filtering and dilution.

Conductivity Detector

- High-sensitivity detection of inorganic anions, amines, surfactants, organic acids, group I and II metals, oxy-metal ions, and metal cyanide complexes (used in combination with micromembrane suppressor).

- Bipolar-pulsed excitation eliminates the non-linear response with concentration found in analogue detectors.

- Microcomputer-controlled temperature compensation minimises the baseline drift with changes in room temperature.

UV/Visible Detector

- High-sensitivity detection of metals, silica, and other UV-absorbing compounds using either post-column reagent addition or direct detection.

- Non-metallic cell design eliminates corrosion problems.

- Filter-based detection with selectable filters from 214 to 800 nm.

- Proprietary dual wavelength detection for ninhydrin-detectable amino acids and 2-pyridyl resorcinol-detectable transition metals.

Optional Detectors

Dionex also offers visible, fluorescence, and pulsed amperometric detectors for use with the series 4000i. Dionex also supply a wide range of alternative instruments, e.g., single channel (2010i) and dual channel (2020i). The latter can be upgraded to an automated system by adding Autoion 100 or Autoion 300 controllers to control two independent ion chromatograph systems. Dionex also supply 2000i series equipped with conductivity pulsed amperometric, UV/visible, visible, and fluorescence detectors.

1.1.15.2 Applications

A typical system for the determination of metals is shown in **Figure 1.6**. A liquid sample is introduced at the top of the ion exchange analytical column (the separator column, **Figure 1.6**). An eluent (containing a complexing agent in the case of metal determination) is pumped through the system. This causes the ionic species (metal ions) to move through the column at rates determined by their affinity for the column resin. The differential migration of the ions allows them to separate into discrete bands.

As these bands move through the column they are delivered, one at a time, into the detection system. For metals, this comprises a post-column reactor that combines a colouring reagent (pyridyl azoresorcinol; PAR) with the metal bands. The coloured bands can then be detected by the appropriate detection mode. In the case of metal–PAR complex detection, visible wavelength absorbance is employed.
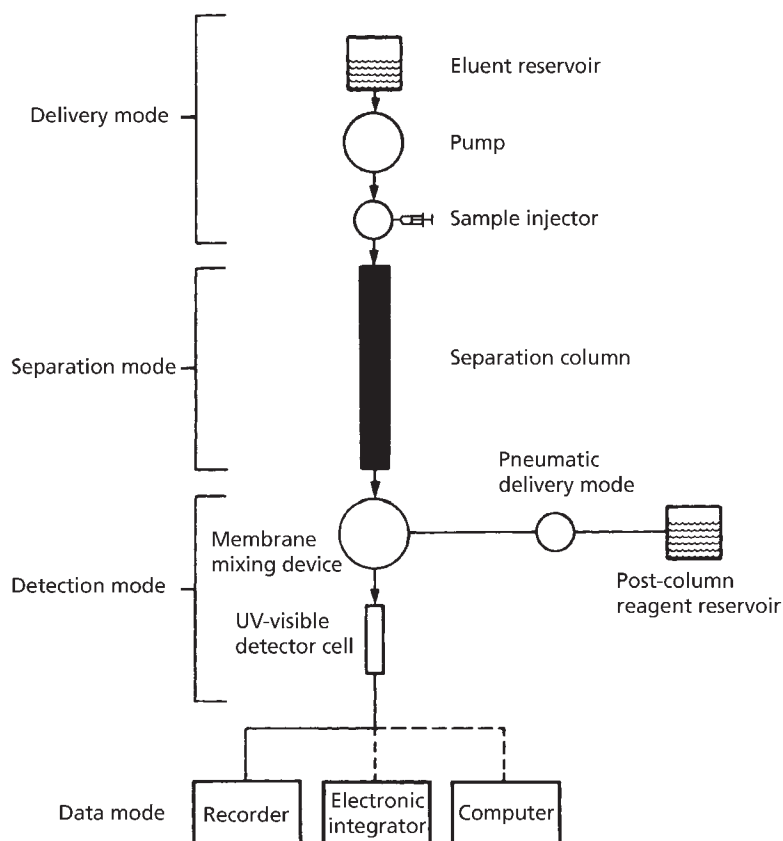
Figure 1.6 Ion chromatography with post-column reaction configuration for metals analysis. (*Source: Author's own files*)

The detector is set to measure the complexed metal band at a pre-selected wavelength. The results appear in the form of a chromatogram, essentially a plot of the time the band was retained on the column versus the signal it produces in the detector. Each metal in the sample can be identified and quantified by comparing the chromatogram against that of a standard solution.

Because only the metal ions of interest are detected, ion chromatography is less subject to interferences compared with other methods. Since individual metals and metal compounds form distinct ions with differing retention times, it is possible to analyse several of them in a single run – typically less than 20 minutes.

By selecting the appropriate column for separating the ions of interest in a sample, it is possible to separate and analyse the oxidation state of many metals, and determine Group I and II metals, metal complexes, and a complete range of inorganic and organic ions in a sample with excellent speed and sensitivity.

Table 1.9 shows a comparison of the detection limits of ion chromatography *versus* flame AAS for ideal, single components in deionised water. On small-volume injections (50 µl), ion chromatography compares well with AAS. With sample pre-concentration techniques, the detection limits for ion chromatography can surpass those of GFAAS. While high concentration of acids or bases can limit the applicability of AAS, ion chromatography allows direct injection of up to 10% concentrated acids or bases. This is extremely convenient in the direct analysis of acid-digested samples such as digests of polymers (**Figure 1.7**). Utilising ion exchange pre-concentration methods, extremely low concentrations of metals in polymer digests can be measured with ion chromatography. These detection limits are typically in the sub-picogram range.

1.2 Non-destructive Methods

1.2.1 X-ray Fluorescence Spectrometry

1.2.1.1 Theory

The XRF technique has a true multi-element analysis capability and requires no foreknowledge of the elements present in the sample. As such it is very useful for the examination of many types of samples encountered in the plastics laboratory.

This technique is very useful for solid samples especially if the main constituents (matrix) are made of low-atomic-weight elements and the sought impurities or constituents are of relatively high atomic weight.

Samples are irradiated with high-energy radiation, usually X-rays, to produce secondary X-rays which are characteristic of the individual elements present. The

Table 1.9 Metal detection limits by ion chromatography				
Metal species detected by ion chromatography		Detection limit (mg/l)		
		Direct	Preconcentrated	Flame AA
Aluminium	Al^{3+}	56	0.5	20
Barium	Ba^{2+}	100	0.1	20
Cadmium	Cd^{2+}	10	0.1	1
Calcium	Ca^{2+}	50	0.5	3
Caesium	Cs^+	100	0.1	20
Chromium	Cr(III) as CrEDTA	1000	10	3
Chromium	Cr(VI) as CrO_4	50	1	3
Cobalt	Co^{2+}	3	0.03	5
Copper	Cu^{2+}	5	0.05	2
Dysprosium	Dy^{3+}	100	1	60
Erbium	Er^{3+}	100	1	60
Europium	Eu^{3+}	100	1	-
Gadolinium	Gd^{3+}	100	1	2000
Gold	Au(I) as $Au(CN)^-$	100	10	10
Gold	Au(III) as $Au(CN)_4^-$	100	10	10
Holmium	Ho^{3+}	100	1	60
Iron	Fe(II)	10	0.1	5
Iron	Fe(III)	3	0.03	5
Lead	Pb^{2+}	100	1	1
Lithium	Li^+	50	0.5	2
Lutetium	Lu^{3+}	100	1	-
Magnesium	Mg^{2+}	50	0.5	0.2
Molybdenum	as MoO_4	50	1	10
Nickel	Ni^{2+}	25	0.3	8
Palladium	as $PdCl_4^{2-}$	10	1	20
Platinum	as $PtCl_6^{2-}$	10	1	50
Potassium	K^+	50	0.5	1

Table 1.9 Continued				
Metal species detected by ion chromatography		**Detection limit (mg/l)**		
		Direct	**Preconcentrated**	**Flame AA**
Rubidium	Rb^+	100	1	2
Samarium	Sm^{3+}	100	1	700
Silver	as $Ag(CN)_2^-$	100	10	2
Sodium	Na^+	50	0.5	0.4
Strontium	Sr^{2+}	100	1	6
Terbium	Tb^{3+}	100	1	2000
Thulium	Tm^{3+}	100	1	-
Tin	Sn(II)	100	1	80
Tin	Sn(IV)	100	1	80
Tungsten	as WO_4^{2-}	50	1	100
Uranium	as UO_2^{2+}	5	0.05	7000
Ytterbium	Yb^{3+}	100	1	-
Zinc	Zn^{2+}	10	0.1	0.6
Source: Author's own files				
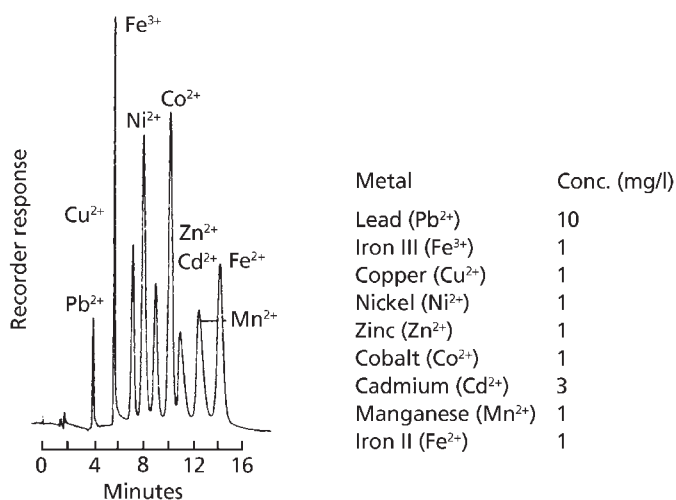
Figure 1.7 Ion chromatography: determination of nine transition metal ions. (*Source: Author's own files*)

X-ray intensity due to a particular element is proportional to the concentration of that element in the sample. There are two types of instrument in production: those in which the emitted radiation is separated by wavelength using crystals as gratings, i.e., total reflection XRF (wavelength dispersive XRF; WDXRF or total reflection XRF; TRXRF); and those in which the radiation is not separated but identified by energy dispersive electronic techniques using solid-state detectors and multi-channel analysers, i.e., energy dispersive XRF (EDXRF).

Energy dispersive instruments rely on solid-state energy detectors coupled to energy discriminating circuitry to distinguish the radiation by its energy level and measure the amount at each level. Most X-ray detectors now in use are solid-state devices which emit electrons when X-rays are absorbed, the energy of the electrons being proportional to that of the incident X-rays and the quantity proportional to the intensity.

Typically, instruments will determine from a few percent down to parts per million in a solid sample.

WDXRF tend to be most accurate and precise for trace element determinations. EDXRF instruments tend to lose precision for traces of light elements in heavy element matrixes unless longer counting times are used. With short counting times, for example, the coefficient of variation for a minor constituent element determination by an energy dispersive instrument should be better than 10%, but for a light trace element it may only be 50%. The advantage of the energy dispersive instrument is that it can be made so that almost all the radiation emitted hits the detector. Qualitative analysis is made by comparison with standard samples of known composition using total line energy. This is given by the total detector output of the line, or line peak area depending on the method of read-out used.

Due to the simple spectra and the extensive element range (sodium upwards in the periodic table) that can be covered using an Si(Li) detector and a 50 kV X-ray tube, EDXRF spectrometry is perhaps unparalleled for its qualitative element analysis power.

Qualitative analysis is greatly simplified by the presence of few peaks that occur in predictable positions and by the use of tabulated element/line markers which are routinely available from computer-based analysers.

To date, the most successful method of combined background correction and peak deconvolution has been the method of digital filtering and least squares (FLS) fitting of reference peaks to the unknown spectrum [46]. This method is robust, simple to automate, and is applicable to any sample type.

The major disadvantage of conventional EDXRF has been poor elemental sensitivity, a consequence of high background noise levels resulting mainly from instrumental

geometries and sample matrix effects. TRXRF is a relatively new multi-element technique with the potential to be an impressive analytical tool for trace element determinations for a variety of sample types. The fundamental advantage of TRXRF is its ability to detect elements in the picogram range in comparison to the nanogram levels typically achieved by traditional EDXRF spectrometry.

The principles of TRXRF were first reported by Yoneda and Horiuchi [47] and further developed by Aiginger and Wadbrauschek [48] and others [49–52]. In TRXRF the exciting primary X-ray beam impinges upon the specimen prepared as a thin film on an optically flat support of synthetic quartz or Perspex at angles of incidence in the region of 2 to 5 minutes of arc below the critical angle. In practice the primary radiation does not (effectively) enter the surface of the support but skims the surface, irradiating any sample placed on the support surface. The scattered radiation from the sample support is virtually eliminated, thereby drastically reducing the background noise. A further advantage of the TRXRF system, resulting from the geometry used, is that the solid-state energy dispersive detector can be accommodated very close to the sample (0.3 mm), which allows a large solid angle of fluorescent X-ray collection, thus enhancing the signal sensitivity and enabling the analysis to be carried out in air at atmospheric pressure.

Instruments include the Philips PW 1404 spectrometer, which is a powerful, versatile sequential X-ray spectrometer system developed from the PW 1400 series and incorporating many additional hardware and software features that further extend its performance. All system functions are controlled by powerful microprocessor electronics, which make routine analysis a simple, push-button exercise and provide extensive safeguards against operator error. The microprocessor also contains sufficient analytical software to permit stand-alone emergency operation, plus a range of self-diagnostic service-testing routines. The layout of the Philips PW 1404 instrument is shown in **Figure 1.8**.

An example of the detection limits achieved by the Seifert EXTRA III (3σ above background, counting time 1000 s) is shown in **Figure 1.9**, for a molybdenum anode X-ray tube and for excitation with the filtered Bremsstrahlung spectrum from a tungsten X-ray tube. The data shown were obtained from diluted aqueous solutions which can be considered to be virtually free from any matrix effects. A detection limit of 10 pg for a 10 µl sample corresponds to a concentration of 1 µg/l. A linear dynamic range of four orders of magnitude is obtained for most elements; for example, lead at concentrations of 2–20,000 µg/l using cobalt as an internal standard at 2000 µg/l.

Seifert manufactures a TRXRF spectrometer [49–52]. Detection limits obtained for 60 elements by this technique are listed in **Table 1.10**.

Programmable channel masks eliminate radiation from sample holders when anaysing different sized samples

Surface-down geometry and small airlock aids liquid analysis and reduces He consumption

Programmable collimator allows for optimisation for resolution or intensity

Tandem scintillation and flow counters maximise detection efficiency for all elements

Scintillation detector

Programmable tube filter removes tube lines and improve peak/background ratios

High-resolution auxillary collimator removes line overlaps and reduces background for heavy elements

Sample

Range of side window tubes gives optimal performance

Flow counter

High-speed measuring electronics permit counting at up to 10^6 Hz

Ultra-stable compact programmable 100 kV generator

Secondary collimator

Supervising microprocessor

Terminal   Computer

Bidirectional six-position crystal changer

Crystal choice includes special multilayer monochromators for enhanced light-element performance

Compact 6 litre spectrometer chamber allows rapid changeover from air to vacuum or helium atmosphere

Figure 1.8 Layout of Philips PW 1404 energy-dispersive X-ray fluorescence spectrometer (*Source: Phillips Electronic Instruments, Mahwah, NJ, USA*)

1.2.1.2 Applications

This technique can be used to conduct destructive or non-destructive analysis of polymers. XRF spectrometry has been used extensively for the determination of traces of metals and non-metals in polyolefins and other polymers. The technique has also been used in the determination of major metallic constituents in polymers, such as cadmium selenide pigment in polyolefins.

Specimen preparation is simple, involving compressing a disc of the polymer sample for insertion in the instrument, measurement time is usually less than for other methods, and X-rays interact with elements as such, i.e., the intensity measurement of a constituent element is independent of its state of chemical combination. However, the technique does have some drawbacks, and these are evident in the measurement of cadmium and selenium. For example, absorption effects of other elements present, e.g (the carbon and hydrogen of a polyethylene (PE) matrix) and excitation of one
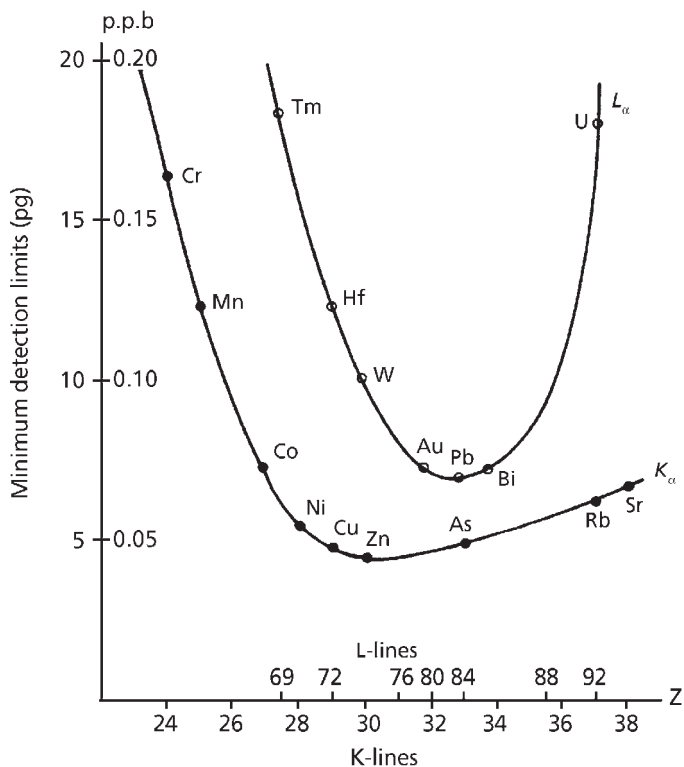
Figure 1.9 Minimum detection limits of TXRF spectrometer (Mo-tube 13 mA/60 kV; counting time 1000) (*Source: Phillips Electronic Instruments, Mahwah, NJ, USA*)

element by X-rays from another (e.g., cadmium and selenium) affect one another. The technique has been applied to the determination of metals in polybutadiene, polyisoprene, and polyester resins [53]. The metals determined were cobalt, copper, iron, nickel and zinc. The samples were ashed and the ash dissolved in nitric acid prior to X-ray analysis. Concentrations as low as 10 ppm can be determined without inter-element interference.

Many investigators have found much higher recoveries using various ashing aids such as sulfuric acid [54], elemental sulfur [55, 56], magnesium nitrate [33, 57], and benzene and xylene sulfonic acids [58].

Leyden and co-workers [59] used XRF spectrometry to determine metals in acid digests of polymers. The aqueous solutions were applied to filter paper discs. They found that recoveries of metals by the X-ray technique were 101–110% compared to 89–94% by chemical methods of analysis.

Table 1.10 Detection limits using the Seifert Extra II X-ray spectrometer	
	Detection limit (pg)
Atomic numbers 18 - 38 (argon to strontium) and 53 - 57 (iodine - lanthanum) and 78 - 83 (osmium to bismuth)	<5
Chlorine atomic numbers 39 - 43 (yttrium to technetium), 47 - 52 (silver to tellurium), 65 - 71 (terbium to lutetium) and 90 - 92 (thorium to uranium)	5 - 10
Phosphorus (15)	10 - 30
Sulfur (16)	
Ruthenium (44)	
Rhodium (45)	
Palladium (46)	
Neptunium (93)	
Plutonium (94)	
Aluminium (13)	30 - 100
Silicon (14)	
Sodium (11)	>100
Magnesium (12)	
Source: Author's own files	

XRF spectrometry has been applied very successfully, industrially, to the routine determination in hot-pressed discs of PE and PP down to a few parts per million of the following elements: aluminium, bromine, calcium, chlorine, magnesium, potassium, sodium, titanium and vanadium.

Ellis and Leyden (private communication) used dithiocarbamate precipitation methods to determine between 2 mg/l and 2 µg/l of five elements. **Table 1.11** shows the excellent agreement generally found between the X-ray instrument and AAS techniques in the analysis of pre-concentrates. Agreement does not extend over the whole concentration range examined for manganese. Some disparity also occurs in zinc determinations and it is believed here that the error is in the graphite furnace results.

Wolska [60] has reviewed recent advances in the application of XRF spectroscopy to the determination of antimony, bromine, copper, iron, phosphorus, titanium, and zinc, in various plastics. The new ED2000 high-performance EDXRF spectrometer

Table 1.11 The analysis of polymer digests by dibenzyldithiocarbamate precipitation - energy-dispersive X-ray spectrometry and electrothermal atomisation atomic absorption spectrometry										
Sample	Mn		Fe		Ni		Cu		Zn	
	XRF	AA	XRF	AA	XRF	AA	XRF	AA	XRF	AA
1	96	104	22	22	4	37	10	4	76	17
2	195	158	75	38	18	23	5	6	44	30
3	114	182	59	56	0.9	2.3	nd	nd	7	nd
4	450	450	46	42	0.9	2.2	1.8	5	61	51
5	2400	2700	15	22	20	25	5	14	1059	342
6	360	335	76	62	12	2.4	6	6	104	92

nd: not determined
Source: Author's own files

manufactured by Oxford Instruments can determine up to 80 elements qualitatively and up to 50 elements quantitatively between sodium and uranium in various materials, including polymers [61]. Workers at Spectra Analytical Instruments GmbH [62] have described a rapid X-ray spectroanalytical fluorescence technique for the determination of cadmium in polymers.

1.2.2 Neutron Activation Analysis

This is a very sensitive technique. Due to the complexity and cost of the technique most laboratories do not have facilities for carrying out NAA. Instead, samples are sent to one of the organisations that possess the facilities.

An advantage of the technique is that a foreknowledge of the elements present is not essential. It can be used to indicate the presence and concentration of entirely unexpected elements, even when present at very low concentrations.

In NAA, the sample in a suitable container, often a pure PE tube, is bombarded with slow neutrons for a fixed time together with standards. Transmutations convert analyte elements into radioactive elements, which are either different elements or isotopes of the original analyte. After removal from the reactor the product is subjected to various counting techniques and various forms of spectrometry to identify the elements present and their concentrations.

1.2.2.1 Applications

This technique is capable of determining a wide range of elements, e.g., chlorine in polyolefins, metals in polymethylmethacrylate [63], total oxygen in polyethylene–ethylacrylate and polyethylene–vinylacetate copolymers [64], and total oxygen in polyolefins.

In many cases the results obtained by NAA can be considered as reference values and these data are of great value when these samples are analysed by alternative methods in the originating laboratory.

To illustrate this, some work is discussed on the determination of parts per million of sodium in polyolefins. It was found that replicate sodium contents determined on the same sample by a flame photometric procedure were frequently widely divergent. NAA offers an independent non-destructive method of checking the sodium contents which does not involve ashing.

In the flame photometric procedure the sample is dry ashed at 650–800 °C in a nickel crucible and the residue dissolved in hot water before determining sodium by evaluating the intensity of the line emission occurring at 589 nm.

NAA (flux of 10^{12} neutrons/cm/s) for sodium was carried out on PE and PP moulded discs containing up to about 550 ppm sodium which had been previously analysed by the flame photometric method. The results obtained in these experiments (**Table 1.12**) show that significantly higher sodium contents are usually obtained by NAA, and this suggests that sodium is being lost during the ashing stage of the flame photometric method. Sodium can also be determined by a further independent method, namely emission spectrographic analysis, which involves ashing the sample at 500 °C in the presence of an ashing aid consisting of sulfur and the magnesium salt of a long-chain fatty acid [56, 65–67]. **Table 1.13** shows the results by NAA and emission spectrography agree well with each other. The losses of sodium in the flame photometric ashing procedure were probably caused by the maximum ashing temperature used exceeding the temperature used in the emission spectrographic method by some 150–300 °C.

The results in **Table 1.14** show clearly that flame photometry following dope ashing at 500 °C gives a quantitative recovery of sodium. Direct ashing without an ashing aid at 500 °C causes losses of 10% or more of sodium, while direct ashing at 800 °C causes even greater losses.

Commonly, nowadays, the active catalyst (based on chromium, titanium, or vanadium) used in HDPE manufacture is adsorbed onto a highly porous silica support. Determination of the silica catalyst support content of the final polymer gives an assessment of the economic productivity of the reactor, i.e., its output of PE

Table 1.12 Interlaboratory variation of flame photometric sodium determinations in polyolefins (sodium content, ppm)		
Neutron activation analysis		Flame photometry
Powder	Moulded discs	Moulded discs
Polyethylene		
207	211, 204	35, 165, 140
177	175, 172	100, 140, 148
266	267, 263	85, 210, 221
203	187, 191	70, 160, 150
Polypropylene		
165	151, 161	50, 130, 133
198	186, 191	95, 173
322	333, 350	95, 138
Source: Author's own files		

Table 1.13 Comparison of sodium determination in polyolefins by neutron activation analysis, emission spectrography and flame photometry (sodium ppm)			
Sample description	By neutron activation analysis	By emission spectrography	By flame photometry
Polyethylene	99, 96, 99	95	60, 76, 55
Polyethylene	256, 247, 256	258, 259	160, 178, 271
Polyethylene	343, 321, 339	339, 287	250, 312
Polyethylene	213, 210, 212	218, 212	140, 196
Polypropylene	194, 189, 192	209, 198	80, 158, 229
Polypropylene	186, 191, 198	191, 191	95, 173
Source: Author's own files			

per gram of catalyst, and also enables the very low concentration of active catalyst metal in the polymer to be calculated.

Battiste and co-workers [68] have described three methods based on NAA, infrared spectroscopy, and ashing for the determination of silica catalyst supports in PE.

		By flame photometry		
By neutron activation	**By emission spectrography**	**Original (ashed between 650 and 800 °C)**	**Dope ash at 500 °C**	**Direct ash at 500 °C**
99, 96, 99	95	60, 75, 55	200	75
256, 247, 259	258, 259	160, 178, 271	225	208
343, 321, 339	339, 287	250, 312	282	265
213, 210, 212	218, 212	140, 196	210	191
194, 189, 192	209, 198	80, 158, 229	196	169
186, 191, 198	191, 191	95, 95, 173	193	173
Source: Author's own files				

Table 1.14 The effects of modification of ashing procedure on the flame photometric determination of sodium (sodium ppm)

In the NAA method approximately 2 g of PE powder is irradiated with neutrons obtained with a 500 keV neutron activator according to the following reaction:

$$^3H(D,n)\ ^4He$$

Silicon is activated by the reaction:

$$^{28}Si(N,p)\ ^{28}Al$$

and the concentration of silicon is then measured by the 1.78 MeV γ-ray emission from the decay of ^{28}Al. A Conostan 5000 pm Si standard is used for the instrument calibration. Two 7.5 cm sodium iodide detectors are used to measure the 1.78 MeV γ-rays. Silica can be estimated by direct measurement of the silica absorbance at the 21.27 μm absorbance band of silica. This is the region of the infrared spectrum that is relatively free from polyethylene absorbance bands. The absorbance of the 21.27 μm band is calculated for each standard by use of the peak height determined by means of the baseline technique between minima near 28.57 and 17.24 μm.

Results of analysis of PE samples containing residual silica supports of three different catalysts are shown in **Table 1.15**. Infrared results differ from NAA results by 0–5 % while ashing and weighing techniques differ from neutron activation by 5–21 % and 5–28 %, respectively.

Table 1.15 Catalyst productivity of some test samples				
Sample	IR at 21.27 μm	NAA	Ashing at 650 °C	Weight
1ᵃ	1893(3.3)d	1833	1923(4.9)	1923(4.9)
2ᵃ	4165(0)	4165	4545(9.1)	3571(14.3)
3ᵇ	1759(2.9)	1709	2222(30.0)	2007(17.4)
4ᶜ	1727(5.4)	1825	2000(9.6)	2000(9.6)
5ᶜ	2207(3.5)	2288	2778(21.4)	2941(28.5)
ᵃ Catalyst A; ᵇ Catalyst B; ᶜ Cabosil S.17 *Values in parenthesis are percentage deviation from NAA. Reprinted from D.R. Battiste, J.P. Butler, J.B. Cross and M. P. McDaniel, Analytical Chemistry, 1981, 53, 2232, with permission from the American Chemical Society [66]*				

Method 1.1. Determination of Traces of Cadmium, Chromium, Copper, Iron, Lead, Manganese, Nickel, and Zinc in Polymers. Ashing – Atomic Absorption Spectrometry

Summary

This atomic absorption spectroscopic procedure determines eight heavy metals in polymers in amounts down to 0.03 to 0.13 ppm.

Apparatus

Platinum dishes, 100 cm³
Volumetric flasks, 10, 25 cm³
Atomic absorption spectrometer

Reagents

Nitric acid, 1 M prepared using Aristar nitric acid.

Method

The polymer is ashed in platinum. A nitric acid extract of the ash is examined by atomic absorption spectroscopy for concentrations of cadmium, chromium, copper,

iron, lead, manganese, nickel and zinc at specific wavelengths. The method is calibrated against standard solutions of the heavy metals in nitric acid.

Experimental Procedure

Accurately weigh 10 g of dry polymer into a platinum dish. Place the dish in a cold contamination-free muffle furnace and temperature programme as follows:

Time from start: 0-1 h   Heat to 200 °C
                  1-3 h   Hold at 200 °C
                  3-5 h   Heat to 450 °C
                  5-8 h   Hold at 450 °C

Remove the dish from the furnace and allow to cool in a dessicator. When cool, add 5 cm^3 1 M nitric acid and warm the dish gently on a hot plate to ensure complete dissolution of the metallic salts. Transfer the solution quantitatively with pure water to a 25 cm^3 volumetric flask and make up to the mark (final solution 0.2 M with respect to nitric acid). Blanks and standard solutions should also be prepared in 0.2 M nitric acid.

Atomic Absorption Instrument Operating Conditions

Instrument: Single beam.

Background correction using deuterium arc.

Grating monochrometer.

Burner: Single slot 10 cm long. Burner aligned along optical axis for each metal.

Fuel gas: Acetylene 0.8 Pa.

Support gas: compressed air, oil-less. Compressor model SY 006.

Aspiration rate: 9.5 cm^3/min.

Spoiler left in position for all elements.

Recorder single pen.

Renew the calibration standards every two weeks from 10 μg/cm^3 stock solutions, by dilution with 0.2 M nitric acid (Aristar). Renew the 10 μg/cm^3 stock solutions monthly.

Typical Results and Discussion

The detection limits for metals in polymers achievable by this procedure are in the range 0.03 – 0.13 ppm.

Method 1.2. Determination of Traces of Arsenic in Acrylic Fibres Containing Antimony Trioxide Fire Retardant Agent. Acid Digestion, Atomic Absorption Spectrometry

Summary

This atomic absorption spectrometric method determines down to 0.02% arsenic trioxide fire retardant in acrylic fibres.

Apparatus

Atomic absorption and flame-emission spectrophotometer, 10 cm slit burner, equipped with an arsenic measurement unit or equivalent and an arsenic hollow-cathode lamp. A schematic diagram of the apparatus used for the arsenic measurement is shown in **Figure 1.10**.
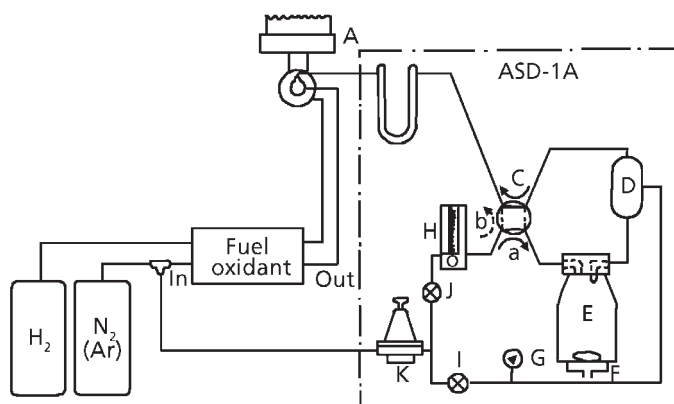
Figure 1.10 Schematic diagram of apparatus used for the arsenic measurement. A: slit burner; B: trap; C: change-over cock; D: buffer tank; E: arsine generator (glass reaction bottle); F: magnetic stirrer; G: pressure gauge; H: gas flow meter; I: back-sweep cock; J: stock-cock; and K: pressure controller, a: sweep; and b: by-pass. (*Reprinted with permission from T. Korenaga, Analyst, 1981, **106**, 40. ©1981, RSC*)

Reagents

All reagents used were of analytical reagent grade.

Arsenic(III) standard solution.

1000 μg/l. Dissolve 132.0 mg of arsenic(III)oxide (purity 99.9%) in 2 cm^3 of 4% *m/v* sodium hydroxide solution. Add dilute sulfuric acid until the solution becomes slightly acidic and then dilute to 100 cm^3 with distilled water.

Arsenic(V) standard solution, 1000 μg/l. Oxidise the arsenic(III) standard solution with a sufficient amount of hydrogen peroxide and evaporate the excess by boiling. Cool the resulting solution and dilute it to the required volume with distilled water.

Nitric acid, concentrated, Analar.

Perchloric acid, concentrated, Analar.

Sulfuric acid, concentrated, Analar.

Benzene, Analar.

Zinc tablet (tablet comprising 1 g of zinc powder containing a binder).

Potassium iodide, 20% UV aqueous made from Analar solid, prepared weekly.

Titanium(III) solution 10% *m/v*.

Dissolve 50.0 g of titanium(III)chloride in concentrated hydrochloric acid* and dilute to 500 cm^3 with concentrated hydrochloric acid. Store this solution in a refrigerator.

*Hydrochloric acid to have an arsenic content less than 0.5 μg/l.

Method

A concentrated nitric acid – perchloric acid – sulfuric acid digest of the polymer is analysed at 193.7 nm by atomic absorption spectrometry. The procedure is calibrated against standards of arsenic free acrylic fibre and pure arsenic trioxide.

Experimental Procedure

Preparation of Sample Solution

Weigh 1 g of sample (to contain less than 2 μg of arsenic) into a Kjeldahl decomposition flask. Add 3 cm^3 of concentrated nitric acid, 3 cm^3 of concentrated perchloric acid and 3 cm^3 of concentrated sulfuric acid. Heat the flask on an electric hot plate (about 1200 W) until the acrylic fibre sample is completely decomposed. If the sample cannot be decomposed completely, add a further 3 cm^3 of concentrated nitric acid and 3 cm^3 of concentrated perchloric acid to the flask and repeat the heating until the solution becomes clear; cool the resulting solution. After the digestion of the sample the amount of sulfuric acid remaining is about 3 cm^3.

Transfer the solution into a 50 cm^3 separating funnel and rinse the Kjeldahl decomposition flask with 7 cm^3 of concentrated hydrochloric acid. Add 5 cm^3 of 10% *m/v* titanium(III)chloride in concentrated hydrochloric acid solution then leave to stand for 30 minutes at 60 °C in a waterbath (the funnel must occasionally be shaken and frequently degassed in order to avoid an explosion). Cool the solution to room temperature, add 10 cm^3 of benzene and shake the funnel for a few minutes. Discard the aqueous phase, add 10 cm^3 of distilled water and shake the funnel for a few minutes. In this way, arsenic(V) in the digested sample is reduced to arsenic(III), and only the arsenic(III) is extracted into benzene and then back-extracted quantitatively into the aqueous phase.

Atomic Absorption Spectrophotometry

Transfer by pipette the aqueous solution containing arsenic(III) (not more than 2 µg of arsenic) obtained by the above procedure into a glass reaction bottle (E in **Figure 1.10**). Add 5 cm^3 of concentrated hydrochloric acid, 1 cm^3 of 20% *m/v* potassium iodide solution and 0.5 cm^3 of 20% *m/v* tin(II)chloride solution. Dilute the solution with distilled water to give a final volume of 25 cm^3 (final concentration of hydrochloric acid 2.4 M). Mix well and allow to stand for 20 minutes. Drop a zinc tablet containing about 1 g of zinc powder into the reaction bottle (E) and immediately connect the bottle to the collection tank (D). Store the generated arsine gas obtained by mixing the sample solutions with a magnetic stirrer (F) to ensure complete arsine generation in the 100 cm^3 collection tank (D) for about 1 minute (until the pressure of arsine generation gas reaches 0.5 kg/cm^2). As soon as the pressure of arsine generation gas (H) reaches 0.5 kg/cm^2 switch the stopcock (C) from the by-pass (b) and introduce the collected arsine into the flame with a stream of nitrogen carrier gas. Use the peak height on the recordings to determine the concentration of arsenic.

According to the analytical conditions given above, arsenic(III) obtained in the aqueous solution was determined at the 193.7 nm absorption line by using arsine generation and atomic absorption spectrophotometry (**Figure 1.10**). A calibration graph was prepared by using 0.25-2.0 µg of standard arsenic(III) solution throughout the procedure for the preparation of the sample solution and was then used for subsequent determinations of arsenic concentrations.

Arsenic(III) separated into the aqueous phase from the matrix antimony after the benzene extraction and back-extraction with distilled water was determined by using arsine generation atomic absorption spectrophotometry as described under Atomic Absorption Spectrophotometry. A calibration graph was prepared by analysing a standard arsenic(V) solution and an acylic fibre containing no antimony oxide by the recommended procedure. Although the calibration graph obtained was not a straight line, amounts of arsenic in the range 0.25-2.0 µg could be determined with good reproducibility under the conditions given above.

Discussion of Results

This method is capable of determining down to 0.02% arsenic in acrylic fibres with an accuracy of ± 5%. Antimony present in the sample does not interfere.

Method 1.3 Determination of Vanadium Catalyst Residues in Ethylene-propylene Rubber. Ashing – Spectrophotometric Procedure

Summary

This spectrophotometric procedure determines vanadium catalyst residues in amounts down to 2 ppm in ethylene-propylene rubbers.

Apparatus

Visible spectrophotometer with 1 and 5 cm cells.

Reagents

Standard vanadium solution. Prepare 5 µg per cm^3 or 50 µg per cm^3 from ammonium metavanadate.

3,3′-diaminobenzidine tetrachloride solution. 0.5% *w/v* store at 4 °C under nitrogen.

Phosphoric acid, 85%.

Nitric acid, concentrated.

Potassium, pyrosulfate, AR solid.

Method

The polymer is ashed then dissolved in nitric acid - phosphoric acid. 3,3′-diaminobenzidine tetrachloride is added and the colour produced evaluated spectrophotometrically at 470 nm. Calibration is achieved against similarly prepared solutions of pure vanadium.

Experimental Procedure

Ash a 10 g sample of elastomer solution in a platinum crucible by charring on a hot plate followed by heating over a meker burner. Add 10 cm^3 of water and 2 cm^3 of

nitric acid then transfer to a 100 cm^3 beaker. To ensure complete removal of vanadium, melt a gram of potassium pyrosulfate in the crucible, cool, then wash the salt into the beaker with hot water. Evaporate to about 10 cm^3 and transfer the contents to a 25 cm^3 volumetric flask. Before diluting to the mark, add 1 cm^3 of 85% phosphoric acid and 1 cm^3 of 3,3′-diaminobenzidine tetrachloride solution. Measure the absorbance at 470 nm in a suitable cell, using a reagent blank, after standing for 15 minutes in the dark.

Calibration

Add suitable aliquots of standard vanadium solution to 100 cm^3 beakers which contain 50 cm^3 of water, 2 cm^3 of nitric acid and 1 g of potassium pyrosulfate. Reduce the volume to about 10 cm^3 by boiling and transfer the contents to a 25 cm^3 volumetric flask. React with phosphoric acid and 3,3′-diaminobenzidine tetrachloride solution as described for sample analysis. For vanadium contents from 5 to 50 μg measure the absorbance in a 4 cm cell using a reagent blank.

Typical Results

Data in **Table 1.16** shows good agreement between data obtained by this method and neutron activation analysis for a range of ethylene-propylene copolymer samples.

Discussion of Results

This method is capable of determining down to 2 ppm vanadium in ethylene-propylene elastomers with an accuracy of ± 5%.

Table 1.16 Results obtained for vanadium (ppm)		
Sample	Dry Ashing	Neutron Activation
A	10.2	9.9 ± 0.2
B	14.0	14.1 ± 0.1
C	14.6	15.6 ± 0.3
D	0.5	0.14 ± 0.01
E	13.0	14.8 ± 0.2
F	0.9	0.27 ± 0.01
G	15.2	18.8 ± 0.3
H	18.2	17.9 ± 0.3

Acknowledgements

References

1. A. Ritter, E. Michel, M. Schmidt and S. Affolter, *Polymer Testing*, 2004, **23**, 4, 467.

2. R.J. Watling, *Analytica Chimica Acta*, 1977, **94**, 181.

3. C. Hallam and K.G. Thompson, *Determination of Lead and Cadmium in Potable Waters by Atom Trapping Atoms Absorbance Spectroscopy*, Divisional Laboratory, Yorkshire Water Authority, Sheffield, UK, 1986.

4. R.G. Godden and D.R. Thomenson, *Analyst*, 1980, **105**, 1137.

5. B.W.J. Rence, *Automatic Chemistry*, 1982, **4**, 61.

6. P.D. Goulden and P. Brooksbank, *Analytical Chemistry*, 1974, **46**, 1431.

7. P.B. Stockwell in *Topics in Automatic Chemical Analysis*, Ellis Horwood, Chichester, UK, 1979.

8. A.L. Dennis and D.G. Porter, *Automatic Chemistry*, 1981, **2**, 134.

9. B. Pahlavanpour, M. Thompson and L. Thorne, *Analyst*, 1981, **106**, 467.

10. B.W.J. Rence, *Automatic Chemistry*, 1980, **105**, 1137.

11. M. Thompson, B. Pahlavanpaur and L. Thorne, *Analyst*, 1981, **106**, 468.

12. W.T. Corus, L. Ebdon and S.J. Hill, *Analyst*, 1992, **117**, 717.

13. W.T. Corus, P.B. Stockwell, L. Ebdon and S.J. Hill, *Journal of Analytical Atomic Spectroscopy*, 1993, **8**, 71.

14. P.B. Stockwell and W.T. Corus, *Spectroscopy World*, 1992, **411**, 14.

15. S. Greenfield, I.L. Jones and C.T. Berry, *Analyst*, 1964, **89**, 713.

16. R.H. Wendt and V.A. Fassel, *Analytical Chemistry*, 1965, **37**, 920.

17. R.H. Scott, *Analytical Chemistry*, 1974, **46**, 75.

18. M. Thompson and J.N. Walsh in *A Handbook of Inductively Coupled Plasma Spectrometry*, Blackie, London & Glasgow, 1983, 55.

19. R.F. Suddendorf and K.W. Boyer, *Analytical Chemistry*, 1978, **50**, 1769.

20. B.L. Sharp, inventor; B.L. Sharp, assignee; GB. 8, 432, 338, 1984.

21. A.M. Gunn, D.L. Millard and G.F. Kirkbright, *Analyst*, 1978, **103**, 1066.

22. H. Matuslavicz and R.M. Barnes, *Applied Spectroscopy*, 1984, **38**, 745.

23. M.W. Tikkanen and K.M. Niemczyk, *Analytical Chemistry*, 1984, **56**, 1997.

24. E.D. Salin and G. Horlick, *Analytical Chemistry*, 1979, **51**, 2284.

25. E.D. Salin and R.L.A. Szung, *Analytical Chemistry*, 1984, **56**, 2596.

26. A.L. Briseno, A. Baca, Q. Zhou, R. Lai and F. Zhou, *Analytica Chimica Acta*, 2001, **441**, 123.

27. S. Ruzicka and E.H. Hansen, *Analytica Chimica Acta*, 1978, **99**, 37.

A.M. Dobney, A.J.G. Monk, K.H. Grobecker, P. Conneely and C.G. de Koster, *Analytica Chimica Acta*, 2000, **423**, 9.

A.M. Riquet and A. Feigenbaum, *Food Additives and Contaminants*, 1997, **14**, 53.

30. H. Narasaki and K. Umezawa, *Kobunshi Kogaku*, 1972, **29**, 438.

31. A.J. Smith, *Analytical Chemistry*, 1964, **36**, 944.

32. T. Gorsuch, *Analyst*, 1962, **87**, 112.

33. T. Gorsuch, *Analyst*, 1959, **84**, 135.

34. E.L. Henn, *Analytica Chimica Acta*, 1974, **73**, 273.

35. T. Korenaga, *Analyst*, 1981, **106**, 40.

36. H. Ogure, *Bunseki Kogaku*, 1975, **24**, 197.

37. R. Reverz and E. Hasty, *Recovery Study Using an Elevated Pressure Temperature Microwave Dissolution Technique*, Pittsburgh Conference and Exposition of Analytical Chemistry and Applied Spectroscopy, March 1987.

38. R.A. Nadkarni, *Analytical Chemistry*, 1984, **56**, 2233.

39. H.M. Kingston and L.B. Jassie, *Analytical Chemistry*, 1986, **58**, 2534.

40. *Parr Manual*, 207M, Parr Instruments Co., Moline, IL, USA.

41. R.A. Nadkarni, *American Laboratory*, 1981, **13**, 22.

42. *Ultraviolet and Visible Solution Spectrometry and Colorimetry 1980*, An Essay Review, Her Majesty's Stationery Office, London, UK, 1981.

43. L.M. Mal'kova, A.I. Kalanin and E.M. Derepletchikove, *Zhurnal Analiticheskoi Kimii*, 1972, **27**, 56.

44. H. Small, T.S. Stevens and W.C. Bauman, *Analytical Chemistry*, 1975, **47**, 1801.

45. *High Performance Liquid Chromatography, Ion Chromatography, Thin-Layer and Column Chromatography of Water Samples*, Her Majesty's Stationery Office, London, UK, 1983.

46. P.J. Statham, *Analytical Chemistry*, 1977, **49**, 2149.

47. Y. Yoneda and T. Horiuchi, *Review of Scientific Instruments*, 1971, **42**, 1069.

48. H. Aiginger and P. Wadbrauschek, *Nuclear Instruments and Methods*, 1974, **114**, 157.

49. J. Knoth and H. Schwenke, *Fresenius' Zeitschrift Analytische Chemie*, 1978, **291**, 200.

50. J. Knoth and H. Schwenke, *Fresenius' Zeitschrift Analytische Chemie*, 1980, **201**, 7.

51. H. Schwenke and J. Knoth, *Nuclear Methods*, 1982, **193**, 239.

52. D.A. Pella and R.C. Dobbyn, *Analytical Chemistry*, 1988, **60**, 684.

53. W.S. Cook, C.O. Jones and A.G. Altenau, *Canadian Spectroscopy*, 1968, **13**, 64.

54. A.A. Vasilieva, Yu V. Vodzinskii and I.A. Korschunov, *Zavodskaia Laboratoriia*, 1968, **34**, 1304.

55. J.S. Bergmann, C.H. Ehrhart, L. Grantelli and L.J. Janik in *Proceedings of the 153rd ACS Meeting*, Miami Beach, FL, USA, 1967.

56. W.A. Rowe and K.P. Yates, *Analytical Chemistry*, 1963, **35**, 368.

57. L.W. Gamble and W.H. Jones, *Analytical Chemistry*, 1955, **27**, 1456.

58. J.E. Shott, Jr., T.J. Garland and R.O. Clarke, *Analytical Chemistry*, 1961, **33**, 506.

59. D.E. Leyden, J.C. Lennox and C.U. Pittman, *Analytica Chimica Acta*, 1973, **64**, 143.

60. J. Wolska, *Plastics Additives and Compounding*, 2003, **5**, 90.

61. *Rubber World*, 1999, **219**, 4, 79.

62. O.J. Kabayashi, *Polymer Science A-1*, 1979, **17**, 293.

63. D. Hull and J. Gilmore in the *Proceedings of the 141st ACS Division of Fuel Chemistry Meeting*, Washington, DC, USA, 1962.

64. J.S. Bergmann, C.H. Ekhart, L. Grantelli and J.L. Janik, private communication, 1967.

65. E. Barendrecht, *Analytica Chimica Acta*, 1961, **24**, 498.

66. J.E. Shott Jr., T.J. Garland and R.O. Clarke, *Analytical Chemistry*, 1961, **33**, 507.

67. D.R. Battiste, J.P. Butler, J.B. Cross and M.P. McDaniel, *Analytical Chemistry*, 1981, **53**, 2232.

68. *Additives for Polymers*, Spectroanalytical Instruments GmbH, April 2003.

2 Determination of Non-metallic Elements

Non-metallic elements such as boron, halogens, nitrogen, oxygen, phosphorus and sulfur, can occur in polymers either as major constituents or as impurities or as components of low-percentage additions of additives containing the element, for example, the addition of 0.5% dilauryl thiodipropionate antioxidant to a polymer during processing will introduce parts per million concentrations of sulfur into the final polymer. Another source of non-metallic elements in polymers is catalyst residues and processing chemicals.

It is advisable when commencing the analysis of a polymer to determine the content of various non-metallic and metallic elements first. Initially, these tests could be qualitative, simply to indicate the presence or absence of the element. All that is required here is that the test is of sufficient sensitivity such that elements of importance are not missed. If an element is found in these tests, it may then be necessary to determine it quantitatively as discussed next. The analytical methods used to determine elements should be sufficiently sensitive to determine about 10 ppm of an element in the polymer, i.e., should be able to detect in a polymer a substance present at 0.01% and containing down to 10% of the element in question.

This requirement is met for almost all the important elements by the use of optical emission spectroscopy and X-ray fluorescence spectrometry (XRFS). XRFS is applicable to all elements with an atomic number greater than 12. Using these two techniques, all metals and non-metals down to an atomic number of 15 (phosphorus) can be determined in polymers at the required concentrations [1-4].

Nitrogen is determinable by micro Kjeldahl digestion techniques. A cautionary note is that, in addition to the polymer itself, the polymer additive system may contain elements other than carbon, hydrogen, and oxygen. The detection of an element such as boron, halogens, nitrogen, phosphorus, silicon, or sulfur, in a polymer is indicative that the element originates in the polymer and not the additive system if the element is present at relatively high concentrations such as several percent. This is highlighted by the example of a high-density polyethylene which might contain 0.2–1% chlorine originating from polymerisation residues and polyvinyl chloride (PVC) homopolymer which contains more than 50% chlorine.

Commercial instrumentation available for the determination of the following total elements is the subject of this chapter: halogens; sulfur; halogens and sulfur; nitrogen; nitrogen, carbon, and sulfur; carbon, hydrogen, and nitrogen; and total organic carbon (TOC).

2.1 Halogens

2.1.1 Combustion Methods

2.1.1.1 Furnace Combustion

The Dohrmann DX 20B system is based on combustion of a sample to produce a hydrogen halide, which is then swept into a microcoulometric cell and estimated. It is applicable at total halide concentrations up to 1000 µg/l with a precision of ±2% at the 10 µg/l level. The detection limit is about 0.5 µg/l. Analysis can be performed in five minutes. A sample boat is available for carrying out analysis of solid samples.

Mitsubishi also supplies a microprocessor-controlled automatic total halogen analyser (model TOX-10) which is very similar in operating principles to the Dohrmann system discussed previously, with, combustion at 800–900 °C followed by coulometric estimation of the hydrogen halide produced.

2.1.2 Oxygen Flask Combustion

Oxygen flask combustion methods have been used to determine traces of chlorine in PVC [5] and in polyolefins and chlorobutyl rubber [6].

Traces of chlorine have been determined in polyolefins [5] at levels between 0 and 500 ppm. The Schoniger oxygen flask combustion technique requires a 0.1 g sample and the use of a 1 litre conical flask. Chlorine-free polyethylene (PE) foil is employed to wrap the sample, which is then supported in a platinum wire attached to the flask stopper. Water is used as the absorbent. Combustion takes place at atmospheric pressure in oxygen. The chloride formed is potentiometrically titrated in nitric acid/acetone medium with 0.01 M mercuric nitrate solution (See Method 2.1 at the end of this chapter).

In the method of determining chlorine in chlorobutyl and other chlorine-containing polymers [6] the sample is combusted in a 1–2 litre oxygen-filled combustion flask containing 0.01 M nitric acid. After the combustion the flask is allowed to cool and 0.01 M silver nitrate added. The combustion solution containing silver chloride is evaluated turbidometrically at 420 mm using a grating spectrophotometer.

Alternatively, to determine bromine, chlorine, iodine, or mixtures thereof, the combustion solution can be titrated with dilute standard silver nitrate solution or can be evaluated by ion chromatography (see Method 2.2).

An oxygen flask combustion method for the determination of between 2 and 80% of chlorine, bromine and iodine in polymers is described in Methods 2.2 and 2.3 at the end of this chapter.

A method for the determination of fluorine in fluorinated polymers such as polytetrafluoroethylene (PTFE) is based on decomposition of the sample by oxygen flask combustion followed by spectrophotometric determination of the fluoride produced by a procedure involving the reaction of the cerium(III) complex of alizarin complexan (1,2-dihydroxy-anthraquinone 3-ylmethylamine *N,N*-diacetic acid). The blue colour of the fluoride-containing complex (maximum absorption, 565 nm) is completely distinguishable from either the yellow of the free dye (maximum absorption, 423 nm) or the red of its cerium(III) chelate (maximum absorption, 495 nm).

A method has been described [7] for the determination of fluorine in polymers containing chlorine, phosphorus and sulfur, which involves oxygen flask combustion over water, addition of ethanol, and titration to the diphenylcarbazide indicator end point with 0.005 M mercuric nitrate:

$$2HF + Hg(NO_3)_2 = HgF_2 + 2HNO_3$$
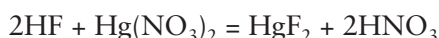
Using this method Johnson and Leonard [7] obtained from PTFE 75.8% of fluorine using a silica or boron-free glass combustion flask against a theoretical value of 76%. Using a borosilicate glass combustion flask they obtained a low fluorine recovery of 72.1%. This method is described in Method 2.4 at the end of this chapter.

2.1.3 Alkali Fusion Methods

Sodium peroxide is another useful reagent for the fusion of polymer samples preparatory to analysis for metals such as zinc and non-metals such as chlorine [8, 9] and bromine. In this method the polymer is intimately mixed either with sodium peroxide in an open crucible or with a mixture of sodium peroxide and sucrose in a micro-Parr bomb. After acidification with nitric acid, chlorine can be determined [9]. In a method for the determination of traces of bromine in polystyrene in amounts down to 100 ppm bromine, a known weight of polymer is mixed intimately with pure sodium peroxide and sucrose in a micro-Parr bomb which is then ignited. The sodium bromate produced is converted to sodium bromide by the addition of hydrazine as the sulfate:

$$2NaBrO_3 + 3NH_2NH_2 = 2NaBr + 6H_2O + 3N_2$$
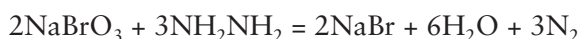
The combustion mixture is dissolved in water and acidified with nitric acid. The bromine content of this solution is determined by potentiometric titration with standard silver nitrate solution.

Fusion with sodium carbonate is a very useful method for the fusion of polymers that, upon ignition, release acidic vapours, e.g., PE containing traces of chlorine or PVC, both of which, upon ignition, release anhydrous hydrogen chloride. To determine chlorine accurately in the polymer in amounts down to 5 ppm the hydrogen chloride must be trapped in a solid alkaline reagent such as sodium carbonate. In this method PE is mixed with pure sodium carbonate and ashed in a muffle furnace at 500 °C. The residual ash is dissolved in aqueous nitric acid, and then diluted with acetone. This solution is titrated potentiometrically with standard silver nitrate. **Table 2.1** compares results for chlorine determinations in PE obtained by this method with those obtained by XRFS. The averages of results obtained by the two methods agree satisfactorily to within ±15% of each other. This method is described in Method 2.5 at the end of this chapter.

| Table 2.1 Comparison of chlorine contents by X-ray method and chemical method (averages in parenthesis)		
X-ray on discs	**Chemical methods on same discs as used for X-ray analysis**	**Chemical method on powder***
865, 841 (840)	700	786, 761 (773)
535, 570 (522)	606	636, 651
785, 675 (730)	598	650, 654 (652)
625, 675 (650)	600	637, 684 (660)
895, 870 (882)	733	828, 816 (822)
*Analysis carried out on samples which had been treated with alcoholic potash to avoid losses of chlorine when preparing discs. Source: Author's own files.		

2.1.4 Physical Methods for Determining Halogens

Manatt [10] has used ^{13}C NMR to determine chlorine in polystyrene. Williams and co-workers [11] determined bromine in brominated PS and poly(2,6-dimethyl, 1,4-phenylene oxide) using ^{13}C NMR. X-ray emission analysis has been used to determine the ratio of chlorine to sulfur in copolymers based on poly (3-methylthiophen) [12].

2.2 Sulfur

2.2.1 Combustion Methods

The Mitsubishi trace sulfur analyser models TS-02 and TN-02(S) again involve a microcombustion procedure in which sulfur is oxidised to sulfur dioxide, which is then titrated coulometrically with triiodide ions generated from iodide ions:

$$SO_2 + I_3^- + H_2O \rightarrow SO_3 + 3I^- + 2H^+$$

$$3I^- \rightarrow I_3^- + 3e^-$$
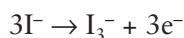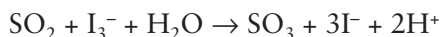
2.2.2 Sodium Peroxide Fusion

Colson has described an alkali fusion method for the determination of down to 500 ppm of sulfur in polymers [13] (See Method 2.6 at the end of this chapter) in which the sulfate in the digest is determined by titration either with 0.01N sodium hydroxide or by photometric titration with 0.01 barium perchlorate.

2.2.3 Oxygen Flask Combustion

To determine sulfur in amounts down to 500 ppm in polyolefins the sample is wrapped in filter paper and burnt in a closed conical flask filled with oxygen at atmospheric pressure. The sulfur dioxide produced in the reaction reacts with dilute hydrogen peroxide solution contained in the reaction flask to produce an equivalent amount of sulfuric acid [14]:

$$H_2SO_3 + H_2O_2 = H_2SO_4 + H_2O$$
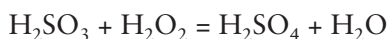
The sulfuric acid is estimated by visual titration with M/500 or M/50 barium perchlorate using Thorin indicator. The repeatability of this method is ±40% of the sulfur content determined at the 500 ppm sulfur level, improving to ±2% at the 1% level. Chlorine and nitrogen concentrations in the sample may exceed the sulfur concentration several times over without causing interference. Fluorine does not interfere unless present in concentrations exceeding 30% of the sulfur content. Phosphorus and metallic constituents interfere when present in moderate amounts (see Method 2.7 (direct titration) or Method 2.8 (photometer titration) at the end of this chapter).

The use of a photoelectric method of end-point detection overcomes the difficulties associated with visual end-point detection, as it makes the assessment of end-point independent of individual operators.

2.3 Phosphorus

2.3.1 Acid Digestion

Phosphorus has been determined [15, 16] in thermally stable polymers by mineralisation with a nitric–perchloric acid mixture and subsequent titration with lanthanum nitrate or by photometric determination of the phosphomolybdic blue complex [17] (see Method 2.9 at the end of this chapter).

2.3.2 Oxygen Flask Combustion

Two oxygen flask methods are described in Methods 2.10 and 2.11 for the determination of phosphorus in polymers. The first is applicable in the range 0.01 to 2% phosphorus and the second in the range 2 to 13% phosphorus.

2.4 Nitrogen

2.4.1 Combustion Methods

Mitsubishi supply two total nitrogen analysers: the model TN-10 and the model TN-05 microprocessor-controlled chemiluminescence total nitrogen analysers. These measure down to micrograms per litre amounts of nitrogen in solid and liquid samples.

The sample is introduced into the combustion tube packing containing oxidative catalyst under oxygen carrier gas. High-temperature oxidation (800–900 °C) occurs and all chemically bound nitrogen is converted to nitric oxide (NO): $R–N \rightarrow CO_2$ + NO. Nitric oxide then passes through a drier to remove water formed during combustion and moves to the chemiluminescence detector, where it is mixed with ozone to form excited nitrogen dioxide (NO_2^*):

$$NO + O_3 \rightarrow NO_2^* + O_2 \rightarrow + O_2 + h\nu$$
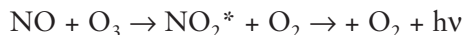
Rapid decay of the NO_2^* produces radiation in the 590–2900 nm range. It is detected and amplified by a photomultiplier tube. The result is calculated from the signal produced and is given in milligrams per litre or as a percentage.

Dohrmann also supplies an automated nitrogen analyser with video display and data processing (model DN-1000) based on similar principles which is applicable to the determination of nitrogen in solid and liquid samples down to 0.1 mg/l.

Hernandez [18] has described an alternative procedure based on pyro-chemiluminescence which he applied to the determination of 250–1500 ppm nitrogen in PE. In this technique the nitrogen in the sample is subjected to oxidative pyrolysis to produce nitric oxide. This when contacted with ozone produces a metastable nitrogen dioxide molecule, which as it relaxes to a stable state emits a photon of light. This emission is measured quantitatively at 700–900 nm.

The Dohrmann DN-1000 can be converted to the determination of sulfur and chlorine by adding the MCTS 130/120 microcoulometer detector modules. The control module, furnace module, and all the automated sample inlet modules are common to both detectors. The system automatically recognises which detector and sample inlet is present and sets the correct operating parameters for fast, simple conversion between nitrogen, sulfur, and chlorine detection.

Equipment for automated Kjeldahl determinations of organic nitrogen in water and solid samples is supplied by Tecator Ltd. Its Kjeltec system 1 streamlines the Kjeldahl procedure resulting in higher speed and accuracy compared to classic Kjeldahl measurements.

Apart from the chemical Kjeldahl digestion procedure for the determination of organic nitrogen, acid digestion of polymers has found little application. One of the problems is connected with the form in which the polymer sample occurs. If it is in the form of a fine powder, or a very thin film, then digestion with acid might be adequate to enable the relevant substance to be quantitatively extracted from the polymer. However, low nitrogen results would be expected for polymers in larger granular form, and for the analysis of such samples classic microcombustion techniques are recommended.

2.4.2 Acid Digestion

Method 2.12, based on Kjeldahl digestion – boric acid titration, is suitable for the determination of high concentrations of nitrogen (1–90%) in nitrogen containing copolymers. Method 2.13 has a wide range of application (0.002–75% nitrogen) and is based on Kjeldahl digestion with spectrophotometric indophenol blue finish for the determination of the ammonia produced on digestion of the polymer.

2.4.3 Physical Method for the Determination of Total Nitrogen

Wirsen [19] used size exclusion chromatography and infrared spectroscopy, and size exclusion chromatography, low angle light scattering to determine the nitrogen content of cellulose nitrate.

2.5 Silica

Silica has been determined in PE films by a method based on near-infrared spectroscopy. For peak height measurements a single baseline point at the minimum near 525 cm^{-1} was found to be best. An additional baseline point below 430 cm^{-1} gave poorer results because of the increased noise at longer wavelengths due to atmospheric absorption. For the same reason peak area measurements were confined to the range 525–469 cm^{-1} [20]. Both height and area measurements gave an error index close to 1%, but derivative methods were considerably poorer. Derivative spectra generally show increased noise levels so that they are unlikely to be useful except when they are overlapping bands. The results obtained with the ratio program also showed a higher error index. The band index ratio method avoids uncertainty associated with measuring the film thickness, but in this case the error resulting from using a rather weak reference band appears greater.

Combustion in a Parr Bomb with sodium peroxide, sucrose and benzoic acid in a gelatine capsule is the basis of a method for determining silica in polymers. Boron, halogens, nitrogen, phosphorus, and sulfur do not interfere.

2.6 Boron

Yoshizaki [21] has described a method for determining boron in which 0.1 g of polymer is digested with concentrated nitric acid in a sealed ampoule to convert organoboron compounds to boric acid. The digest is dissolved in methyl alcohol and boron estimated flame-photometrically at 595 cm^{-1}. Chlorine and nitrogen do not interfere.

2.7 Total Organic Carbon

Dohrmann supplies a TOC analyser. Persulfate reagent is continuously pumped at a low flow rate through the injection port (and the valve of the autosampler) and then into the ultraviolet reactor. A sample is acidified, sparged, and injected directly into the reagent stream. The mixture flows through the reactor where organics are oxidised by the photon-activated reagent. The light-source envelope is in direct contact with the flowing liquid. Oxidation proceeds rapidly; the resultant carbon dioxide is stripped from the reactor liquid and carried to the carbon dioxide-specific non-dispersive infrared detector.

The Shimadzu TOC-500 total organic carbon analyser is a fully automated system capable of determining between 1 and 3000 µg/l TOC.

OIC Analytical Instruments produce the fully computerised model 700 TOC analyser. This is applicable to solids. Persulfate oxidation at 90–100 °C followed by non-dispersive infrared spectroscopy is the principle of this instrument.

2.8 Total Sulfur/Total Halogen

The Mitsubishi TSX-10 halogen–sulfur analyser expands the technology of the TOX-10 to include total chlorine and total sulfur measurement. The model TSX-10, which consists of the TOX-10 analyser module and a sulfur detection cell, measures total sulfur and total chlorine in liquid and solid samples over a sensitivity range of milligrams per litre to a percentage.

Dohrmann also produces an automated sulfur and chlorine analyser (models MCTS 130/120). This instrument is based on combustion microcoulometric technology.

2.9 Nitrogen, Carbon, and Sulfur

The NA 1500 analyser supplied by Carlo Erba is capable of determining these elements in 3–9 minutes in amounts down to 10 mg/l with a reproducibility of ±0.1%. A 196-position autosampler is available.

'Flash combustion' of the sample in the reactor is a key feature of the NA 1500. This results when the sample is dropped into the combustion reactor, which has been enriched with pure oxygen. The normal temperature in the combustion tube is 1020 °C and it reaches 1700–1800 °C during the flash combustion.

In the chromatographic column the combustion gases are separated so that they can be detected in sequence by the thermal conductivity detector (TCD). The output signal is proportional to the concentration of the elements. A data processor plots the chromatogram, automatically integrates the peak areas, and gives retention times, percentage areas, baseline drift, and attenuation for each run. It also computes blank values, constant factors, and relative average elemental contents.

2.10 Carbon, Hydrogen, and Nitrogen

Perkin Elmer supplies an analyser (model 2400 CHN or PE 2400 series II CHNS/O analysers) suitable for determining these elements in polymers. In this instrument the sample is first oxidised in a pure oxygen environment. The resulting combustion gases are then controlled to exact conditions of pressure, temperature, and volume.

Table 2.2 Automated determination of carbon, hydrogen and nitrogen in polymers						
Compound	Theoretical			Found, %		
	C	H	N	C	H	N
Nylon 6	63.68	9.80	12.38	63.58	9.85	12.35
				63.55	9.91	12.32
Styrene/25% acrylonitrile	86.10	7.24	6.60	86.00	7.28	6.62
				86.05	7.20	6.65
Teflon	24.00	–	–	23.97	–	–
				24.10	–	–
Reproduced by kind permission of Perkin Elmer Ltd., Beaconsfield, UK.						

Finally the product gases are separated under steady-state conditions and swept by helium or argon into a gas chromatograph for analysis of the components. The equipment is supplied with a 60-position autosampler and microprocessor controller covering all system functions, calculation of results, and on-board diagnostics. Analysis time is 6 minutes for the CHN mode, 8 minutes for the CHNS mode, and 4 minutes for the oxygen mode [22-28].

Table 2.2 gives theoretical *versus* determined carbon, nitrogen, and hydrogen values obtained by this instrument for three polymers.

2.11 Oxygen Flask Combustion: Ion Chromatography

Combustion of polymers in an oxygen-filled flask over aqueous solutions of appropriate reagents converts elements such as halogens, phosphorus and sulfur into inorganic anions. For example:

• chlorine, bromine, iodine → chloride, bromide, iodide

• sulfur → sulfate

• phosphorus → phosphate

Subsequent analysis (see Method 2.14) of these solutions by ion chromatography [29] enables the concentrations of mixtures of these anions (i.e., the original elements) to be determined rapidly, accurately, and with great sensitivity.
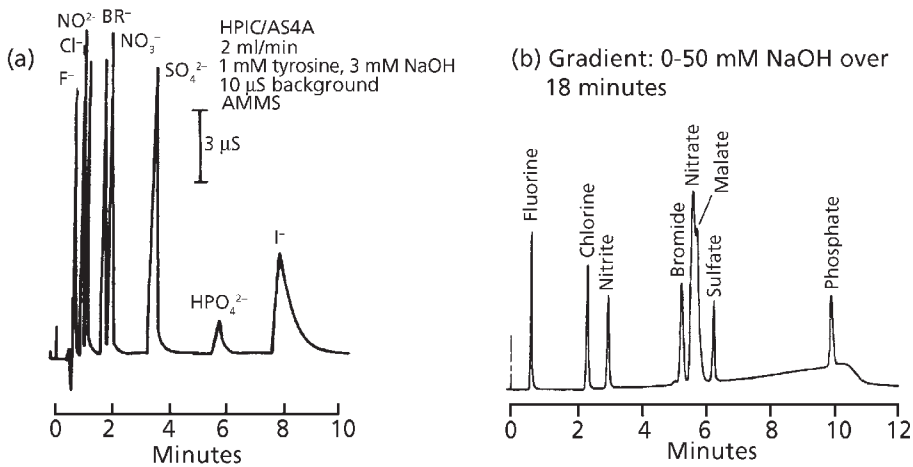
Figure 2.1 Ion chromatograms obtained with Dionex instrument using (anodic) AMMS and CMMS micromembrane suppression, (a) anions with micromembrane suppressor; (b) multi-component analysis by ion chromatography. (*Source: Author's own files*)

Figure 2.1(a) shows a separation of halides, nitrate, phosphate and sulfate, obtained in six minutes by ion chromatography using a Dionex A54A anion exchange separator.

A further development is the Dionex HPLC AS5A-SU analytical anion exchange column. Quantitation of all the anions in **Figure 2.1(b)** would require at least three sample injections under different eluent conditions.

2.12 X-ray Fluorescence Spectroscopy

The X-ray fluorescence (XRF) technique, already discussed in Chapter 1, has been applied extensively to the determination of macro- and micro-amounts of non-metallic elements in polymers.

An interesting phenomenon has been observed in applying the XRF method to the determination of parts per million of chlorine in hot-pressed discs of low-pressure polyolefins. In these polymers the chlorine is present in two forms, organically bound and inorganic, with titanium chloride compounds resulting as residues from the polymerisation catalyst. The organic part of the chlorine is determined by XRF without complications. However, during hot processing of the discs there is a danger that some inorganic chlorine will be lost. This can be completely avoided by intimately mixing

Table 2.3 Determination of chlorine by X-ray procedure		
A: Polymer not treated with alcoholic potassium hydroxide before analysis, ppm chlorine, X-ray fluorescence on polymer discs. Average of 2 discs (A)	**B: Polymer treated with alcoholic potassium hydroxide before analysis, ppm chlorine, X-ray fluorescence on polymer discs. Average of 2 discs (B)**	**Difference between average chlorine contents obtained on potassium hydroxide-treated and untreated samples (B) – (A), ppm chlorine**
510	840	330
422	552	130
440	730	290
497	650	153
460	882	422
Source: Author's own files.		

the powder with alcoholic potassium hydroxide, then drying at 105 °C before hot pressing into discs. The results (**Table 2.3**) illustrate this effect. Considerably higher total chlorine contents are obtained for the alkali-treated polymers.

A further example of the application of XRF spectroscopy is the determination of tris(2,3-dibromopropyl) phosphate on the surface of flame retardant polyester fabrics [30]. The technique used involved extraction of the fabric with an organic solvent followed by analysis of the solvent by XRF for surface bromine and by high-pressure liquid chromatography for molecular tris(2,3-dibromopropyl) phosphate. The technique has been applied to the determination of hydroxy groups in polyesters [31, 32]:
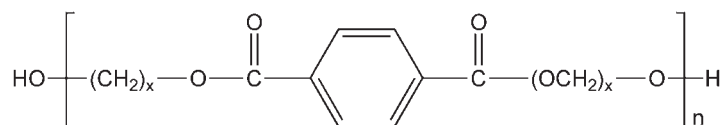
with $n = 1$–100 and $x = 2$ (polyethylene terephthalate) or 4 (polybutylene terephthalate) and ester-interchange elastomers of 4-polybutylene terephthalate and polypropylene glycol. The hydroxyl groups in these products are determined by acetylation with an excess of dichloroacetic anhydride in dichloroacetic acid and measurement of the amount of acetylation by a chloride determination carried out on the derivative.

The XRF method of Wolska [33] discussed in Section 1.2.1 has been applied to the determination of bromine and phosphorus in polymers. Various other workers have

applied this technique to the determination of chlorine and sulfur [34] and various other elements [2, 5, 35, 36].

Niino and Yabe [37] used XRF to determine the chlorine content of products obtained in the photoirradiation of polyvinylidene chloride film.

2.13 Thermogravimetric Analysis

This technique was used by Cambon and co-workers [38] to determine chlorine in chlorinated rubbers.

Method 2.1 Determination of Chlorine in Polymers Containing Chloride and Sulfur and/or Phosphorus and/or Fluorine. Oxygen Flask Combustion – Mercurimetric Titration

Summary

This oxygen flask combustion – titration method is capable of determining down to 5 ppm chlorine in polymers without interference from any fluorine, phosphorus, or sulfur present in the polymer sample.

Apparatus

Oxygen flask – 500 ml capacity, see **Figure 2.2**

A conical flask provided with B24 ground glass stopper, sealed at the lower end to a glass tube 5 mm in external diameter. The lower end of this tube is sealed and flattened to form a slight flange. The length from the lower edge of the ground portion of the stopper to the flanged end of the tube is 70 mm. The sample holder is constructed from 80 mesh platinum gauze in the form of a cylinder 6 mm in diameter and about 10 mm long. It is closed at one end and fastened to the flanged tube by a length of 0.5 mm diameter wire, one end of which is bent over the edge of the open end of the cylinder and pinched, so that the gauze is firmly gripped. The arrangement has significant advantages over the usual type of sample holder. The platinum gauze and wire can be renewed with ease and the thermal capacity of the assembly is relatively small.

Magnetic stirrer.

Content pipette, 2.0 ml capacity – conforming to BS 1428.

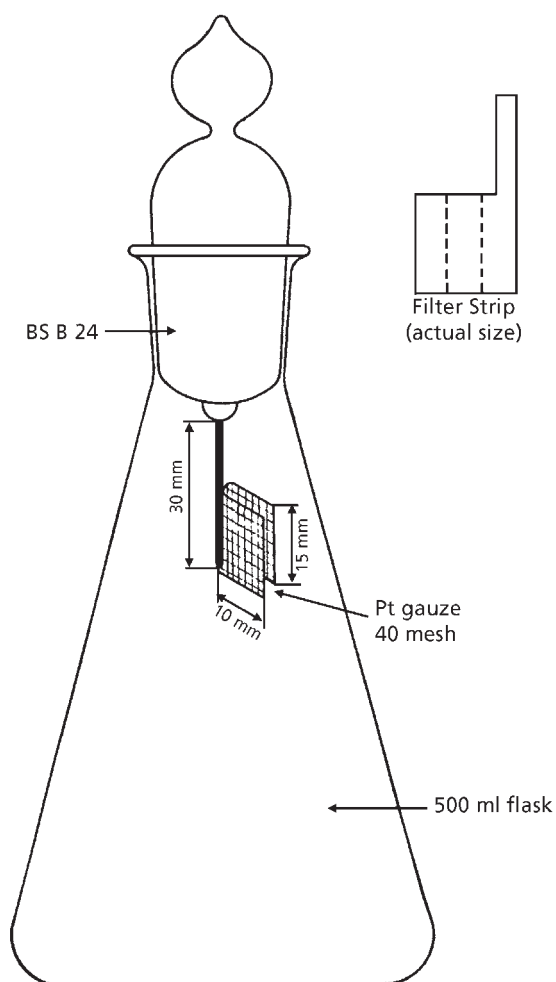Microburette, 10 ml capacity – conforming to BS 1428.

Figure 2.2 Stoppered conical flask with platinum wire gauze to suspend the sample. (*Source: Author's own files*)

Reagents

Sodium hydroxide, 0.1 N.

Nitric acid, 0.1 N.

Bromophenol blue indicator solution, dissolve 50 mg of bromophenol blue in 500 ml of ethanol.

Diphenylcarbazone indicator solution: dissolve 20 mg of diphenylcarbazone in 20 ml of ethanol. Keep the solution in the dark and renew it after 2 weeks.

Sulfur dioxide solution, saturate 50 ml of water with sulfur dioxide. Renew it after 2 to 3 days.

Hydrogen peroxide, 100 volume, micro-analytical reagent grade.

Barium nitrate solution, a saturated aqueous solution of analytical reagent grade barium nitrate.

Thorium nitrate solution, dissolve 15.0 g of analytical reagent grade thorium nitrate tetrahydrate in water and dilute the solution to 1000 ml.

Ethanol, absolute.

Mercuric nitrate, approximately 0.005 M, dissolve 3.5 g of mercuric nitrate in 570 ml of 0.01 N nitric acid and set the solution aside for at least 2 days. Filter off any precipitate and dilute the filtrate to 2 litres.

Sodium chloride, 0.025 M.

Standardisation of the mercuric nitrate solution. Measure out 2.0 ml of 0.025 M sodium chloride solution by means of a content pipette. Dilute to 15.0 ml with water and add 0.05 ml of bromophenol blue indicator solution. Add 0.1 N nitric acid until the yellow colour of the indicator appears and then add a further 0.5 ml of acid. After the addition of 100 ml of ethanol and 0.5 ml of diphenylcarbazone indicator solution, titrate the solution with the mercuric nitrate solution to the first appearance of a permanent violet colour. The solution should be stirred magnetically throughout the titration period. The use of a content pipette for measuring the sodium chloride solution is recommended, since it has been found that the reproducibility of repeated titrations is better than that obtained with, for example, a 5.0 ml delivery pipette, in conjunction with 0.01 M sodium chloride solution. The titration carried out as described must be corrected for the indicator blank value, obtained by the titration of 15.0 ml of water. This blank value is usually less than 0.05 ml of mercuric nitrate solution but much higher values have been obtained occasionally and these have been found to be due to the presence of chloride in the ethanol. In such instances, a suitable stock of ethanol may be mixed with a predetermined volume of the mercuric nitrate solution, sufficient to reduce the blank value to less than 0.05 ml.

Method

The polymer sample is combusted in an oxygen filled flask over water. After neutralisation to the bromophenol blue end-point and the addition of thorium nitrate

and diphenyl carbazide and ethanol, the solution is titrated to the violet end-point with standard mercuric intrate solution:

$$2HCl + Hg\,(NO_3)_2 = HgCl_2 + 2HNO_3$$
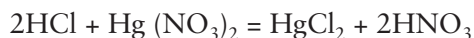
The chlorine content of the polymer can then be calculated from the consumption of standard mercuric nitrate solution. Modifications to the method are described for overcoming interferences by any sulfur, phosphorus or fluorine present in the polymer.

Experimental Procedure

The procedures described next are restricted to the determination of chlorine in organic compounds containing phosphorus or fluorine, or both, in the presence or absence of sulfur. For compounds containing little, if any, hydrogen a preferred alternative procedure is given. The determination of iodine or bromine in the presence of phosphorus or fluorine is not included since the determination of these halogens is, in this instance, best completed by other well known volumetric methods, such as Leipert's method for iodine and oxidation to bromate for bromine.

Compounds Containing Phosphorus or Fluorine, or Both

Weigh out an amount of sample corresponding to 1.0 to 2.0 mg of chlorine and decompose it in an oxygen flask containing 5.0 ml of water. Wash the stopper and sample holder with 10.0 ml of water, add 0.1 ml of bromophenol blue indicator solution and neutralise the solution with 0.1 N sodium hydroxide to the blue colour of the indicator. Add 0.75 ml of thorium nitrate solution, 0.5 ml of diphenylcarbazone indicator solution and 100 ml of ethanol and titrate the stirred solution with standard mercuric nitrate solution to the appearance of a permanent violet colour.

Compounds Containing Sulfur and Either Phosphorus or Fluorine or all Three Together

Proceed as before up to the washing of the stopper, and so on. Boil the solution for 60 seconds, holding the flask directly over a small bunsen burner flame and swirling the solution continuously. Add 0.5 ml of barium nitrate solution, 0.1 ml of bromophenol blue indicator solution and sufficient 0.1 N sodium hydroxide to produce the blue colour of the indicator. After the addition of thorium nitrate, complete the determination as before.

Compounds Containing Phosphorus or Fluorine or Both, and Little Hydrogen

Decompose the weighed sample in an oxygen flask containing 5.0 ml of water and 0.25 ml of saturated solution of sulfur dioxide. Wash the stopper and so on with 10.0 ml of water and complete the determination as described for the analysis of compounds containing sulfur. In this procedure the volume of barium nitrate should be increased if 0.5 ml is found to be insufficient for complete precipitation of the sulfate.

Blank determinations on the reagents and so on, should be carried out in conjunction with each of the procedures described previously. These blank values should not exceed about 0.2 ml of 0.005 M mercuric nitrate.

Discussion of Results

The method has a precision of approximately 0.1 ppm at the 22% chlorine level.

Method 2.2 Determination of Chlorine in Chlorobutyl and Other Chlorine Containing Polymers. Oxygen Flask Combustion – Turbidimetry [6]

Summary

This oxygen flask combustion-turbidimetric method is capable of determining total chlorine in amounts down to 5 ppm in chlorobutyl and other chlorine containing polymers.

Apparatus

Conventional 1 and 2 litre Schoniger type oxygen combustion apparatus.

The absorbance measurements were obtained using a spectrophotometer with a 1 cm cell and a tungsten lamp as the energy source, or equivalent.

Reagents

Standard aqueous potassium chloride solution in demineralised water to contain 1000 ppm chloride. Dilutions made from this standard stock solution to those containing very low chloride levels.

Silver nitrate, 0.01 M aqueous.

Nitric acid, 0.01 M

Potassium nitrate 0.01 M aqueous.

Method

A weighed sample is combusted in an oxygen filled flask over dilute nitric acid. Silver nitrate solution is then added and the resulting silver chloride, i.e., chlorine, estimated turbidimetrically at 420 nm using a grating spectrophotometer.

Experimental Procedure

The preparation of the calibration curve involves the preparation of six standard chloride solutions to contain 0 to 4 ppm chloride. Acidified 0.01 M silver nitrate is added to each solution to form a silver chloride suspension. All the solutions are swirled briefly and allowed to stand for at least 35 minutes with occasional shaking. The absorbance of each of these solutions is then measured at 420 nm in a 1 cm cell. A straight line curve passing through the origin is obtained covering chloride concentrations from 0 to 4 ppm. The ideal absorbance is in the range of approximately 0.03 to 0.2 absorbance units.

During the preparation of standards, swirling each solution for a few seconds is sufficient. Prolonged agitation tends to agglomerate the silver chloride particles.

Generally, about 100 mg of a weighed sample are combusted in a 2 litre Schoniger flask containing 10 ml of 0.01 M nitric acid. After the combustion, the flask is allowed to stand for at least 15 minutes with occasional shaking before 5 ml of 0.01 M silver nitrate solution is added.

If the polymeric sample is difficult to combust, the normal platinum sample basket may be wrapped with 52 mesh platinum gauze to prevent hot and partially burned sample from dripping out of the sample basket. For subsequent combustions of this sample, a smaller sample size and the use of twice the normal volume of nitric acid absorbent are recommended.

The measurement of the absorbance of the silver chloride suspensions should be done within 35-60 minutes of turbidity development of both the sample and standard chloride solutions. The absorbances of the standard solutions are measured first, followed by the sample solutions, then the standard solutions are measured again.

The calculation of results is made in two different ways. For samples of low halogen level and if the combustion results in a clear solution, no removal of a solution aliquot is necessary and the calculation is as follows:

% CI = ppm chloride × 15 × 100/sample weight (mg) × 1000

The value for ppm chloride is obtained from the calibration curve.

If combustion of the sample is such that a clear solution is not obtained and an organic film results in the combustion flask, an 8 ml aliquot is usually removed and only 4 ml silver nitrate is added to the clear aliquot. Here again, the ratio of sample solution aliquot volume to that of silver nitrate is still 1:1 and the calculation for chloride is the same as previously.

Discussion of Results

This method can determine down to 5 ppm total chlorine in chlorine containing polymers with an accuracy of +5%.

Method 2.3 Determination of Up to 80% Chlorine, Bromine and Iodine in Polymers. Oxygen Flask Combustion – Titration

Summary

This oxygen flask combustion – titration procedure is capable of determining between 2 and 80% of total bromine, chlorine or iodine in polymers.

Apparatus

Combustion flask – Pyrex, 500 ml capacity conical flask with B24 conical ground stopper.

Stopper B24 – with a fixed in platinum wire (30 mm long, 0.8 mm diameter) carrying a 15×20 mm piece of 40 mesh platinum gauze or carrying a 1.6 cm long × 0.64 cm diameter bucket fabricated in 40 mesh platinum gauze.

Safety jacket – for combustion flask to serve as a protection during the combustion. Conical shaped, detachable metal wire gauze fitting around the conical flask (**Figure 2.2**).

Automatic titrimeter – with silver/glass electrode system.

Wick lighter, small burner fed with sulfur and halogen free fuel.

Cellulose capsules – halogen free.

Reagents

Silver nitrate solution standard, 0.1 N.

Sodium hydroxide solution, 0.01 N approximately, dissolve 0.4 g of sodium hydroxide in distilled water and dilute to 1 litre.

Sodium metabisulfite solution, 0.05% *w/v*, (Micranalytical Reagent Grade, available from British Drug Houses Ltd., Poole, Dorset) dissolve 0.05 g of sodium metabisulfite in distilled water and dilute to 100 ml.

Barium nitrate, AnalaR, solid.

Oxygen, cylinder.

Nitric acid, AnalaR, concentrated.

Methyl alcohol, AnalaR.

Acetone, pure grade, redistilled.

Water, deionised, halogen content less than 0.05 ppm.

Filter paper, any grade with a halogen content less than 50 ppm.

Method

The sample is burnt in oxygen in a sealed Schoniger flask and the resultant volatiles are absorbed in a suitable absorption solution. This solution is acidified and titrated potentiometrically with standard silver nitrate solution.

Experimental Procedure

Combustion Technique

The method requires different absorption solutions for the various halogens as follows:

Chlorine	10 ml of 0.01 N sodium hydroxide solution.
Bromine and/or iodine	10 ml 0.05% *w/v* solution metabisulfite solution.
Chlorine and bromine and/or iodine	5 ml 0.01 N sodium hydroxide solution and 5 ml 0.05% *w/v* sodium metabisulfite solution.

Pipette the required absorption solution into the flask and fill with oxygen; stopper securely. Accurately weigh out 10-30 mg of sample into a cellulose capsule and place the capsule in the Schoniger basket, with a strip of filter paper to act as a fuse. Light the fuse and quickly insert the basket into the oxygen filled flask. During the combustion hold the basket in the flask firmly and at the same time lift the flask off the bench. Allow the mist formed in the flask to subside with periodic shaking over 15 to 30 minutes. Transfer the solution to a 250 ml beaker using 50 ml of distilled water and 120 mg of methanol. (If the halogen content of the sample is less than 5% then 120 ml acetone should be used instead of methanol.)

If any carbonaceous matter is evident in the solution then the determination should be abandoned and a further combustion carried out using a smaller sample weight.

Carry out a reagent blank combustion including the paper and all reagents but omitting the sample.

Add 1 drop of concentrated nitric acid and, if a mixture of halogens is present, a few crystals of barium nitrate. Titrate the solution potentiometrically using 0.1 N silver nitrate solution.

Calculations

The halogens are titrated in the following order: chlorine, bromine, iodine. Calculate the halogen content as follows:

$$\text{Chlorine \% } w/w = (T_s\text{-}T_b) \times N \times 35.46 \times 100/W \times 1000$$

$$\text{Bromine \% } w/w = (T_s\text{-}T_b) \times N \times 79.92 \times 100/W \times 1000$$

$$\text{Iodine \% } w/w = (Ts\text{-}Tb) \times N \times 126.91 \times 100/W \times 1000$$

where:

T_s = sodium nitrate titration (ml) obtained in sample combustion
T_b = silver nitrate titrations (ml) obtained in blank combustion
N = normality of silver nitrate.
W = weight (g) of sample taken for analysis.

Discussion of Results

This method can determine micro amounts (2-80%) of bromine, chlorine or iodine in halogenated polymers with an accuracy of ±3%.

Method 2.4 Determination of Fluorine in Fluorinated Polymers. Oxygen Flask Combustion - Spectrophotometric Procedure [39]

Summary

This oxygen flask combustion spectrophotometric procedure is capable of determining fluorine in fluorinated polymers such as PTFE in amounts down to 0.5%.

Apparatus

The combustion apparatus consists of a silica or boronfree glass 500 ml Erlenmeyer flask constructed of suitable glass (see Method 2.2). Into the stopper is fused one end of a length of platinum wire, 1 mm in diameter, to the free end of which is attached a piece of 36 mesh platinum gauze, 1.5 cm × 2 cm to act as a sample holder. The flask shall be essentially free from boron and aluminium. Low results are obtained using borosilicate glass flasks.

Optical densities were measured in 4 cm cells with a Unicam SP600 visual range spectrophotometer.

Reagents

Alizarin complexan, 0.0005 M, transfer 0.385 g of alizarin complexan to a 2 litre calibrated flask by means of 20 ml of recently prepared 0.5 N sodium hydroxide and set aside for 5 minutes with occasional swirling, to ensure complete solution. Dilute to about 1500 ml with water, add 0.2 g of hydrated sodium acetate and adjust the pH to about 5 by careful addition of 1 N hydrochloric acid. Dilute to the mark and filter into a brown glass bottle. This solution is stable for at least 4 months.

Cerous nitrate, 0.0005 M, standardise approximately 0.02 M cerous nitrate by titration against standard ethylenediaminetetraacetic acid solution at pH 6 with xylenol orange as indicator. To a suitable volume of this solution (about 50 ml) add 0.2 ml of concentrated nitric acid, 0.1 g of hydroxylamine hydrochloride and sufficient water to produce 2 litres and filter.

Acetate buffer solution, pH 4.6, dissolve 150 g of hydrated sodium acetate in about 600 ml of water, add 75 ml of glacial acetic acid, dilute to 1 litre with water and filter.

Standard fluoride solution, 5 μg per ml, dissolve about 22 mg (accurately weighed) of dried analytical reagent grade sodium fluoride in water and adjust the volume to 2 litres. Store in a polythene container.

Method

The method for the determination of fluorine is based on decomposition of the sample by oxygen flask combustion, followed by spectrophotometric determination of the fluoride produced by a spectrophotometric procedure involving the reaction with the cerium(III) complex of alizarin complexan (1,2-dihydroxy-anthraquinone 2-ylmethyl-amine *N,N*-diacetic acid). The blue colour of the fluoride containing complex (absorption maximum, 565 nm) is completely distinguishable from either the yellow of the free dye (maximum absorption, 423 nm) or the red of its cerium(III) chelate (maximum absorption, 495 nm).

Experimental Procedure

Preparation of Calibration Graph

In each of a series of 100 ml calibrated flasks place 50 ml of distilled water, an accurately measured volume between 2 and 8 ml of standard fluoride solution, 10 ml of alizarin complexan solution and 3 ml of acetate buffer solution. Mix each solution thoroughly, add 10 ml of 0.0005 M cerous nitrate, dilute to the mark with distilled water and set aside, protected from direct light for 1 hour. At the same time, prepare a blank solution in a similar fashion by omitting the standard fluoride solution. Measure the optical densities of the test solutions against the blank in 4 cm cells at 610 nm and plot a graph of optical density against amount of fluoride present.

Procedure

Accurately weigh an appropriate amount of the sample (5 to 25 mg) on a strip of filter paper approximately 3 cm × 4 cm (Whatman No. 1 grade is suitable) that has been folded into three along its length. Enclose the sample in the paper, insert a narrow strip of filter paper to act as a fuse and fix it in the platinum gauze sample holder. Place 20 ml of water in the combustion flask, fill the flask with oxygen, ignite the fuse and immediately insert the stopper. Carefully tilt the flask and when combustion is complete, set it aside the 10 minutes, with intermittent shaking. Quantitatively transfer the liquid to a 250 ml calibrated flask, dilute to the mark and treat an aliquot expected to contain about 25 mg of fluoride by the procedure described for colour development under Preparation of Calibration Graph. At the same time prepare a standard colour from 5 ml of standard fluoride solution to serve as a check on the calibration graph.

Liquid samples can be satisfactorily decomposed by burning in a small gelatin or preferably, methylcellulose capsule containing approximately 30 mg of powdered cellulose.

For solutions derived from the combustion of sulfur containing compounds, boil gently for about 10 seconds with 1 ml of 100 volume hydrogen peroxide, neutralise to phenolphthalein with 1 N sodium hydroxide and then add 1 ml in excess; boil to destroy excess of peroxide, cool and adjust the pH to about 4 with 1 N hydrochloric acid.

Typical Results

Using this method Johnson and Leonard [39] obtained from polytetrafluoroethylene a content of 75.8% fluorine using a silica or boron-free glass combustion flask against a theoretical value of 76%. Using a boroscilicate glass combustion flask they obtained a low fluorine recovery of 72.1%.

Discussion of Results

This procedure is capable of determining down to 0.5% total fluorine in fluorinated polymers with an accuracy of ±5%.

Method 2.5 Determination of Traces of Chlorine in Polyalkenes and Polyalkene Copolymers. Sodium Carbonate Fusion – Titration Procedure

Summary

This sodium carbonate fusion – titration procedure is capable of determining chlorine residues in amounts down to 50 ppm in polyalkenes and polyalkene copolymers.

Apparatus

Titration burette, 10 ml

Platinum crucible

Reagents

Silver nitrate, 0.1 M

Silver nitrate, 0.01 M

Nitric acid, 30% aqueous, dilute 30 cm concentrated nitric acid (MAR) with 100 cm^3 distilled water.

Sodium carbonate, solid microanalytical reagent grade.

Xylene cyanol/methyl orange mixed indicator, alcoholic solution.

Acetone, AR grade.

Acid buffer solution: to approximately 200 cm^3 of distilled water, in a 500 cm^3 volumetric flask add 100 cm^3 glacial acetic acid and 6.5 ml concentrated nitric acid (SG 1.42), dilute to the mark with distilled water.

Gelatine solution: add to 250 cm^3 of deionised water, 2.5 g gelatine and 5 g thymol blue. Heat slowly to the boil and stir until solution is complete. Add 0.5 g thymol as preservative and dilute to 500 cm^3 with distilled water. The solution is stable for up to 3 months at room temperature.

Method

In this method, polyethylene is mixed with pure sodium carbonate and ashed in muffle furnace at 500 °C. The residual ash is dissolved in aqueous nitric acid and then diluted with acetone. This solution is titrated potentiometrically with standard silver nitrate.

Experimental Procedure

Accurately weigh 5 g of polymer into a platinum crucible and cover the polymer with a layer of 2 g sodium carbonate. Place in a cold muffle furnace and increase the temperature gradually to 500 °C, maintaining this temperature for four hours. Allow the crucibles to cool then dissolve the residue in 15–20 ml distilled water. Transfer this solution with crucible washings to a 100 cm^3 beaker. Adjust the final volume of water to 30 cm^3. Add 5 drops of screened methyl orange indicator solution and neutralise the mixture by dropwise addition of 30% nitric acid to the purple red coloured end point. Add a further 10 drops of 30% nitric acid solution to the beaker and then add 30 cm^3 of acetone. Titrate the resultant solution potentiometrically with silver nitrate solution (0.001 M) using an automatic titrator equipped with a silver measuring electrode and glass reference electrode. Carry out a blank determination exactly as described above, omitting only the sample addition.

Typical Results

Calculation: ppm (*w/w*) chlorine in polymer = $(T_s - T_B) \times M \times 35.46 \times 10^3 / W$

where:

T_B = titration of silver nitrate (ml) in blank determination
T_s = titration of silver nitrate (ml) in sample determiantion

M = molarity of silver nitrate solution

W = weight (g) of polymer sample.

Note: If a polyolefin sample does not contain any free residual alkali left in the manufacturing process then there exists a danger that some chlorine will be lost during the ignition process and low chlorine analyses will result. If this is suspected to be the case the polymer sample (50 g) should first be contacted with twice its volume of 2% *w/v* alcoholic potassium hydroxide solution and left in an oven at 70 °C until the polymer is dry. The above method is then applied.

Discussion of Results

This method is capable of determining down to 50 ppm chlorine in polyalkenes and polyalkene copolymers with an accuracy of ±5%.

Method 2.6 Determination of Macro-amounts of Sulfur in Polymers. Sodium Peroxide Fusion - Titration Procedure

Summary

This sodium peroxide fusion – titration procedure [40] is capable of determining total sulfur in polymers in amounts down to 500 ppm.

Apparatus

Nickel 'fluorine bomb' capacity 2 ml – obtainable from Charles W. Cook and Sons Ltd., 97 Walshall Road, Perry Barr, Birmingham.

Conical flask with ground glass stopper, capacity 150 or 200 ml.

Magnetic stirrer.

Microburette, capacity 10 ml – conforming to BS 1428.

Reagents

Sodium peroxide, MAR grade.

Ethanol, absolute.

Barium perchlorate, 0.01 N aqueous, adjust to about pH 3.0 by adding perchloric acid.

Thorin indicator solution, dissolve 25 mg of Thorin in 5 ml of distilled water.

Methylene blue indicator solution, dissolve 15 mg of methylene blue in 50 ml of water.

Cation exchange resin, Amberlite IR-120 (H).

Pre-treatment of the resin. By the column method, wash about 400 g of the analytical grade resin with about 700 ml of 3.0 N hydrochloric acid and then with 4 or 5 litres of water. Transfer the resin to a 1 litre flask, remove most of the water by decantation and shake the resin thoroughly for several minutes with three succesive 100 ml portions of ethanol. Remove the residual ethanol by repeated washing with water and shake the resin vigorously with 400 ml of 0.5 N sodium hydroxide for about 10 minutes. Decant the slightly turbid solution, wash the resin with water until all suspended fine particles have been removed, and filter on a Buchner funnel. Press the resin between filter papers and store it in a glass stoppered bottle sealed with adhesive tape.

Method

The polymer sample is fused with sodium peroxide in a sealed bomb. The fusion product is dissolved in water and sodium ions removed on a cation exchange column. The sodium-free eluate is titrated with standard barium perchlorate solution to the thorinmethylene blue end-point to estimate the amount of sulfate present.

Experimental Procedure

Fusion of the Sample with Sodium Peroxide

Place in the dry bomb 0.5 g of powdered sodium peroxide, a suitable weighed amount of the sample (5 to 15 mg) and a further 0.5 g of sodium peroxide. Close the bomb and mix the contents by rotation. Heat the bomb in a muffle furnace for 3 minutes at 650 °C. Cool the bomb, remove the lid, and extract the fusion product by placing the bomb in a small beaker containing 10 to 15 ml of water and warming until effervescence ceases. Remove the bomb, rinse it with water and then rinse the lid. Transfer the combined solutions quantitatively to a 50 ml calibrated flask and dilute to the mark.

Removal of Sodium from Fusion Product and Titration

Place about 30 g of the cation exchange resin in a conical flask. Add about 25 ml of ethanol, shake the stoppered flask for about 1 minute, remove the ethanol by decantation and repeat the operation with a further 20 ml of ethanol. Transfer 25 ml of the fusion product extract to the resin, shake for about 5 minutes and decant the solution into a suitable conical titration flask containing a magnetic stirrer bar. Rinse the

resin with four successive 25 ml portions of ethanol, add all washings to the contents of the titration flask. Add 0.1 ml each of Thorin and methylene blue indicator solutions and titrate with 0.01 N barium perchlorate to a pink end-point colour persisting for about 20 seconds. Carry out a blank determination in the same manner, omitting only the sample. The blank value should lie between 0.1 and 0.2 ml.

Precautions

When the sodium peroxide fusion is carried out as described, only a small amount of insoluble matter should be found in the aqueous extract of the fusion product, but this material can interfere with the detection of the end-point of the titration. For the best results the extract should be set aside overnight, so that a clear portion can be withdrawn for titration.

End-points in the barium perchlorate titration may be unsatisfactory if the ethanol washed resin is set aside for more than about 2 hours before use. If such a delay is unavoidable, the resin should be washed once more with about 20 ml of ethanol immediately before use.

With some batches of resin it has been observed that after pre-treatment in the prescribed manner, unsatisfactory end-points are obtained in the titration of the resin treated sample solution. If this defect is found with any portion of a given batch of resin, it is recommended that all subsequent portions should be vigorously shaken with about 25 ml of 0.5 N sodium hydroxide for about 10 minutes and then washed with water and ethanol in succession before use.

Discussion of Results

This procedure is capable of determining down to 500 ppm of total sulfur in sulfur containing polymers with an accuracy of + 5%.

Chlorine, fluorine and nitrogen in amounts up to 2 mg in the sample are without serious effect on the determination of sulfur. The effect of larger amounts of fluorine can be suppressed by the addition of boric acid.

Method 2.7 Determination of Sulfur in Polymers. Oxygen Flask Combustion – Titration Procedure

Summary

This oxygen flask combustion – titration method is capable of determining total sulfur in amounts down to 50 ppm in sulfur containing polymers.

Apparatus

Conical flask – Pyrex or Jala glass, 500 ml capacity, provided with conical ground joint BS-B24 (see Method 2.2).

Stopper, BS-B24, with fused in platinum wire (30 mm long, 0.8 mm diameter) carrying a 15×20 mm piece of 40 mesh platinum gauze.

Safety jacket, to serve as a protection during the combustion. Detachable metal wire gauze jacket fitting around the conical flask.

Syringe – 0.05 ml capacity, with 0.001 ml divisions.

Lighter – any suitable small flame fed with sulfur-free fuel, e.g., alcohol.

Micro burette assembly, with 10 ml burette and Pyrex supply bottle, two required.

Ultramicro burette, with 0.001 ml divisions and provided with a glass capillary delivery tube.

Photoelectric colorimeter equipped with two 100 ml optical cells and two 520 nm interference filters in rim, or equivalent.

Electric stirrer, of suitable dimensions to fit on and close the colorimeter compartment, provided with small glass propeller-shaped stirrer.

Filter paper for sample wrapping. Any grade with sulfur content less than 100 ppm e.g., Whatman No.41 or 42. Cut out paper, sized and shaped according to **Figure 2.2**. Fold them along the dotted line to the U shape and store in a closed bottle to protect from any sulfur present in the atmosphere. As the paper contains a small amount of sulfur it is necessary to ensure that the same weight (30 to 40 mg) is used in the sample and the blank combustions.

Reagents

Barium perchlorate standard solution 0.0005 M, dissolve 0.17 g barium perchlorate in 200 cm^3 of deionised water and make up to 1 litre with redistilled isopropanol. Adjust to pH 3.5 by additions of 10% perchloric acid solution. Standardise in an optical cell against sulfuric acid using 1 cm^3 of isopropanol. Add 1 drop (approximately 0.05 cm^3) of perchloric acid solution 3% and $200 \pm 1 \text{ μl}$ of 0.07% *w/v* Thorin indicator solution and proceed as described under Procedure. Run a blank titration in the same way using exactly the same amounts of reagents but omitting the sulfuric acid and applying $20 \pm 0.5 \text{ cm}^3$ of deionised water instead of 10 cm^3. Obtain the net normality of the barium perchlorate solution.

Barium perchlorate solution standard 0.005 M. Dissolve 1.7 g barium perchlorate in 200 cm of deionised water and make up to 1 litre with redistilled isopropanol. Adjust to pH 3.5 by additions of 10% perchloric acid. Standardise in an optical cell against sulfuric acid using 10 cm of standard 0.005 M sulfuric acid solution. Dilute with 10 ± 0.5 cm^3 of deionised water and add 80 ± 2 cm^3 of isopropanol. Add 1 drop (approx 0.05 cm^3) of perchloric acid solution 3% and 200 ± 1 µl (1 µl = 0.001 cm) of 0.02% *w/v* Thorin indicator solution and proceed as described under Procedure. Run a blank titration in the same way using exactly the same amounts of reagents but omitting the sulfuric acid and applying 20 ± 0.5 ml of deionised water instead of 10 cm^3. Obtain the net normality of the barium perchlorate solution.

Hydrogen peroxide: 100 volume Microanalytical reagent grade.

Isopropyl alcohol, redistilled.

Oxygen, free from sulfur compounds.

Perchloric acid, 0.01 M microanalytical reagent grade in glacial acetic acid.

Sulfuric acid, 0.005 M prepared by accurate dilution of 0.05 M acid.

Sulfuric acid, 0.00025 M, prepared by accurate dilution of 0.005 M acid. Prepare the 0.0005 N reagent at least once daily as required.

Thorin indicator solution: 0.02% aqueous Thorin (sodium salt of 2(2-hydro-3,6-disulfo-1-napthylazo) benzene arsonic acid).

Water, deionised, sulfate content less than 0.05 ppm.

Method

The sample is wrapped in a piece of filter paper and burnt in a closed conical flask filled with oxygen at atmospheric pressure. The sulfur dioxide produced in the reaction reacts with dilute hydrogen peroxide solution contained in the reaction flask to produce an equivalent amount of sulfuric acid which is estimated by visual titration with 0.005 M or 0.0005 M barium perchlorate using Thorin indicator.

Experimental Procedure

Sample Combustion

The weight of sample taken should be sufficient to produce a titration of about 4 cm^3 of 0.005 or 0.0005 M barium perchlorate. The maximum permissible sample weight

for complete combustion is 30 mg. Weigh a blank piece of filter paper of similar size and check that its weight is within ± 5% of the weight of the paper used in the sample analysis. Wrap the sample up in the following way. First cover the sample with the raised edges of the paper strip and then roll up the body of the strip towards the narrow strip at the end, which will serve as a fuse. Now clamp the packet in the platinum gauze or bucket on the flask stopper, keeping the fuse free from, and in line with, the platinum suspension wire. Repeat this operation with the blank piece of filter paper. Pipette 4.0 ± 0.5 ml deionised water and 0.15 cm^3 hydrogen peroxide solution into a clean combustion flask. Place the flask in the safety jacket. Replace the air in the conical flask with a rapid stream of oxygen. Ignite the end of the fuse of the sample packet and immediately insert the sample into the combustion flask. Keep the flask firmly closed and keep it upside down for a minute. Shake the flask for one minute and allow it to stand for 15 minutes. When all the mist has disappeared, wet the rim of the flask with isopropyl alcohol, carefully open the flask and transfer the flask contents quantitatively to a 100 cm^3 beaker by means of 65 cm^3 isopropyl alcohol and 12 cm^3 water. To the beaker add 2 cm^3 0.02% Thorin indicator, 3 drops of 0.05 M perchloric acid and 1 cm^3 of 0.00025 M sulfuric acid (by pipette). Carry out a blank combustion including the paper and all the reagents but omitting the sample.

Titrate the sample and blank solutions with 0.005 M or 0.0005 M barium perchlorate solution using a 5 cm^3 syringe.

Calculations

Calculate the sulfur content of the sample as follows:

$$\text{Sulfur (ppm)} (V-B) \times M \times 16 \times 10^3/W$$

where:

V = volume (cm^3) of barium perchlorate solution consumed in actual determination
B = volume (cm^3) of barium perchlorate solution consumed in blank determination
W = weight of sample in g
M = molarity of barium perchlorate

Discussion of Results

The procedure is capable of determining sulfur in amounts from 500 ppm upwards in polyolefins and in other polymers. The repeatability of the method is ± 40% of the determined sulfur content at the 500 ppm sulfur level, improving to ± 2% at the 1% level. Chlorine and nitrogen concentrations in the sample may exceed the sulfur concentration several times over without causing interferences. Fluorine does

not interfere unless present in concentrations exceeding 30% of the sulfur content. Phosphorus interferes even when present in moderate amounts. Metallic constituents also interfere when present in moderate amounts.

Method 2.8 Determination of Sulfur in Polymers. Oxygen Flask Combustion – Photometric Titration Procedure

Summary

This oxygen flask combustion photometric titration procedure [40] is capable of determining total sulfur in polymers in amounts down to 50 ppm.

Apparatus

A general view of the titration arrangement is given in **Figure 2.3**.

Conical flask – Pyrex or Jena glass, 500 cm^3 capacity, provided with conical ground joint B24 (see **Figure 2.2**).

Stopper, B24 with fused in platinum wire (30 mm long, 0.8 mm diameter) carrying a 15×20 mm piece of 40 mesh platinum gauze (see **Figure 2.2** and Method 2.2).

Safety jacket, to serve as a protection during the combustion. Detachable metal wire gauze jacket fitting around the conical flask.

Syringe – 0.05 cm capacity, with 0.001 cm^3 divisions.

Lighter – any suitable small flame fed with sulfur-free fuel, e.g., alcohol.

Microburette assembly, with 10 cm^3 burette and Pyrex supply bottle, two required. Ultramicro burette, with 0.001 cm divisions and provided with a glass capillary delivery tube.

Photoelectric colorimeter equipped with two 100 cm^3 optical cells and two 520 nm interference filters in rim.

Electric stirrer of suitable dimensions to fit on and close the colorimeter compartment, provided with small glass propeller-shaped stirrer (**Figure 2.3**).
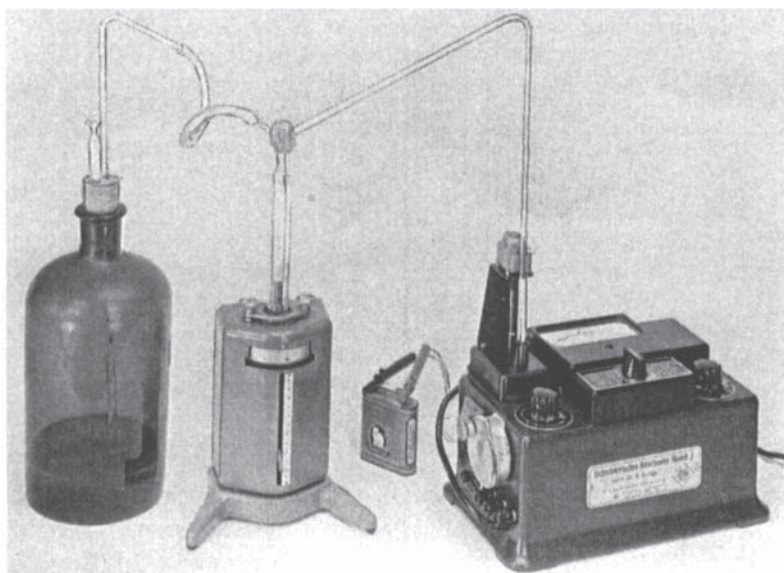
Figure 2.3 Titration assembly for the photometric sulfate titration.
(*Source: Author's own files*)

Reagents

Barium perchlorate solution, standard 0.005 M, prepare as described in Method 2.7.

Barium perchlorate solution standard 0.0005 M, prepare as described in Method 2.7.

Filter paper, ash-free. Seilacher and Schill No. 5892 is recommended. Store in a closed bottle.

Hydrogen peroxide, 30% AR.

Isopropanol, cp, denatured.

Oxygen, compressed, free of sulfur compounds.

Perchloric acid, 10% AR.

Perchloric acid, 3%, AR.

Sulfuric acid solution, standard, 0.01 N prepare by accurate dilution of standardised 0.1 N sulfuric acid solution.

Sulfuric acid solution, 0.0005 N, prepare by accurate dilution of 0.01 N sulfuric acid solution.

Thorin indicator solution, 0.2% aqueous solution of Thorin (sodium salt of 2(2-hydroxy-3, 6-disulfo-l-naphthylazo) benzene-arsenic acid). The Thorin quality marketed by Merck, Darmstadt, West Germany, is recommended.

Water, deionised.

Method

The sample, contained in a piece of filter paper and suitably suspended, is rapidly and completely burnt in a closed conical flask filled with oxygen at atmospheric pressure. The products of combustion are allowed to enter a hydrogen peroxide solution. The amount of sulfuric acid formed is determined by titration with barium perchlorate, using Thorin as the indicator. The equivalence point is obtained photoelectrically by comparing the optical density of the solution with that of a standard reference solution.

Experimental Procedure

Sample Combustion

Weigh a filter strip to the nearest 0.1 mg. Place approximately 30 mg of sample onto the middle of the filter strip and weigh again. Wrap the sample up in the following way: first cover the sample with the raised edges of the strip and then roll up the body of the strip towards the end, which will serve as a fuse. Now clamp the packet in the platinum gauze of the stopper, keeping the fuse free and in line with the platinum suspension wire.

Introduce 4 ± 0.4 ml of deionised water and 3 drops of hydrogen peroxide solution 30% into the conical flask. Install the safety jacket.

Replace the air in the conical flask by oxygen by introducing a rapid stream of oxygen at a point near the bottom for 30 seconds. (Place a G 3 porosity glass filter in the outlet end of the oxygen line to prevent contamination of the absorption liquid.)

Place the flame of the lighter close to the top of the conical flask, ignite the end of the fuse of the sample packet and immediately insert the stopper.

Keep the flask firmly closed and keep it upside down to prevent the flame from touching the walls or bottom of the flask. When the combustion slows down bring

the flask in an inclined position to promote complete combustion also of any dropping particles. Remove the safety jacket, shake the bottle for one minute and allow it to stand for 15 minutes.

Spectrophotometric Evaluation

In an optical cell prepare a colour reference solution by mixing 100 ml of deionised water and 200 ± 1 µl of Thorin indicator solution (measured from the ultramicro burette). Measure the optical density using the deflection method. This value should be 0.17 ± 0.01, adjust if necessary by adding a known amount of either 0.0005 N sodium hydrogen carbonate solution or 0.0025 N sulfuric acid solution.

Prepare a double amount of the colour reference solution described in the previous paragraph in a beaker. Introduce half of it into each optical cell and check the optical density of the solution. With both cells in the compartments and the photometer adjusted for highest sensitivity bring the pointer at position 50 of the linear scale marked 'abs'. Check whether the cells are matched by interchanging them. During the actual determination keep the right-hand cell in its place and titrate in the left-hand cell.

Prepare and measure a fresh colour reference solution at least once a day and whenever a new batch of deionised water or Thorin indication solution is used. Switch on the photometer at least two hours before use.

Introduce 1 ml of 0.00025 N sulfuric acid solution by means of a pipette and 15 ± 0.5 ml of deionised water into the optical cell. Wet the rim between flask and stopper with some isopropanol and open the flask to draw the liquid in. Use 80 ± 2 ml of isopropanol to wash the stopper and the platinum gauze and to transfer the solution under test quantitatively to the cell. Add 1 drop (approximately 0.05 ml) of 3% perchloric acid solution and 200 ± 1 ul of Thorin indicator solution.

Discussion of Results

The following data should be used for judging the acceptability of results (95% probability). Duplicate results by the same operator should not differ by more than the following amounts:

Sulfur content	Repeatability
Above 0.5%	0.05
Below 0.5%	2% of amount present but not better than 0.005

Chlorine and nitrogen concentrations in the sample may exceed the sulfur concentrations several times over without causing interference. Fluorine does not interfere unless present in concentrations exceeding 30% of the sulfur content. Phosphorus and metallic constituents interfere even when present in moderate amounts.

Place the optical cell in the photometer and install the electric stirrer. Immerse the burette tip into the cell solution and stir. Titrate at a slow rate with barium perchlorate solution, until the pointer reaches 50 again. Use the 0.005 M barium perchlorate solution for sulfur contents exceeding 0.15% and the 0.0005 M barium perchlorate solution for the lower sulfur concentrations.

Especially in the lower sulfur range, a minimum titration time of two minutes is recommended. Run a blank determination including all reagents used (with filter paper) but omitting the sample.

Calculation

Calculate the sulfur content by means of the following equation:

$$\text{Sulfur } \%w = (V - B) \times N \times 16 \times 10^3/W$$

where:

V = volume of barium perchlorate solution consumed in the actual determination, millilitres

B = volume of barium perchlorate solution consumed in the blank determination, millilitres

N = normality of the barium perchlorate solution.

W = weight of sample milligrams

Method 2.9 Micro Determination of Phosphorus in Polymers. Acid Digestion – Spectrophotometric Method

Summary

This acid digestion – spectrophotometric method determines phosphorus in amounts down to 0.5% in polymers.

Apparatus

Hot plate capable of maintaining a temperature of 250-300 °C.

Fume chamber connected to water vacuum pump.

Pyrex flasks, 100 ml.

Spectrophotometer with matched cells (1 cm).

Small glass sample cups, with ground glass lids.

Reagents

Ammonium molybdate, 10% *w* aqueous.

Ammonium vanadate, 1% *w/v* in 2 N HNO_3.

Perchloric acid, 70% AR

Sulfuric acid, AR

Standard phosphate solution, 0.1 mg P/cm^3.

Method

The sample is decomposed and oxidised in sulfuric acid-perchloric acid. After cooling, water, ammonium vanadate and ammonium molybdate are added to form the yellow phosphovanadomolybdate complex, which is measured colorimetrically at 430 nm.

Experimental Procedure

Sample Digestion

Weigh out a suitable amount of polymer (ranging from 25-50 mg at the 0.1 to 0.5% phosphorus level to 3-5 mg at the 20% phosphorus level).

Place the weighed sample in the flask. Add 3 cm^3 of concentrated sulfuric acid, then 0.5 cm^3 perchloric acid and digest on the hotplate at 250-300 °C. After about 15 seconds the perchloric acid decomposes with formation of dense white fumes and the solution becomes yellow. Heating is continued for a further two minutes.

Remove the flask from the hotplate, allow to cool and then cautiously add a few drops of water and mix. Dilute to about 50 cm^3 with distilled water.

Spectrometric Evaluation

Add 5 cm^3 of ammonium vanadate solution, followed by 10 cm^3 of ammonium molybdate solution; make up to 100 cm and mix. Allow 15 minutes for colour development and read off the optical density at 430 nm. Carry out a blank determination.

Preparation of Calibration Curve

Transfer by use of pipettes or a burette 0, 2, 5, 8, 10, 12, 15 and 20 cm^3 aliquots of standard phosphate solution into separate 100 cm volume reaction flasks. Add 3 cm^3 of concentrated sulfuric acid and 0.5 ml of 70% perchloric acid.

Add a small glass bead to each flask and boil off the water by heating on the hotplate. Continue heating until the dense cloud of decomposing perchloric acid appears and then for a further two minutes.

Cool, add water cautiously to a volume of 50-60 cm^3. Add 5 cm^3 ammonium vanadate solution followed by 10 cm of ammonium molybdate, make up to 100 cm and leave for at least 15 minutes.

Read off the optical densities of the solutions using 1 cm cells at 430 nm. Plot milligrams of phosphorus/cm^3 against optical density. The average factor (F) may be calculated from the expression:

$$F = \text{mg P per cm}^3/\text{OD reading}$$

Calculation of Results

$$\text{Phosphorus, \% w} = (OD_1 - OD_2) \times F \times 100/W$$

where:

OD_1 = optical density of test solution

OD_2 = optical density of blank

F   = factor obtained by standardisation against known concentrations of standard phosphate solution

W   = sample weight in mg

Discussion of Results

This method is capable of determining total phosphorus in polymers in amounts down to 0.5% and up to 20% with an accuracy of ± 5%.

Method 2.10 Determination of Low Levels of Phosphorus in Polymers. Oxygen Flask Combustion – Spectrophotometric Method

Summary

This oxygen flask combustion – spectrophotometric method determines 0.01 to 2% total phosphorus in phosphorus-containing polymers.

Apparatus

500 ml conical combustion flask fitted with a reducing adaptor and joint carrying approximately 2.5 cm square platinum quaze (see Method 2.2).

Unicam SP 500 spectrophotmeter with 1 cm and 4 cm glass cells and tungstan lamp.

Methyl cellulose capsules – No. 4 small.

Sodium carbonate scoop – fabricated from glass tubing – 4 mm in outside diameter and marked to contain 50 ± 10 mg of anhydrous sodium carbonate powder.

Filter paper fuses approximately 38×3.2 mm in size made ferom ashless filter paper.

100 ml volumetric flasks, 150 ml conical flasks, pipettes etc.

Reagents

Demineralised water used throughout.

Ammonium molybdate solution: dissolve 40 g reagent grade ammonium molybdate $(NH_4)Mo_7O_{24}. 4H_2O)$ in a cooled mixture of 450 ml concentrated sulfuric acid and 1 litre water. Dilute to 2 litres with water.

Hydrazine sulfate solution, 1.5 g/litre.

Molybdate-hydrazine reagent, dilute 50 ml of ammonium molybdate solution with 130 ml of water, add 20 ml of hydrazine sulfate solution and mix well. Use 50 ml for each determination and prepare no earlier than 1 hour before use as this mixture is unstable.

Stock standard phosphorus solution, dissolve 4.393 g of dried AnalaR potassium dihydrogen phosphate (KH_2PO_4) in 150 ml of 1:10 sulfuric acid and dilute to 1 litre with water (1.0 mg/ml phosphorus). From this prepare solutions containing 0.01 mg P/ml and 0.001 mg P/ml.

Oxygen.

Sodium carbonate, anhydrous, AnalaR.

Method

The ground polymer mixed with sodium carbonate is decomposed by igniting in an oxygen filled flask containing dilute sulfuric acid. The solution is treated with molybdate-hydrazine reagent and the phosphate measured colorimetrically as its heteropoly-blue equivalent.

Experimental Procedure

Sample Digestion

Place one scoop of anhydrous sodium carbonate in the bottom half of a methyl cellulose capsule. Weigh a sample of not more than 32 mg, estimated to contain between 0.001 and 0.06 mg phosphorus, directly onto the sodium carbonate bed. Cover the sample with another scoop of sodium carbonate. Insert a filter paper fuse between the top and bottom halves of the capsule after making a small slit in the top half to give the clearance required. Secure the capsule in the platinum gauze with the wick towards the stopper.

Pass oxygen into the flask containing 10 ml of 1:10 sulfuric acid for 30 seconds. Holding the flask horizontally remove the oxygen lead, light the sample fuse and quickly insert the stopper in the flask (Gloves and goggles should be worn and the ignition carried out behind a protective glass screen). Tilt the flask immediately at an angle of 135° from the vertical so that the absorbing solution forms a liquid seal at the neck of the flask. During the period of maximum flame height completely invert the flask to prevent impingement of the flame on the flask walls. Hold the stopper firmly in place during the combustion. After combustion allow the flask to stand for 10 to 15 minutes.

Open the flask and wash the platinum gauze and surfaces of the reducing adaptor with a maximum of 35 ml of water. Remove the adaptor and lower the gauze into the solution.

Spectrophotometric Evaluation

Add 50 ml molybdate hydrazine reagent (it is essential that the solution is diluted before the molybdate hydrazine reagent is added). Heat the solution rapidly to boiling and boil for 2-3 minutes. Cool to room temperature in an ice-water bath, transfer to 1000 ml volumetric flask and dilute to volume.

Measure the absorbance against water in appropriate cells at 830 nm. Carry out a blank determination.

Calibration Curve

Prepare separate calibrations from standard phosphorus solutions for 1 cm and 4 cm cells containing 0-0.06 mg P/100 ml and 0-0.015 mg P/100 ml, respectively, as follows:

Measure appropriate amounts of the phosphorus standards into 150 ml conical flasks and dilute to approximately 30 ml with water. Add 10 ml of 1:10 sulfuric acid and 50 ml of molybdate/hydrazine reagent and develop the colour as before.

Measure the absorbance against water in appropriate cells at 830 μm.

Carry out a blank determination.

Prepare graphs of corrected absorbance against weight of phosphorus (mg/100 ml). Linear calibration graphs are obtained.

Discussion of Results

This method is capable of determining total phosphorus in polymers in amounts down to 0.01% and up to 2% with an accuracy of ± 5%.

Method 2.11 Determination of 2-13% Phosphorus in Polymers. Oxygen Flask Combustion – Spectrophotometric Method

Summary

This oxygen flask combustion – spectrophotometric procedure determines total phosphorus in polymers in the concentration range 2 to 13% phosphorus.

Apparatus

A 500 ml conical flask fitted with a reducing adaptor and joint carrying approximately 2.5 cm square of platinum gauze (see Method 2.2).

Methyl cellulose capsules – No. 4 small.

Sodium carbonate scoop, fabricated from glass tubing 4 mm in outside diameter and marked to contain 50 ± 10 mg of anhydrous sodium carbonate powder.

Filter paper fuses, approximately 38 × 3.2 mm in size made from ashless filter paper.

Unicam SP 500 spectrophotometer with 1 and 4 cm cells and tungsten lamp.

100 volumetric flasks, 150 ml conical flasks, pipettes, etc.

Reagents

Oxygen.

Sodium hydroxide, 0.5 N.

Saturated bromine water.

Percolated water, prepared by percolating distilled water through a mixed resin bed containing Amberlite IR 120 (H) and Amberlite IRA 400 (OH).

Ammonium molybdate 5% *v/v*. Dissolve 50 g ammonium molybdate in a litre of warm distilled water.

Ammonium vanadate, 0.25% *w*. Dissolve 2.5 g of ammonium vandate in 500 ml hot water. Cool and add 20 ml of concentrated nitric acid. Cool and dilute to 1 litre.

Aqueous sulfuric acid, 25% *w*.

Method

The ground polymer, mixed with sodium carbonate, is decomposed by igniting in an oxygen-filled flask containing saturated bromine water and sodium hydroxide. The solution is acidified, boiled and made up to 100 ml. The phosphorus is determined colorimetrically as molybovanadophosphoric acid.

Experimental Procedure

Sample Digestion

Pass oxygen into a flask containing 5 ml of 0.5 N sodium hydroxide and 4 ml saturated bromine water for 30 seconds.

Place one scoop of anhydrous sodium carbonate in the bottom half of a methyl cellulose capsule supported in a bored cork. Weigh a sample of not more than 32 mg, estimated to contain between 0.05 and 2.5 mg phosphorus, directly onto the sodium carbonate bed. Cover the sample with another scoop of sodium carbonate. Insert a filter paper fuse between the top and bottom halves of the capsule (after making a small slit in the top half to give the clearance required.). Secure the capsule in the platinum gauze with the wick towards the stopper.

Holding the flask horizontally remove the oxygen lead, light the sample fuse and quickly insert the stopper in the flask. Tilt the flask immediately at an angle of 135°

from the vertical, so that the absorbing solution forms a liquid seal at the neck of the flask. During the period of maximum flame height, completely invert the flask to prevent impingement of the flame on the flask walls. Set aside until the mist has cleared (10 to 15 minutes is usually sufficient).

Open the flask and wash down the platinum gauze and surfaces of the reducing adaptor with demineralised water. Remove the adaptor and lower the gauze into the solution.

Spectrophotometric Evaluation

Add to the solution 6 ml of 25% *v/v* sulfuric acid and boil the solution for 15 minutes. Cool and transfer the solution to a 100 ml graduated flask. Add 10 ml of ammonium vanadate, followed by 10 ml of ammonium molybdate and make up to 100 ml. Allow 30 minutes for colour development.

Using either 1 or 4 cells, read off the optical density at 460 nm. Carry out a blank determination.

Preparation of Calibration Curve

Prepare separate calibration curves from standard phosphorus solutions for 1 cm and 4 cm cells containing 0-0.25 mg $P/100$ cm^3 and 0-0.06 mg $P/100$ cm^3, respectively, as follows:

Measure appropriate amounts of phosphorus standards into 100 cm^3 graduated flasks. Add 10 cm^3 of ammonium molybdate and 10 cm^3 of ammonium vanadate and make up to 100 cm^3. Allow 30 minutes for colour development.

Using either 1 cm or 4 cm cells, read off the optical density at 460 nm. Also make measurement using a reagent blank.

Prepare graphs of corrected absorbance against weight of phosphorus (mg/100 cm^3).

Discussion of Results

This method is capable of determining phosphorus in polymers in amounts down to 2% and up to 13% with an accuracy of ± 5%.

Method 2.12 Determination of Between 0.002% and 75% Organic Nitrogen in Polymers. Kjeldahl Digestion – Spectrometric Indophenol Blue Method

Summary

This Kjeldahl digestion – spectrophotometric method is capable of determining organic nitrogen in polymers in amounts between 0.002 and 75%.

Apparatus

Kjeldahl digestion apparatus (see **Figure 2.4**).

Kjeldahl digestion flasks 100 cm^3 Pyrex glass, B19 sockets.

Kjeldahl flask glass bulbs, with inlet and outlet and B19 cone.

Kjeldahl digestion flask heaters, with flask supports (100 ml flask size).

Nitrogen purifying train (see **Figure 2.4**) for purifying nitrogen supply to digestion flasks.

Two glass tubes (approximately 46 × 5 cm) of approximately 1 cm^3 capacity with No. 1 sintered glass discs and gas inlet at base and gas outlet at top. Third tube (with
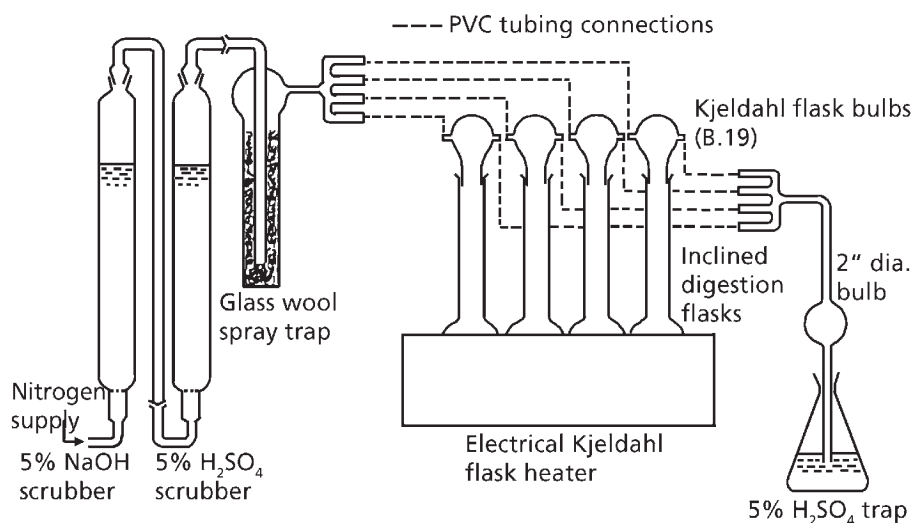
Figure 2.4 Kjeldahl digestion apparatus. (*Source: Author's own files*)

gas inlet and outlet) packed with glass wool to remove spray. Glass connections by ball and socket joints.

Ammonia recovery apparatus:

Condenser, Liebig l2 in (B24 cone and socket) round bottomed steam generator flask B24, central and 2 × B19 side, 1 dm³. Three-way stopcock, with vertical arm connected to B24 cone. Separatory funnel with B19 cone, 250 cm³, conical flasks B24, 250 cm³ (see **Figure 2.4**).

Recovery apparatus proper:

Consisting of steam stripping vessel (interior vessel large enough to hold 150 cm³ solution). Separatory funnel 50 cm³ with B14 cone and short delivery stem, steam trap leading to vertical condenser. Guard tube containing activated silica gel connected by suitable adaptors to lower end of condenser (silica gel to be regenerated daily).

Activated silica gel:

Self indicating, mesh 6-20, to regenerate gel: heat for 6 h at 150 °C in a vacuum oven.

Apparatus for concentration of ammonia steam distillate, consisting of:

Concentration apparatus B24 to B24 (70 degree bend) distillation flask head connected to slightly (horizontally) inclined 30 cm Liebig condenser with B24 cone and socket. Connected to outlet end of Liebig condenser (i.e., to B24 cone) a 20 cm vertical delivery tube (B24 socket) with 2.5 cm diameter bulb, 10 cm from the open end. Open end of delivery tube dipping in dilute sulfuric acid solution.

Silica gel guard tubes, 20 cm × 2.5 cm with B24 cone at base, packed with freshly activated silica gel.

Apparatus for preparation of ammonia free distilled water:

Round bottomed flask (2 dm³) in electric mantle: connected via adaptor and steam trap to slightly (horizontally) inclined 14 in Liebig condenser (B24 cone and socket). Delivery end of condenser (B24 cone) connected by suitable B24 socket to B24 cone) adaptor to 2 dm³ separatory funnel receiver (with activated silica gel guard tube connected by PVC tubing on side arm of the adaptor). The apparatus is totally enclosed – the only exit to atmosphere being via the silica gel guard tube (silica gel tube regenerated daily).

Colorimetric determination of ammonia:

Stoppered cylinders graduated, 50 cm^3. Pipette 5 cm^3 bulb, 1 cm^3 graduated.

Spectrophotometer – 4 cm glass cells.

Reagents

Ammonia free water. Use water which has been redistilled from 100 cm^3 5% sulfuric acid and fresh boiling chips, in an apparatus which is sealed from atmosphere by a guard tube containing freshly regenerated silica gel.

Sulfuric acid, (93%) – nitrogen free quality.

Dextrose, AnalaR.

Kjeldahl digestion catalysts:

Tablets each consisting of 1 g sodium sulfate and the equivalent of 0.05 g selenium as selenium dioxide.

Tablets each consisting of 1 g sodium sulfate and the equivalent of 0.05 g mercury as mercuric oxide.

Tablets each consisting of 1 g sodium sulfate and 0.05 g hydrated cupric sulfate.

Tablets each consisting of 1 g sodium sulfate.

The following reagents may also be required for Kjeldahl digestion:

Copper(II)sulfate (25% *w/v*), prepared from $CuSO_4.5H_2O$, aqueous.

Potassium sulfate (nitrogen free). Purify AnalaR potassium sulfate by recrystallisation in the following way:

Introduce into a 4 cm^3 beaker, 3 cm^3 of distilled water, 2 g sodium hydroxide and fresh boiling chips, heat to incipient boiling and add 675 g of AnalaR potassium sulfate. Adjust to pH 10 or higher by sodium hydroxide addition. Boil for 20 minutes to expel ammonia. Filter the boiling solution on a Buchner funnel through (previously hot water washed) Whatman No. 42 filter paper. Cool the filtrate to 5 °C and vacuum filter off the small uniform crystals. Dry the crystals in an air oven (yield 450 g). Allow to cool in a desiccator and store in well stoppered glass bottle.

Sodium hydroxide (use when mercury free catalysts are used for Kjeldahl digestion). Pour 1600 cm^3 distilled water into a 4 litre beaker and add 1500 g sodium hydroxide AnalaR. When dissolved allow to cool and transfer to a Winchester.

Sodium hydroxide – sodium thiosulfate (use when mercury containing catalysts are used for Kjeldahl digestion (see Method 2.13).

Sulfuric acid 0.25 M. Prepare by dilution of nitrogen-free concentrated sulfuric acid.

Phenol, 8% in ammonia-free water. Store in a brown glass bottle.

Sodium hypochlorite (6 *w/v* available chlorine). Made by diluting sodium hypochlorite solutions: (10-14% available chlorine) to 6.0 ± 0.1% *w/v* available chlorine content with ammonia free water.

Standard nitrogen solution (for calibration of the indophenol blue method).

Stock solution, dry ammonia sulfate AnalaR at 100 to 110°C for 1 hour and weigh out exactly 0.118 g. Transfer to a 250 cm^3 volumetric flask and make up to volume with ammonia free water. This solution contains 100 µg nitrogen per cm^3.

Working solution: for calibration purposes take 25 cm of the solution and dilute to 250 cm^3 with ammonia free water. The solution contains 10 µg nitrogen per ml. Prepare this solution daily by dilution of the stock solution.

Method

A known weight of sample is digested with 'nitrogen free' sulfuric acid, dextrose, potassium or sodium sulfate and digestion catalysts for 1.5 to 2 hours using an electrical heater. A suitable blank digestion is also carried out. The cooled digestion mixture, after dilution, is transferred to a semimicro steam distillation apparatus. Steam is passed through the sample and excess sodium hydroxide added. The liberated ammonia is collected in slightly acidulated water.

To a standard volume of this solution, add phenol and sodium hypochlorite reagents. An indophenol blue colour, proportional in intensity to the concentration of ammonia present, is produced. This colour is evaluated spectrophotometrically at 625 nm using a spectrophotometer which has been calibrated against a standard ammonia solution.

Experimental Procedure

Analytical Conditions

Choose an approximate weight of sample as indicated in **Table 2.4**.

Table 2.4 Quantities of digestion reagent					
Approximate nitrogen content of sample		Amount of sample required for analysis		Volume of H_2SO_4 needed in Kjeldahl digestion	Dilution to be applied to 50 ml of steam distillate
%w/w	ppm	g	mg	cm^3	cm^3
0.0025	25	0.6	600	10	nil
0.005-0.05	50-500	0.3	300	5	nil
0.075	750	0.15	150	5	nil
0.1	1000	0.1	100	5	nil
0.15	1500	0.075	75	5	nil
0.2	2000	0.05	50	5	nil
0.2-2	-	0.05	50	5	nil or × 10
1.0-2.5	-	0.01-0.005	10	5	× 10
75	-	0.005		5	× 50
Source: Author's own files					

Setting up Nitrogen Purifying Train

Charge the first bubbler with 250 to 300 cm^3, 5% sodium hydroxide solution and the second bubbler with 250 to 300 cm^3, 5% sulfuric acid solution (replace these solutions daily). Connect four digestion flask bulbs (see **Figure 2.4**) in parallel, at the outlet end of the nitrogen purifying train by means of PVC tubing. Purge the system by passing nitrogen for one hour before commencing sample digestion.

Sample Digestion

Into two 100 cm^3 digestion flasks containing a suitable weight of sample and two blank flasks containing no sample, (i.e., perform sample and blank determinations in duplicate), introduce 0.05 g dextrose and one small piece of clean porous pot. Keep the flasks stoppered between reagent additions to prevent contamination with any ammonia in the laboratory atmosphere. From this point treat the blank and sample determinations in an identical manner throughout the whole determination. Now add alkali metal sulfate, digestion catalysts and concentrated sulfuric acid to sample and blank digestion flasks, as indicated in **Table 2.5**.

Table 2.5 Amounts of reagents for the digestion of up to 0.3 g sample	
Digestion reagents, g	**Concentrated sulfuric acid, cm^3**
Sodium sulfate, 1 g (selenium, 0.05 g copper(II)sulfate.5H$_2$O), 0.05 g	5 ± 0.2
Sodium sulfate, 1 g mercury added as metal or mercury(II)oxide, 0.05-0.1 g	5 ± 0.2
Sodium sulfate, 1 g: copper(II)sulfate.5H$_2$O, 0.05-0.1 g	5 ± 0.2
Sodium sulfate, 1 g: mercury 0.05 g Copper(II)sulfate.5H$_2$O, 0.05 g	5 ± 0.2
Source: Author's own files	

Digest the samples gently and at an even rate for 20 minutes. Now increase the digestion temperature steadily at five minute intervals over a period of one hour so that eventually the acid is condensing about half way up the neck of the digestion flask. Ensure that the carbon char is completely oxidised (maximum digestion temperature 380 °C). Continue digestion for 15 to 20 miutes at maximum temperature after the solution has clarified.

Maintain a gentle purge of pure nitrogen through the bulbs during the acid digestion and also during the cooling period which follows digestion. If the nitrogen compound is known to be refractory then extend the total acid digestion period to 4 hours. Switch off the heaters and allow the flasks to cool to room temperature with the pure nitrogen stream still flowing. At least half of the original sulfuric acid additions should remain in the digestion flasks at this stage. Carefully add 5 cm^3 of ammonia free distilled water to each flask, remove the flasks from the digestion rack and stopper tightly.

Recovery by Steam Distillation

To the 1 litre steam generator (**Figure 2.4**) add some pellets of sodium hydroxide and boiling chips. Three-quarters fill the flask with distilled water. Turn stopcock T1 to connect A to C. Boil the contents of the generator for 5 to 10 minutes on an electric hotplate, to sweep dissolved ammonia impurity into the waste flask. Then turn stopcock T1 to connect B to C thereby passing steam through the steam stripper for 5 minutes to clean the stripper (stopcock at D and clip at E closed). Again divert the steam supply to the waste flask.

Quickly transfer the contents of a digestion flask with two or three 5 cm^3 ammonia free water washings together with 0.2 ml 25% copper(II)sulfate solution via the

funnel on the steam stripper to the interior of the sample vessel. Close stopcock D immediately. Open outlet E to waste and turn stopcock T1 to reconnect B and C. Pass steam until it exits at E. Meanwhile pour an excess of 40% sodium hydroxide into the (closed) funnel at D. Use 20 cm^3 or 40 cm^3, depending on whether 5 cm^3 or 10 cm^3 of concentrated sulfuric acid was used for acid digestion. If, however, the digestion catalyst used contains mercury or mercury(II)oxide use the same volumes of sodium hydroxide-sodium thiosulfate instead. Use the same amount of alkali in both sample and blank determinations.

Connect to the vertical condenser of the steam stripper a clean 250 cm^3 flask. Connect a guard tube containing freshly activated silica gel in position above this receiving flask.

When steam is emitting from the steam stripper outlet E close the clip thereby allowing steam to pass through the sample solution. Steam distill until about 50 cm^3 distillate has been collected. Disconnect the flask from the apparatus and replace immediately by a clean 250 cm^3 ammonia receiving flask containing 50 cm^3 ammonia-free water and 6 drops of 0.25 M nitrogen free sulfuric acid (silica gel guard tube still in position). Open stopcock D and slowly admit the alkaline reagent in several portions. Leave 1 cm^3 of alkali in the funnel to act as a seal.

It is necessary to ensure that an excess of alkali is added at this stage. Alkalinity is indicated by the formation of first, a soluble deep blue cupramine salt then a precipitate of brown copper oxide (formed by reaction between free ammonia or sodium hydroxide, respectively, with the previously added copper(II)sulfate).

Steam distill for about 20 minutes, i.e., until about 100 cm^3 to 120 cm^3 of liquid is in the receiver. Remove the B24 neck ammonia receiving flask from the apparatus and tightly connect an 20 cm vertical guard tube (24 cone) containing activated silica gel to prevent contamination of the distillate by any ammonia impurity in the laboratory atmosphere.

Remove the silica gel guard tube from the ammonia receiver flask and stand on an electric hotplate. Connect the flask immediately to a horizontally inclined Liebig condenser fitted with a delivery tube immersed in dilute sulfuric acid solution.

Boil until the contents of the distillation flask reduce to 20 to 25 cm^3. Immediately disconnect the flask and connect a B24 silica gel guard tube and leave to cool. If up to 150 μg of nitrogen is present in the concentrated sample solution, transfer this solution and the blank solution (with 2 × 5 cm^3 ammonia free water washings) to two clean 50 cm^3 graduated cylinders and make up to 40 cm^3 with ammonia free water. If more than 100 to 150 μg of nitrogen is present in the sample solution, transfer this solution and the blank solution to two 50 cm^3 volumetric flasks and make up to the mark with ammonia free water. Then transfer to a 50 cm^3 graduated cylinder,

a volume of the sample solution containing 100 to 150 µg nitrogen. Transfer the same volume of blank solution from the 50 cm^3 volumetric flask to a further 50 cm^3 graduated cylinder. Make the volume of the sample and blank solutions in the graduated cylinders up to 40 cm^3 with ammonia-free water.

Spectrophotometric Evaluation

Pipette into the 50 cm^3 graduated cylinders containing the blank and the sample solutions, 5 cm^3 of 8% phenol solution and mix. Then pipette 5 cm^3 of sodium hypochlorite solution into each cylinder and again mix. Immerse the two cylinders up to the neck (stoppers loosened) into a 2 dm^3, beaker of water which has been brought previously to the boil. Remove the cylinders from the water bath after exactly 7 minutes and cool to 20 ± 1 °C by standing in a beaker of water.

Determine the optical density of the indophenol blue colour produced between 15 and 30 minutes after addition of the phenol and sodium hypochlorite reagents.

Spectrophotometer conditions:

Instrument: Visible Spectrophotometer
Wavelength: 625 nm
Cells: 4 cm glass

Blank solution: Use the reagent blank referred to in the text, i.e., a test solution prepared identically to the sample test solution omitting only the addition of sample at the Kjeldahl digestion stage in the determination. To determine the magnitude of the blank optical density (as a check the reproducibility obtained in duplicate determinations), measure the optical density of the blank solution at 625 nm relative to distilled water in the comparison cell.

Preparation of Calibration Graph

Accurately pipette 2, 5, 10, 15 and 20 cm^3 of a freshly prepared standard nitrogen solution (containing 10 µg nitrogen per cm^3) into five clean 50 cm^3 graduated cylinders, i.e., between 20 to 200 µg nitrogen. Include a further 50 cm^3 graduated (blank) cylinder containing no standard nitrogen solution addition.

Dilute the contents of the cylinders up to 40 cm^3 with ammonia-free distilled water. Continue as described under spectrophotometric evaluation.

Measure the optical densities of the standard nitrogen solutions at 625 nm in 4 cm glass employing the reagent blank solution (i.e., containing no addition of standard

nitrogen solution), in the comparison cell. Construct a weekly calibration graph relating these optical densities to the number of micrograms of nitrogen present in the nitrogen calibration solutions.

Calculations

Refer the optical density (reagent blank solution in comparison cell), given by the sample solution to the nitrogen calibration graph and read off the number of micrograms of nitrogen present. Calculate the nitrogen content of the sample from the following equations:

Nitrogen, % = N × 10^6 × 100/W

Nitrogen, ppm = N/W

where:

N = number of micrograms of nitrogen present in 50 cm^3 final test solutions used for colour development

W = weight of sample (g) which contains N microgram nitrogen

Note, any dilution of the test solution prior to the development of colour with phenol and sodium hypochlorite must be allowed for when calculating W.

Discussion of Results

The overall reproducibility of this nitrogen determination method is ± 5% in the nitrogen content range 0.002 to 75%. The sodium sulfate-selenium-copper sulfate mixture is particularly suitable for the quantitative digestion of all compounds in which the nitrogen is present in an easily decomposed form (e.g., as amine, amino compounds, amino acids, amide or nitrile and their simple derivatives). Forms of nitrogen for which accurate results are not usually obtained include those with -N-N (e.g., diazo) and N-O (e.g., nitro) linkages and some resistant heterocyclic structures.

Method 2.13 Determination of 1 to 90% Organic Nitrogen in Polymers. Kjeldahl Digestion – Boric Acid Titration Method

Summary

This Kjeldahl digestion – titration procedure can determine between 1 and 90% of organic nitrogen in polymers.

Apparatus

a) Kjeldahl digestion apparatus consisting of:

Kjeldahl digestion flasks – 100 ml Pyrex glass.

Electric heating 'Bun ray' electric bunsens suitable (minimum loading 375 watts) or Kjeldahl digestion flask heaters with flask supports (100 ml flask size).

b) Ammonia recovery apparatus consisting of (see **Figure 2.5**):

Condenser (B24 cone and socket), Leibig 30 cm. Round bottomed steam generation flask, 1000 ml central B24 and 2 × B19 side. Three way stopcock, vertical arm connected to B24 cone. Separatory funnel 250 ml with B19 cone.

Recovery apparatus proper:

Consisting of steam stripping vessel (interior vessel large enough to hold 150 ml solution). Separatory funnel 50 ml with B14 cone and short delivery stem. Steam trap leading to vertical condenser and guard tube containing activated silica gel which is connected by a suitable adaptor (Note 1). Activated silica gel. Self indicating, mesh 6-20, available from British Drug Houses Ltd., Poole. To regenerate gel, heat for 6 hours at 150 °C in a vacuum oven.
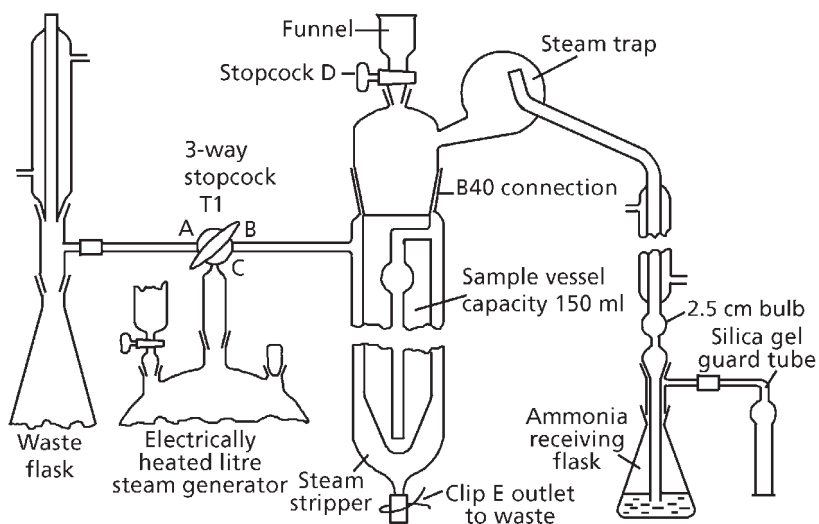
Figure 2.5 Ammonium recovery steam stripper assembly.
(*Source: Author's own files*)

c) Apparatus for determination of ammonia in distillate, miscellaneous glassware:

Burette, 50 ml pipettes.

Reagents

Sulfuric acid, preferably nitrogen-free quality.

Glucose, micro analytical reagent (MAR) grade.

Kjeldahl digestion catalysts:

Tablets each consisting of 1 g sodium sulfate and the equivalent of 0.05 g selenium (as selenium dioxide).

Tablets each consisting of 1 g sodium sulfate and equivalent of 0.05 g of mercury (as mercuric oxide).

Cupric sulfate, 25% w, dissolve 25 g $CuSO_4.4H_2O$ AnalaR in water and make up to 100 ml (0.2 ml of this solution contains 0.05 g $CuSO_4.5H_2O$.

Mercuric oxide, pure grade.

Potassium sulfate, AnalaR.

Sodium hydroxide (use when mercury-free catalysts are used for Kjeldahl digestion). Pour 1600 ml distilled water into a 4 litre beaker and add 1500 g of sodium hydroxide AnalaR. When dissolved allow to cool and transfer to a Winchester.

Sodium hydroxide-sodium thiosulfate (use when mercury containing catalysts are used for Kjeldahl digestion). Pour 1400 ml distilled water into a 4 litre beaker and add 1500 g sodium hydroxide AnalaR. When dissolved, allow to cool. In another beaker dissolve 150 g sodium thiosulfate.$5H_2O$ AnalaR in 200 ml distilled water. Mix the two solutions and transfer to a Winchester. Remove nitrogenous impurities from either reagent as follows: add 5 g zinc powder and pass a slow stream of nitrogen for 48 hours to sweep out ammonia. Filter the cold solution through a 40 cm Whatman No. 1 filter paper to remove sodium carbonate. Store the reagent in polyethylene bottles. Carry out these operations in a fume cupboard to avoid contamination of the solutions by any ammonia impurity present in the laboratory atmosphere.

Boric acid, 4% w, dissolve 40 g boric acid (H_3BO_3) AnalaR in 1000 ml distilled water contained in a 2 litre round bottomed flask. Boil for 20 minutes to expel

carbon dioxide. Connect a carbon dioxide absorbing guard tube and cool. Transfer to a 1 litre volumetric flask. Make up to 1 litre with cold boiled out distilled water and mix.

Methyl red, bromocresol green indicator: mix 5 volumes of 0.2% bromocresol green with 1 volume of 0.2% methyl red, both in 95% ethanol.

Hydrochloric acid, 0.05 N.

Hydrochloric acid, 0.02 N prepared daily by dilution of the stock 0.05 N hydrochloric acid.

Method

The procedure involves Kjeldahl digestion followed by collection of generated ammonia in boric acid.

A suitable weight of sample is digested with concentrated sulfuric acid, sodium or potassium sulfate and digestion catalysts using an electrical heater (Note 2). A reagent blank determination is alos carried out. The digested sample, after dilution, is transferred to a steam distillation apparatus. The addition of sodium hydroxide liberates ammonia equivalent to the nitrogen content of the sample. Liberated ammonia is collected in boric acid solution and determined by titration with standard hydrochloric acid.

Experimental Procedure

The weights of sample required for the determination of nitrogen in compounds containing between 1% and 90% of nitrogen are shown in **Table 2.6**. Also shown is the normality of the hydrochloric acid required for the titration of ammonia at the end of the determination.

Methods of sample transfer into Kjeldahl digestion:

• Solids: These may be transferred directly to the Kjeldahl flask or wrapped in a cigarette paper (use potassium nitrate free brand of paper), which is dropped into the flask.

• Aqueous solutions of polymers: pipette a suitable aliquot of test solution into the flask and add 6 drops of 0.5 N sulfuric acid (include in blank). Heat at 50 °C under vacuum to reduce the volume to approximately 1 ml. The sample is now ready for analysis.

113

Table 2.6 Recommended sample size and normality of hydrochloric acid used in final ammonia titration		
Nitrogen content of sample (%)	**Weight of sample for digestion (g)**	**Strength of hydrochloric acid to be used in titration of ammonia (normality, N)**
1-3	0.2	0.02
5	0.2-0.1	0.02
10	0.1	0.02
20	0.1 -0.05	0.02
40	0.03 or 0.05	0.02 or 0.05
60	0.05	0.05
80-90	0.03	0.05
All weighing done with a 4-place balance. *Source: Author's own files*		

Into the Kjeldahl flask containing the sample, introduce a small piece of clean porous pot. Depending on the weight of sample to be digested, add the recommended quantities of a suitable catalyst mixture and of concentrated sulfuric acid as indicated in **Table 2.7,** also 0.05 g glucose (Note 3).

To the flask used for the reagent blank determination introduce the same amount of catalyst mixture, sulfuric acid and glucose. Suitable catalysts and length of sulfuric acid digestion time for the digestion of various types of nitrogen compounds and polymers are shown in **Table 2.7**.

Mount the digestion flask containing sample, sulfuric acid, catalysts and glucose on an electrical heater (Note 1) and insert a small funnel in the neck of the flasks. Digest gently at first and then increase the digestion temperature steadily, at five or ten minute intervals over the recommended digestion period (**Table 2.7**). After the first 45 minutes digestion, the heating rate should be such that the acid is condensing about half way up the neck of the digestion flask (maximum digestion temperature 380 °C). Ensure that the carbon char becomes completely oxidised during digestion. Continue the digestion for at least 20 minutes, at maximum temperature after the solution has clarified. When digestion is complete, switch off the heaters. Leave to cool at room temperature. At least half of the original sulfuric acid addition should remain in the digestion flasks at this stage (Note 5). Add distilled water to the contents of each digestion flask.

Table 2.7 Catalyst and sulfuric acid additions		
Weight of sample digested (g)	**Catalyst and alkali sulfate mixture**	**Volume of concentrated sulfuuric acid used for digestion (ml)**
0.1-0.3*	A** 0.4 g Sodium sulfate 0.02 g Selenium (as dioxide) 0.02 g $CuSO_4.5H_2O$, or	2
	B 0.4 g Sodium sulfate 0.02 g Selenium (as dioxide), or 0.02 g Mercury (as oxide), or	2
	C 1.3 g Potassium sulfate 0.04 g Mercuric oxide	2
0.03 - 0.08*	A** 1 g Sodium sulfate 0.05 g Selenium (as dioxide) 0.05 g $CuSO_4.5H_2O$, or	5
	B 1 g Sodium sulfate 0.05 g Selenium (as dioxide) 0.05 g Mercury (as oxide), or	5
	C 3 g Potassium sulfate 0.1 g Mercuric oxide	5
0.08-0.2	A** 2 g Sodium sulfate 0.1 g Selenium (as dioxide) 0.1 g $CuSO_4.5H_2O$, or	10
	B 2 g Sodium sulfate 0.01 g Selenium (as dioxide) 0.01 g Mercury (as oxide)	10
* *Use a micro or semi-micro balance when weighing out 0.01-0.03 g samples*		
** *Recommended as a good general digestion catalyst. The sodium sulfate – selenium catalyst is available in tablet*		

Ammonia Recovery by Steam Distillation

Set up the distillation apparatus shown in **Figure 2.5**. To the 1 litre steam generation flask add several pellets of sodium hydroxide and some boiling chips, then three quarters fill with distilled water. Turn stopcock T1 to connect A to C. Boil the contents of the generator for 5 minutes (note 1) to sweep out dissolved ammonia into the waste flask. Then turn stopcock T1 to connect B to C thereby passing steam through the steam stripper (stopcock D and clip at E closed). Again divert the steam supply to the waste flask.

Transfer the contents of a digestion flask with two or three 5 ml distilled water washings together with 0.2 ml 25% cupric sulfate solution via the funnel on the steam stripper to the interior sample vessel and close the stopcock D. Open the outlet E to waste and turn stopcock T1 to reconnect B and C. Pass steam until it exits at E. Meanwhile pour an excess of 40% sodium hydroxide into the (closed) funnel at D. Use 10 ml, 20 ml or 40 ml sodium hydroxide (depending on whether 2 ml, 5 ml or 10 ml of concentrated sulfuric acid was used for the acid digestion.) If the digestion catalyst used contains mercury or mercuric oxide use instead, the same volumes of sodium hydroxide-sodium thiosulfate solution (Note 6). Use the same amount of alkali in both sample and blank determinations.

Connect a 250 ml flask to the vertical condenser of the steam stripper. Connect a guard tube containing freshly activated silica gel in position above this receiving flask (Note 2). When steam is emitting from the steam stripper outlet E close the clip thereby allowing steam to pass through the sample solution. Steam distill until about 50 ml distillate has been collected (Note 7) and disconnect the flask from the apparatus. Into a clean 250 ml ammonia receiving flask, pipette 25 ml 4% boric acid solution and add 4 drops of bromocresol green – methyl red mixed indicator. If this solution is blue-green in colour (due to the presence of a trace of dissolved ammonia), then add single drops of 0.01 N hydrochloric acid from a burette until the solution becomes neutral grey in colour. Connect this flask to the vertical condenser of the steam stripper (silica gel guard tube still in position).

When steam is emitting from the steam stripper outlet E, close the clip thereby allowing steam to pass through the sample solution. Open stopcock D and slowly admit the alkaline reagent in several portions. Leave 1 ml of alkali in the funnel to act as a seal. It is necessary to ensure that an excess of alkali is added at this stage. Alkalinity is indicated by the formation of, first, a soluble deep blue cupramine salt then a precipitate of brown copper oxide.

Steam distil until the volume of liquid in the receiver is approximately 100 ml, i.e., for about 20 minutes. Remove the receiver flask from the apparatus. Clean the steam stripper ready for the next analysis (Note 8).

Titrate the contents of the receiver flask with either 0.05 N or 0.02 N hydrochloric acid, depending on the amount of sample digested and its nitrogen content.

The colour change at the end-point is from green to neutral grey. The addition of a further drop of hydrochloric acid beyond this end-point should produce a pale pink colour.

Calculation

The nitrogen content of the sample is given by:

$$N\ (\%) = (T_a\text{-}T_b) \times f \times 14/W \times 10$$

where:

T_a = titration (ml) of hydrochloric acid, sample
T_b = titration (ml) of hydrochloric acid, blank
f = normality of hydrochloric acid
W = weight (g) of sample taken for analysis

Note 1. Pick up of ammonia impurity from laboratory atmosphere. The apparatus used for steam distillation from alkali to recover ammonia from the acid digest is fitted with an activated silica gel guard tube. This prevents contamination of the distillate with any ammonia impurity that is present in the laboratory atmosphere.

Note 2. Electrical heating during the Kjeldahl digestion and ammonia recovery is preferable to gas heating. The chance of contamination of the sample by nitrogenous impurities in coal gas is thereby avoided.

Note 3. Addition of glucose in Kjeldahl digestion. Normally no organic matter would be present in the blank digestion flask. If the nitrogen impurity in the reagents is in both oxidised and reduced forms, therefore, it is necessary to add some organic material to the contents of the blank flask in order to ensure that nitrogen impurity is completely reduced. The addition of 0.05 g pure glucose to the blank (and sample) is sufficient for this purpose.

Note 4. Reduction of nitrogen compounds prior to Kjeldahl digestion. Nitro, nitroso and azo compounds, also hydrazones, oximes and some heterocyclic compounds are not quantitatively digested by the catalysts A, B or C shown in **Table 2.8**. If compounds of these types are being analysed either add 0.5 g pure sucrose (or glucose) to the mixture of catalyst A or B, sulfuric acid and a suitable weight of sample (or carry out a preliminary reduction of the sample with hydriodic acid and red phosphorus as described next.)

Transfer a suitable weight of sample (catalysts and sulfuric acid absent) and 5 ml of pure hydriodic acid (AnalaR about 55%) to a clean Kjeldahl flask with B19 quickfit socket. Warm gently and introduce 50 mg pure red phosphorus and some porous pot. Reflux for 45 minutes and then dilute with 5 ml water. Add 5 ml concentrated sulfuric acid and mix. Boil the mixture rapidly (without condenser) to remove hydriodic acid and iodine vapour. If iodine is not completely removed add a further 5 ml of water and boil again until the mixture fumes. Carry out an identical reagent blank omitting only the sample additions. Add a suitable quantity of Kjeldahl digestion catalysts A or B (**Table 2.8**), concentrated sulfuric acid and 0.05 g glucose (note 3) to the reduced sample and blank solutions.

Suitable quantities of catalyst and acid for the digestion of various sample weights are shown in **Table 2.8**. Continue by the normal Kjeldahl digestion as described in section (b) under procedure.

Table 2.8 Selection of suitable catalysts and digestion times		
Type of compound digested	**Catalyst and alkali metal sulfate mixture recommended* (see Table 2.6)**	**Total digestion time with sulfuric acid (h)**
Amines, amino compounds amino acids, amides and their simple derivatives	A, B or C	1.5-2
Nitriles and their simple derivatives also: styrene-acrylonitrile copolymers and polyacrylonitrile	A	3
Refractory nitrogen compounds	C	4
Nitro, nitroso and azo compounds hydrozones, oximes and some heterocyclic nitrogen compounds	See Note 4	4
Many azo compounds, volatile nitro compounds, diazo ketones and certain semicarbazones	No successful Kjeldahl digestion procedure known	
Source: Author's own files		

Various other methods have been proposed for the reduction of nitro groups prior to digestion. These include the use of thiosalicylic acid, salicylic acid-sodium thiosulfate, sodium hydrosulfite-ethanolic hydrochloric acid and zinc dust-pyrogallic acid.

To obtain satisfactory results in the digestion of pyridine it is necessary to leave the sample in contact with catalysts and sulfuric acid for 8 hours at room temperature. Then digest at a low temperature for 1 hour and at a higher temperature for 4 hours. Alternatively add a crystal of iodine to the sample, sulfuric acid and catalysts and digest in the normal manner.

No satisfactory general method for the digestion of nitrogen compounds with an N-N linkage is known.

Note 5. Loss of nitrogen during digestion. Some sulfuric acid is usually lost during digestion. The boiling temperature of the digestion mixture then increases due to the increase in the alkali metal sulfate concentration in the digestion mixture. If the temperature of the mixture becomes too high, due to loss of acid, then a partial loss of nitrogen also occurs. No loss of nitrogen occurs, however, provided the volume of sulfuric acid left at the end of the digestion is at least half of the amount originally added.

Note 6. Modification of ammonia recovery stage when mercury containing catalysts are used for digestion. Low ammonia recoveries result during steam distillation from sodium hydroxide when mercury containing catalysts are used in the Kjeldahl digestion. This is due to the partial formation of a mercuric-amine which is not completely decomposed by sodium hydroxide. The addition of a mixture of sodium hydroxide and sodium thiosulfate completely degrades this complex and quantitative ammonia recoveries result.

Note 7. Volatile acids in digestion mixture. It has been found that traces of steam volatile acids remain in the acid digestion mixture after digestion of certain organic materials. These are removed by passing steam through the diluted digestion mixture prior to sodium hydroxide addition. This acidic distillate is rejected.

Note 8. Cleaning of steam distillation apparatus. Clean the steam stripper ready for the next determination as follows. With clip E closed, turn stopcock T1 to divert the steam supply to the waste flask (i.e., connect A to C). The sample solution now syphons from the sample vessel into the outer vessel and is disposed of by opening clip E. Now fill the sample vessel with water via the funnel (clip E again closed) and pass steam through this water until it boils. Syphon the water from the sample vessel as before. Repeat this cleaning operation until the interior of the vessel is perfectly clean.

Discussion of Results

The method is capable of determining nitrogen in polymers which contain between 1% and 90% of this element. The accuracy of results obtained is of the order of ± 1.0% of the true nitrogen content.

The Kjeldahl digestion procedure described quantitatively decomposes amines, amino compounds, amino acids, amides, nitriles and their simple derivatives and also many refractory nitrogen compounds. Quantitative decomposition of nitrogen containing polymers, e.g., styrene-acrylonitrile copolymers and polyacrylonitrile, is achieved.

Reduction of nitrogen compounds prior to Kjeldahl digestion – nitro, nitroso and azo compound, also hydrazones, oximes and some heterocyclic compounds are not quantitatively digested by the catalysts A, B or C shown in Table 2.8. If compounds of these types are being analysed, either add 0.5 g pure sucrose (or glucose) to the mixture of catalyst A or B, sulfuric acid and a suitable weight of sample; or carry out a preliminary reduction of the sample with hydriodic acid and red phosphorus.

Normally no organic matter would be present in the blank digestion flask. If the nitrogen impurity in the reagents is in both oxidised and reduced forms, therefore, it is necessary to add some organic material to the contents of the blank flask in order to ensure that nitrogen impurity is completely reduced. The addition of 0.05 g pure glucose to the blank (and sample) is sufficient for this purpose.

Method 2.14 Qualitative Detection of Elements in Polymers. Oxygen Flask Combustion

Summary

This qualitative oxygen flask combustion method [29] enables nitrogen, fluorine, chlorine, bromine, iodine, sulfur and phosphorus to be identified in polymers in amounts down to 0.01%.

Apparatus

Combustion unit – the electrically fired combustion unit was used in this work, although there is no reason why other forms of oxygen flask should not be used, with appropriate calibration.

Filter paper – Whatman No. 541 filter paper. When not in use, store filter paper in a sealed container out of contact with the laboratory atmosphere.

Cotton wool – BPC super quality.

Reagents

Sodium hydroxide, N.

Nitrogen.

Resorcinol – AnalaR

Acetic acid, glacial.

Ammonium ferrous sulfate - AnalaR.

Fluorine.

Reagents. Buffered alizarin and complexan solution: weigh 40 mg of 3-amino-ethylalizarin-*N,N′*-diacetic acid (Hopkins and Williams Ltd.) into a beaker and add 2 drops of N sodium hydroxide and approximately 20 ml of distilled water. Warm the solution to dissolve the reagent, cool and dilute to 208 ml. Weigh into another beaker 4.4 g of sodium acetate ($CH_3COONa3H_2O$) and dissolve in water. Add 4.2 ml of glacial acetic acid and dilute to 42 ml. Pour this sodium acetate solution into the alizarin complexan solution and mix to give the final buffered alizarin complexan solution.

Cerous nitrate, 0.0005 M: dissolve 54.3 mg of cerous nitrate ($Ce(NO_3)_36H_2O$) in water and dilute to 250 ml.

Chlorine.

Reagents. Ammonium ferric sulfate solution – dissolve 12 g of AnalaR ammonium ferric sulfate in water and add 40 ml of AnalaR nitric acid. Dilute to 100 ml and filter.

Mercuric thiocyanate solution – dissolve 0.4 g of recrystallised mercuric thiocyanate in 100 ml of absolute ethanol.

Bromine.

Reagents. Fluorescein solution – dissolve 0.1 g of fluorescein in 25 ml of 0.1 N sodium hydroxide and dilute to 100 ml with water.

Sodium acetate buffer solution – mix 100 ml of N sodium acetate with 15 ml of N acetic acid.

Chloramine-T solution – dissolve 12 g of chloramine-T in 100 ml of distilled water.

Sodium thiosulfate solution – prepare a 0.5% *w/v* solution of sodium thiosulfate in 5% *w/v* sodium hydroxide solution.

Hydrochloric acid, N.

Iodine.

Starch solution – dissolve 0.2 g of soluble starch in 100 ml of distilled water.

Sulfuric acid, dilute – prepare an approximately 10% *w/v* solution of concentrated sulfuric acid in distilled water.

Quantitative Determination of Sulfur - Barium Chloride Method

Reagents

Hydrochloric acid, N

Precipitating reagent solution A – dissolve 0.2 g of peptone in 50 ml of 1% barium chloride ($BaCl_2 2H_2O$) solution. Buffer to a pH of 5.0 with 0.02 N hydrochloric acid, add 20 g of sodium chloride (AnalaR) and dilute to 100 ml. Heat on a water bath for 10 minutes, and add a few drops of chloroform. Filter if necessary.

Precipitating reagent solution B – dissolve 0.04 g of gum ghatti in 200 ml of distilled water by warming slightly. When solution is complete, add 2.0 g of barium chloride ($BaCl_2 2H_2O$). Filter if necessary.

Store solutions A and B separately and prepare the final reagent just before use by diluting 10 ml of solution A to 100 ml with solution B.

Hydrogen peroxide, 100 volume – AnalaR.

Qualitative Determination of Sulfur-4-Amino -4′-Chlorodiphenyl Hydrochloride Method

Reagents

Solution A – 4-amino-4′-chlorodiphenyl hydrochloride - peptone solution. Dissolve 0.025 g of peptone and 0.125 g of 4-amino-4′-chlorodiphenyl hydrochloride as completely as possible by warming with 50 ml of 0.05 N hydrochloric acid. Cool, and filter through a double Whatman No. 40 filter paper.

Solution B – 4-amino-4′-chlorodiphenyl hydrochloride - gum ghatti solution. Dissolve

0.20 g of gum ghatti (finely ground) and 1.00 g of 4-amino-4′-chlorodiphenyl hydrochloride as completely as possible by warming to about 70 °C with 400 ml of 0.05 N hydrochloric acid. Cool and filter through a double Whatman No. 40 filter paper.

Final precipitation reagent: dilute 10 ml of solution A to 100 ml with solution B. This solution should be freshly prepared.

Hydrochloric acid, N.

Qualitative Determination of Hydrolysable Phosphorus

Reagents

Ammonium molybdate solution – dissolve 10 g of AnalaR ammonium molybdate ($NH_4MO_7O_{24}4H_2O$) in about 70 ml of water and dilute to 100 ml. Add this solution with stirring to a cooled mixture of 150 ml of sulfuric acid and 150 ml of water.

Ascorbic acid – laboratory reagent grade.

Method

Approximately 20 mg of polymer is combusted in an oxygen filled flask over dilute sodium hydroxide solution (See **Figures 2.2 and 2.3** and Methods 2.1–2.4). Specific colorimetric tests for nitrogen, sulfur and phosphorus and the four halogens are applied to reveal the presence or absence of these elements.

Experimental Procedure

Combustion Procedure

Weigh out approximately 20 mg of sample and transfer it to the centre of a small piece of the Whatman No. 541 filter paper weighing approximately 0.1 g. Fold the filter paper so that the sample is completely enclosed and before making the final fold, insert a small wick of cotton wool weighing about 6 mg.

Carry out the combustion using 5 ml of N sodium hydroxide in the bottom of the flask as absorption solution. Set the flask aside for 15 minutes to allow the gases formed in the combustion to be absorbed and then wash the contents of the flask quantitatively into a 25 ml measuring cylinder with distilled water. Dilute the solution to 25 ml and mix well. This constitutes the test solution, aliquots of which are taken for the

detection of the individual elements by the colorimetric methods detailed next. For comparison purposes in the tests, prepare a blank test solution by carrying out the combustion procedure on the filter paper and cotton wool only.

Determination of Nitrogen

Weigh 0.1 g of resorcinol into a clean dry 50 ml beaker and dissolve in 0.5 ml of glacial acetic acid. Add 5 ml of the test solution and, after mixing, add 0.1 g of ammonium ferrous sulfate. Carry out the same test on the blank test solution. The development of a green colour in the sample test solution, compared with a pale yellow in the blank, indicates the presence of nitrogen in the sample.

If a semi-quantitative estimation of the nitrogen content of the sample is required, set both sample and blank solutions aside for 20 minutes. Add 10 ml of distilled water to each, mix and measure the optical density of the sample solution against the blank at 690 nm in a 4 cm cell. The blank in this test is low, giving an optical density of 0.07 measured against water at 690 nm in the 4 cm cells.

Determination of Fluorine

Transfer 20 ml of distilled water and 2.4 ml of buffered alizarin complexan solution to a 50 ml beaker. Add 1 ml of test solution and mix swirling the solution. Finally, add 2 ml of cerous nitrate solution and mix again. Treat the blank solution in a similar manner. When fluorine is present in the sample a mauve colour will be developed in the test solution (compared with the pink coloured blank solution). If a semi-quantitative estimation of fluorine is required, set the solutions aside for 10 minutes and measure the optical density of the test solution against the blank solution at 600 nm in 1 cm cells. Sulfur, chlorine, phosphorus and nitrogen do not interfere in this procedure.

Determination of Chlorine

Transfer 5 ml of the test solution to a 50 ml beaker and add 1 ml of ammonium ferric sulfate solution. Mix the solution and add 1.5 ml of mercuric thiocyanate solution. Mix and dilute to 10 ml. Treat the blank solution in a similar manner. When chlorine is present in the sample an orange colour will be developed in the test solution compared with yellow coloured blank solution. If a semi-quantitative estimation of chlorine is required, set the solutions aside for 10 minutes and measure the optical density of the test solution against the blank solution at 460 nm in 2 cm cells.

Determination of Bromine

Transfer 5 ml of the test solution to a 50 ml beaker. Add 1 ml of N hydrochloric acid and then 0.5 ml of sodium acetate buffer solution and 1 drop of fluorescein solution. Mix thoroughly and then add 1 drop of chloramine T solution. Mix by swirling and set aside for 30 seconds, then stop the reaction by adding 2 drops of alkaline thiosulfate reducing agent. Treat the blank solution in a similar manner. When bromine is present in the sample, a rose-pink colour will be developed in the test solution compared with the yellow-green blank solution. (Note: Iodine also gives a positive result with this test.)

Determination of Iodine

Transfer 5 ml of test solution to a 50 ml beaker and add a few drops of starch solution. Mix the solution and then acidify with dilute sulfuric acid. Treat the blank in a similar manner. When iodine is present in the sample, the characteristic blue colour of starch iodide will be developed in the test solution compared with the colourless blank solution.

Determination of Sulfur (Barium Chloride Method)

Transfer 5 ml of the test solution to a 15 cm × 2.5 cm test tube and add 2 drops of 100 volume hydrogen peroxide, then add 1.2 ml of N hydrochloric acid. Mix well and add 2.0 ml of precipitating reagent A or B with continued shaking. A distinct turbidity will be produced in the mixed solution if hydrogen peroxide decomposable sulfur is present in the sample; the blank test under the same conditions will be perfectly clear. If a semi-quantitative estimation of the sulfur content is required, add 5 ml of distilled water to both blank and test solutions, mix, and set aside for 30 minutes. Mix the solutions and measure the optical density of the test solution in a 4 cm cell at 700 nm with the blank solution in the comparison cell.

Determination of Sulfur (4 Amino-4′-Chlorodiphenyl Hydrochloride Method)

Transfer 5 ml of the test solution to a 15 cm × 2.5 cm test tube and add 1-2 ml of N hydrochloric acid. Mix well and add 10.0 ml of the prepared final precipitation reagent. A distinct turbidity will be produced in the mixed solution if hydrolysable sulfur is present in the sample. A blank test under the same conditions will be perfectly clear.

Determination of Phosphorus

Transfer 2 ml of the test solution to a 100 ml beaker. Add 40 ml of distilled water and 4 ml of ammonium molybdate solution. Mix thoroughly, then add 0.1 g of ascorbic

acid and boil the solution for 1 minute. Cool in running water for 10 minutes and dilute to 50 ml with distilled water. Treat the blank solution in a similar manner. When hydrolysable phosphorus is present in the sample, a blue colour will be developed in the test solution as compared with a pale yellow in the blank. If a semi-quantitative estimation of the phosphorus is required, measure the optical density of the test solution against the blank solution at 820 nm in 2 cm cells.

Discussion of Results

Nitrogen, fluorine, chlorine, bromine and iodine, sulfur and phosphorus are quantitatively detected in polymers in the solution resulting from a single oxygen combustion. Semi quantitative data can be obtained on the same solutions for nitrogen, fluorine, chlorine, sulfur and phosphorus.

References

1. W.S. Cook, C.O. Jones and A.G. Altenau, *Canadian Spectroscopy*, 1968, **13**, 64.

2. H.W. Houk and L. Silverman, *Analytical Chemistry*, 1959, **31**, 6, 1069.

3. B.J. Mitchell and H.J. O'Hear, *Analytical Chemistry*, 1962, **34**, 12, 1620.

4. J.S. Bergmann, C.H. Ekhart, L. Grantelli and J.L. Janik in *Proceedings of the 153rd ACS Meeting*, Miami Beach, FL, USA, 1967.

5. K. Tanaka and T. Morikawat, *Kagaku*, 1974, **48**, 387.

6. J.Z. Falcon, J.L. Love, L.J. Gaeta and A.G. Altenau, *Analytical Chemistry*, 1975, **47**, 1, 171.

7. C.A. Johnson and M.A. Leonard, *Analyst*, 1961, **86**, 1019, 101.

8. W.D. Mitterberger and R. Gross, *Kunststoff-tecknik*, 1973, **12**, 7, 176.

9. M.L. Bakroni, N.K. Chakavarty and S. Chopra, *Indian Journal of Technology*, 1975, **13**, 576.

10. S.L. Manatt, D. Horowitz, R. Horowitz and R.P. Pinell, *Analytical Chemistry*, 1980, **52**, 9, 1529.

11. E.A. Williams, E.M.S. Frarne, P.E. Donahue, N.A. Marotta and R.P. Kambour, *Applied Spectroscopy*, 1990, **44**, 7, 1107.

12. Z. Qi and D.G. Pickup, *Analytical Chemistry*, 1993, **65**, 6, 696.

13. A.F. Colson, *Analyst*, 1963, **88**, 1042, 26.

14. A.F. Colson, *Analyst*, 1963, **88**, 1051, 791.

15. H. Narasaki, V. Hijaji and A. Unno, *Bunseki Kagaku*, 1973, **22**, 541.

16. L.S. Kalinina, N.I. Nikitina, M.A. Matorina and I.V. Sedova, *Plasticheskie Massy*, 1976, **5**, 66.

17. T. Salvage and J.P. Dixon, *Analyst*, 1965, **90**, 1066, 24.

18. H.A. Hernandez, *International Laboratory*, 1981, 84.

19. A. Wirsen, *Makromolecular Chemistry*, 1988, **189**, 4, 833.

20. F. Mocker, *Kautschuk und Gummi*, 1964, **11**, 1161.

21. T. Yoshizaki, *Analytical Chemistry*, 1963, **35**, 13, 2177.

22. *The Elemental Analysis of Various Classes of Chemical Compounds Used with Perkin Elmer PE2400 CHN Elemental Analyser*, Perkin Elmer Elemental Newsletter EAN-5, Perkin Elmer, Norwalk, CT, USA.

23. *Principles of Operation – the Perkin Elmer PE2400 CHN Elemental Analyser*, Perkin Elmer Elemental Newsletter EAN-2, Perkin Elmer, Norwalk, CT, USA.

24. *Principles of Operation – Oxygen Analysis Accessory for the PE2400 CHN Elemental Analyser*, Perkin Elmer Elemental Newsletter EAN-4, Perkin Elmer, Norwalk, CT, USA.

25. *Calculation of Weight Percentages for Organic Elemental Analysis*, Perkin Elmer Elemental Newsletter EAN-6, Perkin Elmer, Norwalk, CT, USA.

26. *Analysis of a Copolymer or Polymer Blend when One Component Contains a Heteroelement*, Perkin Elmer Elemental Analysis Newsletter EAN-13, Perkin Elmer, Norwalk, CT, USA.

27. *Application of the PE2400 CHN Elemental Analyser for the Analysis of Plasticizers,* Perkin Elmer Elemental Analysis Newsletter EAN-23 Perkin Elmer, Norwalk, CT, USA.

28. H. Small, T.S. Stevens and W.C. Bauman, *Analytical Chemistry*, 1975, **47**, 11, 1801.

29.   J. Haslam, J.B. Hamilton and D.C.M. Squirrell, *Analyst*, 1961, **86**, 1021, 239.

30.   T.L. Smith and B.N. Whelihan, *Textile Chemist and Colorist*, 1978, **10**, 35.

31.   G.D.B. Van Houwelingen, *Analyst*, 1981, **106**, 1057.

32.   G.D.B. Van Houwelingen, M.W.M.G. Peters and W.G.B. Huysmans, *Fresenius' Journal of Analytical Chemistry,* 1978, **293**, 5, 396.

33.   J. Wolska, *Plastics Additives and Compounding*, 2003, **5**, 3, 50.

34.   F. Blockhuys, M. Claes, R. Van Grieken and H.J. Geise, *Analytical Chemistry*, 2000, **72**, 14, 3366.

35.   L.M. Sherman, *Plastics Technology*, 1998, **44**, 1, 56.

36.   J.M. Bruna and S.A. Izasa, *Revista de Plásticos Modernos*, 1995, **65**, 550.

37.   N. Niino and A. Yabe, *Journal of Polymer Science – Polymer Chemistry Edition*, 1998, **36**, 14, 2483.

38.   C. Cambon and B. Loiseau, *Double Liasion-Chim Peint*, 1987, **34**, 33, 385.

39.   C.A Johnson and M.A. Leonard, The Analyst, 1961, 86, **1019**, 101.

40.   A.F. Colson, *The Analyst,* 1963, **88**, 791.

3 Determination of Functional Groups in Polymers

A variety of instrumental techniques have been used to determine functional groups in polymers and to elucidate the detail of polymer structure. These include infrared spectroscopy, near-infrared spectroscopy including Raman spectroscopy, Fourier transform infrared spectroscopy (FTIR), nuclear magnetic resonance (NMR) and proton magnetic resonance (PMR) spectroscopy, chemical reaction gas chromatography, pyrolysis gas chromatography (PyGC), pyrolysis gas chromatography–mass spectrometry, pyrolysis–NMR spectroscopy, X-ray fluorescence spectroscopy (XRFS), and also newer techniques such as time-of-flight secondary ion mass spectrometry (ToF-SIMS), X-ray photoelectron spectroscopy (XPS), tandem mass spectrometry (MS-MS), matrix-assisted laser desorption/ionisation mass spectrometry (MALDI-MS), microthermal analysis, atomic force microscopy (AFM), and various X-ray methods including scanning electron microscopy (SEM) and energy dispersive analysis using X-rays (EDAX).

Functional groups that may have to be determined include unsaturation, hydroxy, carbonyl, carboxyl, alkyl, aryl, alkoxy, oxyalkylene, nitrile, ester, amino, nitro, amide, amido, imino, and epoxy groups. Comonomer ratios, isomers, and short-chain branching are all structural features of polymers that may have to be elucidated in order to obtain a complete picture of polymer structure.

3.1 Hydroxy Groups

3.1.1 Acetylation and Phthalation Procedures

Chemical methods for the determination of hydroxyl groups in polymers are based on acetylation [1-12], phthalation [2], perchloric acid catalysed acetylation [2, 4, 5], reaction with beta-nitro phthalic, anhydride [5, 8], pyromellitic anhydride [6] and reaction with phenyl isocyanate [2, 5] or when two adjacent hydroxyl groups are present in the polymers, by reaction with potassium periodate [1].

The reactions on which these methods are based are as follows:

Acetylation:

$$2R\text{—}OH + (CH_3CO)_2O \longrightarrow 2CH_3COOR + H_2O$$
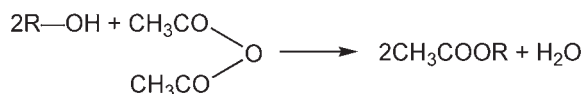
Phthalation:

Reaction with phenyl isocyanate:

Reaction with potassium periodate:

$$R\text{—}CH(OH)\text{—}CH(OH)\text{—}R' + HIO_4 \longrightarrow RCHO + R'CHO + H_2O + HIO_3$$
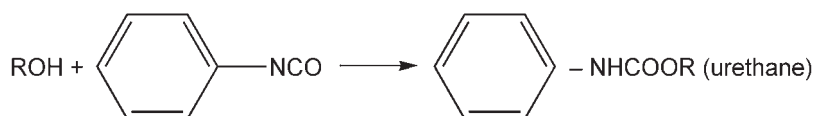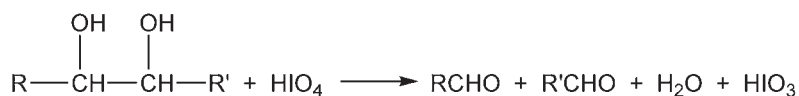
In all procedures the hydroxyl-containing polymer is reacted with an excess of a standard non-aqueous solution of the acetylation or phthalation reagent, sometimes in the presence of a catalyst such a *p*-toluene sulfonic acid. After the formation of the ester is complete, an excess of water is added to convert excess anhydride to the free carboxylic acid. The acid is titrated with aqueous or alcoholic standard potassium hydroxide to the phenolphthalein end-point, to determine unconsumed acid. A blank run is carried out in which the sample is omitted. The hydroxyl content of the polymer can then be calculated from the difference between the sample and blank titratrions.

Table 3.1 compares hydroxyl values obtained by three methods. It is seen that in every case the acid-catalysed acetylation method gives a higher result than that obtained by phthalation, the average difference between the two methods being 2.5% of the determined value. It will be seen from the table that the agreement between the *p*-toluene sulfonic acid method and the phenyl isocyanate method is good.

Table 3.1 Hydroxy values obtained on polypropylene glycol by catalysed acetylation, phthalation and phenyl isocyanate reaction			
Molecular weight	***p*-Toluene sulfonic acid catalysed acetylation method**	**Phthalation method [2]**	**Reaction with phenyl isocyanate**
	Average hydroxyl value (mg KOH/g)	**Average hydroxyl value (mg KOH/g)**	**Average hydroxyl value (mg KOH/g)**
700	353	346	
1260	276	265	
5000	34.9	34.0	34.9
5000	34.3	33.8	35.1
2890	58.3	57.0	
Source: Author's own files			

The Stetzler and Smullin [2] method is applicable to polyoxyethylene, polyoxypropylene and ethylene oxide tipped glycerol/propylene oxide condensates. Compounds of this type in the molecular range 500 to 5000 can be analysed by this procedure.

Houwelingen [13] has described a procedure for the determination of hydroxyl groups in the following types of polyesters:
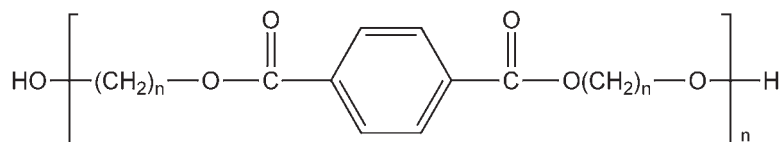
with $n = 100$ and $\times = 2$ (polyethylene terephthalate) or 4-polybutylene terephthalate and ester-interchange elastomers of 4-polybutylene terephthalate and polypropylene glycol.

The method has also been applied to the determination of polyamides.

The hydroxyl groups in polyesters are determined by acetylation with an excess of dichloroacetic anhydride in dichloroacetic acid and measurement of the amount of acetylation by a chlorine determination. Owing to the low concentration of hydroxyl groups, especially in high relative molecular weight materials, the determination of the excess is inaccurate and the determination of the amount of reagent incorporated is much more attractive.

Table 3.2 Hydroxyl end group content of several PETP, PBTP and PBTP-PPG samples
Sample	**Viscosity ratio[a]**	**Hydroxyl end groups/mmol/kg**	**Remarks**
PETP A	1.80	30.9-29.8 30.6-30.4	Total end groups[b] 76.6 mmol/kg
PETP B	1.82	14.4-14.8	Total end groups 79.1 mmol/kg
PBTP A	2.07	70.7-70.6	Total end groups 95.2 mmol/kg
PBTP B	2.08	50.6-49.3	Total end groups 92.6 mmol/kg
PBTP C	1.24	664-653	
PBTP-PPG A	1.25	742-729	M_N (calc)[c] 2700; M_N (measured) 2400[d]
PBTP-PPG B	1.34	329-345	
PBTP-PPG C	1.50	229-212	M_N (calc) 9000; M_N (measured) 10100
PBTP-PPG D	2.38	51-57	M_N (calc) 35000; M_N (measured) 44800

[a] *Measured for a 1% m/m solution in m-cresol at 25 °C (PETP and PBTP), or for a 1% m/v solution in o-chlorophenol at 25 °C (PBTP-PPG)*

[b] *Total end groups in sum of OH + COOH + methyl ester end groups*

[c] *MN measured by gel permeation chromatography in m-cresol as a solvent*

[d] *Calculated from OH + COOH content*

Reprinted with permission from G.D.B. von Houwelingen, Analyst, 1981, 106, 1267, 1057. ©1981, Royal Society of Chemistry [13]

The derivatisation of the polyester is carried out in a 10% *m/m* solution of dichloroacetic anhydride in dichloroacetic acid at 60 °C. A reaction time of 1 hour suffices. After the reaction the solution is poured into water and the precipitated polymer is washed out. To remove the last traces of solvent and acetylation agent, reprecipitation of the derivatised polymer from a hexafluoroisopropanol solution into water is carried out. For polymers with a low hydroxyl content (below 100 mmol/kg), the reprecipitation is carried out from a solution in nitrobenzene into cold light petroleum, in order to obtain more reproducible results.

The content of hydroxyl groups is subsequently determined by measurement of the chlorine content of the purified derivative. This is done either by potentiometric titration with silver ions after combustion or by x-ray fluorescence spectroscopy of a compressed disc of the polymer.

The suitability of this method for a number of samples is demonstrated in **Table 3.2**.

The standard deviation of the method for high relative molecular weight polymers is 0.7 mmol/kg whereas for the low relative molecular weight materials, it is about 10 mmol/kg.

Groom and co-workers [8] employed trichloroacetyl isocyanate and trifluoroacetic anhydride acetylations to determine hydroxy end-groups in polyester polyols. The isocyanate reagent was best suited for samples having molecular weights of less than 4500; this anhydride method was more sensitive and applicable to higher molecular weight polymers than is a ^{19}F-NMR method.

3.1.2 Spectrophotometric Methods

A method the determination of hydroxy groups in polyethylene glycols (PEG) has been described by Fritz and co-workers [9] (see Method 3.1 at the end of the chapter). The method consists of substituting the hydroxyl group with a chromophoric siloxy group, purification of the silylated polymer, and a photometric determination of the chromophor concentration. The silanisation of the primary hydroxyls with dimethylaminosilanes proceeds quantitatively under very mild conditions and elimination of the excess reagent by precipitation is easy. The precision of the method is ± 4.5% (95% confidence level) down to 5×10^{-4} mol/kg. The method has about the same precision as acylation methods but yields a 1000 fold gain in sensitivity.

In a further spectrophotometric method, the polyester is reacted with a dimethyl formamide-monochlorbenzene solution of vanadium 8-hydroxyquinolinate (V8HQ). According to Tanaka and Kojima [10] a coloured complex with the following structure is formed:
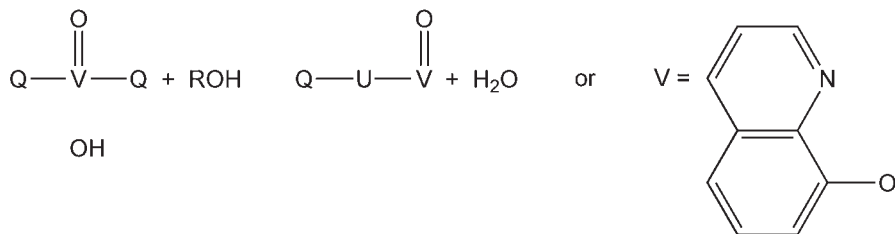
After removal of the excess reagent by extraction, the complex is acidified with dichloroacetic acid and the blue colour formed is measured at 620 nm. Calibration is carried out with an alcohol as internal standard.

Table 3.3 Comparison of the V8HQ method with the acetylation method		
Sample	OH content mmol/kg	
	V8HQ	Acetylation
I	47.9-47.6 43.1-46.8	50-70
II	35.5-34.9	35-50
III	130.1-126.7	170-120
IV	73.8-74.9	50-70
Reprinted with permission from M. Tanaka and I. Kojima, Analytica Chimica Acta, 1968, 41, 75. ©1968, Elsevier [10]		

The application of this method to some esters of new types of acids showed that a precise determination is possible (**Table 3.3**). The standard deviation of this method is 1.5 mmol/kg which is about ten times more precise than that of the classical acetylation procedure.

Spectrophotometry using ceric ammonium nitrate has been used to determine hydroxyl groups in polycarbonates [11] and hydroxypolybutadiene [12].

3.1.3 Nuclear Magnetic Resonance Spectrometry

A further method for distinguishing between different types of hydroxy groups in polymers is the NMR method described by L'Ho [14]. This procedure is based on the reaction of the hydroxy compound with hexafluoroacetone to form the adduct shown below which is amenable to ^{19}F-NMR spectroscopy:

$$(CF_3)_2\, C = O + ROH = C(CF_3)_2\, OHOR$$

A fluorine resonance spectrum of a mixture of several hexalfuoroacetone adducts is shown in **Figure 3.1**. There are two interesting features in this spectrum. First, it illustrates clearly the high resolution and the information on structural aspects of the molecules one can obtain by this method. The hydroxyl adduct from each alcohol gives a sharp resonance, with the tertiary adducts at high field, followed by secondary and then primary. The chemical shift of the hexafluoroacetone alcohol adduct is determined by the structural environment of the hydroxyl. For example, the gradual upfield shift observed in the series methanol, ethanol, isopropanol and *tert*-butanol, results from the increase in shielding caused by replacing a hydrogen atom with a
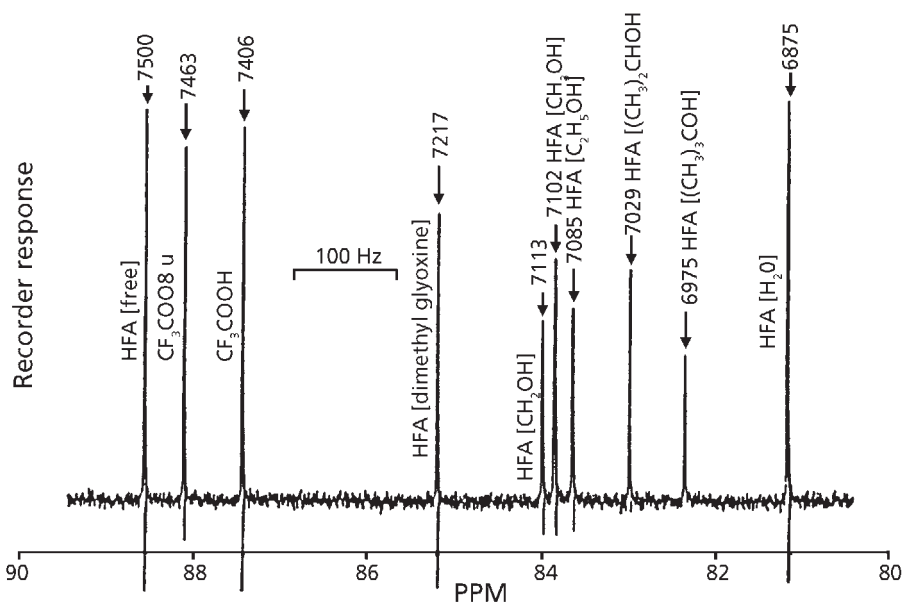
Figure 3.1 Fluorine-19 NMR spectra of several HFA adducts. From left: HFA (free), butyl trifluoroacetate, trifluoroacetic acid, HFA dimethyl glyoxime, HFA (benzyl alcohol), HFA (methanol), HFA (ethanol), HFA (isopropanol), HFA (*tert*-butanol) and HFA H_2O. The numbers on top are Hz downfield from C_8F_8 lock. (*Reprinted with permission from F.F-L. Ho, Analytical Chemistry, 1973, 45, 3, 603. ©1973, ACS*) [14]

methyl group. The high degree of resolution under **Figure 3.1** was also observed for polymeric materials. Therefore, not only can the total hydroxyl concentration be determined but also the type or types present in the polymer.

The quantative aspect of hydroxyl determination is illustrated in **Table 3.4** for the analysis of hydroxyl in some polymeric materials. In most cases, the fluorine resonance from *n*-butyl trifluoroacetate (at 7463 Hz in **Figure 3.1**) was used as internal standard to calibrate the spectral integral. From the data shown in **Table 3.4** it seems that the adduct formation is quantitative for primary and secondary hydroxyls. The reaction normally requires less than 20 minutes at room temperature. However, as with the chemical acylation methods, tertiary hydroxyl was found to react only partially, and the reaction for *tert*-butanol required about 24 hours to reach equilibrium. The method can be used for the determination of hydroxyl groups in polymers of unknown structure.

^{13}C-NMR has been used to determine primary and secondary hydroxyl groups in polyethers [15].

135

Table 3.4 Quantitative determination of hydroxyl groups in several commercial polymers		
Polymers	**Hydroxyls (%)**	
	Found	**Expected**
Aliphatic polyethers-polyethylene glycol		
Carbowax 200	17.40	16.2-17.9[a]
Carbowax 1000	3.54	3.24-3.58[b]
Polypropylene glycol		
Voranol P1010	3.46	3.37[c]
Voranol P4000	0.85	0.85[d]
Polyepichlorohydrin[e]	0.84	0.85
Aromatic polyethers		
Bakelite phenoxy resin PKHC	5.8	6.0[f]
Monosanto R, J-100 resin	5.4	5.4-6.0
Polyesters		
Atlac 382E	0.92	0.93
Aromatic ester resin No. 1[g]	8.20	8.30
Aromatic ester resin No. 2[g]	12.20	12.35

[a] Based on literature molecular weight of 190 to 210.

[b] Based on literature molecular weight of 950 to 1050.

[c] Based on an average molecular weight of 1010

[d] Based on an average molecular weight of 4000

[e] Polyepichlorihydrin 2000 from Shell Chemical Co.

[f] Calculated from the idealised molecular structure with a unit weight of 284

[g] Experimental resin from Hercules Incorporated

Reprinted with permission from F.F-L. Ho, Analytical Chemistry, 1973, 45, 3, 603. ©1973, American Chemical Society [14]

3.1.4 Infrared Spectroscopy

3.1.4.1 Determination of Hydroxy Groups in Dinitropropyl Acrylate Prepolymer

The dinitropropyl acrylate polymer has the following structure:

$$HO-CH_2\sim(CH_2-CH_n\sim CH_2OH)$$
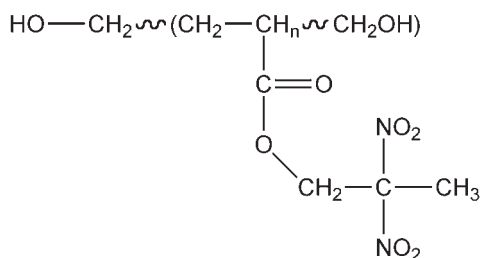
This method [16-18] utilises the strong infrared absorption band at 2.90 μm. The hydroxyl concentration of approximately 30 mequiv/l is low enough that the hydroxyl groups are completely associated with the tetrahydrofuran spectroscopic solvents, and there are no apparent free self-associated hydroxy peaks. It is essential in this method that the sample is dry, as water absorbs strongly in the 2.9 μm region of the spectrum. A further limitation of the method is that any other functional group in the sample, such as phenols, amides amines, and sulfonic acid groups, that absorb in the 2.94-2.86 μm region are likely to interfere in the determination of hydroxyl groups.

Kim and co-workers [18] studied variables such as temperature, concentration, bulk dielectric properties, and the structure of the alcohols to determine their effects on the characteristics of the THF-associated OH absorption peak. These studies show that the infrared method has a general applicability. The hydroxy equivalent weight values by this method compare well with expected values on a variety of dinitroacrylate polymers [18]. This method is subject to interferences (see **Table 3.5**).

Brako and Wexler [19] have described a useful technique for differentiating the presence or absence of functional groups such as hydroxyl, carboxylic acid or ester in polymers containing small percentage components of such groups. Films of latexes or polymers are subjected to chemical treatment which results in marked changes in the infrared spectrum and which can be associated with the disappearance of a functional group. Infrared data may be readily interpreted negatively so that one may definitely preclude the presence of hydroxyl, carbonyl, amine, amide, nitrile, ester, carboxylic, aromatic, methylene, tertiary butyl, and terminal vinyl groups if the corresponding group vibrations are absent in the infrared spectrogram. More difficult is the assignment of functional groups where multiple or several alternative

Table 3.5 OH equivalent weights of prepolymers: comparison of IR method with other methods			
Prepolymers	Vendor's eqivalent weight	IR method	Chemical methods*
Hydroxy terminated polybutadiene	1300	1280	1350
Hydroxy terminated butadiene acrylonitrile copolymer	1820	1770	
Hydroxy terminated polycaprolactone	980	970	970
Polyethylene glycol	1660	1630[a]	1670
Hydroxy terminated polytetrahydrofuran	500	480	500

[a] Alkoxyethanols used for calibration

* Reaction with excess acid anhydride in presence of base catalyst PA - phthalic anhydride, AA - acetic anhydride. Excess anhydride hydrolysed at end of reaction and carboxylate groups titrated with standard potassium hydroxide

Reprinted with permission from C.S.Y. Kim, A.L. Dodge, S.F. Lau and A. Kowasaki, Analytical Chemistry, 1982, 54, 2, 232. ©1982, American Chemical Society [18]

possibilities exist, as in the mixture of a carboxylic and keto group or in the assignment of a band to an olefinic group.

Figure 3.2(a) shows the infrared spectra of a sodium polyacrylate film before and after exposure to hydrochloric acid vapour. Exposure to acid results in the disappearance of the broad, intense band associated with the carboxylate group in the polyacrylate ion at around 6.25 μm. Appearance of a broad intense absorption at about 5.8 μm is associated with carbonyl of the carboxylic acid group. Changes are also observed in the 9.09-8.33 μm region. Heating the acidified film resulted in minor changes in the spectrum. **Figure 3.2(b)** shows the changes in the infrared spectrum resulting from the exposure of acrylic acid-vinylidene chloride copolymer film to ammonia vapour. Bands associated with the carboxylic acid carbonyl stretching frequencies at 5.83-5.75 μm disappear on exposure to ammonia vapour. A well-defined carboxylate band appears at 6.37 μm. This change is sufficient to confirm that the copolymer contains carboxylic acid groups.
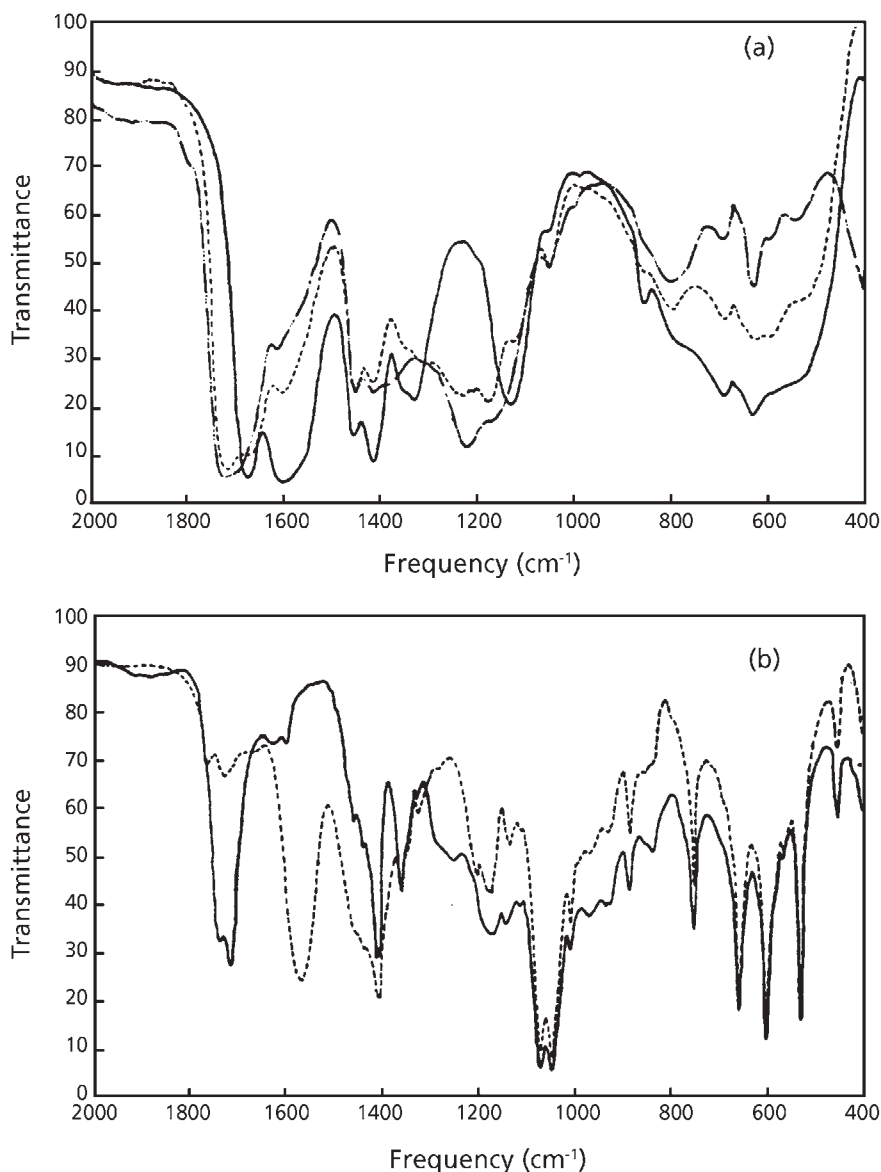
Figure 3.2 Infrared spectra of chemically treated polymers: (a) spectrum of sodium polyacrylate before and after exposure to hydrogen chloride vapour and the heated film of the hydrogen chloride treated acrylate, sodium polyacrylate film, sodium polyacrylate film exposed to HCl vapour, sodium polyacrylate film exposed to HCl vapour and then heated; (b) spectra of copolymer of acrylic acid and vinylidene chloride and the film after exposure to ammonia vapour, acrylic acid-vinylidene chloride copolymer film, acrylic acid-vinylidene chloride copolymer film exposed to ammonia vapour. (*Source: Author's own files*)

Infrared spectroscopy has also been used to determine hydroxyl groups in polyethers [20], polyethylene ether carbonate [21], and carboxy terminated polybutadiene [22, 23] and hydroxybutadienes [24].

3.1.5 Direct Injection Enthalpimetry

This technique involves the reaction of a small portion of sample with a large excess of acetic anhydride under conditions where reaction is rapid (less than 1 s). The change in temperature associated with the reaction, dT, is recorded using a thermistor bridge. Under conditions of constant heat capacity, dT should be directly proportional to the number of reactive groups per unit mass of the sample. The main advantages of the technique are, firstly, that it is relatively simple to operate and secondly, that only a few minutes are required in order to perform an analysis.

Kaduji and Rees [16] and others [25] employed direct injection enthalpimetry to determine the hydroxy value of glycerol - alkylene oxide polyethers and butane-1,4-diol-adipic acid polyesters (see Method 3.2 at the end of this chapter).

Direct injection enthalpimetry has great potential as a method for determining the hydroxyl values of polyethers and polyesters. The method is rapid, the temperature rises for two samples and a standard being recorded in duplicate in about 10 minutes.

These methods determine total hydroxy groups and are applicable to many types of hydroxy containing polymers including polyethylene glycol, polypropylene glycol and glycol/alkylene oxide condensates.

3.1.6 Kinetic Method – Primary and Secondary Hydroxyl Groups

In many practical situations, it is necessary to be able to distinguish between prmiary and secondary hydroxyl groups in polymers. Thus, the reaction product of a glycerol-ethylene oxide condensate with propylene oxide would contain both types of hydroxy group:

$$CH_2(CH_2CH_2O)_l\,OH + CH_3CH_2CH_2O \rightarrow CH_2(CH_2CH_2O)_l - CHCH_3CH_2OH^{**}$$
$$|\qquad\qquad\qquad\qquad\qquad\qquad\qquad\qquad |$$
$$CH(CH_2CH_2O)_mOH + CH_2 - CHCH_3O \rightarrow CH(CH_2CH_2O)_m - CH_2CHCH_3OH^{*}$$
$$|\qquad\qquad\qquad\qquad\qquad\qquad\qquad\qquad |$$
$$CH_2(CH_2CH_2O)_nOH \qquad\qquad\qquad CH_2(CH_2CH_2O)_n$$
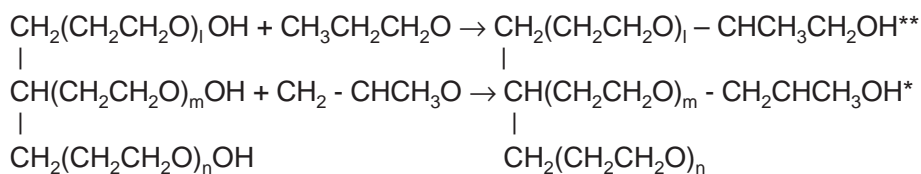
*secondary hydroxyl, **primary hydroxyl

Reaction rate differences of primary and secondary hydroxyl groups with phenyl isocyanate are basis of a kinetic method for carrying out this determination [26] (see Method 3.3).

3.1.7 Miscellaneous Techniques

Dickie and co-workers [27] derivitised surface hydroxy groups on acrylic copolymers with ammonia then characterised them by x-ray photoelectron microscopy.

Hydroxyl groups in epoxy resins have been determined by a method based on the use of lithium aluminium hydride [28].

3.2 Carboxyl Groups

3.2.1 Titration Method

Most methods for the determination of carboxyl groups in polymers are based on titration techniques including, for example, the following copolymers: acrylic acid - itaconic acid [29], acrylic acid - ethyl acrylate [30] and maleic acid-styrene [31]. High-frequency titration has been applied [32] to the analysis of itaconic acid - styrene and maleic acid - styrene copolymers and ethyl esters of itaconic anhydride - styrene copolymers. The method can also be used to detect traces of acidic impurities in polymers and in the identification of mixtures of similar acidic copolymers. Titration indicates that the acid segments in the copolymers of itaconic acid - styrene and maleic acid - styrene, and the homopolymer polyitaconic acid, act as dibasic acids. The method has a sensitivity that permits identification and approximate resolution of two carboxylate species in the same polymer, for example:

Polyitaconic acid

High frequency titration gives a precise location of the inflection points related to the polymer carboxyl groups and is a sensitive method for the determination of the freedom of the copolymer samples from monbasic acid impurities (comonomer acids), since mixtures of copolymer acids with monobasic and dibasic acids show definite inflection points that can be related to the individual carboxylate species present.
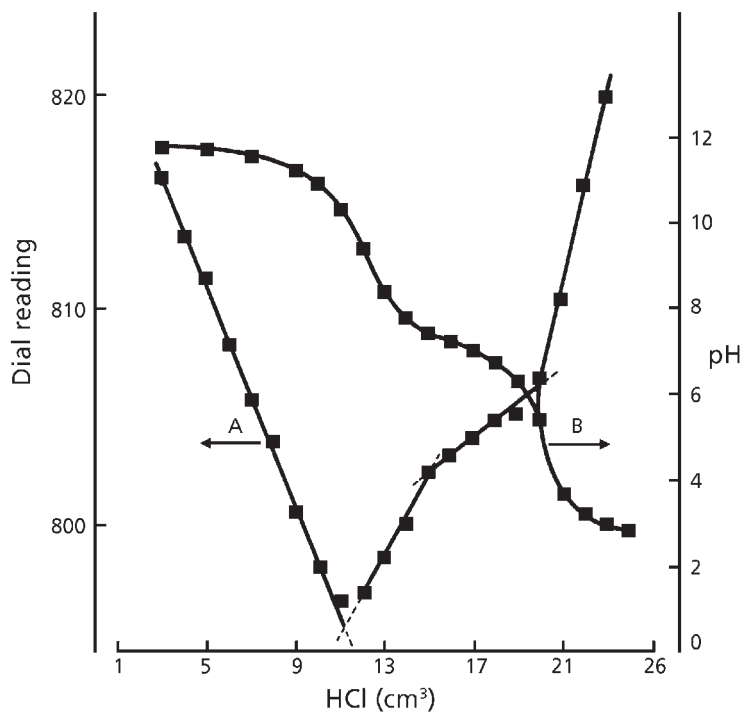
Figure 3.3 High frequency (A) and potentiometric (B) displacement titration of the monosodium salts of the monomethyl esters of polyitaconic acid-costyrene. Titration of 0.2345 g 57:43 anhydride styrene copolymers + MeOH (heat) + excess NaOH with 0.1286 N HCl.

A titration curve (**Figure 3.3**) is shown for a monomethyl ester of an itaconic acid-styrene copolymer.

Potentiometric titration provides a method of investigating changes of conformation undergone by polyelectrolytes in solution, since the environment of the dissociating groups is dependent on the conformation of the polymer chain helix-coil transitions of polyacids. Thus, precise potentiometric titration of solutions of high molecular weight polyacrylic acid at constant ionic strength indicate the presence of such conformational transition [33-35].

Figure 3.4(a) shows the titration results for polyacrylic acid plotted at pH + log((l —α)/α) *versus* degree of dissociation, as points connected by full curves. The four curves at the different ionic strengths all show the same features. The first short region, labelled A in the figure, is probably due to some instability in the solution,
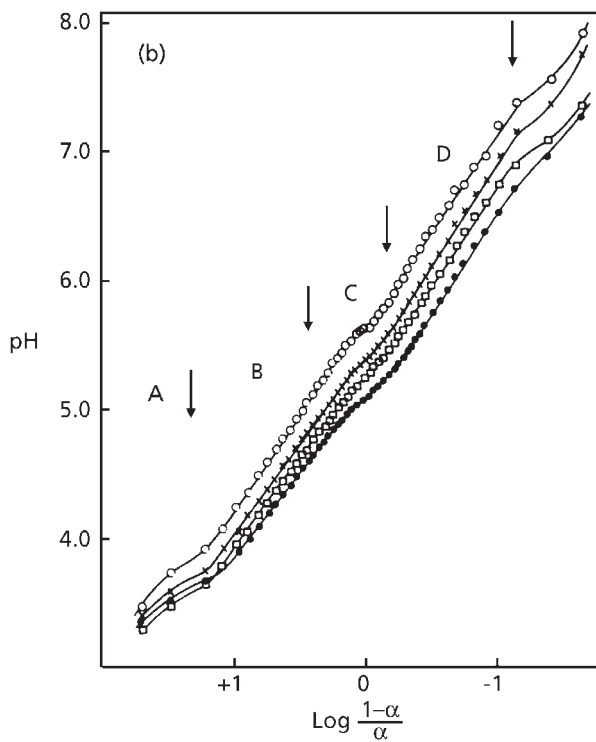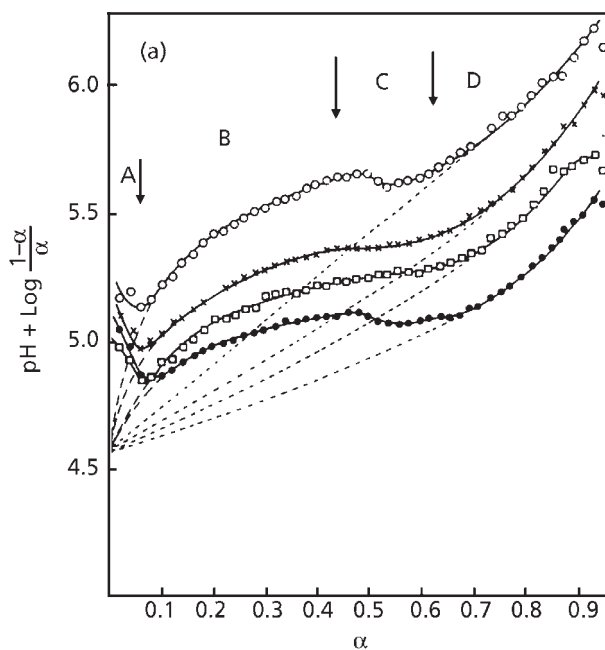
Figure 3.4 Titration of polyacrylic acid: (a) dependence of the function pH + log (1-α)/α at various ionic strengths. u: (O) u = 0.02; (×) u - 0.065; (□) u = 0.11; (●) u = 0.20. (b) pH versus log (1-α)/α at various ionic strengths u: (O) u = 0.02; (×) u = 0.065; (□) u = 0.11; (●) u = 0.20. (*Reprinted with permission from A.R. Mathieson and J.V. McLaren, Journal of Polymer Science Part A: General Papers, 1965, 3, 7, 2555. ©1965, John Wiley and Sons*) [33]

such as aggregation preceding precipitation. This region extends to higher values of α at the higher ionic strengths. The second region, B, represents the ionisation of the first conformation of the polymer; the third, C, the conformational transition; and the fourth, D, the ionisation of the second conformation. The first conformation, which exists at the lower degree of dissociation, has presumably the more tightly coiled, is denoted polyacrylic acid (a). The four curves of polyacrylic acid (a) in **Figure 3.4(a)** have extrapolated (dashed curves) semi-empirically to zero alpha, and they meet there at a value of pH + log((l — α)/α) shown in **Figure 3.4(b)**. These plots, though almost linear over the whole range, as previously reported by Mandel and Leyte [36, 37], are not quite so, and regions A, B , C and D can be distinguished here also. Linear extrapolation of region B, which represents PAA (curve 3.4(a)), to higher values of log((l — α)/α) was used to obtain the extrapolations of the PAA(a) curves of **Figure 3.4** to zero alpha.

An attractive method for determining carboxyl groups is based on the Schmidt reaction, in which the carboxyl group is subjected to reaction with sodium azide in sulfuric acid [38]. The acylazide formed rearranges to an amine, with the liberation of nitrogen and carbon dioxide:

$$\sim\sim\sim COOH \xrightarrow[\text{H}_2\text{SO}_4]{\text{NaN}_3} NH_2 \ + \ CO_2 \ + \ N_2$$
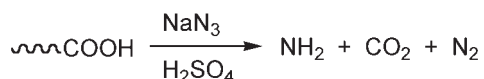
The carbon dioxide evolved is measured quantitatively by an automatic non-aqueous titration. This method is applicable to poly(*m*-phenylene isophthalmide) which is soluble in dimethylformamide, but is not applicable to poly(*p*-phenylene) terephthalamide for which no organic solvent could be found.

The suitability of this method has been investigated with the model compound *N,N'*-bis-(*p*-carboxybenzol)-*p*-phenylenediamine:
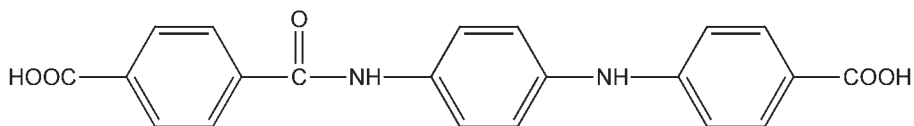
The conversion of this polymer in 100-101% sulfuric acid at 50 °C and a reaction time of 2 hours gives a quantitative conversion, which also suffices for polymer solutions.

The determination of groups in high relative molecular weight polyesters and polyamides gives, in combination with other data, information about the degree of polymerisation, chain branching, degradation and thermal stability. The choice of

the method depends on the solubility of the polymer. Most methods are based on titration in non-aqueous media with visual, potentiometric or photometric indication of the end-point.

A very convenient technique for the determination of carboxyl groups in polyethylene terephthalate and Nylon 6 is photometric titration. The sample is dissolved in *o*-cresol at 125 °C, cooled, diluted with chloroform and, after addition of bromophenol blue or bromocresol green, the titration is carried out in a spectrophotometer with tetrabutyl ammonium hydroxide. The change in absorbance is recorded continuously and the end-point is determined graphically. A detailed description has been given by Van Lingen [39].

Table 3.6 surveys applications of the photometric titration method together with a comparison with a potentiometric titration method. Generally the agreement is very satisfactory.

Table 3.6 Determination of carboxyl groups					
Sample		**% Carboxyl groups**			
		Photometric titration		**Potentiometric titration**	
		X	**Standard deviation**	**X**	**Standard deviation**
PETP (MN low)	C	4.3	0.25	4.0b	0.10
	D	12.0	0.34	12.0b	0.30
	E	17.4	0.56	17. 5b	0.49
PETP (MN high)	F	36.8	0.32	35.2	0.9
	G	68.3	0.29	68.2	1.2
	H	113.4	0.52	112.8	1.8
Nylon 6	I	73.3	0.31	72.4c	1.0
	J	53.2	0.22	52. 5c	0.37
	K	35.3	0.45	36. 2c	0.32
Mean of four independent determinations					
Titration in aniline at 40 °C					
Titration in benzyl alcohol – methanol – water					
Reprinted with permission from G.D.B. Houwelingen, G.M. Albaro and A.J. De Hoog, Fresenius' Zeitschrift für Analytische Chemie, 1980, 300, 12. © 1980 Springer Verlag [38]					

3.2.2 Nuclear Magnetic Resonance Spectroscopy

In titrating copolymers of methyl methacrylate and methacrylic acid with standard base to determine composition, a number of deficiencies have been encountered. For example, there were two common sources of 'contamination' that gave rise to under determination of the acid content: 1) the copolymers tended to be hygroscopic and hence, could on occasion contain 5% absorbed moisture, and 2) they could, on occasion, retain solvents and/or monomers. Additionally, the method has been found to be inapplicable to copolymers of high molecular weight (MW>1,000,000) and/or high acid content (> 60% acid) because of the tendency of such systems to reprecipitate during the titration procedure.

Because of these limitations, Johnson and co-workers [40] examined the applicability of Fourier transform proton NMR to the compositional analysis of methylmethacrylate acid copolymers (see Method 3.4). By using the integral of the ester, methoxy protons and combining this result with the total integral for CH_2 and CH_3 protons (the overlap between CH_2 and CH_3 resonances was enough at 100 MHz to prevent separate determination of these integrals), the copolymer composition could be ascertained. However, it was necessary to carry out the determinations at 100 °C or higher to attain resolution sufficient for reliable integrals. An additional problem was that the reaction solvents (toluene and hexane) and comonomers had resonances that overlapped those of the CH_2 and CH_3 of the copolymers introducing considerable inaccuracy in the total CH_2 CH_3 integral. For this reason they investigated the applicability of ^{13}C-NMR. Because of the greater spectral dispersion and narrower resonance lines obtained with ^{13}C-NMR relative to proton NMR problems associated with resonance overlap can be resolved. Excellent agreement was obtained between carboxyl values obtained by this procedure and conventional titration in 1:1 ethanol water with standard potassium hydroxide to the phenolphthalein end-point even the acid content range 13% to 100%.

In pyridine solutions of these copolymers, the resonances arising from acid carboxyl and ester carbonyl carbons are sufficiently resolved to allow the determination of relative integrals.

3.2.3 Pyrolysis Gas Chromatography – Mass Spectrometry

Sharp and Paterson [41] have described a pyrolysis - gas chromatographic - mass spectrometric procedure for the determination of 1-10% of copolymerised acrylic acid and methacrylic acid in acrylic polymers (see Method 3.5). The acid groups are propylated and the polymer pyrolysed according to the following reaction scheme:

```
 ┌ CH₃        ┐  ┌ R          ┐                  ┌ CH₃        ┐  ┌ R          ┐
 │ │          │  │ │          │                  │ │          │  │ │          │
─┤ C—CH₂     ├──┤ C—CH₂     ├─propylation────┤ C—CH₂     ├──┤ C—CH₂     ├──
 │ │          │  │ │          │                  │ │          │  │ │          │
 │ C=O        │  │ C=O        │                  │ C=O        │  │ C=O        │
 │ │          │  │ │          │                  │ │          │  │ │          │
 └ OCH₃      ┘ₙ └ OH        ┘ₘ                 └ OCH₃      ┘ₙ └ OC₃H₇     ┘ₘ
```

Pyrolysis:

```
  CH₃          R
  │            │
  C=CH₂  +   C=CH₂
  │            │
  C=O          C=O
  │            │
  OCH₃         OC₃H₇
```
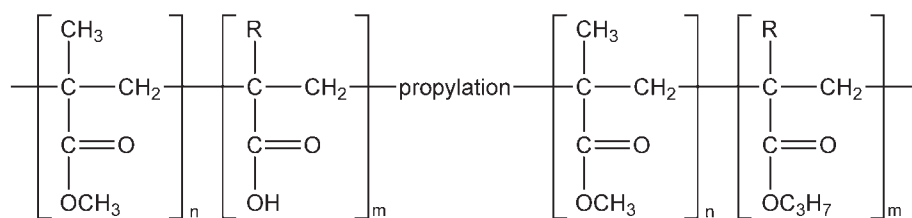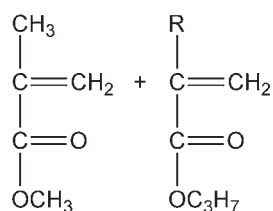
Jander and co-workers [42] used PyGC to characterise carbonyl groups in humic substances.

3.2.4 Infrared Spectroscopy

This technique has had limited application in the determination of hydroxyl groups in polyacrylamides [43, 44] caboxy terminated butadienes [24] and polyethylene [45].

3.2.5 Miscellaneous

Precipitation as the copper or uranyl salt has been used to determine carboxyl groups [12] in carboxy methyl cellulose.

Nissen and co-workers [46] have described a method for determining carboxyl groups in polyethylene terephthalate. Hydrazinolysis led to formation of terephthalomonohydrazide from carboxylated terephthalyl residues to provide a selective analysis for carboxyl group via ultraviolet absorbance at 240 nm.

3.3 Carbonyl Groups

Germanenko [47] determined low concentrations for carbonyl groups in PVC and vinyl chloride - vinyl acetate copolymers. In this method the carbonyl groups in the
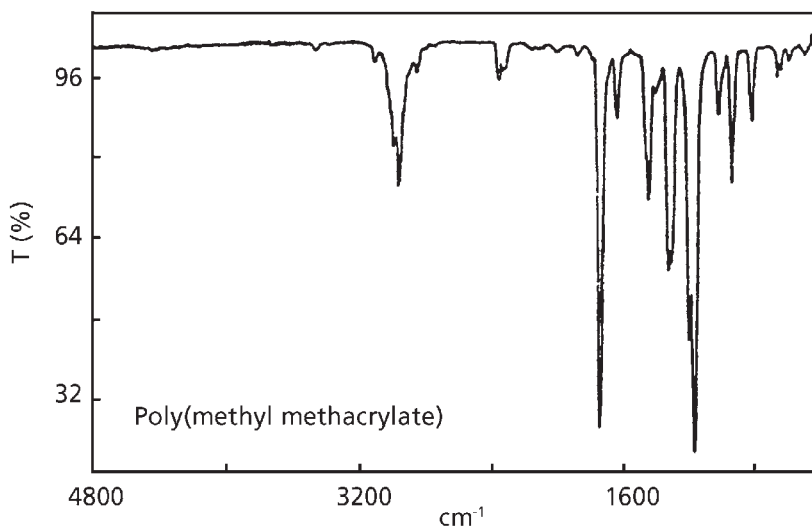
Figure 3.5 Infrared spectrum of pyrolysed polymethacrylic acid.
(*Source: Author's own files*)

polymer are reacted with 2,4-dinitrophenyl hydrazine to produce the corresponding phenyl-hydrazone. Excess reagent is washed away from the polymer, which is then digested with concentrated sulfuric acid to convert the bound hydrazone to ammonium sulfate, which is then estimated using Nessler's reagent.

Direct spectrophotometry in the visible and ultraviolet region been used to determine low concentrations of functional groups on the surface of polymer films. Thus, Kato [48] has followed the regeneration of carbonyl groups from 2,4-dinitrophenyl-hydrazones formed on the surface of irradiated polystyrene films by absorption measurements at 378 nm.

In the infrared spectrum of pyrolysed polymethacrylic acid a carbonyl stretching band is clearly visible at 5.73 μm. Also evident is the ester stretching band at 9.82 μm (**Figure 3.5**).

3.4 Ester Groups

Most methods for the determination of ester groups in polymers are based on the following procedures:

a) Saponification.

b) Zeisel procedures, based on hydriodic acid.

c) Pyrolysis - gas chromatography.

d) Physical methods, e.g., infrared spectroscopy and nuclear magnetic resonance spectroscopy.

3.4.1 Saponification Methods

Ester groups occur in a wide range of polymers (e.g., polyethylene terephthalate) and in copolymers such as, for example, ethylene vinyl acetate. The classical chemical method for the determination of ester groups, namely, saponification, can be applied to some types of polymer. For example, copolymers of vinyl esters and esters of vinyl esters and esters of acrylic acid, can be saponified in a sealed tube with 2 M sodium hydroxide. The free acids from the vinyl esters were determined by potentiometric titration or gas chromatography. The alcohols formed by the hydrolysis of the acrylate esters were determined by gas chromatography. Vinyl acetate ethylene copolymers can be determined by saponification with 1 N ethanolic potassium hydroxide at 80 °C for 3 hours and back titration with standard acid or by saponification with *p*-toluene sulfonic acid and back titration with standard acetic acid [49, 50].

Polymethyl acrylate can be hydrolysed rapidly and completely under alkaline conditions. On the other hand, the monomer units in polymethyl methacrylate prepared and treated similarly are resistant to hydrolysis [51] although benzoate end-groups react readily [52]. Only about 9% of the ester groups in polymethyl methacrylate reacted even during prolonged hydrolysis; hydrolysis of polymethyl acrylate was complete in 0.5 hours. Although only about 9% of the ester groups in methyl methacrylate homopolymers are hydrolysed in several hours reflux with alcoholic sodium hydroxide, this proportion is increased by the introduction of comonomer units into the polymer chain. Thus, saponification techniques should be applied with caution to polymeric materials.

A copolymer of ethylene and vinyl acetate has the following structure which, upon hydrolysis in the presence of excess standard potassium hydroxide/*p*-toluene sulfonic acid catalyst reacts as follows:

$$\text{---}(CH_2\text{---}CH_2\text{---}CH_2\text{---}CH\text{---})_n + nKOH \longrightarrow$$
$$\qquad\qquad\qquad\qquad | $$
$$\qquad\qquad\qquad OOCCH_3$$

$$\text{---}(CH_2\text{---}CH_2\text{---}CH\text{---}CH\text{---})_n + nCH_3COOK$$
$$\qquad\qquad\qquad\qquad\quad | $$
$$\qquad\qquad\qquad\qquad OH$$

Excess potassium hydroxide is then determined by titration with standard acetic acid, and hence the vinyl acetate content of the polymer is calculated from the amount of potassium hydroxide consumed. Vinyl acetate ethylene copolymers can be determined by saponification with 1 N ethanolic potassium hydroxide at 80 °C for 3 hours [53, 54].

Saponification methods have been applied to the determination of ester groups in alkyd resins [55-57], polyesters, cellulose, polyvinyl esters, polyacrylates and polymethacrylates [58-60].

3.4.2 Zeisel Hydriodic Acid Reduction Methods

Hydrolysis using hydriodic acid has been used for the determination of the methyl ethyl, propyl and butyl esters of acrylates, methacrylates or maleates [61] and the determination of polyethyl esters in methyl methacrylate copolymers [62, 63]. First the total alcohol content is determined using a modified Zeisel hydriodic acid hydrolysis [64]. Secondly, the various alcohols, after being converted to the corresponding alkyl iodides, are collected in a cold trap and then separated by gas chromatography. Owing to the low volatility of the higher alkyl iodides the hydriodic acid hydrolysis technique is not suitable for the determination of alcohol groups higher than butyl alcohol. This technique has also been applied to the determination of alkoxy groups in acrylate esters [61].

Anderson and co-workers [65] have used combined Zeisel reaction - gas chromatography to analyse acrylic copolymers. Acrylic esters were cleaved with hydriodic acid and gas chromatography was used for analysing the alkyl iodides so formed:

R = H, CH$_3$, C$_2$H$_5$, C$_4$H$_9$, R′ = H, OH$_3$
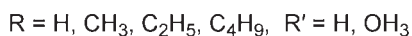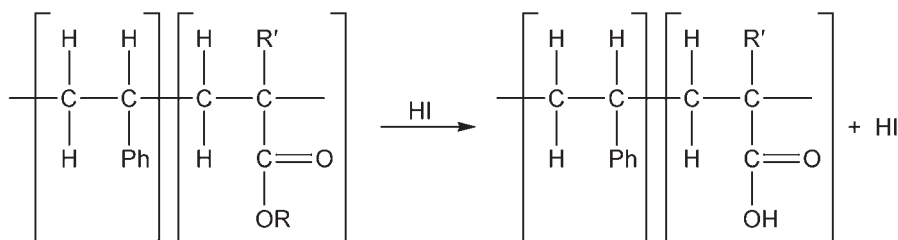
Using this procedure, the recovery of alkyl iodides is greater than 95% for polymers containing between 10 and 90% of the methyl, ethyl and butyl esters of acrylic and methacrylic acid. In addition, the use of isopropylbenzene as the trapping solvent allows the determination of all C$_1$ to C$_4$ alkyl iodides. Quantitative cleavage by hydriodic acid

	Methyl-acrylate (%)	Methyl-methacrylate (%)	Ethyl-acrylate (%)	Ethyl-methacrylate (%)	Butyl-acrylate (%)	Butyl-methacrylate (%)
Polymer						

Table 3.7 Recovery of alkyl iodides from the Zeisel cleavage of acrylic polymers[a]

Polymer	Methyl-acrylate (%)	Methyl-methacrylate (%)	Ethyl-acrylate (%)	Ethyl-methacrylate (%)	Butyl-acrylate (%)	Butyl-methacrylate (%)
1	33.7 (33.3)		33.0 (33.3)		32.7 (33.3)	
2		33.6 (33.3)		33.4 (33.3)		31.9 (33.3)
3			19.5 (20.0)			
4		50.1 (50.0)	30.5 (30.0)			
5		59.9 (60.0)			39.8 (40.0)	
6		29.7 (30.0)			29.8 (30.0)	
7		59.8 (60.0)				9.8 (10.0)
8	19.9 (20.0)		19.8 (20.0)			19.8 (20.0)
9		30.1 (30.0)		30.0 (30.0)	29.8 (30.0)	
10		29.9 (30.0)	29.6 (30.0)		39.7 (40.0)	
11		60.1 (60.0)	30.1 (30.0)			9.5 (10.0)

[a] All values are the average of at least three determinations and are reported as:
  % monomer found (% monomer in polymer)

Theoretical values are in brackets

Reprinted with permission from D.G. Anderson, K.E. Jackson, D.L. Smew, D.J. Tessari and J.T. Vandeberg, Analytical Chemistry, 1971, 43, 7, 894. © 1971, ACS [65]

of the acrylate and methacrylate esters is also observed in the presence of the modifying monomer units such as styrene, vinyl acetate, vinyl chloride and acrylamide.

Table 3.7 shows some results obtained by applying this method to a range of acrylic polymers. The calculated recoveries are greater than 95% for polymers containing

between 10% and 100% acrylic monomer. The method has a 99% confidence interval of 0.8. The presence of comonomers such as styrene, acrylonitrile, vinyl acetate, acrylamide or acrylic acid does not change the recovery of acrylate or methacrylate esters. Non-quantitative results are obtained, however, for polymers containing hydroxy-propyl methacrylate.

3.4.3 Pyrolysis Gas Chromatography

Barrall and co-workers [66] have described a pyrolysis - gas chromatographic procedure for the analysis of polyethylene - ethyl acrylate and polyethylene - vinyl acetate copolymers and their physical mixtures. They used a specially constructed pyrolysis chamber as described by Porter and co-workers [67]. Less than 30 seconds is required for the sample chamber to assume block temperature. This system has the advantages of speed of sample introduction, controlled pyrolysis temperature and complete exclusion of air from the pyrolysis chamber. The pyrolysis chromatogram of polyethylene - vinyl acetate contains two principal peaks due to methane and acetic acid:

$$\text{---OCH}_2\text{---CH}_2\text{---CH}_2\text{---CH} \quad \xrightarrow[\text{300--480 °C}]{\text{pyrolysis}} \quad CH_3COOH + CH_4$$
$$\underset{\underset{\displaystyle OOCCH_3}{|}}{}$$
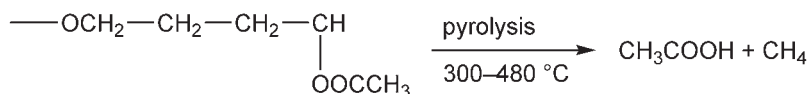
Table 3.8 Pyrolysis results on physical mixtures of polyethylene – ethyl acrylate and polyethylene – vinyl acetate						
Mixture	Acetic acid found	wt% calculated	Ethylene found	wt% calculated[a]	Oxygen found	wt% calculated
50% PEEA-1 and 50%						
PEVA-2	9.10	9.05	2.65	2.62	7.88	8.25
33.3% PEEA-2						
and 66.6%						
PEEA-3	12.15	12.33	0.75	0.70	7.33	7.49
[a] *Calculated from results for acetic acid and ethylene content for individual samples on weight% basis*						
Reprinted with permission from E.M. Barrall, R.S. Porter, D.E. Johnson, Analytical Chemistry, 1963, 35, 1,73. ©1963, ACS [66]						

Variations from 350 °C to 490 °C in pyrolysis temperature produced no change in the area of the acetic acid peak, but did cause an area variation in the methane peak. The pyrolysis chromatogram of polyethylene - ethyl acrylate at 475 °C shows one principal peak due to ethanol. No variation in peak areas was noted in the temperature range 300 °C to 480 °C. **Table 3.8** shows results obtained the analysis of 0.5 g samples of polyethylene - ethyl acrylate (PEEA) and polyethylene - vinyl acetate (PEVA) obtained at a pyrolysis temperature of 475 °C.

Pyrolysis - gas chromatography - mass spectrometry has been used to identify ester groups in acrylic polymers [68].

3.4.4 Infrared Spectroscopy

3.4.4.1 Determination of Bound Vinyl Acetate in Ethylene-Vinyl Acetate Copolymers

There are two methods for this determination, depending on the concentration of vinyl acetate. At levels below 10% a band at 2.89 μm is used. This band is not suitable for higher concentrations because the necessary film thickness is less than 0.1 mm. For higher concentrations the carbonyl overtone band at 16.39 μm can be used, since much thicker films are needed to give suitable absorbance levels. Here the carbonyl overtone band was used for a series of standards with vinyl acetate concentrations up to 35%, the nominal thickness being about 0.5 mm.

A combination of CDS and QUANT software on a Perkin Elmer model 683 infrared spectrometer has been used to establish the calibration for this analysis. Once the calibration has been carried out, the simplest way to measure an unknown sample would be with an OBEY routine in the CDS II software. This would incorporate the calibration data so that the single routine would measure the spectrum and calculate the vinyl acetate concentration with an error of approximately 5%.

The vinyl acetate content of films of ethylene - vinyl acetate copolymers can be determined by methods based on the measurement of absorbances at 16.1 and 13.9 μm [69] and at 5.73 μm [68]. The acrylate salt in acrylate salt - ethylene ionomers has been determined from the ratio absorbances at 6.41 μm (asymmetric vibration of the carboxylate ion) and 7.24 μm [70, 71].

3.4.4.2 Determination of Free and Combined Vinyl Acetate Groups in Vinyl Chloride-Vinyl Acetate Copolymers

Infrared spectroscopy has been applied to the determination of free and combined vinyl acetate in vinyl chloride-vinyl acetate copolymers [72]. This method is based upon the quantitative measurement of the intensity of absorption bands in the near-infrared spectral region arising from vinyl acetate. A band at 1.63 µm due to vinyl groups enables the free vinyl acetate content of the sample to be determined. A band at 2.15 µm is characteristic for the acetate group and arises from both free and combined vinyl acetate. Thus, the free vinyl acetate content may be determined by difference at 2.15 µm. Polymerised vinyl chloride does not influence either measurement.

Anderson and co-workers [65] have described an infrared procedure for distinguishing between copolymerised acrylic and methacrylic acids in acrylic polymers containing more than 10% of the acid. This method is based on precise measurement of the wavelength of the carboxylic acid absorption maximum at about 5.9 µm. The identification of the acid in compositions containing less than 10% of acid has hitherto not been possible, except when unpolymerised acid residues can be separated from the polymer [73].

3.4.5 Nuclear Magnetic Resonance Spectroscopy

NMR has been used to determine ethyl acrylate in ethyl acrylate - ethylene and vinyl acetate - ethylene copolymers [74]. Measurements were made on 10% solutions in diphenyl ester at an elevated temperature. Resolution improved with increasing temperature and lower polymer concentration in the solvent. NMR spectra for an ethylene - ethyl acrylate copolymer indicate clearly both copolymer identification and monomer ratio (**Figure 3.6**). A distinct ethyl group pattern (quartet, triplet), with methylene quartet shifted downfield by the adjacent oxygen, is observed. The oxygen effect carries over to the methyl triplet which merges with the aliphatic methylene peak. No other end-group would give this characteristic pattern. The area of the quartet is a direct and quantitative measure of the ester content. All features are consistent with an identification of an ethylene-rich copolymer with ethyl acrylate. Ethyl acrylate contents obtained by NMR (6.0%) agreed well with those obtained by PMR (6.2%) and neutron activation analysis for oxygen (6.1%).

NMR spectroscopy has been applied to the determination of ester groups in polyethylene terephthalate (PET) [74]. A blend of a protic solvent (dimethyl sulfoxide), sodium hydroxide, and methanol hydrolyses ester groups in this polymer much more rapidly than do hydrolysis reagents previously used.
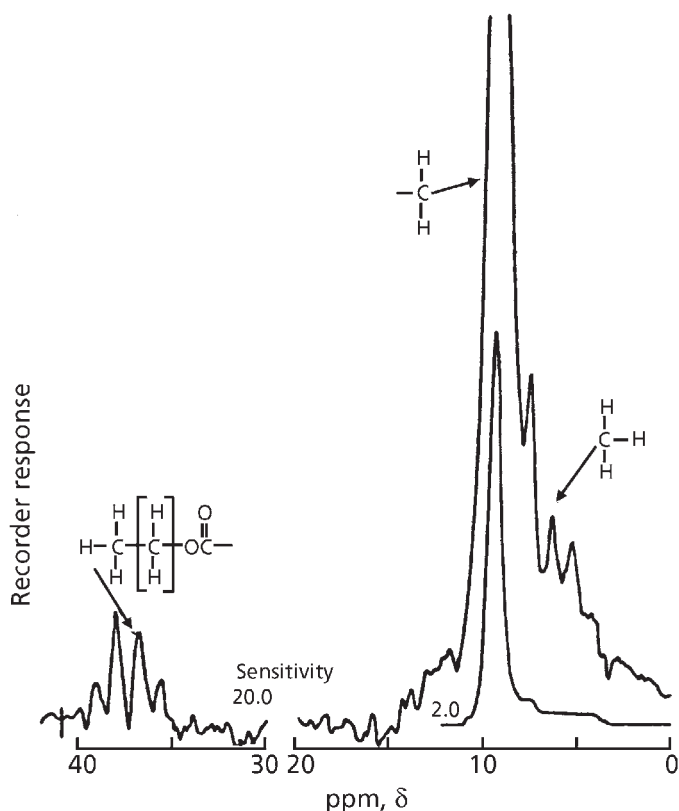
Figure 3.6 NMR spectrum, polyethylene ethyl acrylate copolymer. (*Reprinted with permission from R.S. Porter, S.W. Nicksic and J.F. Johnson, Analytical Chemistry, 1963, **35**, 12, 1948. ©1963, ACS*) [74]

NMR spectroscopy has been used for the determination of isophthalate in PET – isophthalate dissolved in 5% trichloroacetic acid. The NMR spectra of these polymers were measured on a high resolution NMR spectrometer at 80 °C. A singlet at 7.74 ppm is due to the four equivalent protons attached to the nucleus of the terephthalte unit. The complicated signals which appear at 8.21, 7.90, 7.80, 7.35, 7.22 and 7.10 ppm are due to the four protons attached to the nucleus of the isophthalate unit. The content of the iosphthalate unit can be calculated from the integrated intensities of these peaks. Aydin and co-workers [49] hydrolysed polyesters and converted the product acids and glycols including 1,4-cyclohexane di-methanol and isophthalic acid to the corresponding trimethylsilyl esters and ethers which were then analysed by gas chromatography.

3.4.6 Gas Chromatography

3.4.6.1 Succinate Ester Groups

Esposito and Swann [76] published a technique involving methanolysis of succinate ester groups in polyester resin with lithium methoxide as a catalyst. The methyl esters formed were separated from the polyols and identified by gas chromatography:

$$HOOC\!-\!\!-\!\!((CH_2)_2CO[O(CH_2)_2OCO(CH_2)_2CO]OH \; + \; 3CH_3OH \xrightarrow{\; (LiOCH_3) \;}$$

succinic acid – diethylene glycol polyester

$$2CH_3OOC(CH_2)_2COOCH_3 \; + \; HO(CH_2)_2OH$$
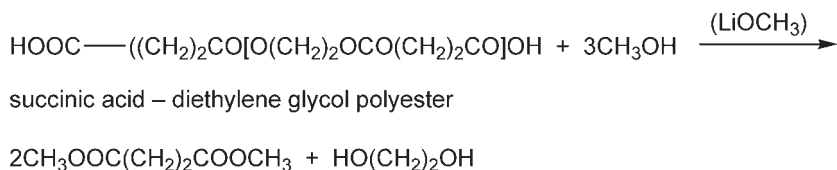
This method was improved by Percival [77] by using sodium methoxide as a catalyst and injecting the reaction mixture of the transesterification directly into the gas chromatograph (without any preliminary separation).

3.4.7 Isotope Dilution Method

Cambell [78] has described an isotope dilution method for the determination of vinyl acetate in vinyl acetate-vinyl chloride copolymers. In this method a known amount of acetic 2-^{14}C acid is added to a solution or suspension of the resin in methyl ethyl ketone and the ester is hydrolysed with sodium hydroxide. The major portion of the sodium acetate ^{14}C is isolated and converted to 2-methyl benzimidazole-methyl ^{14}C by means of the Phillips reaction [79] with *o*-phenylene diamine.

Methyl-labelled acetic acid is used to avoid the kinetic isotope effect that would be expected with the reagent labelled in the carbonyl group:
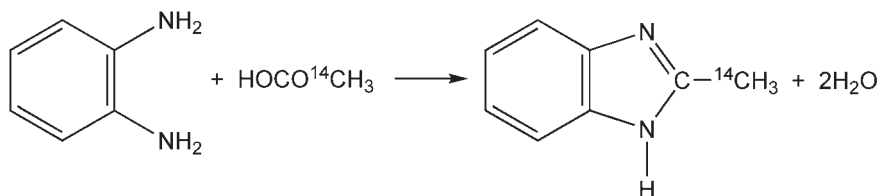
3.5 Ether Groups

Anderson and co-workers [80] have studied the application of an alcohol exchange – gas chromatographic method to the determination of etherification levels in acrylamide interpolymers of the type:
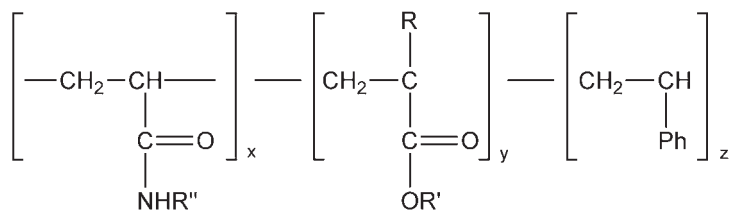
where

R = H or CH$_3$

R′ = H, CH$_3$, C$_2$H$_5$, C$_4$H$_9$ OR C$_8$H$_{17}$

R″ = H, CH$_2$OC$_4$H$_9$ or CH$_2$OH

In this method a cast film of the acrylamide interpolymer is reacted with an alcohol, e.g., octyl alcohol, to exchange with etherifying alcohols present in the polymer backbone as follows:
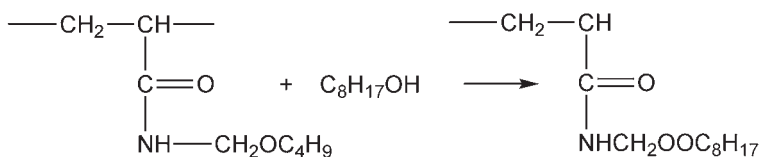
The etherifying alcohol content of the digest, in this case butanol, is determined by gas chromatography. The method is calibrated against standard solutions of the etherifying alcohol and an internal standard.

The level of alcohol obtained during the exchange reaction of acrylamide is correlated with data obtained using Zeisel cleavage of the alkoxy groups. These data are summarised in **Table 3.9**. Comparable results are obtained using both

Table 3.9 Correlation of alcohol exchange and Zeisel cleavage		
Sample	Butylated Acrylamide[a] (%)	
	Alcohol exchange	Zeisel cleavage
14% Acrylamide	100	101
23% Acrylamide	101	100
[a] *Based on experimentally determined butoxy and nitrogen content*		
Reprinted with permission from D.G. Anderson, K.E.Osakson, J.T.Vanderberg, M.Y.T. Jao, D.J. Tessari and L.C. Alfremo, Analytical Chemistry, 1975, 47, 7, 1008. ©1975, ACS [80]		

procedures, however, the Zeisel cleavage reaction will also cleave ester linkages as well as ether functionalities. This presents no problem with polymers which do not contain ester groups. In systems employing both butyl esters and butyl ethers the Zeisel cleavage reaction gives a total $O-C_4H_9$ content in the sample. Alcohol exchange, on the other hand, will cleave only the butyl ether groups in the sample. By subtracting the alcohol exchange data from that obtained from Zeisel cleavage, one can assess the relative amounts of alkyl ester and alkyl ether in the sample.

Smith and Dawson [17] determined traces of ether linkage in polyethylene glycol and polypropylene glycol by reacting the sample with hydrobromic acid then determining the dibromoethane and dibromopropane fission products by gas chromatography.

The Zeisel method has been used to determine ether groups in cellulose and polyvinyl ethers [81].

3.6 Alkoxy Groups

3.6.1 Infrared Spectroscopy

Swaraj and Bengt [82] used infrared spectroscopy to determine epoxy groups in methylmethacrylate - glycidyl methacrylate copolymers.

The infrared analysis was performed on dried potassium bromide pellets containing 0.5 mg sample in 200 mg potassium bromide. An infrared spectrum of a methyl methacrylate - glycolymethyacrylate copolymer is shown in **Figure 3.7**. The peaks at the wave numbers 11.02 and 5.82 µm are the most suitable ones for analysis of epoxy and carbonyl groups, respectively. Using the 'base line density' method, the values of the absorbances at 11.02 and 5.82 µm have been determined in triplicate. The average values of the absorbances, their ratio and the glycidylmethylacrylate mole fraction determined chemically are presented in **Table 3.10**.

The absorbance ratio at 11.02 *versus* 5.82 µm is linearly related to the GMA content in the copolymer and can be expressed by the following equation:

$$R = 0.250 \, X_G - 0.033$$

where R is the absorbance ratio at 11.02 and 5.82 µm, X_G is the mole fraction of GMA containing the epoxy group in the copolymer. The term 0.033 is considered to be a correction factor arising from the very weak absorption due to polymethyl methacrylate at wave numbers near 11.02 µm.
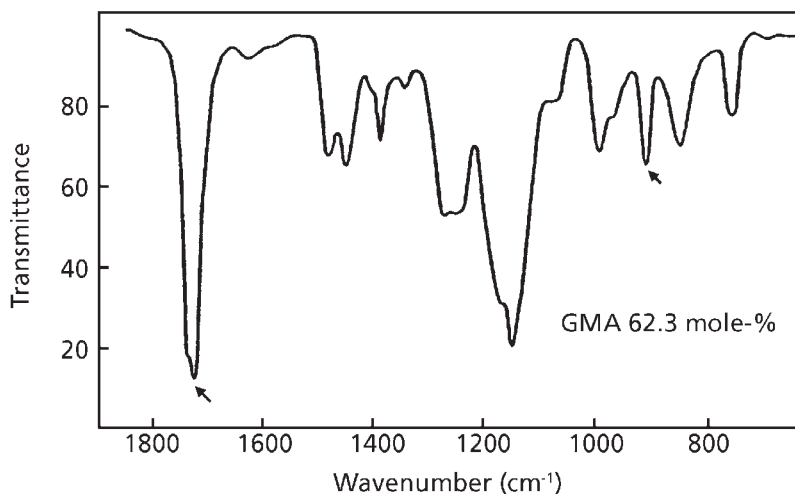
Figure 3.7 Infrared spectrum of methylmethacrylic acid – glycol methyl-acrylate copolymer containing 62.3 mole% of glycolmethylacrylate.
(*Reprinted with permission from S. Paul and B. Ranby, Analytical Chemistry, 1975, 47, 8, 1428. ©1975, ACS*) [82]

Table 3.10 Analytically determined mole fraction of glycidyl methacrylate (GMA) in the methylmethacrylate – glycidyl methacrylate copolymers and the infrared absorbance at 5.82 and 11.02 μm				
Experiment number	Mole fraction of GMA in the copolymer determined chemically	A, 5.82 μm	A, 11.02 μm	Absorbance ratio, A 11.02 μm/A 5.82 μm
R50	0.218	1.366	0.128	0.093
R51	0.394	0.911	0.120	0.131
R52	0.584	0.629	0.115	0.182
R61	0.623	0.921	0.177	0.192
R53	0.706	0.955	0.204	0.213
Reprinted with permission from S. Swarej, B. Ranby, Analytical Chemistry, 1975, 47, 8, 1428. ©1975, ACS, [82]				

Hard epoxy resins of the diglycidylether-bisphenol A type, (e.g., Epikote 1004 (Shell Chemicals) and Bakelite epoxy resin ERL 1774) are manufactured by the reaction of bisphenol and epichlorohydrin as shown:
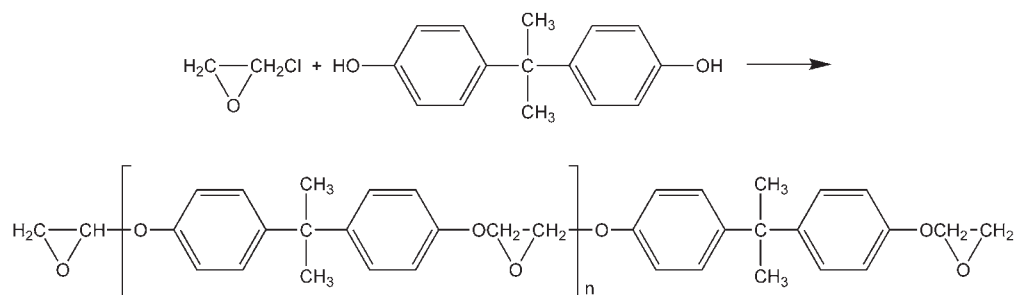
Peltonen and co-workers [83] have described an infrared method for determining epoxy resins and their thermal degradation products in workspace air samples which have been collected by filtration on glass-fibre filters. Epoxy residues were extracted from the filters with chloroform, the extract evaporated to dryness and the residue dissolved in 0.5 ml deuterochloroform ($CDCl_3$). An infrared spectrum of an elute epoxy resin (Epicote 1004) is shown in **Figure 3.8**. If thermal degradation products of epoxy resins were present, the initial chloroform extract was washed with 1 N sodium hydroxide, then water to remove phenolic products, then evaporated and the residue dissolved in $CDCl_3$ prior to infrared spectroscopy. $CDCl_3$ was used instead of chloroform for preparing the extract for infrared spectroscopy as chloroform has a strong absorption at 6.62 μm which precludes the use of this aromatic absorption for the determination of epoxy resin in the extract. The absorbance at 6.62 μm is linear with concentration in the concentration range 50-740 μg epoxy resin per 0.5 ml with a detectton limit of 50 μg per 0.5 ml and recoveries ranging from 70% at the 72 μg per 0.5 ml level to 97% at the 288 μg per 0.5 ml level.

The high relative molecular mass fraction, derived from the cracked epoxy network, contains the same aromatic substances as the intact epoxy resin. This enabled Peltonen and co-workers [83] to use pure epoxy resin as a standard for quantification of the high relative molecular mass fraction of the thermal degradation products. High performance liquid chromatography revealed the presence of phenolic compounds. These were washed off because they also absorb strongly at 6.62 μm. The removal efficiency of phenols (100%) was confirmed by HPLC. The removal of phenols was also observed in the infrared spectrum as decreased absorption by hydroxy groups. The remaining absorption was probably due to the secondary aliphatic alcohol groups in the chains. Secondary aliphatic alcohols are not acidic and therefore they are not removed by sodium hydroxide extraction.
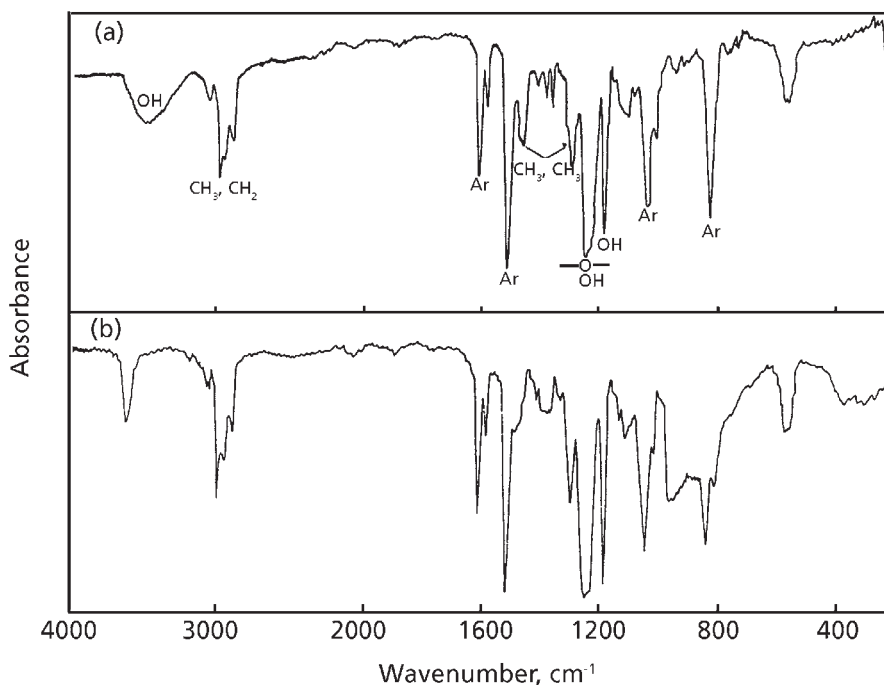
Figure 3.8 IR spectrum of a solid epoxy resin (Epicote 1004) in (a) potassium bromide and (b) chloroform-d. (*Reprinted with permission from K. Peltonen, P. Pfäffli and A. Itkonen, Analyst, 1985, **110**, 9, 1173. ©1985, RSC*) [83]

Miyauchi and co-workers [84] determined methoxy groups in methylated melamine-formaldehyde resins by establishing the infrared spectroscopic correlation between area ratio 12.27 μm (triazine) and 10.95 μm (methoxy and ethoxy contents) as established by gas chromatography.

3.6.2 Nuclear Magnetic Resonance Spectroscopy

Hammerich and Willeboordse [85] compared repeat unit (n) values obtained by PMR spectroscopy and those obtained by chemical methods of analysis. In the PMR method areas were excluded whose integrals were overlapped.

NMR determinations are usually consistently lower than the corresponding titrimetric determinations.

3.6.3 Miscellaneous Methods

Epoxy groups have also been determined spectrophotometrically using 2,4 dinitrobenzene sulfamic acid [86] and by the Ziesel method [87-89].

3.7 Oxyalkylene Groups

3.7.1 Cleavage – Gas Chromatography

Several mixed anhydrides of carboxylic and sulfonic acids, as proposed by Karger and Mazur [90], act as reagents for the cleavage of ether linkages, particularly that of acetic anhydride toluene-*p*-sulfonic acids, which is not only a powerful reagent for the cleavage of ether linkages but is also an active acetylating agent. For example, when the propylene oxide adduct of glycerol is treated with this reagent, the polyether is split, thus giving glycerol triacetate and propylene glycol which are easily identified by gas chromatography. Tsuji and Konishi [91] extended this method to the identification of base compounds and the determination of their oxyethylene and oxypropylene group contents.

In this method the cleavage reagent comprises a solution of acetic anhydride (80 g) in 120 g of *p*-toluene sulfonic acid. This mixture is refluxed at 120 °C for 30 minutes. The product obtained is used as the reagent without removal of the acetic acid produced and the excess of acetic anhydride.

Figure 3.9(a) shows gas chromatograms obtained with reaction products of several polyurethane polyethers.

The gas chromatogram of the acetate peaks are satisfactorily separated from each other and the peak of propylene glycol diacetate produced by the cleavage of the polyoxypropylene groups did not overlap those of the derivatives from polyol base compounds except that for the polyether based on propylene glycol. These base compounds could therefore be easily distinguished and identified. By decreasing the temperature of the gas chromatographic column, the peak for propylene glycol diacetate can be accurately identified.

Polyethers based on sorbitol yielded complex products that consist of the acetates of sorbitans and sorbides produced by dehydration. However, the gas chromatograms always showed similar patterns, so that the base compound (sorbitol) can be identified from the chromatogram.

In order to obtain the peaks of the reaction products of polyethers based on 1,2-diaminomethane and 2,2′-diaminodiethylamine, the SE-30 column is operated
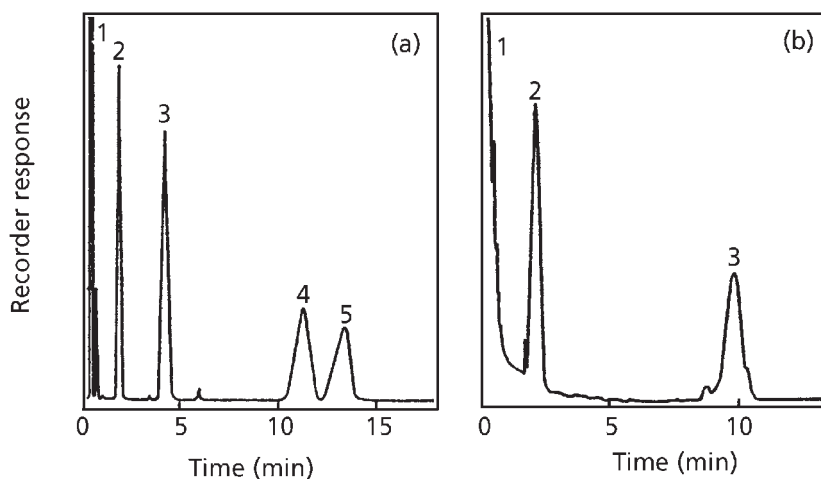
Figure 3.9 Reaction of polyethers with *p*-toluene sulfonic acid – gas chromatography. Gas chromatogram of reaction products of polyurethane polyethers (1) propylene glycol diacetate; (2) glycerol triacetate; (3) trimethylpropane triacetate; (4) triethylanolamine triacetate; (5) pentaerythritol tetracetate. Gas chromatographic conditions: column 1 m × 3 mm, coated with 15% FFAQ on Uniport B, oven 170 °C; chart speed 1 cm/s. (b) Gas chromatogram of reaction products of polyurethane polyethers based on amines (1) pyropylene glycol diacetate; (2) derivative from 1,2 diaminoethane; (3) derivative from 2,2′-diaminodiethylamine. Gas chromatographic conditions: Column 1 m × 3 mm packed with 15% SE-30 on Uniport B; oven 230 °C; chart speed, 1 cm/min. (*From authors's own files*)

isothermally at 230 °C and the flow-rate of the carrier gas was maintained at 60 ml/min. A typical gas chromatogram is shown in **Figure 3.9(b)**. These base compounds can also be distinguished and identified.

To determine oxyethylene and oxypropylene groups in the ethylene oxide propylene oxide copolymers, and polyols, the samples were oxypropylated and then oxyethylated, and these were then decomposed as described above for the determination of the polyol base compounds. The FFAP column is operated isothermally at 65 °C and the flow-rate of the carrier gas is regulated at 60 ml/min.

A typical chromatogram for the reaction of the 1,2-diaminoethane ethylene oxide-propylene oxide adduct is shown in **Figure 3.9(b)**. The ethylene glycol diacetate and propylene glycol diacetate peaks, produced from polyoxyethylene and

polyoxypropylene groups, respectively, are completely separated. The proportions of ethylene and propylene oxide can be determined by measuring the two peak areas, (i.e., of the ethylene glycol and propylene glycol diacetates) and applying the appropriate calculations. The derivative from the base compound itself (1,2-diaminoethane) do not appear in the chromatogram and so do not interfere in the determination of the ratio of oxyethylene to oxypropylene groups.

Cervenka and Merrall [92] have investigated the application of acidic dehydration of ethylene oxide - propylene oxide condensates in bromonaphthalene in the presence of *p*-toluene sulfonic acid to the elucidation of the molecular structure and monomer sequence of these polymers. Gas chromatography was used to determine dehydration products.

Studies on polyethylene glycol and polypropylene glycol homopolymers showed that dioxane and its derivatives, (e.g., methyl dioxone 1.4) are not the only reaction products. Dehydration of polyethylene glycol gave three products; that of polypropylene glycol, six products. The majority of them were identified.

Cervenka and Merrall [92] conclude that results on homopolymers, their blends and model copolymers of different chain architectures demonstrate that acidic dehydration is capable of distinguishing ethylene oxide - propylene oxide copolymers of different structures, giving correct absolute values of overall monomer contents and also ranking polyols according to their degrees of randomness.

Ethylene oxide and propylene oxide adducts of polyhydric alcohols and amines are widely used as polyethers in the production of polyurethane foams by reaction with diisocyanate. The physical properties of their foams depend to a certain extent on the chemical structure of these polyethers, so it is very important to establish a method for the identification of the base compounds and for the determination of the proportions of their oxyethylene and oxyproylene groups.

Mathias and Mellor [93] split the polyethers with hydrobromic acid - acetic acid to give bromo compounds, which were analysed by gas chromatography:

$$-CH_2-CH_2O + 2HBr = BrCH_2CH_2Br + H_2O$$

$$-CH-CH_3-CH_2O + 2HBr = BrCH(CH_3)-CH_2Br + H_2O$$
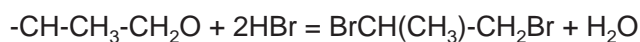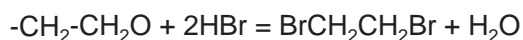
In this way, the content of oxyethylene groups, and therefore, the original polyhydric alcohols, can be determined. Stead and Hindley [94] modified this method and obtained good results for the determination of the oxyethylene group contents of ethylene oxide - propylene oxide copolymers.

3.7.2 Pyrolysis Gas Chromatography

Various workers have described methods for determining alkoxy groups based on thermal degradation of oxyalkylene groups to the corresponding olefin, which is determined by gas chromatography [95-97].

Neumann and Nadeau [96] and Swann and Dux [97] studied the pyrolysis of ethylene oxide, propylene oxide condensates containing various proportions of ethylene oxide. There were no significant differences in the pyrolysis chromatograms of samples heated for 0.5 to 2 hours. The only effect of time of pyrolysis is the total amount of gas produced. The relative concentrations of components are not significantly changed. The temperature of pyrolysis, however, does play a large part in both the amount and type of components in the volatile gases. Between 390 °C and 410 °C there was no noticeable change in products. As the ethylene oxide content of the copolymer increases, so does the amount of ethylene produced. The curve is linear up to about 50% ethylene oxide, then turns sharply upward to an ethylene content of 38.6% for pure PEG. The relative contents of ethylene oxide and propylene oxide in polyethylene - polypropylene glycols has been determined using combined pyrolysis-gas chromatography calibrated with PEG and polypropylene glycol standards [91].

3.7.3 Infrared Spectroscopy

Simak [98] investigated absorptions of the C-O-C group in polyethylene terephthalate in the infrared at 15.82, 15.62 and 26.3 μm. Oxyethylene groups have also been determined [99].

3.7.4 Nuclear Magnetic Resonance Spectroscopy

The determination of the content of oxyethylene groups in ethylene oxide – propylene oxide can also easily be carried out by nuclear magnetic resonance spectrometry [93, 100] without chemical splitting of the ether linkage. However, it is difficult to identify the base compounds by this method. A number of methods for the cleavage of ethers have been studied but few were applied to the identification of the base compounds of the polyurethane polyethers.

Chu and co-workers [101] showed, using ^{1}H- and ^{13}C-NMR, that chlorobutyl rubber and bromobutyl rubbers contained oxymethylene groups.

Bisphenol-A - epichlorohydrin condensates of the following type have been determined by NMR spectroscopy [85], also polycaprolactone polyols (see below), diethylene glycol started caprolactone ester diols:

$$H\,[OCH_2(CH_2)_3{-}CH_2{-}\overset{\displaystyle O}{\overset{\|}{C}}]_xOCH_2CH_2{-}OCH_2CH_2O[\overset{\displaystyle O}{\overset{\|}{C}}{-}CH_2(CH_2)_3CH_2O]$$
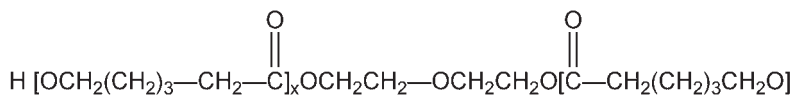
Trimethylol propane started caprolactone, ester triols
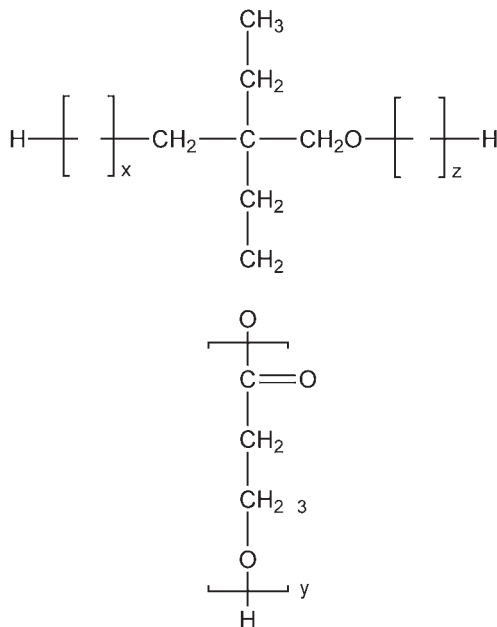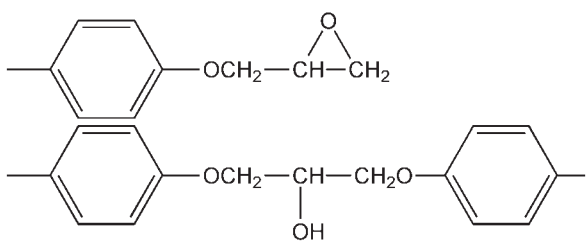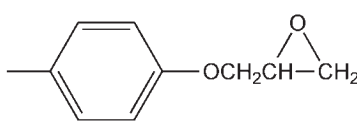
NMR spectroscopy provided information on the number of repeat units (n) in these polymers as well as a set of statistical parameters inherent to the choice of ratioing. The PMR spectra of these three types of polymers are shown in **Figure 3.10 (a) to (c)**.

As an example of the treatment of PMR data proposed by Hammerich and Willeboordse [85] consider the cases of epichlorohydrin - bisphenol-A condensates. **Figure 3.10(a)** exhibits the PMR spectrum of Bakelite epoxy resin ERL-2774, typical of that observed for the diglycidyl ethers of bisphenol A (DGEBA) where the multiplet at 2 ppm is attributable to pentadeuteroacetone. If n represents the number of repeat units, then the assignment and the number of protons contributing to each lettered area are portrayed in **Table 3.11**.

As the unreacted epoxy protons yield two separable areas, areas C and D in Figure 3.10(c) then a total of five distinct areas are observed for DGEBA polymers. Every conceivable ratio of a linearly independent combination of these areas yields a function, f(R), for n. (The ratio of aromatic to gem dimethyl protons is linearly dependent with a constant value of 4/3.)
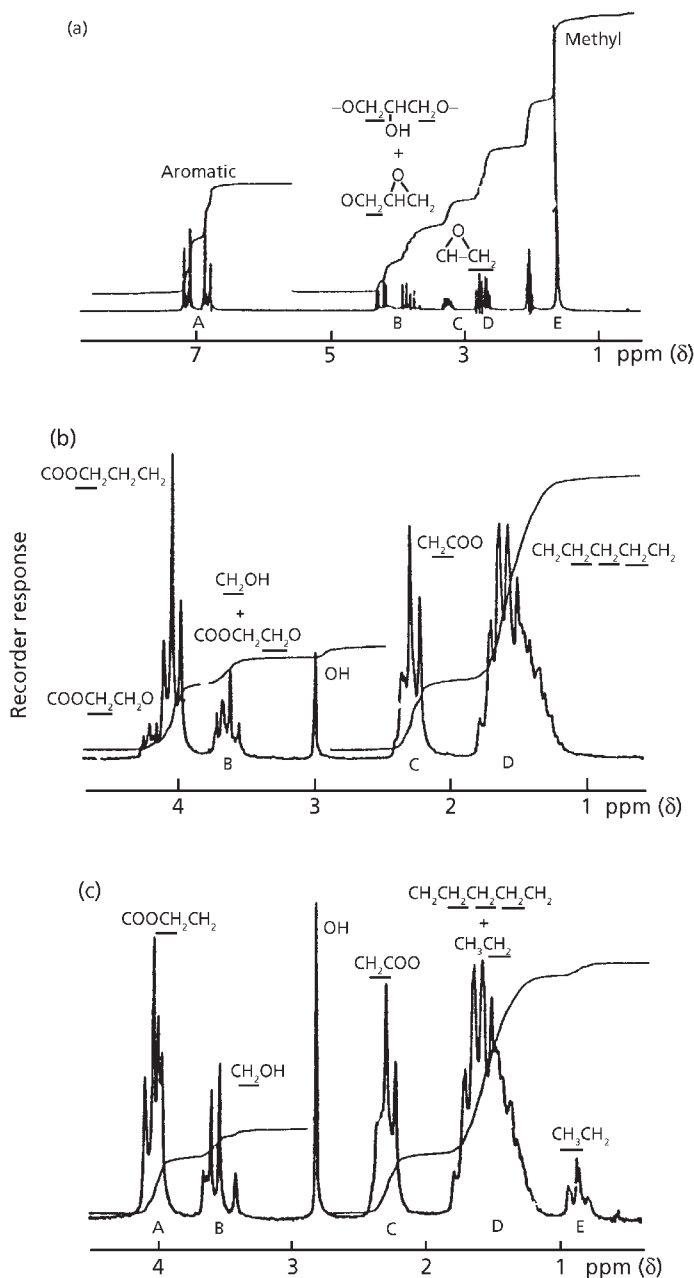
Figure 3.10 PMR spectra of: (a) bisophenol-epichlorohydrin condensate (Bakelite epoxy ERL 2774); (b) Ethylene glycol started caprolacone ester diol (Niox polyol, PCP-0230); (c) Trimethylol propane started caprolactone ester triols (Niax polyol, PCP-0310). (*Reprinted with permission from A.D. Hammerich and F.G. Willeboordse, Analytical Chemistry, 1973, 45, 7, 1696. ©1973, ACS*) [89]

Area	Assignment	No. of protons
Table 3.11 Peak assignments for diglycidl ethers of bisphenol A-based resin (DGEBA) polymers	
A	Aromatic	$6n + 8$
B		$6n + 4$
C + D		6
E	Methyl	$6n + 6$
Reprinted with permission from A.D. Hammerlich, F.G. Willeboorde, Analytical Chemistry, 1973, 45, 7, 1096. ©1973 American Chemical Society [85]	

3.8 Anhydride Groups

Van Houwelingen [13] discussed the determination of anhydride groups in a resin derived from octadecene-1 and maleic anhydride:
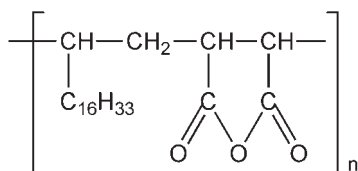
The common method for anhydride groups involving reaction with an excess of aniline and subsequent backtitration of the excess [102] is unsuitable, as the reactivity of the anhydride group is low. Even after hydrolysis with aqueous pyridine (containing 40% *v/v* of water) in a Parr bomb at 150 °C for 4 hours, anhydride groups are still seen in the infrared spectra.

A suitable method for determining the anhydride group is titration with aqueous potassium hydroxide in pyridine after previous esterification of the carboxyl group with diazomethane. This esterification is carried out in diethyl ether methanol (9 + 1). After methylation, which takes about 10 minutes for 0.5 g of sample, the solvents are removed by evaporation and a portion of the derivatised polymer is dissolved in pyridine and titrated. In the infrared spectra of the resin before and after methylation it can be seen that the absorption band of the acid group at 5.84 μm disappears and a carbonyl band of the ester at 5.74 μm is formed. The acid content of the sample is found from the difference in titres of an unmethylated and a methylated product.

3.9 Total Unsaturation

The methods described in this section cover only the determination of total unsaturation. Distinction between different types of unsaturation, (e.g., *cis*, *trans* 1,2, *trans* 1,4) will be discussed in a subsequent volume.

3.9.1 Hydrogenation Methods

Unsaturation in polymers is usually measured by physical techniques, as discussed later. This is especially so in the case of low levels of unsaturation, or in instances where a distinction has to be made between different types of unsaturation. Hydrogenation techniques have been used, however, to measure higher levels (0.5-5.0 mole%) of total unsaturation in polymers, a good example of which is the determination of terminal unsaturation in polystyrene oligomers [103-105] (low molecular weight polymers), e.g., polystyrene dimer:

$$2PhCH = CH_2 \rightarrow PhCH_2 - CH = CH - CH_2Ph$$

3.9.2 Halogenation Methods

In acidic medium potassium, bromide and potassium bromate produce bromine stoichiometrically, and this is the basis of a titration method [106] for determining double bonds in polymethylmethacrylate. After bromination, excess bromine is estimated by the addition of potassium iodide, and the iodine produced estimated by titration with standard sodium thiosulfate to the starch end-point:

$$KBrO_3 + 5KBr + 6HCl = 3Br_2 + 3H_2O + 6KCl$$
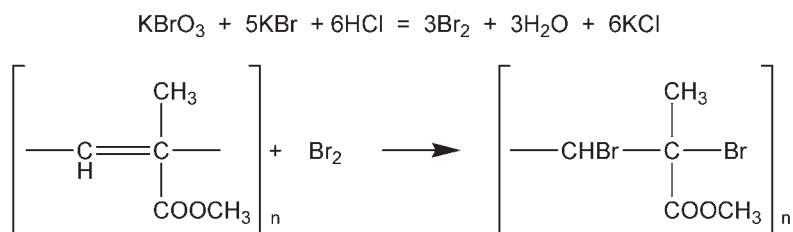
Hensen and Eatough [107] have described a direct injection enthalpimetric determination of residual total unsaturation in polymers which is based on the heat produced during the bromination of double bonds. Koltoff and Mitarb [108] and Boyers [109] both discuss the application of bromination to the determination of total unsaturation in di and polyolefins. McNeil [110, 111] has discussed methods for the determination of total unsturation based on chlorination with radiochlorine (^{35}Cl). This method, with slight modification, is capable of determining unsaturation at the 0.01 to 0.1 mole% level. If the specific activity of the radiochlorine in the gas phase is known, the weight of chlorine in the polymer can be found by counting. The mole% unsaturation of the polymer is calculated from the weight% unsaturation by assuming that one atom of chlorine enters the polymer per double bond producing a monocholoro compound. With this assumption it was found that polyisobutene consumes a mean of 1.2 chlorine atoms per double bond producing a monocholoro compound. This is probably an indication that side-reactions, such as addition of chlorine, are occurring to a small extent. Since the true unsaturation is close to one double bond per chain it follows that the main chain-breaking reaction during the cationic polymerisation of isobutene is proton transfer.

Chemical methods for the determination of unsaturation are often based on halogenation or hydrogenation. An elegant method for determining unsaturated compounds is the *in situ* generation of a halogenating agent (e.g., bromine) by constant-current coulometry. The amount of reagent consumed is proportional to the amount of electricity used to generate the reagent. The reaction between the double bond and bromine is catalysed by mercury(II) chloride. The advantages of a coulometric method are that a standard reagent is not needed, minimum side-reactions (substitution) occur because the bromine concentration is kept low, and the method is precise and is suitable for low levels and can be readily automated.

A survey of applications has been given by Hirozawa and co-workers [112].

Von Houwelingen [13] has used coulometric bromination to determine vinyl ester end-groups in polyethylene terephthalate formed by thermal chain scission with the subsequent liberation of acetaldehyde:
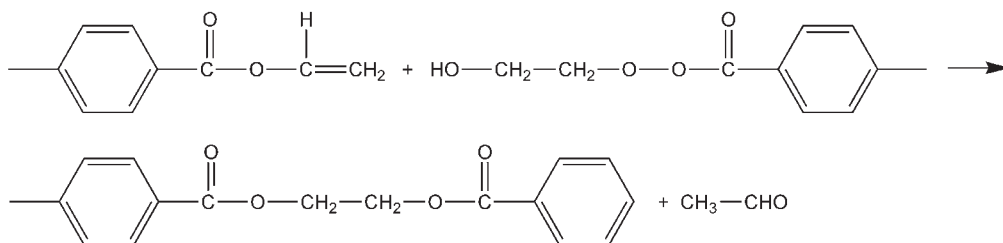
The constant-current generation of bromine is carried out in a medium of dichloroacetic acid, hexafluoroisopropanol, water, potassium bromide and mercury(II) chloride. To this medium an amount of the polymer, previously dissolved in hexafluoroisopropanol and diluted with anhydrous dichloroacetic acid, is added and bromine is generated. The end of the reaction is detected biamperometrically. The suitability of this method was tested against methyl vinyl terephthalate:
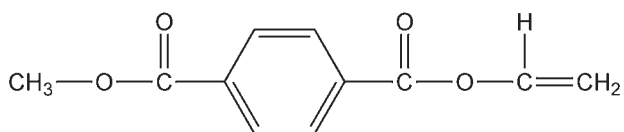
Additions of 14.2 and 1.0 μmol of methyl vinyl terephthalate (corresponding to 30 and 2 μmol of vinyl ester end groups per kilogram of polymer) were recovered quantitatively (recoveries of 99.8 and 98.5%, respectively). The coulometric analysis must be completed within 30 minutes because after longer times the hydrolysis of the vinyl ester end group is no longer negligible.

The vinyl ester end group is not the only reactive moiety in polyethylene terephthalate that consumes bromine, as impurities present also do so. To determine this background in a second sample the vinyl ester end group is previously hydrolysed at 80 °C in a dichloroacetic acid - water medium, **Figure 3.11 (a)** shows the relationship between the bromine consumption and the hydrolysis time for methyl vinyl terephthalate and **Figure 3.11 (b)** represents the same relationship for two polymers containing a high and negligible amount of vinyl ester end groups.

It can be seen that the vinyl ester end group in methyl vinyl terephthalate is hydrolysed completely after 4-6 hours at 80 °C. For polymer A shown in **Figure 3.11**, a sharp decrease occurs, which can mainly be attributed to the hydrolysis of the vinyl ester end group in the polymer. In addition, a much smaller effect is observed due to the hydrolysis of the consuming impurities (see relationship for polymer B, **Figure 3.11 (b)**). This small effect is corrected by extrapolating this relationship from time 6 hours to time zero, i.e., 0.7 mmol/kg.
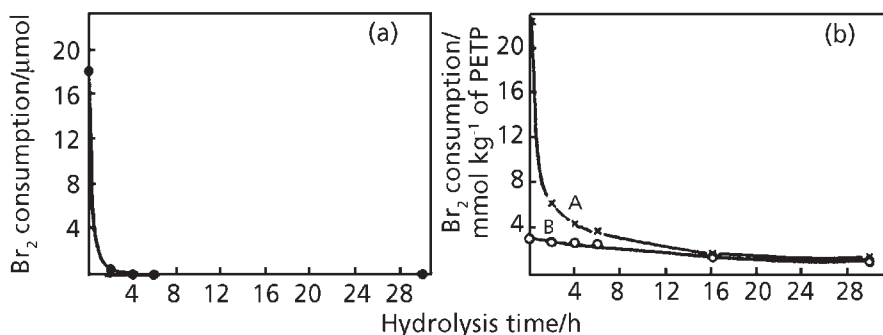
Figure 3.11 (a) Hydrolysis of methylvinyl terephthalate; (b) hydrolysis of vinyl ester end groups in PET; (A) PET with a high vinyl ester end group level; (B) PET with a negligible vinyl ester end group level. (*Reprinted with permission from G.D.B. van Houwelingen, Analyst, 1981, **106**, 1267, 1057. ©1981, RSC*) [13]

The vinyl ester end-group content is calculated by subtracting the background, i.e., the value measured after 6 hours hydrolysis + 0.7 mmol/kg, from the content originally measured. The standard deviation of the method is 0.2 mmol/kg.

3.9.3 Iodine Monochloride Procedures

Most of the published work on the determination of functional groups, not unexpectedly, has been carried out on copolymers. This is because the determination of a functional group that is specific to one of the copolymer constituents is the key to the determination of the monomer ratios in the copolymer, see Chapter 4.

Styrene-butadiene copolymers contain residual double bonds which enable the butadiene content of the copolymer to be determined:

$$Ph-CH=CH_2 \ + \ CH_2=CH-CH=CH_2 \ \longrightarrow \ -CH-CH_2-CH_2-CH=CH-CH_2-$$
$$\qquad\qquad\qquad\qquad\qquad\qquad\qquad\qquad\qquad\qquad | $$
$$\qquad\qquad\qquad\qquad\qquad\qquad\qquad\qquad\qquad\quad Ph$$
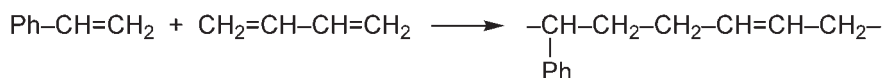
In this procedure the polymer is reacted with an excess of standard iodine monochloride dissolved in glacial acetic acid (Wijs reagent):

$$-CH-CH_2-CH_2-CH=CH-CH_2- \ + \ ICl \ \longrightarrow \ -CH-CH_2-CH_2-CHI-CH-CH_2-$$
$$\ \ |\qquad\qquad\qquad\qquad\qquad\qquad\qquad\qquad\qquad\qquad\qquad\quad | $$
$$\ \ Ph\qquad\qquad\qquad\qquad\qquad\qquad\qquad\qquad\qquad\qquad\quad Ph$$
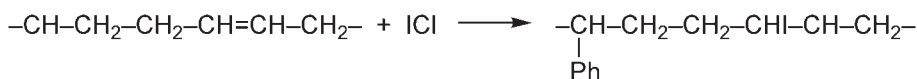
After completion of the reaction, excess iodine monochloride is reacted with potassium iodide and the liberated iodine estimated by titration with standard sodium thiosulfate:

ICl + KI = KCl + I$_2$
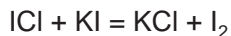
The double bond content of the original polymer can be then calculated from the measured consumption of iodine monochloride.

Crompton and Reid [113] have described procedures for the separation of high impact polystyrene, i.e., styrene-butadiene copolymer, into the free rubber plus rubber grafted polystyrene plus copolymerised rubber and a gel fraction and for estimating total unsaturation in the two separated fractions. To separate a sample into gel and soluble fractions it was first dissolved in toluene. Only gel remains undissolved. Methanol is then added, which precipitates the polystyrene - rubber graft, ungrafted rubber and polystyrene. Any styrene monomer, soap or lubricant remain in the liquid phase, which is separated from the solids and rejected.

The addition of toluene to the solids dissolved all the polymeric material with the exception of the gel. The toluene solubles are separated from the solid gel by centrifuging and made up to a standard volume with toluene. The gel is then dried in vacuum and weighed.

Both the gel and toluene soluble fractions are reserved for determination of unsaturation by the iodine monochloride method. To determine unsaturation in styrene-butadiene rubbers with good accuracy using the iodine monochloride procedure, it was found necessary to contact the sample with chloroform for 15 hours before reaction with iodine monochloride. Even with a 30 hour reaction period, a constant iodine-value is obtained only when a five-fold excess of iodine monochloride reagent is used.

The solid gel, separated from a high impact polystyrene by solvent extraction procedure, is completely insoluble in chloroform and in the iodine monochloride reagent solution. A contact time with chloroform of 90 hours then a 75 hour reaction period with reagent is required.

Crompton and Reid [113] used these procedures to study the distribution of rubber added in several laboratory preparations of high impact polystyrene containing 6 wt% of a styrene-butadiene rubber and 94% styrene, i.e., theoretical 4.1% butadiene. The results in **Table 3.12** show the way in which the added unsaturation of 4.1% butadiene distributes between the gel and soluble fractions; the butadiene content of the separated gel remains fairly constant, in the 20-25% region, regardless of the quantity of gel present in the sample. As the gel content

Table 3.12 Distribution of butadiene between soluble and gel fractions obtained from polystyrenes containing different amounts of gel					
Gel content of sample (wt%)	Butadiene content isolated gel (wt%)	Soluble graft butadiene content A (calculated on original sample) (wt%)	Gel butadiene content B (calculated on original sample) (wt%)	Total butadiene (A + B) (calculated on original sample) (wt%)	Amount of original rubber unsaturation in the sample C = (A + B) × 100%
		3.5		3.5	85
4.7	19.5	2.8	0.0	3.7	90
5.6	16.2	2.9			
	0.9	3.8	93		
8.9	23.3	1.5	2.1	3.6	88
11.8	20.0	1.5	2.4	3.9	95
Source: Author's own files					

increases, therefore, so more of the rubber becomes incorporated into the gel and less remains as free rubber or soluble graft. The recovered unsaturation lies mainly in the 90-95% region, indicating that loss of unsaturation due to grafting or crosslinking reactions occurs only to the extent of some 5-10%.

The iodine monochloride method has been used for a variety of polymers. These polymers include those which are highly unsaturated, such as polybutadiene and polyisoprene [114-117] and polymers having low unsaturation such as butyl rubber [118] and ethylene propylene diene terpolymer. Considerable work has been done investigating the side reactions of iodine monochloride with different polymers [118]. These side reactions are substitution and splitting out rather than the desired addition reaction.

Albert [119] has compared determinations of butadiene in high-impact polystyrene (HIPS) by an infrared method and by the iodine monochloride method described by Crompton and Reid [113]. The infrared method is based on a characteristic absorbance in the infrared spectrum associated with the transconfiguration in polybutadiene:

Transpolybutadiene units

cis polybutadiene units

Since different grades of HIPS may contain elastomers with different *trans*-butadiene contents, calibration curves based on the standard rubber are not always suitable for analysing these products. The results obtained by the two methods for several high-impact grades are compared in **Table 3.13**. The rubber content of HIPS sample 1 determined by titration is lower than the value obtained by the infrared method.

Table 3.13 Rubber content of HIPS (based on PBD)		
Sample	**Polybutadiene %w (iodine monochloride)**	**Polybutadiene %w (IR method)**
Standard: 6.0%w diene 55	6.2	-
Standard: 12%w diene 55	12.2	-
Standard: 15%w diene 55	14.8	-
HIPS 1	8.6	9.7
HIPS 2	5.6	5.8
HIPS3	9.0	1.2
HIPS 4	11.2	11.4
HIPS 5	5.8	5.9
Reprinted from N.K. Albert, Woodbury Research Laboratory, Shell Chemical Company, Woodbury, USA, private communication		

This is expected on interpolymerised polymers because of crosslinking, which reduces the unsaturation of the rubber. The other polymers (except sample 3), appear to contain diene-55 type rubber of high *trans*-butadiene content, since reasonable agreement was obtained between the iodine monochloride and infrared methods. HIPS 3, however, must contain a polybutadiene of high *cis*-content to explain the low (1.2%w) amount of rubber found by the infrared method compared to the 9.0% found by the titration method.

3.9.4 Infrared Spectroscopy

Fraga [120] has described an infrared thin-film area method for the analysis of styrene-butadiene copolymers. The integrated absorption area between 6.6 and 7.2 µm has been found to be essentially proportional to total bound butadiene, and is independent of the isomeric type of butadiene structure present. This method can be calibrated for bound styrene contents ranging from 25 to 100%.

Infrared spectroscopy and pyrolysis gas chromatography have been used for the determination of unsaturation in ethylene-propylene-diene terpolymers [121]. Determination of extinction coefficients for the various terpolymers is required for quantitive work.

Brako and Wexler [122] have described a useful technique for testing for the presence of unsaturation in polymer films such as polybutadiene and styrene-butadiene. They expose the film to bromine vapour and record its spectrum before and after exposure (**Figure 3.12**). This results in marked changes in the infrared spectrum. Noteworthy is the almost complete disappearance of bands at 13.691, 10.99, 10.36, and 6.10 µm associated with unsaturation. A pronounced band possibly associated with a C-Br vibration appears at 12.02 µm which is due to exposure to bromine vapour. Exposure of butadiene-styrene copolymer (**Figure 3.12**) to bromine vapour results in the disappearance of bands at 10.99 and 10.36 µm associated with unsaturation in the butene component of the copolymer. Some alteration of the phenyl bands at 14.28 and 10.37 µm is evident. The loss of a band at 6.45 µm and the appearance of a band at 5.88 µm are probably due to the action of acidic vapours on the carboxylate purifactant of the latex.

Raman spectroscopy has been applied to the determination of unsaturation in styrene - butadiene – methylmethacryalate terpolymers [120,123,124].

Panyszach and Kovar [125] have shown that results accurate to within 2.5% can be obtained in determinations by FTIR of the butadiene content of styrene – butadiene copolymers. Infrared methods are reported to have serious disadvantages when applied to the determination of unsaturation in vulcanisates [126–130].
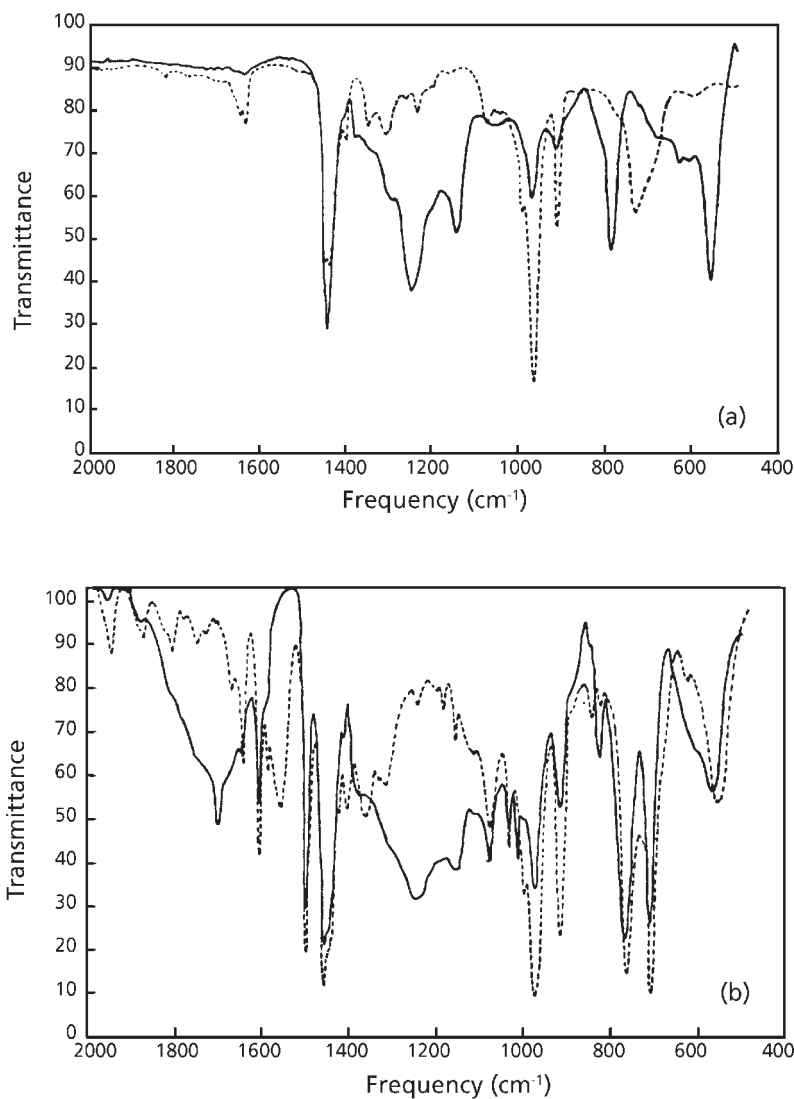
Figure 3.12 (a) Spectra of polybutadiene and of the film after exposure to bromine: --- polybutadiene; — polybutadiene after exposure to bromine vapour; (b) Spectra of styrene-butadiene copolymer film and of copolymer film after exposure to bromine vapour: --- styrene-butadiene copolymer; — copolymer after exposure to bromine vapour. (*Reprinted with permission from F. D. Brako and A. S. Wexler, Analytical Chemistry, 1963, 35, 12, 1944. ©1963, ACS*) [122]

3.9.5 Nuclear Magnetic Resonance Spectroscopy

NMR spectroscopy is capable of distinguishing between the different types of unsaturation that can occur in a polymer and has been used to determine unsaturation in acrylonitrile-butadiene-styrene (ABS) terpolymers [131, 132], 1, 2-polybutadiene [122, 132], ethylene-propylene terpolymers [122], and vinyl chloride-vinylidene chloride copolymers [120, 133, 134].

Regarding ABS terpolymers [135], NMR is capable of determining ungrafted butadiene rubber in solvent extracts of these polymers. No aromatic protons of styrene or acrylonitrile protons are seen in the NMR spectra. The vinyl content of the polybutadiene is about 20%.

Sewell and Skidmore [136] used time averaged NMR spectroscopy at 60 MHz to identify low concentrations of non-conjugated dienes such as cyclopentadiene, 1,4-hexadiene, or ethylidene norbornene introduced into ethylene-propylene copolymers to permit vulcanisation. Although infrared spectroscopy [137] and iodine monochloride unsaturation methods [138] have been used to determine or detect such dienes, these two methods can present difficulties. The spectra obtained by time averaged NMR are usually sufficiently characteristic to allow identification of the particular third monomer incorporated in the terpolymer. Moreover, as the third monomer initially contains two double bonds, differing in structure and reactivity, the one used up in copolymerisation may be distinguished from the one remaining for subsequent use in vulcanisation. Therefore, information concerning the structure of the remaining unsaturated entity may be obtained. **Table 3.14 s**hows the chemical shifts of olefinic protons of a number of different third monomers in the terpolymers.

Altenau and co-workers [139] applied time averaging NMR to the determination of low percentages of termonomer such as 1,4 hexadiene, dicyclopentadiene, and ethylidene norbornene in ethylene-propylene termonomers. They compared results obtained by NMR and the iodine monochloride procedure of Lee and co-workers [140]. The chemical shifts and splitting pattern of the olefinic response were used to identify the termonomer. **Table 3.15** compares the amount of termonomer found by the NMR method of Altenau and co-workers [139] and by iodine monochloride procedures. The termonomers were identified by NMR and IR spectroscopy.

Table 3.15 shows that the data obtained by the NMR method agree more closely with the Lee [140] iodine monochloride method than with the iodine monochloride method [141]. The difference between the latter two methods is best explained on the basis of side reactions occurring between the iodine monochloride and the polymer because of branching near the double bond [140]. The reason for the difference between the NMR method and the method of Lee and co-workers [140] is not clear.

Table 3.14 Determination of non-conjugated dienes in copolymers	
Third monomer	**Chemical shift (ppm)**
1,5-Cyclooctadiene	4.55
Dicyclopentadiene	4.55
1,4-Hexadiene	4.7
Methylene norbornene	5.25 and 5.5
Ethylidene norbornene	4.8 and 4.9

Table 3.15 Determination of termonomer in ethylene-propylene diene terpolymers - comparison of methods (data shown as weight % terpolymer)			
NMR	**Iodine monochloride [140]**	**NMR [139, 141]**	**Termonomer**
7.3	3.0		Dicyclopentadiene
1.1	1.6		1,4-Hexadiene
5.7	5.9	9.0	Ethylidene norbornene
2.8	3.6	4.5	Ethylidene norbornene
1.7	2.3	4.8	Ethylidene norbornene
4.6	5.4	6.0	Ethylidene norbornene
Reprinted with permission from A.G. Altenau, L.M. Headley, S.O. Jones and S.C. Rensaw, Journal of Polymer Science A-1, 1970, 42, 1280. ©1970, John Wiley and Sons [139]			

The reproducibility of the NMR method was ± 10-15 %.

3.9.6 Pyrolysis Gas Chromatography

Van Schooten and Evenhuis [142, 143] applied their pyrolysis (500 °C) – hydrogenation-gas chromatographic technique to unsaturated ethylene-propylene

copolymers, i.e., ethylene-propylene-dicyclopentadiene and ethylene-propylene-norbornene terpolymers. The programs show that very large cyclic peaks are obtained from unsaturated rings: methyl cyclopentane is found when methyl norbornadiene is incorporated; cyclopentane when dicyclopentadiene is incorporated; methylcyclohexane and 1,2-methylcyclohexane when the addition compounds of norbornadiene with isoprene and dimethylbutadiene, respectively, are incorporated; and methylcyclopentane when the dimer of methylcyclopentadiene is incorporated. The saturated cyclopentane rings present in the same ring system in equal concentrations, however give rise to peaks which are in order of magnitude smaller. Therefore, the peaks which stem from the termonomer could be used to determine its content if a suitable calibration procedure could be found.

Van Schooten and Evenhuis [142, 143] subjected a number of terpolymers containing dicyclopentadiene, and having different amounts of unsaturation, to pyrolysis-gas chromatographic analysis, and plotted the height of the characteristic peaks (or ratio of the heights of these peaks to the height of the *n*-C peak) against unsaturation measured by ozone absorption [144]. A linear relationship was found between peak height ratio and ozone unsaturation up to about 16 double bonds per 1000 atoms. Similar curves were found for the methylcyclopentane or ethylcyclopentane peaks.

McKillop [145] found that the application of pyrolysis – gas chromatography to the determination of unsaturation in vulcanisates had serious disadvantages. Vinyl groups in styrene-divinyl benzene copolymer have been determined by pyrolysis – mass spectrometry [146].

3.10 Ethylene Glycol, 1,4-Butane Diol, Terephthalic Acid and Isophthalic Acid Repeat Units in Terylene

Terylene is manufactured from terephthalic acid and ethylene glycol as follows:
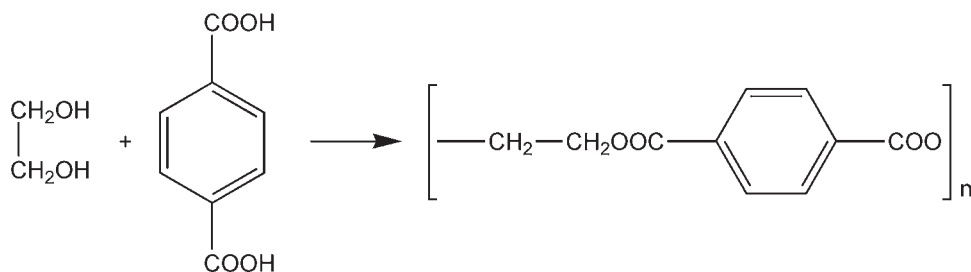
Such polymers contain repeat units based on ethylene glycol (and indeed other glycols such as 1,4-butane diol) and terephthalic acid and proportions of isophthalic acid.

Allen and co-workers [147] developed a precise quantitative method for determining such units in Terylene. The sample is subject to an alkaline hydrolysis and glycol and acidic products after conversion to the trimethylsilylderivatives are analysed by gas chromatography.

In this method the sample is weighed into a 100 ml flask and 50 ml of 1 N potassium hydroxide in 2-ethoxyethanol is added. A condenser cooled by chilled water is attached and the reaction mixture is protected from carbon dioxide by means of a tube packed with Ascarite absorbent and Drierite desicant. The contents of the flask are heated and maintained at reflux temperature for 10 minutes with constant stirring. The flask is allowed to cool to room temperature and the hydrolysate is adjusted to a pH of 1 using concentrated hydrochloric acid (5 ml). An internal standard is added to the flask. Pyridine (25 ml) is added to dissolve the acids present and an aliquot is centrifuged to remove the potassium chloride. Approximately 50 µl of hydrolysed sample is allowed to react at room temperature for 5 to 10 minutes with 500 µl of *N,O*-bis(trimethylsilyl) trifluoracetamide to form silyl ethers and esters of the glycols and acids, respectively. The silyated hydrolysate is chromatographed by injecting 0.1 µl of sample into the gas chromatograph.

The silyl derivative of diethylene glycol is separated from the silyl derivative of ethylene glycol using a 3 m × 3.2 mm stainless steel column packed with 100-200 mesh Chromosorb G-HP solid support containing 3% by weight of Versilube F-50 liquid phase, (a mixture of trichlorophenyl silicone (10%) and methyl silicone manufactured by General Electric).

Figure 3.13(a) is a chromatogram obtained for the silyl derivatives of the hydrolysate of a polyethylene terephthalate. Dodecane is used as an internal standard and the column is operated isothermally at 127 °C with a nitrogen carrier gas flow rate of 10 ml/min.

Figure 3.13(b) is a chromatogram of the silyl derivatives of ethylene glycol, 1,4-butanediol and the *cis* and *trans* isomers of 1,4-cyclohexanedimethanol from the hydrolysate of an experimental polyester. A 1.8 m × 6.4 mm glass column packed with 100-200 mesh Chromosorb W-HP solid support containing 10% by weight of Versilube F-50 liquid phase is used for this separation. Nonyl alcohol is used as an internal standard and the column is operated at 120 °C for 8 minutes and programmed to 210 °C at 4 °C/min with a nitrogen carrier gas flow rate of 20 ml/min.

High-boiling acids, such as terephthalic and isophthalic acids, are separated using a 1.8 m × 3.2 mm stainless steel column packed with 100-200 mesh Chromosorb W-HP solid support containing 10% by weight Versilube F-50 liquid phase. **Figure 3.13(c)** is the chromatogram obtained for the separation of the silyl derivatives of isophthalic and
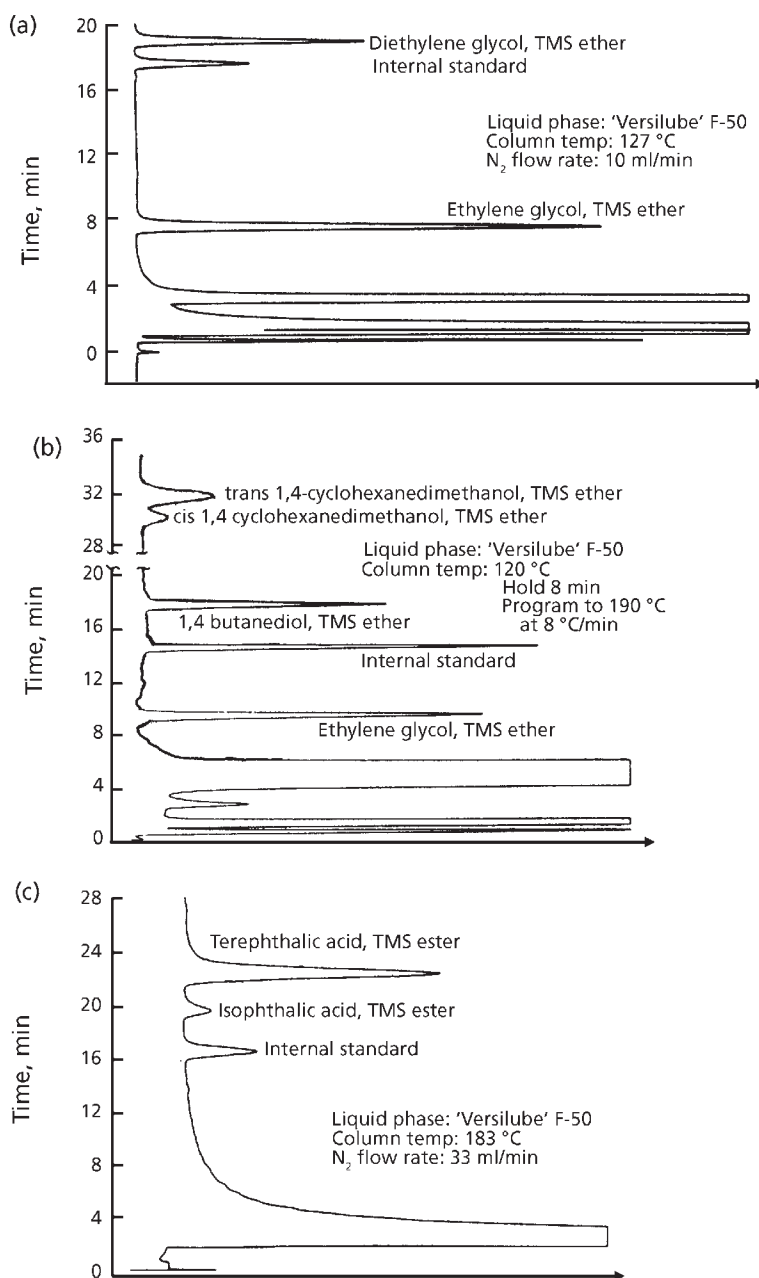
Figure 3.13 Chromatogram of (a) trimethylsilyl derivatives of the glycols from the hydrolysis of PET; (b) silylated glycols from experimental polyesters; (c) iso and terephthalaic acids, (*n*-heptadecane as internal standard). (*Reprinted with permission from B.J. Allen, G.M. Elsea, K.P. Keller and H.D. Kinder, Analytical Chemistry, 1977, 49, 6, 741. ©1977, ACS*) [147]

terephthalic acid from an experimental polyester. The column is operated isothermally at 183 °C with a nitrogen carrier gas flow rate of 33 ml/min. *N*-Heptadecane was added as an internal standard to permit the calculations of the weight per cent acids.

Another important use of the alkaline hydrolysis/gas chromatographic procedure is the determination of methyl ester end groups. If the polyester is terminated with methyl ester end groups, then methyl alcohol is produced when the polyester is hydrolysed. By determining the concentration of methyl alcohol, one can calculate the number of methyl ester end groups in polyethylene terephthalate. The hydrolysis procedure for determining methyl ester end groups is the same as discussed for the glycols and acids. The gas chromatographic procedure is different in that no silylation reagent is used. The hydrolysed sample is separated using a 1.8 m × 6.4 m glass column containing 60-80 mesh Chromosorb 102 column packing.

Propyl alcohol is used as the internal standard, and the column is operated isothermally at 145 °C with a nitrogen carrier gas flow rate of 10 ml/min.

The precision of the overall method is good. This method is relatively simple and fast. It has been used to analyse experimental polyester for the amount of monomers present in the repeat units and for determining the composition of copolymers and polymer blends.

It has been observed that in the preparation of polyester for compositional analysis by NMR spectroscopy, much higher rates of hydrolysis are achieved by refluxing polyethylene terephthalate with a mixture of sodium hydroxide, an alcohol (methanol) and a protic solvent (dimethyl sulfoxide) than is achieved with the usual alcoholic alkali reagents [148].

3.11 Oxirane Rings

Oxirane rings in epoxy resins have been determined by ring cleavage with pyridine-hydrochloric acid [149]. Cleavage with pyridine-hydrochloric acid, glacial acetic acid, hydrobromic acid or dioxin-hydrochloride have all been employed as methods of cleavage [150, 151] of oxirane rings prior to their determination.

3.12 Amino Groups

Amino groups have been determined by acetylation with acetic hydride in dimethyl acetamide. Diethylamine was added and the excess amine was titrated potentiometrically [152].

Two indirect titration procedures have been described for the determination of amino end groups in aromatic polyamides. One method involves the reaction of the amine with salicylaldehyde to form the Schiff base. After precipitation of the polymer, the excess, unreacted aldehyde is titrated with potassium hydroxide [153].

Heterogeneous derivitivisation with 1-fluoro,2,4-dinitrobenzene has been used to determine amino groups in polyethylene terephthalate [13]:
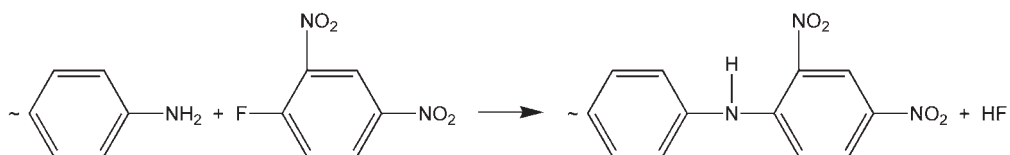
The polymer is treated for 4 hours at 80 °C with 1-fluoro-2,4-dinitrobenzene in an ethanol hydrogen carbonate medium. After washing out the excess of reagent, the dinitrophenyl group introduced is measured spectrophotometrically at 430 nm after dissolution of the derivatised polymer in methane sulfonic acid.

The spectrophotometric method was calibrated with the 1-fluoro-2,4-dinitrobenzene derivative of the model compound *N,N'*-bis(*p*-amino-phenyl) terephthalamide:
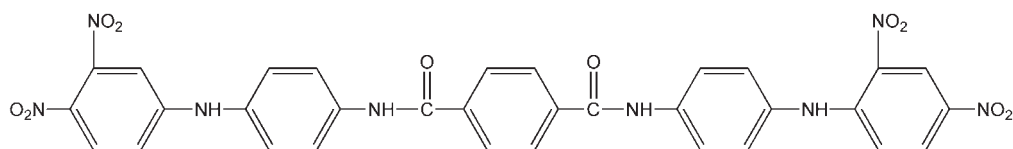
The correctness of the whole procedure was confirmed by the use of ^{14}C labelled 1-fluoro-2,4-dinitrobenzene and measurement of the incorporated activity.

Spectroscopy using *p*-aminobenzaldehyde [154] or ninhydrin [155] or dimethoxytrityl chloride [156] has been used to estimate primary amino groups in polymers. A spectrofluorimetric method has also been described [157].

3.13 Amido and Imido Groups

3.13.1 Alkali Fusion Reaction Gas Chromatography

Schleuter and Siggia [158, 159] and Frankoski and Siggia [160] used the technique of alkali fusion reaction gas chromatography for the analysis of imide monomers
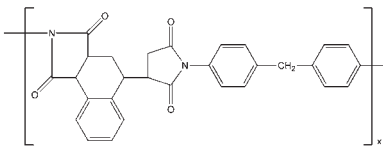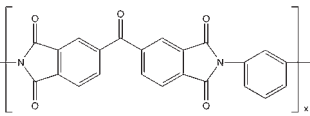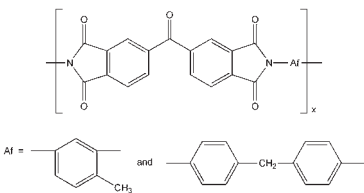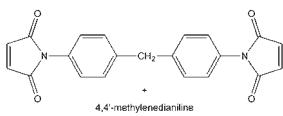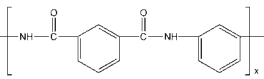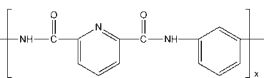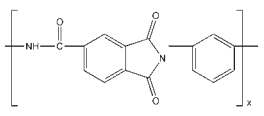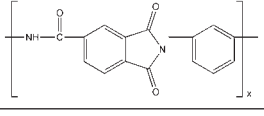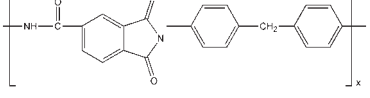
and aromatic polyimides, polyamides and poly(amide-imides) (see Method 3.6 at end of this chapter).

Samples are hydrolysed with a molten potassium hydroxide reagent at elevated temperatures in a flowing inert atmosphere. Volatile reaction products are concentrated in a cold trap before separation by gas chromatography. The identity of the amine and/or diamine products aids in the characterisation of the monomer or polymer; the amount of each compound generated is used as the basis for quantitative analysis:
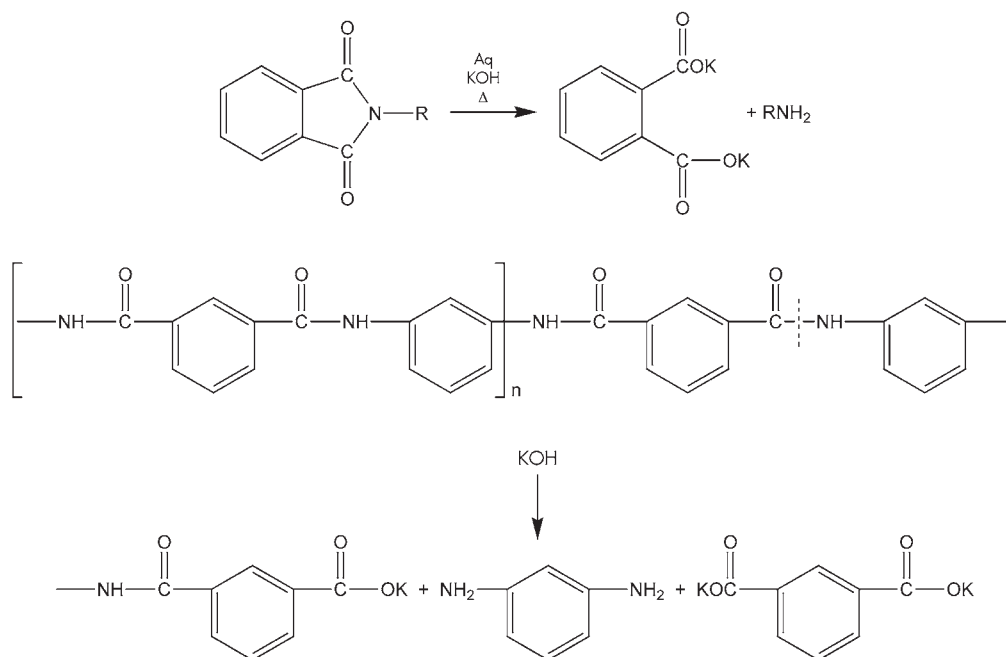
The average relative standard deviation of the method is ± 1.0%.

Table 3.16 summarises the chemical structures and sample designations of the polymers studied. The weight percent of adsorbed water and the decomposition temperature, both determined by thermogravimetric analysis, are also included. The water content was needed to calculate the dry weight of polymer in each sample. It was not possible to simply dry and weigh the polymers, because they tended to reabsorb moisture from the atmosphere too rapidly. **Table 3.17** summarises the diamine recoveries obtained with isothermal (5 minutes at 380 °C) and programmed reaction temperatures (100 to 390 °C over 30 minutes). These numbers represent the mole per cent of theoretical diamine based on the dry weight of sample and the idealised linear polymer repeat units depicted in **Table 3.16**. Recoveries were, in all cases, between 90 and 101% of theory. The amount of diamine recovered from a polymer reacted isothermally, was within ± 3%

Table 3.16 Structure, water content and decomposition temperature of the polymers studied			
Designation	Structure of repeat unit	Wt% water	Decomposition temperature, °C
PI-1		6.5	385
PI-2		2.2	410
PI-3		3.4	410
PI-4		0.6	310
PA-1		5.8	315
PA-2		9.7	330
PAI-1		6.2	340
PAI-2		12.6	395
PAI-3		8.9	340
Reprinted with permission from S.P. Frankoski and S. Siggia, Analytical Chemistry, 1972, 44, 3, 507. ©1972, American Chemical Society [160]			

Sample	Diamine produced	Mol % of theoretical[a] ± RSD[b]	
		5 min at 380 °C	**30 min from 100 to 390 °C**
PI-1	4,4′-Methylenedianiline	98.3 ± 0.8	97.5 ± 0.9
PI-2	*m*-Phenylenediamine	89.1 ± 0.7 91.2 ± 0.9 91.6 ± 1.3	91.0 ± 0.8 91.0 ± 0.7
PI-3	2,4-Toluenediamine 4,4′-Methylenedianiline	73.1 ± 0.2 97.8 ± 0.5 24.8 ± 0.3	73.2 ± 1.0 99.1 ± 1.2 25.9 ± 0.2
PA-1	*m*-Phenylenediamine	100.7 ± 0.6	97.0 ± 1.7 97.7 ± 1.7 97.9 ± 1.0 99.6 ± 2.6
PA-2	*m*-Phenylenediamine	100.7 ± 0.6 96.4 ± 1.5	92.9 ± 1.0 93.3 ± 0.6
PAI-1	*m*-Phenylenediamine	93.5 ± 0.9	93.1 ± 0.7 95.3 ± 0.5
PAI-2	*m*-Phenylenediamine	93.5 ± 1.1 94.1 ± 0.6 95.1 ± 1.2	97.4 ± 0.9
PAI-3	4,4′-Methylenedianiline	98.0 ± 1.1	98.8 ± 1.1

Table 3.17 Analysis of polyimides, polyamides and poly(amide-imides by alkali fusion reaction gas chromatography

[a] *These recovery values are based on the structure shown in Table 3.16, which assume that one mole of diamine is produced foreach mole of repeat unit.*
[b] *The relative standard deviation is based on five or more determinations.*
Reprinted with permission from S.P. Fronkoski and S. Siggia, Analytical Chemistry, 1972, 44, 3, 507. ©1972, American Chemical Society [160]

of the amount produced by the programmed temperature approach. Average percentage relative standard deviations were similar in both cases (± 0.9% *versus* 1.1%).

Figure 3.14(a) shows the reaction gas chromatogram obtained from poly(amide-imide) PAI-2. Only one diamine was produced. The chromatogram in **Figure 3.14(b)** obtained from the fusion reaction of the polyamide terpolymer PI-3, contains peaks for each diamine. The quantitative analysis of both products revealed that the weight ratio of 2,4 toluene diamine to 4,4′-methylenedianiline in the polymer was 2:1.
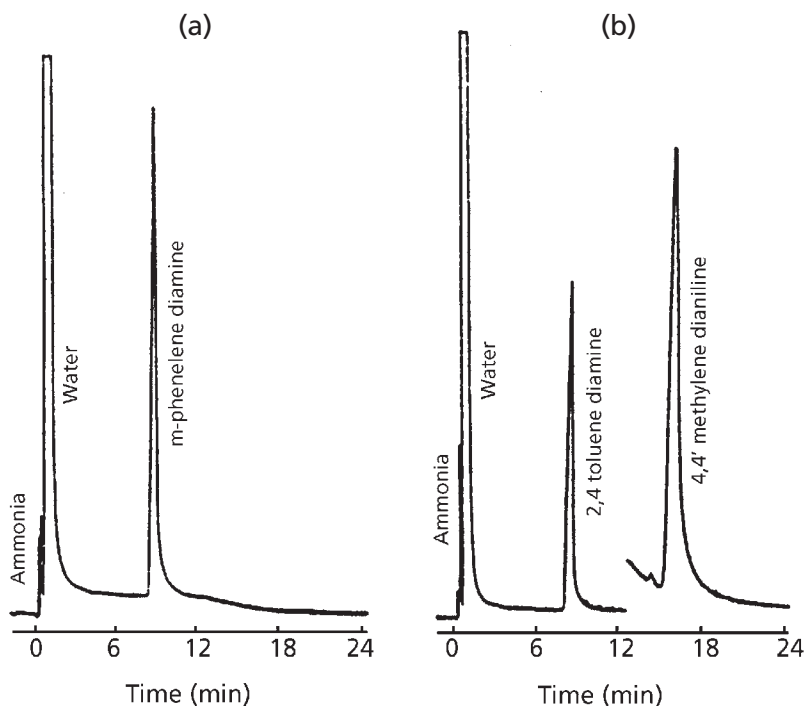
Figure 3.14 Alkali fusion reaction gas chromatogram produced from (a) polyamide-imide (PAI-2). The column temperature was programmed from 100 to 250 °C at 12 °C/min; (b) polyamide terpolymer (PI-3). The column temperature was programmed from 100 to 250 °C at 12 °C/min. (*Reprinted with permission from S.P. Frankoski and S. Siggia, Analytical Chemistry, 1972, 44, 3, 507. ©1972, ACS*) [160]

In an attempt to correlate the alkali fusion recoveries (expressed as weight percent nitrogen) with the elemental nitrogen analyses of the polymers, it was noted that the elemental nitrogen analyses of the polymers were higher. Analysis of the fusion residue indicated that no detectable amounts of nitrogen were present. This led to the discovery that ammonia was also produced from the samples. When the nitrogen contribution from ammonia was added to that of the diamine, the total was in good agreement with the elemental value. **Table 3.18** lists the results obtained from the analysis of mixtures of polymers. The amount of *m*-phenylenediamine produced was, in all cases, within 1.2% of the theoretical value.

Haken and co-workers [161] described an analytical procedure for the rapid qualitative analysis of polyurethane elastomers, based on polycaprolactonediols (CAPA). These thermoplastic polyurethanes are a complex reaction product of an

Polymer mixture	Micromoles of *m*-phenylenediamine			Recovery (%)
	Taken*		Found	
PI-2	2.24			
PAI-2	9.26	11.50	11.36	98.8
PA-1	7.23			
PA-2	7.43	14.66	14.71	100.3
PAI-1	4.99			
PI-2	7.67	12.66	12.58	99.4
PAI-1	5.28			
PAI-2	7.09	12.37	12.48	100.9
PA-1	5.51			
PAI-2	5.81	14.21	14.33	100.8
PI-2	2.89			
PA-2	8.79			
PAI-1	3.25	14.80	14.98	101.2
PA-1	2.76			

Table 3.18 Analysis of polymer mixtures by alkali fusion reaction gas chromatography

* These values were calculated from the weight of polymer taken and were corrected for the weight of adsorbed water (Table 3.16) and the average experimental recovery (Table 3.17).

Reprinted with permission from S.P. Fronkoski and S. Siggia, *Analytical Chemistry*, 1972, 44, 3, 507. ©1972, American Chemical Society [160]

isocyanate-terminated linear CAPA-based polyester prepolymer, extended with a 1,4-butanediol chain extender. The polymer is cleaved into the corresponding diamine, polyester, 6-hydroxycaproic acid, and 1,4-butanediol fragments by alkali fusion at high temperature. The fragments formed were analysed by gas and size-exclusion chromatography, after separation and derivatisation. The polyethers were further cleaved into the corresponding polyol acetates by using a mixed anhydride reagent, before the gas chromatographic analysis.

Gomoryova [162] hydrolysed amide and imide linkages with hydrochloric acid and identified the diamines using paper or thin-layer chromatography. The diamine portion

or polyamides has also been determined by fusing the sample with an alkali reagent and separating the products by thin-layer chromatography [163]. Acidification of the melt allowed the separation and identification of the diacid components. Polyimides have been decomposed with hydrazine hydrate and the diamine products identified by gas chromatography. Polyamides and poly(amide-imides) required a prehydrolysis step. The di, tri- or tetracarboxylic acid segments were determined by reaction of the polymer with a 10% aqueous solution of tetramethylammonium hydroxide, pyrolysis of the resulting salt and identification of the volatile methyl ester by gas chromatography [164]. Kalinina and Doroshina [165] have reviewed the qualitative and quantitative methods for the analysis of polyamides and polyimides.

Infrared spectroscopy [165-168] and mass spectroscopy have been used to estimate the degree of conversion of polyimides and the extent of polyamic acid ring closure [169].

3.14 Nitrile Groups

3.14.1 Determination of Bound Nitrile Groups in Styrene – Acrylonitrile Copolymers

An infrared method has been described [170] for the compositional analysis of styrene-acrylonitrile copolymers. In this method the relative absorbance between a nitrile $\upsilon(CN)$ mode at 4.4 μm and a phenyl $\upsilon(CC)$ mode at 6. 2 μm is used.

A near infrared method using combination and overtone bands has been used [171] for carrying out the same analysis. Near infrared spectra of random acrylonitrile containing copolymers are shown in **Figure 3.15**.

The bands which occur in the region 1.6-2.2 μm result form overtones and combination tones which occur in the regions 1.6-1.8 μm and 1.9-2.2 μm, respectively.

The band near 1.68 μm is assigned as an overtone of phenyl $\upsilon(CH)$ mode near 3.3 μm and its absorbance is directly proportional to the styrene content of the copolymer and the film thickness. The band near 1.75 μm is assigned as an overtone of the aliphatic $\upsilon(CH)$ mode 3.45 μm and both acrylonitrile and styrene absorb at this wavelength. Bands at 1.910 and 1.952 μm and are combination tones of acrylonitrile and are assigned as (1) $\upsilon(CN) = \upsilon_{asym}(CH_3(2237 + 2940 = 5177$ cm^{-1} = 1.932 μm) and (2) $\upsilon(CN) + \upsilon_{asym}(CH_3)2237 + 2870 = 5107$ cm^{-1} = 1.958 μm), respectively. For calculation of the absorbance of these four characteristic bands, two different baseline methods were used. The method using the extrapolated baseline from (2) introduces less deviation than the other baseline method. The absorbance ratio $A_{1.675}/A_{1.910}$ proved to be the best one for analytical measurements.
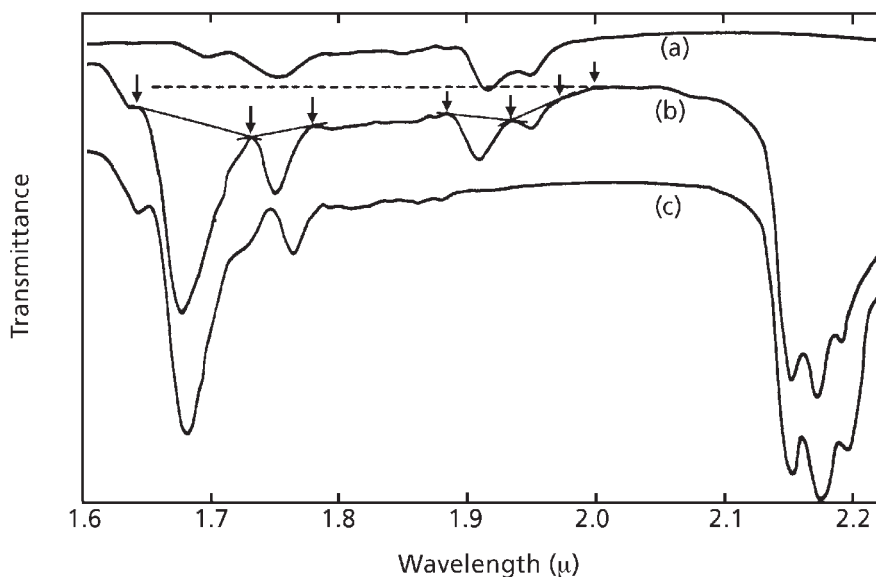
Figure 3.15 Near infrared spectra: (a) polyacrylonitrile; (b) styrene-acrylonitrile copolymer (acrylonitrile content 25.7 wt.%); (c) polystyrene. (*Reprinted with permission from A. Krishen, Analytical Chemistry, 1972, 44, 3, 494. ©1972, ACS*) [170]

A dye partition method has been decribed for the determination of low levels of nitrile groups in polystyrene [172].

3.15 Nitric Ester Groups

These have been determined in nitrocellulose by saponification, followed by reduction of the nitro group with Devada's alloy and determination of the ammonia produced [173].

3.16 Silicon Functions

Total silanol (SiOH), silane hydrogen (SiH) groups and tetrapropyoxy-silane and diphenylmethyl silanol crosslinking agents.

Dubiel and co-workers [174] described methods for determining these reactive components in room temperature vulcanised silicone foams. Total SiOH and SiOH are determined by Fourier transform infrared (FTIR) spectrometry, the SiOH

peak at 2.71 μm and the SiH peak at 4.61 μm were used for quantitation. The tetrapropoxysilane content was determined by gas chromatography using a solid capillary open tubular (SCOT) column and linear programmed temperature control. The diphenylmethylsilanol content was determined by gel permeation chromatography using the tetrahydrofuran solvent.

The preferred approach is to use secondary standards, i.e., well characterised compounds or polymers that quantitatively react with the reagent to give the desired product. For example, when only methane is determined, GE Viscasil 60,000, a high molecular weight polydimethylsiloxane (PDMS) is used. DC 704, a polymethylphe nylsiloxane, is used as the secondary standard when both methane and benzene are determined.

In all cases, the standards are trapped and chromatographed in exactly the same manner as the reaction products. The best straight line calibration curves are determined by a least-squares regression curve fitting computer programme.

Gaboury and Urban [175] have described an attenuated total reflection method for the determination of SiH groups in PDMS.

The technique of alkali fusion reaction gas chromatography has been applied to the determination of alkyl and aryl groups in polysiloxanes [158, 159]. The method involves the quantitative cleavage of all organic substituents bonded to silicon, producing the corresponding hydrocarbons:
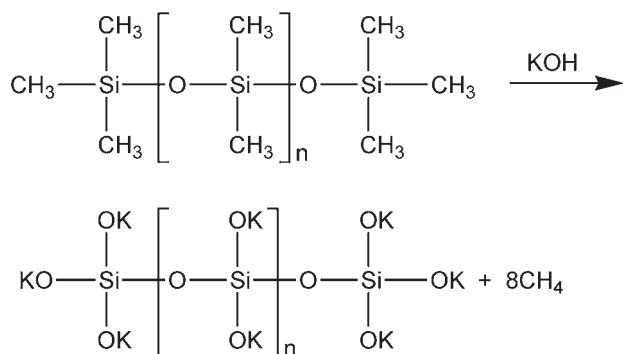
Reactions are driven to completion, with no apparent decomposition, in less then 10 minutes by fusing the sample with potassium hydroxide in an inert atmosphere. After concentration of the volatile products, they are separated and determined by gas chromatography. Sample losses are minimised by performing the total analysis in a single piece of apparatus. Fluids, gum rubbers, and resins are handled with equal

Table 3.19 Reaction methods for the quantitative determination of organic substituents bonded to silicon

Group determined	Reagent	Reaction conditions	Product	Analysis	Reference
Phenyl	60% aqueous KOH in DMSO	2 h at 120 °C	Benzene	GC	[176]
Phenyl	Bromine in glacial acetic acid	Boiling solution	Bromobenzene	Titration of excess bromine	[177]
Ethyl and phenyl	Phosphorus pentoxide and water	30-580 °C over 45 min	Ethane and benzene	GC-FID	[178]
Methyl and ethyl	Powdered potassium hydroxide	2 h at 250-270 °C	Methane and ethane	Gas burette	[179]
Methyl	Sulfuric acid	20 min at 280-300 °C	Methane	Gas burette	[180, 181]
Phenyl	Ethylbromide in the presence of aluminium chloride	…	Hexaethyl benzene	Gravimetric	[182]
Vinyl	Phosphorus pentoxide and water	80-600 °C over 40 min	Ethylene	GC-FID	[183]
Vinyl	Phosphorus pentoxide	Ambient to 500 °C	Ethylene	GC-FID	[184]
Vinyl	90% sulfuric acid	75-250 °C at 10 °C/min and 1 h at 250 °C	Ethylene	GC-TC	[185]
Vinyl	Sodium hydroxide pellets	300 °C for 15 min	Ethylene	Colorimetric	[186]
Vinyl	Potassium hydroxide pellets	Heat with Meker burner	Ethylene	GC-FID	[187]

TC: *Thermal conductivity detector*
Source: Author's own files

ease. The percentage relative standard deviation of the method is 1.00%; the average deviation between experimental and the theoretical result is 0.5% absolute.

Various other reagents have been used for the determination of organic substituents bonded to silicon in organosilicon polymers (**Table 3.19**).

Seino and Kawakami [188] used proton magnetic resonance spectroscopy and MALDI-ToF mass spectrometry to determine hexenyl groups in silsesquioxanes.

Method 3.1 Determination of Hydroxyl Groups in Polyethylene Glycol. Silation – Spectrophotometry [9]

Summary

This silation spectrophotometric method is capable of determining down to 0.1% of hydroxy groups in a polyethylene glycol (PEG) with a molecular weight of 3000.

Apparatus

Gas chromatograph equipped with flame ionisation detectors. The carrier gas was helium.

Spectrographs: IR spectrometer, UV spectrophotometer.

Reagents

Pentane, spectroscopic grade.

Petroleum ether, 40:60.

Ethanol, spectroscopic grade.

1-Napthyl dimethyl (dimethylamino) silane (preparation). A 10% solution of 1 equiv monochlorosilane (naphthyl dimethyl chlorosilane) in hexane (in benzene if necessary for solubility reasons) is stirred in a flask equipped with a reflux condenser cooled at –20 °C. From a communicating flask 2.2 equiv of dimethylamine vapour is slowly introduced over the solution and the mixture kept at room temperature overnight. After filtration and evaporation of the solvent, the residue is distilled.

Purification of the hydroxyl terminated PEG (H-PEG)
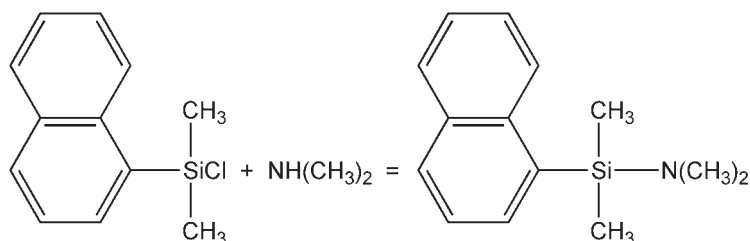
A solution of 100 g of commercial practical grade polymer in 400 ml of 0.01 M sodium hydroxide is digested at 40 °C for 24 h, then passed through two ion-exchange columns, the first containing 50 cm^3 of Amberlite IR 120 (H^+ form) and the second 50 cm^3 of Lewatite MP 7080 (base form). After evaporation of the water, the residue is dissolved in 1 cm^3 of toluene and filtered on an aluminium oxide column (50 g). The agitated solution is then thermostated at the temperature indicated below and 5.0 cm^3 of petroleum ether added dropwise. The slurry is cooled to 0 °C, allowed to stand for 15 minutes and the precipitate filtered. The temperature of precipitation is critical: it was 0 °C for H-PEG of molecular weight 600 (H-PEG-600), 10 °C for H-PEG-1000), 20 °C for H-PEG-2000 and 30 °C for polymers of higher molecular weight. The purified product is dried at room temperature and 13 Pa pressure.

Method

A 1,2 dimethoxyethane solution of the PEG is silylated with naphthyl dimethyl dimethylamino-silane. After some working up the extract is dissolved in ethanol and the chromophore concentration evaluated spectrophotometrically. The method is calibrated against PEG of known equivalent weight.

Experimental Procedure

Determination of the Hydroxyl Content of PEG

For polymers with expected equivalent weights higher than 1000, a sample of 1 g (0.5 g for lower equivalent weights) is dissolved in 5 cm^3 of dry 1,2-dimethyoxyethane. The dissolution is omitted if the melting point of the polymer is less than 60 °C. The flask is purged with dry argon (or nitrogen) and three equivalents for each expected equivalent hydroxyl (but not less than 200 mg) of 1-naphthyl dimethylaminosilane is added. The homogenised mixture is kept at 60 °C for 30 minutes. The sample

is then diluted at room temperature to 10 cm^3 with 1,2-dimethyloxyethane. After cooling to 0 °C it to an appropriate temperature, the silyated polymer is precipitated by adding dropwise, 50 cm^3 of low boiling petroleum ether to the stirred solution (the temperature of the precipitation is critical). After precipitation, the mixture is stirred at 0 °C for 15 minutes, then filtered on a sintered glass filter (G3) and washed with 5 cm^3 portions of petroleum ether. The precipitate is redissolved on the filter in 5 cm^3 of warm 1,2-dimethyloxyethane and precipitated a second time as above. If the expected hydroxyl content of the polymer is lower than 10^{-1} mol/kg, the precipitation should be repeated a third time. After the last precipitation, the polymer is washed on the filter with 20 cm^3 of spectroscopic grade pentane, dried for 5 hours at room temperature/13 Pa or in a stream of dry nitrogen. A portion of the dry sample is dissolved in spectroscopic grade ethanol so as to yield an absorbance of 0.2-0.8. The absorbance of the solution is measured *versus* ethanol as reference at 282.5 nm. If the sample concentration is higher than 1 g/cm^3 (= c), an ethanolic solution of the pure PEG of about the same concentration must be used as a reference.

Typical Results

The molarity of the silyl groups in the solution M_{sol}, is given by:

$$M_{sol} = A/a = c/EW_{Psil} \text{ mol/l}$$

where A is the absorbance of the solution, c is the concentration of the silylated polymer in dm^3, a is the molar absorptivity of the silylating agent and EW_{Psil} is the equivalent weight of the silylated polymer which can be calculated by:

$$EW_{Psil} = Ca/A \text{ g/mol}$$

In order to obtain the equivalent weight of the hydroxy terminated polymer, EW_{POH} the molecular weight of the silyl group MW_{sil} and that of the substituted proton must be taken into account:

$$EW_{POH} = Ca/A - (MW_{Sil} - 1) \text{ g/mol}$$

The molarity of the hydroxyl groups in 1 kg of original polymer, m_{OH} is then given by:

$$m_{OH} = 1000/EW_{POH} = 1000 \text{ A}/(Ca - A (MW_{Sil} - 1)) \text{ mol/kg}$$

For the 1-naphthyldimethylsilyl substituent, $MW_{Sil} = 185$

Table 3.20 Physical Data of R′, R″ and R‴ (2′-methoxyethoxy) silanes					
R′, R″ and R‴	**bp (°C)/ Pa**	**mp (°C)**	**d 20 (g/cm³)**	**20$_D$**	**ε(λ)/mol**
1-Naphthylydimethyl	111/4	-	1.051	1.5582	7.33×10^3 (282.5)
The purity of the samples controlled by gas chromatography was better than 99.8% *Reprinted with permission from D.E. Fritz, A. Sahil, H.P. Keller and E. Kovat, Analytical Chemistry, 1979, 51, 1, 7. ©1979, American Chemical Society [9]*					

The values of the molar absorptivities are given in **Table 3.20**. 1-Naphthyldimethyl(dimethylamino) silane quantitatively silated primary and secondary groups at 60 °C but little of tertiary hydroxyl groups.

The above procedure with 1-naphthyldimethyl(dimethylamino)silane was applied to four polymers, two of them hydroxyl terminated, the other two with methoxy end groups of unknown, but very low, hydroxyl content. Two nominal molecular weights were chosen for both types of polymers, 600 and 20,000 representing extreme types regarding the difficulties involved in the purification of the silylated polymers by precipitation and filtration. For this operation, the best pair of solvents proved to be 1,2-dimethyloxyethane and low boiling petroleum ether. The samples were redissolved and precipitated repeatedly and each time a portion of the precipitate was subjected to photometric analysis. Apparent hydroxyl contents expressed as a function of the number of precipitations showed that in the case of the hydroxyl terminated polymers, a constant silyl concentration is attained after the first precipitation. Three precipitations were necessary, however, for the methylated polymers in order to obtain consistent results.

Discussion of Results

This method is capable of determining down to 0.01% of hydroxy groups in a 3000 molecular weight PEG (or 1% of hydroxy groups in a 30,000 molecular weight PEG), with a precision of ± 45%.

Method 3.2 Determination of Hydroxyl Number of Glycerol-Alkylene Oxide Polyethers and Butane, 1,4-Diol Adipic Acid Polyesters. Direct Injection Enthalpimetry [9]

Summary

This direct injection enthalpimetric method is capable of determining hydroxy values of polyesters and polyethers in less than 10 minutes.

Apparatus

The basic electrical circuit is a simple DC Wheatstone bridge incorporating in one arm a thermistor of nominal resistance 10 kohm at 25 °C. The off-balance voltage is recorded on a recording potentiometer (10 mV full-scale deflection) with a chart speed of 4 cm/min.

A glass bottle (of about 25 ml capacity) is used for titrations, it was thermally insulted in a block of polystyrene. The titrand is stirred at a constant rate by a PTFE covered magnet.

Reagents

Titrant for polyethers. 2% *v/v* sulfuric acid (98% *v/v*); 23% *v/v* acetic anhydride, 25% *v/v* carbon tetrachloride and 50% *v/v* glacial acetic acid.

Titrant for polyesters. 2% *v/v* sulfuric acid (98% *v/v*); 23% *v/v* acetic anhydride, 25% *v/v* glacial acetic acid and 50% *v/v* methylene chloride.

Carbon tetrachloride.

Methylene chloride.

Experimental Procedure

The titrand consists of 100 to 200 µl of a solution of a sample dissolved in either carbon tetrachloride (for polyethers) or methylene chloride (for polyesters) delivered from a microlitre syringe. These organic solvents are dried over a molecular sieve (grade 5A). When the hydroxyl value is less than 100 mg/g of potassium hydroxide, the titrant is used at a 33.3% *m/V* solution; for hydroxy values exceeding 100 mg/g it is made up to 20% *m/V*.

Six portions, each 200 μl in volume, of a titrant added separately to one sample of titrand yields the same recorder deflection after each addition. The deflections produced by two samples and one standard can thus be determined in duplicate without renewing the titrand. All samples are examined in duplicate or triplicate and deflections on the recorder are usually reproducible to ± 0.025% of full-scale deflection.

Typical Results

Plots of dT (defined as the height of the recorder deflection) against hydroxyl value (determined by the conventional phthalic anhydride method) for five glycerol - propylene oxide condensates ranging in molecular weight between 300 and 4000 pass very near to the origin.

Discussion of Results

This method is capable of determining hydroxy values of polyethers and polyesters down to 10 mg/kg with an accuracy of ± 2%.

Method 3.3 Determination of Primary and Secondary Hydroxyl Groups in Ethylene Oxide Tipped Glycerol-Propylene Oxide Condensates. Phenyl Isocyanate Kinetic Method

Summary

In many situations it is necessary to be able to determine both primary and secondary hydroxy groups in polymers. This kinetic method, based on the difference in reaction rate of primary and secondary hydroxy groups with phenyl isocyanate enables both groups to be determined.

The reaction is carried out under standard conditions in which a calculated weight of the polyol (depending on its hydroxyl number) is reacted under standard conditions with an excess of a standard toluene solution of phenyl isocyanate in the presence of a basic catalyst:
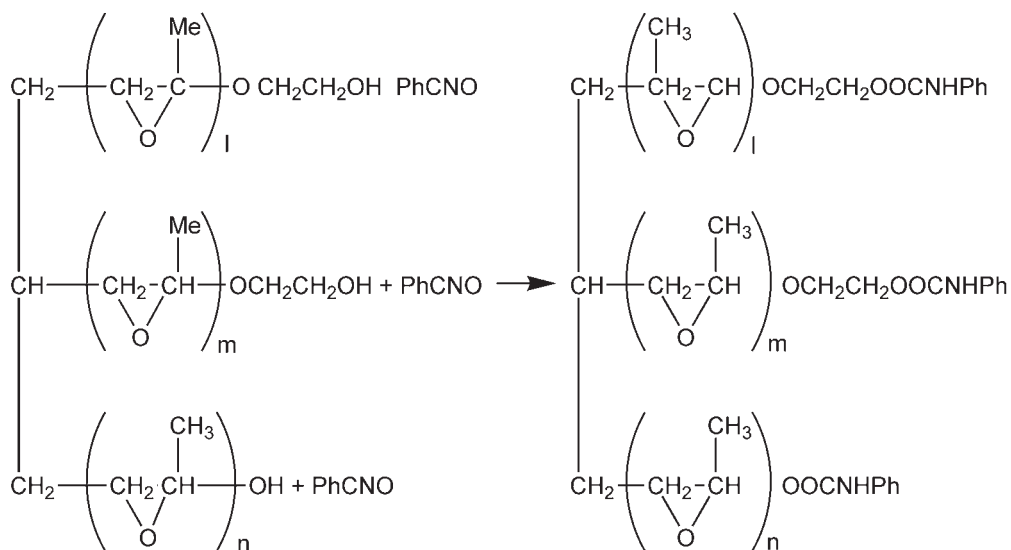
Unconsumed phenyl isocyanate is then reacted with excess standard potassium hydroxide:

$$PhCNO + 2KOH = K_2CO_3 + PhNH_2$$
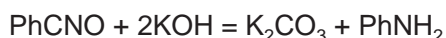
Excess potassium hydroxide is estimated by titration with standard acetic acid to the phenolphthalein end-point. A blank run is performed in which the sample is omitted. From the difference between the sample and the blank titrations it is possible to calculate the hydroxyl content of the original polymer:

1 mole hydroxyl groups ≡ 1 mole phenyl isocyanate ≡ 2000 ml N KOH

Reactivity is calculated by a kinetic procedure in which the percentage of the original phenyl isocyanate addition, which reacts with the sample in a given time, is taken as an index of its reactivity. A calibration graph can be prepared in which the determined phenyl isocyanate reactivity is plotted against the ethylene oxide content, and this enables a determination to be made of the ethylene oxide content of unknown samples from the calibration graph by interpolation.

Apparatus

(a) Apparatus for preparation, storage and dispensing of dry toluene (containing less than 15 ppm water). A description of the apparatus required is given with
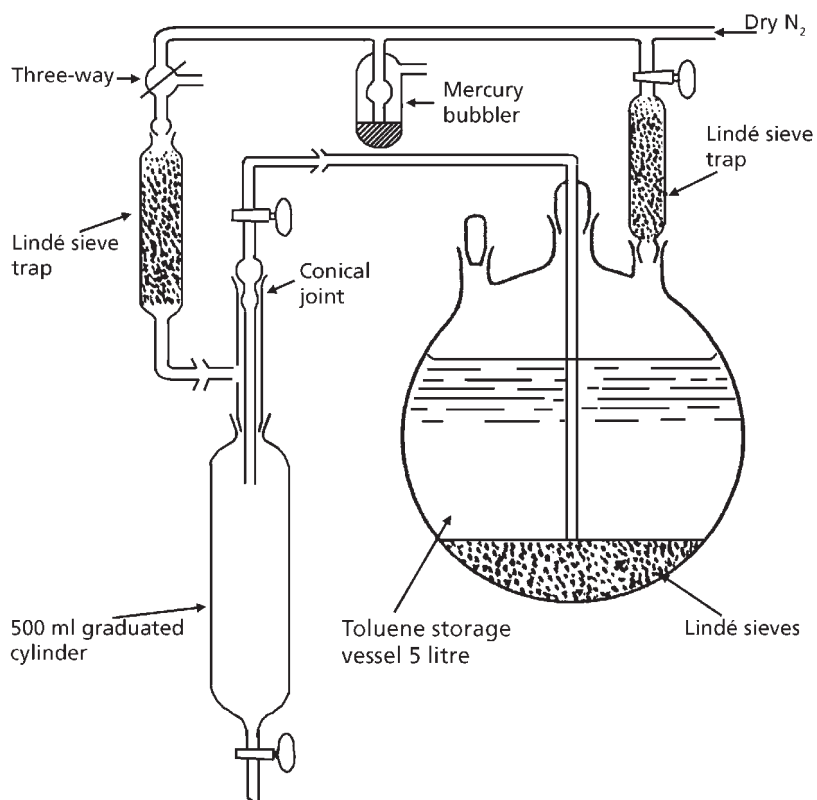
Figure **3.16** Apparatus for preparation, storage and dispensing of dry toluene.
(*Source: Author's own files*)

the method of drying toluene described later. **Figure 3.16** shows the apparatus required for storing and dispensing the dried toluene.

(b) Apparatus for reducing water content of polyol sample to 100-150 ppm (**Figure 3.17**). The water content of the neat polyol is reduced to 100-150 ppm by subjecting it to vacuum treatment for 2 hours at 70-80 °C. Connect a vacuum pump of approximately $1.4m^3$/min capacity (capable of attaining a vacuum of 0.005 mm mercury) to a 700 ml Quickfit flange type flask assembly and a Manostat gauge (via a Cardice/isopropanol filled cold trap, see **Figure 3.17**). Provision is made for feeding dry nitrogen into the flask when the vacuum treatment is completed. During vacuum treatment the temperature of the reaction flask is maintained at 70 to 80° C by immersion in a Simmerstat controlled water bath.
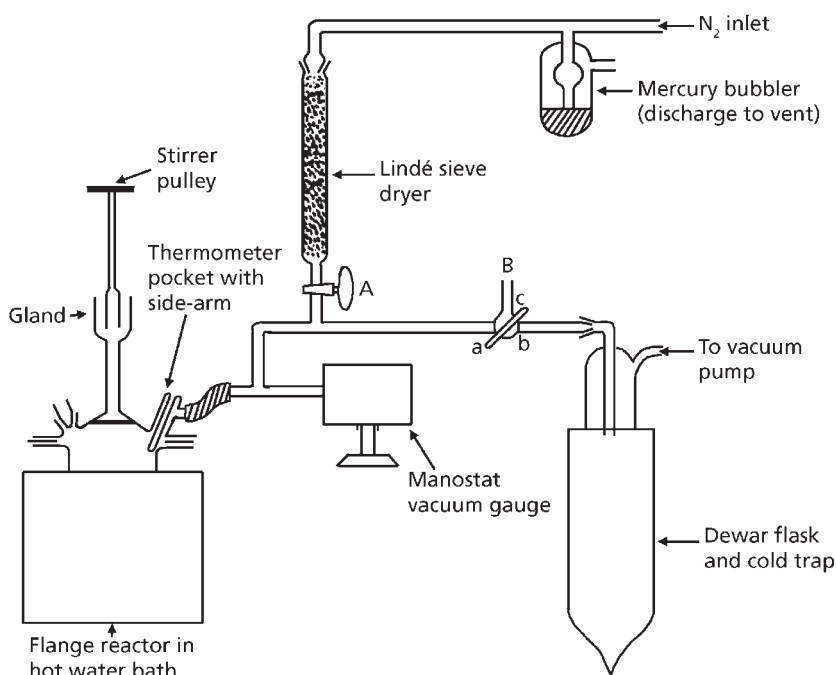
Figure 3.17 Apparatus for reducing water content of polyol sample.
(*Source: Author's own files*)

(c) Apparatus for reaction of polyol with phenyl isocyanate (**Figure 3.18**). The reaction of the polyol with phenyl isocyanate is carried out in a 700 cm³ Quickfit flange type vessel (as described above). This apparatus is mounted in a rectangular aluminium tank (dimensions 61 cm × 18 cm high), thermostatted at 40 ± 0.1 °C. The tank is fitted with a Perspex top having holes cut to accommodate two reaction flasks and the thermostatted heater/stirrer.

(d) Miscellaneous apparatus. Precision torsion balance, capacity 4000 g, scale divisions 1 g; Stopwatches; Long stemmed sampling pipette, capacity 10-12 cm³ from tip to graduation on top of bulk; Miscellaneous volumetric glassware.

Reagents

(a) Preparation and storage of dry toluene (containing less than 15 ppm water). Reflux 4 cm³ of toluene with 30 g calcium hydride for 6 to 8 hours in a 5 cm³ B24 neck flask with a 24 in vertical condenser attached. Connect a horizontal condenser
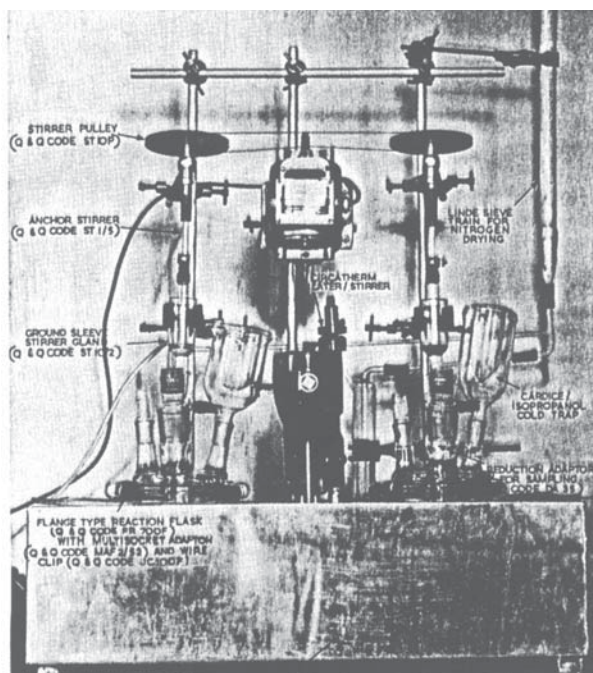
Figure 3.18 Apparatus for reaction of polyol with phenyl isocyanate.
(*Source: Author's own files*)

to the 5 cm^3 flask, (excluding moist air). To the end of this condenser connect a dry three-neck B25 5 litre flask containing 100 g freshly ignited molecular sieves (15 cm × 2.5 cm molecular sieve trap also connected to a 5 litre flask - molecular sieves dried 3 to 4 h at 120 °C). Now distil 3 to 3.5 cm^3 of the toluene from the calcium hydride into the dry receiver containing molecular sieves. Deactivate the calcium hydride remaining in the distillation flask by slowly adding a 10:1 hexane:ethanol solution and dispose of this solution in an open drain.

Connect the toluene receiver to a dry dispensing system as shown in **Figure 3.16**. In this apparatus the solvent is kept dry (i.e., less than 15 ppm water) by standing over molecular sieves under an atmosphere of dry nitrogen. To the outlet end of this dispensing apparatus connect a dry 500 cm^3 graduated cylinder. By suitable adjustment of stopcocks keep this cylinder dry by continuously purging with dry nitrogen when the apparatus is not in use.

Immediately before dry toluene is required for an analysis, syphon a suitable volume into the dry 500 cm^3 graduated cylinder by adjustment of the stopcocks.

The water content of the toluene stock should be checked periodically by a Karl Fischer procedure to ensure that it is below the required limit of 15 ppm.

(b) Toluene solution of phenyl isocyanate, 1.00 ± 0.005 M. Weigh 120 ± 0.2 g phenyl isocyanate into an oven dried, stoppered, 1 litre volumetric flask. Run dry toluene (less than 15 ppm water) into this flask from the dispenser (see section (a) and Figure 3.16) until approximately 950 cm³ of liquid is present in the volumetric flask. Immerse the stoppered volumetric flask in a water bath, thermostatted at 25 ± 1 °C and leave for 15 minutes with occasional mixing. Finally make the volume of liquid in the flask up to 1 litre at 25 °C with dry toluene. Stopper and mix well. This solution is to be maintained in a water bath thermostatted at 25 ± 1 °C when portions of it are withdrawn for standardisation or for use in the determination of the reactivity of polyols. A measured volume of the solution then contains a constant weight of phenyl isocyanate.

Standardisation of phenyl isocyanate solution.

Hydrochloric acid, 0.1 M aqueous.

Bromophenol blue indicator, 0.1%. Dissolve 0.1 g bromophenol blue in 100 cm distilled water, add 1.5 ml of 0.1 M sodium hydroxide solution.

Methanol redistilled.

Di-*n*-butylamine 0.2 M (approximately) in dry toluene (less than 15 ppm water). Transfer 9.3 cm³ di-*n*-butylamine AnalaR to a dry 250 cm³ volumetric flask. Make up to the mark with dry toluene and thoroughly mix the solution. Keep this reagent well stoppered when not in use and renew weekly.

Adjust the temperature of the 1 cm³ flask of 1 M phenyl isocyanate solution by immersing it in a water bath at 25 ± 1 °C with dry toluene (less than 15 ppm water) and thoroughly mix the contents of the 250 cm³ flask.

Pippette 25 cm³ 0.2 M di-*n*-butylamine solution into two dry stoppered 250 cm³ conical flasks (i.e., a sample and a blank flask). Allow a 15 s pipette draining time during these operations. Into one of the flasks pipette 25 cm³ of the ten-fold diluted phenyl isocyanate solution (sampled at 25 °C using a 15 s draining time) and into the blank flask pipette 25 cm³ of toluene. Leave both solutions for 15 minutes to react, then add to each 100 cm³ methanol and 5 drops bromophenol blue indicator. Using 0.1 M hydrochloric acid titrate the sample (T_S ml of normal hydrochloric acid) and the blank solutions (T_B ml of normal hydrochloric acid) to the yellow-green end point.

The normality (F) of the 1 cm³ undiluted stock phenol isocyanate solution of 25 ± 1 °C is then given by:

$$F = \frac{10 \times f_x (T_S - T_B)}{25}$$

The molarity of the phenyl isocyanate solution at 25 ± 1 °C, prepared as described previously, should be slightly greater than 1000 M. Finally, adjust the strength of the 1 cm³ of stock phenyl isocyanate solution to within the range 1.000 ± 0.005 M by addition of a calculated volume of dry toluene. Mix the 1 cm³ stock solution well in the thermostatted 25 ± 1 °C water bath and recheck the normality of a ten-fold dilution as described previously.

Due to the high coefficient of cubical expansion of toluene, the normality of a toluene solution of phenyl isocyanate varies as its temperature is changed. It is for this reason that the solution is prepared at 25 ± 1 °C and subsequently standardised at the same temperature.

For the purpose of calculating results, it is necessary to know the weight of 50 cm³ of the phenyl isocyanate at 25 ± 1 °C. This may be obtained by weighing 50 cm³ of the reagent from the thermostatted stock flask in a dry 50 cm³ stoppered volumetric flask.

The normal phenyl isocyanate stock solution should be well stoppered when not in use and should be left open for a minimum period when sampling (to exclude atmospheric moisture). Recheck the normality of the solution at 25 ± 1 °C at frequent intervals.

(c) Dabco catalyst solution (0.56% *w/v*) Dabco is the trade name for triethylene diamine. Weigh out 6 ± 0.1 g Dabco and transfer to an oven-dried 1 litre volumetric flask. Add dry toluene (less than 15 ppm water) from the dispenser (see **Figure 3.16**) to make the volume up to approximately 950 cm³. Dissolve the Dabco by shaking and stand the flask in a water bath thermostatted at 25 ± 1 °C. When the solution has reached 25 °C make up to the 1 litre mark with dry toluene and mix thoroughly. Stand the solution in a water bath, thermostatted at 25 ± 1 °C. A measured volume of this solution then contains a constant weight of Dabco catalyst.

Standardisation of the Dabco Solution

Immerse the 1 litre flask of stock solution of Dabco in a water bath thermostatted at 25 ± 1 °C and leave until the solution reaches this temperature. Pipette 25 cm³ of this solution (15 s draining time) into a 250 cm³ conical flask containing 100 cm³

methanol and 5 drops of 1% aqueous bromophenol blue indicator. Using 0.1 M hydrochloric acid, titrate the sample solution (T cm^3 of M hydrochloric acid; f) to the yellow-green end point. The reaction which has occurred at the bromophenol blue indicator end point is:

$$N (C_2H_4)_3N + HCl = N(C_2H_4)_3N.HCl$$
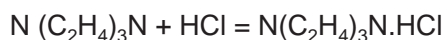
The strength (% *w/v*) of the 1 litre of Dabco solution at 25 ± 1°C is given by:

Dabco (% *w/v*) = 4 × 112 × T × f/1000

The strength of the Dabco solution at 25 ± 1 °C must be in the range 0.56 ± 0.01 % *w/v*.

For the purpose of calculating results it is necessary to know the weight of 50 cm^3 of the Dabco catalyst solution at 25 ± 1 °C. This may be obtained simply by weighing 50 cm^3 of the reagent from the thermostatted stock flask into a dry 250 cm^3 stoppered conical flask.

This solution should be well stoppered when not in use and should be left open for a minimum time when sampling (to exclude atmospheric moisture).

Method

The described kinetic procedure, based on the difference in the reaction rates with phenyl isocyanate of the terminal primary and secondary hydroxyl groups present in ethylene oxide tipped glycerol/propylene oxide condensates, must be carried out under rigidly standardised conditions. Primary hydroxyl groups react with phenyl isocyanate to form a urethane faster than do secondary hydroxyl groups. The greater the amount of terminal ethylene oxide units in a glycerol/propylene oxide condensate, therefore, the greater its reactivity, (i.e., rate of reaction) with phenyl isocyanate. The method may be used, therefore, for evaluating the reactivity of ethyiene oxide tipped polyols.

Experimental Procedure

(a) Calculation of the weight of polyol required for analysis.

It is explained in note 1 that the analysis is carried out using a toluene solution of the polyol which is exactly decimolar with respect to total primary and secondary hydroxyl groups in the sample. First determine the hydroxyl value (H, mg KOH/g) of the polyol sample by a modified catalysed acetylation procedure. Calculate

the weight W (g) of polyol required to produce 500 cm^3 of a decinormal toluene solution (at 25 °C ± 1 °C) from the following equation:

$$W \text{ (g)} = 56.1 \times 50/H$$

Transfer approximately 95 g of polyol sample to a clean 100 cm^3 conical flask and weigh to the nearest 0.01 g. Transfer from this flask exactly the calculated weight (W)of polyol into a 700 cm^3 Quickfit flanged reaction vessel (see **Figure 3.18**). Reweigh the conical flask to check that the weight of polyol added to the reaction vessel is correct to within 0.01 g.

(b) Removal of water from polyol.

Assemble the reaction apparatus with multineck adaptor, stirrer and gland, thermometer pocket and vacuum assembly as shown in **Figure 3.17**.

Mount the flask in a suitable water bath and connect the stirrer motor and vacuum line. Maintain the Cardice - isopropanol cold trap at –60 °C and operate the stirrer at approximately 200 rpm.

Close stopcock A (**Figure 3.17**) and connect (a) to (c) with stopcock B. Heat the water bath up to 70 to 80 °C and allow the stirred reactor contents to reach this temperature. Switch on the vacuum pump. Reduce the pressure in the reaction flask to 2 mm over a period of 5 minutes by momentarily turning tap B to connect (a) to (b) several times (if the pressure is reduced too rapidly to 2 mm then violent de-gassing of the polyol may take place due to the presence of dissolved propylene oxide in the sample). When de-gassing is complete turn tap B to connect (a) to (b) and continue the vacuum treatment for 2 hours. After half an hour the pressure in the flask should be less than 0.1 mm.

When the vacuum treatment is completed switch off the bath heater and the stirrer motor. Isolate the flask from the vacuum line by turning tap B to connect (c) to (b). Now apply a rapid purge of dry nitrogen at the nitrogen inlet and cautiously open stopcock A to allow nitrogen to fill the reaction vessel. Replace the thermometer pocket by a stopper, remove the flask from the water bath and dry the outside of the flask. The moisture content of the polyol should now be in the range 80-150 ppm.

(c) Toluene dilution of polyol.

Stand the stoppered reaction flask on a cork ring placed on a balance. Fill the 500 cm^3 graduated cylinder of the dry toluene dispensing unit (**Figure 3.16**) with toluene and attach a molecular sieve filled guard tube to the top of this cylinder.

Run a suitable weight (W_g) of toluene (to the nearest 1 g) from the graduated cylinder into the reaction flask and immediately stopper the flask to exclude atmospheric moisture. The weight (W_g) of toluene required is given by the following expression.

Weight of toluene required to make the volume of test solution up to 400 cm^3 at 25 °C:

$$W_g = 0.861 \times (400 - W_1/S)$$

where:

W_1 = weight (g) of polyol used in experiment

S = specific gravity of neat polyol at 25 °C (usually assumed to be 1.00)

0.861 = specific gravity of pure toluene at 25 °C

(d) Commencement of the reaction.

Immerse the reaction flask with multineck adaptor in an aluminium water tank of the type shown in **Figure 3.18**. This tank is thermostatted at 40 ± 1 °C. Insert the cold trap and sampling fitting with Gaco seal into the multineck adaptor. Maintain the cold trap at –60 °C with Cardice/isopropanol during the whole run.

Connect to the top of the cold trap a supply of dry nitrogen and maintain a slight pressure of nitrogen in the reaction flask. The nitrogen stream should be very gentle, otherwise some loss of toluene vapour, with consequential analytical errors, may occur when the reaction flask is opened for sampling. Adjust the stirrer speed to 200 rpm and leave the contents of the flask for 30 minutes to reach thermal equilibrium with the bath at 40 °C.

Whilst the reaction flask is reaching thermal equilibrium carry out the following two operations:

(1) Place the two 1 litre reagent flasks containing the stocks of 1.000 ± 0.005 M phenyl isocyanate solution and of 0.56% *w/v* Dabco catalyst solution in a separate water bath thermostatted at 25 ± 1 °C, and allow these flasks to reach this temperature over a period of 30 minutes.

(2) Pipette 10 ml of 0.2 N di-*n*-butylamine solution into each of twelve dry 100 cm^3 conical flasks and quickly replace the stoppers (15 s pipette draining time). Ensure that the same amount of di-*n*-butylamine is introduced into each flask

by keeping the temperature of the stock di-*n*-butylamine solution constant during the pipetting. These flasks will be used later for the determination of the phenylisocyanate content of samples withdrawn from the polyol/phenyl isocyanate reaction at various times.

When the reaction flask containing the toluene solution of polyol has reached 40 °C, pipette into this flask 50 cm^3 of normal phenyl isocyanate stock solution (at 25 °C), allowing a 15 s pipette draining time. No reaction occurs between polyol and phenyl isocyanate in the absence of Dabco catalyst. Leave the mixture for 15 minutes to reach thermal equilibrium. Transfer, by pipette, 50 cm^3 of stock 0.56% *w/v* Dabco solution from the storage vessel (thermostatted at 25 °C) into a dry 50 cm^3 volumetric flask. Remove the B34/B24 sampling adaptor from the reaction flask assembly and insert the neck of the 50 cm^3 volumetric flask into the B34 socket to introduce the Dabco catalyst into the reaction mixture. Allow a 15 s draining time for the Dabco flask and replace the B34/B24 sampling adaptor. Start the stopwatch at the same moment that the Dabco solution is first tipped into the reaction flask, (i.e., at the exact moment that the Dabco catalysed reaction between polyol and phenyl isocyanate commences).

(e) Sampling the polyol/phenyl isocyanate reactor.

Samples are now withdrawn periodically from the reactor for determination of residual phenyl isocyanate. Immediately before starting the reaction between polyol and phenyl isocyanate by the addition of Dabco catalyst, (i.e., time zero) weigh to the nearest 1 mg, one of the twelve 100 cm^3 conical flasks containing 10 cm^3 of 0.2 M di-*n*-butylamine (referred to in section 2 – see 1 above). Withdraw approximately 10 cm^3 of the polyol/phenyl isocyanate reaction mixture by means of a long stemmed 10 cm^3 pipette via the Gaco seal on the sampling point and exactly one minute after starting the reaction, (i.e., addition of Dabco) run this solution into the di-*n*-butylamine solution contained in the weighed flask. Stopper and reweigh the conical flask to obtain the weight of polyol/phenyl isocyanate reaction mixture withdrawn for analysis (this weight is needed in the calculation of results). Leave the mixture for 15 minutes, or longer, to react. Transfer the contents of this flask quantitatively to a 250 cm^3 conical flask with 100 cm^3 redistilled methanol and add 5 drops of 0.1% bromophenol blue indicator. Using 0.1 M hydrochloric acid, titrate the sample to the yellow-green end-point and record this titration.

To one of the blank flasks referred to in Section 2 previously, add 10 cm^3 toluene and transfer the contents of a 250 cm^3 conical flask with 100 cm^3 methanol. Add 5 drops of bromophenol blue indicator and titrate with 0.1 N hydrochloric acid to the yellow-green end-point.

Table 3.21 Phenyl isocyanate kinetic method – determination of polyols		
Di-*n*-butylamine flask number	Test	Time interval between adding Dabco catalyst (i.e., start of reaction) and sampling for phenyl isocyanate determination (min)
1	Blank run	-
2	Sample run	1
3	Sample run	15
4	Sample run	30
5	Sample run	55
6	Sample run	60
7	Sample run	65
8	Sample run	95
9	Sample run	100
10	Sample run	105
11	Sample run	120
12	Blank run	-
Source: Author's own files		

Similarly, withdraw samples from the polyol/phenyl isocyanate reaction solution at various other time intervals (see **Table 3.21** after commencement of the reaction and immediately introduce the sample into 10 ml di-*n*-butylamine in order to analyse it for phenyl isocyanate content as described previously. Tabulate the titrations obtained. Titrations of the 10 cm³ 0.2 M di-*n*-butylamine blank solution carried out at the beginning and at the end of the experiment usually agree within 0.05 cm³.

The small amount of Dabco catalyst present in samples taken from the reaction flask interferes slightly in these determinations of residual phenyl isocyanate. This interference is allowed for in the method of calculation.

(f) Graphical plotting of experimental data.

The method of calculating % of the original phenyl isocyanate addition consumed under standard conditions (denoted by P%) is given next. On graph paper plot P% *versus* the corresponding time (in minutes) from the commencement of reaction

of each of the ten samples withdrawn from the reaction flask. Draw a smooth line through the 10 points. From this graph read (P%) corresponding to 60 minutes and P% corresponding to 100 minutes, i.e., $(P\%)_{60min}$ and $(P\%)_{100min}$.

(g) Correlation of reactivities with ethylene oxide content of sample.

As $(P\%)_{60min}$ and $(P\%)_{100min}$ are determined under rigidly standardised test conditions these quantities are dependent upon the reactivity of the polyol sample analysed and therefore, constitute a parameter by which it is possible to compare one batch of polyol with another. In ethylene oxide tipped condensates prepared under specified conditions, the reactivity of the polyol increases with its ethylene oxide content.

A series of molecular weight 5000 glycerol/propylene oxide condensates containing between nil and 9 moles of ethylene oxide per mole of glycerol can be used to prepare a calibration graph. The procedure under calculations was then used to determine $(P\%)_{60min}$ and $(P\%)_{100min}$ for the standard samples.

Prepare plots of $(P\%)_{60min}$ and $(P\%)_{100min}$, respectively, *versus* the weight addition ethylene oxide content (expressed in moles of ethylene oxide per mole glycerol). The ethylene oxide contents of ethylene oxide tipped glycerol/propylene oxide condensates of unknown ethylene oxide content may be determined by referring their determined $(P\%)_{60min}$ and $(P\%)_{100min}$ reactivity figures to this calibration graph. The two determinations usually agree within ± 0.1 ethylene oxide units.

It is necessary to ensure that the samples used to prepare the calibration curve were manufactured in the same way as the unknown samples being analysed, thus the standard samples should be manufactured using the same polymerisation catalyst that is used to manufacture the unknown samples.

Typical Results

Calculations.

(a) To calculate total weight of initial reaction flask charge let:

$W_1(g)$ = weight of neat polyol taken for analysis

$W_2(g)$ = weight of toluene required to make the volume of polyol/toluene test solution up to 400 cm^3 at 25 ± 1 °C

$W_3(g)$ = weight of 50 cm^3 1.000 ± 0.005 normal phenyl isocyanate (in toluene) reagent at 25 ± 1 °C

211

$W_4(g)$ = weight of 50 cm^3 of 0.56% Dabco (in toluene) reagent at 25 ± 1 °C

$W_A(g)$ = total weight of initial reaction flask charge

$= W_1 + W_2 + W_3 + W_4$

(b) To calculate weight of phenyl isocyanate in total initial weight of reaction flask charge before the polyol/phenyl isocyanate reaction is started.

Let F = normality of phenyl isocyanate stock solution at 25 ± 1 °C.

Then the original weight of phenyl isocyanate present $W_B(g)$ in the total reaction flask charge $W_A(g)$ (i.e., before reaction with polyol commences) is given by:

$W_B(g) = 50 \times F \times 119.13/1000$ g phenyl isocyanate present in $W_A(g)$ of reaction flask charge.

(c) To calculate initial weight of phenyl isocyanate (i.e., before reaction with polyol is started) in the portion of reaction solution withdrawn for phenyl isocyanate determination.

Let W_c = weight (g) of an approximately 10 cm^3 sample taken from the reactor during the run for determination of phenyl isocyanate.

Then calculate the weight of phenyl isocyanate $W_D(g)$ present in the $W_c(g)$ portion of reaction solution withdrawn for phenyl isocyanate determination (i.e., before reaction between polyol and phenyl isocyanate is started by addition of Dabco) is given by:

$W_D(g) = W_B \times W_c / W_A$

(d) To calculate the titration correction (T_D cm^3) required to allow for the presence of Dabco catalyst in the portion of reaction solution $W_c(g)$ withdrawn for phenyl isocyanate determination.

112 g Dabco = 1000 cm^3 of 1.0000 M hydrochloric acid (Dabco titrated to the bromophenol blue end-point).

In the reactivity determination there is 50 cm^3 of 0.56% *w/v* Dabco solution (i.e., 0.28 g pure Dabco) present in $W_A(g)$ of initial reaction flask charge.

Now 0.28 g pure Dabco consumes $0.56 \times 50 \times 1000/100 \times 112$ cm^3 = 2.5 cm^3 of 1.0000 M hydrochloric acid, i.e., the Dabco present in $W_A(g)$ of initial reaction flask charge consumes 2.5 cm^3 of 1.000 M hydrochloric acid.

The hydrochloric acid titration correction (T_D cm^3) required to allow for the presence of Dabco catalyst in the portion of reaction solutions W_c(g) withdrawn for phenyl isocyanate determination is given by:

T_D (cm^3) = 2.5 × W_c/W_A cm^3 of 1.000 M hydrochloric acid

To obtain the actual weight of phenyl isocyanate, W_E(g) (corrected for Dabco present) remaining in W_c(g) portion of reaction solution withdrawn for phenyl isocyanate determination after time T minutes (i.e., T minutes after the Dabco catalysed reaction of polyol and phenyl isocyanate has been started).

If, in the phenyl isocyanate determination by the di-*n*-butylamine method:

T_B = volume of hydrochloric acid (cm^3) required in blank titration of 10 cm^3 of 0.2 M di-*n*-butylamine solution

T_A = volume of hydrochloric acid (cm^3) required to titrate a mixture of 10 cm^3 of 0.2 M di-*n*-butylamine and the W_c(g) of reactor sample which was withdrawn for phenyl isocyanate determination after time T minutes.

f = normality of hydrochloric acid used in phenyl isocyanate determination

T_D = Dabco titration correction, referred to under typical results.

119.13 = molecular weight of phenyl isocyanate

Then the actual weight W_E(g) of phenyl isocyanate (corrected for Dabco present) in a W_c(g) portion of reaction solution withdrawn for phenyl isocyanate determination after time T min is given by:

W_E(g) = (T_B × f - (T_A × f - T_D)) 119.13/1000 g phenyl isocyanate

or

W_E(g) = (T_B × f - (T_A × f - 2.5 × W_c))/W_A 119.13/1000 g phenyl isocyanate

The equation to calculate the percentage (p) of the original addition of phenyl isocyanate consumed in the reaction solution after time T minutes denoted by (P_T min) = (W_D-W_F)100/W_D.

This method has been applied to a range of glycerol/propylene oxide adducts containing various accurately known amounts of ethylene oxide tipping, up to 5.3 moles (**Table 3.22**). Increasing the ethylene oxide tip content of a polyol leads to a distinct increase in the reactivity of the polyol with phenyl isocyanate. As expected,

				Reactivity, i.e., percentage of original phenyl isocyanate addition consumed in:	
Sample identification	Approximate molecular weight	Hydroxyl number (mg KOH/g polyol)	Ethylene oxide tipping, moles ethylene oxide/ mole glycerol (by weight addition)	60 min reaction	100 min reaction
A	3000	59.0	0	25.2	35.2
B	5000	34.9	0	27.1	36.8
C	5000	34.3	3.0	41.5	46.6
D	5000	35.9	3.5	44.4	51.0
E	5000	36.0	4.3	47.5	54.1
F	5000	33.3	5.3	51.9	57.4

Table 3.22 Application of reactivity method to standard ethylene oxide tipped polyols

Source: Author's own files

'untipped' polyols which are relatively free from primary hydroxyl groups react comparatively slowly with phenyl isocyanate. Decinormal solutions of 'untipped' glycerol/propylene oxide condensates of molecular weight 3000 and 5000 has an identical rate of reaction with phenyl isocyanate. Thus, the rate of reaction with phenyl isocyanate of the terminal isopropanol end groups in polyols is independent of molecular weight in the molecular weight range 3000 to 5000 and depends only on proportions of primary and secondary end groups present.

A calibration curve is prepared by plotting moles of ethylene oxide per mole of glycerol for the range of standard tipped polyols of known ethylene oxide content against % of original phenyl isocyanate addition consumed after 60 and 100 minutes, i.e., P60% and P100%. This curve can be used to obtain from P60% and P100% data obtained for tipped glycerol propylene oxide polyols of unknown composition their tipped ethylene oxide contents (in moles of ethylene oxide per mole glycerol).

Discussion of Results

For polyols which contain less than 4 moles of ethylene oxide per mole of glycerol the reactivity method has an accuracy of better than ± 5% of the determined value. For polyols which contain between 5 and 15 moles of ethylene oxide per mole of glycerol, the accuracy is in the range ± 10%.

Method 3.4 Determination of Compositional Analysis of Methylmethacrylate - Methacrylic Acid Copolymers. Fourier Transform ^{13}C-NMR Spectroscopy [40]

Samples are prepared by dissolving or swelling approximately 0.3 g of copolymer in 2 g of solvent – both components being weighed directly into a 10 mm NMR sample tube. A 50/50 mixture of pyridine and pyridine–d_5 is used as the solvent and provided the deuterium internal lock for the spectrometer. Spectra are obtained on a Varian CFR-20 pulse Fourier transform spectrometer operating at 18.7 kg (20.0 MHz ^{13}C frequency). The pulse power delivered to the single coil 10 mm od probe is sufficient to rotate the ^{13}C magnetisation by 90° in 15 μs. Probe temperature under these conditions was 38 °C. Spectrometer parameters for the determination of spectra are: approximately 65 degree (10 μs) pulse, 4 KHz spectral width, 1 second data acquisition time and 3 seconds delay between repetitive pulses (i.e., a total experiment recycle time of 4 seconds). Typically 12,000-15,000 free induction decays (FID) are accumulated (i.e., an 'overnight' run mode was employed) for each quantitative determination. The accumulated FID is digitally-filtered with a time constant that produces a 1.7 Hz line

broadening. The 8 K data table is then Fourier transformed to yield a 4 KHz spectrum defined by 4 K real points (i.e., digital resolution approximately 1 Hz).

Spin lattice relaxation times (T 1) for the carbonyl carbides are estimated from 180-5-90 pulse sequences and found to be in the range 0.8-1.1 seconds. It should be noted that the solutions were not degassed and that the presence of dissolved oxygen may influence the observed relaxation rate. (If samples were degassed, the carbonyl relaxation could be longer in which case a longer delay between repetitive pulses would be required). The imposition of a 3 second pulse delay and employment of a 65° pulse ensured the recovery of the carbonyl magnetisation during the recycle time, thus eliminating possible errors in quantitation resulting from differential relaxation times. Spectra are obtained under fully proton decoupled conditions using a gated-decoupling scheme in which the proton decoupler was off during the 3 seconds delay time and gated on at the start of the 1.0 seconds acquisition period. In this manner, problems associated with differential nuclear Overhauser enhancements (NOE) for different carbonyl carbons are avoided.

A method of checking that the spectrometer conditions are sufficient to yield quantitative data is to compare the total integral of the carbonyl region with those obtained for α-CH$_3$>C< CH$_2$ since all integrals should be the same under quantitative conditions. In all cases examined by Johnson and co-workers [40], the integral values for all four resonance regions are within 2-3% with the deviations being random from sample to sample - i.e., in one case the carbonyl might be the greatest of the four in magnitude and in another case the lowest.

A ^{13}C-NMR spectrum of a polymethylmethacrylate - methacrylic acid copolymer is shown in **Figure 3.19 (a)**. The spectrum demonstrates the acidic group and the ester group resonances.

In **Figure 3.19(b)** is shown the fully proton decoupled ^{13}C spectrum obtained in pyridine at 38 °C of a (MMA/MAA) copolymer of approximately 33% acid composition. While the spectrum resolves into α-CH$_3$, CH$_2$, OCH$_3$ >C<, and C - O regions, the structural similarity of the comonomers results in resonance overlap (at 20 MHz) between ester and acid carbons in all regions but the carbonyl. The complete structure in the carbonyl region arises from the sensitivity of the carbons to the microstructural features of the copolymer chain, i.e., sequence and tacticity effects. To be sure that these effects do not lead to overlap of ester and acid carbonyl resonance, chemical shifts of both homopolymers and homosteric copolymers were examined with the result that the carbonyl resonance region does separate into distinct acid and ester regions in pyridine.
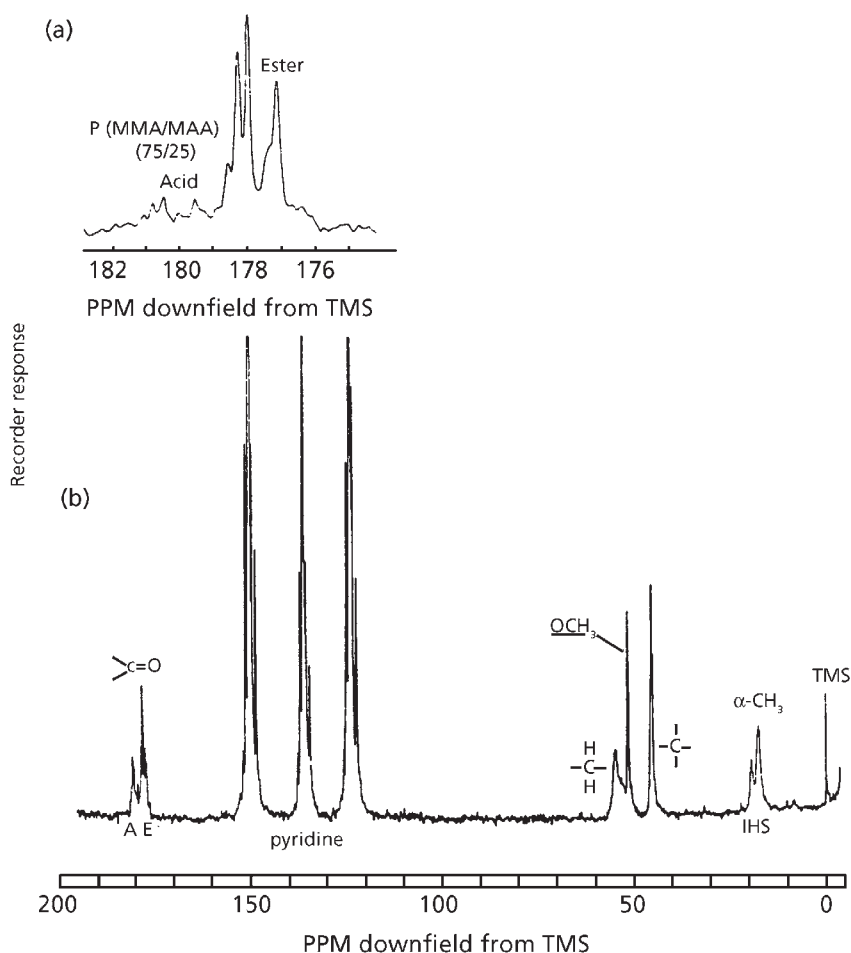
Figure 3.19 20 MHz ^{13}C-NMR spectra of: (a) P(MMA-*co*-MAA) - 25% acid dissolved in pyridine; (b) (MMA-*co*-MAA) - 33% acid dissolved in 50:50 *v/v* pyridine; pyridine d$_5$. Assignment of the various resonance regions is given in the figure; the I, H, S rotation refers to isotactic, heterotactic and syndiotactic stereochemical triads; A and E refer to ester and acid. (*Reprinted with permission from D.E. Johnson, J.R. Lyerla, Jr., T.T. Horikawa and L.A. Pederson, Analytical Chemistry, 1977, 49, 1, 77. © 1977, ACS*) [40]

In order to test the reliability of compositional results obtained by the ^{13}C NMR, analyses of several copolymers were carried out by both ^{13}C NMR and titration. Titrations were carried out in 50% aqueous ethanol medium to the phenolphthalein end-point using 0.15 N aqueous potassium hydroxide as the titrant. There is an

excellent correlation between the compositional analysis by NMR and titration (correlation coefficient = 0.998) with most of the comparative analyses differing by 2% or less.

Method 3.5 Identification of Acrylic Acid and Methacrylic Acid in Acrylic Copolymers. Propylation - Pyrolysis - Gas Chromatography [41]

Apparatus

Glass vials of capacity 15-30 ml with Teflon-lines septa (Pierce Hypo-vials) are suitable.

A thermostatically controlled oven at 60 °C capable of being evacuated in less than 2 kPA was used.

Pyrolysis - gas chromatographic - mass spectrometric equipment

Sharp and Paterson [41] used a Perkin Elmer filament pyrolysis unit fitted in a Perkin Elmer F11 gas chromatograph (pyrolysis temperature control 250-550 °C). The gas chromatographic column used is a 1.7 m × 3 mm od stainless steel column packed with 30% m/m silicone oil (Embaphase) on acid washed Celite, operated at 80 °C with a helium flow rate of 30 ml/min. The column effluent is split in the ratio 2:1 between a flame ionisation detector and an AFI MS12 mass spectrometer equipped with a glass fit type of molecular separator at 150 °C. Mass spectra are scanned from *m/e* 200 to 20 at 8 seconds per decade under standard electron bombardment conditions, electron energy 70 eV, emission current 500 μA, accelerating voltage 8 kV and source temperature 200 °C.

Reagents

Dimethylformamide dipropyl acetal (2 mequiv/ml in pyridine) (Propyl-8).

Procedure

Direct Pyrolysis

Transfer 1 mg of polymer or an amount of latex or solution containing this mass of polymer onto the pyrolysis filament. Remove any water, or solvent by blowing

with hot air from a hair-drier. Insert the filament into the pyrolysis chamber and connect the carrier gas and gas chromatographic apparatus. Heat the filament at 250 °C for 15 seconds to ensure the removal of water, solvent or volatile additives. Pyrolyse the polymer by heating the filament at 550 °C for 15 seconds.

Propylation and Pyrolysis

Transfer about 0.25 g of polymer or an amount of the acrylic latex or solution containing this mass of polymer into a glass vial and dry by evacuation at 60 °C for 15 hours. Seal the vial and inject by means of a hypodermic syringe, 1 ml of the Propyl-8 reagent onto the the dried polymer film. Heat at 60 °C for 16 hours then let the vial and contents cool to ambient temperature. Transfer a smear of the gel or viscous solution produced on to the pyrolysis filament and remove the bulk of the propylation reagent by blowing with warm air from a hairdryer. Heat the filament for 15 second periods at 250 °C in the stream of carrier gas until the chromatogram indicates the complete removal of reagent residues and finally pyrolyse at 550 °C. Identify by mass spectrometry any eluted compounds that were not observed in the original direct pyrogram or that occur to a significantly greater extent in the pyrogram of the propylated polymer.

The presence of propyl acrylate or propyl methacrylate in the pyrogram of the propylated polymer indicates that the original polymer contained acrylic or methacrylic acid, respectively.

The mass to charge (*m/e*) ratio and relative abundance of the molecular and fragment ions observed are listed in **Table 3.23**.

Figure 3.20 shows a pyrogram of polymethylmethacrylate copolymerised to contain 1 and 10% of acrylic or methacrylic acid. By this procedure, copolymerised acrylic or methacrylic acid has been identified in terpolymers with (a) butyl acrylate and styrene, (b) methylmethacrylate and ethyl acrylate and, (c) ethylene and propylene. A methyl methacrylate - methylstyrene - maleic acid terpolymer, when examined by this propylation - pyrolysis procedure, yielded dipropyl fumerate and a smaller amount of dipropyl maleate.

Table 3.23 Charge/mass ratio in propylated acrylic acid – methacrylic acid copolymer

Propyl acrylate (C$_6$H$_{10}$O$_2$) M$_n$ = 114

m/e	55	73	29	42	41	43	27	85	31	39	59
relative abundance	100	46	15	11		9	7	6	55	5	4
m/e	15	99	114								
relative abundance	1	1	0.2								

Propyl methacrylate ~(C$_7$H$_{12}$O$_2$) M$_n$ = 128

m/e	41	69	43	87	39	42	27	59	29	86	70
relative abundance	100	91	66	66	38	34	25	9	6	6	5
m/e	31	38	88	26	99	13	128				
relative abundance	4	3	3	2	2	2	2				

Figure 3.20 Pyrograms of polymethylmethacrylates and some acid copolymers after propylation. Polymethylmethacrylate containing the following amounts of copolymerised acid: A: 10% methacrylic; B: 1% methacrylic acid; C: 10% acrylic acid; D: 1% acrylic acid; E: no acid; elution times: methylmethacrylate: 9 min, propyl acrylate: 15 min, propylmethacrylate: 28 min. (*Reprinted with permission from J.L. Sharp and G. Paterson, Analyst, 1986, **105**, 1250, 517. ©1986, RSC*) [41]

Method 3.6 Determination of Amino Groups in Aromatic Polyamides, Polyimides and Polyamides-imides. Potassium Hydroxide Fusion Gas Chromatography [158, 159]

Reagents

Fusion Reagent

The alkali fusion is a prefused mixture of potassium hydroxide (Analytical reagent grade) and 0.5% sodium acetate.

Typically, the mixture melts around 110 °C and contains 13–14% of water. When preparing this reagent, it is important to avoid excessive heating. If too much water is lost, the molten reaction mass may solidify before the hydrolysis reaction is complete. On the other hand, too much water will make the reagent sticky and difficult to handle. Additionally, it is possible to plug the cold trap if large amounts of water are released. To prevent adsorption of moisture from the atmosphere, the powdered reagent is stored in a small desiccator within a nitrogen-filled glove bag.

Apparatus

The total analysis (reaction, trapping, separation and quantitation) is performed in a single piece of apparatus. The reaction portion consists of a pyrolysis tube, combustion furnace assembly, and a mounting frame taken from a commercial unit (Perkin Elmer Pyrolysis Accessory 154-0825, Norwalk, CN 06856). Samples, standards and reagent are contained in miniature platinum boats (10 mm × 4 mm × 4 mm, Fisher Scientific Co., Pittsburgh, PA 15219) and are magnetically manipulated within the confines of the glass tubing with metal cylinders and a hoe-shaped retriever. The combustion furnace assembly monitors and controls the temperature within the reaction zone.

A loop-shaped piece of 316 grade stainless steel tubing (3.2 mm od, 2.4 mm inch id) connected between the outlet of the reaction furnace and a special low dead volume GC injector assembly serves as a trap for efficiently concentrating most volatile reaction products. All of the transfer tubing from the reaction zone to the injection port, except the lower section of the loop, is heated to 300 °C by a clam-shell type combustion furnace clamped around the tubing. The exposed piece of tubing, which is loosely packed with quartz wool, is cooled in a liquid nitrogen-filled Dewar flask when concentrating the evolved products and heated with a 400 °C Nichrome wire heater when 'injecting' the products into the gas chromatograph. Helium carrier gas flows (60 ml/min) through the reaction unit and cold trap before entering the chromatographic column.

Procedure

One to five milligrams (± 1 μg) of powdered sample or standard is weighed into the tared platinum micro-boats. The boats are then filled with the powdered caustic reagent in the nitrogen-purged glove bag and quickly loaded into the storage arm of the reaction tube with a metal cylinder behind each. When making quantitative analysis, the first sample reacted in a series of runs is used to condition the apparatus. Boats are usually loaded at the end of a work day, thus permitting entrapped air to be purged from the system overnight. When samples are loaded in the morning, the tube is purged for 1 hour before turning on the thermal conductivity detector current.

Once a stable baseline is obtained, the liquid nitrogen-filled Dewar flask (–196 °C) is position around the unheated section of the trap. The first metal cylinder is magnetically moved forward, pushing the boat in front of it into the heated reaction zone. The cylinder is removed to storage area. The optimum reaction temperature profile for a fusion reaction will depend on the reactivity of the samples. The furnace temperature was programmed from 100 to 300 °C over a period of 10 minutes. As the reaction occurs, the volatile reaction products and water, liberated from the molten mixture, are carried by the flowing helium carrier gas and concentrated in the trap. At the end of the reaction period, i.e., 10 minutes, the boat is withdrawn from the furnace with the magnetic retriever and deposited with its cylinder. After adjusting the furnace control to its initial temperature setting, the trapped compounds are revolatilised and directed into the gas chromatograph by replacing the Dewar flask with the heater (400 °C). When the separation and integration are completed and the initial conditions re-established, the procedure is repeated for each sample and standard. Matched 1.8 m × 6.4 mm od stainless steel columns packed with 60/80 mesh Chromosorb 103 were used to separate the amine reaction products. Diamines were chromatographed on 1.3 m × 3.2 mm od stainless steel columns packed with 10% FFAP on 60/70 mesh Anakrom AB.

Calibration curves were prepared daily for each compound determined. Anhydrous ammonia was injected with a calibrated 1000 µl gas tight syringe through the septum inlet of the reaction tube. Ambient temperature and pressure corrections were made to determine the actual amount of gas injected. Benzylamine was generated from reaction of the hydrochloride salt with potassium hydroxide. The diamine standards were weighed into boats, covered with caustic reagent, and volatilised by moving the boat into the heated furnace. In each case, the standard compounds were trapped and chromatographed in the same manner as the volatile reaction products. The best straight line calibration curves were determined by a least-square regression curve fitting computer programme.

References

1.   J. Majewski, *Polimery Tworzywa Wielkoczasteczkowe*, 1973, **18**, 3, 142.

2.   R.S. Stetzler and C.F. Smullin, *Analytical Chemistry*, 1962, **34**, 2, 194.

3.   B. Haszczyc and W.Walczyk, *Chemia Analtyczna*, 1975, **20**, 885.

4.   J.S. Fritz and G.H. Schenk, *Analytical Chemistry*, 1959, **31**, 11, 1808.

5.   J.A. Floria, I.W. Dobratz and J.H. McClure, *Analytical Chemistry*, 1964, **36**, 11, 2053.

6. S. Siggia, J.G. Hanna and R. Culmo, *Analytical Chemistry*, 1961, **33**, 7, 900.

7. Yu L. Spririn and T.A. Yatsimirskaya, *Vysokomolekulyarnye Soedineniya Series A*, 1973, **15**, 11, 2595.

8. T. Groom, J.S. Babiec and B.G. Van Leuwen, *Journal of Cellular Plastics*, 1974, **10**, 1, 43.

9. D.F. Fritz, A. Sahil, H.P. Keller and E. Kovats, *Analytical Chemistry*, 1979, **51**, 1, 7.

10. M. Tanaka and I. Kojima, *Analytica Chimica Acta*, 1968, **41**, 75.

11. M.A. Motorina, L.S. Kalinina and E.I. Metalkina, *Plasticheskie Massy*, 1973, **6**, 74.

12. R.D. Law, *Journal of Polymer Science – A1*, 1971, **9**, 589.

13. G.D.B. van Houwelingen, *Analyst*, 1981, **106**, 1267, 1057.

14. F.F. L'Ho, *Analytical Chemistry*, 1973, **45**, 3, 603.

15. J. Loccufier, M. Bos and E. Schacht, *Polymer Bulletin*, 1991, **27**, 2, 201.

16. I.I. Kaduji and J.H. Rees, *Analyst*, 1974, **99**, 1180, 435.

17. R.M. Smith and M. Dawson, *Analyst*, 1980, **105**, 1246, 85.

18. C.S.Y. Kim, A.L. Dodge, S-F. Lau and A. Kawasaki, *Analytical Chemistry*, 1982, **54**, 2, 232.

19. F.D. Brako and A.S. Wexler, *Analytical Chemistry*, 1963, **35**, 12, 1944.

20. K.A.B. Lee, S.M. Hurley, R.A. Siepler, R.D. Mills, K.A. Handrich and J.J. Conway, *Journal of Applied Spectroscopy*, 1990, **44**, 10, 1719.

21. R.F. Storey, K.R. Herring and D.C. Hoffman, *Polymer Preprints*, 1990, **31**, 1, 20.

22. A.Z. Conner and R.W. Eyler, *Analytical Chemistry*, 1950, **22**, 9, 1129.

23. C.V. Francis, Analytical Chemistry, 1953, **25**, 6, 941.

24. R.D. Law, *Journal of Polymer Science Part A-1: Polymer Chemistry*, 1971, **9**, 3, 589.

25. L.S. Bark and J.K. Grime, *Analyst*, 1972, **97**, 1160, 911

26. T.R. Crompton, unpublished work.

27. R.A. Dickie, J.S. Hammond, J.E. De Vries, and J.W. Holubka, *Analytical Chemistry*, 1982, **54**, 12, 2045.

28. G.A. Stenmark and F.T. Weiss, *Analytical Chemistry*, 1950, **28**, 11, 1784.

29. S. Crisp, B.G. Lewis and A.D. Wilson, *Journal of Dental Research*, 1975, **54**, 6, 1238.

30. J.S. Tan and S.P. Gasper, *Macromolecules*, 1973, **6**, 5, 741.

31. E.R. Garrett and R.L. Guile, *Journal of American Chemical Society*, 1951, **73**, 10, 4533.

32. J. Douglas, A. Timnick and R.L. Guile, *Journal of Polymer Science Part A: General Papers*, 1963, **1**, 5, 1609.

33. A.R. Mathieson and J.V. McLaren, *Journal of Polymer Science Part A: General Papers*, 1965, **3**, 7, 2555.

34. A. Katelhalsky, N. Shavit and H. Eisenberg, *Journal of Polymer Science*, 1954, **13**, 68, 69.

35. A.R. Mathieson and J.V. McLaren, *Journal of the Chemical Society A: Inorganic, Physical, Theoretical*, 1960, **9**, 3581.

36. J.C. Leyte and M. Mandel, *Journal of Polymer Science*, A2, 1964, 4, 1879.

37. M. Mandel and J.C. Leyte, *Journal of Polymer Science*, 1962, **56**, 823.

38. G.D.B. Houwelingen, J.G.M. Aalbers and A.J. Hoog, *Fresenius' Journal of Analytical Chemistry*, 1980, **300**, 2, 112.

39. R.L.M. Van Lingen, *Fresenius' Journal of Analytical Chemistry*, 1969, **247**, 3-4, 232.

40. D.E. Johnson, J.R. Lyerla, Jr., T.T. Horikawa and L.A. Pederson, *Analytical Chemistry*, 1977, 49, **1**, 77.

41. J. L. Sharp and G. Paterson, *Analyst*, 1980, **105**, 1250, 517.

42. R. Jander, S. Pompe, M. Bubner and R.H. Heise, *Forschungzent Rossendorf FZR*, 1996, **123**, 60.

43. J.C. Oxley and W.D. Perkins, *Analysis*, 1987, **15**, 61.

44. J.E Tackett, *Applied Spectroscopy*, 1990, **44**, 9, 1581

45. G.M. Whiteside, Report D8RED4 – TRI Order No. AD A 173988/7/GAR, Aval NTIS, From Government Report Announcement, 1987, 87, Abstract No. 705, 582.

46. D. Nissen, V. Rossbach and H. Zahn, *Journal of Applied Polymer Science*, 1974, **18**, 7, 1953.

47. E.N. Gemerenko and E.M. Perepletchikova, *Zhurnal Analiticheskoi Khimii*, 1974, **29**, 4, 830.

48. K. Kato, *Journal of Applied Polymer Science*, 1973, **17**, 1, 105.

49. V.O. Aydin, B. Kaczmar and R.C. Schulz, *Angewandte Makromolekulare Chemie*, 1972, **24**, 1, 171.

50. G.Lenkrath, *Gummi Asbest Kunststoffe*, 1976, **29**, 585.

51. J.C. Bevington, D.E. Eaves and R.L. Vale, *Journal of Polymer Science*, 1958, **32**, 317.

52. J.K. Allen and J.C. Bevington, *Transactions of the Faraday Society*, 1960, **56**, 1762.

53. J. Majer and J. Sodomka, *Chemicky Prumysl*, 1975, **25**, 11, 601.

54. D. Muntenau and N. Savu, *Revista de Chimie (Bucharest, Romania)*, 1976, **27**, 10, 902.

55. C.P.A. Kappelmeier, *Farbon Zeitung*, 1935, **40**, 1141.

56. C.P.A. Kappelmeier, *Verfkroniek*, 1954, **27**, 291.

57. F.W. Ferskow, *Farbon Zeitung*, 1939, **44**, 33.

58. G. Bandel, *Angewandte Chemie*, 1938, **51**, 570.

59. C.J. Malin, L.B. Genung and R.F. Williams, *Industrial & Engineering Chemistry, Analytical Edition*, 1942, **14**, 935.

60. C.J. Malm, L.J. Tanghe, B.C. Laird and G.D. Smith, *Analytical Chemistry*, 1954, **26**, 1, 188.

61. D.L. Miller, E.P. Samsel and J.G. Cobler, *Analytical Chemistry*, 1961, **33**, 6, 677.

62. J. Haslam, J.B. Hamilton and A.R. Jeffs, *Analyst,* 1958, **83**, 983, 66.

63. J. Haslam and A.R. Jeffs, *Journal of Analytical Chemistry*, 1957, **7**, 24.

64. E.P. Samsel and J.A. McHard, *Industrial Engineering Chemistry, Analytical Edition*, 1942, **14**, 750.

65. D.G. Anderson, K.E. Isakson, D.L. Snow, D.J. Tessari and J.T. Vandeberg, *Analytical Chemistry*, 1971, **43**, 7, 894.

66. E.M. Barrall II, R.S. Porter and J.F. Johnson, *Analytical Chemistry*, 1963, **35**, 1, 73.

67. R.S. Porter, A.S. Hoffman and J.F. Johnson, *Analytical Chemistry*, 1962, **34**, 9, 1179.

68. D.C.M. Squirrel, *Automotive Methods in Volumetric Analysis*, Hilger and Watts, London, UK, 1964, p.94.

69. J. Haslam, M.A. Willis and D.C.M. Squirrel, *Identification and Analysis of Plastics*, 2nd Edition, Ilcliffe, London, UK, 1972, p.57.

70. K. Czaja, M. Nowakowska and J. Zubek, *Polimery Tworzywa Wielkoczasteczkowe*, 1976, **21**, 4, 158.

71. A.G. Siryuk and R.A. Bulgakova, *Vysokomolekulyarnye Soedineniya Series B*, 1977, **19**, 2, 152.

72. J. Helmroth, *Polychromarium Plast*, 1973, **3**, 7.

73. C.B. Puchalsky, *Analytical Chemistry*, 1979, **51**, 8, 1343.

74. R.S. Porter, S.W. Nicksic and J.F. Johnson, *Analytical Chemistry,* 1963, **35**, 12, 1948.

75. G.W. Tindall, R.L. Perry, J.L. Little and A.T. Spaugh, *Analytical Chemistry*, 1991, **63**, 13, 1251.

76. G.G. Esposito and M.H. Swann, *Analytical Chemistry*, 1962, **34**, 9, 1048.

77. D.F. Percival, *Analytical Chemistry*, 1963, **35**, 2, 236.

78. D.R. Campbell, *Analytical Chemistry*, 1975, **47**, 8, 1477.

79. M.A. Phillips, *Journal of the Chemical Society*, 1928, 1, 2393.

80. D.G. Anderson, K.E. Isakson, J.T. Vandeberg, M.Y.T. Jao, D.J. Tessari and L.C. Afremow, *Analytical Chemistry*, 1975, **47**, 7, 1008.

81. F. Viebak and C. Brechaer, *Berichte der Bunsen-Gesellschaft für Physikalische Chemie*, 1930, **63**, 3207.

82. S. Paul and B. Ranby, *Analytical Chemistry*, 1975, **47**, 8, 1428.

83. K. Peltonen, P. Pfäffli and A. Itkonen, *Analyst*, 1985, **110**, 9, 1173.

84. N. Miyauchi, T. Takeshita, M. Akashi and R. Machida, *Journal of Applied Polymer Science*, 1987, **34**, 7, 2601.

85. A.D. Hammerich and F.G. Willeboordse, *Analytical Chemistry*, 1973, **45**, 7, 1696.

86. J. Urbanski, *Plaste Kautschuk*, 1968, **15**, 260.

87. R. Kretz, *Fresenius' Journal of Analytical Chemistry*, 1960, **176**, 6, 421.

88. A. Steyermark, *Journal of Agricultue and Food Chemistry*, 1955, **38**, 367.

89. S. Ehrlich-Rogozinski and A. Patchornik, *Analytical Chemistry*, 1964, **36**, 4, 840.

90. M.H. Karger and Y. Mazur, *Journal of the American Chemical Society*, 1968, **90**, 14, 3878.

91. K. Tsuji and K. Konishi, *Analyst*, 1974, **99**, 1174, 54.

92. Y.Y. Huang and C.H. Wang, *Journal of Chemical Physics*, 1975, 62, 1, 120.

93 A. Mathias and N. Mellor, *Analytical Chemistry*, 1966, **38**, 3, 472.

94. J.B. Stead and A.H. Hindley, *Journal of Chromatography A*, 1969, **42**, 470.

95. I. Zeman, L. Novak, L. Mitter, T.T. Stekla and O. Holendova, *Journal of Chromatography A*, 1976, **119**, 581.

96. E.W. Neumann and H.G. Nadeau, *Analytical Chemistry*, 1963, **35**, 10, 1454.

97. W.B. Swann and J.P. Dux, *Analytical Chemistry*, 1961, **33**, 4, 654.

98. P. Simak, *Die Makromolekulare Chemie Macromolecular Symposia,* 1986, **5**, 61.

99.   G. Meszlenyi, E. Juhasz and M. Lelkes, *Tenside, Surfactants, Detergents*, 1994, **31**, 83.

100.   Konische and Y. Konoh, *Japan Analyst*, 1966, **15**, 1110.

101.   C. Chu, K. Watson and R. Vukov, *Rubber Chemistry and Technology*, 1987, **60**, 4, 636.

102.   I. Gyenes, *Titration in Non-aqueous Media*, Illiffe Books, London, UK, 1967, p.261.

103.   D.C. Pepper and P.H. Reilly, *Proceedings of the Chemical Society*, 1961, **1**, 460.

104.   S.G. Gallo, H.K. Wiese and J.F. Nelson, *Industrial and Engineering Chemistry,* 1948, **40**, 1277.

105.   T.S. Lee, I.M. Kolthoff and E. Johnson, *Analytical Chemistry*, 1950, **22**, 8, 995.

106.   E.C. Kuryolnikov, R.V. Vizyert, A.A. Berlin and L. Vigne, *Viv Politetihy Inst Nosv*, 1971, **36**, 242.

107.   L.D. Hensen and D.J. Eatough, *Thermochimica Acta*, 1987, **117**, 37.

108.   J.M. Koltoff and J. Mitarb, *Journal of Polymer Science*, 1947, **2**, 199, 220.

109.   R.F. Boyers, *Journal of Physics–Colloid Chemistry*, 1947, **51**, 80.

110.   I.C. McNeill, *Polymer*, 1963, **4**, 15.

111.   R. McGuchan and I.E. McNeill, *Journal of Polymer Science A-1: Polymer Chemistry*, 1966, **4**, 9, 2051.

112.   S.T. Hirozawa, *Treatise on Analytical Chemistry: Part II: Analytical Chemistry of Inorganic and Organic Compounds, Volume 16: Functional Groups*, Eds., I.M. Kolthoff and P.J. Elving, Wiley Interscience, New York, NY, USA, 1971, p.23.

113.   T.R. Crompton and V.W. Reid, *Journal of Polymer Science, Part A1*, 1963, **1**, 347.

114.   A. Basch and M. Lewin, *Journal of Polymer Science,* 1973, **11**, 1707.

115.   D. Dollimore and B. Holt, *Journal of Polymer Science, Polymer Physics Edition*, 1973, **11**, 1703.

116. S.D. Varma and V. Narashimhan, *Journal of Polymer Science,* 1972, **16**, 3325.

117. J.M., Funt and J.H. Magill, *Journal Polymer Science - Polymer Physics Edition*, 1974, **12**, 217.

118. B.V. Kokta, J.L. Valade and W.N. Martin, *Journal of Applied Polymer Science*, 1973, **17**, 1, 1.

119. N.K. Albert, Woodbury Research Laboratory, Shell Chemical Company, Woodbury, USA, *private communication*.

120. D.W. Fraga, Shell Chemical Company, Ltd., Emeryville Research Laboratories, CA USA, *private communication*.

121. R. Hank, *Rubber Chemistry and Technology*, 1967, **40**, 3, 936.

122. F. D. Brako and A. S. Wexler, *Analytical Chemistry*, 1963, **35**, 12, 1944.

123. C. Shihota, M. Yamazaki and T. Tabenchi, *Bulletin of the Chemical Society of Japan*, 1977, **50**, 311.

124. H.J. Sloane and R. Bramston-Cooke, *Applied Spectroscopy*, 1973, **27**, 3, 217.

125. M. Panyszach and J. Kovar, *Canadian Journal of Spectroscopy*, 1986, **31**, 130.

126. H.C. Dinsmore and D.C. Smith, *Rubber Chemistry and Technology*, 1949, **22**, 527.

127. D.L. Harms, *Analytical Chemistry*, 1953, **25**, 8, 1140.

128. D. Hummel, *Rubber Chemistry and Technology*, 1959, **32**, 854.

129. M. Lerner and R.C. Gilbert, *Analytical Chemistry*, 1964, **36**, 7, 1382.

130. M. Tyron, E. Horowicz and J.J. Mandel, *Journal of Research of National Bureau of Standards*, 1955, **55**, 219.

131. R.R. Turner, S.W. Carlson and A.G. Altenau, *unpublished work*.

132. H.J. Sloane and R. Bramstone-Cooke, *Applied Spectroscopy*, 1973, **27**, 3, 217.

133. S. Chujo, S. Satoh, T. Ozaka and E. Nagai, *Journal of Polymer Science*, 1962, **61**, 171, 512.

134. S. Chujo, S. Satah and E. Nagai, *Journal of Polymer Science*, Part A, General Papers, 1964, **A2**, 895.

135. S.C. Paltcini and J.J. Porro, *Identification of Polymer Laminates using Diamond Bell Techniques*, Perkin Elmer Infrared Bulletin, No.1RD121, Perkin Elmer, Boston, MA, USA.

136. P.R. Sewell and D.W. Skidmore, *Journal of Polymer Science* A-1, 1968, **6**, 8, 2425.

137. W. Cooper, D.E. Eaves, M.E. Tunnicliffe and G. Vaughan, *European Polymer Journal,* 1965, **1**, 2, 121.

138. M.E. Tunnicliffe, D.A. MacKillop and R. Hank, *European Polymer Journal,* 1965, **1**, 4, 259.

139. A.G. Altenau, L.M. Headley, C.O. Jones and H.C. Ransaw, *Analytical Chemistry,* 1970, **42**, 11, 1280.

140. T.S. Lee, I.M. Kolthoff and E. Johnson, *Analytical Chemistry,* 1950, **22**, 8, 995.

141. A.R. Kemp and H. Peters, *Industrial and Engineering Chemistry, Analytical Edition,* 1943, **15**, 1, 52.

142. J. Van Schooten and J.K. Evenhuis, *Polymer*, 1965, **6**, 11, 561.

143. J. Van Schooten and J.K. Evenhuis, *Polymer*, 1965, **6**, 7, 343.

144. H. Boer and E.C. Kooyman, *Analytica Chimica Acta*, 1951, **5**, 550.

145. D.A. MacKillop, *Analytical Chemistry*, 1968, **40**, 3, 607.

146. N. Svob and F.Flajsman, *Croatic Chemica Acta*, 1970, **42**, 417.

147. B.J. Allen, G.M. Elsea, K.P. Keller and H.D. Kinder, *Analytical Chemistry*, 1977, **49**, 3, 741.

148. G.W. Tindall, R.L. Perry, J.L. Little and A.T. Spaugh, *Analytical Chemistry*, 1991, **63**, 13, 1251.

149. G.A. Stenmark, *Analytical Chemistry*, 1957, **29**, 9, 1367.

150. M. Cohen, *Industrial Engineering Chemistry,* 1955, **47**, 2496.

151. A.J. Durbetaki, *Analytical Chemistry*, 1956, **28**, 12, 2000.

152. E.A. Emelin, V. Savinov and L.B. Sakolov, *Journal of Analytical Chemistry USSR,* 1973, **28**, 1188.

153.   A.P. Freskkov, L.N. Shudsova and E.A. Emelin, *Soviet Plastics*, 1968, **10**, 53. *Chemical Abstracts*, 1969, **70**, 20345q.

154.   Z.V. Gershenko, V.F. Blinov and Yu.B. Zimin, *Plasticheskie Massy*, 1975, **12**, 12.

155.   L. Pohaseilsky and J. Heran, *Chemicky Prumysl*, 1977, **27**, 630.

156.   R.K. Gaur, P. Sharma and K.C. Gupta, *Analyst*, 1989, **114**, 9, 1147.

157.   Y. Eckstein and P. Dreyfuss, *Analytical Chemistry*, 1980, **52**, 3, 537.

158.   D.D. Schlueter and S. Siggia, *Analytical Chemistry*, 1977, **49**, 14, 2349.

159.   D.D. Schlueter, *Application of Alkali Fusion Reaction Gas Chromatography to Organic Functional Group Analysis*, University of Massachusetts, Amherst, MA, USA, 1976.

160.   S.P. Frankoski and S. Siggia, *Analytical Chemistry*, 1972, **44**, 3, 507.

161.   J.K. Haken, P.A.D.T. Vimalasiri and R.P. Burford, *Journal of Chromatography*, 1987, **399**, 1, 295.

162.   A. Gomoryova, *Chemical Abstracts*, 1975, **83**, 596924.

163.   E. Stahl and L.S. Oey, *Kunststoffe*, 1974, **64**, 11, 657.

164.   O. Mleinek and L. Cveckova, *Journal of Chromatography*, 1974, **94**, 135.

165.   L.S. Kalinina and L.I. Doroshina, *Chemical Abstracts*, 1973, **79**, 54100g.

166.   R.J. McGowan, *Analytical Chemistry*, 1969, **41**, 14, 2074.

167.   R.J. McGowan, *Analytical Chemistry*, 1970, **42**, 8, 942.

168.   N.P. Kulikova and L.E. Shahlygin, *Khimicheskie Volokna*, 1973, **3**, 24.

169.   A.S. Teleshova, E.N. Teleshar and A.N. Pravednikov, *Vyskomol Soedin Seria A*, 1971, **13**, 2309. [*Chemical Abstracts*, 1972, 76, 46644.]

170.   A. Krishen, *Analytical Chemistry*, 1972, **44**, 3, 494.

171.   T. Tukuchi, S. Tauge and Y. Sigmura, *Journal of Polymer Science A1*, 1968, **6**, 1, 3415.

172.   G. Nonjilal, B.Mitra and S.R. Palet, *Makromolekulare Chemie*, 1977, **178**, 1707.

173. T. Berl and K. Hefler, *Cellulose Chemistry*, 1933, **14**, 67.

174. S.V. Dubiel, G.W. Griffith, C.L. Long, G.K. Baker and R.E. Smith, *Analytical Chemistry,* 1983, **55**, 1533.

175. S.R. Gaboury and M.W. Urban, *Polymer*, 1992, **33**, 23, 5085.

176. R.D. Parker, Dow Corning Corporation, Barry, Wales, unpublished procedure.

177. G.Gritz and H. Hurcht, *Zeitschrift für Anorganische und Allgemeine Chemie,* 1962, **317**, 35.

178. V.M. Krasikova, A.N. Kaganova and V.D. Lobtov, *Journal of Analytical Chemistry USSR*, 1971, **28**, 1458.

179. M.G. Voronkov and V.T. Shemyatenkova, *Bulletin of the Academy of Science USSR, Division of Chemical Science*, 1961, 178. [*Chemical Abstracts*, 1961, **55**, 16285b.]

180. J. Franc and K. Placek, *Collection of Czechoslovak Chemical Communications*, 1973, **38**, 513.

181. J. Franc, *Chemical Abstracts*, 1975, **82**, 67923q.

182. A.P. Kreshkov, V.T. Shemyatenkova, S.V. Syavtsillo and N.A. Palamarchuck, *Journal of Analytical Chemistry USSR*, 1960, **15**, 727. [English Translation]

183. G.W. Heymun, R.L. Bujalski and H.B. Bradley, *Journal of Gas Chromatography*, 1964, **2**, 300.

184. V.M. Krasikova and A.N. Kaganova, *Journal of Analytical Chemistry USSR*, 1970, **25**, 1212. [English Translation]

185. E.R. Bissell and D.B. Fields, *Journal of Chromatographic Science*, 1972, **10**, 164.

186. J. Franc and K. Placek, *Mikrochimica Acta*, 1975, **64**, 1, 31.

187. C.L. Hanson and R.C. Smith, *Analytical Chemistry*, 1972, **44**, 9, 1571.

188. M. Seino and Y. Kawakami, *Polymer Journal*, 2004, **36**, 5, 422.

4 Monomer Ratios in Copolymers

4.1 Olefinic Copolymers

4.1.1 Ethylene-propylene

4.1.1.1 Determination of Bound Propylene in Ethylene – Propylene Copolymers

Tosi and Simonazzi [1] have described an infrared method for the evaluation of the propylene content of ethylene-rich, ethylene-propylene copolymers. This is based on the ratio between the absorbance of the 7.25 μm band and the product of the absorbances by the half width of the 6.85 μm band obtained on diecast polymer film at 160 °C (**Table 4.1**).

The calibration curve, based on a series of standard copolymers prepared with either ^{14}C-labelled ethylene or propylene, is obtained by plotting the 7.25 absorbance:6.85 absorbance ratio against the C_3 weight fraction. The basis for the calibration of many methods for the analysis of ethylene – propylene copolymers is the work published by Natta and co-workers [2] which involves measuring the infrared absorption of polymer solutions at 7.25 μm presumably due to methyl vibrations which is related to the propylene concentration in the copolymer. In some cases the dissolution of copolymers with low propylene content or some particular structures is difficult [3, 4]. Moreover, Natta's solution method was calibrated against his radiochemical method [2] for which the precision of the method was not stated; a considerable amount of scatter is evident in the data presented. Typical methods that have used Natta's solution procedure [2] for calibration are described in publications by Wei [5] and Gössl [6]. These infrared methods avoid the solution problems by employing intensity measurements made on pressed films. The ratio of the absorption at 13.95 μm to that at 8.70 μm is related to the propylene content of the copolymer. Some objections [7] to the use of solid films have been raised, based on the effect of crystallinity on the absorption spectra in copolymers with low propylene content. These film methods are reliable only over the range 30-50 mol% propylene.

Other infrared methods for the determination of the ethylene – propylene ratio in copolymers are reviewed in **Table 4.2**.

Table 4.1 Calibration points for the composition analysis of C_2-C_3 copolymers (spectra recorded at 160 °C)		
Sample	C_3 (wt%)[a]	$A_{7.25}/A_{6.85}$
3137-25	40.5	0.652 ± 0.011
3629-48	32.9	0.561 ± 0.053
3629-44	32.0	0.548 ± 0.032
3137-38	30.7	0.606 ± 0.024[b]
3137-31	20.7	0.416 ± 0.018
3297-55	18.2	0.365 ± 0.037
3297-59	18.0	0.357 ± 0.015
3274-53	14.2	0.318 ± 0.015
Blend No. 1	11.0	0.315 ± 0.022
Blend No. 2	6.0	0.204 ± 0.013
Polyethylene	6.0	0.036 ± 0.007

[a] *Radiochemical analysis*

[b] *The standard deviation has been multiplied by the Student's $t_{95\%}$ coefficient to the number of replications (on average 5) for each calibration point.*

*Reproduced with permission from G. Tosi and T. Simonazzi, Die Angewandte Macromolecular Chemie, 1973, **32**, 1, 153 [1]*

Table 4.2 Application of infrared spectroscopy to the determination of propylene in ethylene – propylene copolymers			
Wavelength	Related to	Comments	Reference
7.25 μm (CCl_4 solution) Ratio 13.95/8.7 μm (solid film)	7.25 μm methyl groups Propylene content in range 30–50% propylene	High scatter in results Results adversely affected by polymer crystallinity	[3–5] [4–6]
Ratio 7.25 μm band (solid diecast film) and product of absorbance by the halfwidth of 6.85 μm band	Propylene content	Calibrated *versus* [14]C labelled ethylene or propylene copolymers by plotting ratio 7.25/6.55 μm *versus* % propylene weight fraction	[7]

Table 4.2 Continued			
Wavelength	Related to	Comments	Reference
7.25 µm and ratio 8.6/2.32 µm (CCl$_4$ solution)	7.25 µm methyl groups	Copolymers containing 30% propylene	[10]
Ratio 1.692/1.764 µm (CCl$_4$ solution)	1.692 µm CH$_3$ groups 1.764 µm CH$_2$ groups	Applicable to copolymers containing 15–52% propylene	[11]
13.7 µm and solid film scanned at 180 °C	13.70–13.89 crystalline phase 13.89 amorphous phase	Calibrated *versus* known composition copolymers prepared with[14]C labelled ethylene	[12-14]
Ratio 11.00/11.25 µm pyrolysis of film at 450 °C	11.00 µm vinyl groups 11.25 µm vinylidine groups	Ratio 11.00/11.25 µm varies with propylene content of copolymer Copolymers containing >8% propylene	[15] [16, 17]
Ratio 1.465/ 1.378 µm	-	Measurement of ethylene – propylene ratio	[18]
Propylene content correlated with ratio A$_1$/A$_1$ + A$_2$ where A$_1$ and A$_2$ are absorbances at 8.62 and 13.89 µm	-	Measurement of propylene content in isotactic polyethylene – polypropylene blends	[19]
ATR near IR specroscopy	-	Measurement of ethylene – propylene ratio	[20]
Measurement of absorbances at 14.49, 13.85, 13.66, 13.30, and 11.75 µm	-	Measurement of ethylene – propylene ratio	[21, 22]
Source: Author's own files			

4.1.1.2 Determination of Bound Ethylene in Ethylene Copolymers

Paxton and Randall [8] used Fourier transform infrared (FTIR) spectroscopy to measure the concentration of ethylene in ethylene propylene copolymers by amounts down to 0.1%. These polymers contained greater than 95% propylene, with the ethylene units present as isolated entities between two head-to-tail propylene units. These workers point out that most infrared bands used for determining copolymer compositions are sensitive to sequences of both monomers. This infrared method for compositional analysis can be calibrated if: (a) known standards of similar constitution to the copolymers being analysed are available and (b) assignments and behaviour of the calibration bands are well established; preferably the absorptivities of these bands should be relatively independent of the position of monomer units in the chain. Thus, quantitative infrared analysis of copolymers depends primarily on the standards employed, whose composition can be determined directly and reliably. Paxton and Randall used ^{13}C-NMR (carbon nuclear magnetic resonance) to provide such reference standards for the less time consuming infrared measurements. An excellent correlation is obtained between ^{13}C-NMR and infrared results on a series of ethylene – propylene copolymers containing greater than 95% wt% propylene.

Determination of infrared spectra of moulded films of the polymer at 13.66 μm enables the propylene unit content of the polymer to be determined. The absorbance is measured of the 13.66 μm infrared band, attributed to gamma $(CH_2)_3$ is characteristic of an ethylene unit isolated between two head-to-tail propylene units. The method is calibrated against known copolymers of similar constitution to the copolymers being analysed:

i.e. $—CH—CH_3—CH_2—CH_2—CH_2—CHCH_3—CH_2—$

$\quad\quad\quad\quad\quad\quad\quad$ α $\quad$ β $\quad$ γ

$\quad$ propylene $\quad\quad\quad\quad$ ethylene $\quad\quad\quad\quad$ propylene
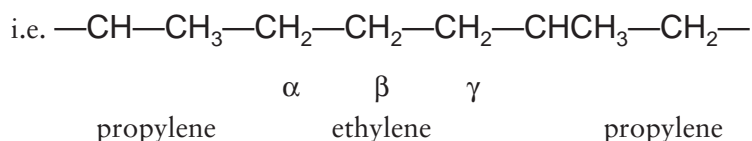
The absorbance of the 13.66 μm infrared band attributed to γ_r $(CH_2)_3$ is recorded.

The equation relating the infrared absorbance to the ethylene content is:

Y = 2.465 X + 0.451

where Y is the infrared absorbance at 13.66 μm divided by the film thickness in centimetres and X is the wt% ethylene. The standard errors are 0.110 and the intercept is 0.051 for the slope.

The infrared absorbance at 13.66 μm is sufficiently sensitive to the ethylene incorporation to determine the wt% ethylene within 0.1–0.2% at the 95% confidence level. From the ^{13}C-NMR data, it can be concluded that the propylene units occur in predominantly isotactic, head-to-tail sequences and that the ethylene units are incorporated as isolated units only. Thus, this structural prequisite is a requirement for application of this method because it has not been tested on copolymers containing propylene configurational irregularities or ethylene sequences two units and longer.

Lomonte and Tirpak [9] have developed a method for the determination of the percentage of ethylene incorporated in ethylene-propylene block copolymers. Standardisation is taken from mixtures of the homopolymers. Both standards and samples are scanned at 180 °C in a spring-loaded demountable cell. The standardisation is confirmed by the analysis of copolymers of known ethylene content prepared with ^{14}C-labelled ethylene. By comparison of the infrared results from the analyses performed at 180 °C, and also at room temperature, the presence of ethylene homopolymer can be detected. These workers derived an equation for the quantitative estimation of the percentage of ethylene present as copolymer blocks.

This method distinguishes between true copolymers and physical mixtures of copolymers. It makes use of a characteristic infrared rocking vibration due to sequences of consecutive methylene groups. Such sequences are found in polyethylene (PE) and in the segments of ethylene blocks in ethylene-propylene copolymers. This makes it possible to detect them at 13.70 and 13.89 um. There are bands at both these locations in the infrared spectrum of the crystalline phase, but only at 13.89 um in the amorphous phase. The ratio of these two bands in the infrared spectrum of a polymer film at room temperature is a rough measure of crystallinity. As seen by this ratio, the infrared spectra of the copolymers show varying degrees of PE-type crystallinity, dependent on the ethylene concentration and method of incorporation. It is this varying degree of crystallinity that allows the qualitative detection of ethylene homopolymer in these materials. A calibration curve of absorbance at 13.89 μm *versus* ethylene is made from known mixtures for both hot and cold runs. Both plots result in straight lines from which the following equations are calculated:

% Ethylene at 180 °C = A/(0.55b)

% Ethylene at room temperature = A/(3.0b)

where A is the absorbance measured at 13.89 μm and b the thickness of the specimen in centimetres.

A series of ethylene-propylene block copolymers prepared with ^{14}C-labelled ethylene was analysed for percentage of ethylene incorporation by radiochemical methods.

Table 4.3 ^{14}C-labelled ethylene-propylene copolymers ethylene, %			
Sample	Radiochemistry	Hot infrared scan	Cold infrared scan
3401	2.4	2.9	0.9
3402	4.0	3.65	1.3
3403A	22.4	20.7	14.7
3403B	24.5	22.2	15.3
3404	12.4	13.0	7.1
3405	14.0	14.1	7.5
From J.N. Lomonte and J.A. Tirpak, Polymer Science, 1964, A2, 705 [9]			

Table 4.4 Samples with hydrogen-reduced active sites		
Sample no.	Ethylene %	
	Hot infrared scan	Cold infrared scan
1487	5.0	5.3
1553	7.1	6.9
From J.N. Lomonte and J.A. Tirpak, Polymer Science, 1964, A2, 705 [9]		

When scanned at 180 °C, these samples gave infrared results that agreed with the radiochemical assay quite well. However, when the cooled samples were scanned, the results from the cold calibration were low in comparison with the known ethylene content. These data are shown in **Table 4.3**.

A pair of samples were prepared in which the active sites on the growing propylene polymer were eliminated by hydrogen before addition of ethylene. Practically identical values for percentage of ethylene incorporation were calculated for both the hot and cold scans. These data are shown in **Table 4.4**.

Ciampelli and co-workers [10] have developed two methods based on infrared spectroscopy of carbon tetrachloride solutions of polymers at 7.25, 8.65, and 2.32 μm for the analysis of ethylene – propylene copolymers containing greater than 30% propylene. One method can be applied to copolymers soluble in solvents for infrared analysis; the other can be applied to solvent-insoluble polymer films. The absorption band at 7.25 μm due to methyl groups is used in the former case, whereas the ratio
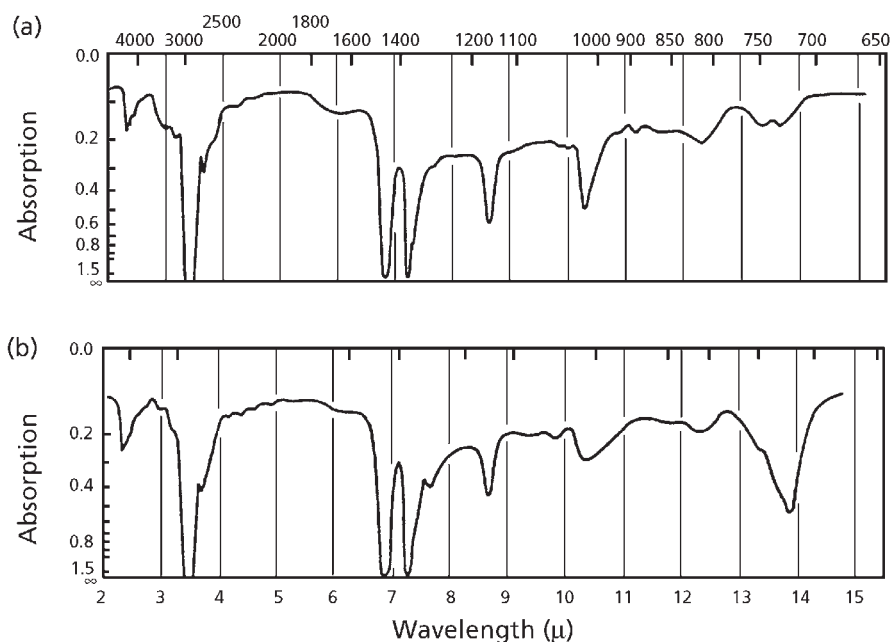
Figure 4.1 Infrared spectra of ethylene-propylene copolymers of various compositions: (a) 85.5% polyethylene; (b) 55.5% polyethylene. (*Reprinted with permission from F. Ciampelli, G. Bucci, A. Simonazzi and A. Santambroglio, Chimica et L'Industria, 1962, **44**, 489*) [10]

of the band at 8.6 µm to the band at 2.32 µm is used in the latter. Infrared spectra of polymers containing 55.5 and 85.5% ethylene are shown in **Figure 4.1**.

4.1.1.3 Nuclear Magnetic Resonance Spectroscopy

For the determination of ethylene copolymers containing more than 95% propylene Paxton and Randall [8] have described a method wherein a 1,2,4 trichlorobenzene – perdeuterobenzene solution of the polymer is examined on a nuclear magnetic resonance (NMR) spectrometer to evaluate methine resonances. The method is calibrated against known copolymers of similar constitution to the copolymers being analysed.

The best results are obtained using methine resonances 4 and 5 (**Table 4.5**) to determine copolymer composition. This is because the methane carbon resonance is the least sensitive towards configurational differences and also the least affected by overlap from neighbouring resonances. Similar results are obtained whether one uses peak heights or peak areas.

Table 4.5 Observed and reference ^{13}C-NMR chemical shifts in ppm for ethylene – copolymers and reference polypropylenes as measured with respect to an internal IMS standard

Resonance line	Carbon	3/97 E/P[a]	E/P	97/3[a] E/P	Sequence assignment	Reference crystalline polypropylene	Amorphous polypropylene
1	alpha alpha CH$_2$	46.4	46.3		PPPP	46.5	47.0–47.5 r / 46.5 m
2	alpha alpha CH$_2$	46.0	45.8		PPE		
3	alpha gamma CH$_2$	37.8	37.8		PPEP		
4	CH	30.9	30.7		PPE		
5	CH	28.8	28.7		PPP	28.5	28.6 mmmr / 28.5 rmmr / 28.4 mr + rr
6	beta beta CH$_2$	24.5	24.4		PPEPP		
7	CH$_3$	21.8	21.6		PPPP	21.8	21.3–21.8 mm / 20.6–21.0 mr / 19.9–20.3 rr
8	CH$_3$	21.6	21.4		PPPE		
9	CH$_3$ CH$_3$ CH alpha CH$_2$ beta CH$_2$ (CH$_2$)$_n$	20.9	20.7 19.8 33.1 EPE 29.8	19.8 33.1 37.4 27.3 29.8	PPPEP EPE EPE EPE EPE EEE		

From the NMR data it can be concluded that the propylene units occur in predominantly isotactic head-to-tail sequences and that the ethylene units are incorporated as isolated units only. The NMR method can be used to provide reference standards for the less time consuming infrared method. Provided the infrared method is calibrated in this way, excellent agreement is obtained between the infrared and NMR methods for copolymers containing >95% propylene. No corrections need to be made for differential nuclear Overhauser effects since these have been shown to be constant for the major resonances in low ethylene – propylene copolymers.

Cheng and Kakugo [23] and Zhang and co-workers [24] have also discussed the application of ^{13}C-NMR to the measurement of monomer ratios in ethylene – propylene copolymers.

De Pooter and co-workers [25] point out that the quantitative analysis of branching in polyethylene has been a subject of much investigation due to the commercial importance of this material [26–33]. The primary analysis tools for the determination of the level and type of branching have been infrared (IR) and ^{13}C-NMR spectroscopy. The IR method utilises the absorbance of the methyl group at about 7.25 µm for the determination. This method suffers from limitations, namely, that the absorbance must be corrected due to interferences of the methylenes and other bands. The absorbance frequency and absorptivity of the methyl groups are also somewhat dependent upon the type of branch, and upon crystallinity [34]. This presents a problem for the quantitative analysis of branching in ethylene copolymers of two or more comonomers. However, the IR method has some distinct advantages over the ^{13}C-NMR method; these include precision and analysis time. There is a need to provide well-defined and accepted standards for this analysis in order that the IR method might be routinely practiced.

The NMR method lists as an advantage that it is an absolute method, not requiring standards. Also it suggests the benefit of specificity, since the location of the resonance identifies it as being from a given type of branch. In fact, branches shorter than six carbons in length can be unambiguously assigned from their ^{13}C-NMR spectrum. Branches longer than five carbons in length cannot be differentiated from long chain branches [30]. Therefore, the advantages of the NMR technique, accuracy and specificity, can be utilised to define standard materials which can then be used to standardise the IR method.

De Pooter and co-workers [25] described a comprehensive ^{13}C-NMR method for the analysis of composition in the most common commercial polyethylene copolymers. The method covers ethene copolymers with propene, also butene-1, hexene-1, octene-1, and 4-methyl pentene-1 in the composition range of 1–10 mol%. The chemical shift assignments and T_1 values of the resonances of the copolymers are presented
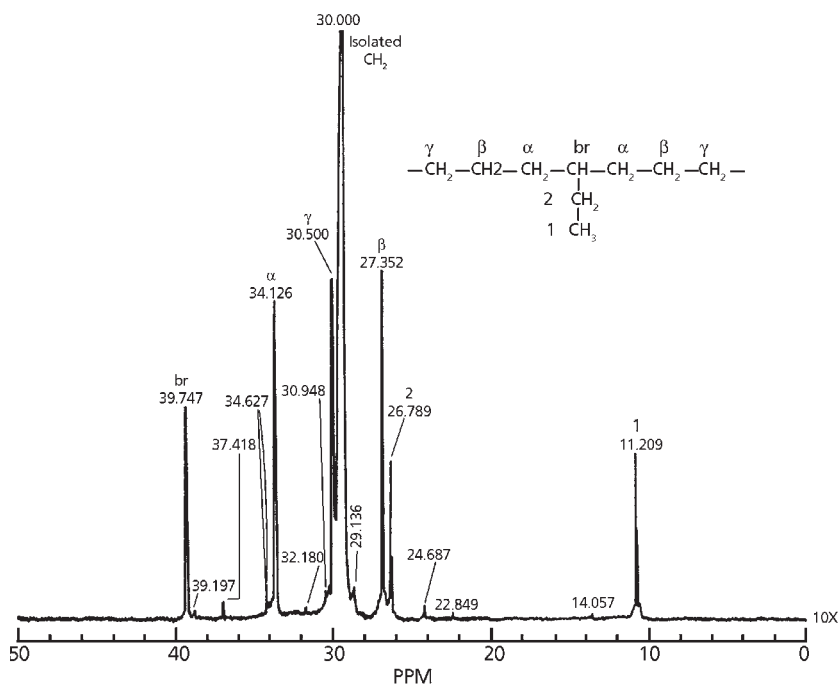
Figure 4.2 The ^{12}C-NMR spectrum of an ethylene-butene-1 copolymer.

(see **Figures 4.2–4.5**). Results of precision studies and interlaboratory analyses showed that the molar composition could be determined with a relative precision at 2σ of about 6%.

The method involves measurements between 10 and 50 ppm. **Figure 4.6** shows the NMR spectrum obtained for an ethylene – propylene copolymer. The method is valid for products containing 1–10 mol % of the second alkene-1 excluding products containing an extraordinary amount of blocky alkene-1.

4.2 Pyrolysis Gas Chromatography

The consensus of opinion is that, particularly in the cases of those polymers such as the polyolefins where complex pyrograms are produced, filament pyrolysis is the preferred method. For the purposes of fundamental studies, pyrolysis at a variety of temperatures and heating rates is preferred. Smaller sample weights of the order of 1–2 mg are preferred as these prevent or reduce the occurrence of secondary side
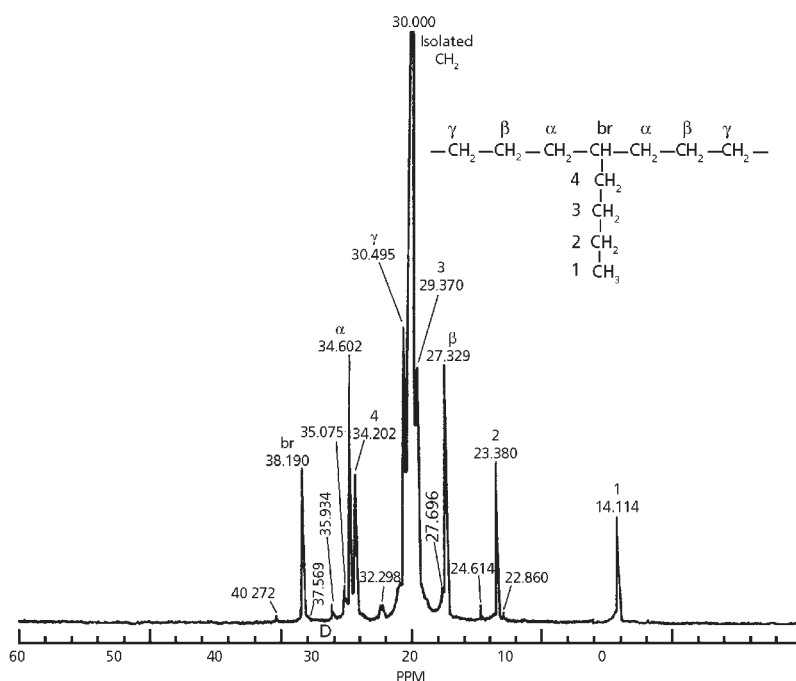
Figure 4.3 The ^{13}C-NMR spectrum of an ethylene-hexene-1 copolymer.

reactions in the pyrolysis which might confuse the interpretation of the pyrogram when carrying out polymer structural studies. Certainly, sample weights above 3 mg should be avoided. The use of small sample sizes necessitates the use of the more sensitive types of gas chromatograph detectors, such as flame ionisation. In particular circumstances where the occurrence of a microstructural feature is being studied, failure to use a sufficiently sensitive detector could result in the pyrolysis product being missed. To improve sensitivity in such studies, a limited increase in sample weight, say from 1–2 mg to 4 might be permitted.

In-line hydrogenation is a useful innovation for simplifying the pyrogram obtained for those polymers which produce complicated mixtures, but should be used with caution in fundamental studies. More information might be obtained by carrying out studies with and without in-line hydrogenation. Finally, the type of gas chromatography separation column used should be the subject of close scrutiny. The information gained in pyrolysis studies is only as good as the degree and type of separation achieved on the column and, particularly in the early stages of investigation work, a variety of columns should be studied.
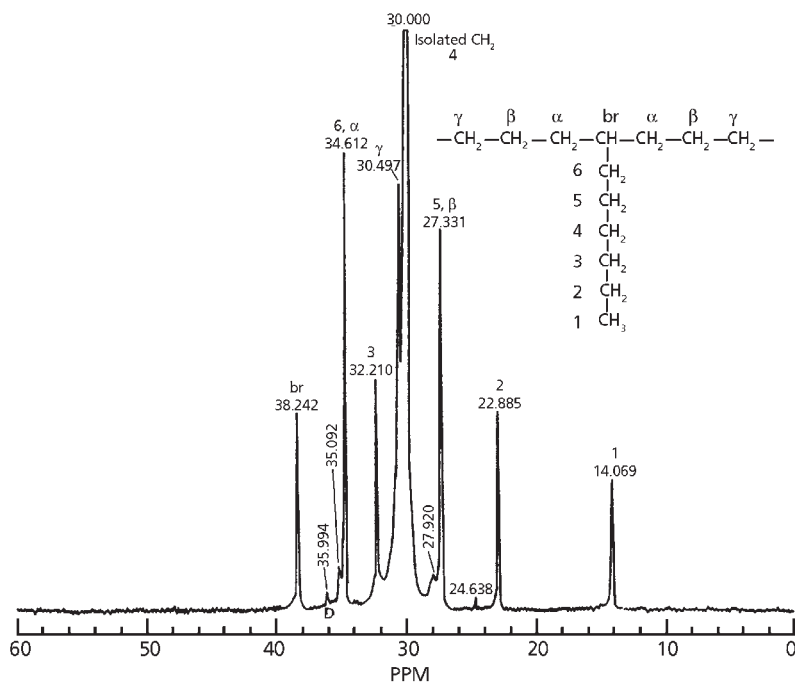
Figure 4.4 The ^{13}C-NMR spectrum of an ethylene-octene-1 copolymer.

Quantitative measurements of the amounts of various pyrolysis products can, in many instances, be correlated with the percentage composition of a copolymer, or with the concentration or a particular microconstituent in the polymer. Thus, Van Schooten and co-workers [35, 36] applied their pyrolysis-hydrogenation-gas chromatography technique to the quantitative determination of copolymer composition of ethylene – propylene copolymers, an analysis which presents difficulties in solvent solution-infrared methods, especially with samples that are only partly soluble in suitable solvents such as carbon tetrachloride. Since the hydrogenation pyrogram of polyethylene consists almost exclusively of normal alkanes and that of polypropylene isoalkanes, the ratio of the peak heights of a *n*-alkane to an iso-alkane is a good measure of the copolymer composition. The ratio *n*-C_7/(2-methyl C_7 + 4-methyl C_7) was found to be a good measure of ethylene – propylene ratio in copolymers.

4.2.1 Pyrolysis – Infrared Spectroscopy

Brown and co-workers [15] showed that pyrolysis of ethylene – propylene copolymers at 450 °C produces derivatives that are rich in unsaturated vinyl and
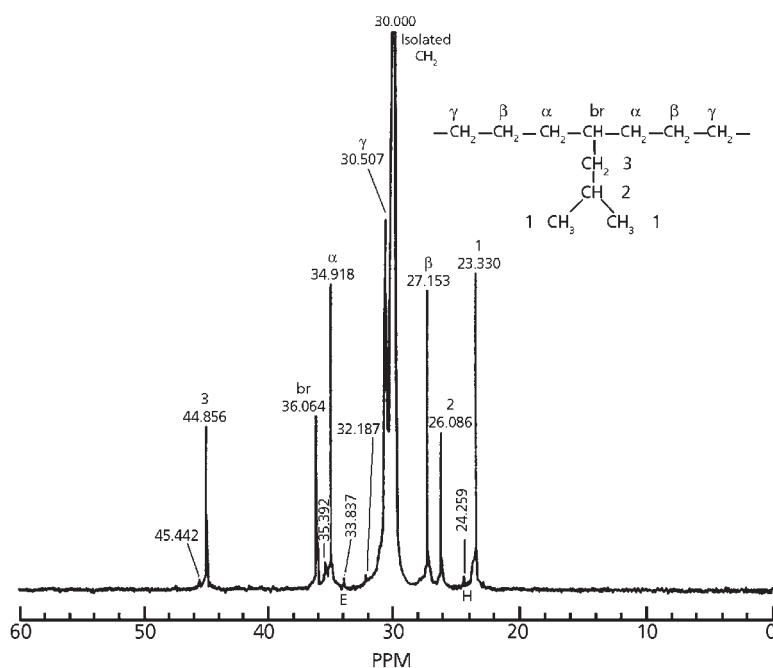
Figure 4.5 The ^{13}C-NMR spectrum of an ethylene-4-methyl pentene copolymer.

vinylidene groups, similar to those obtained in the pyrolysis of natural rubber and styrene-butadiene rubber mixtures [37], which produce vinyl groups derived from the butadiene part of the molecule and the vinylidene groups from the methyl branch of the isoprene units. This unsaturation exhibits strong absorption of the infrared region. The ratio for the absorption of the vinyl groups to that of the vinylidene groups varies with the mole fraction of propylene in saturated ethylene-propylene copolymers. Making use of this ratio, an analytical method for determining propylene in both raw and vulcanised ethylene – propylene copolymers was developed. The vinyl group absorbs at about 11.00 μm and the vinylidene at about 12.25 μm.

Figure 4.7 shows some typical spectra obtained on the pyrolysates in the region of 10.50-11.76 μm. The values of the ratio, R (X 100) range from 9.977 to 0.0290, respectively, for 0 to 100 mole% propylene for the raw samples and from 5.400 to 0.0431, respectively, for 10 to 100 mole% propylene for the vulcanised samples. The common logarithm of the ratio, R, can be represented by a liner function of the mole % of propylene in the copolymer.
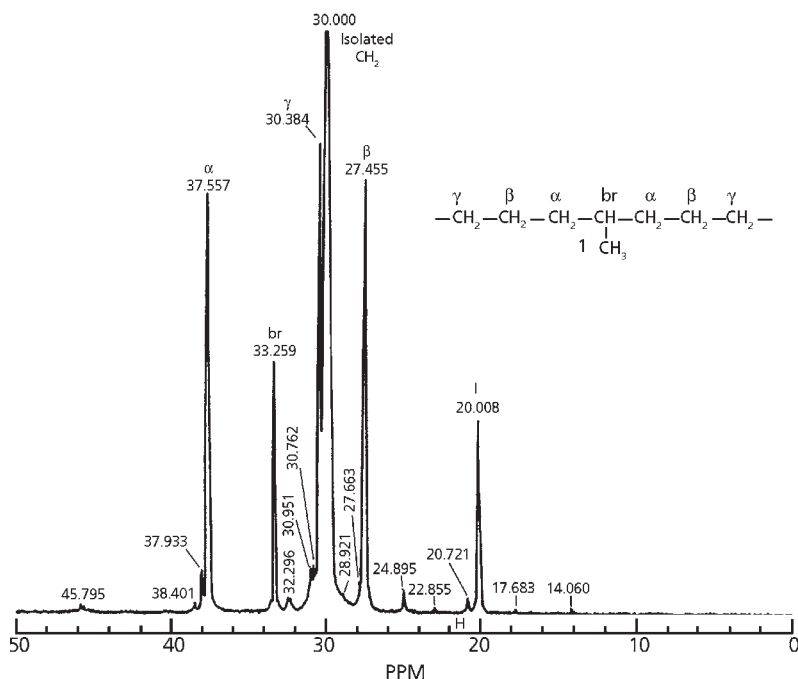
Figure 4.6 The ^{13}C-NMR spectrum of an ethylene-propylene copolymer.

4.2.2 Ethylene – Butane-1 Copolymers

The NMR spectroscopy has also been applied to the analysis of copolymers of ethylene with butane-1, hexane-1, octane-1 and 4-methyl pentene-1 [27]. Cheng [38] and Fisch and Dannenberg [39] have also discussed the application of ^{13}C-NMR to the measurement of ethylene – butane-1 copolymers. They analysed copolymers containing up to 11% bound to propylene.

Hatfield and co-workers [40] applied melt state magic angle spinning (MAS) ^{13}C-NMR to the determination of comonomer types and composition in ethylene-alpha olefin copolymers. Melt state ^{13}C-NMR with MAS and dipolar coupling was used for this analysis and gave the advantages of reduced analysis time, and the ability to analyse samples which were not amenable to solution state NMR. Hatfield and co-workers [40] examined five different ethylene-alpha olefin copolymers (one crosslinked, i.e., insoluble). Good agreement was obtained between melt and solution NMR methods.

NMR spectroscopy has also been used to elucidate the composition of butane - ethylene - propylene [41], ethylene - butene-1 [42] and 4-methyl pentene-1-pentene copolymer [42, 43].
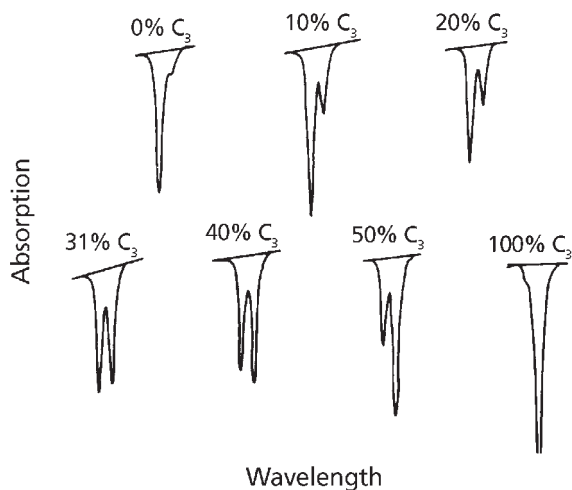
Figure 4.7 Typical infrared spectra of pyrolysates obtained from raw ethylene-propylene copolymers. The position of the absorption peaks from left to right are near 909 cm^{-1} and 889 cm^{-1}, respectively, for each pair, and the nominal compositions are indicated in mole% propylene. (*Reprinted with permission from J.E. Brown, M. Tryon and J. Mandel, Analytical Chemistry, 1963, 35, 13, 2172. ©1963, ACS*) [15]

A pyrolysis – gas chromatography method has been described [44–46] for the determination of the composition of an ethylene-butene-1 copolymer containing up to about 10% butene. Pyrolyses were carried out at 410 °C in an evacuated gas vial and the products swept into the gas chromatograph. Under these pyrolysis conditions, it is possible to analyse the pyrolysis gas components and obtain data within a range of about 10% relative standard deviation. The peaks observed on the chromatogram were methane, ethylene, ethane, combined propylene and propane, isobutane, 1-butene, trans-2-butene, *cis*-2-butene, 2-methyl-butane and *n*-pentane.

A straight line relationship exists between the amount of ethylene produced on pyrolysis and the amount of *i*-butene in the ethylene – butene copolymer. The y intercept of 16.3% ethylene should represent that amount of ethane which would result from a purely linear polyethylene. An essentially unbranched Phillips-type polyethylene polymer yielded 14.5% ethylene, which is fairly close to the predicted 16.3%.

Other methods for analysing ethylene – butane-1 copolymers include x-ray crystallography and melting point fractionation [47]. The most widely adopted technique is infrared spectroscopy using either a heated cell to eliminate the effects of crystallinity, or more simply by scanning a film of known thickness and comparing the absorbance to those

of standards [47–51]. Infrared is the easiest method to run and the least demanding in equipment. It requires, however, a set of standards for calibration of the instrument used. These standards have in the past been frequently obtained by copolymerisation of ^{14}C tagged monomer and radioassay [52]. This technique introduces additional manipulations and the possibility of isotope effects. It is also time-consuming.

4.2.3 Ethylene – Hexane-1

Kissin and Brandolini [53] reported on the ^{13}C-NMR spectra of ethylene – hexane-1 copolymers and assigned chemical shifts for these copolymers which enabled them to determine the ratio of the two comonomers. They assign the 29.4 and 29.3 ppm peaks to be hexane-1-β CH_2 carbon atoms. Cheng [54] also used this technique to analyse ethylene – hexane-1 copolymers.

4.2.4 Other Olefin Polymers

Aoki and co-workers [55] and others [56–58] used ^{13}C-NMR spectroscopy to study the microstructure of propylene-butene-1 copolymers.

4.2.5 Ethylene – Vinyl Acetate Copolymers

There are two methods for this determination, depending on the concentration of vinyl acetate. At levels below 10% a band at 2.89 μm is used. This band is not suitable for higher concentrations because the necessary film thickness is less than 0.1 mm. For higher concentrations, the carbonyl overtone band at 16.39 μm can be used, since much thicker films are needed to give suitable absorbance levels. Here, the carbonyl overtone band was used for a series of standards with vinyl acetate concentrations up to 35%, the nominal thickness being about 0.5 mm.

A combination of CDS and QUANT software on a Perkin Elmer model 683 infrared spectrometer was used to establish the calibration for this analysis. Once the calibration has been carried out, the simplest way to measure an unknown sample would be with an OBEY routine in the CDS II software. This would incorporate the calibration data so that the single routine would measure the spectrum and calculate the vinyl acetate concentration with an error of approximately 5%.

Pallacini and co-workers [59] and Jones and McClelland [60] also used infrared spectroscopy to analyse ethylene vinyl acetate copolymers. ^{13}C-NMR has also been used [61-63].

Other ethylene copolymers that have been studied include those with vinyl alcohol [64], acrylates [65] tetrafluoroethylene [66], 4-methyl pentene [67, 68], propylene – vinyl chloride [69], ethylene vinyl cyclohexane [70] and ethylene – vinyl acetate [71].

4.3 Vinyl Chloride Copolymers

4.3.1 Vinyl Chloride – Vinyl Acetate

Infrared spectroscopy has been applied to the determination of free and combined vinyl acetate in vinyl chloride – vinyl acetate copolymers [72]. This method is based upon the quantitative measurement of the intensity of absorption bands in the near-infrared spectral region arising from vinyl acetate. A band at 1.63 μm due to vinyl groups enables the free vinyl acetate content of the sample to be determined. A band at 2.15 μm is characteristic for the acetate group and arises from both free and combined vinyl acetate. Thus, the free vinyl acetate content may be determined by difference at 2.15 μm. Polymerised vinyl chloride does not influence either measurement.

Campbell [73] used an isotope dilution method – derivative method to determine down to 0.2% of combined vinyl acetate in the copolymers. In this method, a known amount of methyl labelled acetic 2-^{14}C acid is added to a solution or suspension of the resin in methyl ethyl ketone and the ester is hydrolysed with sodium hydroxide. The major portion of the sodium acetate ^{14}C is isolated and converted to 2-methylbenzimidazole-methyl ^{14}C by means of the Phillips reaction with *o*-phenylene diamine:
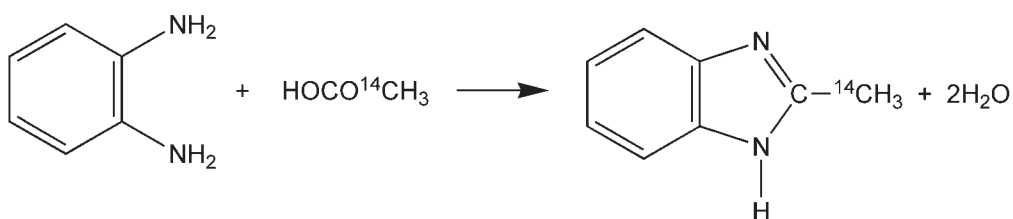
The product is radioassayed following addition of a scintillator, and the vinyl acetate content calculated from the determined specific activities.

4.3.2 Vinylidene Chloride – Vinyl Chloride

Wang and Smith [74] used pyrolysis – gas chromatography to elucidate the composition of, and carry out structural studies on, vinyl chloride-vinylidene chloride copolymers.

The number average sequence length, which reflects monomer arrangement in the copolymer, was calculated using formulae that incorporate pure trimer and hybrid trimer peak intensities.

Due to the difference in reactivity between vinyl chloride and vinylidene chloride monomers the structure of the polymer was further investigated on the basis on the percentage of grouped monomers (i.e., the number average sequence length for vinyl chloride and vinylidene chloride repeat units). The results obtained for compositional analysis achieved by this method and by ^{1}H-NMR were in excellent agreement. In the method 2.5 mg of sample was pyrolysed in a quartz tube, equilibrated for 5 minutes at 180 °C, then pyrolysed at 700 °C for 20 seconds using a pyroprobe with a platinum coil. Gas chromatography was carried out using a flame ionisation or mass spectrometric detector.

In further work Wang and Smith [75] used pyrolysis – gas chromatography (Py-GC) to study the composition and structure of vinylidene chloride/vinyl chloride copolymers. The composition and number average sequence length, which reflects the monomer arrangement in the polymer, were calculated using formulae that incorporate the pure trimer peak intensities and hybrid trimer peak intensities. The structure of the polymer was further investigated on the basis of the percentage of grouped monomers (i.e., the number average sequence length for vinyl chloride and vinylidene chloride repeat units.) The composition and number average sequence length elucidated from the Py-GC study were compared with the product composition specification and/or the composition measured by hydrogen ion NMR.

Figure 4.8 shows the typical pyrogram of a vinylidene chloride/vinyl chloride copolymer. The identification of all four trimers was accomplished by comparing retention times with those of standard compounds, as well as identification by Py-GC/MS in the electron ionisation (El) mode.

Benzene, chlorobenzene, dichlorobenzene, and trichlorobenzene are four major products formed in the pyrolysis of vinylidene chloride/vinyl chloride copolymer. To make the composition calculation, the first assumption is that all trimer peak intensities generated from the Py-GC after correction for pyrolysis efficiency and detection efficiency accurately represent the triad distribution of the vinylidene chloride/vinyl chloride copolymer. If a close relationship exists between the triad distribution in the polymer chain and the production of trimers in pyrolysis, the composition and number average sequence length can be calculated on the basis of the trimer production in the pyrolysis.

Results were in good agreement with those obtained by ^{1}H-NMR (**Table 4.6**). Copolymers containing between 11 and 95% vinyl chloride, and 5 to 89% of vinylidene chloride were successfully analysed.
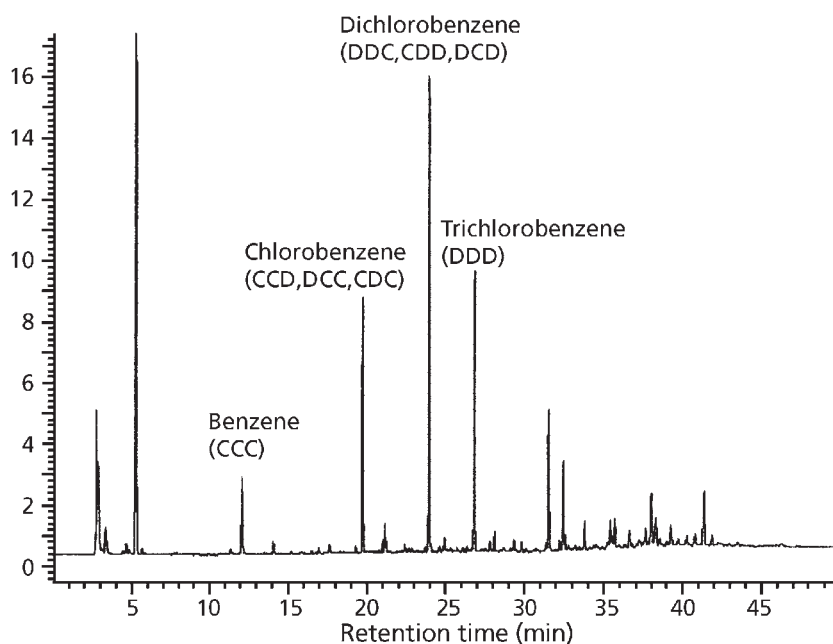
Figure 4.8 Typical pyrogram of a vinylidene chloride/vinyl chloride copolymer. (*Reprinted with permission from F.C-Y. Wang and P.B. Smith, Analytical Chemistry, 1996, 68, 3, 425. ©1996, ACS*) [75]

		Sample					
Pyrolysis (wt%)	VC(C)	11	12	14	17	50	95
	VDC(D)	89	88	86	83	50	5
^{1}H-NMR	VC(C)	11	12	14	17	48	95[§]
	VDC(D)	89	88	86	83	52	5[§]

Table 4.6 Composition results calculated from pyrolysis peak intensities compared with the ^{1}H-NMR results of five different compositions of vinylidene chloride/vinyl chloride copolymer

[§]*Weight percentage data from commercial product specification*

VC: vinyl chloride

VDC: vinylidene chloride

*Reprinted with permission from F.C-Y. Wang and P.B. Smith, Analytical Chemistry, 1996, **68**, 3, 425 [75]. ©1996, ACS*

Other vinyl polymers that have been examined include vinylidene chloride – methyl methacrylate [76], vinylidene chloride – phenyl acetate [77], vinyl chloride – butadiene [78], vinyl copolymers [79] and vinylidene chloride – polyethylene [80].

4.4 Styrene Copolymers

4.4.1 Styrene Acrylate and Styrene Methacrylate

Anderson and co-workers [81] have described an infrared method for the determination of down to 1% of bound styrene units in styrenated acrylate resins.

Styrene units were determined, as described below (by infrared spectroscopy at 14.28 μm) which is the phenyl ring out of mode. This frequency provides specficity, freedom from interferences, and an absorption that is directly proportional to the styrene content.

Table 4.7 Infrared analysis for bound styrene in styrenated acrylic polymers		
Sample	Styrene	
	Calculated (%)	Observed (%)
1	5. 0	5.0, 4.9
2	7.5	7.1, 6.9
3	10.0	19.6, 19.5
4	24.3	24.4, 24.3
5	24.3	25.6, 24.6
6	25.0	25.1, 25.8, 24.2[§]
7	35.0	36.3, 35.6
8	35.0	34.7, 35.2
9	40.0	38.9, 40.1
10	60.7	59.1, 60.3, 59.7[§]
11	70.0	69.3, 70.3, 69. 5[§]

[§]Percent styrene values, determined in tetrahydrofuran.

Values: all the remaining values were determined using acetone as the solvent.

*Reproduced with permission from D.G. Anderson, K.E. Isakson, D.L. Snow, D.J. Tessari and J.T. Vandeberg, Analytical Chemistry, 1971, **43**, 7, 894 [80]. ©1971, ACS*

The accuracy of this method on typical acid modified styrenated acrylic polymers is shown in **Table 4.7**. In the 5 to 70% styrene range determined values are better than 95% relative.

Urban and co-workers [82] studied the structure of styrene-acrylic acid copolymers using attenuated total reflection Fourier transform infrared spectroscopy. Kandu and El Gamel [83] correlated the relative intensities of the carbonyl frequencies of the methyl acrylate units in styrene methyl acrylate copolymers with copolymer composition. The positions and shapes of the carbonyl bands in the infrared absorption spectra of the copolymers dissolved in chloroform, were shown to depend on the composition of the copolymers and upon the presence of different proportions of methyl acrylate centred triads. The results obtained by infrared spectroscopy were compared with those obtained by ^{13}C-NMR. Infrared spectra may be used to yield information about both the copolymer composition and the triad sequence distribution.

4.4.2 Styrene – Methacrylate and Styrene – Methyl Methacrylate Copolymers

Both infrared spectroscopy [84, 85] and ^{13}C-NMR have been used in compositional studies in these copolymers.

4.2.2.1 Nuclear Magnetic Resonance Spectroscopy

Evans and co-workers [86] have described techniques employing pyrolysis – gas chromatography, proton NMR and carbon analyses for the determination of styrene and methacrylate units in styrene – methylmethacrylate and styrene-*n*-butyl methacrylate copolymers with an accuracy of ±2%. Agreement between the three independent methods is excellent. The comparison stresses the complementary nature of all three methods. The pyrolysis – gas chromatography method possesses advantages such as simplicity and rapidity.

In the NMR method a deuterated chloroform solution of the polymer containing trimethylsilane internal standard is run on the NMR spectrometer. Integration of peak areas at delta 8 and delta 1-4, gives a measure of signal strengths from aliphatic protons (methacrylate units) and aromatic protons (styrene), respectively. These areas can be used as a basis for calculating the methacrylate and styrene unit contents of the polymer.

The analysis of comonomer composition does not appear to be significantly affected by the extent of randomness observed for these materials. The difference between NMR and pyrolysis – gas chromatography results are in the range of 0-4% and 0-4.8% for styrene-*n*-butyl methacrylate and styrene – methyl methacrylate, respectively. The difference in carbon analysis and pyrolysis – gas chromatography results is also in the same range

for both the copolymers. Standard deviation for pyrolysis – gas chromatography ranges from 1.2-2.1%. Precision for NMR analyses is better than 1%.

Pyrolysis of methyl methacrylate – ethylene dimethacrylate copolymer gives only one major peak (methyl methacrylate) using a hot filament detector. The composition of methyl methacrylate – ethylene dimethacrylate copolymer can, however, be determined by pyrolysing a weighed sample and using the ratio of sample weight to area of the methyl methacrylate peak for obtaining a standard analysis curve. Under favourable conditions, with careful control of the pyrolysis column and detector variables, constituents can be determined to within ±0.5%.

The differences in the pyrograms of block and random copolymers allows estimation of the comonomer distribution. Random copolymers of ethylene with methyl acrylate or methyl methacrylate yield on pyrolysis a lower ratio of methanol/methyl or methanol/methyl methacrylate, respectively, than block polymers of the same composition. Differential thermal analysis measurements give a first-order transition for block polymers only, and by measuring the area under the transition an indication of the minimum chain length between acrylate units can be obtained.

Subrahmanyam and co-workers [87] used ^{1}H-NMR spectroscopy to determine the composition of behenyl acrylate – vinyl acetate copolymers. The reactivity ratios were evaluated by different methods and were found to be 0.021 for vinyl acetate and 1.76 for behenyl acrylate. Fineman-Ross and Kelen-Tüdos methods gave similar values. The *Q* and *e* values for behenyl acrylate were calculated as 0.25 and 0.94, respectively. The experimental copolymer composition was found to be in close agreement with calculated values.

Figure 4.9 compares ^{1}H-NMR spectra obtained for the two monomers and for the copolymer.

4.4.3 Styrene Acrylic Acid Copolymer NMR Spectroscopy

Wang and Poehlein [88] showed that ^{1}H-NMR is a valuable tool for the quantitative determination of monomer ratios in styrene – acrylic acid copolymers.

In this work, results from ^{1}H- and ^{13}C-NMR were obtained and compared.

The measurement of NMR spectra of S-AA copolymers was complicated because of the difficulties in dissolving the samples. Copolymers with high acrylic acid content cannot be dissolved in $CDCl_3$. If the styrene content is high, the copolymer cannot be dissolved by DMSO-D_6. Hence the NMR spectra were recorded using DMSO-D_6 or $CDCl_3$-DMSO-D_6 solvent mixtures. ^{1}H-NMR spectra were obtained using a Varian XL-400 spectrometer operating at 400 MHz at 50 °C. The recording conditions for
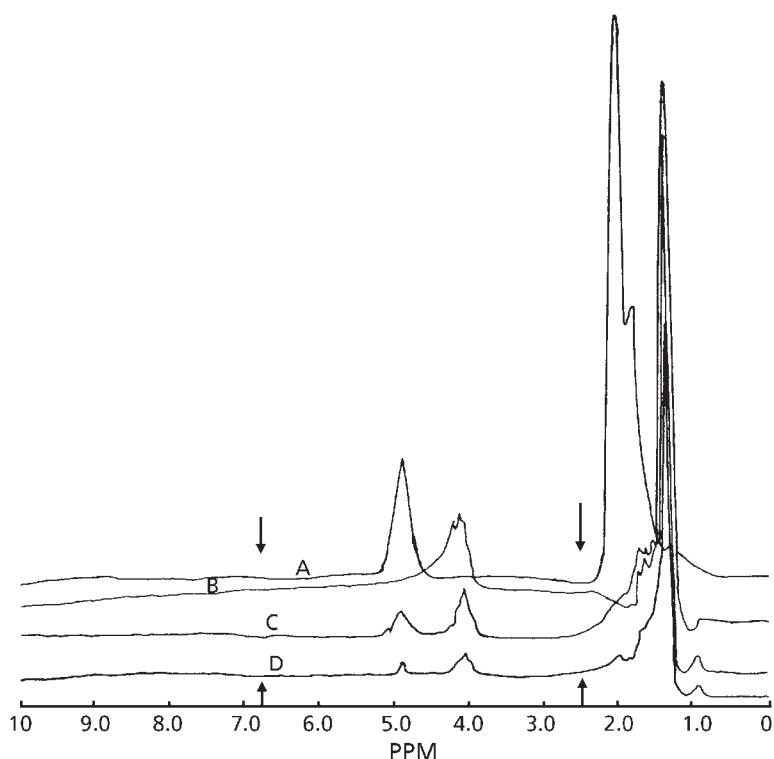
Figure 4.9 ^{1}H-NMR spectra of (A) polyvinylacetate, (B) polybehenyl acrylate and copolymers of vinyl acetate and behenyl acrylate: [VA]/[BA] C = 12.4 (D) = 0.74.

^{1}H-NMR were: sample concentration 1% (g/ml), spectral width 4798.5 Hz, acquisition time 1.67 s, pulse delay 5 s, and number of scans 16. The ^{13}C-NMR spectra were obtained with the same spectrometer at 100 MHz at 90 °C. The conditions for ^{13}C-NMR measurements were: sample concentration 10% (g/ml), spectral width 20000 Hz, acquisition time 0.4 s, flip angle 45°, pulse delay 1.6 s, and number of scans 512. DMSO was used as the locking agent for all NMR spectra.

4.4.4 Styrene Methacrylate Copolymers, NMR Spectroscopy

Van Doremaele and co-workers [89] applied ^{1}H-NMR spectroscopy to the determination of monomer ratios in styrene methyl acrylate copolymers. **Figure 4.10** depicts, as a typical example, the 400 MHz ^{1}H-NMR spectrum of a low-conversion solution styrene – methyl acrylate copolymer dissolved in CDCl$_3$ at 25 °C, whereas in
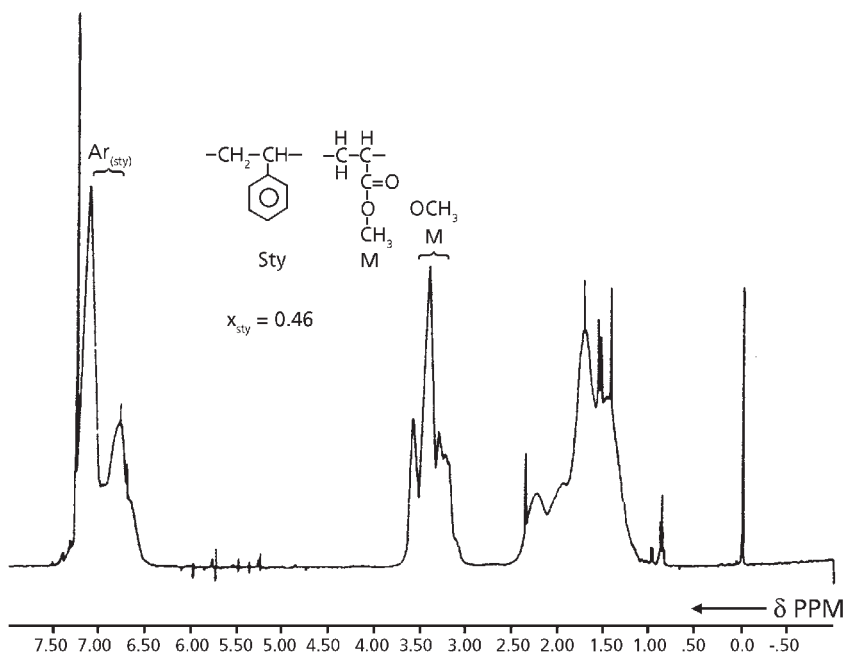
Figure 4.10 400 MHz ^{1}H-NMR spectrum of a low-conversion solution of styrene (S)-methyl acrylate (M) copolymer in CDCl3 at 25 °C. The mole fraction of styrene (Fs) is indicated on the left. (*Reprinted with permission from G.H.J. Van Doremaele, A.L. German, N.K. De Vries and G.P.M. Van der Velden, Macromolecules, 1990, 23, 19, 4206. ©1990, ACS*) [89]
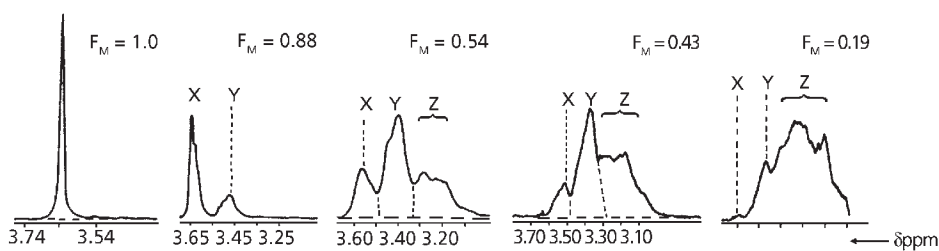
Figure 4.11 Expanded 400 MHz ^{1}H-NMR spectra of low-conversion solution styrene-methyl acrylate copolymers and homopolymer PM showing the methoxy region only. Spectra were recorded in CDCl3 at 25 °C. Copolymer compositions are indicated for each copolymer. Area measurements have been performed for the regions X, Y, and Z by using the dotted areas. (*Reprinted with permission from G.H.J. Van Doremaele, A.L. German, N.K. De Vries and G.P.M. Van der Velden, Macromolecules, 1990, 23, 19, 4206. ©1990, ACS*) [89]

q_0*	F_s	Conversion, mol%
0	0	20
0.038	0.12	7
0.11	0.33	5
0.36	0.46	12.6
0.85	0.57	14.3
1.98	0.67	16.1
2.97	0.77	10.2
4.78	0.81	9.7

Table 4.8 Observed cumulative average copolymer compostion (F_s = mole fraction of styrene) and final conversions of some low-conversion solution styrene – methyl acrylate copolymers

Initial monomer feed ratio q_0 = [S]/[M]

*Reprinted with permission from G.H.J. Van Doremaele, A.L. German, N.K. De Vries and G.P.M. Van der Velden, Macromolecules, 1990, **23**, 19, 4206 [89]. ©1990, ACS*

Figure 4.11 expanded 400-MHz spectra are shown for four copolymers and polymethyl acrylate (PM). Expansions of the methoxy region are shown since in particular this region displays additional fine splittings due to combined configurational (= tacticity) and compositional sequence effects. The average copolymer composition (mole fraction styrene, F_s) can be readily obtained by using:

$$\overline{F}_s = \frac{3A_1}{3A_1 + 5A_2}$$

where A_1 and A_2 represent the total peak areas of the aromatic and methoxy proton resonances, respectively. The initial feed (q_0 = [S]/[M]), the average copolymer composition, and the conversion are summarised in **Table 4.8**, where [S] = concentration of styrene in feed, [M] = concentration of methyl acrylate in feed.

4.4.4.1 Pyrolysis – Gas Chromatography

Wang and co-workers [90] applied pyrolysis – gas chromatography to the determination of the structure of styrene-*n*-butyl acrylate copolymers. The number average sequence length which reflects monomer arrangement was calculated using formulae that incorporate pure trimer peak intensities and hybrid trimer peak intensities.

The degree of structure, i.e., number average sequence lengths, also composition were determined for styrene-*n*-butyl acrylate copolymers and compared to those obtained for homogenous, i.e., non-structured (random), copolymers.

4.4.5 Styrene-n-butyl Acrylate Copolymers

4.4.5.1 Pyrolysis – Gas Chromatography

Wang and co-workers [90] showed that pyrolysis – gas chromatography of styrene-*n* butyl acrylate can be used to obtain the number average sequence length which can be further used to calculate the percentage of monomer in these copolymers.

4.4.6 Styrene Methacrylate Copolymers

In a procedure described by Sharp and Patterson [91] the acrylic acid and methacrylic acid groups in acrylic copolymers are first propylated using dimethyl formamide dipropyl acetal; then this product pyrolysed according to the following scheme:
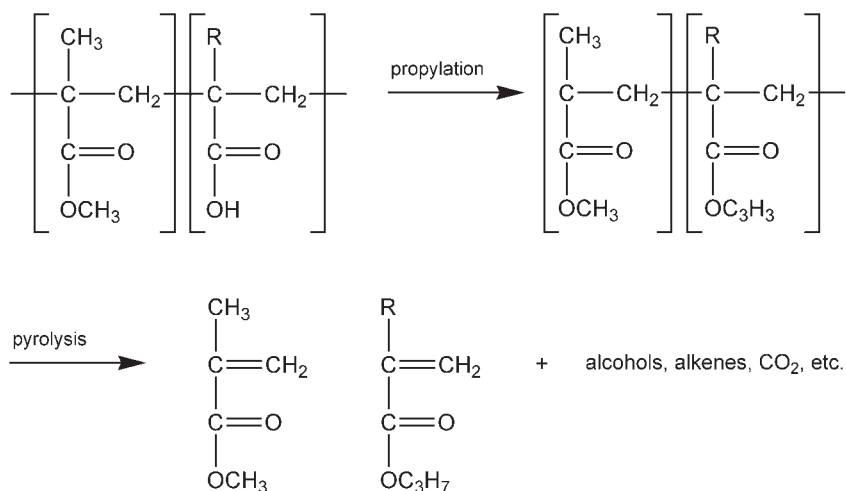
The resulting pyrolysis products (propylacrylate and methacrylate) are separated on a gas chromatograph and analysed by mass spectrometry.

By this procedure, copolymerised acrylic or methacrylic acid has been identified in terpolymers with (a) butyl acrylate and styrene (b) methyl methacrylate and ethyl

acrylate and (c) ethylene and propylene. A methyl methacrylate – methylstyrene – maleic acid terpolymer, when examined by this propylation – pyrolysis procedure, yielded dipropyl fumarate and a smaller amount of dipropyl maleate.

This method enables acrylic acid and methacrylic acid units to be determined in acrylic copolymers in amounts down to 0.1% with an accuracy of ±5%.

Wang and Smith [74] studied the composition and microstructure of styrene/methyl methacrylate copolymers. The composition was quantified by Py-GC using monomer peak intensity. Because of the poor stability of methyl methacrylate oligomers, neither methylmethacrylate dimer nor methylmethacrylate trimers were detected under normal pyrolysis conditions. The number average sequence length for styrene was determined by pure and hybrid trimer peak intensities. The number average sequence length for methylmethacrylate was determined by using formulas that incorporate composition and the number-average sequence length of styrene. This method is a new approach for the investigation of the microstructure of those copolymers that do not produce dimer and trimer peaks upon pyrolysis.

Figure 4.12 shows a typical program of a 39.61 wt% styrene – methylmethacrylate copolymer. The identification of all dimer and trimer peaks was accomplished by
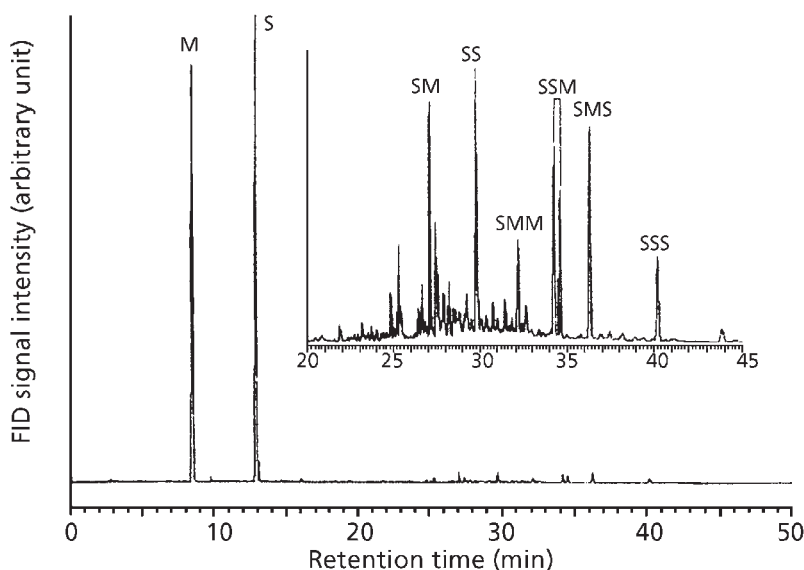
Figure 4.12 Typical pyrogram of a styrene-methylmethacrylate (39:61 by wt%) copolymer. (*Reprinted with permission from F.C-Y. Wang and P.B. Smith, Analytical Chemistry, 1996, 68, 17, 3033. ©1996, ACS*) [74]

comparing chromatogram retention times with a chromatogram from the literature [90] as well as by comparing mass spectra obtained from Py-GC/MS in the El mode and CI mode. The distinction of hybrid trimer peaks of styrene – styrene – methyl methacrylate (SSM) and styrene – methyl methacrylate – stryrene (SMS) was accomplished by comparing chromatograms of styrene/methyl methacrylate homogeneous copolymer and styrene/methylmethacrylate alternating copolymer [92].

The composition of styrene/methyl methacrylate copolymer systems has been studied by liquid absorption chromatography [105-116]. The structure styrene/methylmethacrylate random copolymer systems has also been studied by combining Py-GC with a modelling method [117]. In this study, Py-GC has been used to produce very clear and distinguishable monomer peaks that are used in the determination of the composition. In addition, the partially available dimer and trimer peaks, also from Py-GC, are used in combination with the composition to determine the number-average sequence length and percentage of grouped monomers [90]. The trimer peaks of styrene/methylmethacrylate copolymers were identified by Py-GC/MS in both El and CI mode. The compositions of the copolymers were compared to the recipe amounts that were incorporated into the polymer or compared with ^{13}C-NMR results.

4.4.7 Miscellaneous Styrene Copolymers

Table 4.9 presents information concerning the measurement of comonomer ratios in a variety of styrene containing copolymers, and other copolymers based on acrylate and methacrylate monomer units.

4.4.8 Vinyl Acetate – Methyl Acrylate NMR Spectroscopy

Brar and Charan [118] established the vinyl acetate:methyl acrylate monomer ratio in copolymers by ^{1}H-NMR.

The ^{1}H-NMR spectrum of the vinyl acetate – methyl acrylate copolymer (vinyl acetate content = 44 mol % in the copolymer) with the signal assignments is shown in **Figure 4.13**. The copolymer composition was calculated using the expression:

$$F_v = -\frac{\left[3I(-CH)_v\right]}{\left[3I(-CH)_v + I(-OCH_3)_M\right]}$$

where F_y is the mole fraction of V in the copolymer and $I(-CH)_v$ and $I(-OCH_3)_M$ are the intensities of methine and methoxy proton resonance signals due to vinyl acetate and methyl acrylate monomenc units, respectively.

Table 4.9 Miscellaneous styrene copolymers		
Copolymer	Technique	Reference
Glycidyl methyl methacrylate – glycidyl methacrylate	IR	[93]
Methacrylic acid – methyl methacrylate styrene isoprene	^{13}C – FT NMR Thermogravimetric analysis - MS	[94] [95]
Styrene – divinyl benzene	^{13}C-NMR	[96-99]
Styrene-α-methyl styrene Styrene-butadiene	^{13}C-NMR	[100]
Styrene – acrylonitrile	Py-GC	[101]
Methacrylic acid – ethyl acrylate	^{13}C-NMR	[102]
Glycidyl methacrylate – poly(2-vinyl-selonophane)	^{13}C-NMR	[103]
Propylene – methylmethacrylate	IR and Raman spectroscopy	[104]
Methyl methacrylate – butyl acrylate	IR	[105]
Acrylamide - acrylate	Py-MS	[106]
Butyl methacrylate – methyl methacrylate	IR	[107]
Butylacrylate – methyl methacrylate	FT MS	[108]
Methylacrylate – 2,3-dibromopropyl acrylate, methyl acrylate-2,3-dibromopropyl methacrylate	GC-MS	[109]
Source: Author's own files		

4.5 Butadiene-based Polymers

4.5.1 Styrene Butadiene and Polybutadiene

Krishen [119] has described a procedure for the determination of these monomer units. He quantitatively analysed the gaseous pyrolysis products from natural rubber, styrene-butadiene rubber and ethylene-propylene diene terpolymer rubber by gas chromatography. He showed that the 2-methyl-2-butene peak was linear with the natural rubber content of the sample. Styrene-butadiene rubber was determined from the peak area of the 1,3-butadiene peak. The ethylene-propylene-terpolymer content was deducted from the 1-pentane peak area of the pyrolysis products. Some of the pyrolysis products identified are shown in **Table 4.10**.
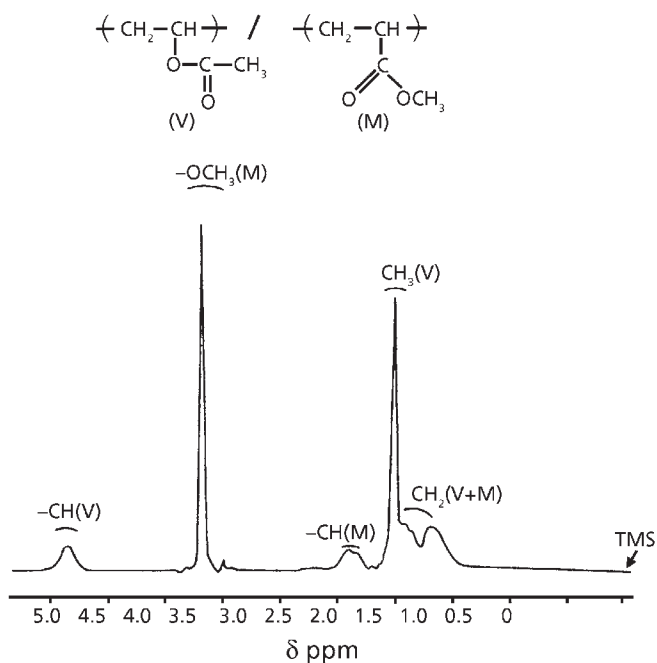
Figure 4.13 300 MHz ^{1}H-NMR spectrum of the vinyl acetate/methyl acrylate copolymer (V = 44 mol% in the copolymer) in CDCl$_3$ at room temperature.

Near-infrared spectroscopy has been used to determiners *cis*-1,4, *trans*-1,4, and 1,2 butadiene groups in these polymers [120].

Miller and co-workers [121] used near-infrared spectroscopy to determine the microstructure and composition of polybutadiene and styrene-butadiene copolymers. The procedure was capable of distinguishing between *cis*-1,4, *trans*-1,4, and 1,2 butadiene groups. Geyer [122] has given details of a Bruker Spectrospin P/ID.28 used for the identification of plastics using mid-infrared spectroscopy.

Pandey and co-workers [123] describe a novel approach to the non-destructive evaluation of various physicomechanical properties of propylene copolymer. A single-step measurement of the infrared spectrum followed by chemometric operation of the predetermined characteristic region of the spectrum enables one to obtain various property parameters of melt flow index, impact and flexural modulus, required for quality evaluation of the copolymer.

Cheng and co-workers [124] determined bromobutyl isomers and isoprene in bromobutyl rubbers by IR spectroscopy.

Table 4.10 Peak identification and relative retention data. (Tricresylphosphate column at 35 °C)		
Peak numer	Compound	Relative retention nonane = 1.0000
1	Methane	0.0009
2	Ethane + Ethane	0.0082
3	Propane	0.0268
4	Propene	0.0347
5	2-Methylpropane	0.0849
6	Propadiene + Butane	0.0948
7	1-Butene + 2- Methylpropene	0.1048
8	Trans-2-Butene	0.1409
9	*Cis*-2-Butene	0.1649
10	1,3-Butadiene	0.1769
11	2-Methyl-1-Butene	0.2074
12	1-Pentene	0.3038
13	2-Methyl-1-Butene	0.2074
14	Trans-2-Pentene	0.3848
15	*Cis*-2-Pentene	0.3993
16	2-Methyl-2-Butene	0.4476
17	Isoprene	0.5397
*Reprinted with permission from A. Krishen, Analytical Chemistry, 1972, **44**, 3, 494 [119]. ©1972, American Chemical Society*		

Ramarao and co-workers [125] used an ozonisation technique to characterise hydroxyl terminated polybutadiene.

4.6 Styrene-butadiene-acrylonitrile

Kranz and co-workers [126] have shown that acrylonitrile can be determined in styrene – butadiene – acrylonitrile terpolymers via a determination of organic nitrogen by the Kjeldahl procedure. Styrene units can be can be determined by infrared spectroscopy. Butadiene units can be determined by the iodine monochloride procedure. The compositional analysis and details of the microstructure of butadiene – acrylonitrile copolymers can be obtained by Raman spectroscopy [127].

4.7 Vinylidene Chloride – Methacrylonitrile and Vinylidene Chloride Cyanovinylacetate Copolymers

Montheard and co-workers [128] studied the structure of these copolymers by ^{13}C-NMR spectroscopy and showed that the macromolecules prepared from equimolar amounts of the monomers are mostly alternating with only a small proportion of homosequences of methacrylonitrile or cyanovinyl acetate.

The nitrile groups of *p*-vinyl chloride and of *p*-vinyl acetate give three peaks which can be referred to the three configurations of triads denoted MM_1, MR or RR in **Figure 4.14**.

Dong and Hill [129] and Nagata and co-workers [130] used infrared spectroscopy to study the structure and composition of styrene – methacrylonitrile copolymers.
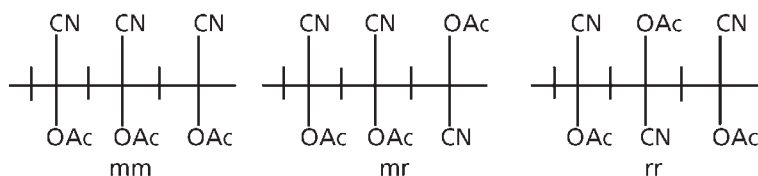
Figure 4.14 Triads of *p*(cyanovinylacetate(CVA)) homopolymer. (*Reprinted with permission from J.P. Montheard, A. Mesli, M. Raihane, A. Belfkira, M. Raihone and Q.T. Phan, Macromolecular Reports, 1994, A31, Supplement 1-2, 1. ©1994, Taylor & Francis*) [128]

4.8 Acrylonitrile-*cis* (or *Trans*) Penta-1,3-diene

Petit and Neel [131] investigated the possibility of using the method of flash pyrolysis – gas chromatography for the quantitative determination of the composition of free-radically prepared *cis*- or *trans*-1,3-pentadiene – acrylonitrile copolymers and for evaluation of their comonomer sequence distributions in terms of the run numbers. The experiments (sample weight: 50 µg, pyrolysis time: 4 s) were carried out, under a flow of helium, at a thermolysis temperature ranging from 450 to 900 °C with a Curie-point pyrolyser. The pyrolysis – gas chromatographic characterisation of the primary structure of copolymers was studied, between 500 and 800 °C, through the quantitative treatment of the corresponding liberated monomers which appeared on the pyrograms. By applying the both-side boundary effect theory on the molar amounts of these degradation products, which depend both upon copolymer composition and triad sequence distributions in the chain, the relative values of the monomer formation

probability constants were calculated. The composition and the run number of each pyrolysed sample were then determined using these parameters. The analytical data obtained by means of the procedure suggested are in very good agreement with those predicted, from reactivity ratios, by the usual theory of copolymerisation (terminal-unit model) and with the evaluations provided by the ^{13}C-NMR spectroscopy.

4.9 Hexafluoropropylene – Vinylidene Fluoride

Two methods have been described for determining the compositional analysis of these copolymers; one based on high resolution continuous and Fourier transform ^{19}F-NMR and the other on pyrolysis – gas chromatography.

4.9.1 ^{19}F-NMR

To measure the composition of a single component in a mixture, it is necessary to relate the component resonance to that of another compound (an internal standard) which is of known chemical composition and has been added in known weight to a known weight of unknown. Brame and Yeager [132] used dichlorobenzotrifluoride as an internal standard in the continuous wave method for determining the compositional analysis of both repeat units in hexafluoropropylene – vinylidene fluoride copolymers. This work demonstrated the utility of the Fourier transform NMR method in quantitative analysis of the copolymer, in relation to results obtained by continuous wave ^{19}F-NMR and proton NMR.

The lines observed are attributed to the following:

CF_3 group (delta = -70 to -75), CF_2 groups (delta = -90 to -120) and CF group (delta = -180 to -185).

The value obtained was in excellent agreement with those obtained by mass balance.

4.9.2 Pyrolysis – Gas Chromatography

Blackwell [133] used a Curie point pyrolyser to carry out quantitative analysis of monomer units in polyhexafluoropropylene – vinylidene fluoride (**Figure 4.15**). The polymer composition is calculated from the relative amounts of monomer regenerated and the trifluoromethane (CHF_3) produced during pyrolysis. The exact mechanism by which trifluoromethane is produced during pyrolysis is not known but it is presumed that the free trifluoromethyl group is cleaved from the polymer
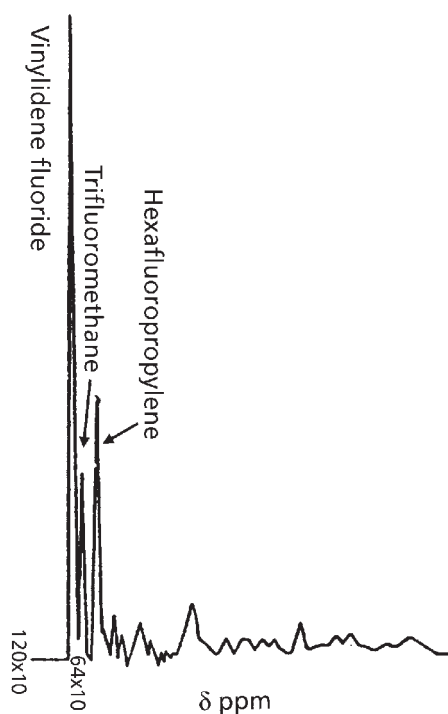
Figure 4.15 Typical chromatogram of the pyrolysis products for hexafluoropropylene-vinylidene fluoride copolymer. (*Reprinted with permission from J.T. Blackwell, Analytical Chemistry, 1976, 48, 13, 1883. ©1976, ACS*) [133]

backbone. The trifluoromethyl group then extracts a proton from the polymer chain to form trifluoromethane:
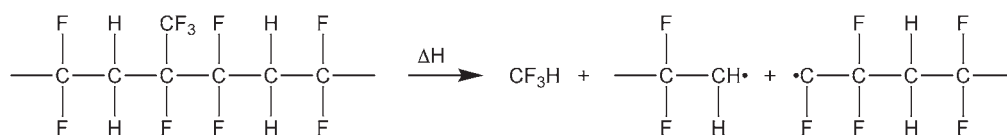
The monomer composition of the series of copolymers was calculated from the pyrolysis data and compared to that calculated from the NMR data. These data are summarised in **Table 4.11**. The difference in weight% calculated for the two techniques, averaged for hexafluoropropylene ± 6.0% and for vinylidene fluoride ± 0.85%.

Table 4.11 Comparison of the monomer composition of HFP/VF$_2$ copolymer as calculated by pyrolysis data and NMR data						
Weight % HPF			Weight % VF$_2$			SD for curie point pyrolyser
^{19}F-NMR	Pyrolysis		^{19}F-NMR	Pyrolysis		
28.6	28.8	0.2	71.4	70.9	0.5	1.04
29.0	28.8	0.2	71.0	71.0	0	0.34
34.79	36.04	1.25	65.21	62.63	2.58	0.52
36.46	36.73	0.27	63.96	62.91	1.05	0.82
37.24	37.33	0.11	62.76	62.61	0.1	0.39
39.04	39.07	0.03	60.96	60.88	0.08	0.67
39.04	38.35	0.69	60.96	61.55	0.59	0.63
39.82	38.46	1.36	60.18	61.89	1.71	0.30
40.10	39.45	0.65	59.90	61.49	0.57	0.10
42.4	43.2	0.8	57.6	56.7	0.9	0.39
44.8	46.2	0.2	55.2	53.8	1.4	0.48
44.8	45.4	1.4	55.2	54.3	0.9	0.59
47.3	47.0	0.3	52.7	52.8	0.1	0.92
49.95	49.45	0.50	50.05	50.55	0.50	0.30

SD: standard deviation

HPF: hexafluoropropylene

VF$_2$: vinylidene fluoride

*Reprinted with permission from J.T. Blackwell, Analytical Chemistry, 1976, **48**, 13, 1883 [133]. ©1976, American Chemical Society [133]*

4.10 Ethylene Glycol Terephthalic Acid, Ethylene Glycol Hydroxyl Benzoic Acid

The ratio of comonomers in these has been determined by NMR spectroscopy [134].

4.11 Ethylene Oxide Copolymers

4.11.1 Ethylene Oxide – Propylene Oxide

The composition of ethylene oxide – propylene oxide copolymers has been determined by infrared spectroscopy [133].

4.11.2 Ethylene Oxide – Polyacetal

The ethylene oxide contents of ethylene oxide – polyacetal copolymers were determined on the basis of cyclic ether intensities by reactive pyrolysis – gas chromatography in the presence of cobalt sulfate [135].

4.12 Maleic Anhydride Copolymers

Various methods have been applied to the determination of chloroprene – maleic anhydride [137], maleic anhydride polypropylene [138] by Fourier transform infrared spectroscopy and NMR [139] and maleic anhydride – styrene – methyl methacrylate, maleic anhydride – styrene – vinyl acetate and maleic anhydride – *S*-allyl propionate copolymers by FTIR spectroscopy [140].

Wang [141] developed a pyrolysis-gas chromatography method to study composition and microstructure of a styrene – maleic anhydride (SMA) copolymer. Since the anhydride functional group is not stable under normal pyrolysis conditions, a derivatisation technique was developed to study the composition and microstructure. Because of the unique structure of SMA copolymers, the number average sequence length can be used to indicate the polymer chain length or average molecular mass. This method demonstrated a feasible approach to studying the composition and structure by pyrolysis-GC for those polymers containing functional groups which are not stable under pyrolysis conditions.

4.13 Acrylamide – Methacryloyl Oxyethyl Ammonium Chloride, and Acrylamid – Acyloxyethyl Ammonium Chloride

Vu and Cabestany [142] determined the composition of water soluble polyacrylamides (acrylamide – methacryloylethyl trimethyl ammonium chloride and acrylamide – acryloyloxyethyltrimethyl ammonium chloride) by ^{1}H-NMR and ^{13}C-NMR of

deuterium oxide solutions of the copolymers. Good agreement was obtained between these results and those obtained by Kjeldahl nitrogen determinations. This ^{1}H-NMR method involves integration of the $N(CH_3)_3$, the CH_2, the carbonyl and the CH signals in deuterium oxide solution of either polymer. There was reasonably good agreement of the results obtained by NMR methods with the theoretical values.

References

1. C. Tosi and T. Simonazzi, *Die Angewandte Makromolekulare Chemie*, 1973, **32**, 1, 153.

2. G. Natta, G. Mazzanti, A. Valvassori and A. Pajaro, *Chimica et L'Industria*, 1957, **29**, 773.

3. H.V. Drushel and F.A. Iddings, *Analytical Chemistry*, 1963, **35**, 1, 28.

4. H.V. Drushel and F.A. Iddings in *Proceedings of the 142nd ACS Meeting*, Atlantic City, NJ, USA, 1962, Paper 20.

5. P.E. Wei, *Analytical Chemistry*, 1961, **33**, 2, 215.

6. T. Gössl, *Die Makromolekulare Chemie*, 1961, **42**, 1, 1.

7. P.J. Corish, R.M.B. Small and P.E. Wei, *Analytical Chemistry*, 1961, **33**, 12, 1798.

8. J.R. Paxton and J.C. Randall, *Analytical Chemistry*, 1978, **50**, 13, 1777.

9. J.N. Lomonte and J.A. Tirpak, *Journal of Polymer Science*, 1964, 2, 7, 705.

10. F. Ciampelli, G. Bucci, A. Simonazzi and A. Santambroglio, *Chimica et L'Industria*, 1962, **44**, 489.

11. G. Bucci and T. Simonazzi, *Chimica et L'Industria*, 1962, **44**, 262.

12. G.V. Fraser, P.J. Hendra, J.H. Walker, M.E.A. Cudby and H.A. Willis, *Makromolekulare Chemie*, 1973, **173**, 7, 205.

13. C. Tosi, *Makromolekulare Chemie*, 1973, **170**, 6, 231.

14. U.P. Popov and A.P. Duvonov, *Zhurnal Prikladnoi Spektroskopii*, 1973, **18**, 1077.

15. J.E. Brown, M. Tryon and J. Mandel, *Analytical Chemistry*, 1963, **35**, 13, 2172.

16. H.V. Drushel, *Critical Reviews in Analytical Chemistry*, 1970, **1**, 161.

17. C. Tosi and G. Ciampelli, *Advances in Polymer Science*, 1973, **12**, 87.

18. M. Johnson-Plaumann, H. Plaumann and S. Keeler, *Rubber Chemistry and Technology*, 1986, **59**, 4, 580.

19. R.M. Paroli, J. Lara, J-J. Hechler, K.C. Cole and I.S. Butler, *Applied Spectroscopy*, 1987, **41**, 2, 319.

20. E. Nishio, M. Morimoto and K. Nishikida, *Applied Spectroscopy*, 1990, **44**, 10, 1639.

21. M.M. Partnov, S.F. Salova, M.G. Matveer and V.S. Stein, *Vysokomolekulyarnye Soedineniya Seriya B*, 1987, **29**, 243.

22. J.M Sanders and K. Komoroski, *Macromolecules*, 1977, **10**, 6, 1214.

23. H.N. Cheng and M. Kakugo, *Macromolecules*, 1991, **24**, 8, 1724.

24. X. Zhang, H. Chen, Z. Zhou, B. Huang, Z. Wang, M. Jiang and Y. Yang, *Macromolecular Chemistry and Physics*, 1994, **195**, 3, 1063.

25. M. De Pooter, P.B. Smith, K.K. Dohrer, K.F. Bennett, M.D. Meadows, C.G. Smith, H.P. Schouwenaars and R.A. Geerards, *Journal of Applied Polymer Science*, 1991, **42**, 2, 399.

26. J.C. Randall and E.T. Hsieh, *NMR and Macromolecules: Sequence, Dynamic, and Domain Structure*, Ed., J.C. Randall, ACS, Washington, DC, USA, 1984, p.101.

27. D.E. Axelson, G.C. Levy and L. Mandelkern, *Macromolecules*, 1979, **12**, 1, 41.

28. D.C. Bugada and A. Rudin, *European Polymer Journal*, 1987, **23**, 10, 809.

29. H.N. Cheng, *Polymer Bulletin*, 1986, **16**, 5, 445.

30. M.E.A. Cudby and A. Bunn, *Polymer*, 1976, **17**, 4, 345.

31. C. Baker and W.F. Maddams, *Makromolekulare Chemistry*, 1976, **177**, 2, 437.

32. M.A. McRae and W.F. Maddams, *Makromolekulare Chemistry*, 1976, **177**, 2, 449.

33. ASTM D2238, *Standard Method of Test for Absorbance Due to Methyl Groups at 1378 cm^{-1}*, 1968.

34. W.F. Maddams and S.F. Parker, *Makromolekulare Chemistry,* 1988, **2**, 189, 333.

35. J. van Schooten, E.W. Duck and R. Berkenbosch, *Polymer*, 1961, **2**, 1, 357.

36. J. van Schooten and S. Mostert, *Polymer*, 1961, **4**, 1, 135.

37. N. Tyron, Z. Horowicz and E. Mandel, *Journal of Research of the National Institute of Standards and Technology*, 1955, **55**, 219.

38. H.N. Cheng, *Macromolecules*, 1991, **74**, 17, 4813.

39. M.H. Fisch and J.J. Dannenberg, *Analytical Chemistry*, 1977, **49**, 9, 1405.

40. G.R. Hatfield, W.E. Killinger and R.C. Zeigler, *Analytical Chemistry*, 1995, 67, 17, 3082.

41. F.A. Yur'eva, F.O. Guseinova, A.E. Portyanskii, N.M. Seidov, V.M. Namedova, A.T. Abasov and H.G. Malova, *Vysokomolekulyarnye Soedin Seriya A,* 1977, **19**, 2410.

42. G.G. Wanless, *Journal of Polymer Science*, 1962, **62**, 174, 263.

43. G.G. Wanless, *Journal of Polymer Science*, 1965, **8**, 1, 137.

44. E.W. Neumann and H.G. Nadeau, *Analytical Chemistry*, 1963, **35**, 10, 1454.

45. J.C. Verdier and A. Guyot, *Makromolekulare Chemie*, 1974, **175**, 5, 1543.

46. E.M. Barrall II, R.S. Porter and J.F. Johnson, *Journal of Applied Polymer Science*, 1965, **9**, 9, 3061.

47. D.F. Slonaker, R.L. Combs and H.W. Coover, Jr., *Journal of Macromolecular Science*, *Part A*, 1967, **1**, 3, 539.

48. A.T. Jons, *Journal of Polymer Science – Polymer Letters Edition*, 1965, **3**, 2, 591.

49. T. Huff, C.J. Bushman and J.W. Cavender, *Journal of Applied Polymer Science*, 1964, **8**, 2, 825.

50. C. Tosi, M.P. Lachi and A. Pinto, *Macromolecular Chemistry*, 1968, **120**, 1, 225.

51. N.J. Wegemer, *Journal of Applied Polymer Science*, 1970, **14**, 573.

52. J. Lomonte, *Journal of Polymer Science – Polymer Letters Edition*, 1963, **1**, 4, 645.

53. Y.V. Kissin and A.J. Brandolini, *Macromolecules*, 1991, **24**, 9, 2632.

54. H.N. Cheng, *Polymer Bulletin*, 1991, **26**, 3, 325.

55. A. Aoki, T. Hayashi and T. Asakura, *Macromolecules*, 1992, **25**, 1, 155.

56. E.M. Barrall, R.S. Porter and J.F. Johnson, *Journal of Chromatography*, 1963, **11**, 177.

57. E.M. Barrall II, R.S. Porter and J.F. Johnson, *Analytical Chemistry*, 1963, **35**, 1, 73.

58. R.S. Porter, A.S. Hoffman and J.F. Johnson, *Analytical Chemistry*, 1962, **34**, 9, 1179.

59. S. Pallacini, T. Porro and J. Pavlek, *American Laboratory*, 1991, **23**, 10, 38.

60. R.W. Jones and J.F. McClelland, *Analytical Chemistry*, 1990, **62**, 19, 2074.

61. M. Burbak, H.P. Voegele and H.J. Winkets, *Macromoleculare Chemie – Makromolecular Symposia*, 1986, **187**, 3, 569.

62. K. Beshah, *Macromolecules*, 1992, **25**, 21, 5597.

63. H.N. Cheng and G.H. Lee, *Polymer Bulletin*, 1988, **19**, 1, 89.

64. M.D. Bruch, *Macromolecules*, 1988, **21**, 9, 2707.

65. M. Buback, M. Busch, T. Droge, F.O. Mahling and C. Prellberg, *European Polymer Journal*, 1997, **33**, 3, 375.

66. J.J. Morelli, M.A. Grayson and C.J. Wolf, *Analytical Chemistry*, 1989, **61**, 8, 802.

67. G.G. Wanless, *Journal of Polymer Science*, 1965, **8**, 137.

68. S.L. Manett, D. Horowitz, R. Horowitz and R.P. Pinnell, *Analytical Chemistry*, 1980, **52**, 9, 1529.

69. I. Kubic, M. Singbar and Y. Navratil, *Petrochemia*, 1977, **17**, 10.

70. M.H. Grasley and E.E. Barnum, Martinez Research Laboratory, Shell Chemical Company, *private communication*.

71. D. Munteanu, M. Toader and M. Laiber, *Materiale Plastice*, 1976, **13**, 2, 97.

72. J. Helmruth, *Polyvehromarium Plast*, 1973, 73.

73. D.R. Campbell, *Analytical Chemistry*, 1975, **47**, 8, 1477.

74. F.C-Y. Wang and P.B. Smith, *Analytical Chemistry*, 1996, **68**, 17, 3033.

75. F.C-Y. Wang and P.B. Smith, *Analytical Chemistry*, 1996, **68**, 3, 425.

76. T.C. Chiang, Q.T. Pham and A. Guyot, *Journal of Polymer Science: Polymer Chemistry Edition 1*, 1977, **15**, 9, 2173.

77. B.A. Howell and P.B. Smith, *Journal of Polymer Science: Polymer Physics Edition s*, 1988, **26**, 6, 1297.

78. H.N. Cheng and M.A. Bennett, *Analytical Chemistry*, 1984, **56**, 13, 2320.

79. R. Salzer, H. Hoyer, A. Kaezmarch, A. Kerst and Z. Huppe, *Plaste Kautsch*, 1986, **33**, 444.

80. D.G. Anderson, K.E. Isakson, D.L. Snow, D.J. Tessari and J.T. Vandeberg, *Analytical Chemistry*, 1971, **43**, 7, 894.

81. W. Wasilewska, E. Grzywa and M. Rajkiewicz, *Chemia Analityczna (Warsaw)*, 1974, **19**, 89.

82. M.W. Urban, J.L. Koenig, L.B. Shih and J.R. Allaway, *Applied Spectroscopy*, 1987, **41**, 4, 590.

83. S.H. Kandu and M.A. El-Gamel, *Journal of Polymer Science, Part A - Polymer Chemistry*, 1986, **24**, 2765.

84. T.C. Schuk, S.T. Salke and P. Cheung, *Journal of Chromatography A*, 1994, **661**, 1-2, 227.

85. G.V.S. Shashidhar, K.R. Rao, N. Satyanarayana and E.V. Sundaram, *Journal of Polymer Science: Polymer Letters Edition*, 1990, **28**, 5, 157.

86. D.L. Evans, J.L. Weaver, A.K. Mukherji and C.L. Beatty, *Analytical Chemistry*, 1978, **50**, 7, 857.

87. B. Subrahmanyam, S.D. Baruah, M. Rahman, J.N. Baruah and N.N. Dass, *Journal of Polymer Science, Part A: Polymer Chemistry*, 1992, **30**, 10, 2273.

88. S. Wang and G.W. Poehlein, *Journal of Applied Polymer Science*, 1993, **49**, 6, 991.

89. G.H.J. Van Doremaele, A.L. German, N.K. De Vries and G.P.M. Van der Velden, *Macromolecules*, 1990, **23**, 19, 4206.

90. F.C-Y. Wang, B.B. Gerhart and P.B. Smith, *Analytical Chemistry*, 1995, **67**, 19, 3536.

91. J.L. Sharp and G. Patterson, *Analyst*, 1986, **105**, 1250, 517.

92. S. Tsuge and H. Ohtani, *Pyrolysis Gas Chromatography of High Polymers – Fundamentals and Data Compilation*, Techno-System, Tokyo, Japan, 1989, p104.

93. S. Paul and B. Ranby, *Analytical Chemistry*, 1975, **47**, 8, 1428.

94. D.E. Johnson, J.R. Lyerla, T.T. Horikawa and L.A. Pederson, *Analytical Chemistry*, 1977, **49**, 1, 77.

95. R.B. Prime and B. Shushan, *Analytical Chemistry*, 1989, **61**, 11, 1195.

96. M. Periyasamu, W.T. Ford and F. McEnroe, *Journal of Polymer Materials Science Engineering*, 1987, **56**, 184.

97. A.T. Jackson, K.R. Jennings and J.H. Scrivens, *Rapid Communications in Mass Spectrometry*, 1996, **10**, 12, 1449.

98. A.T. Jackson, A. Buzy, K.R. Jennings and J.H. Scrivens, *European Mass Spectrometry*, 1996, **2**, 2, 115.

99. J. Bonilla in *Proceedings of 53rd SPE Annual Technical Conference*, USA, 1995, **2**, 2745.

100. J. Muehl, V. Srica, V. Jarm and M. Kovac Filipovic, *Industrial and Engineering Chemistry Research*, 1990, **29**, 4, 707.

101. H.J. Cortes, G.L. Jewett, C.D. Pfeiffer, S. Martin and C. Smith, *Analytical Chemistry*, 1989, **61**, 9, 901.

102. P. Bajaj, M. Goyal and R.B. Chavan, *Journal of Applied Polymer Science*, 1994, **53**, 13, 1771.

103. D.L. Trumbo, *Polymer Bulletin*, 1993, **31**, 2, 191.

104. R.M. Henry, A.R. Druhe and M.K. Debe, *Applied Surface Science*, 1987, **28**, 1, 63.

105. A.J. Palacios, M.J. Aronda and G. Claver, *Journal of the Mexican Chemical Society*, 1985, **29**, 101.

106. W.M. Leung, D.E. Axelson and J.D. Van Dyke, *Journal of Polymer Science: Polymer Chemistry Edition,* 1987, **25**, 7, 1825.

107. R.W. Jones and J.F. McClelland, *Analytical Chemistry*, 1990, **62**, 20, 2247.

108. L.M. Nuwaysir, C.L. Wilkins and W.J. Simonsick, *Journal of American Society of Mass Specrometry*, 1990, **1**, 1, 66.

109. N. Grassie, M.A.M. Diab and A. Scotney, *Polymer Degradation and Stability*, 1987, **18**, 1, 45.

110. S. Mori, Y. Uno and M. Suzuki, *Analytical Chemistry*, 1986, **58**, 2, 303.

111. S. Mori, Y. Uno and M. Suzuki, *Analytical Chemistry*, 1987, **59**, 1, 90.

112. S. Mori, *Analytical Chemistry*, 1988, **60**, 11, 1125.

113. S. Mori, *Journal of Chromatography*, 1987, **411**, 355.

114. G. Glöckner and J.H.M. Van der Berg, *Journal of Chromatography,* 1987, **385**, 135.

115. G. Glöckner, M. Stickler and W. Wunderlich, *Fresenius' Journal of Analytical Chemistry*, 1988, **330**, 1, 46.

116. K. Kretschmer, W.Heibig, H. Kroschwic and G. Gloeckner, *Plaste Kautsch*, 1987, **34**, 1, 441.

117. T. Shimono, M. Tanaka and T. Shono, *Analytical Applied Pyrolysis*, 1979, 1, 1, 77.

118. A.S. Brar and S. Charan, *Journal of Applied Polymer Science*, 1994, **53**, 13, 1813.

119. A. Krishen, *Analytical Chemistry*, 1972, **44**, 3, 494.

120. E. Klesper, A. Corwin and D. Turner, *Journal of Organic Chemistry*, 1962, **27**, 700.

121. C.E. Miller, B.E. Eichinger, T.W. Gurley and J.G. Hermiller, *Analytical Chemistry*, 1990, **62**, 17, 1778.

122. I. Geyer, *Revue Generale des Caoutchoucs et Plastiques*, 1996, **1751**, 34.

123. G.C. Pandey, A. Kumar and R.K. Garg, *European Polymer Journal*, 2002, **38**, 4, 745.

124. P. Cheng, I. Gardner, H. Wong, C. Frederick, A. Dekmezin and P. Haus, *Rubber Chemistry and Technology*, 1990, **63**, 265.

125. M. Ramarao, K. J. Scarish, P. V. Ravindran, G. Chandrasekharan, S. Alwan, K. S. Sastri, *Journal of Applied Polymer Science*, 1993, **49**, 3, 435.

126. D. Kranz, K. Dinges and T. Wendling, *Angewandte Makromolekulare Chemie*, 1976, **51**, 1, 25.

127. H.G.M. Edwards, A.F. Johnson, I.R. Lewis and J.M.G. Cowie, *Polymer International*, 1993, **31**, 4, 391.

128. J.P. Montheard, A. Mesli, M. Raihane, A. Belfkira, M. Raihone and Q.T. Pham, *Macromolecular Reports*, 1994, **A31**, 1 & 2, 1.

129. L. Dong and D.J.T. Hill, *Polymer Bulletin*, 1995, **34**, 3, 323.

130. A. Ngata, K. Ohta and R. Iwamoto, *Macromolecular Chemistry and Physics*, 1996, **197**, 6, 1959.

131. A. Petit and J. Neel, *Journal of Applied Polymer Science*, 190, **41**, 1/2, 267.

132. E.G. Brame, Jr., and F.W. Yeager, *Analytical Chemistry*, 1976, **48**, 4, 709.

133. J.T. Blackwell, *Analytical Chemistry*, 1976, **48**, 13, 1883.

134. L. Abis, R. Po, P. Schimperna and E. Merlo, *Makromolekulare Chemie*, 1994, **195**, 1, 181.

135. G. Mezzienyl, M. Sipos, E. Jahazz and M. Leikas, *Acta Chimica Academiae Scientarium Hungaricae*, 1990, **127**, 495.

136. Y. Ishida, H. Ohtani, K. Abe, S. Tsuge, K. Yamamoto and K. Katoh, *Macromolecules*, 1995, **28**, 19, 6528.

137. W.J. Cho, C.H. Choi and E. Hass, *Journal of Polymer Science*, *Part A: Polymer Chemistry*, 1994, **32**, 6, 2301.

138. A. Galia, R. De Gregorio, G. Spadaro, O. Scialdone and G. Filardo, *Macromolecules*, 2004, 37, 12, 4580.

139. S.H.P. Bettini and J.A.M. Agnelli, *Journal of Applied Polymer Science*, 2002, **85**, 13, 2706.

140. A. Boztug, S. Basan and O.E. Ekberov, *Materials Research Innovations*, 2004, **8**, 2, 89.

141. F.C-Y. Wang, *Journal of Chromatography*, 1997, **765**, 2, 229.

142. C. Vu and J. Cabestany, *Journal of Applied Polymer Science*, 1991, **42**, 11, 2857.

5 Analysis of Homopolymers

5.1 Infrared Spectroscopy

Infrared (IR) spectra of thin films of a polymer in the region up to 2.5 μm are characteristic of the polymer. Computerised retrieval from data in a library of standard polymers has been used in the IR fingerprinting technique to facilitate polymer identification [1].

Alexander [2] has described a method for obtaining spectra of thin films of polymer that are free of interference fringes.

Various methods have been used to prepare polymers for IR spectroscopy:

- Potassium bromide discs [3]: the spectra were run either as potassium bromide discs (1.5–2 μg polymer per 400 mg potassium bromide) or as polymer films of varying thickness, up to 12 μm, using a sodium chloride prism.

- Hot pressed film [4]: Osland [5] has described a heated press for the preparation of plastic films for analysis by IR spectroscopy. The press can produce films of reproducible thickness, as thick as 500 μm.

Alternatively, the sample material can be dissolved in a suitable organic solvent and a film cast onto glass or a cell window.

A new sample handling accessory with which films of constant thicknesses can be prepared has been introduced by Phillips Analytical. The plastic film press contains a thermostatically controlled oven unit that is calibrated up to 300 °C. It also contains a cooling facility which may be connected to a low-pressure compressed air supply to cool the prepared films rapidly. Reproducible thickness is ensured by using a set of brass dies that can be heated and cooled quickly. The dies can produce films of 20, 50, 100, 200, and 500 μm thickness.

Deschant [6] has discussed in detail the IR spectra of 35 polymers, whilst Hippe and Kerste [7] developed an algorithm for the IR identification of vinyl polymers. Pyrolysis followed by IR spectroscopy is a particularly useful technique for application to polymers

that are rendered opaque or completely non-transparent by the presence of pigments or fillers. Leukoth [8] used this technique to determine the chemical composition of plastics and rubbers containing high proportions of pigments or fillers.

5.1.1 Determination of Low Concentrations of Methyl Groups in Polyethylene

This analysis is based on the 7.24 μm methyl absorption which appears on the side of the strong methylene bands at 7.29 and 7.58 μm.

A wedge of polymethylene, or high-density polyethylene (HDPE) with very low methyl group content, is placed in the reference beam and moved until the methylene absorptions are cancelled. A computerised equivalent of the wedge method was used, in which the PECDS program was employed to subtract the methylene absorption bands before applying the QUANT program. Subtraction of the methylene absorption left an uneven baseline; visual inspection of this baseline proved the most satisfactory method of choosing the optimum scaling factor.

A set of six standards was prepared with methyl group concentrations ranging from 0.8 to 28.9 CH_3 groups per thousand carbon atoms. The film thickness was approximately 0.12 mm.

When the QUANT program is used directly the best results are clearly given by the first derivative maximum (D1MAX). The first derivative spectrum shows that the maximum at 7.22 μm is relatively free from overlap by the CH_2 bands, and is much larger than the minimum at 7.26 μm. The relative success of the D1MAX measurement is therefore not surprising. Despite considerable band overlap, the simple peak height measurement gives an error index of only 2.6%. This implies that the background due to the CH_2 bands is fairly constant, or varies with CH_2 concentration in a roughly linear fashion.

5.1.2 Bond Rupture in HDPE

Hammond and co-workers [9] studied the effect of elongation, time and temperature on the concentration of carbonyl and vinyl end groups formed during the plastic deformation of HDPE using IR spectroscopy. The data obtained confirmed the experimental evidence given by Peterlin [10, 11] but demonstrated the incongruity of his theory of plastic deformation. An alternative explanation for the processes that occur when spherulitic materials become oriented and fibrillar is offered, namely, that mechanical work is concentrated into very small volumes in the neck region, leading to localised melting and recrystallisation.

Homolytic breakage leads to the formation of primary radicals ($-CH_2$ in polyethylene) and then of secondary radicals by abstraction of hydrogen ($-CH_2-CH-CH_2-$ in polyethylene), or reaction with oxygen (R-O-O). Owing to the high reactivity of the primary radicals, it is often difficult to assess the number originally formed, because several secondary reactions may occur after the generation of one primary radical.

Vinyl and carbonyl groups are the functions most likely to occur as the result of chain scission of polyethylene in air. Both are readily detectable by infrared spectroscopy, using the characteristic frequencies [12] listed in **Table 5.1**. In the case of the carbonyl group, it is now well established that the observed peak in the thermally or photochemically oxidised polyethylene is a composite band, probably containing three components specific for the saturated aldehydic, ketonic and carboxylic groups [13]. There is also evidence that the first of these is the least abundant [14, 15]. There is a readily detectable shoulder near 1740 cm^{-1} and this has been assigned to ester groups [13].

In the work of Hammond and co-workers [9], the peak maximum occurred at 5.74 µm suggesting that ester groups are the major carbonyl containing species present.

The influence of four variables upon the concentrations of carbonyl and vinyl groups formed during plastic deformation was assessed. Thus, the effects of (1) the atmosphere surrounding the sample during deformation; (2) the time elapsed between deformation and spectroscopic examination; (3) the sample temperature during deformation; and (4) the sample thickness were measured, by carrying out a series of connected, and in other cases interrelated, experiments as follows.

For example, in a study of the effect of atmosphere surrounding the sample during draw, samples about 350 µm thick were selected and degassed under a vacuum of 0.05 bar for 3 days. They were then placed in an atmosphere of nitrogen or oxygen, as relevant, for 2–3 days before being drawn. The results, presented in **Figure 5.1**, show that vinyl group formation is favoured in nitrogen, (in fact, quite markedly so). In both cases, the concentration of the two types of functional group increases with increasing draw ratio. In three out of four cases, the rate of formation of the functional group increases quite considerably at high draw ratios, indicating, as was anticipated, that chain scission is more prevalent under these conditions.

Particular studies of the IR spectra of homopolymers include isotactic poly(1-pentane), poly(4-methyl-1-pentene), and atactic poly(4-methyl-pentene) [16], chlorinated polyethylene (PE) [17], aromatic polymers including styrene, terephthalic acid, isophthalic acid [18], polystyrene (PS) [19–21], *trans* 1,4-polybutadiene [22], polyether-carbonate-silica nanocomposites [23], polyhydroxyalkanoates [24], poly(4-vinyl-*n*-butyl) [25], polyacetylenes [26], polyester urethanes [27], miscellaneous

Table 5.1 Characteristic infrared frequencies for functional groups that may be formed in polyethylene by chain rupture			
Functional group	**Vibrational mode**	**Frequency (cm⁻¹)**	**Frequency (µm)**
CH_3	$\delta(CH_3)$	1370-1380	7.29-7.24
$R–CH=CH_2$	$\delta(CH_2)$	910, 990	10.99, 10.10
R₁\R₂ C=CH₂	$\delta(CH_2)$	890	11.23
C=C	$\nu(C=C)$	1640-1660	6.10, 6.02
—C(=O)—CH=CH—	$\nu(C=C)$	1680-1690	5.95
R—C(=O)—R	$\nu(C=O)$	1715-1720	5.83-5.92
R—C(=O)—OH	$\nu(C=O)$	1710-1715	5.84-5.83
R—C(=O)—H	$\nu(C=O)$	1730-1745	5.78-5.73
R—C(=O)—OR	$\nu(C=O)$	1735-1745	5.76-5.93
R—C(=O)—OOR	$\nu(C=O)$	1763	5.67
R—C(=O)—OOH	$\nu(C=O)$	1785	5.60
Reprinted with permission from C.L. Hammond, P.J. Hendra, B.G. Lator, W.F. Maddams and H.A. Willis, Polymer, 1988, 29, 1, 49 [9] ©1988, Elsevier			

polymers [28], polyurethanes [29], polyphenylene [30], vinylene [31], acrylic grafted polyethylene [32], polyamidoamine [33], benzocyclobutene [34], polyvinyl chloride [35], chloropolymers [36], polypropylene [37], polyethylene [38, 39], polyacetal [40], dimethylsiloxane rubber [40]. Some important spectral lines associated with particular polymers are given in **Table 5.2.**
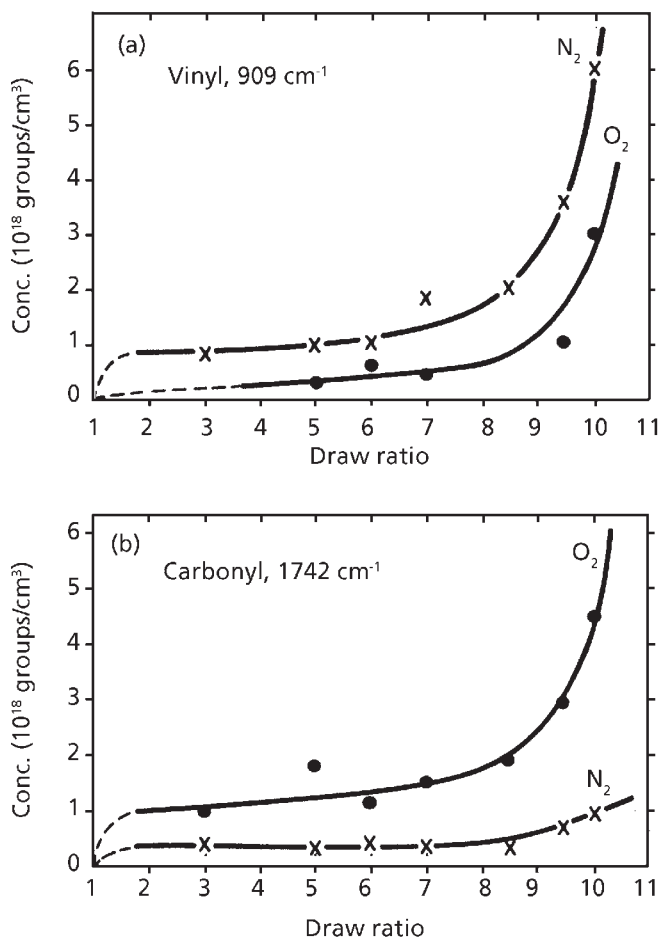
Figure 5.1 New end-group concentrations as a function of draw ratio and atmosphere for samples 350 µm thick at 20 °C. (*Reprinted with permission from C.L. Hammond, P.J. Hendra, B.G. Lator, W.F. Maddams and H.A. Willis, Polymer, 1988, 29, 1, 49. ©1988, Elsevier*) [9]

Table 5.2 Some infrared spectral lines of polymers (µm)	
1. Polyacrylonitrile	C=N, 4.47 Aliphatic C–H, 3.41, 3.49 C=O stretching, 5.78 Others 6.01, 6.90, 3.34, 3.41
2. Polyformaldehyde	C–H stretching, 4.90, 6.80, 7.0, 7.23, 8.08, 9.15 Others, 3.34, 3.41, 11.15 (strong)
3. Polyisobutylene	Aliphatic CH, 3.35-3.50, 6.70 - 6.90 Others, 7.20, 7.32, 8.15 Doublet at 10.56, 10.87
4. Polyester resin	Aliphatic CH, 3.30, 3.40 C=O stretching, 5.80 (strong) C=O stretching ester, 7.65 - 8.03 Others, 6.09, 6.15, 6.50, 6.61, 6.70, 7.65 and 12.90 and 14.35 (characteristics)
5. Buna rubber	Aliphatic CH, 3.40 Double bond, 5.90 Others, 6.10, 6.25, 6.69, 6.90 - 6.96 Strong, 10.36, 11.0, 13.22, 14.33
6. Vinylite polymers (Union Carbide) copolymerised vinyl chloride – vinyl acetate	Vinylite VMCH aliphatic CH, 3.40 C=O stretching, 3.65, 5.76 H O H binding absorbed water, 6.16 C–O stretching, 7.00, 7.32, 7.56, 8.1 Others, 9.17, 9.28
7. Vinylite VAGH	Aliphatic CH, 3.45, 3.56 C=O stretching, 5.79 Adsorbed water, 6.16 C–O stretching, 7.02, 7.55, 8.05 Others, 9.16, 10.42 On comparing with above spectra for Vinylite VMCH it is seen that there are sufficient differences to make positive identification possible in the region 7.0-7.5 and 9.5-10
8. Vinylite XYHL	The difference between this and the spectra of Vinylite VMCH and Vinylite VAGH is the strong absorption at 8.73
9. Silicone oil	Methyl in Si–CH$_3$, 7.95, 9-10, 12.6 Si–O–Si, 12. 6 Aliphatic CH, 3.36, 3.43 - vibrations

10. Methyl cellulose	OH stretching, 2.90 Aliphatic CH stretching, 3.42, 3.51 Adsorbed water, 6.15 (similar spectrum to cellulose)
11. Ethyl cellulose	Splitting of aliphatic CH stretching vibration at 3.37-3/50 Others, 6.94, 7.27 (strong), 10.90, 11.37 (weak)
12. Carboxy methylcellulose sodium salt	Resembles spectrum of cellulose Carboxy, 3-4
13. Carboxy methylcellulose (free)	C=O stretching, 5.57 (strong)
14. Nitrocellulose	$R-O-NO_2$, 6.05, 7.80 (characteristic)
15. Phenol formaldehyde (asbestos filled)	C–H groups, 3.3 (weak) Double bond plus C–H absorption, 6.25 double peak –Si O (from asbestos), 9.5-10.0
16. Melamine formaldehyde (asbestos filled)	N-H groups 2.75 Si O (from asbestos), 9.5-10.0
17. Polycarbonate	OH, 2.90, 6.12 (adsorbed water) CH adjacent to double bond, 3.28 (aromatic CH) Aliphatic C–H, 3.37, 3.48 C=O stretching, 5.88 (strong) CH, 6.9, 7.10-7.37 Carbonyl ester, 8.0 1,4 disubstitution, 12.1, 13.8
18. Polyethylene glycol	OH, 2.90 weak Aliphatic C - H, 3.45 (strong), 6.75-7.50 $-CH_2-O-CH_2$ band, 9
19. Polypropylene glycol	CH adsorption, 2.90 Triple C–H, 3.35-3.50 CH, 6.9 CH_3, 7.3 (strong) C–O–C, 9 (strong) Others, 10.8, 11.6, 12.0
20. Polyvinylidene chloride	Aliphatic C–H, 3.4-3.5 C=O absorption, 5.75 (impurity) CH, 7.10, 7.31 C–CI, 13.35 (usually 13.3-14.3)

21. Chlorinated polypropylene	Absorbed water, 2.93, 6.16 Aliphatic C–H, 3.40, 6.96, 7.25 Methyl C–CI 13.15, 13.65, 12.75 (probably)
22. Polyvinylacetal	OH, 2.91 Aliphatic CH, 3.4 C=O ester, 5.76 Methyl groups, 7.28 –CH$_2$–O–CR, 8.8
23. Polyacrylamide	C=O, 6.00 C=N (probably), 4.5 OH (moisture), 2.95
24. Cellulose propionate	Moisture, 2.9, 6.13 Triple C–H adsorption, 3.4 Ester carbonyl, 5.7, 8.6 Others (characteristic), 7.25-8.5, 11.4, 2.45, 13.45
25. Cellulose acetate butyrate	Characteristic absorptions, 10.5, 11.1, 12.0, 12.6, 13.4, 14.5
26. Butyl rubber	Aliphatic CH, 3.4 (strong), 6.8 Two methyls attached to carbon, 7.19, 7.31 CH adjacent to aliphatic double band, 10.55, 10.85
27. Nitrile rubber	CH adjacent to double band, 10.3 (strong), 3.25, 6.00, 6.10, 6.25 (strong) Aliphatic C–H, 3.40, 3.49, 6.9 C=N, 4.46
28. Styrene-butadiene rubber	Polystyrene bands, 3.25, 3.30, 3.35 (C–H adjacent to double band) Monosubstituted benzene ring, 5.6, 13.2, 14.33 C–H adsorption, 10.35
29. Styrene-butadiene acrylonitrile	Moisture, 2.92, 6.12 Aromatic C–H, 3.28, 3.31, 6.28 and C–H adjacent to double bond Aliphatic C–H, 3.41, 3.50, 6.88, C=N, 4.47 Monosustituted benzene ring, weak 13.2, 14.35
30. Ethylene-propylene copolymer	Closely resembles polyethylene spectrum plus double bonds, 10.3 Aliphatic C–H, 3.4 CH adjacent to double bond, 3.3 Methyl groups, 7.25

31. Ethylene-propylene-diene terpolymer	Closely resembles spectrum of ethylene propylene copolymer. Addition spectral lines Aliphatic double bands, 3.3 (weak) 10.65
32. Epoxy resin (Araldite)	Hydroxy, 2.9, 9.04 C–H, 3.27, 3.34, 6.20, 6.30 Split methyl group, 7.20, 7.32 1,4-di-substituted benzene ring, 5.6 (weak) 12.3 Aliphatic C–H, 3.39, 3.43, 3.45,6.84
33. Coumarone-indene resin	Adsorbed water, 2.92 Aromatic C–H, 3.31,6.49 Substituted benzene ring, 13.4, 14.3 Aliphatic C–H, 3.42, 3.50, 6.90
34. Polyvinylacetate	C=O, 5.75 Ester, 8.0, 9.8
35. Polyvinyl butyral	Characteristic absorptions, 7.25, 8.05, 8.9, 10.0
36. Polytetrafluorethylene	CF_2, 8.4 Others, 8.4, 4-5 OH stretching, 2.82 C=O, 2.90, 5.80
37. Polyethylene terephthate (Terylene)	H stretching, 3.25 CH_2 stretching, 3.35, 3.43 CH_2 deformation, 7.08, 7.20 CH deformation, 7.90 C–O–C stretching, 8.51, 9.59 C–C, 6.80 Others, 5.80, 6.19,11.45, 13.77, 6.65, 7.30, 7.45, 8.86, 9.10, 9.80, 10.3, 11.15, 11.45, 11.80, 12.62, 13.75
38. Polymethlmethacrylate	Ester carbonyl, 5.75 C–O–C stretching, 6.70-6.95, 8.30-8.80 Other, 10.00, 10.40
39. Cellulose (Cellophane)	Water absorption, 2.8 - 3,4 OH stretching, 3.4 CH stretching, 3.4 C=O stretching, 5.8 COO - ion stretching, 6.28 CH_2 deformation, 7.0 CH deformation, 7.3,7.6,11.1

	OH deformation, 7.5, 8.9, 15.4 C–O stretching, 8.6 OH bending, 9.4 C–OH stretching, 9.8 C–OH, 8.9 C–O, C–C stretching, 10.0 Other absorption, 9.0, 6.1
40. Cellulose acetate	Adsorbed water, 2.9 Ester carbonyl, 5.75 Other absorption, 3.5-5.35, 8.0, 7.5-10.0
41. Melamine	Characteristic absorptions, 3.0, 6.0-6.5, 9.7, 12.3
42. Urea formaldehyde	Characteristic absorptions, 6.0-6.2, 6.9, 8.0, 10.0
43. Natural rubber	C=C, 6.08 CH_2 and CH_3 deformation, 7.0, 7.25, 12.00 Other absorption, 7.5 -11
Source: Author's own files	

5.2 Fourier Transform Infrared (FTIR) Spectroscopy

5.2.1 Instrumentation

Fourier transform infrared spectroscopy, a versatile and widely used analytical technique, relies on the creation of interference in a beam of light. A source light beam is split into two parts and a continually varying phase difference is introduced into one of the two resultant beams. The two beams are recombined and the interference signal is measured and recorded as an interferogram. A Fourier transform of the interferogram provides the spectrum of the detected light.

A FTIR spectrometer consists of an infrared source, an interference modulator (usually a scanning Michelson interferometer), a sample chamber, and an infrared detector. Interference signals measured at the detector are usually amplified and then digitised. A computer initially records and then processes the interferogram; it also allows the spectral data that result to be manipulated.

The principal reasons for choosing FTIR spectroscopy are that (i) the instruments record all wavelengths simultaneously and thus operate with maximum efficiency, and (ii) Fourier transform infrared spectrometers have a more conventional optical geometry than do dispersive infrared instruments. These two factors lead to the following advantages:

1. Much higher signal-to-noise ratios can be achieved in comparable scanning times.

2. Wide spectral ranges can be covered with a single scan in a relatively short scan time, thereby permitting the possibility of kinetic time-resolved measurements.

3. Higher resolution is possible without undue sacrifice in energy throughput or signal-to-noise ratios.

4. None of the stray light problems usually associated with dispersive spectrometers are encountered.

5. A more convenient focus geometry – circular rather than slit-shaped – is provided at the sample focus.

Perkin Elmer supply a range of Fourier transform infrared spectrometers.

Vibrational spectra contain vast amounts of molecular or microscopic structure information about polymeric materials. Geometric and steric isomerism, molecular orientation, conformational regularity, crystallinity, and the local microscopic environment of specific functional groups of polymeric materials can be elucidated with vibrational spectroscopic analysis. Particularly, Fourier transform infrared spectrometry is a convenient and powerful means of measuring vibrational spectra of polymeric materials.

Stress- or strain-induced molecular orientation is one of the most significant factors determining the microscopic properties of polymeric materials. Noda and co-workers developed the infrared spectral measurement method of dynamic orientation change under a sinusoidal strain perturbation, i.e., dynamic infrared linear dichroism (DIRLD) [41, 42] more than a decade ago. This novel method, also combined with two-dimensional analysis [43], has been applied to various polymeric materials including isotactic polypropylene [44], polyethylene [45], polyurethane (PU) [46], polyethylene terephthalate (PET) [47, 48], and several composite materials [49, 50]. All these experiments were performed in the transmission mode, either with a dispersive IR spectrometer in the 1980s or with a step-scan FTIR spectrometer in recent years. In the IR transmission measurement the preparation of thin film samples is critical. To obtain a linear response from dynamic strain perturbation, band absorbance must be controlled at under roughly 0.7 absorbance units in order to permit use of the Beer-Lambert law [51]. For example, isotactic polypropylene films with a thickness of a few tens of micrometers can easily be prepared, and yet the C–C chain stretching (8.56 μm) and CH_3 rocking (11.89 μm) absorbance bands can still be kept low enough due to the relatively low absorption coefficient. However, in the case of polymer materials consisting of the functional groups with strong absorption coefficients of 0.3 or more (such as C=O, COO, and Si–O, including PET, polyethylene naphthalate,

polydimethyl siloxiane, and acetyl cellulose) very thin, normally less than 2 µm thick, film samples should be prepared so that the absorbance is less than 0.7 au and the dynamic response would be in the linear region. The preparation of such thin films is, of course, very difficult and even if it is successful, the sample may be easily broken under dynamic stress. In practice, the observations of the dynamic spectra of PET films have traditionally been restricted to the weak absorbing regions [47, 48] with the transmission method.

In the dynamic transmission mode, information about two-dimensional dynamic dichroic differences can be attained [46]. It is useful to study uniaxially oriented polymers such as strongly elongated fibres. However, the orientation of most polymer films should be considered biaxial, even with uniaxially drawn films, which still show slight biaxial orientation at the surface [52]. This fact suggests that the two-dimensional dynamic dichroic data obtained from transmission mode is not necessarily adequate for evaluating most (biaxially oriented) polymer films.

Attenuated total reflection (ATR) FTIR is one of the most useful tools for characterising the chemical composition and physical characteristics of polymer surfaces [53]. One useful application is the measurement of molecular orientation using polarised infrared ATR spectroscopy [54, 55]. The polarised infrared ATR spectra normally include three-dimensional (e.g., machine, transverse, and thickness direction) orientational information in contrast to the polarised transmission infrared linear dichroism. In addition, band absorbance of less than 0.7 au is easily achieved, even with the strong absorption bands, because the penetration depth of ATR from sample surfaces can be adjusted to a few micrometers by changing the internal reflection element and/or the angle of incidence. If successful combination of the dynamic infrared spectroscopy and the ATR methods can be achieved, more useful dynamic orientational information can be obtained.

In dynamic ATR spectroscopy, periodic compression (instead of strain) is applied to the polymeric materials against the internal reflection element. The combination of a piezoelectric transducer and ATR to induce dynamic compressive deformation was initially reported by Marcott and co-workers [50] and Ekgasit and Padermshoke [56] with some primitive results. When applying this technique to various rigid polymeric materials, several problems are present; these were addressed by Nishikawa and co-workers [57]. The purpose of their paper was to develop a compression modulation ATR-based FTIR method and then apply it to the measurement of dynamic orientational changes of polymeric materials.

These workers developed dynamic compression modulation attenuated total reflection Fourier transform infrared spectroscopic methods for characterising polymer films. To obtain dynamic compression polarised ATR spectra, internal reflection element (IRE) secure assemblies made of tungsten carbide with very high hardness were designed.

These assemblies were mounted on the Harrick Seagull ATR attachment and measured by step-scan FTIR spectroscopy. Effects of static compression, air gaps and refractive index changes were examined. Experimental and simulated results show that the effect of air gaps between the sample and IRE, and refractive index changes of the sample and IRE, are negligible at values larger than a static torque of 40 cN m and that good signal-to-noise ratios and reproducible data can be obtained. Uniaxially and biaxially drawn polyethylene terephthalate were measured by this method. Both bipolar and unipolar bands were observed in the dynamic in-phase ATR spectra, which can be associated with their microstructural environmental changes. This technique shows promise in evaluating various polymer film materials, including biaxially oriented films, multilayer coated film surfaces and molecular interactions between polymer-polymer and polymer additives at the film surface.

Figure 5.2 shows the Fourier transform infrared spectrum of polymethylmethacrylate (PMMA). **Figure 5.3** (top spectrum) shows a spectrum of an acrylonitrile-butadiene copolymer of unknown composition. The lower spectrum is a match obtained from one of a range of standard copolymers of known composition to demonstrate that the unknown copolymer contains between 30% and 32% acrylonitrile and between 70% and 68% butadiene.
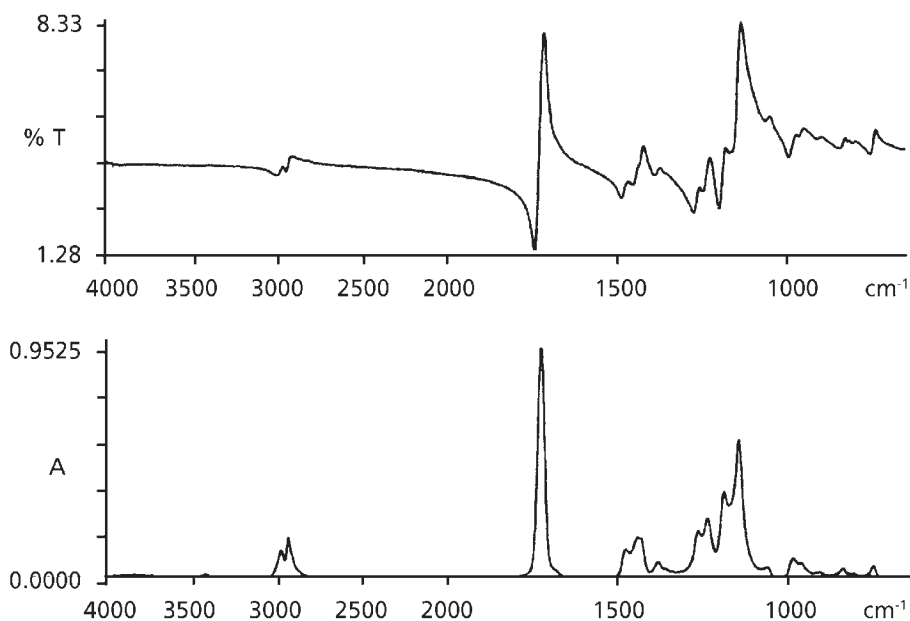
Figure 5.2 Specular reflectance (top) and Kramers-Kronig transformation (bottom) spectra of polymethylmethacrylate. (*Source: Author's own files*)

```
COMPARE X Disk 4000.0 650.0 ON
unknown:
correlation  factor   name    comment
0.998579     0.5444   std11   30-32% acrylonitrile/butadiene
0.973323     1.1819   std15   37-39% acrylonitrile/butadiene
0.956112     1.6101   std12   43-45% acrylonitrile/butadiene
0.892559     4.9056   std10   19-22% acrylonitrile/butadiene
0.776770     0.3678   std8    23% styrene/butadiene copolymer
0.774302     0.3827   std7    5% styrene/butadiene copolymer
0.740537     0.8742   std9    45% styrene/butadiene
0.422132     8.0718   std1    ethylene 12% vinylacetate
0.413650     4.1568   std2    ethylene 18% vinylacetate
0.411130     0.8564   std15   plastic bag#1 - polyethylene
```

Figure 5.3 An example of the COMPARE function. Top spectrum: unknown. Bottom spectrum: match from hits list shown above. (Sample is 30–32% acrylonitrile/butadiene copolymer.) (*Source: Author's own files*)

A further example of the application of Fourier transform infrared spectroscopy is the determination of total silanol (SiOH), silane hydrogen (SiH), and tetrapropoxysilane and diphenylmethylsilanol crosslinking agents in room temperature vulcanised silicone foams [58]. Total SiOH and SiH are determined by FTIR spectroscopy; the SiOH peak at 2.71 μm and the SiH peak at 4.61 μm are used for quantitation. The tetrapropoxysilane content is determined by gas chromatography using a solid capillary open tubular (SCOT) column and linear programmed temperature control. The diphenylmethylsilanol content is determined by gel permeation chromatography using a tetrahydrofuran solvent.

A technique for the identification of components or polymer laminates is the diamond anvil cell technique supplied by Perkin Elmer [59]. A laminate is separated by cutting
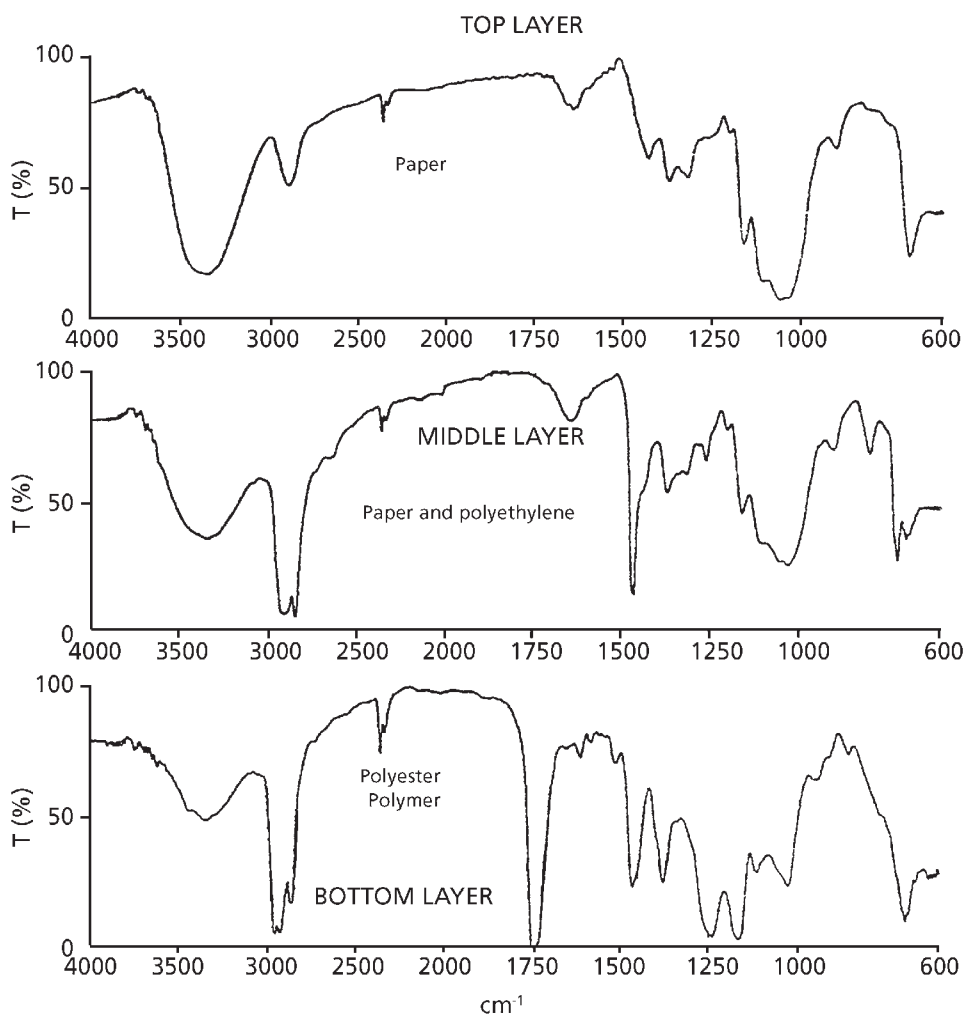
Figure 5.4 Infrared spectrum of three layer polymer laminate using the diamond cell technique. (*Source: Author's own files*)

a small portion of the sample with a razor blade. The layers are then separated by sectioning each piece with the blade. All sample preparation is performed under a stereo microscope. The separated layers are then individually placed in the diamond cell and a spectrum is obtained. This work was performed using a Perkin Elmer model 1650 instrument at 8 cm^{-1} resolution and 16 scans. **Figure 5.4** shows spectra identifying the components of a three-layer polymer laminate.

Garside and Wyeth [60] have used Fourier transform infrared spectroscopy to characterise cellulose fibres such as jute, sisal, and cotton. The technique has also been used to determine low levels of polyvinyl pyrrolidinone in polysulfone [61]. Weiss and co-workers [62] used Fourier transform infrared microspectroscopy in the study of organic and inorganic phases of an injectable hydroxypropylmethylcellulose-calcium phosphate composite for bone and dental surgery.

Other applications of FTIR in microstructural analysis of homopolymers include 1,4-diazophenylene – bridged Cu-phthalocyanine [63], isobornyl methacrylate [64], polypropylene [65, 66], polyaniline [67, 68], polycaprolactone [69], viscose fibres [70], Kevlar [71], polystyrene sulfonic acid [66, 72], syndiotactic polystyrene [73], isotactic polypropylene [66, 74, 75], polyurethane [76], PMMA [75, 77], polyurethane ether [78], PE [79–80], fluorinated acrylates [81], rigid PU [82], *N*-(2-biphenyl)4-(2´ phenylethynyl)phthalamide [83], polyacrylic acid [84], polysodium styrene sulfonate [84], and polyacrylic acid [85].

FTIR spectroscopy has been applied in the study of polymer blends including Neoprene rubber, chlorosulfonated PE, nitrile rubber, polyvinyl chloride (PVC) containing carbon black and other fillers [86], Nylon 6 inorganic [87], polyhydroxyether sulfone/poly(*N*-vinyl pyrrolidone) [88], graphite-based low-density polyethylene [89], caprolactone/Nafion blends [90], polybutylene terephthalate/polyamide [91], polyphenylene sulfide/acrylonitrile – butadiene – styrene [92], PMMA/polypyrrol [93], and lower or high performance liquid chromatography (LDPE/HDPE) [94].

Nanocomposites examined include PP/PP – styrene – butadiene [95], PA – clay [96], dicyanate – clay [97, 98], polypropylene carbon [99], and the following composites: polyfuran/poly(2-fluoroaniline) [100], polyvinyl alcohol – cadmium sulfide [100, 101], polyhydroxybutyrate – polyvinyl alcohol (PVOH) [102], HDPE – wood flour [103], polyaniline – gold [104] and PU – casein [105].

5.3 Fourier Transform Raman Spectroscopy

5.3.1 Theory

Raman spectroscopy is an emission technique which involves irradiating a sample with a laser and collecting the scattered radiation. Most of the scattered radiation has the same wavelength as the laser. A very small fraction (approximately one millionth) of the scattered radiation is displaced from the laser wavelength by values corresponding to the vibrational frequencies of the sample. This is the Raman signal.

The major features of Raman spectroscopy are:

1. The information on molecular structure is complementary to that obtained from infrared spectroscopy.

2. Functional groups that give weak absorptions in the infrared, such as S-S, C=C, and N=N, give strong Raman signals.

3. It is a non-contact, non-destructive technique.

4. No sample preparation is required.

5. Glass is an ideal optical window material.

6. Dangerous or delicate samples may be examined in sealed containers.

Conventional Raman spectrometers use visible lasers to irradiate the sample with wavelengths between 400 and 800 nm. At these wavelengths 90% of 'real-world' samples fluoresce, and no useful Raman data can be collected. When a near-infrared laser (i.e., near-infrared Raman spectroscopy) is used to irradiate a sample, fluorescence is unlikely to occur and at least 80% of samples will give useful Raman spectra. Thermal degradation of coloured and delicate samples is also reduced. The intensity of Raman scattering is dependent on the wavelength of the excitation source; therefore a near-infrared laser produces a much weaker Raman signal than a visible laser. Fourier transform technology provides the signal-to-noise advantage necessary to overcome this low signal level. In addition, circular apertures in a Fourier transform spectrometer make sample alignment much less critical than with a dispersive system.

The advantages of Fourier transform near-infrared Raman spectroscopy are:

1. Fluorescence is minimised.

2. Thermal degradation of coloured or delicate samples is reduced.

3. 80% of 'real-world' samples give useful Raman spectra.

4. Multiplex advantage: complete spectra, fast.

5. Real-time display of complete spectra.

6. Signal-to-noise optimisation in real time.

7. Abscissa accuracy: Raman shift calibration uses HeNe laser referencing.
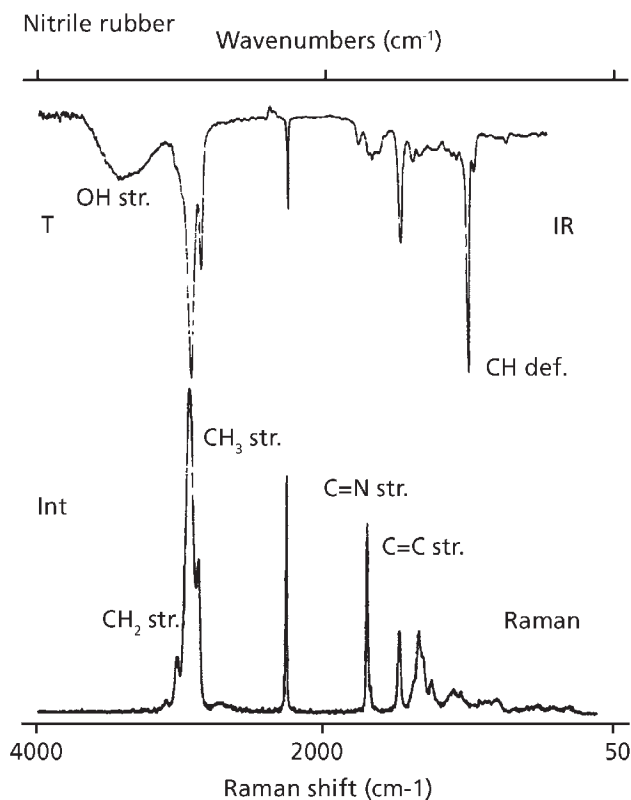
Figure 5.5 Nitrile rubber. In Raman spectroscopy the C=C stretching vibration is particularly sensitive to its environment in a similar way to C=O in the IR. (*Source: Author's own files*)

Figure 5.5 shows a Raman spectrum of nitrile rubber demonstrating the sensitivity of the C=C stretching vibration to its environment in the polymer molecule.

5.3.2 Applications

Agbenyega and co-workers [105] have investigated the applicability of Fourier transform near-infrared Raman spectroscopy in the synthetic polymer field. Their investigations covered the following areas:

1. Crystallinity in polymers, e.g., atactic and crystalline isotactic polystyrene, polypropylene, PE, polyurethane sulfide, and polytetrafluoroethylene (PTFE).

2. Raman spectra of different polyamides, showing that the spectra are sufficiently different to be of use for characterisation purposes and evaluation of crystallinity.

3. Raman spectra of polyaryl ether ether ketone and polyaryl ether ketones.

4. Raman spectra of polyaryl ether ether sulfone and polyaryl ether sulfones.

5. Curing of epoxy resins, study of chemical reactions occurring during cure, and effect of temperature.

6. Determination of monomer ratios in copolymers, e.g., ethylene oxide – vinyl chloride, tetrafluoroethylene – hexafluoropropylene (see Chapter 6).

7. Raman spectra of polythioethers.

8. Study of the structure of polyvinyl chloride gels.

These workers concluded that this technique has a great future in polymer analysis problems.

Fourier transform near-infrared spectroscopy had been used to determine traces of hydroxy and carboxy functional groups and water in polyesters. Bowden and co-workers [106] monitored the degradation of PVC using Raman microline focus spectrometry. They demonstrated that PVC decomposition is accompanied by the formation of modal polyene chains containing 11-12 or 13-19 double bonds. Bloor [107] has discussed the Fourier transform Raman spectroscopy of polydiacetylenes. Koenig [108] discusses results obtained by the application of infrared and Raman spectroscopy to polymers.

Yoshino and Shinomiya [20] have published Raman spectra of solutions of various polymers. Raman spectroscopy has many applications in the identification of polymers in which additives obscure the polymer peaks obtained in the IR spectrum.

The appearance of the Raman spectra is essentially independent of the physical form of the sample. The only obvious difference between spectra of pellets, powders, films, fibres, and foams is in the signal intensity. For constant laser power these intensities reflect the packing of the solid into the region being observed, and the path of the exciting radiation. As would be expected, powders give stronger spectra than solids. Fibres and films give poorer spectra, presumably because of inefficient packing. The spectra of foams vary.

The quality of the spectra obtained in two minutes is more than adequate for qualitative identification. Differences in crystallinity are readily seen for both PP and polyester samples. Some common inorganic fillers such as glass and talc are weak Raman scatterers and are not evident in the spectra. In other cases inorganic fillers are seen, for example, $BaSO_4$ in voided polyethylene terephthalate film.

The Raman spectra shown in **Figure 5.6** were obtained with a modified Perkin Elmer 1720 FTIR spectrometer using a Nd:YAG laser at 1.064 μm and a liquid nitrogen-cooled InGaAs detector. Excitation and collection of radiation were at 180°, the samples being held in a metal cup at one focus of an ellipsoidal mirror.

Most samples absorb 1.064 μm radiation only weakly. Even so there is sufficient sample heating to limit the laser power that can be used. The measurements were made using a focused laser which emphasises the heating effects. Samples were examined
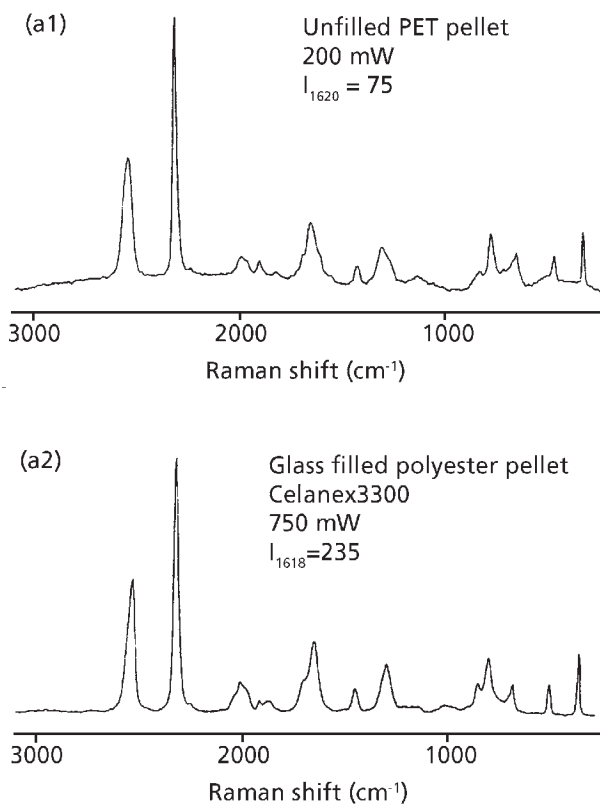
Figure 5.6 Raman spectra of polyesters and polypropylene: (a) PET = polyethylene-terephthalate; (b) polypropylene. (*Source: Author's own files*)

(a3)

PET film
750 mW
$I_{1620}=116$

3000   2000   1000

Raman shift (cm^{-1})

(a4)

PET fibres
200 mW
$I_{1618}=12$

3000   2000   1000

Raman shift (cm^{-1})

(a5)

PET voided film
750 mW
$I_{1618}=60$

$*BaSO_4$

$*$

3000   2000   1000

Raman shift (cm^{-1})

Figure 5.6 (*Continued*)

(b1)

Polypropylene

Unfilled pellet
750 mW
$I_{2887}=229$

3000   2000   1000

Raman shift (cm⁻¹)

(b2)

Polypropylene

Powder
750 mW
$I_{2887}=627$

3000   2000   1000

Raman shift (cm⁻¹)

(b3)

Polypropylene

Glass filled moulding
750 mW
$I_{2876}=69$

3000   2000   1000

Raman shift (cm⁻¹)

Figure 5.6 (*Continued*)

(b4)

Polypropylene

Talc filled moulding
200 mW
$I_{2887}=20$

Raman shift (cm^{-1})

3000   2000   1000

(b5)

Polypropylene

Voided film
200 mW
$I_{2887}=16$

Raman shift (cm^{-1})

3000   2000   1000

Figure 5.6 (*Continued*)

using laser powers of 200 and 750 mW. In most cases there were no changes in the spectra but in some filled samples bands broadened at the higher power. Strongly absorbing samples, notably all carbon-filled materials, were damaged at low laser power and gave no spectra.

Raman spectroscopy has been used in structural studies of a wide range of homopolymers and copolymers [109–122] including crystalline PE [123], polyaniline [124], polystyrene-*co*-*p*-(hexafluoro-2 hydroxyisopropyl)-alpha methyl styrene/polypropylene carbonate blends [125], PE [126], PP [126], polylactide [127], polyacrylonitrile [128], Nylon-6 – polyvinyl alcohol blends [129], poly(4-vinyl pyridine cupric salt complexes [130] and regenerated cellulose [131].

5.4 Mass Spectrometry

Mass spectrometry (MS) involves the study of ions in the vapour phase. This analytical method has a number of features and advantages that make it an extremely valuable tool for the identification and structural elucidation of organic molecules, including synthetic polymers:

1. The amount of sample needed is small (microgram level or less).

2. The molar mass of the material can be obtained directly by measuring the mass of the molecular (or quasimolecular) ion.

3. Molecular structures can be elucidated by examining molar masses, ion fragmentation patterns, and atomic compositions determined by mass spectrometry.

4. Mixtures can be *analysed by using 'soft' ionisation* methods and hyphenated techniques such as gas chromatography MS, liquid chromatography MS and tandem MS (GC/MS, LC/MS, and MS/MS, respectively).

Mass spectrometry in recent years has rapidly become an indispensable tool in polymer analysis, and modern MS today complements in many ways the structural data provided by nuclear magnetic resonance (NMR) and IR methods. Contemporary MS of polymers is capable of changing the established protocols for the molecular and structural analysis of macromolecules.

Some of the most significant applications of modern MS to synthetic polymers are:

• Chemical structure and end-group analysis

• Direct measurement of molar mass and molar mass distribution

• Copolymer composition and sequence distribution

• Detection and identification of impurities and additives in polymeric materials

Scrivens has reviewed the applications of MS to polymer characterisation [132].

In order to analyse any material by MS, the sample must first be vapourised (or desorbed) and ionised into the instrument's vacuum system. Since polymers are generally nonvolatile, many mass spectral methods have involved degradation of the polymeric material prior to analysis of the more volatile fragments. Two traditional methods to examine polymers have been flash-pyrolysis GC/MS and direct pyrolysis in the ion source of the instrument.

In recent years, however, there has been a marked tendency toward the use of direct MS techniques. While a continued effort to introduce MS as a major technique for the structural analysis of polymers has been made over the past three decades, MS analysts did not have a great impact upon the polymer community until the past five years or so. During this period outstanding progress has been made in the application of MS to some crucial problems involving the characterisation of synthetic polymers.

Developments in two general areas have spurred this progress. Sector and quadrupole mass analysers, the traditional methods of separation of ions in mass spectrometry, have recently been complemented by the development of powerful Fourier transform (FT-MS) and time-of-flight (ToF-MS) instruments. The ToF analysers are particularly well-suited for detecting higher molar-mass species present in polymers.

Parallel to this, new ionisation methods have been developed that are based on the direct desorption of ions from polymer surfaces. With the introduction of 'desorption/ionisation' techniques, it has become possible to eject large molecules into the gas phase directly from the sample surface, and thereby mass spectra of intact polymer molecules have been produced. The term 'desorption/ionisation' refers to a method in which the desorption/vapourisation and ionisation steps occur essentially simultaneously. Much progress to date has been made using matrix-assisted laser desorption/ionisation (MALDI-MS), which is capable of generating quasimolecular ions in the range of a million Daltons and beyond.

Until around 1970, the only ionisation method in common use was electron impact (EI). Field ionisation (FI) was developed in the 1950s, but it was never very popular, and chemical ionisation (CI) was just getting started. These three methods (EI, FI, CI) depend upon vaporisation of the sample by heating, which very much limits polymer applications to small, stable oligomers or to polymer degradation products (formed by pyrolysis or other methods). Field desorption (FD), invented in 1969, was the first 'desorption/ionisation' method. FD- and FI-MS are often very useful (particularly for analysis of less polar polymers), but they have never been in widespread use.

The 1970s and 1980s saw the advent of several new 'soft' desorption/ionisation methods, many of which are now well-established in analytical MS. MALDI, electrospray ionization (ESI), and a few other desorption/ionisation techniques have important applications in polymer analysis.

5.4.1 Time-of-Flight Secondary Ion Mass Spectrometry

SIMS is the most commonly used of the surface MS techniques. SIMS analyses the secondary ions ejected from a sample following bombardment with a primary ion

beam, usually argon ions. The impact of the primary ion causes an atomic-scale collision cascade within the surface layers of the sample and, at points remote from impact, secondary ions are ejected from the surface. These ions are then determined by MS.

Time-of-Flight Secondary Ion Mass Spectrometry (ToF-SIMS) uses a primary ion beam, usually argon ions, which is pulsed and focused onto the sample. The secondary ions emitted from the sample are accelerated by a field to the same kinetic energy, and mass separation is achieved by measuring the flight time necessary for the passage of the ions along a path of known length. The secondary ions reach a detector in order of increasing mass, the detector consisting of a multi-channel plate in combination with a scintillation counter and a photomultiplier. The relationship between kinetic energy and flight time may be used to determine the mass of the secondary ion and therefore identify it. The sensitivity of the instrument requires great care to avoid sample contamination.

There are two modes of operating SIMS: static and dynamic.

Static SIMS (SSIMS) operates under non-damaging conditions. It gives good information on molecular content and, like Auger spectroscopy, can be used for surface micro-analysis at high spatial resolution.

The most widely used method of static SIMS is ToF-SIMS. This uses ToF-MS which provides optimum sensitivity and mass resolution for secondary ions.

With the latest ToF-SIMS instruments mass resolutions of 10^{-3} to 10^{-4} amu are achievable with sampling depths of greater than 1 nm. This has two main advantages. Firstly, the sensitivity is increased, allowing peaks to be resolved where previously there had been overlap (i.e., two peaks at nominally the same mass) which enables ToF-SIMS to be sensitive to ppm/ppb levels of surface species. Secondly, high mass resolution enables very accurate mass measurement so that empirical formulae can be calculated from the measured accurate mass, making unknown peak identification more certain.

Dynamic SIMS (DSIMS) operates under conditions designed to remove surface layers sequentially during the analysis. This is achieved by rastering a primary ion beam over the area of analytical interest and collecting the emitted secondary elemental or cluster ions in the MS system. The erosion rates can be controlled from a few nanometres per hour to several tens of micrometres. The technique provides high sensitivity, quantitative elemental information in the form of mass spectra, depth profiles, and two- and three-dimensional images. All elements in the periodic table can be detected with sensitivities in the parts per million to parts per billion range.

High mass resolution analysis can be used to separate elemental and molecular species with the same nominal mass values.

This technique has been used in the examination of structural details, and in some cases molecular weight determination of various types of polymers, and is extremely useful in polymer surface studies. The technique has also been used to provide new information and establish relations between species in monolayers, e.g., in the bonding of plastic films to metal or glass.

The ToF-SIMS technique is used either on its own or, as is the growing trend, in conjunction with X-ray photoelectron spectroscopy (XPS). Often the combination of these two techniques provides better solutions to problems than either technique alone.

5.4.1.1 Applications of ToF-SIMS Alone to Problem Solving (XPS Not Used)

A study has been carried out of hydrogen-deuterium exchange in PS using ToF-SIMS [20].

Cox and co-workers [133] analysed PS/polyvinyl methyl ether blends by coincidence counting ToF mass spectrometry. This technique gave information on the chemical and spatial relationships between secondary ions. Thompson [134] carried out a quantitative surface analysis of organic polymer blends (e.g., miscible polycarbonate (PC)/PS blends) using ToF-SIMS. Lin and co-workers [135] used supersonic beam/multiphoton ionisation/ToF mass spectrometry to analyse photoablation products resulting from styrene-containing polymers such as styrene-butadiene, acrylonitrile-butadiene-styrene (ABS), and PS foams. Photoablation products were examined by supersonic beam spectrometry and the results were compared with those obtained by thermal decomposition.

The high selectivity provided by supersonic beam spectrometry allowed the detection of minor species such as styrene, resulting from ablation of poly-α-methylstyrene produced by cleavage of a methyl group and by proton rearrangement.

Because ablation is carried out at high temperatures it is possible to examine thermally static polymers such as poly-*p*-methylstyrene. Other recent applications of ToF-SIMS include the examination of PS [136–139], carbon-fibre reinforced epoxy resins [140], polyalkylacrylates [141], alkylketene dimers [142], perfluorinated polymers [143], siloxanes [144–150], rubbers [151], ethylene – tetrafluoroethylene copolymers [151], Nylon 6 [152], PC [153], polydimethylsiloxane [154], polypyrrole coated PS [156], poly-*p*-phenylene vinylene [157], butyl rubber [158], poly(4-vinyl

phenol)/poly(4-vinyl pyridine) blends [159], polypyrrole – silica gel composites [160], γ-glycidyloxypropyltrimethoxy silane [161], triblock copolymer polyethylene (ethylene glycol β-poly(phenylene ethnylene)-β-polyethylene glycol) [162], ethylene terephthalate – hydroxybenzoate copolymer [163], sulfenylene – siloxane [164], polyethylene phthalate [165], polytetrafluoroethylene [165, 166], PMMA [165, 166], poly(bis-trifluoroethoxyphosphazine [165, 166], PU [167], polyethyleacrylate [168], polyacrylonitrile [168], PC [166], polyarylates [166] and PET [166].

5.4.1.2 Applications of Both ToF-SIMS and XPS [169]

These techniques have been applied to PTFE [170, 171], polybutadiene [172], rubbers [173, 174], acrylics [175, 176], PE [177, 178, 179], PU [180], PS [181], polyvinyl carbazole [182], polymalic acid [183], poly-β-hydroxy butyrate [184], poly-β-hydroxy valerate [184], γ-glycidyloxypropyltrimethoxy silane [185], polypyrrole [186], acrylonitrile – butadiene rubber [187], polyferrocenyl silanes [188], polyamides [189], polyarylates [178, 190] and epoxy resins [191].

5.4.1.3 Further Applications of ToF-SIMS

Adhesion Studies

ToF-SIMS, and also in some cases XPS, has been applied to a range of polymer problems such as adhesion studies of elastomers based on brominated poly(isobutylene-*co*-4-methylstyrene) and diene elastomers [192], PVC [193], epoxy resin aluminium [194, 195], glass rubber [196], squalene brass [197], and sealants [198].

Tse and co-workers used this technique to study the effects of migration on adhesion between different polymers [199].

Chain Diffusion Studies

Lin and co-workers [196] studied the chain diffusion behaviour and microstructure at an interface between the rubbery polymer PS and the glassy polymer polyphenylene oxide by depth-resolved SIMS. The interface region demonstrated a very sharp symmetric profile before annealing, with a thickness of 25–30 nm. As chain diffusion took place the interfacial region widened asymmetrically, moving into the polyphenylene oxide region, and the chain diffused across the interface in a manner that simultaneously showed both Fickian and Case II non-Fickian behaviour. The interfacial region could be divided into a rubbery and glassy region using the local

glass transition temperature, which could be calculated by the Flory-Fox equation. The Fickian behaviour predominated at the rubbery side, and the non-Fickian behaviour at the glassy side. The effect of temperature on the interfacial diffusion agreed with the WLF (Williams-Landel-Ferry) equation. The average velocity of the interface decreased with the molecular weight according to a negative power law. The precise exponents of the power law were different above and below the critical molecular weight of PS, which was 38,000. The mutual diffusion coefficients were calculated from the MS data, and showed a good agreement with the predictions of the 'slow theory', which deals with the case where the diffusion coefficient is dominated by the effect of the slower-moving component.

Polymer Surface Characterisation

ToF SIMS has been applied to the measurement of surface chemical composition in blends or complexes of polystyrene-*co*-4-vinyl phenol/polystyrene-*co*-4-vinylpyridine blends [200] and rubbers [201].

5.4.2 Tandem Mass Spectrometry

Jackson and co-workers [202] have used tandem mass spectrometry (MS/MS) in an AutoSpec 5000-orthogonal acceleration-time of flight (oa-ToF) instrument to generate end group and structural information from a variety of polymers. These systems include PMMA, polyethyl methacrylate, and polybutyl methacrylate. Matrix-assisted laser desorption/ionisation-collision-induced dissociation (MALDI-CID) data have been obtained from polymeric precursor ions with mass-to-charge ratios of up to approximately 5000. It is shown that end group and structural information may also be obtained from copolymers using MALDI-CID. Sequence information is generated for a MMA/butyl methacrylate block copolymer synthesised by group transfer polymerisation.

Bouajila and co-workers [203] used a technique based on liquid chromatography - ultra violet spectroscopy - mass spectrometry - mass spectrometry (LC-UV-MS-MS) to elucidate the structure of phenol oligomers in resols by fragmenting the monomers. The progression of resin crosslinking was determined by solid-state ^{13}C-NMR (constant potential (CP)/MAS), and the residual percentage of monomers and oligomers was determined in leachates and characterised by LC-UV-MS-MS. Results for crosslinking advancement were then correlated with the various synthesis parameters [204].

Tandem MS has been used to identify end-groups in polyaniline [205] and for the characterization of polyperfluoroethylenes [206].

5.4.3 Matrix Assisted Laser Desorption/Ionisation Mass Spectrometry

This is a relatively new technique developed amongst other things, for the determination of repeat groups and end groups in polymers and copolymers, also molecular weight distribution.

In matrix assisted laser desorption/ionisation (MALDI) the material to be analysed (the analyte) is mixed with an analysis aid (the matrix) which is easily volatilised by the appropriate laser light [206–208]. In electrospray ioniation [209-211] the analyte is sprayed from a small orifice in a high electric field. Both techniques have been developed to introduce non-volatile materials into a mass spectrometer. These revolutionary techniques have effectively opened polymers to mass spectrometric characterisation.

Mass spectrometers are instruments that measure the mass to charge ratio of charged particles. There are a variety of methods to measure mass to charge. The most common mass spectrometers used with MALDI and ESI sources for the study of polymer materials are ToF instruments [212]. ToF mass spectrometers measure mass to charge by accurately measuring the time required for an ion to traverse the instrument after acceleration from a known voltage. Modern ToF instruments have very high mass ranges (up to 10^6 D), high mass resolution (up to 20,000 using full width at half maximum, FWHM), high mass accuracy (as good as 5 ppm), and have the multiplex advantage (the mass spectrometer is not scanned, all of the ions are detected). These instruments are particularly well suited to the analysis of low mass polymers.

Hanton [213] has discussed in detail the application of these techniques to the analysis of polymers and polymer coatings.

The mass differences between the ions determine the mass of the polymer repeat units. While mass alone is not sufficient to determine the repeat units, the context of the sample often provides enough information to generate high confidence in the polymer identity.

The masses of the specific oligomer ions also generate information about the polymer end groups. If we subtract the mass of all of the repeat units from the ion mass, the residual mass includes the mass of the end groups and the cation. The chemical identity of the end groups can then be determined either from combining the mass data with some spectroscopy data (like NMR or IR), or by measuring the accurate mass of the oligomer. The accurate mass measurement can help determine the most likely elemental composition responsible for the residual mass.

Figure 5.7 shows a small segment of MALDI mass spectra of two surfactants. Both the upper and lower mass spectra show two oligomers cationised by both Na^+ and K^+ resulting in ion peaks spaced by 16 D. Calculations for the end group mass can easily determine
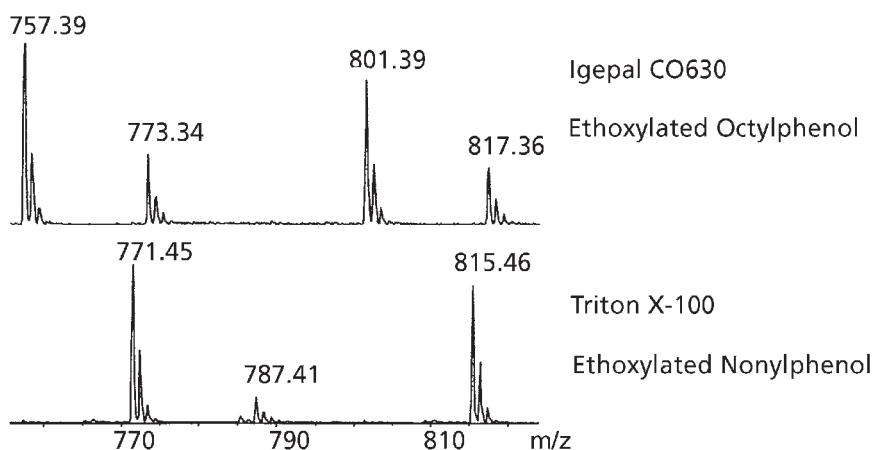
Figure 5.7 Small segments of MALDI mass spectra for two different ethoxylated surfactants. Residual mass calculations show that the upper spectrum is an ethoxylated octophenol and the lower spectrum is an ethoxylated nonylphenol. MALDI can easily differentiate these materials. (*Reprinted with permission from S.D. Hanton, JCT Coatings Technology, 2004, **1**, 62. ©2004, Federation of Societies for Coatings Technology*) [213]

that the upper spectrum corresponds to ethoxylated octylphenol (Igepal CO630) and that the lower spectrum corresponds to an ethoxylated nonylphenol (Triton X-100).

Gel permeation chromatography can be coupled with MALDI to help generate data for samples with broad dispersivity.

Figure 5.8 shows a series of MALDI mass spectra obtained from the gel permeation chromatography (GPC) separation of a sample of PTMEG 1000. Each mass spectrum corresponds to a particular elution time from the GPC column. These GPC fractions were collected continuously. At each position along the transform track, a high quality MALDI mass spectrum can be generated.

Combined MALDI-MS and ion exclusion chromatographic techniques: in most of these techniques described in the literature, the MALDI is not directly coupled off-line with the ion exclusion column. An exception is that of the work of Esser and co-workers [214], in which the two units are interfaced via a robotic interface. This technique was applied to studies of PS, PMMA, and butylmethacrylate – methylmethacrylate copolymers. Mehl and co-workers [215] combined ion exclusion with MALDI-MS to provide accurate molecular weight determinations on polyether and polyester polyurethane soft blocks.
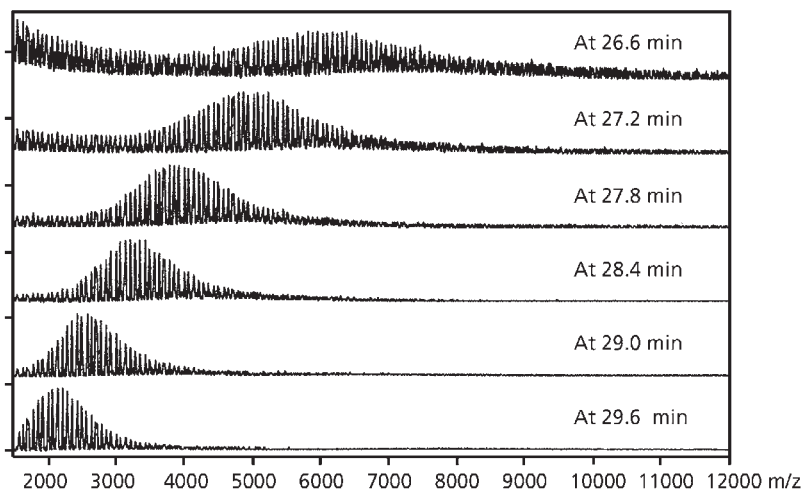
Figure 5.8 MALDI mass spectra obtained from the GPC separation of PTMEG 1000 using an LC Transform instrument. Each spectrum was obtained from a distinct position on the foil. (*Reprinted with permission from S.D. Hanton, JCT Coatings Technology, 2004, 1, 62. ©2004, Federation of Societies for Coatings Technology*) [213]

It is seen that MALDI-MS represents a unique tool for the simultaneous determination of molecular weight distribution and chemical structure of oligomers and polar and non-polar low-molecular-weight homopolymers. This includes end-group analysis fragmentation studies, molar mass analysis, analysis of copolymers, and fundamental studies. However, MALDI analysis of multifunctional polymers and block copolymers has some drawbacks, which are caused by the different ionisation behaviour of structurally different polymers. To obtain both chemical and structural information a coupling of chromatography with MALDI-MS can be applied. Special attention is paid to the principle of chromatography used for polymer separation. Besides size exclusion chromatography (SEC), which can be used for the separation of polymers according to their hydrodynamic volume, some other modes of chromatography can be applied.

The structural and molecular analysis of copolymers is a difficult problem that often cannot be easily dealt with by analysing the intact copolymer, and therefore much effort has been directed at the task of converting SEC traces to molar masses of copolymers. Multiple detectors and SEC/light scattering techniques may provide a solution to the problem, but difficulties remain. Being able to discriminate among different masses and possessing a remarkably high sensitivity, the MALDI-MS detector does not suffer these limitations and, coupled with analytical SEC, MALDI-MS is found to give mass spectra with average molar mass values in excellent agreement with those obtained by conventional techniques.

Advances in methods used in the structural characterisation of redox-active polymers will aid in developing structure/property relationships and in guiding synthetic efforts. MALDI-MS analysis has proved to be a powerful structural characterisation tool for biopolymers. The application of MALDI-MS to synthetic polymers has been primarily limited to polar or polarisable polymers that can be protonated or can form salt/metal adducts. Electron transfer matrices for MALDI-MS of small, non-polar, redox-active analytes have been evaluated and it was found that anthracene and terthiophene are effective MALDI matrices for these analytes and assist in producing analyte molecular ions (not protonated molecules). Thus, non-polar, redox-active polymers might also be similarly ionised.

In most of the published work, the ion-exclusion chromatographic technique was not used, this being limited to the application of ToF MALDI-MS as reviewed here, silicone elastomers [216], PMMA [217, 218], acrylic dienes [219], polyesters [220, 221], polycaprolactone [222, 223], polyhexylthiophene [224], polyether and polyester – PU soft blocks [225], polyisobutylene [226, 227], PS [228], PE [229], polyalkylene oxides [230], polypropylene glycol [231], polyisobutyl vinyl ether [232], polypropylene oxide [233], hindered amine light stabilisers [234], poly-1,2:3,4-di-*O*, isopropylidene-6-*O*-(2-vinyl-oxyethyl)-D-galactopyranose [235], cyclic carbonates [236], vinyl peroxide end groups [237], polyamidoamine dendrimers [238], blue emitting polymers [239], poly-3-methylenehydroxy-bile acid derivatives [240], polylactides [241], furanylene vinyl or cyclopentadienyl vinyl polymers [242], polydimethyl-S-(2-hydroxyethoxy)iso phthalate [243], polyacrylic acid [244], rubbers [245], polyethylene glycol (PEG) [246], PMMA [247–249], poly-*N*-isopropyl acrylamide [250], PS [251–253], polyetherimide [252], *tert*-butyl acrylate [249], polyether ketone [254], epsilon-caprolactone [255, 256], polyisocyanate [257], bisphenol-triphosgene condensates [258], poly(1,3-cyclohexadiene) [259], polyimides [260, 261], 2,2-bis(methylol)propionic acid derivatives [262], polyethylene glycol-lithium perchlorate polymers [263], PET [264], lactones [265], hydroxylated polybutadienes [266], and polyalkenes [264, 265, 267].

Theoretical studies using ToF MALDI-MS have been reported by various workers [245, 253–257, 268–271]. This technique has also been applied to the identification of various polymers including polyglycols [272].

5.4.4 Fourier Transform Ion Cyclotron Mass Spectrometry

Van der Hage and co-workers [273] combined MALDI and Fourier transform ion cyclotron mass spectrometry (FT-ICR-MS) for the characterisation of polyoxyalkyleneamines. MALDI FT-ICR-MS was used to resolve intact, sodium ion cationised oligomer ions in the mass range from *m/z* 500 to 3500. NMR was used to measure the average end-group distribution to provide insight into conformational differences. In this respect, FT-ICR-MS and NMR data were complementary. Combined

results yielded detailed information about chemical composition distributions of polyalkyleneamines that hitherto it was not possible to obtain with either technique separately. Merits and limitations of the data produced with MALDI FT-ICR-MS are discussed and compared with those of ^{1}H and ^{13}C NMR data.

5.4.5 Fast Atom Bombardment Mass Spectrometry

This technique has been used to identify cyclic oligomers formed by polycondensation reactions leading to aromatic, aliphatic and aromatic-aliphatic polysulfides and their complexes with heavy metals [274].

The positive fast atom bombardment (FAB) mass spectra of a mixture of cyclic sulfides extracted from the various crude polymeric samples are reported in **Figure 5.9**.
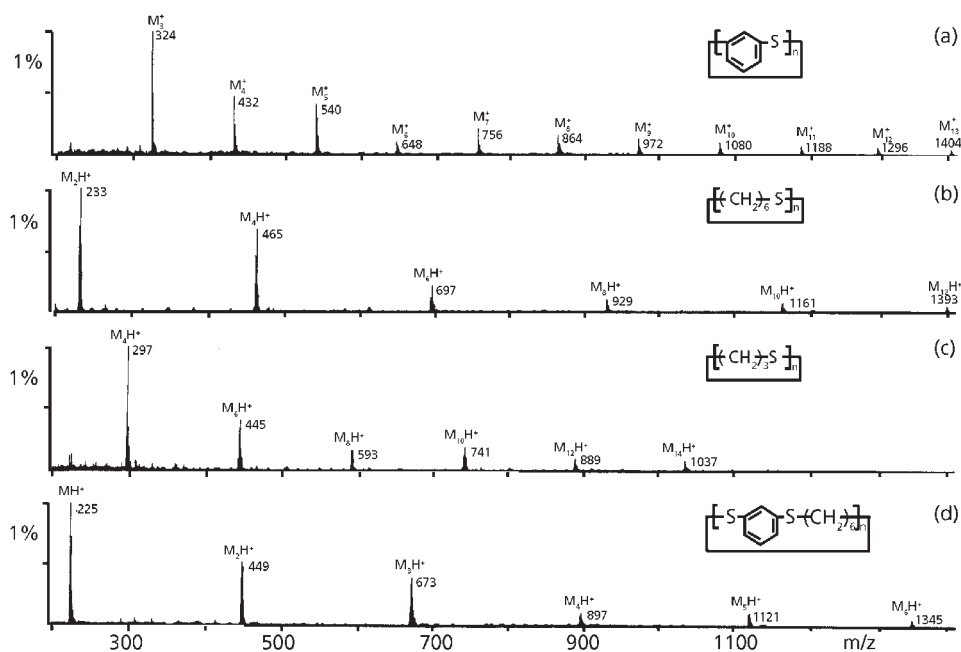
Figure 5.9 FAB mass spectra of the mixtures of cyclic sulfides extracted from the crude polymers: (a) poly(*m*-phenylene sulfide) (polymer I); (b) poly(hexamethylene sulfide) (polymer II); (c) poly(trimethylene sulfide) (polymer III); (d) poly(*m*-phenylene hexamethylene sulfide) (polymer IV). (*Reprinted with permission from G. Montaudo, E. Scamporrino, C. Puglisi and D. Vitalini, Macromolecules, 1988, 21, 6, 1594. ©1988, ACS*) [274]

In the mass spectrum of the poly(*m*-phenylene sulfide) (polymer I, Figure 5.9a), the peaks at *m/z* 324 + n108 correspond to molecular ions (M^+) of cyclic oligomers M_3^+-M_{13}^+. FAB mass spectra of polymers II-IV in **Figure 5.9** (parts b-d, respectively), show peaks due to protonated molecular ions (MH^+) of the oligomers present in mixtures.

In all cases the FAB spectra are constituted exclusively by peaks due to molecular ions (M^+ or MH^+), indicating that these macrocycles are very stable toward the FAB desorption method, without producing fragmentation.

5.5 Gross Polarisation Magic Angle Spinning ^{13}C and ^{15}N

5.5.1 Solid State Nuclear Magnetic Resonance Spectroscopy

This technique has been applied in microstructural studies on polypyrrole and polydiallyldimethyl ammonium chloride [275] and epoxy systems. For polypyrrole the ^{15}N signal consisted of at least four peaks decomposed by line shape analysis.

(a)　　　　　　　　　(b)
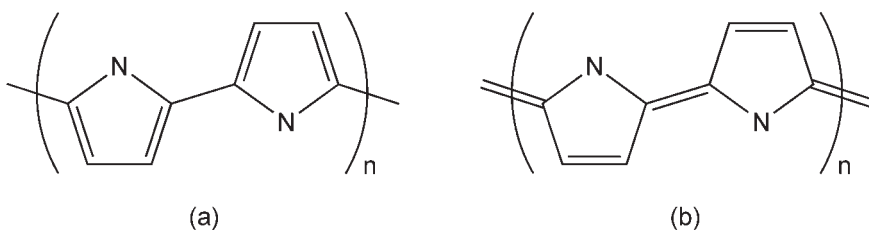
Four peaks (α, β, γ and δ) are assigned to the oxidised structure, the aromatic form, the quinoid form, and the 2,3-bond structure, of polypyrrole, respectively. The half-width of peak γ is a measure of electrical conductivity. Electrical conductivity measurements at room temperature and –23 °C show that the hopping conduction mechanism is the dominant one for polypyrrole.

^{13}C solid state ^{15}N and ^{14}N solid state NMR have been used to investigate the molecular structure of polydiallyldimethyl ammonium chloride [275]. The polymer (see right) was shown to consist of a chain of five-membered pyrrolidinium rings with predominantly *cis* stereochemistry.
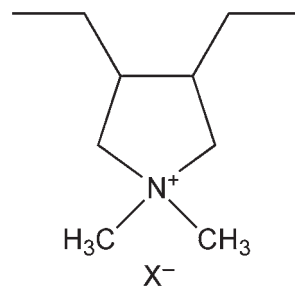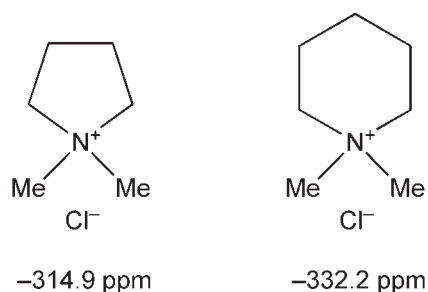
Figure 5.10 ^{14}N-NMR Chemical shifts of quaternary ammonium halide model compounds.

[14]N-NMR data shows that there is a chemical shift dependent on ring size, with five (I) and six (II) membered ring ^{14}N NMR resonances. The resonances are separated by about 17 ppm (**Figure 5.10**). This study has shown that it is possible to gain information concerning the ring size of the units making up poly(diallyldimethylammonium chloride) using solution state ^{14}N NMR spectroscopy. This provides another example of the utility of heteronuclear NMR spectroscopy in the determination of the structure of polymers obtained by cyclopolymerisation of heteroatom-containing α, ω-dienes.

Harris and co-workers [276] have described high temperature (well above transition temperature (T_g)) ^{13}C-NMR techniques for determining the crosslinked network structure formed when the diglycidyl ether of bisphenol A is cured with diphenylsulfone.

The advantage of high temperature studies lies in the fact that above the T_g higher intrinsic line widths resulting from inhomogeneous broadening are obtained.

The stoichiometries in question are based on the functionality of the two components; the difunctional epoxy (I) and the tetrafunctional amine (II).

As a result of the reactions indicated in **Figure 5.11**, it is anticipated that the principal epoxy-derived network linkage for the 100% material will be III, whereas the 66% system should show both III and IV, together with some V. Also, some intramolecular cyclization ('back-biting') might be expected to occur between epoxy units and amine groups (or, with a deficiency of hardener (II), hydroxyl groups) to give a distribution of ring sizes, of which VI is a simple example.

The work of Harris and co-workers [276] confirmed that highly-resolved NMR spectra can be obtained from very rigid amorphous materials such as cured epoxies,
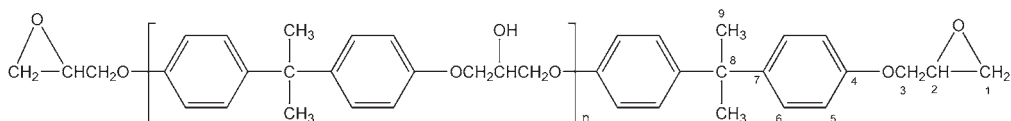
I: Diglycydyl ether of bisphenol A
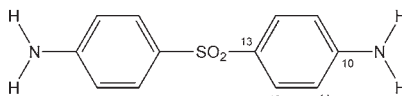
II: 4,4'-diaminodiphenylsulphone
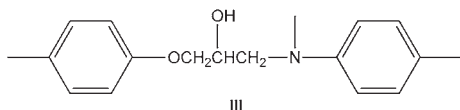
III
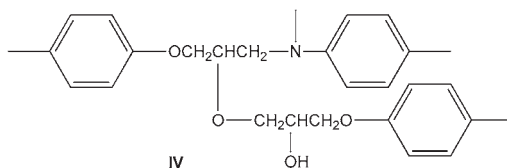
IV
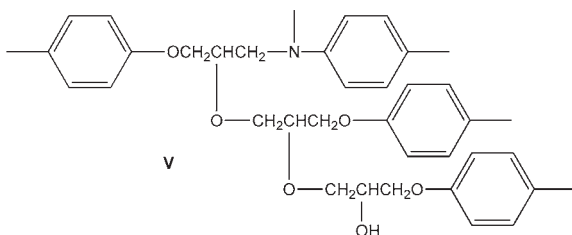
V
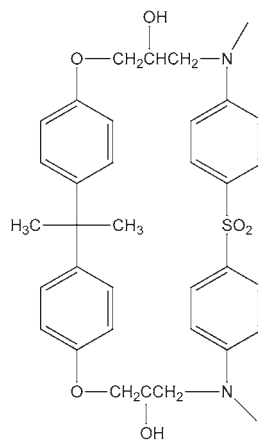
VI

providing the temperature at which the measurement is made is sufficiently high to allow motional narrowing without sample degradation. At these temperatures, features in the spectra reflect the chemistry of the curing process and confirm proposed structures. The details observable in the spectra are such that the completeness of the curing process and the degree of extra ether-link content are clearly visible. Motional narrowing at these temperatures reduces linewidths sufficiently to allow the use of spectral editing techniques to confirm assignments of the peaks. However, in order for these experiments to work the proton-proton dipolar interactions must be reduced sufficiently by molecular motion so that

(a) Epoxy-amine reaction:
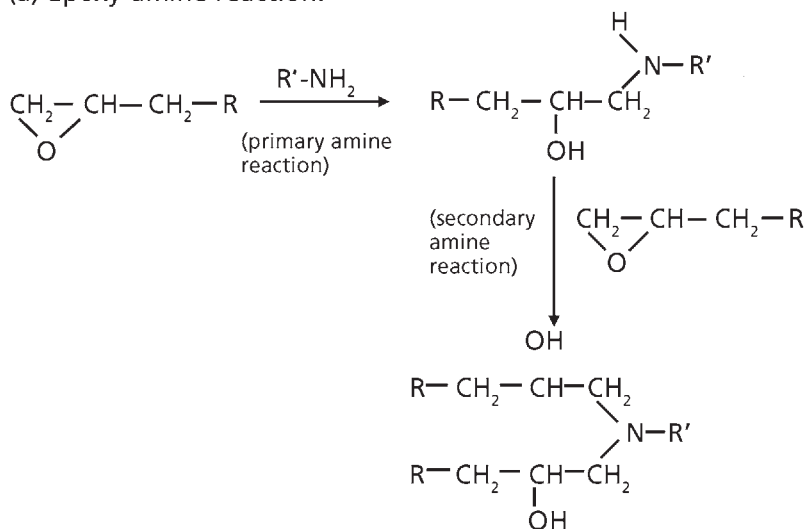
(b) Epoxy-hydroxyl reaction:
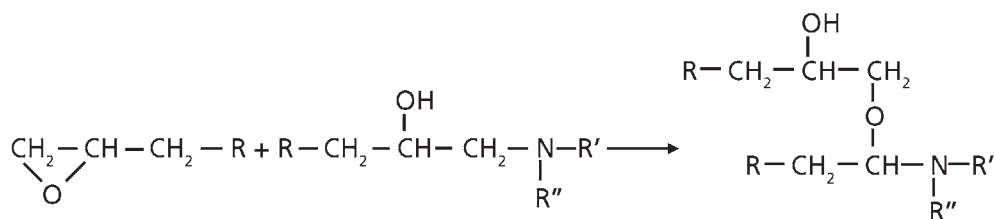
Figure 5.11 Curing reactions of the diglycidyl ether of bisphenol A with amine hardener. (*Reprinted with permission from R.K. Harris, R.R. Yeung, P. Johncock and D.A. Jones, Polymer, 1996, 37, 5, 721. ©1996, Elsevier*) [276]

modulations contained in heteronuclear J-coupling can be converted into sign and intensity information as displayed in the APT spectrum. Similarly, in the absence of dipolar interactions, polarisation transferred via J-coupling can suppress certain carbon signals whilst enhancing others as shown by the distortionless enhancement by polarisation transfer (DEPT) subspectra. Within these constraints, techniques hitherto strictly applicable only to the liquid state can be used to complement the information already available from solid-state spectra.

5.6 Gas Chromatography – Mass Spectrometry

McClennen and co-workers [277] used this technique to determine the structure of poly(α-methylstyrene). The technique has also been used to characterise monocarboxyl end grouped polycaprolactone [278] and in thermal degradation studies of polystyrene at temperatures between 300 and 600 °C [279].

5.7 Proton Magnetic Resonance Spectroscopy

Randall [280, 281] carried out a detailed study of the PP methyl group in triad and pentad configuration environments. Figure 5.12 shows the proton magnetic resonance (PMR) spectrum of a hot *n*-heptane_solution of a PP containing up to 40% syndiotactic placement, and which by Natta's definition may be stereoblock. The spectrum is inherently complex, as a first-order theoretical calculation, and this indicated the possibility of at least 15 peaks with considerable overlap between peaks, because differences in chemical shifts are about the same magnitude as the splitting due to spin-spin coupling.

The largest peak, at high field in **Figure 5.12(a)**, represents pendant methyl moieties in propylene units. It is characteristically split by the tertiary hydrogen. By peak area integration, about 20% of the nominal methyl proton peak is due to overlap of absorption from chain methylenes. This overlap is consistent with a reported syndiotactic triplet, two peaks of which are close to A and B in **Figure 5.12(a)** and a third peak that falls with the low-field branch of the methyl split. The absence of a strong single peak in the methylene range indicates the virtual absences of 'amorphous' polymer in the PP shown in **Figure 5.12(a)**, which could possibly be due to the head-to-head and tail-to-tail units. The low-field peak represents the partial resolution of tertiary protons that are opposite the methyls on the hydrocarbon chain.

Figure 5.12(a) also shows a spectrum for an isotactic polypropylene (iPP) (>95% isotactic by solubility, <5% soluble in boiling heptane). This spectrum has the same general character as the atactic PP. The important difference is a marked decrease of peak intensity in the chain methylene region. This decrease is caused by extensive splitting and the difference in chemical shifts for the non-equivalent methylene hydrogens in isotactic environments. This is in accord with the study of Stehling [282] on deuterated PP, which indicated that much of isotactic methylene absorption is buried beneath the methyl and tertiary hydrogen peaks. The fractional area in the nominal methylene region of the spectrum is thus sensitive to the number of isotactic and syndiotactic diads, and therefore may be used as a measure of PP and linear PE. The low-field absorption in **Figure 5.12(b)**, characteristic of aromatic hydrogens, is due to the polymer solvent, diphenyl ether, which was used throughout. Polymer
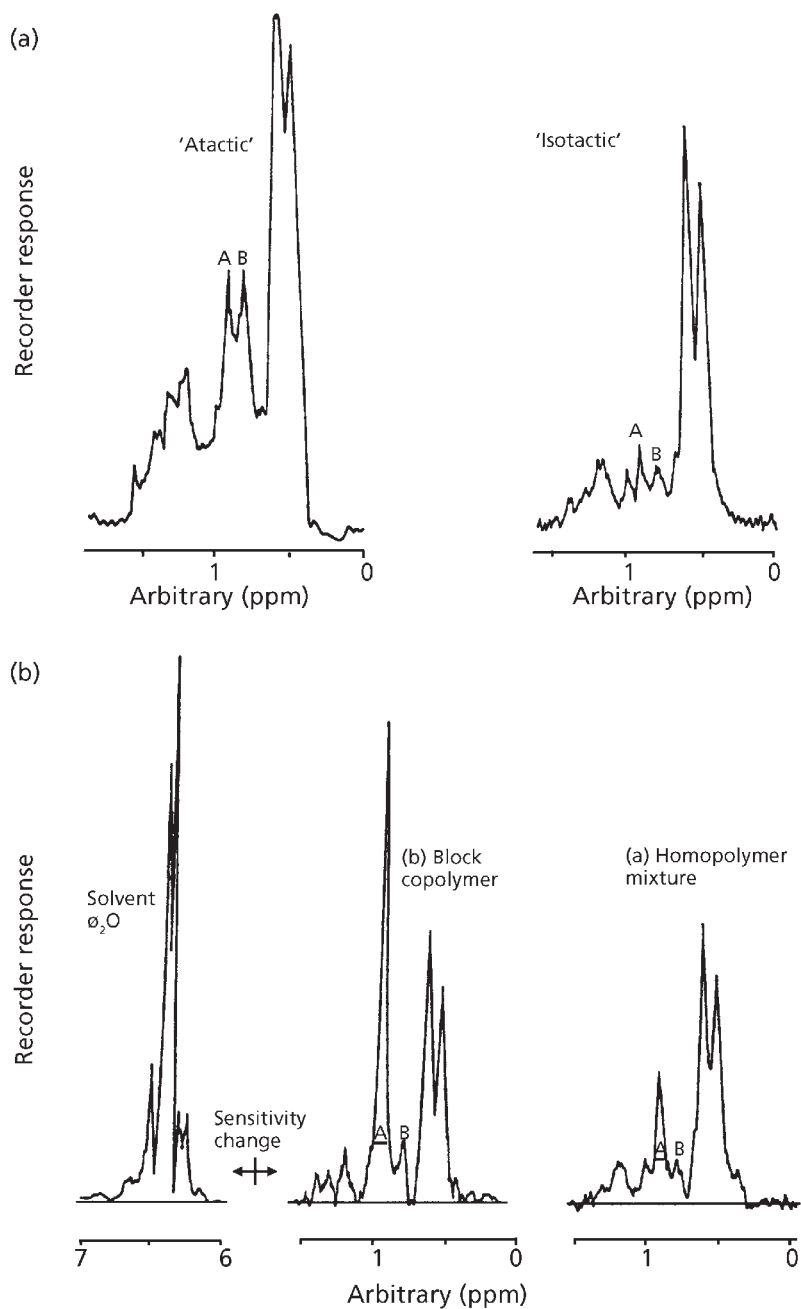
Figure 5.12 PMR spectra of (a) polypropylenes and (b) ethylene-propylene copolymers. (*Source: Author's own files*)

concentrations in solution can be readily calculated from the ratios of peak areas adjusted to the same sensitivity. The superpositions of spectra of the homopolymers, that were obtained separately, show the same pattern as spectra of physical mixtures but with different intensities. The PE absorption falls on the peak (marked A) of the chain methylene complex in PP. Peak B, also due to chain methylenes in PP, is resolved in both spectra in **Figure 5.12(b)**, which also gives the spectrum of an ethylene-propylene block copolymer. The ethylene contribution again falls on peak A.

Various workers have developed analyses for physical mixtures and block copolymers based on the ratio of the incremental methylene area to the total polymer proton absorption.

This concept has been tested by Barrall and co-workers [283, 284] using PMR analyses of a series of physical mixtures and block copolymers synthesised with ^{14}C-labelled propylene and others with ^{14}C-labelled ethylene. A most important feature of this analysis is that the methylene peaks A and B have virtually the same relative heights in PP with a variety of tacticities (note **Figure 5.12 (a)**). This is also true for PMR spectra given by Satoh and co-workers for atactic series of PP [285]. This suggests that PMR analyses for ethylene are independent of tacticity, since the area increment of peak A above peak B has been used for analysis.

Qualitative PP tacticities can be estimated by PMR not only for homopolymers (**Figure 5.12(a)**) but also in the presence of PE and ethylene copolymer blocks. The relative heights of the peaks for secondary and tertiary hydrogen in **Figure 5.12(b)** indicate that PP in the copolymer and the physical mixture is dominantly isotactic.

PMR spectroscopy has been applied to the characterisation of a wide range of homopolymers including PMMA [286-289], PVC [290–294], PS [293, 295, 296], polyvinyl ethers [297–300], polyacrylic acid [301], poly(methyl-α-chloroacrylate) [302], carboxy terminated polybutadiene [303], poly(α-methyl styrene) [304], natural rubber [305–307], chlorinated polyisobutylenes [308], sulfonated PS resins [309, 310], polyvinyl phenyl ether [311], lactone polyester [312], chlorinated PVC [313], PC [314], poly 1,3 butadiene [315], poly-2-allyl phenyl acrylate [316], poly(4-methyl-pentene-1) [317], polymethacrylic acid [318], PP [296], cyclic ethers [319], polymethacrylonitrile [320], poly(α-methyl styrene) tetramer [321], PEG [322], PE [289], polyacrylamide [311], polymethylacrylamide [323], polypyrrolidone [324], polychloroprene [325], phenol formaldehyde resins [326, 327], Nylon 66 [328], polyvinylidene fluoride [329], polyvinyl formate [330], polyacrylonitrile [331], epoxy resins [332], allyl biguanide [333], poly(2-isopropyl-2-oxazollines) [334] and trehalose vinyl benzyl ether [335].

5.8 Electron Spin Resonance Spectroscopy

This technique, in conjunction with gas chromatography and infrared spectroscopy, has been used in studies of degradation of LDPE [336] and in studies of the reaction of polybutylvinylether with elementary sulfur to produce polyacetylene and then polythienothiophene structures [337].

5.9 Infrared Spectra

Infrared spectra of thin films of polymers and copolymers in the region up to 2.5 μm are characteristic of the polymer [338]. Some infrared spectra are shown in **Figures 5.13 to 5.65**. Other information on infrared spectra of polymers and copolymers is shown in **Table 5.2**.
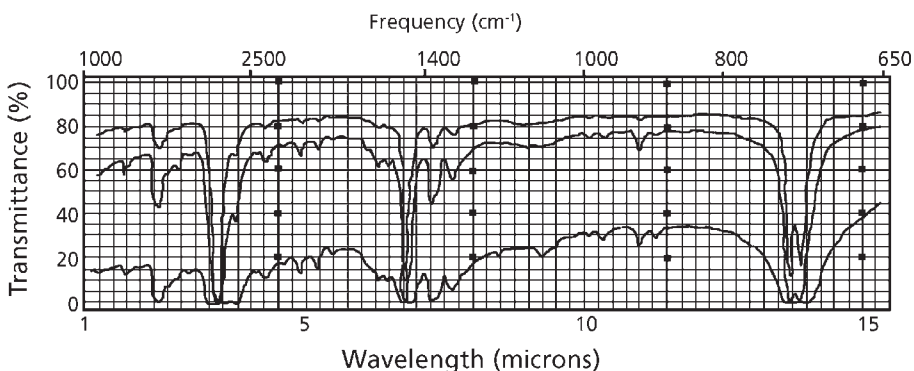
Figure 5.13 High-density polyethylene
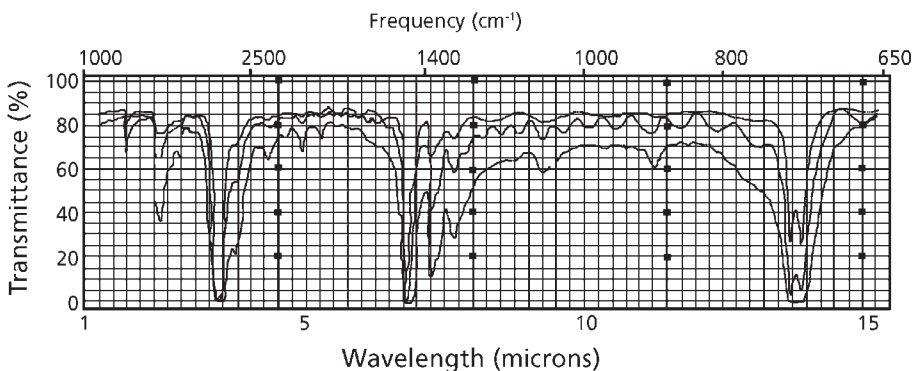
Figure 5.14 Low-density polyethylene
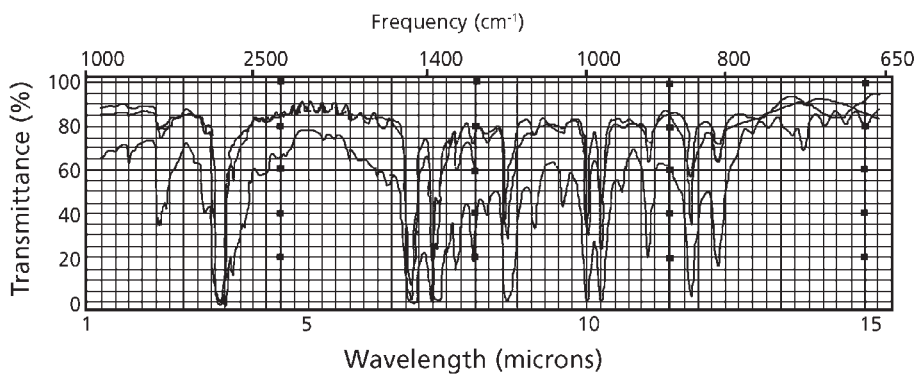
Figure 5.15 Polypropylene
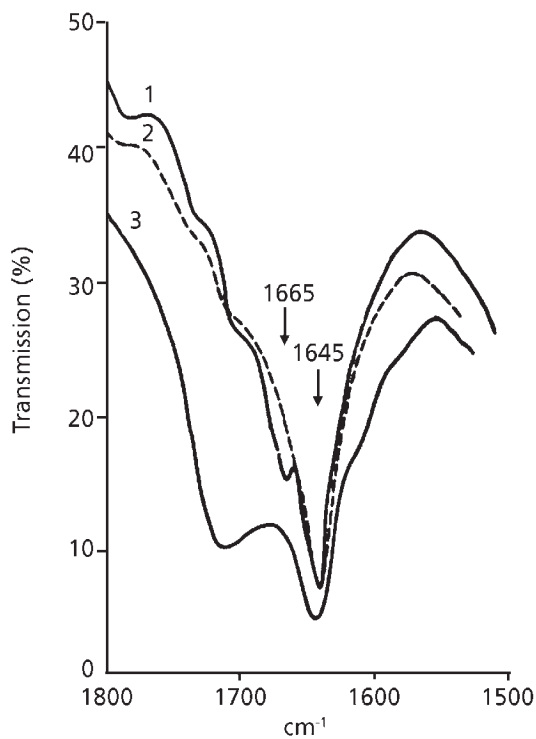
Figure 5.16 Amorphous polypropylene
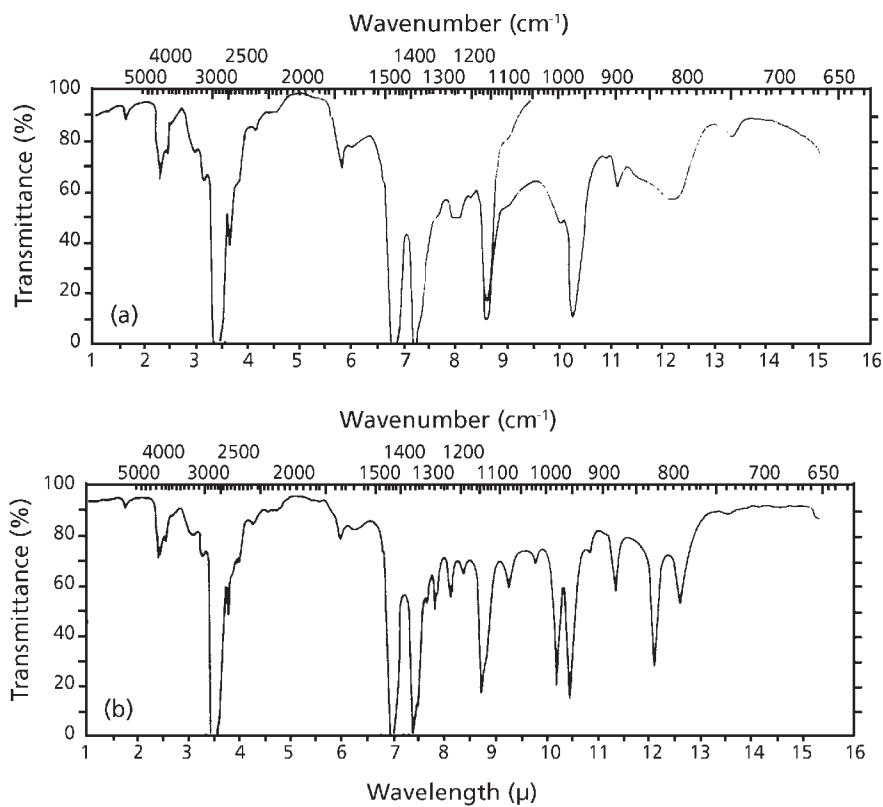
Figure 5.17 Polypropylene prepared with vanadyl based catalysts (a) amorphous; (b) crystalline part
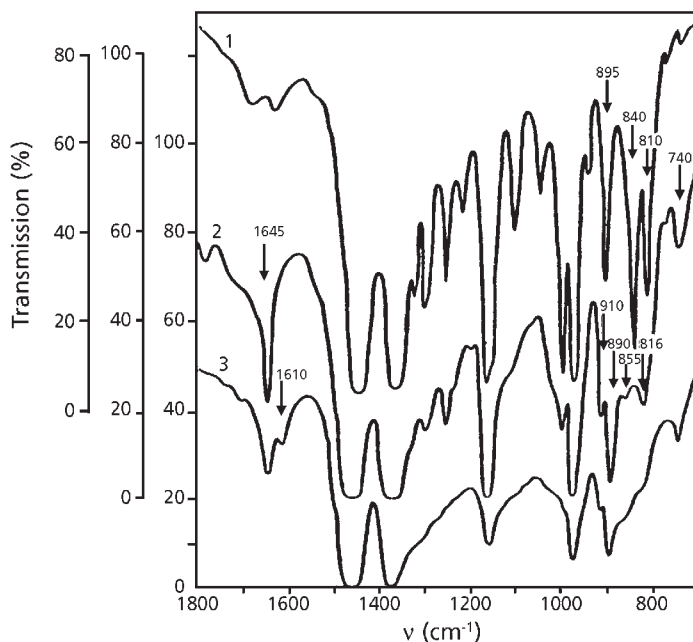
Figure 5.18 Isotactic polypropylene 1 – original; 2 – irradiated with fast electrons: 500 mRad
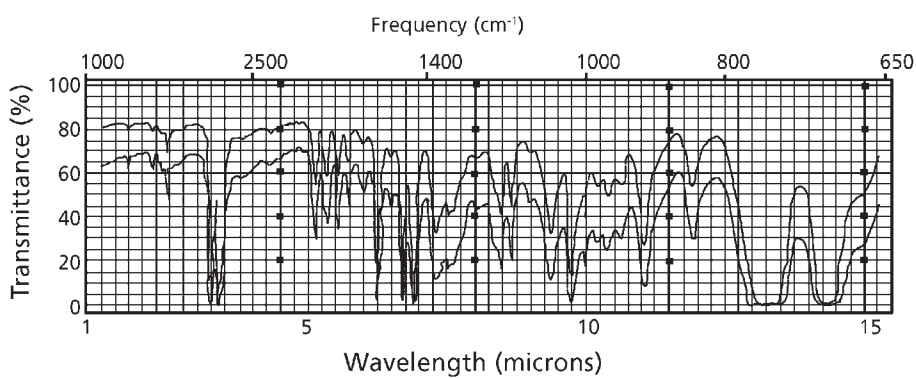
Figure 5.19 Polystyrene
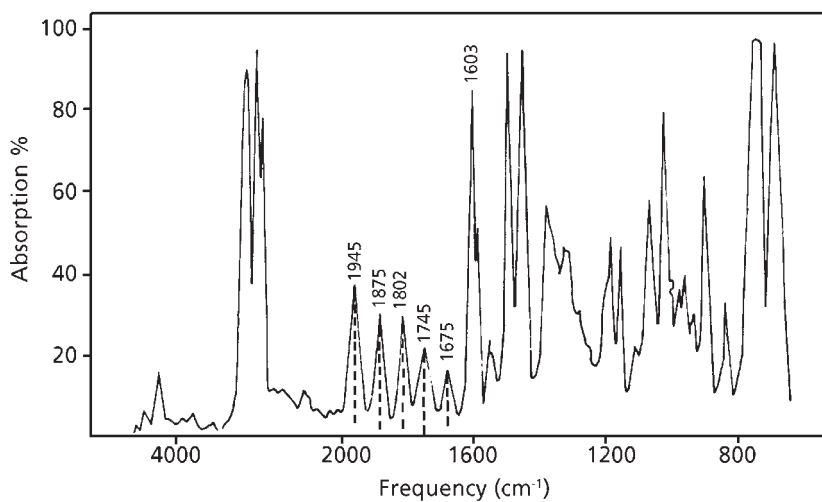
Figure 5.20 Polystyrene
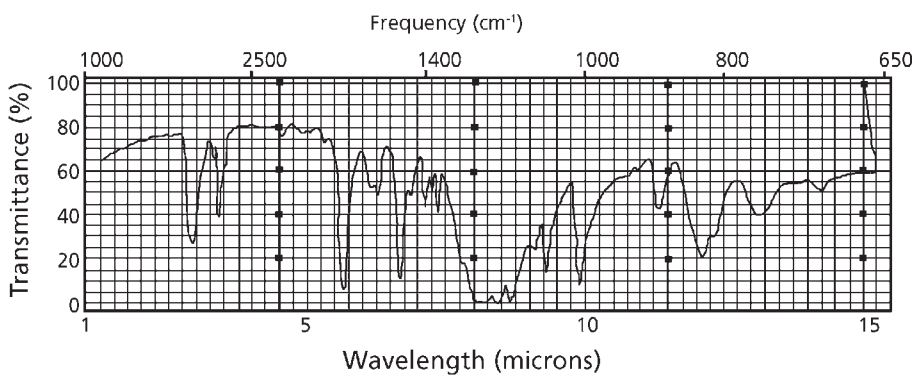
Figure 5.21 Polycarbonate (KBr disc)
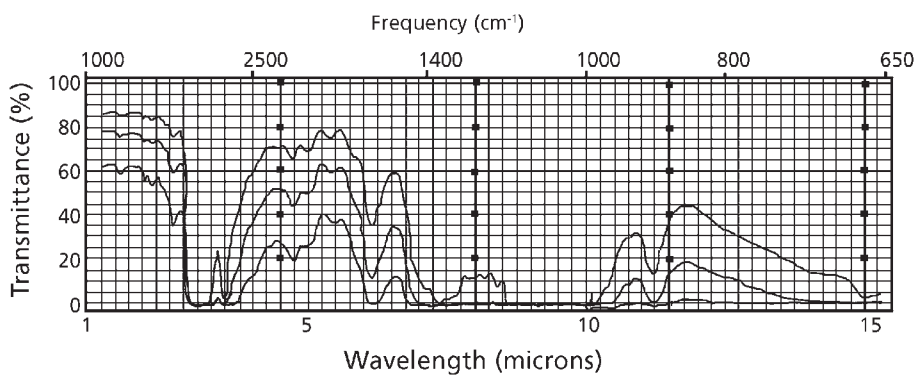
Figure 5.22 Cellophane
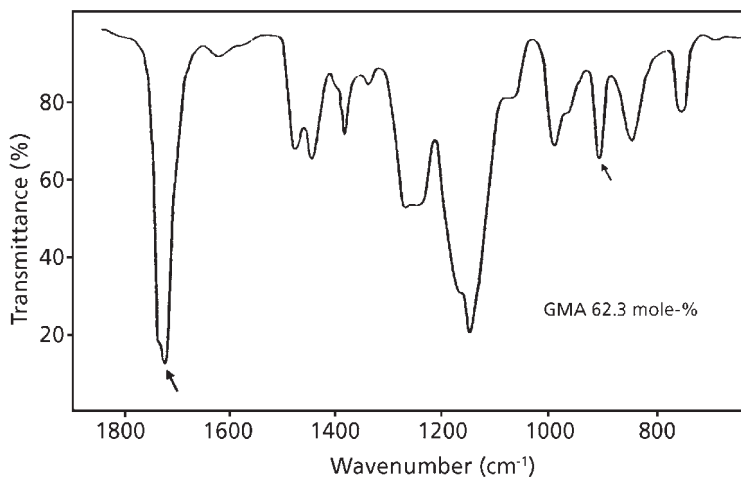
Figure 5.23 Methylmethacrylate-glycidyl methacrylate
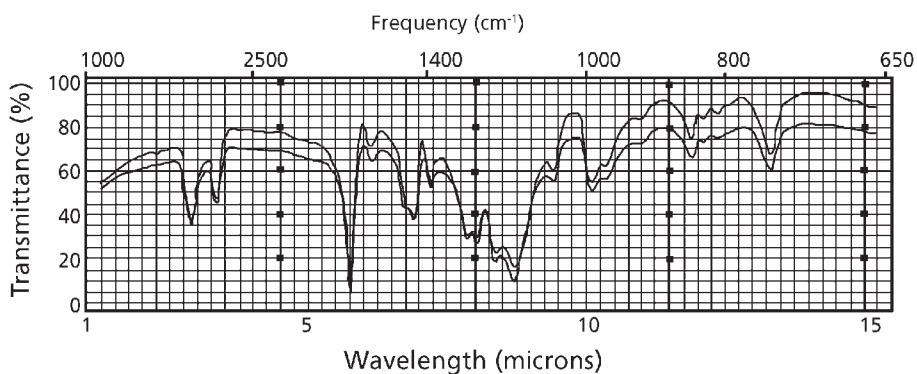
Figure 5.24 Polymethyl methacrylate
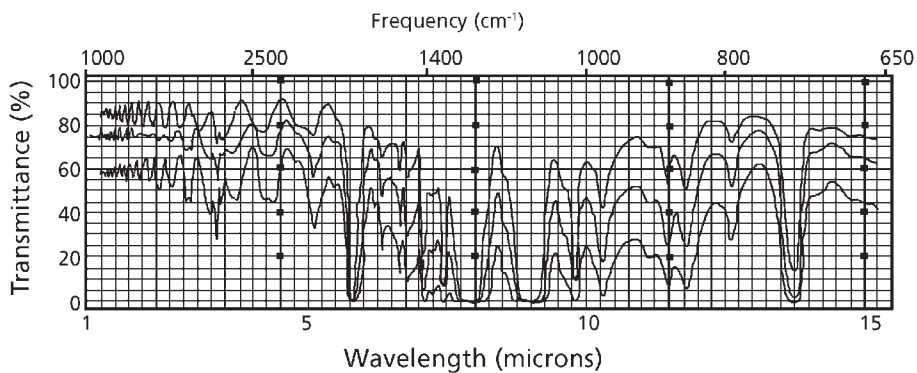
Figure 5.25 Polyethylene terephthalate
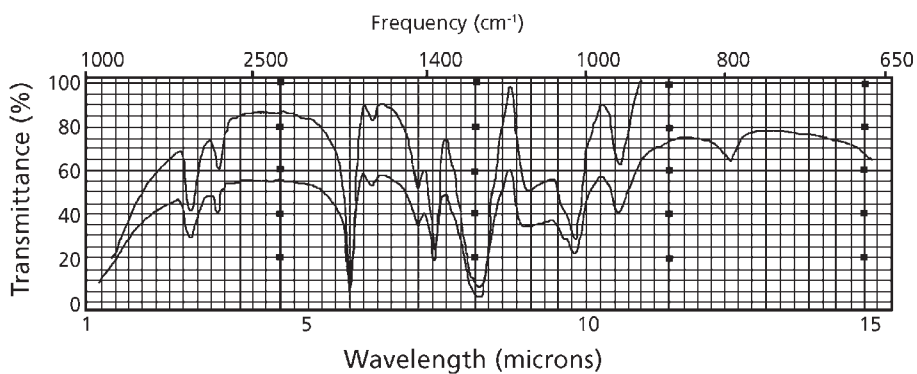
Figure 5.26 Polyvinyl acetate (KBr disc)
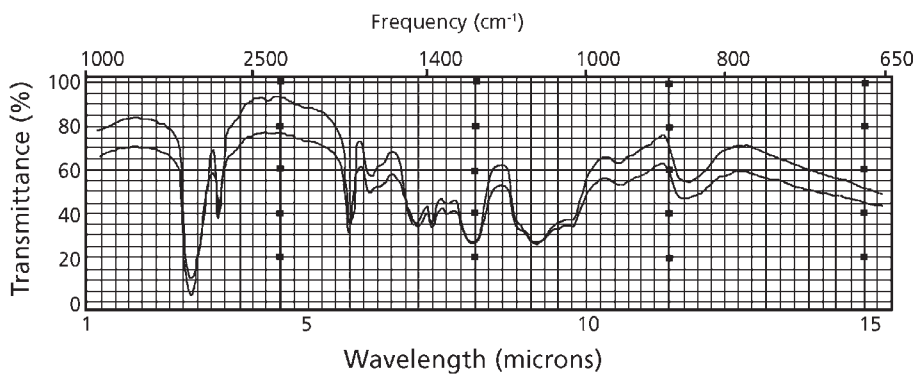
Figure 5.27 Polyvinyl alcohol (KBr disc)
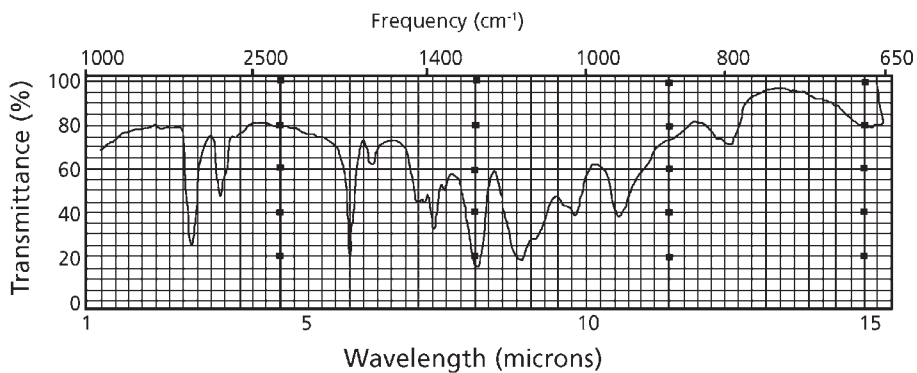
Figure 5.28 Polyvinyl acetate (KBr disc)
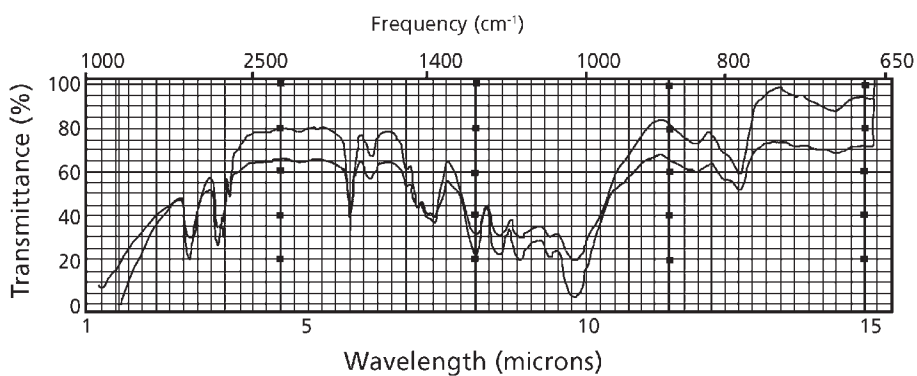
Figure 5.29 Polyvinyl formal (KBr disc)
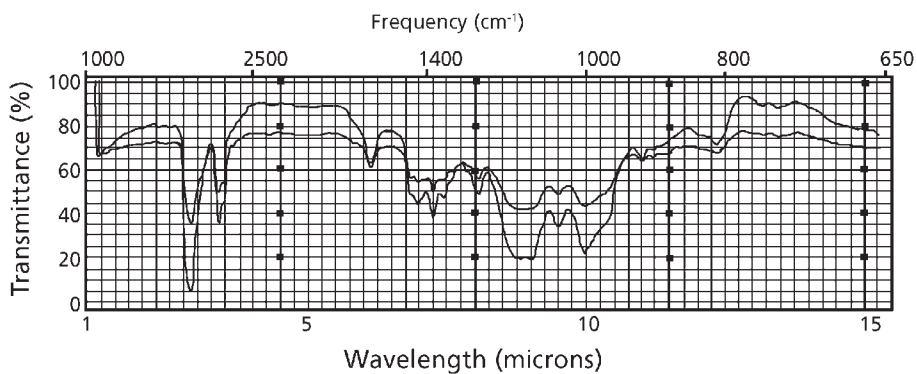
Figure 5.30 Polyvinyl butyrate (KBr disc)
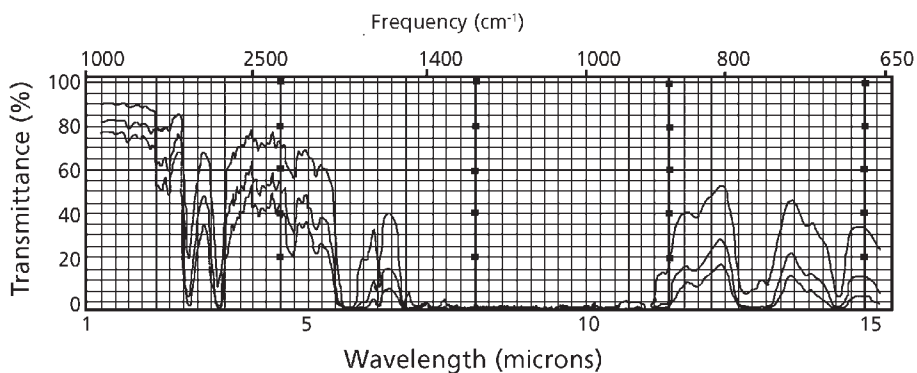
Figure 5.31 Cellulose acetate (0.06, 0.12, 0.18 cm film)
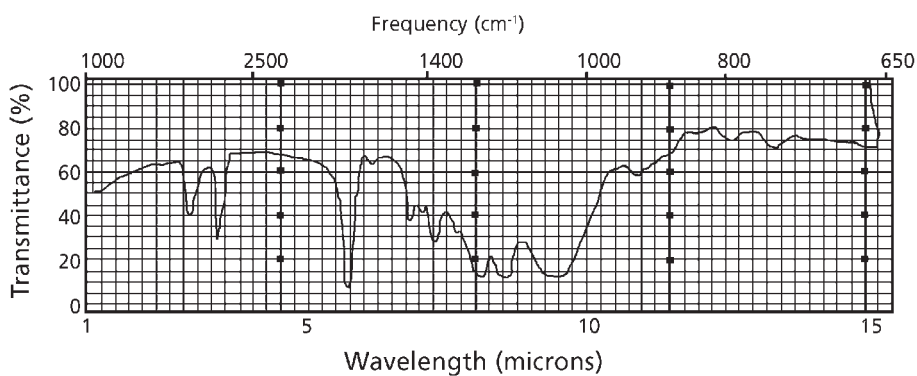
Figure 5.32 Cellulose acetate (KBr disc)
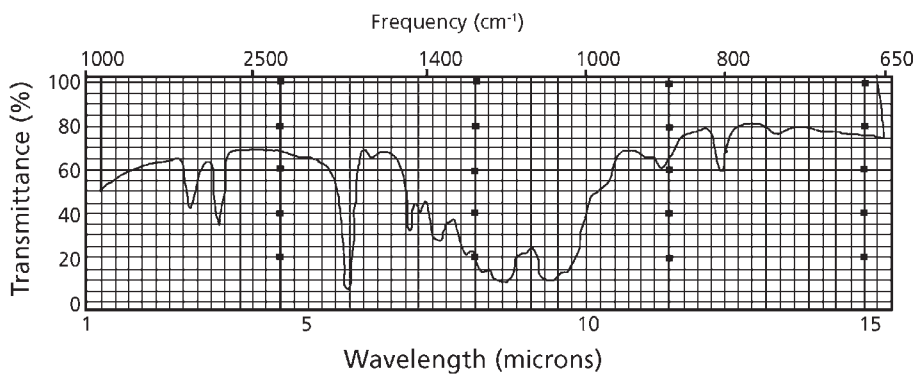
Figure 5.33 Cellulose propionate (KBr disc)
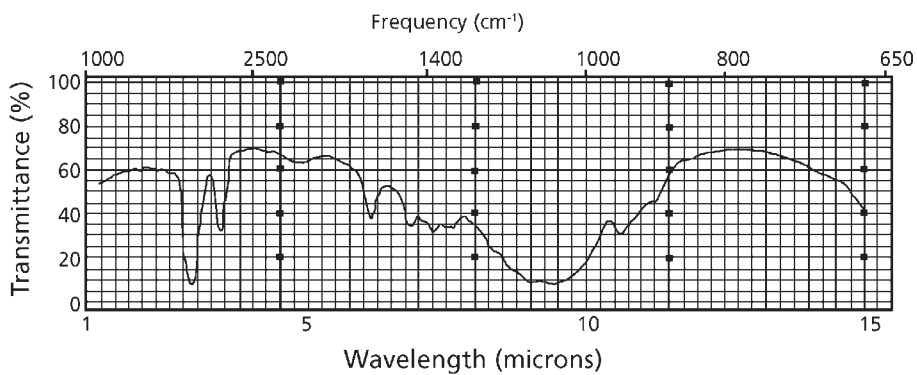
Figure 5.34 Methyl cellulose (KBr disc)
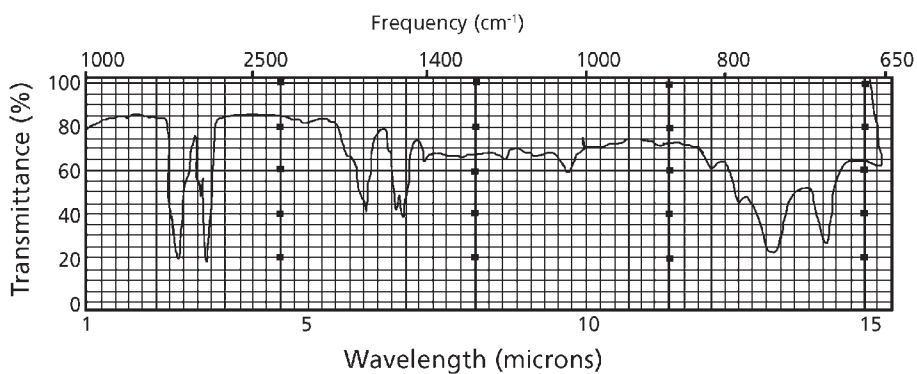
Figure 5.35 Coumarone–indene resin (KBr)
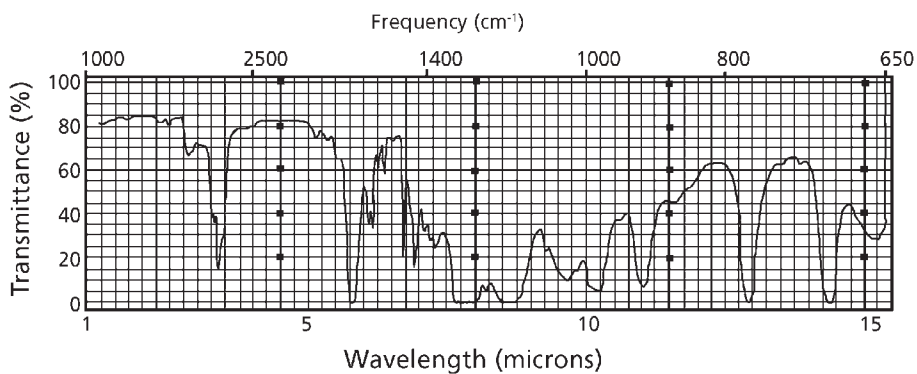
Figure 5.36 Polyester resin, capillary film between NaCl plates
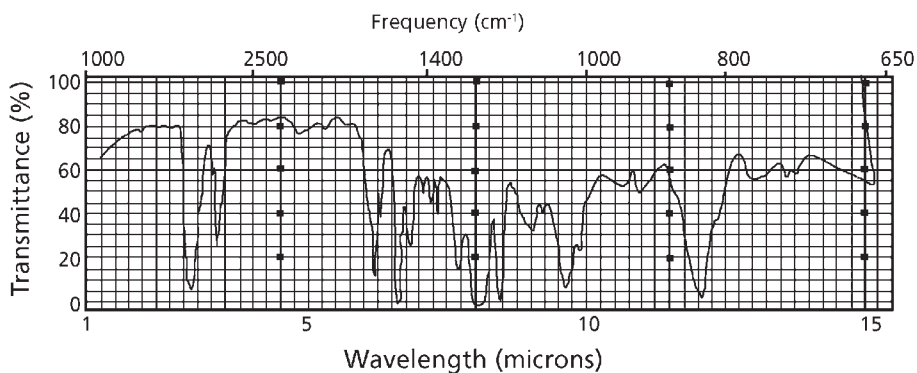
Figure 5.37 Epoxy resin (KBr disc)
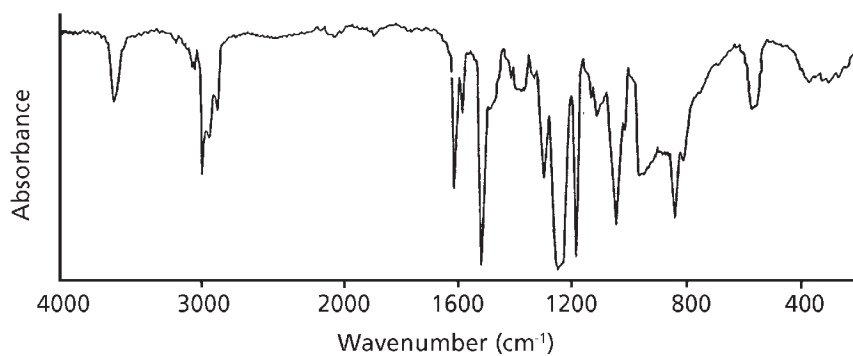
Figure 5.38 Epoxy resin, chloroform solution
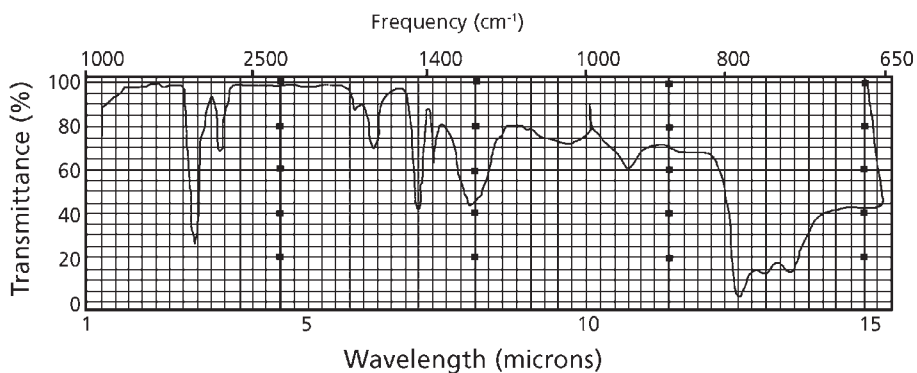
Figure 5.39 Chlorinated polypropylene (KBr disc)
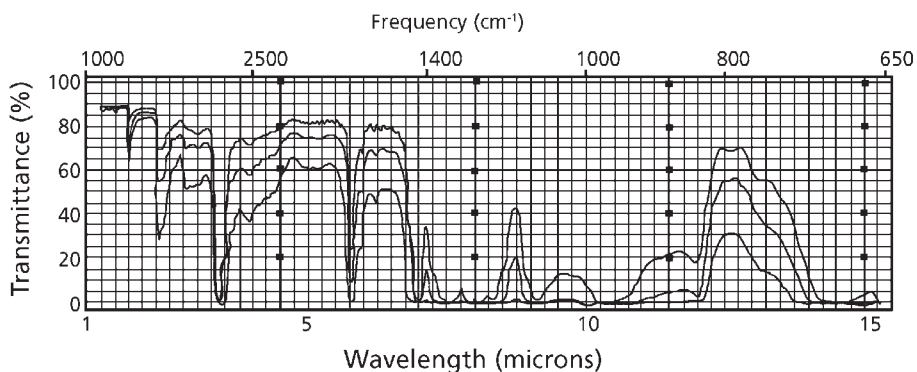
Figure 5.40 Rigid PVC (0.4 mm film)
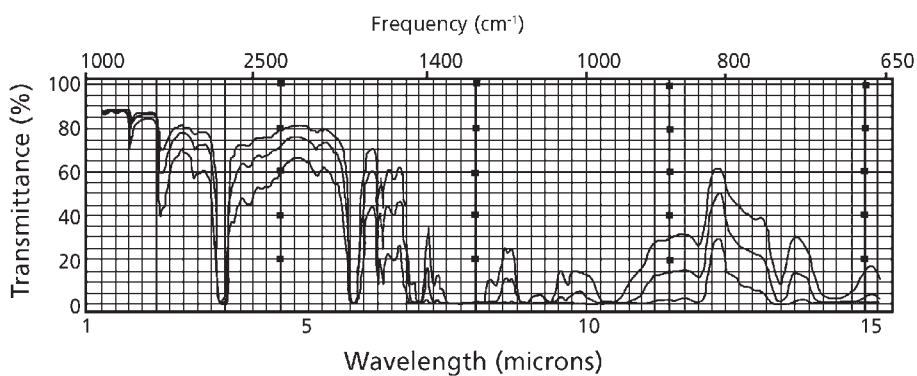
Figure 5.41 Plasticised PVC (0.3 mm film)
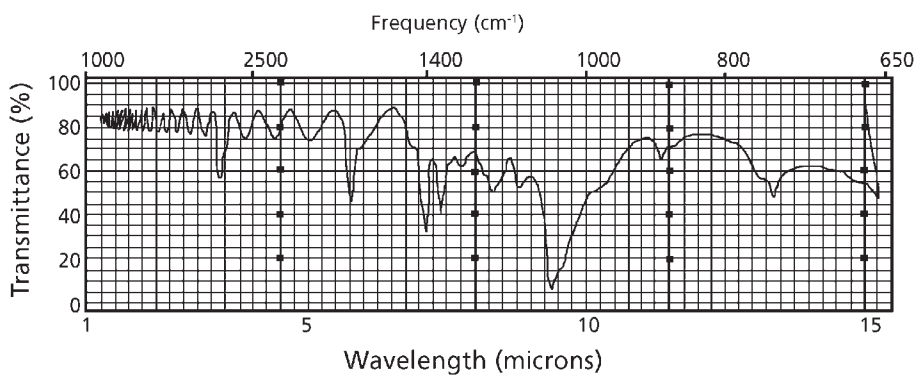
Figure 5.42 Polyvinylidene chloride (1.2 μm film)
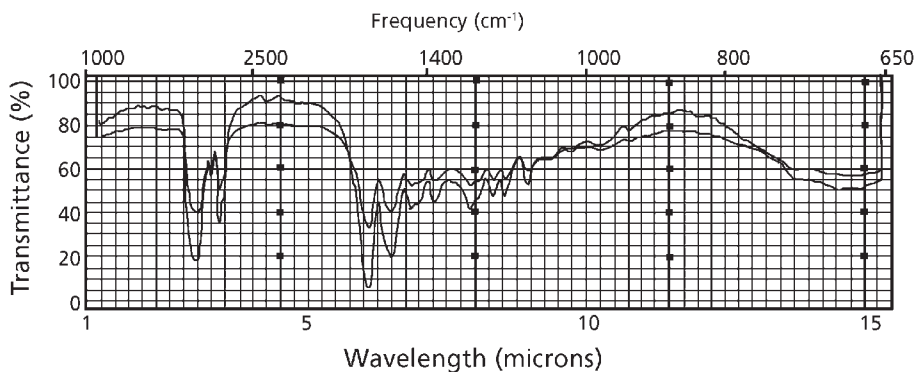
Figure 5.43 Nylon (KBr disc)
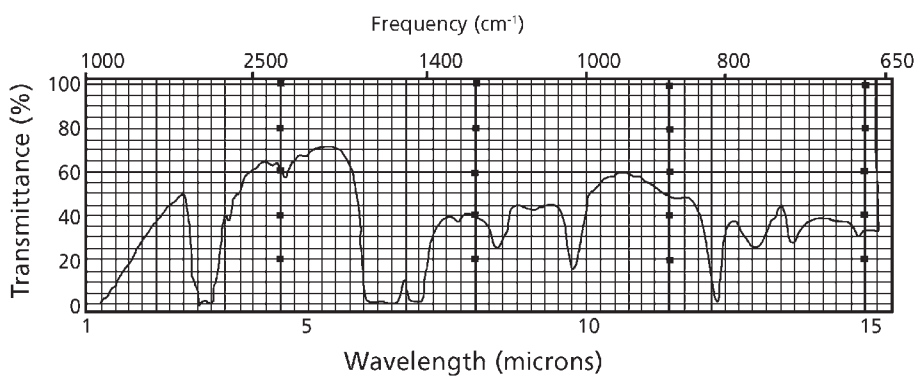
Figure 5.44 Melamine resin (KBr disc)
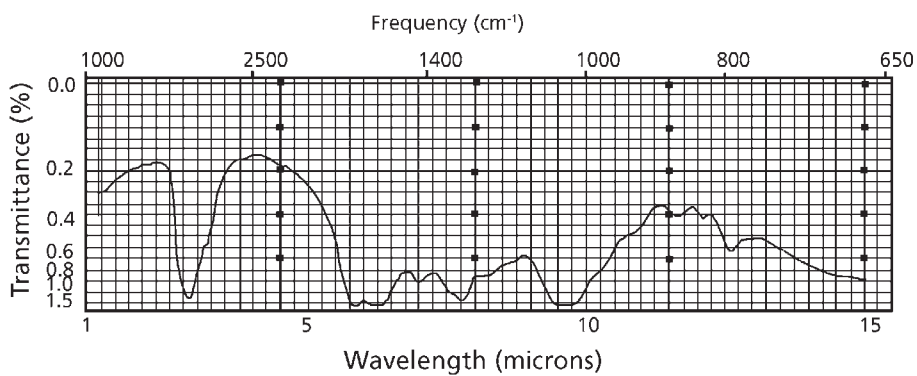
Figure 5.45 Urea-formaldehyde resin (KBr disc)
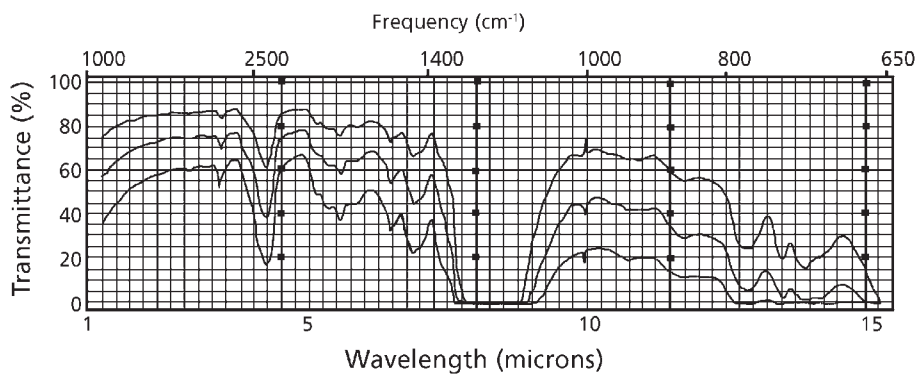
Figure 5.46 Polytetrafluoroethylene (0.055, 0.11, 0.22 mm film)
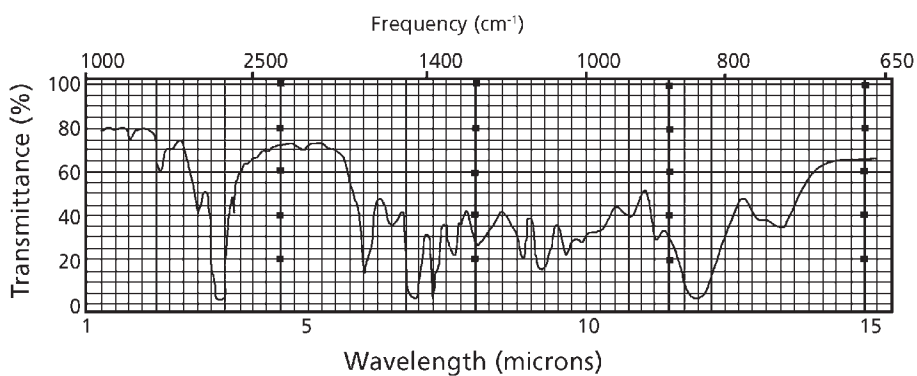
Figure 5.47 Natural rubber (KBr disc)
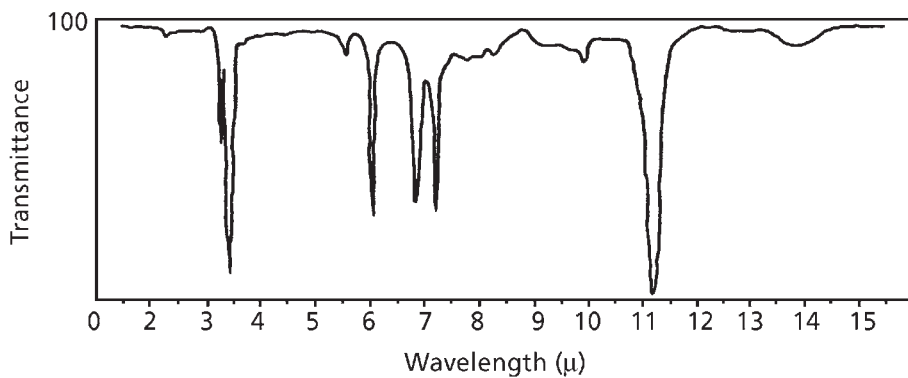
Figure 5.48 Poly 2,4-isoprene (KBr disc)
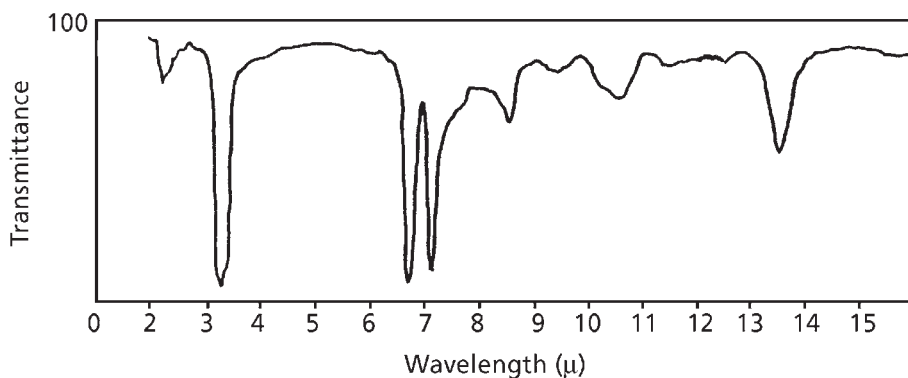
Figure 5.49 Halogenated polyisoprene (KBr disc)
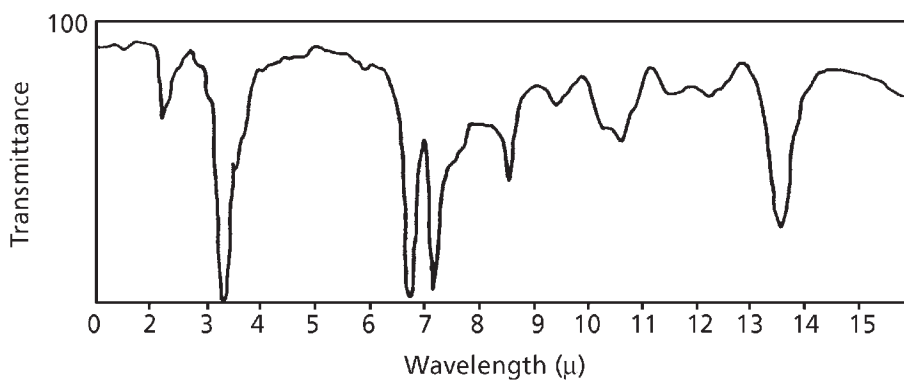
Figure 5.50 Hydrogenated natural rubber (KBr disc)
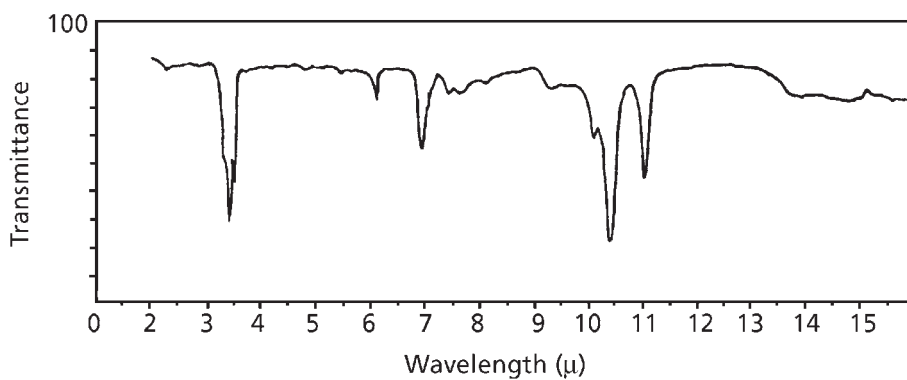
Figure 5.51 Emulsion polybutadiene (KBr disc)
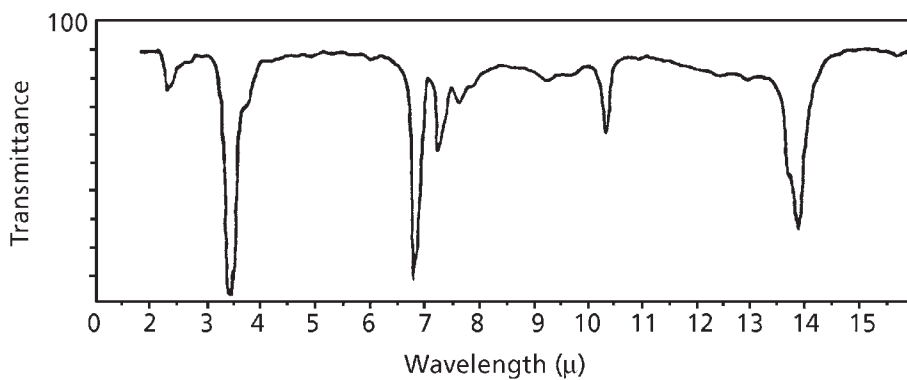
Figure 5.52 Halogenated emulsion polybutadiene (KBr disc)
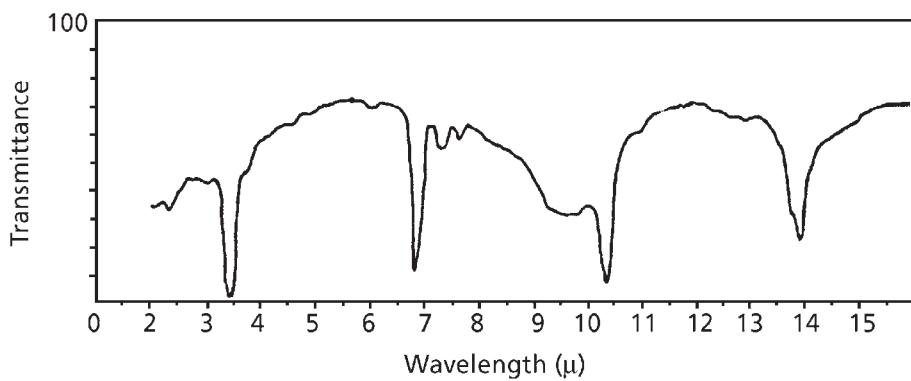
Figure 5.53 Hydrogenated lithium polybutadiene (KBr disc)
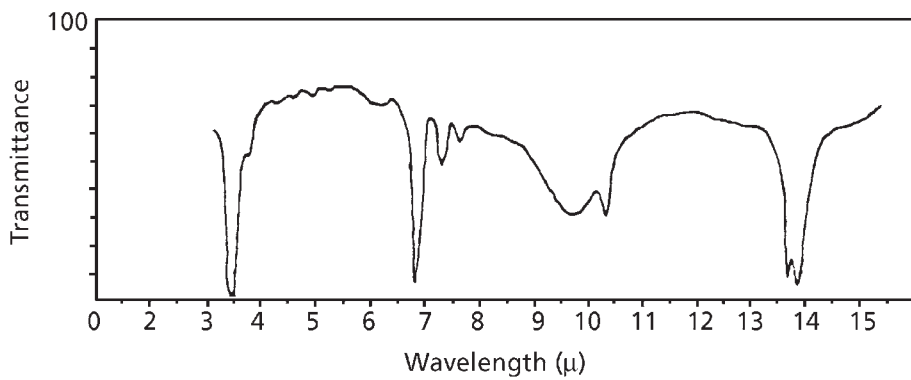
Figure 5.54 Hydrogenated Ziegler polybutadiene (KBr disc)
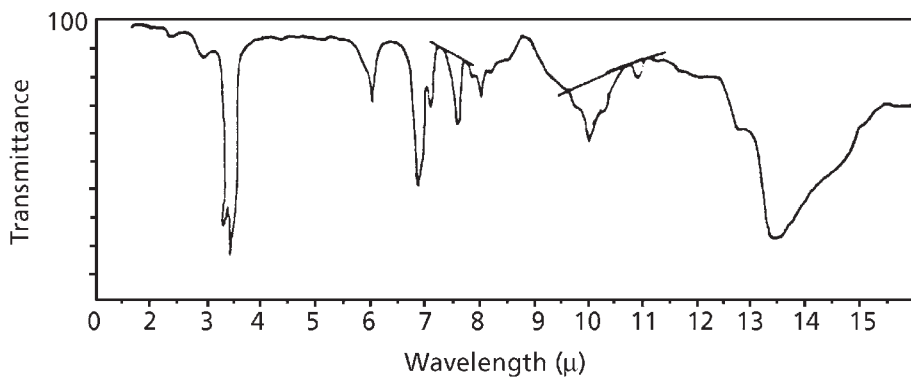
Figure 5.55 *Cis* 1,4 polybutadiene (KBr)
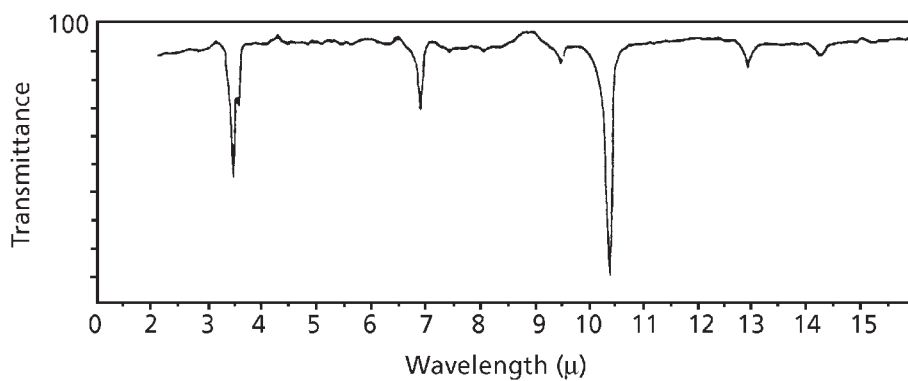
Figure 5.56 *Trans* 1,4-polybutadiene (KBr disc)
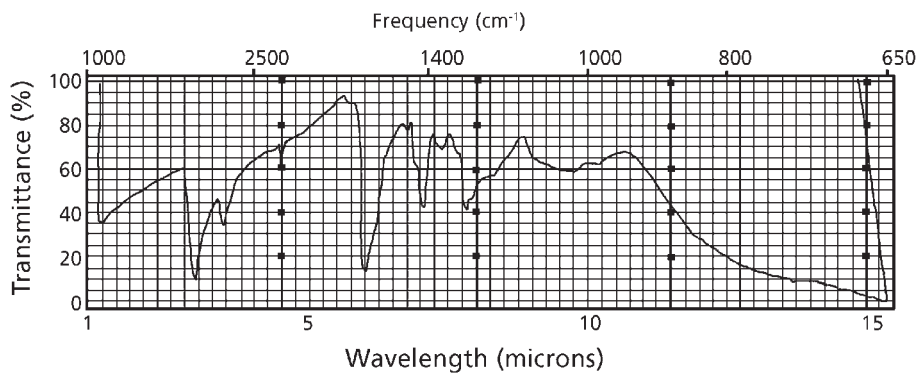
Figure 5.57 Polyacrylamide (KBr disc)
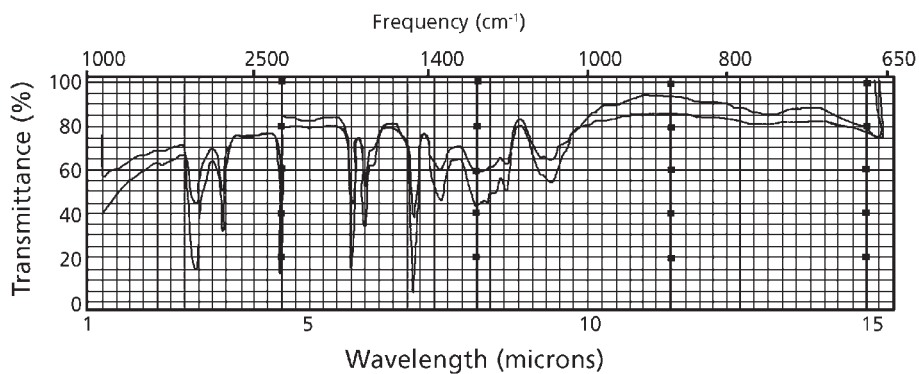
Figure 5.58 Polyacrylonitrile (KBr disc)
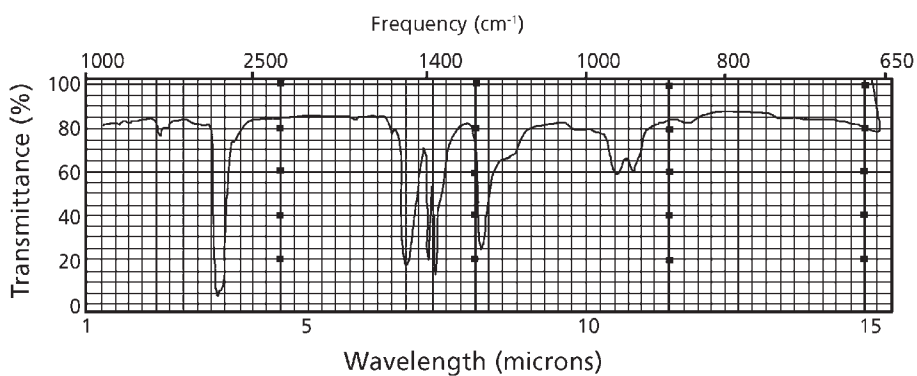
Figure 5.59 Butyl rubber (KBr disc)
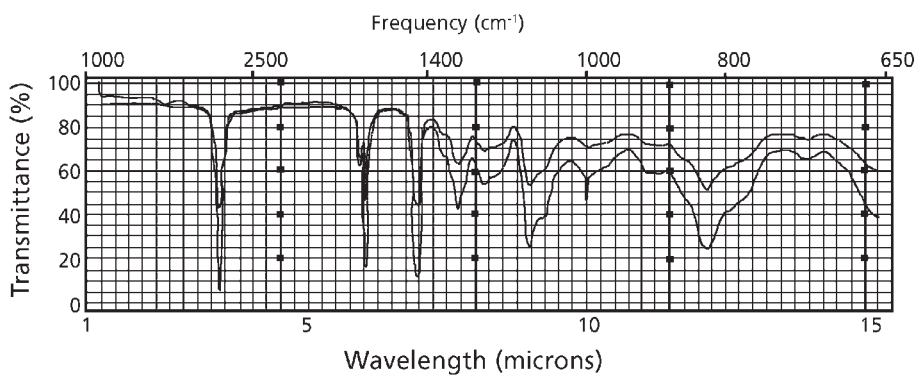
Figure 5.60 Neoprene (NaCl disc)
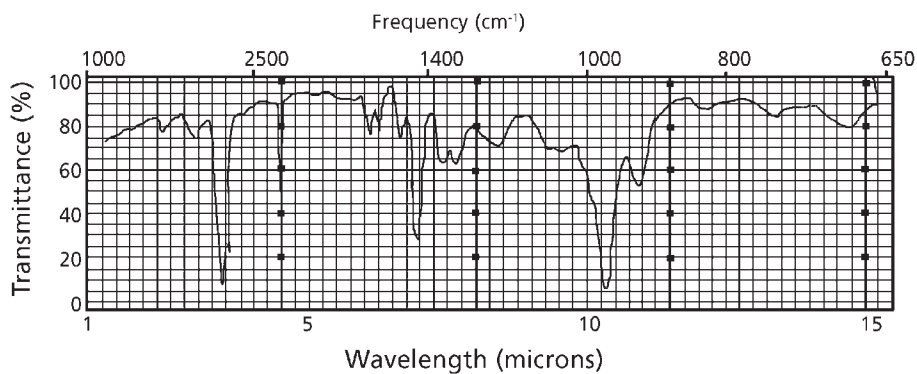
Figure 5.61 Nitrile nubber (NaCl disc)
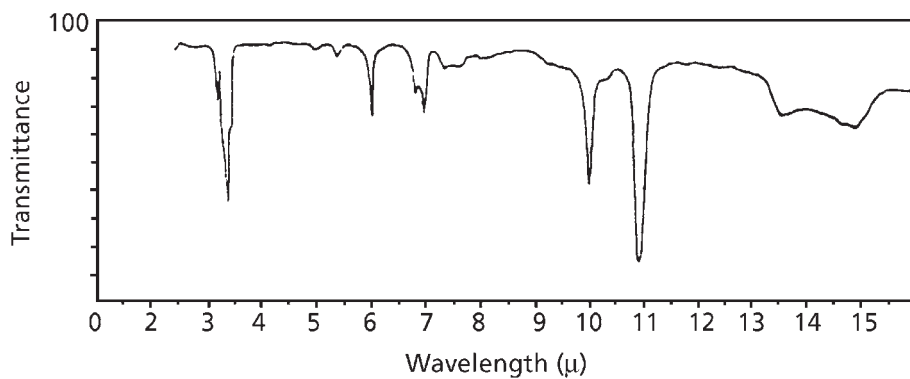
Figure 5.62 Polybutadiene (KBr disc)
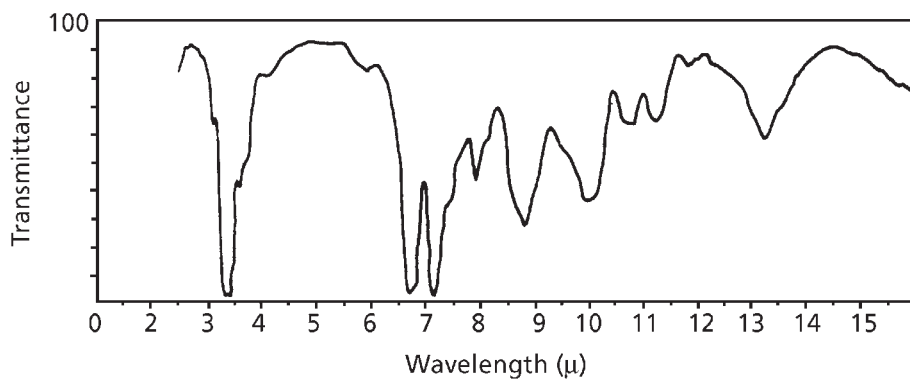
Figure 5.63 Hydrogenated polydimethyl butadiene (KBr disc)
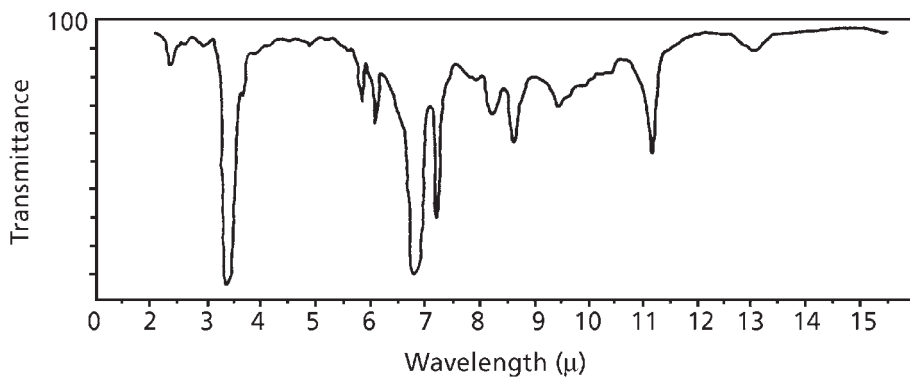
Figure 5.64 Polymethylbutadiene (KBr discs)
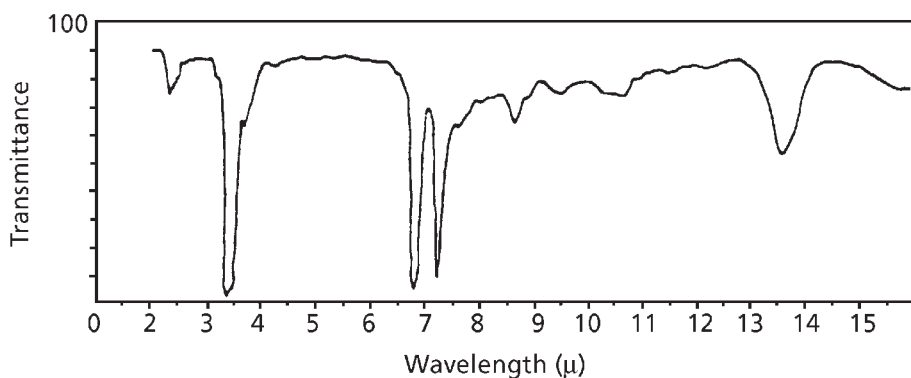
Figure 5.65 Hydrogenated polypiperylene (KBr disc)

References

1.   M. Razinger, M. Penca and J. Zupan, *Analytical Chemistry*, 1981, **53**, 7, 1107.

2.   R. Alexander, *The Analytical Report,* No.7, Perkin Elmer Ltd, Beaconsfield, UK, 1985.

3.   *Perkin Elmer Application & News Bulletin,* 1963, **1**, 1–8.

4.   M. Bowden, P. Donaldson, D.J. Gardiner, J. Birnie and D.L. Gerrard, *Analytical Chemistry*, 1991, **63**, 24, 2915.

5.   R. Osland, *Laboratory Practice,* 1971, **37**, 73.

6.   J. Dechant, *Ultraspektroskopische Untersuchungen an Polymern,* Akadamie Verlag, Berlin, Germany, 1972, p.516.

7.   Z. Hippe and A. Kerste, *Bulletin de I' Academie Polanaise des Sciences: Serie des Sciences Chimiques,* 1973, **21**, 395.

8.   G. Leukoth, *Gummi Asbest Kunststoffe,* 1974, **27**, 91, 794.

9.   C.L. Hammond, P.J. Hendra, B.G. Lator, W.F. Maddams and H.A. Willis, *Polymer*, 1988, **29**, 1, 49.

10.   A. Peterlin, *Journal of Polymer Science Part A-1: Polymer Chemistry Edition*, 1969, **7**, 4, 1151.

11.   A. Peterlin, *Polymer Engineering and Science*, 1969, **9**, 3, 172.

12.   L.J. Bellamy, *The Infrared Spectra of Complex Molecules*, Wiley, London, UK, 1954.

13.   F.M. Rugg, J.J. Smith and R.C. Bacon, *Journal of Polymer Science*, 1954, **13**, 72, 535.

14.   J.V. Benham and T.J. Pullukat, *Journal of Applied Polymer Science*, 1976, **20**, 12, 3295.

15.   Z.S. Fodor, M. Iring, F. Tudos and T.J. Kelen, *Journal of Polymer Science: Polymer Chemistry Edition*, 1984, **22**, 10, 2539.

16.   S.M. Gabbay and S.S. Stivala, *Polymer*, 1976, **17**, 2, 121.

17.   B.M. Quernum, P. Berticat and G. Vallet, *Polymer Journal*, 1975, **7**, 3, 277.

18.   G. Stanescu, *Revista de Chemie, Bucharest*, 1963, **64**, 42.

19.   H.J. Sloane, T. Johns, W.F. Ulrich and W.J. Cadman, *Applied Spectroscopy*, 1965, **19**, 4, 130.

20.   T. Yoshino and M. Shinomiya, *Journal of Polymer Science, Part A: Polymer Chemistry*, 1965, **3**, 8, 2811.

21.   B. Govindaraj, N.V. Sastry and A. Venkataraman, *Journal of Applied Polymer Science*, 2004, **93**, 2, 778.

22.   N. Hongbo, S. Huafeng, H. Baochen, Y. Wei and Z. Xifieng, *China Synthetic Rubber Industry*, 2004, **27**, 1, 21.

23.   C-S. Tan, C-C. Juan and T-W. Kuo, *Polymer*, 2004, **45**, 6, 1805.

24.   A. Padermshoke, Y. Katsumoto, H. Sato, S. Ekgasit, I. Noda and Y. Ozaki, *Polymer*, 2004, **45**, 19, 6547.

25.   C. Liu and C. Xiao, *Journal of Applied Polymer Science*, 2004, **92**, 1, 559.

26.   P. Mastrorilli, C.F. Nobile, R. Grisorio, A. Rizzuti, G.P. Suranna, D. Acierno, E. Amendola and P. Iannelli, *Macromolecules*, 2004, **37**, 12, 4488.

27.   B.O. Lazdina, U.K. Stirna, V.V. Tuprueina, I.V. Sevastyanova and A.V. Dzene, *Journal of Polymer Science, Part A: Polymer Chemistry*, 2004, **46**, 4, 411.

28. J.L. Koenig, *Analytical Chemistry*, 1987, **59**, 19, 1141.

29. Y-Z. Xiao, F-A. He, Q-X. Zhang and H.H. Wang, *Polymer Materials Science and Engineering*, 2004, **20**, 5, 69.

30. G. Kostov, Z. Bakalova and M. Mihailova, *European Polymer Journal*, 1987, **23**, 10, 753.

31. D.D.C. Bradley, G.P. Evans and R.H. Friend, *Synthetic Metals*, 1987, **17**, 1–3, 651.

32. G.S. Irwan, Y. Aoyama, S. Kuroda, H. Kubota and T. Kondo, *European Polymer Journal*, 2004, **40**, 1, 171.

33. Z. Guo, H. Feng, H.C. Ma, Q.X. Kang and Z.W. Yang, *Polymers for Advanced Technologies*, 2004, **15**, 1–2, 100.

34. J.T. Beechinor, E. McGlynn, M. O'Reilly and G.M Crean, *Microelectronic Engineering*, 1997, **33**, 1–4, 363.

35. R.C. Wiebolt, G.E. Adams, D.W. Later and R. Rosenthal, *Journal American Laboratory*, 1988, **20**, 121.

36. A.E. Tonelli and T.N. Bowmer, *Journal of Polymer Science, Part B: Polymer Physics Edition*, 1987, **25**, 5, 1153.

37. T.V. Monakhova, P.M. Nedorezova, V.I. Tsvetkova and Y.A. Shlyapnikov, *Journal of Polymer Science, Part B: Polymer Physics Edition*, 2004, **46**, 3–4, 113.

38. C.E. Miller, *Applied Spectroscopy*, 1993, **47**, 2, 222.

39. A. Valadez-González and L. Veleva, *Polymer Degradation and Stability*, 2004, **83**, 1, 139.

40. J.A.J. Jansen and W.E. Haas, *Analytica Chimica Acta*, 1987, **196**, 69.

41. I. Noda, A.E. Dowrey and C. Marcott, *Journal of Polymer Science, Polymer Letters Edition*, 1983, **21**, 2, 99.

42. I. Noda, A.E. Dowrey and C. Marcott, *Applied Spectroscopy*, 1988, **42**, 2, 203.

43. T. Nakano, S. Shimada, R. Saitoh and *I. Noda, Applied Spectroscopy*, 1993, **47**, 9, 1337.

44. B.O. Budevska, C.J. Manning, P.R. Griffiths and R.T. Roginski, *Applied Spectroscopy*, 1993, **47**, 11, 1843.

45. V.G. Gregoriou, I. Noda, A.E. Dowrey, C. Marcott, J.L. Chao and R.A. Palmer, *Journal of Polymer Science, Part B: Polymer Physics Edition*, 1993, **31**, 12, 1769.

46. H. Wang, D.K. Graff, J.R. Schoonover and R.A. Palmer, *Applied Spectroscopy*, 1999, **53**, 6, 687.

47. M. Sonoyama, K. Shoda, G. Katagiri and H. Ishida, *Applied Spectroscopy*, 1996, **50**, 3, 377.

48. M. Sonoyama, K. Shoda, G. Katagiri and H. Ishida, Applied *Spectroscopy*, 1997, **51**, 3, 346.

49. D.K. Graff, H. Wang, R.A. Palmer and J.R. Schoonover, *Macromolecules*, 1999, **32**, 21, 7147.

50. C. Marcott, A.E. Dowrey and I. Noda, *Analytical Chemistry*, 1994, **66**, 10, 1654.

51. L. Bokobza, T. Buffeteau and B. Desbat, *Applied Spectroscopy*, 2000, **54**, 3, 360.

52. N.J. Everall, *Applied Spectroscopy*, 1998, **52**, 12, 1498.

53. F.M. Mirabella and N.J. Harrick, *Internal Reflection Spectroscopy: Review and Supplement*, Harrick Scientific Corporation, New York, NY, USA, 1985.

54. N.J. Everall and A. Bibby, *Applied Spectroscopy*, 1997, **51**, 8, 1083.

55. J.P. Hobbs, C.S.P. Sung, K. Krishnan and S. Hill, *Macromolecules*, 1983, **16**, 2, 193.

56. S. Ekgasit and A. Padermshoke, *Applied Spectroscopy*, 2001, **55**, 10, 1352.

57. Y. Nishikawa, T. Nakano, H. Miyauchi, K. Nishikida and E.Y. Jiang, *Applied Spectroscopy*, 2004, **58**, 8, 958.

58. S.V. Dubiel, G.W. Griffith, C.L. Long, G.K. Baker and R.E. Smith, *Analytical Chemistry*, 1983, **55**, 9, 1533.

59. S.C. Paltcini, T.J. Porro, *Identification of Polymer Laminates using the Diamond Cell Technique*, *Perkin Elmer Infrared Bulletin*, No. IR P121, Perkin Elmer, Boston, MA, USA.

60. P. Garside and P. Wyeth, *Polymer Preprints*, 2000, **41**, 2, 1792.

61. W.K. Way and G. Gloeckner in *Proceedings of Antec 2002*, San Francisco, CA, USA, 2002, Paper 579.

62. P. Weiss, S. Bohic, M. Lapkowski and G. Daculsi, *Journal of Biomedical Materials Research, Part A*, 1998, **41**, 1, 167.

63. C. Alkan, L. Aras and G. Gunduz, *E-Polymers*, 2004, No. 070.

64. M. Schnell, J. Borrajo, R.J.J. Williams and B.A. Wolf, *Macromolecular Materials and Engineering*, 2004, **289**, 7, 642.

65. N. Wang, L. Zhang and Y. Lu, *Industrial and Engineering Chemistry Research*, 2004, **43**, 13, 3336.

66. Y. Chen, Y. Liu, Q. Wang, H. Yin, N. Aelmans and R. Kierkels, *Polymer Degradation and Stability*, 2003, **81**, 2, 215.

67. J. Stejskal, D. Hlavatá, P. Holler, M. Trchová, J. Prokeš and I. Sapurina, *Polymer International*, 2004, **53**, 3, 294.

68. N. Plesu, A. Kellenberger, N. Vaszilcsin and I. Manoviciu, *Molecular Crystals and Liquid Crystals*, 2004, **416**, 1, 127.

69. M. Catauro, M.G. Raucci, F. de Gaetano, A. Buri, A. Marotta and L. Ambrosio, *Journal of Materials Science in Medicine*, 2004, **15**, 9, 991.

70. F. Carrillo, X. Colom, J.J. Suñol and J. Saurina, *European Polymer Journal*, 2004, **40**, 9, 2229.

71. J.W. Downing Jr and J.A. Newell, *Journal of Applied Polymer Science*, 2004, **91**, 5, 417.

72. M.M. Nasef and H. Saidi, *International Journal of Polymeric Materials*, 2004, **53**, 12, 1027.

73. W. Ma, J. Yu and J. He, *Macromolecules*, 2004, **37**, 18, 6912.

74. Q-J. He, A-M. Zhang and L-H. Guo, *Polymer-Plastics Technology and Engineering*, 2004, **43**, 3, 951.

75. A.H. Yuwono, B. Liu, J. Xue, J. Wang, H.I. Elim, W. Ji, Y. Li and T.J. White, *Journal of Materials Chemistry*, 2004, **14**, 20, 2978.

76. X. Feng and H. Shi-Huai, *Polymeric Materials Science and Engineering*, 2004, **20**, 4, 214.

77. P. Vermette, G.B. Wang, J.P. Santerre, J. Thibault and G. Laroche, *Journal of Biomaterials Science: Polymer Edition*, 1999, **10**, 7, 729.

78. R.A. Prasath, S. Nanjundan, T. Pakula and M. Klapper, *European Polymer Journal*, 2004, **40**, 8, 1767.

79. S.M. Desai and R.P. Singh, *Advances in Polymer Science*, 2004, 169, 231.

80. S. Apone, R. Bongiovanni, M. Braglia, D. Scalia and A. Priola, *Polymer Testing*, 2003, **22**, 3, 275.

81. S-H. Hsiao and H-W. Chiang, *European Polymer Journal*, 2004, **40**, 8, 1691.

82. K. Debski and J. Magiera, *Journal of Polymer Engineering*, 2002, **22**, 2, 137.

83. A. Georgiades, I. Hamerton, J.N. Hay, H. Herman and S.J. Shaw, *Polymer International*, 2004, **53**, 7, 877.

84. C.O. M'Bareck, Q.T. Nguyen, M. Metayer, J.M. Saiter and M.R. Garda, *Polymer*, 2004, **45**, 12, 4181.

85. S. Moulay and R. Mehdaoui, *Reactive and Functional Polymers*, 2004, **61**, 2, 265.

86. A.R. Tripathy, P.K. Patra, J.K. Sinha and M.S. Banerji, *Journal of Applied Polymer Science*, 2002, **83**, 5, 937.

87. S. Zhang, J. Zhao, C. Pang and I. Bonnard, *Journal of Elastomers and Plastics*, 2004, **36**, 3, 241.

88. H. Lü, S. Zheng, B. Zhang and X. Tang, *Macromolecular Chemistry and Physics*, 2004, **205**, 6, 834.

89. B. Qu and R. Xie, *Polymer International*, 2003, **52**, 9, 1415.

90. S.N. Cassu, R.A. Zoppi and M.I. Felisberti, *Journal of Applied Polymer Science*, 2004, **92**, 3701.

91. R. Jeziorska, *Polimery*, 2004, **49**, 5, 350.

92. J-D. Nam, J. Kim, S. Lee, Y. Lee and C. Park, *Journal of Applied Polymer Science*, 2003, **87**, 4, 661.

93. S.M. Ashraf, S. Ahmad and U. Riaz, *Journal of Applied Polymer Science*, 2004, **93**, 1, 83.

94. D. Srivastava, P. Kumar and G.N. Mathur, *Advances in Polymer Technology*, 2004, **23**, 1, 59.

95. W. Wang, M. Fu and B. Qu, *Polymers for Advanced Technologies*, 2004, **15**, 8, 467.

96. G. Chen, D. Shen, M. Feng and M. Yang, *Macromolecular Rapid Communications*, 2004, **25**, 11, 1121.

97. N. Ballav and M. Biswas, *Synthetic Metals*, 2004, **142**, 1–3, 309.

98. D.S. Kim and K.M. Lee, *Journal of Applied Polymer Science*, 2004, **92**, 3, 1955.

99. T. Kashiwagi, E. Grulke, J. Hilding, K. Groth, R. Harris, K. Butler, J. Shields, S. Kharchenko and J. Douglas, *Polymer*, 2004, **45**, 12, 4227.

100. A. Gök, B. Sari and M. Talu, *Journal of Polymer Science, Part B: Polymer Physics Edition*, 2004, **42**, 18, 3359.

101. Y.A. Badr, K.M. Abd El-Kader and R.M. Khafagy, *Journal of Applied Polymer Science*, 2004, **92**, 3, 1984.

102. L. Zhao, K. Tsuchiya and Y. Inoue, *Macromolecular Bioscience*, 2004, **4**, 8, 699.

103. N.M. Stark, L.M. Matuana and C.M. Clemons, *Polymer Degradation and Stability*, 2004, **86**, 1, 1.

104. J.M. Kinyanjui, D.W. Hatchett, J.A. Smith and M. Josowicz, *Chemistry of Materials*, 2004, **16**, 17, 3390.

105. J.K. Agbenyega, G. Ellis, P.J. Hendra, W.F. Maddams, C. Parssingham, H.A. Wills and J. Chalmers, *Spectrochimica Acta, Part A*, 1990, **46**, 2, 197.

106. M. Bowden, P. Donaldson, D.J. Gardiner, J. Birnie and D.L. Garrard, *Analytical Chemistry*, 1991, **63**, 24, 2915.

107. D. Bloor, *Polymer*, 1999, **40**, 14, 3901.

108. J. Koenig, *Infrared and Ramen Spectroscopy*, Rapra Review Report No 134, 2001, **12**, 2, Rapra Technology, Shawbury, Shrewsbury, UK.

109. V.F. Gaylor, A.L. Conrad and J.H. Lander, *Analytical Chemistry*, 1957, **29**, 2, 228.

110. B. Schraeder, *Angewandte Chemie-International Edition*, 1973, **12**, 11, 884.

111. F.J. Boerlo and J.L. Koenig in *Polymer Characterisation: Interdisciplinary Approaches*, Ed., C. Craver, Plenum Press, New York, NY, USA, 1971, p.1–13.

112. F.J. Boerio and J.L. Koenig, *Journal of Polymer Science: Polymer Symposia*, 1973, **43**, 1, 205.

113. J.L. Koenig, *Chemical Technology*, 1972, **2**, 7, 411.

114. N.A. Slovakhotova, *Metody Ispytatelei Kontr Issledovaniya Machinostroit Mater*, 1973, **3**, 41.

115. C.J.H. Schutte, *Fortschritte der Chemischen Forschung*, 1972, **36**, 57.

116. C. Tosi and G. Zerbi, *Chimica e Industria (Milan)*, 1973, **55**, 4, 334.

117. I.V. Kumpanenko and K.S. Kazanskil, *Uspekhi Khimii Fizicheskikh Polimeri*, 1973, 64.

118. R.D. Andrews and T.R. Hart in *Characterisation of Metal and Polymer Surfaces,* Ed., L.H. Lee, Academic Press, New York, NY, USA, 1977, p.207–240.

119. M.G. Chauser, V.D. Ermakova, O.B. Mishenko, V.S. Gunova and M.I. Cherkashin, *Armyanskii Khimicheskii Zhurnal*, 1973, **26**, 608.

120. J.K. Koenig in *Proceedings of the Polymer Characteristaion Conference,* 1975, Cleveland, OH, USA, 73.

121. J.M. Chalmers, *Polymer*, 1977, **18**, 7, 681.

122. W.E. Steper, *Macromolecular Chemistry – Macromolecular Symposium*, 1988, 18, 77.

123. O. Schroeter, *Naturwiss Rekhe,* 1986, **47**, 1, 109.

124. M. Ohira, T. Sakai, M. Takeuchi, Y. Kobayashi and M. Tsuji, *Synthetic Metals*, 1987, **18**, 1–3, 347

125. S. Chen, L. Tan, F. Qiu, X. Jiang, M. Wang and H. Zhang, *Polymer*, 2004, **45**, 9, 3045.

126. K.J. Thurecht, D.J.T. Hill, C.M.L. Preston, L. Rintoul, J.W. White and A.K. Whittaker, *Macromolecules*, 2004, **37**, 16, 6019.

127. N.A. Weir, F.J. Buchanan, J.F. Orr, D.F. Farrar and A. Boyd, *Biomaterials*, 2004, **25**, 28, 3939.

128. T.V. Sreekumar, T. Liu, B.G. Min, H. Guo, S. Kumar, R.H. Hauge and R.E. Smalley, *Advanced Materials*, 2004, **16**, 1, 58.

129. N. Artzi, B.B. Khatua, R. Tchoudakov, M. Narkis, A. Berner, A. Siegmann and J.M. Lagaron, *Journal of Macromolecular Science B*, 2004, **43**, 3, 605.

130. A.L. Santana, L.K. Noda, A.T.N. Pires and J.R. Bertlino, *Polymer Testing*, 2004, **23**, 7, 839.

131. Y. Zhu, X. Ren and C. Wu, *Journal of Applied Polymer Science*, 2004, **93**, 4, 1731.

132. J.H. Scrivens, *Advances in Mass Spectrometry*, 1995, **13**, 2, 447.

133. B.D. Cox, M.A. Park, R.G. Kaercher and E.A. Schweikert, *Analytical Chemistry*, 1992, **64**, 8, 843.

134. P.M. Thompson, *Analytical Chemistry*, 1991, **63**, 21, 2447.

135. C.H. Lin, Y. Murata and T. Imasaka, *Analytical Chemistry*, 1996, **68**, 7, 1153.

136. F. David, L. Vanderroost and P. Sandra, *Proceedings of the 13th International Symposium on Capillary Chromatography*, Riva del Garda, Italy, 1991, 1539.

137. F. Pisciotti, J. Lausmaa, A. Boldizar and M. Rigdahl, *Polymer Engineering and Science*, 2003, **43**, 6, 1289.

138. X.V. Eynde, P.Bertrand and R. Jerome, *Macromolecules*, 1997, **30**, 21, 6407.

139. D.W. Abmayr, Jr in *Proceedings of 2002 PLACE Conference*, Boston, MA, USA, 2002, Paper 95.

140. A.C. Prickett, P.E. Vickers, P.A. Smith and J.F. Watts, *Proceedings of Adhesion '99 Conference*, Cambridge, UK, 1999, 369.

141. P.A. Zimmerman, D.M. Hercules and A. Benninghoven, *Analytical Chemistry*, 1993, **65**, 8, 983.

142. P.A. Zimmerman, D.M. Hercules and W.O. Loos, *Analytical Chemistry*, 1995, **67**, 17, 2901.

143. I.V. Bletsos, D.M. Hercules, D. Van Leyen, A. Benninghoven and D. Fowle, *Analytical Chemistry*, 1990, **62**, 13, 1275.

144. X. Dong, A. Proctor and D.M. Hercules, *Macromolecules*, 1997, **30**, 1, 63.

145. D.E. Fowler, R.D. Johnson, D. Van Leyen and A. Benninghoven, *Analytical Chemistry*, 1990, **62**, 19, 2088.

146. I.V. Bletsos, D.M. Hercules, D. Van Leyen, B. Hagenhoff, E. Niehuis and A. Benninghoven, *Analytical Chemistry*, 1991, **63**, 18, 1953.

147. R.J. Ratway and C.M. Balik, *Journal of Polymer Science, Part B: Polymer Physics Edition*, 1997, **35**, 11, 1651.

148. W.J. van Ooij, J.M. Kim, S. Luo and S. Borros, *Proceedings of the 156th ACS Rubber Division Meeting*, Orlando, FL, USA, 1999, Paper 57.

149. P. Bertrand, L.T. Wang, W. Lauer and R. Zimmer, *Rubber Chemistry and Technology*, 2002, **75**, 4, 627.

150. S. Borros, E. Vidal, N. Agullo and W.J. van Ooij, *Kautschuk und Gummi Kunstoffe*, 2000, **53**, 12, 711.

151. L-T. Weng. T.L. Smith, J. Feng and C-M. Chan, *Macromolecules*, 1998, **31**, 3, 928.

152. S.S. Reddy, X. Dong, R. Murgasova, A.I. Gusev and D.M. Hercules, *Macromolecules*, 1999, **32**, 5, 1367.

153. V.H. Perez-Luna, K.A. Hooper, J. Kohn and B.D. Ratner, *Journal of Applied Polymer Science*, 1997, **63**, 11, 1457.

154. J.T. Cherian and D.G. Castner, *Journal of Advanced Materials*, 2000, **32**, 1, 28.

155. J.T. Cherian, *private communication*.

156. S.F. Lascelles, S.P. Armes, P.A. Zhdan, S.J. Greaves, A.M. Brown, J.F. Watts, S.R. Leadley and S.Y. Luk, *Journal of Materials Chemistry*, 1997, 7, 8, 1349.

157. W. Bijnens, J. Manca, T-D. Wu, M. D'Olicslacger, D. Vanderzande, J. Gelan, W. De Ceuninck, L. De Schepper and L.M. Stals, *Synthetic Metals*, 1996, **83**, 3, 261.

158. X.V. Eynde, P.Bertrand, P. Dubois and R. Jerome, *Macromolecules*, 1998, **31**, 19, 6409.

159. X.M. Zeng, C.M. Chan, L.T. Weng and L. Li, *Polymer,* 2000, **41**, 23, 8321.

160. C. Perruchot, M.M. Chehimi, M. Delamar, J.A. Eccles, T.A. Steele and C.D. Mair, *Synthetic Metals*, 2000, **113**, 1–2, 53.

161. M.L. Abel, I.W. Fletcher, R.P. Digby and J.F. Watts, *Proceedings of Adhesion '99*, Cambridge, UK, 1999, 87.

162. W.Y. Huang, S. Matsuoka, T.K. Kwei, Y. Okamoto, X. Hu, M.H. Rafailovich and J. Sokolov, *Macromolecules*, 2001, **34**, 22, 7809.

163. M.J. Stachowski and A.T. Dibenedetto, *Polymer Engineering and Science*, 1997, **37**, 2, 252.

164. Y. Kawakami, I. Imae, M. Oishi, M. Seino and Y. Liu, *Molecular Crystals and Liquid Crystals*, 2004, **415,** 1, 75.

165. A.D. Appelhans, J.E. Delmore and D.A. Dahl, *Analytical Chemistry*, 1987, **59**, 13, 1685.

166. H. Feld, A. Leute, R. Zurmuehlen and A. Benninghoven, *Analytical Chemistry*, 1991, **63**, 9, 903.

167. I.V. Bletsos, D.M. Hercules, D. Van Leyen, A. Benninghoven, C.G. Karakatsanis and J.N. Rieck, *Analytical Chemistry*, 1987, **61**, 19, 2142.

168. N. Baute, V.M. Geskin, R. Lazzaroni, J.L. Bredas, X. Arys, A.M. Jonas, R. Legras, C. Poleunis, P. Bertrand, R. Jerome and C. Jerome, *E-Polymers*, 2004, No. 063.

169. A. Dhanabalan, S.S. Talwar, A.Q. Contractor, N.P. Kumar, S.N. Narang, S.S. Major, K.P. Muthe and J.C. Vyas, *Journal of Material Science Letters*, 1999, **18**, 8, 603.

170. V. Boittiaux, F. Boucetta, C. Combellas, F. Kanoufi, A. Thiebault, M. Delamar and P. Bertrand, *Polymer*, 1999, **40**, 8, 2011.

171. J. Eccles, R. Williams, T. Markkula and S. Hird in *Proceedings of the Rapra Polymers for the Medical Industry – Innovations in Healthcare Delivery Conference*, Brussels, Belgium, 2001, Paper 19.

172. D.V. Patwardhan, H. Zimmer and J.E. Mark, *Journal of Macromolecular Science*, 1998, **35**, 12, 1941.

173. Y.M. Tsai, F.J. Boerio, W.J. Van Ooij and D.K. Kim, *Journal of Adhesion*, 1997, **62**, 1–4, 127.

174. J. Sidwell in *Proceedings of Rubber Bonding 2001 Conference*, Cologne, Germany, 2001, Paper 10.

175. M.R. Alexandra and T.M. Duc, *Journal of Materials Chemistry*, 1998, **8**, 4, 937.

176. X. van den Eynde, P. Betrand and J. Penelle, *Macromolecules*, 2000, **33**, 15, 5624.

177. D. Pleul, S. Schneider, F. Simon and H.J. Jacobasch, *Journal of Adhesion Science and Technology*, 1998, **12**, 1, 47.

178. K. Endo, N. Kobayashi, M. Aida and T. Hoshi, *Polymer Journal (Japan)*, 1996, **28**, 10, 901.

179. H.H.K. Lo, C.M. Chan and S-H. Zhu, *Polymer Engineering and Science*, 1991, **39**, 4, 721.

180. Y. Deslandes, G. Pleizier, D. Alexander and P. Santerre, *Polymer*, 1998, **39**, 11, 2361.

181. J-B. Lhoest, E. Detrait, P.van den Bosch de Aguilar and P. Bertrand, *Journal of Biomedical Materials Research, Part A*, 1998, **41**, 1, 95.

182. L-T. Weng, P.C.L. Wong, K. Ho, S. Wang, Z. Zeng and S. Yang, *Analytical Chemistry*, 2000, **72**, 20, 4908.

183. S.R. Leadley, M.C. Davies, M. Vert, C. Braud, A.J. Paul, A.G. Shard and J.F. Watts, *Macromolecules*, 1997, **30**, 22, 6920.

184. E.R. Lang, D. Leonard, H.J. Mathieu, E.M. Moser and P. Bertrand, *Macromolecules*, 1998, **31**, 18, 6177.

185. M-L. Abel, A. Rattana and J.F. Watts, *Journal of Adhesion*, 2000, **73**, 2–3, 313.

186. C. Perruchot, M.M. Chehimi, M. Delamar, P.C. Lacaze, A.J. Eccles, T.A. Steele and C.D. Mair, *Synthetic Metals*, 1999, **102**, 1–3, 1194.

187. H. Hirahara, S. Abe, K. Mori, Y. Oishi and I. Tanaka, *Kobunshi Ronbunshu*, 2000, **57**, 2, 95.

188. W.Y. Chan, A.Y. Cheng, S.B. Clendenning and I. Manners, *Macromolecular Symposia*, 2004, **209**, 1, 163.

189. J. Yip, K. Chan, K.M. Sin and K.S. Lau, *Polymer International*, 2004, **53**, 6, 634.

190. C.M. Dekeyser, S. Biltresse, J. Marchand-Brynaert, P.G. Rouxhet and C.C. Dupont-Gillain, *Polymer*, 2004, **45**, 7, 2211.

191. A.N. Rider, N. Brack, S. Andres and P.J. Pigram, *Journal of Adhesion Science and Technology*, 2004, **18**, 10, 1125.

192. M.F. Tse, K.O. McElrath, H-C. Wang and W. Hu, *Proceedings of the 158th ACS Rubber Division Meeting*, Cincinnati, OH, USA, 2000, Paper 94.

193. J.W. Burley, *Proceedings of the SPE Antec 2001*, Dallas, TX, USA, 2001, Paper 606.

194. A. Rattana, J.D. Hermes, M.L. Abel and J.F. Watts, *International Journal of Adhesion and Adhesives*, 2002, **22**, 3, 205.

195. J.F. Watts, A. Rattana, M.L. Abel and J. Hermes, *Proceedings of the 39th Annual Conference on Adhesion and Adhesives*, Oxford, UK, 2001, Paper 3.

196. H.C. Lin, I.F. Tsai, A.C.M. Yang, M.S. Hsu and Y.C. Ling, *Macromolecules*, 2003, **36**, 7, 2464.

197. J.M. Kim and W.J. van Ooij, *Journal of Adhesion Science and Technology*, 2003, **17**, 2, 165.

198. D.A. Cole, *Journal of the Adhesive and Sealant Council Conference Proceedings,* San Francisco, CA, USA, 1996, 6503.

199. M.F. Tse, W. Hu, M.S. Yeganeh and D. Zhang, *Journal of Applied Polymer Science*, 2004, **93**, 1, 323.

200. S. Liu, C.M. Chan, L.T. Weng and M. Jiang, *Polymer*, 2004, **45**, 14, 4945.

201. P. Albers, B. Freund, G. Prescher, K. Seibold and S. Wolff, *Proceedings of the 2nd International Conference*, Mulhouse, France, 1993, 119.

202. A.T. Jackson, J.H. Scrivens, W.J. Simonsick, M.R. Green and R.H. Bateman, *Polymer Preprints*, 2000, **41**, 1, 641.

203. J. Bouajila, G. Raffin, H. Watson, C. Sanglar, J.O. Paisse and M.F. Grenier-Loustalot, *Polymers and Polymer Composites*, 2003, **11**, 4, 233.

204. A.R. Dolan and T.D. Wood, *Synthetic Metals*, 2004, **143**, 2, 243.

205. A. Guarini, G. Guglielmetti, M. Vincenti, P. Guarda and G. Marchionni, A*nalytical Chemistry*, 1993, **65,** 8, 970.

206. M. Karas and F. Hillenkamp, *Analytical Chemistry*, 1988, **60**, 20, 2299.

207. U. Bahr, A. Deppe, M. Karas, F. Hillenkamp and U. Giessman, *Analytical Chemistry*, 1992, **64**, 22, 2866.

208. K. Tanaka, H. Waki, Y. Ido, S. Akita, Y. Yoshida and T. Yoishida, *Rapid Communications Mass Spectrometry*, 1988, **2**, 1, 151.

209. M. Yamashita and J.B. Fenn, *Journal of Physical Chemistry*, 1984, **88**, 1, 451.

210. J.B. Fenn, M. Mann, K. Meng, S.F. Wong and C.M. Whitehouse, *Science*, 1989, **246**, 64.

211. M. Dole, L.L. Mack, R.L. Hines, C. Mobley, L.D. Ferguson and M.B. Alice, *Journal of Physical Chemistry*, 1968, **49**, 2240.

212. R.J. Cotter, *Time-of-Flight Mass Spectrometry Instrumentation and Applications in Biological Research*, ACS, Washington, DC, USA, 1997.

213. S.D. Hanton, *JCT Coatings Technology*, 2004, **1**, 1, 62.

214. E. Esser, C. Keil, D. Braun, P. Montag and H. Pasch, *Polymer*, 2000, **41**, 11, 4039.

215. J.T. Mehl, R. Murgasova, X. Dong, D.M. Hercules and H. Nefzger, *Analytical Chemistry*, 2000, **72**, 11, 2490.

216. H. Goetz, U. Maschke, T. Wagner, C. Rosenauer, K. Martin, S. Ritz and B. Ewen, *Macromolecular Chemistry and Physics*, 2000, **201**, 12, 1311.

217. M.S. Montaudo and G. Montaudo, *Polymer Preprints*, 2002, **43**, 1, 427.

218. D. Cho, S. Park, T. Chang, K. Ute, I. Fukuda and T. Kitayama, *Analytical Chemistry*, 2002, **74**, 8, 1928.

219. V.T. Petkovska, D. Powell and K.B. Wagener, *Polymer Preprints*, 2002, **43**, 1, 427.

220. H.R. Kricheldorf, M. Rabenstein, M. Maskos and M. Schmidt, *Macromolecules*, 2001, **34**, 4, 713.

221. H.R. Kricheldorf and O. Petermann, *Journal of Polymer Science, Polymer Chemistry Edition*, 2002, **40**, 23, 4537.

222. T. Hamaide, M. Pantiru, H. Fessi and P. Boullanger, *Molecular Rapid Communications*, 2001, **22**, 9, 659.

223. T. Hamaide and E. Lavit, *Polymer Bulletin*, 2002, **48**, 2, 173.

224. T.D. McCarley, C.J. Dubois, R.L. McCarley, C. Cardona and A.E. Kaifer, *Polymer Preprints*, 2000, **41**, 1, 674.

225. D.M. Hercules, J.T. Mehl, R. Murgasova and X. Dong, *Polymer Preprints*, 2000, **41**, 1, 639.

226. H. Ji, N. Sato, Y. Nakamura, Y. Wan, A. Howell, Q.A. Thomas, R.F. Storey, W.K. Nonidez and J.W. Mays, *Macromolecules*, 2002, **35**, 4, 1196.

227. P.B. Smith, A.J. Pasztor, Jr., M.L. McKelvy, D.M. Meunier, S.W. Froelicher and F.C-Y. Wang, *Analytical Chemistry*, 1999, **71**, 12, 61.

228. C.M. Guttman, S.J. Wetzel, W.E. Wallace, W.R. Blair, R.M. Goldschmidt, D.L. Vanderhart and B.M. Fanconi, *Polymer Preprints*, 2000, **41**, 1, 678.

229. S. Lin-Gibson, L. Brunner, D.L. Vanderhart, B.J. Bauer, B.M. Fanconi, C.M. Guttman and W.E. Wallace, *Polymer Preprints*, 2002, **43**, 2, 1331.

230. R.P. Lattimer and B.F. Goodrich, *Polymer Preprints*, 2000, **41**, 1, 667.

231. S.M. Weidner, J. Falkenhagen, H. Much, R.P. Krueger and J.F. Freidrich, *Polymer Preprints*, 2000, **41**, 1, 655.

232. H. Katayama, M. Kamigaito and M. Sawamoto, *Journal of Polymer Science, Part A: Polymer Chemistry*, 2001, **39**, 8, 1249.

233. A. Sunder, H. Frey and R. Mulhaupt, *Macromolecular Symposia*, 2000, **153**, 187.

234. G.J. Sun, H.J. Jang, S. Kaang and K.H. Chae, *Polymer*, 2002, **43**, 22, 5855.

235. F. D'Agosto, M-T. Charreyre, F. Delolme, G. Dessalces, H. Cramail, A. Deffieux and C. Pichot, *Macromolecules*, 2002, **35**, 21, 7911.

236. G.Rokicki, T. Kowalczyk and M. Glinski, *Polymer Journal (Japan)*, 2000, **32**, 5, 381.

237. A.K. Nanda, K. Ganesh, K.Kishore and M. Surinarayanani, *Polymer Preprints*, 2000, **41**, 26, 9063.

238. J. Peterson, V. Allikmaa, J. Subbi, T. Pehk and M. Lopp, *European Polymer Journal*, 2003, **39**, 1, 33.

239. H. Chen, M. He, J. Pei and B. Liu, *Analytical Chemistry*, 2002, **74**, 24, 6252.

240. F. Zuluaga, M. Larrahondo and K.B. Wagener, *Polymer Preprints*, 2002, **43**, 1, 627.

241. S. Sosnowski, S. Slomski, A. Lorenc and H.R. Kricheldorf, *Colloid and Polymer Science*, 2002, **280**, 2, 107.

242. H.S. Bazzi and H.F. Sleiman, *Polymer Preprints*, 2002, **43**, 1, 694.

243. W.J. Feast and D. Parker in *Proceedings of the ACS Polymeric Materials Science and Engineering Meeting*, San Diego, CA, USA, 2001, 299.

244. C. Ladavière, N. Dörr and J.P. Claberie, *Macromolecules*, 2001, **34**, 16, 5370.

245. B.V. Rozynov, R.J. Liukkonen, D.O. Becklin, A.L. Noreen and S.D. Ponto, *Polymer Preprints*, 2000, **41**, 1, 692.

246. T.J. Kemp, R. Berridge, M.D. Eason and D.M. Haddleton, *Polymer Degradation and Stability*, 1999, **64**, 2, 329.

247. N.K. Singha, S. Rimmer and B. Klumperman, *European Polymer Journal*, 2004, **40**, 1, 159.

248. E. Ihara, T. Todaka and K. Inoue, *Journal of Polymer Science, Part A: Polymer Chemistry*, 2004, **42**, 1, 31.

249. E. Ihara, J-I. Ikeda, T. Itoh and K. Inoue, *Macromolecules*, 2004, **37**, 11, 4048.

250. G. Masci, L. Giacomelli and V. Crescenzi, *Macromolecular Rapid Communications*, 2004, **25**, 4, 559.

251. H. Zettl, W. Häfner, A. Böker, H. Schmalz, M. Lanzendörfer, A.H.E. Müller and G. Krausch, *Macromolecules*, 2004, **37**, 5, 1917.

252. G.C. Eastmond and J. Paprotny, *Polymer*, 2004, **45**, 4, 1073.

253. T. Biedron and P. Kubisa, *Journal of Polymer Science, Part A: Polymer Chemistry*, 2004, **42**, 13, 3230.

254. H.R. Kricheldorf, M. Garaleeh, G. Schwarz and L. Vakhtangishvili, *High Performance Polymers*, 2004, **16**, 1, 137.

255. M. Pantiru, C. Iojoiu, T. Hamaide and F. Delolme, *Polymer International*, 2004, **53**, 5, 506.

256. C. Iojoiu, T. Hamaide, V. Harabagiu and B.C. Simionescu, *Journal of Polymer Science, Part A: Polymer Chemistry*, 2004, **42**, 3, 689.

257. F. Burel, A. Feldman, C. Loutelier-Bourhis and C. Bunel, *E-Polymers*, 2004, No. 011.

258. H.R. Kricheldorf, S. Böhme, G. Schwarz and C-L. Schultz, *Macromolecules*, 2004, **37**, 5, 1742.

259. R.P. Quirk, F. You, C. Wesdemiotis and M.A. Arnould, *Macromolecules*, 2004, **37**, 4, 1234.

260. X-Z. Fang, Q-X. Li, Z. Wang, Z-H. Yang, L-X. Gao and M-X. Ding, *Journal of Polymer Science, Part A: Polymer Chemistry*, 2004, **42**, 9, 2130.

261. X. Fang, Z. Yang, S. Zhang, L. Gao and M. Ding, *Polymer*, 2004, **45**, 8, 2539.

262. M. Malkoch, H. Claesson, P. Löwenhielm, E. Malmström and A. Hult, *Journal of Polymer Science, Part A: Polymer Chemistry*, 2004, **42**, 7, 1758.

263. T.J. Singh, G. Ganeshsanjeev, K. Siddappa and S.V. Bhat, *Journal of Polymer Science, Part B: Polymer Physics Edition*, 2004, **42**, 7, 1299.

264. S.J. Pastor and C.L. Wilkins, *Journal of the American Society of Mass Specrometry*, 1997, **8**, 3, 225.

265. D. Tillier, H. Lefebvre, M. Tessier, J-C. Blais and A. Fradet, *Macromolecular Chemistry and Physics*, 2004, **205**, 5, 581.

266. L. La Tourte, J.C. Blais, R.B. Cole, G. Bilbeck, B. Escoffier and J.C. Tahat, *Proceedings of the 45th ASTM Conference on Mass Spectrometry and Allied Topics*, Palm Springs, CA, USA, 1997, 536.

267. A. Favier, C. Ladavière, M-T. Charreyre and C. Pichot, *Macromolecules*, 2004, **37**, 6, 2026.

268. C.N. McEwen and P.M. Peacock, *Analytical Chemistry*, 2002, **74**, 12, 2743.

269. S. Karlsson, *Polymer News*, 2002, **27**, 9, 305.

270. A.E. Giannakopulos, A.R. Bottrill, K.S. Lee and P.J. Derrick, *Conference Proceedings of Polymer Preprints*, 2000, **41**, 1, 643.

271. U.S. Schubert and C. Eschbamner, *Conference Proceedings of Polymer Preprints*, 2000, **41**, 1, 676.

272. J.D. Hogan and D.A. Laude, *Analytical Chemistry*, 1992, **64**, 7, 763.

273. E.R.E. van der Hage, M.C. Duursma, R.M.A. Heeren, J.J. Boon, M.W.F. Nielen, A.J.M. Weber, C.G. de Koster and N.K. de Vries, *Macromolecules*, 1997, **30**, 15, 4302.

274. G. Montaudo, E. Scamporrino, C. Puglisi and D. Vitalini, *Macromolecules*, 1988, **21**, 6, 1594.

275. T.C. Masterman, N.R. Dando, D.G. Weaver and D. Seyferth, *Journal of Polymer Science, Part B: Polymer Physics Edition*, 1994, **32**, 13, 2263.

276. R.K. Harris, R.R. Yeung, P. Johncock and D.A. Jones, *Polymer*, 1996, **37**, 5, 721.

277. W.H. McClennen, R.M. Buchanan, N.S. Arnold, J.P. Dworzanski and H.L.C. Meuzelaar, *Analytical Chemistry*, 1993, **65**, 20, 2819.

278. Y. Zhang, Q. Zhang, K. Cheng and J. Xu, *Journal of Applied Polymer Science*, 1992, **92**, 2, 722.

279. M. Krauze, J. Trzeszezynski and M. Dzieciol, *Popular Plastics and Packaging*, 2004, **49**, 11, 100.

280. J.C. Randall in *Carbon 13 NMR Polymer Science*, Ed., W.M. Pasika, ACS, Symposium Series No.103, ACS, Washington, DC, USA, 1979, 235.

281. J.C. Randall, *Journal of Polymer Science, Part B: Polymer Physics Edition*, 1976, **14**, 11, 2083.

282. F.C. Stehling, *Journal of Polymer Science, Part A: Polymer Chemistry*, 1966, **4**, 189.

283. E.M. Barrall II, R.S. Porter and J.F. Johnson, *Polymer Preprints*, 1964, **5**, 2, 816.

284. E.M. Barrall II, R.S. Porter and J.F. Johnson, *Journal of Applied Polymer Science*, 1965, **9**, 9, 3061.

285. S. Satoh, R. Chûjô, T. Ozeki and E. Nagai, *Journal of Polymer Science,* 1962, **62**, 174, S101.

286. M. Nagai and A. Nishioka, *Journal of Polymer Science, Part A: Polymer Chemistry*, 1968, **6**, 6, 1655.

287. S. Amiya, I. Ando and R. Chûjô, *Polymer Journal (Japan)*, 1973, **4**, 4, 385.

288. S. Amiya, I. Ando, S. Watanabe and R. Chûjô, *Polymer Journal (Japan)*, 1974, **6**, 2, 194.

289. A.E. Woodward, *Journal of Polymer Science, Part C: Polymer Symposia,* 1965, **8**, 1, 137.

290. T. Miyamoto and H.T. Contow, *Macromolecular Chemistry*, 1972, **162**, 14, 43.

291. P.Q. Tho and M. Taieb, *Journal of Polymer Science, Part A: Polymer Chemistry*, 1972, **10**, 10, 2925.

292. L. Cavalti, *Relaz Corso-Toer-Prat Rizonenza Mana Nud*, 1973, 351.

293. S. Satoh, *Journal of Polymer Science, Part A: General Papers,* 1964, **2**, 12, 5221.

294. Y. Abe, M. Tasumi, T. Shimanouchi, S. Satoh and R. Chûjô, *Journal of Polymer Science A-1: Polymer Chemistry,* 1966, **4**, 6, 1413.

295. S. Morita, M. Shen, G. Sawa and M. Ieda, *Polymer Preprints, ACS Division Polymer Chemistry*, 1976, **17**, 545.

296. A.E. Woodward, *Journal of Polymer Science, C,* 1965, **8**, 1, 137.

297. H. Yuki, K. Hatada and M. Takeshita, *Journal of Polymer Science, Part A-1: Polymer Chemistry*, 1969, **7**, 2, 669.

298. I. R. Peat and W.F. Reynolds, *Tetrahedron Letters*, 1972, **13**, 14, 1359.

299. H. Girad and P. Monjol, *Comptes Rendus Hebdomadaires de Seances de l'Academie des Sciences Serie C*, 1974, **279**, 13, 553.

300. K. Matsuzaki, T. Kanai, T. Kawamura, S. Matsumoto and T. Uryu, *Journal of Polymer Science: Polymer Chemistry Edition*, 1973, **11**, 5, 961.

301. A. Forchioni and C. Chachaty, *Journal of Polymer Science, Part A-1: Polymer Chemistry*, 1972, **10**, 7, 1923.

302. G. R. Dever, F. E. Karasz, W. J. Macknight and R. W. Lenz, *Journal of Polymer Science: Polymer Chemistry Edition*, 1975, **13**, 8, 1803.

303. A. S. Tompa, R. D. Barefoot and E. Price, *Journal of Polymer Science, Part A-1: Polymer Chemistry*, 1968, **6**, 10, 2785.

304. K-F. Elgert, R. Wicke, B. Stützel and W. Ritter, *Polymer*, 1975, **16**, 6, 465.

305. H. Kusumoto and H.S. Gutowsky, *Journal of Polymer Science, Part A: General Papers*, 1963, **1**, 9, 2905.

306. E. Campos-López and J. Palacios, *Journal of Polymer Science: Polymer Chemistry Edition*, 1976, **14**, 6, 1561.

307. S. Kawahawa, K. Takano, J. Yunyongwattanarorn, Y. Isono, M. Hikosaka, J.T. Sakdapipanich and Y. Tanaka, *Polymer Journal (Japan)*, 2004, **36**, 5, 361.

308. R. McGuchan and I.C. McNeill, *Journal of Polymer Science, Part A-1: Polymer Chemistry*, 1968, **6**, 1, 205.

309. J.E. Gordon, *Journal of Physical Chemistry*, 1962, **66**, 6, 1150.

310. J.E. Gordon, *Chemistry and Industry (London)*, 1962, 267.

311. V.A. Kruglova, G.V. Ratovskii, A.A. Borisenko and A.V. Kalabina, Vysokomol Soedin Seriya A, 1973, **15**, 1967.

312. G. Ceccarelli, F. Andruzzi and M. Paci, *Polymer*, 1979, **20**, 5, 605.

313. D. Doskocilová, B. Schneider, E. Drahorádová, J. Štokr and M. Kolínský, *Journal of Polymer Science, Part A-1: Polymer Chemistry*, 1971, **9**, 10, 2753.

314. O.V. Smirnova, V.V. Korshak, T.Y. Slonim, Y.G. Urman, S.G. Alekseyeva and V.A. Bairomov, *Vysokomole Soedin Seriya A*, 1975, **17**, 11, 2778.

315. D.H. Beebe, C.E. Gordon, R.N. Thudium, M.C. Throckmorton and T.L. Hanlon, *Journal of Polymer Science: Polymer Chemistry Edition*, 1978, **16**, 9, 2285.

316. B. Jasse, F. Laupretre and L. Monnerie, *Makromolekulare Chemie*, 1977, **178**, 7, 1987.

317. P. Crouzet, F. Fine and P. Mangin, *Journal of Applied Polymer Science*, 1969, **13**, 1, 205.

318. F.A. Bovey, *Journal of Polymer Science: Part A, General Papers*, 1963, **1**, 3, 843.

319. G. Pruckmayr and T.K. Wu, *Macromolecules*, 1973, **6**, 1, 33.

320. Y. Koma, K. Limura, S. Kondo and M. Takeda, *Journal of Polymer Science: Polymer Chemistry Edition*, 1977, **15**, 7, 1697.

321. D.H. Richards and R.L. Williams, *Journal of Polymer Science: Polymer Chemistry Edition*, 1973, **11**, 1, 89.

322. T. Okada, *Journal of Polymer Science: Polymer Chemistry Edition*, 1979, **17**, 1, 155.

323. F.A. Bovey and G.V.D. Tiers, *Journal of Polymer Science: Part A, General Papers*, 1963, **1**, 3, 849.

324. G. Filopovich, *Journal of Polymer Science: Part A, General Papers*, 1963, **1**, 7, 2279.

325. R.C. Ferguson, *Journal of Polymer Science A: General Papers*, 1964, **2**, 11, 4735.

326. J.C. Woodbrey, H.P. Higginbottom and H.M. Culbertson, *Journal of Polymer Science A: General Papers*, 1965, **3**, 3, 1079.

327. R. E. Glick and R. C. Phillips, *Journal of Polymer Science A: General Papers*, 1965, **3**, 5, 1885.

328. R.C. Hirst, D.M. Grant, R.E. Hoff and W.J. Burke *Journal of Polymer Science A: General Papers*, 1965, **3**, 6, 2091.

329. J.B. Lando, H.G. Olf and A. Peterlin, *Journal of Polymer Science, Part A-1: Polymer Chemistry*, 1966, **4**, 4, 941.

330. K.C. Ramey, D.C. Lini and G.L. Statton, *Journal of Polymer Science, Part A-1: Polymer Chemistry*, 1967, **5**, 2, 257.

331. R. Yamadera and M. Murano, *Journal of Polymer Science, Part A-1: Polymer Chemistry*, 1967, **5**, 5, 1059.

332. F. Mustata and I. Bicu, *Journal of Polymer Engineering*, 2004, **24**, 4, 391.

333. K. Iio, S. Yamasaki, S. Tasaki, H. Kudoh and M. Matsunaga, *Journal of Polymer Science, Part A: Polymer Chemistry*, 2004, **42**, 7, 1707.

334. C. Diab, Y. Akiyama, K. Kataoka and F.M. Winnik, *Macromolecules*, 2004, **37**, 7, 2556.

335. N. Teramoto and M. Shibata, *Journal of Applied Polymer Science*, 2004, **91**, 1, 46.

336. J.K. Haken, N. Harahap and R.P. Burford, *Journal of Chromatography A*, 1990, **500**, 367.

337. I.V. Morozova, A.I. Mikhaleva, I.V. Tatarinova, G.F. Myachina, T.A. Skathein, T.V. Mamaseva and B.A. Trofimov, *Polymer Science Series B,* 2004, **42**, 5–6, 159.

338. C. Marcott, G.M. Stury, I. Nada, A. Bibby and C.J. Manning in *Fourier Transform Spectroscopy 11th International Conference*, Ed., J.A.D. Baseth, American Institute of Physics, Woodbury, NY, USA, 1998, 379.

6 Analysis of Copolymers

6.1 Infrared Spectroscopy

This technique has been used extensively for the determination of functional groups, in polymers and copolymers (Chapter 3) and in comonomer analysis (Chapter 4). Both these aspects are concerned with the determination of polymer structure. For example: the distinction between free and combined vinyl acetate in vinyl chloride – vinyl acetate copolymers (Section 3.4.4); or the elucidation of the structure of methylmethacrylate (MMA) – glycidyl methacrylate copolymers (Section 3.6.1); or the elucidation of the various types of unsaturation occurring in styrene – butadiene copolymers (Sections 3.9.3, 3.9.4). Typical infrared (IR) spectra of copolymers are shown in **Figures 6.1 to 6.4**.

Johnson-Plaumann and co-workers [1] used infrared and nuclear magnetic resonance spectroscopy (NMR) to quantitate the composition of various ethylene – propylene copolymers. Absolute concentrations were measured by IR spectroscopy. An IR calibration curve was obtained by plotting the absorbance ratio 6.82 μm/7.26 μm *versus* concentration of monomer units.
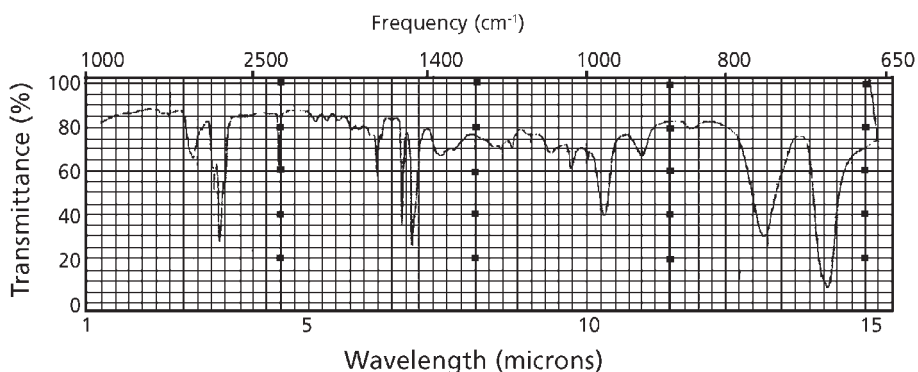
Figure 6.1 Acrylonitrile-butadiene-styrene terpolymer (Novodur W - Bayer Chemicals), benzene solution evaporated on sodium chloride windows. (*Source: Author's own files*)
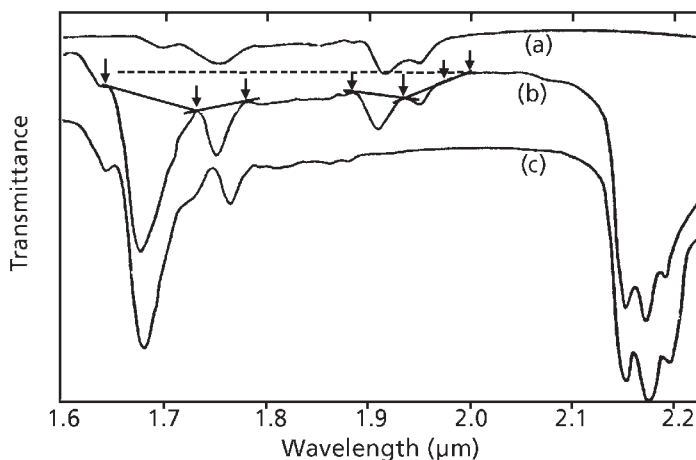
Figure 6.2 Near infrared spectra (a) polyacrylonitrile; (b) styrene-acrylonitrile copolymer (acrylonitrile content 25.7 wt%); (c) polystyrene. (*Source: Author's own files*)
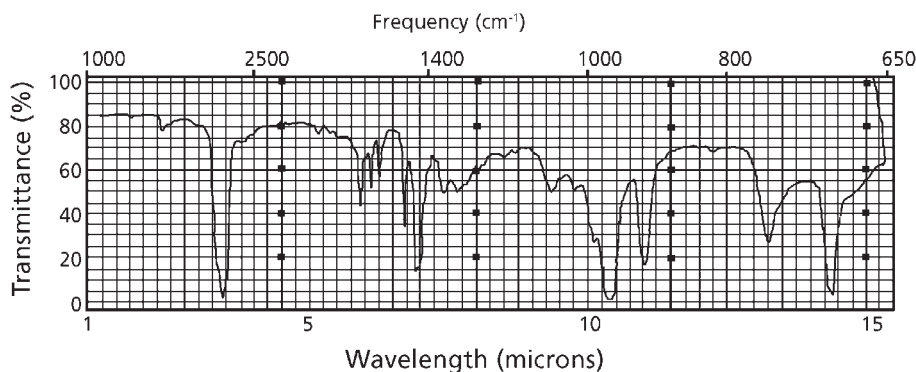
Figure 6.3 Styrene butadiene (SBR 15 M - Phillips Chemical Co.), benzene solution evaporated on sodium chloride window. (*Source: Author's own files*)

Partnov and co-workers [2], on the other hand, measured the ratio of monomer units in ethylene – propylene copolymers by IR measurements at 14.49, 13.85, 13.66, 13.29 and 11.75 μm. Typical IR spectra for copolymers of different composition are shown in **Figure 6.5**.

Kandil and El-Gamal [3] used IR spectroscopy at 5.78 μm to study the composition of methylacrylate – styrene copolymers. The carbonyl band intensity at 5.78 μm was correlated with copolymer composition.
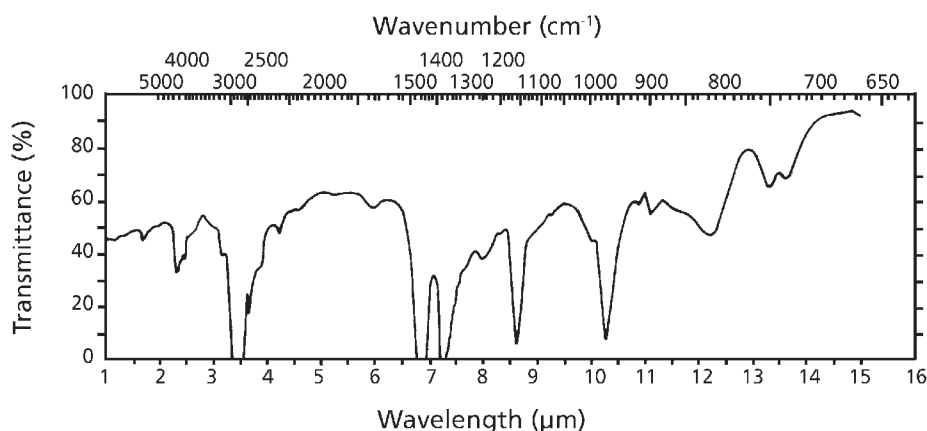
Figure 6.4 Infrared spectrum of ethylene propylene copolymer containing 85 mole% propylene. (*Source: Author's own files*)

Other applications of IR spectroscopy in copolymer characterisation include: styrene-glycidyl-*p*-isopropenylphenyl ether copolymers [4], styrene-isobutylene copolymers [5], vinyl chloride – vinyl acetate – vinyl fluoride terpolymers [6], vinylchloride – vinyl acetate copolymers [7], styrene copolymers [8], ethylene-vinyl acetate copolymers [9], graft copolymers, and butadiene-styrene [10] and acrylonitrile – styrene copolymers [11], polyurethane – polyacrylate [12], polymethylmethacrylate grafted high alpha cellulose [13], bisphenol-polycarbonate (PC) [14], bromobutyl isoprene [15], styrene – methacrylonitrile (SMAN) [16, 17] and styrene – acrylonitrile [18].

6.2 Fourier Transform Infrared Spectroscopy

IR spectra have been shown to be very useful for examining the compositional microstructure of copolymers [19–22]. However, whilst the measurement of the properties of the monomer constituents in a copolymer using characteristic IR absorption bands is comparatively easy (and has been used widely for various copolymer systems) by comparison with the NMR technique, the analysis of the sequence distribution of monomer units which comprise a copolymer is often difficult and complex [18]. Therefore, there have only been a small number of reports of the use of IR spectroscopy for sequence microstructure analysis for a limited number of copolymer systems [23–25].

Dong and Hill [16] analysed the infrared spectra for a series of random SMAN copolymers with various compositions, to determine the dependence of the frequencies
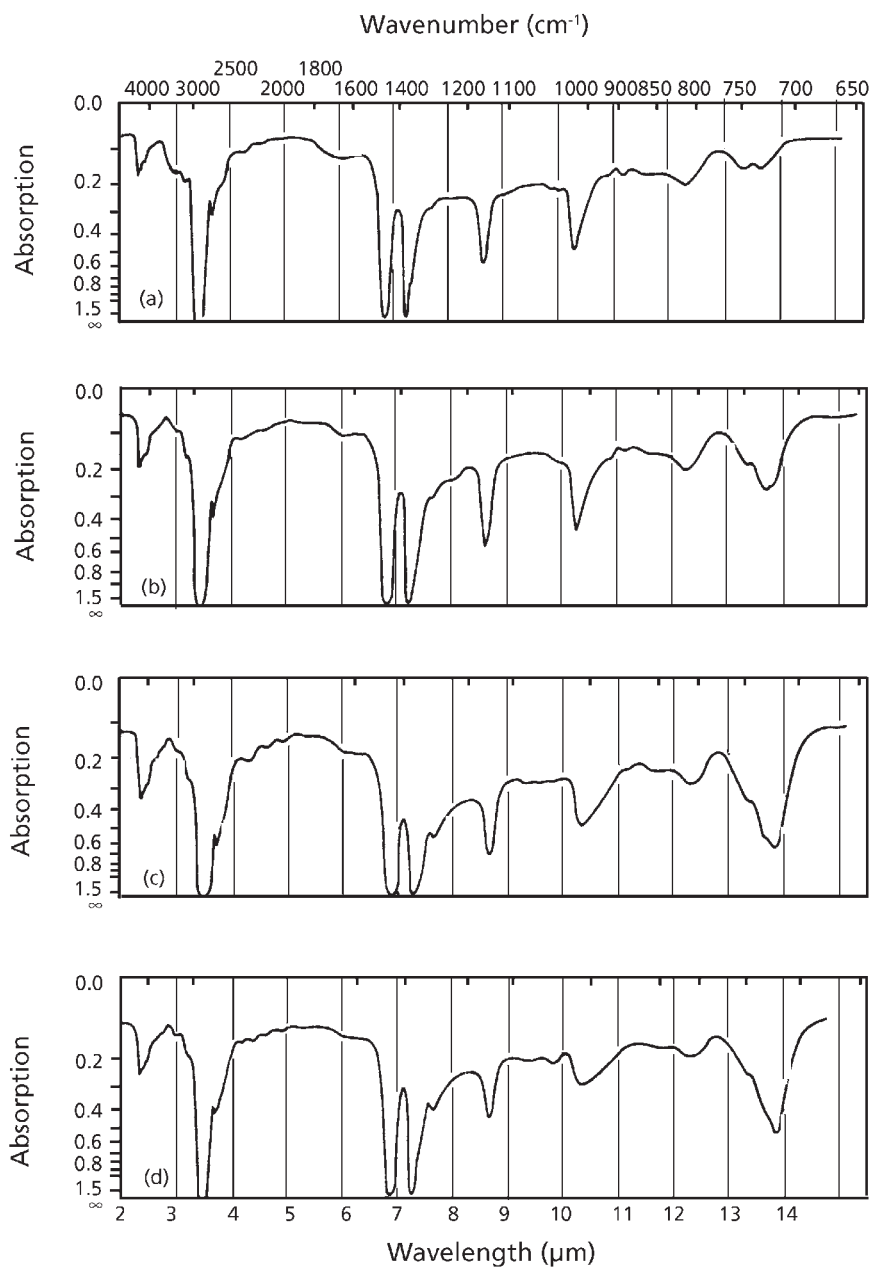
Figure 6.5 Infrared spectra of ethylene propylene copolymers of various compositions: (a) 85.5% polyethylene; (b) 74.0% polyethylene; (c) 65.9% polyethylene; (d) 55.5% polyethylene. (*Source: Author's own files*)

of the individual spectral peaks on the copolymer composition. In particular, the vibration frequencies for the nitrile group is discussed in detail. Correlations were established to relate changes in the peak positions to changes in the copolymer composition and monomer sequence distribution. In addition, the vibration band frequencies for blends of polymethacrylonitrile (PMAN) and polystyrene were examined in order to compare the effects of inter- and intra-chain interactions on these bands.

An important characteristic of PMAN and its copolymers is the presence of the strongly polar nitrile groups. The nitrile groups can interact with their surroundings in a variety of ways. These different interactions between the nitrile groups and their surroundings may lead to a change in the stretching frequency of the carbon nitrogen (CN) bond. Therefore, the stretching frequency of the CN bond may provide information about the microstructure of the SMAN copolymers, providing next neighbour effects are dominant.

The peak located at 4.48 μm, which is the CN bond stretching band for an SMAN copolymer with $Y_M = 0.189$, shifts to higher frequency with increasing methacrylonitrile content in the SMAN copolymers, as shown in **Figure 6.6**.

The high dipole moment (3.9 Debye) for the nitrile group can give rise to either a strong attraction or a strong repulsion (according to orientation) with similar groups or other substituents in a copolymer which possess a high dipole moment [26]. The
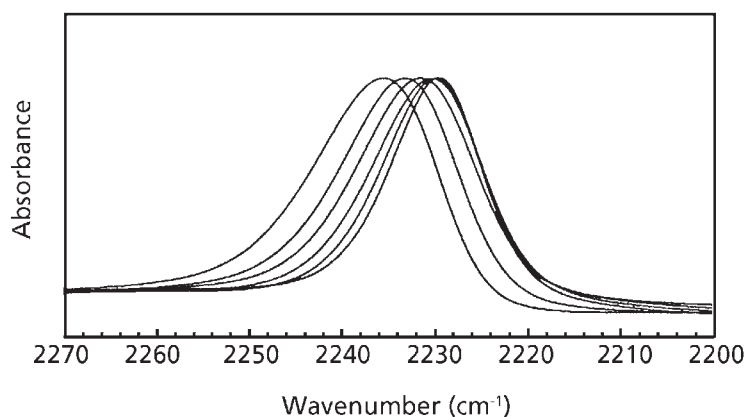
Figure 6.6 The shift of CN frequency of styrene-methacrylonitrile (SMAN) copoymers in KBr-disk (Y_M: 0.189, 0.376, 0.480, 0.651, 0.798, 1.000, from right to left). (*Reprinted with permission from L. Dong and D. Hill, Polymer Bulletin, 1995, 34, 3, 323. ©1995, Springer*) [16]

intra- and inter-molecular forces in a PMAN polymer chain result predominantly from these types of dipolar interactions [27, 28]. The adjacent nitrile groups in PMAN repel one another and force the polymer chain to adopt a conformation in which these repulsive forces are minimised. But nitrile groups on adjacent chains may be involved in attractive interactions. The incorporation of stryrene units into a PMAN chain will reduce the extent of the repulsive interactions of neighbouring nitrile groups and will enhance the mobility of the polymer chain segments, thus allowing more attractive interactions to occur between the polar nitrile groups, as well as other groups in the copolymers.

At low concentrations of nitrile groups in a SMAN copolymer, the frequency of the CN resonance lies in the range of 4.484 to 4.482 µm depending on the nature of the matrix of the polymer (e.g., solution or solid state). Thus, as the CN content of the polymer increases, the probability for the occurrence of adjacent MAN-MAN diad sequences rises, and hence the extent of repulsion between these neighbouring groups also rises. As the concentration of MAN units in the copolymer increases, so does the vibrational frequency of the CN bond, as shown in **Figure 6.7**.

The increasing vibrational frequency with increasing MAN content in the copolymers is consistent with an apparently higher force constant for the CN bond. This can be rationalised in terms of the repulsive forces which exist between the carbon and nitrogen atoms of neighbouring nitrile residues along the polymer chain, and which restrict the vibration of the two atoms in each of the nitrile groups.
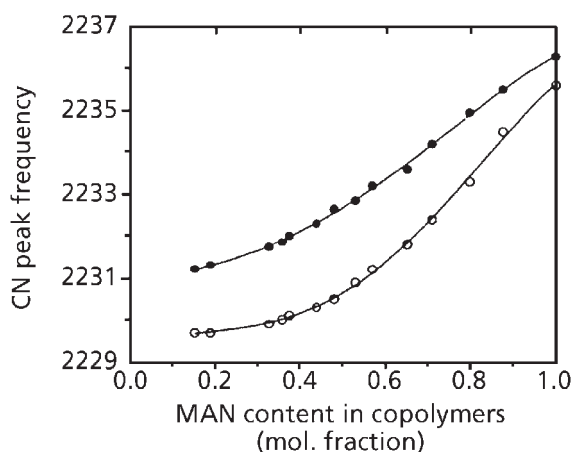
Figure 6.7 Relationship between the CN frequency and the copolymer composition (●: solution sample; ○: KBr disk sample). (*Reprinted with permission from L. Dong and D. Hill, Polymer Bulletin, 1995, **34**, 3, 323. ©1995, Springer*) [16]

Figure 6.7 shows the relationship between the CN bond stretching frequency and MAN content in the copolymers for the solution samples and solid state samples in the form of KBr-disks.

From **Figure 6.7**, the samples determined in dichloromethane solution have a higher stretching frequency for the CN bond than the corresponding solid state samples determined in the KBr-disk form. This may be attributed to the nature of the interaction between the copolymer chains and the dichloromethane solvent. The polar dichloromethane, which has a dielectric constant of 9.7, will interact strongly with the polar CN bonds in the copolymers, leading to an increase in the polarisation of these bonds, and thus to a shift on their stretching frequency towards higher values.

Whilst this study does not provide a method of determining the styrene and acrylonitrile contents of these copolymers, it does provide important structural information regarding sequence distributions in the copolymer.

Fourier transform IR spectroscopy (FTIR) has been applied to the characterisation of pyrrole – ethylamine [29], poly(beta-hydroxybuturate) – beta (hydroxyl valerate) [30], polyethylene terephthalate – bibenzoate [31], polyether oxide – poly(beta-benzyl *L*-aspartate [32], poly(vinylidene fluoride) – trifluoro-ethylene [33], polyacrylamide methyl acrylate [34], ethylene propylene – diene [35], and styrene methacrylate [16, 25].

Applications of IR and Raman spectroscopy to copolymer microstructure studies are also discussed in Sections 3.1.4, 3.3, 3.4.4, 3.6.1, 3.7.3, 3.9.4, 3.14, 3.16, 4.1, 4.7.5, 4.3.1, 4.4.1, and 4.5.

6.3 Raman Spectroscopy

As discussed in Section 5.3, this technique has been applied to the investigation of microstructure of a range of copolymers including ethylene oxide – vinyl chloride and tetrafluoroethylene – hexafluoropropylene [36]. **Figure 6.8** shows the influence of copolymer composition on the Raman spectra of ethylene oxide – vinyl chloride copolymers containing 60%, 80% and 40% ethylene oxide. Similarly Raman spectroscopy has been applied to the study of the microstructure of butadiene – acrylonitrile copolymers [37].
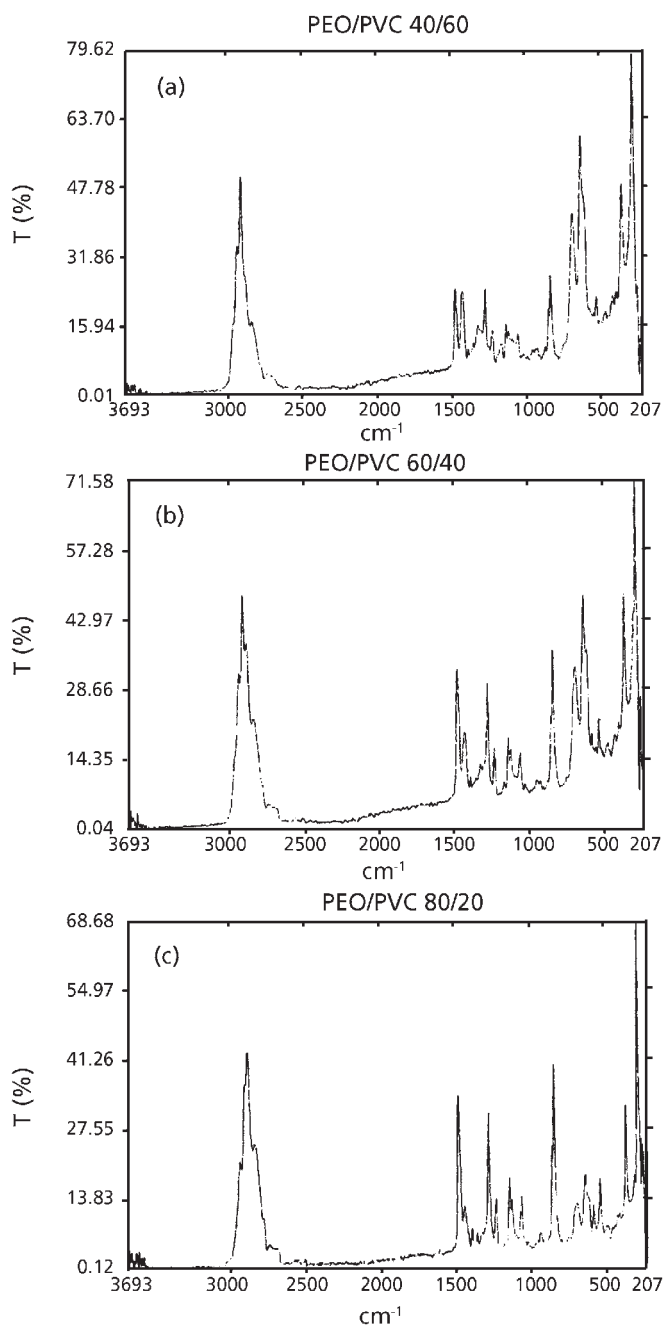
Figure 6.8 The Raman spectra of ethylene oxide/vinyl chloride containing 80, 60 and 40% oxide. (*Reprinted with permission from J.K. Agbenyega, G. Ellis, P.J. Hendra, W.F. Maddams, C. Parssingham, H.A. Wills and J. Chalmers, Spectrochimica Acta, Part A, 1990, 46, 2, 197. ©1990, Elsevier*)

6.4 Mass Spectrometry

6.4.1 Radio Frequency Glow Discharge Mass Spectrometry

Shick and co-workers [38] used this technique for the characterisation of bulk polymers such as polytetrafluoroethylene (PTFE), methyl vinyl ether and PTFE – hexafluoropropylene – polyvinylidene fluoride.

A radio frequency (RF) powered glow discharge atomisation/ionisation source was used to determine the applicability of the technique for direct polymer analysis. The technique provided fingerprint mass spectra for a series of PTFE-based polymers, the mass spectrum being obtained by observing the different base peaks and relative peak intensities. Discharge stabilisation and internal stability were very reproducible (with a standard deviation of less than 5%). On-depth profiles could be obtained by observing the polymers following deposition of a layer of copper on the polymer surface.

6.4.2 Fast Atom Bombardment Mass Spectrometry

Montaudo and co-workers [39] used fast atom bombardment mass spectrometry to identify the cyclic oligomers formed in the polycondensation reactions leading to the aromatic-aliphatic polysulfides. He also used the technique in microstructural studies on copolymers [40, 41].

6.4.3 Laser Desorption – Ion Mobility Spectrometry

In this technique the pulse from a Nd/YAG laser ablates the surface of the polymer generating molecular fragments in the vapour phase that are representative of the target material. These vapour phase components are drawn into the ion mobility spectrometer source where they are ionised. Both positive and negative ions are formed and the spectrometer can operate in either mode. The ions are resolved into a pattern or signature characteristic of the polymer. Simpson and co-workers [42] examined polyvinyl chloride (PVC), Nylon 66, acrylonitrile – butadiene – styrene terpolymer, polyethylene terephthalate (PET) and polyethylene (PE), by this technique.

6.4.4 Gas Chromatography – Mass Spectrometry

This technique has been used in studies on styrene – isoprene block copolymer [43] and poly(vinylalcohol – vinyl acetate – vinyl acetate) copolymer [44].

6.4.5 Matrix-assisted Laser Desorption/Ionisation (MALDI) Mass Spectrometry

This technique has been used [45] in a study of the copolymerisation of allyl butyl ether (ABE) with methyl acrylate and butyl acrylate, using different free radical techniques. MALDI-TOF (time-of-flight) mass spectroscopic techniques are used to elucidate structural details. Well-defined copolymers containing about 20 mol% ABE are obtained using ethyl-2-bromoisobutyrate as initiator. Narrow molecular mass distributions result when atom transfer radical polymerisation is used, but this is much broader for a free radical polymerisation. In addition, free radical polymerisation results in low molar mass products compared with homopolymerisation of acrylates. This suggests that ABE acts as a chain transfer agent for free radical polymerisation. Reversible addition-fragmentation chain transfer copolymerisation also gives excellent control of the polymerisation and shows that ABE acts as a comonomer rather than chain transfer agent under these conditions.

Other applications of this technique include the determination of molecular weights of copolymers of MMA, butyl acrylate styrene, and maleic anhydride [46, 47], cyclic PS [48-50], thiophene – phenylene copolymers [51], methacryloxypropyltrimethoxy silane [52], various copolymers [53], PEG, polyetherimide photooxidation products [54], polyester – polyurethane [55], biodegradable polymers [56] and polyethylene – propylene oxide – ethylene oxide triblock polymers [57], ethylene isophthalate-bis(2-hydroxy ethyl terephthalate [58], MMA-1-octene [59], and acrylamide – acrylate [60].

6.5 NMR and Proton Magenetic Resonance Spectroscopy

Some typical NMR spectra of ethylene propylene copolymers are shown in **Figures 6.9 and 6.10**. The technique has been used in various structural studies on copolymers. Thus Hashidzume and co-workers [61], in an investigation of the spontaneous copolymerisation of 2,6-diisopropyl-*N*-methylene aniline with phthalic anhydride or with itaconic anhydride, showed that in the case of polymerisation of 2,6-diisopropyl-*N*-methylene aniline and phthalic anhydride, the copolymer was formed by a coupling reaction of a zwitterion one to one adduct. Also in the case of copolymerisation of 2,6-diisopropyl-*N*-methylene aniline and itaconic anhydride, the copolymer is formed by the addition polymerisation through the C=C bond in the itaconic anhydride moiety.

Drummond and co-workers [62] used proton magnetic resonance (PMR) spectroscopy to confirm the nature of the chemical linkages between the polyethylene glycol (PEG) segment and the poly(lactic-b-ethylene glycol – lactic acid) segments in poly(lactic acid-ethylene glycol-lactic acid) – PEG – poly(lactic acid-b-ethylene glycol-lactic
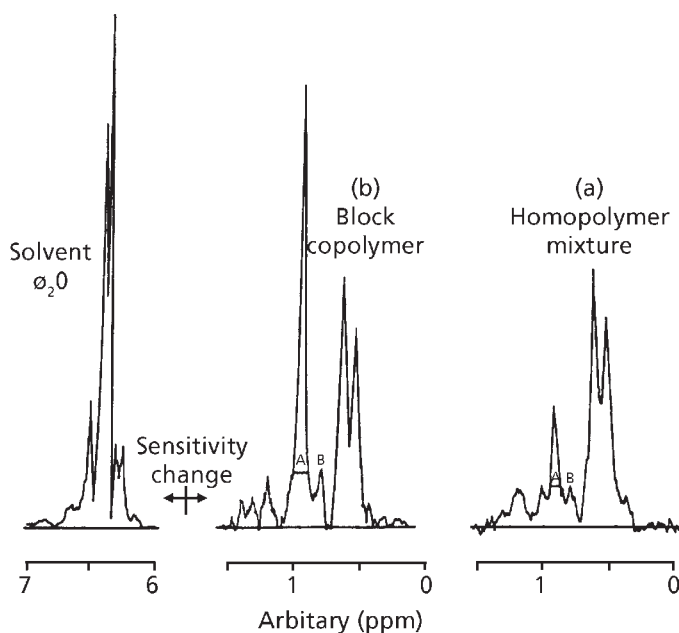
Figure 6.9 PMR spectra of (a) ethylene and propylene copolymers and (b) mixture of polyethylene and polypropylene copolymers. (*Source: Author's own files*)
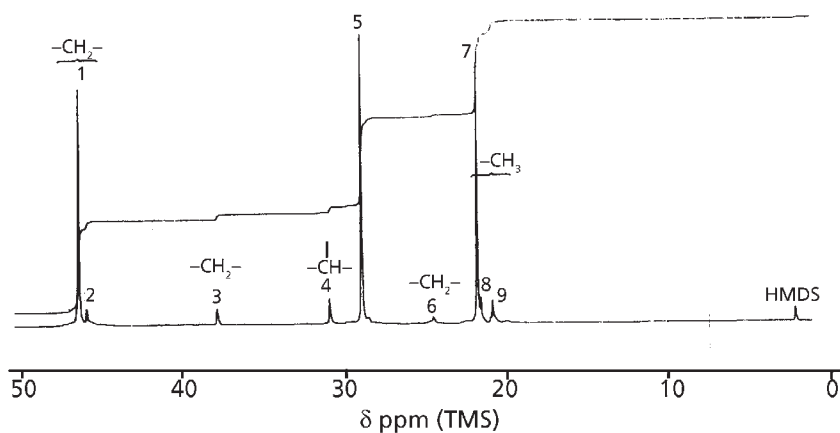
Figure 6.10 252 MHz ^{13}C proton noise decoupled NMR spectrum at 125 °C of 97:3 *w/v* ethylene-propylene copolymer in 1,2,4-trichlorobenzene and perdeutrobenzene. Internal standard: hexamethyldisoloxane. (*Source: Author's own files*)

acid) triblock copolymers. PMR spectroscopy was used to measure the degree of polymerisation of the poly(lactic acid-β-ethylene glycol-lactic acid) segments.

Rivas and Sánchez [63] used PMR in a characterisation of poly(*o* and *m* aminobenzylamine) aniline-Cu to show that polymeristion yield depended on the substituent position in the aromatic ring, and that when copper was incorporated in the copolymers, the amount incorporated was dependent on the side position in the aromatic ring.

Li and co-workers [64] showed that in the synthesis of a aminoquinoline – anisidene copolymer [65], the polymer obtained was a real copolymer containing both monomer units, rather than a mixture of two homopolymers. The 8-aminoquinoline content calculated based on the proton NMR spectra of the copolymers is slightly higher than the feed 8-aminoquinoline content when the feed 8-aminoquinoline content is lower than 70 mol%. However, the 8-aminoquinoline content calculated based on the carbon NMR and elemental analyses was lower than the feed 8-aminoquinoline content when the 8-aminoquinoline feed content was more than 50 mol%. A peculiar dependency of molecular weight and electroconductivity of the copolymers on the 8-aminoquinoline: anisidine ratio was observed.

Kawai and co-workers [66] determined the composition of butyl acrylate – ethyl acrylate copolymers with a narrow chemical composition distribution by ^{1}H-NMR spectroscopy. The components of the copolymers were separated by normal and reversed phase high-performance liquid chromatography (HPLC) using crosslinked acrylamide and styrene beads. Samples containing higher butyl acrylate content eluted faster with normal phase HPLC while the opposite occurred with reversed phase HPLC, indicating that butyl acrylate is less polar than ethyl acrylate.

Cheng and Lee [67] combined the use of 2-dimensional NMR and lanthanide shift reagents for the characterisation of ethylene – vinyl acetate copolymers.

Two-dimensional NMR has been extensively used and the technique is fairly routine for many applications. One consequence of the increasing use of 2-dimensional NMR is a revival of interest in ^{1}H-NMR for polymer studies. Yet, a major drawback of ^{1}H-NMR remains its limited chemical shift range, such that in complex molecules the resonances of different protons are frequently overlapped or incompletely resolved. Cheng and Lee [67] showed that the use of lanthanide shift reagents (LSR) combined with two-dimensional NMR can alleviate this difficulty in suitable cases.

They concluded that the combined use of lanthanide shift reagents with the 2D NMR experiment can provide detailed assignments (at the polymer microstructural level) of the ^{1}H and the ^{13}C spectra of ethylene – vinyl acetate copolymers. In

No.	Assignments			^{13}C shift (ppm)	
				Sample A	Sample B
A. Backbone carbons					
1a	CH		EVE	73.8 – 74.6	73.8-74.6
1b	CH		VVE	70.0 – 71.8	70.0-71.8
1c	CH		VVV	-	ca. 67.7
2a	CH_2		$S_{\alpha\alpha}$ - VVVE[a]	-	39.9
2b	CH_2		$S_{\alpha\alpha}$ - EVVE[a]	-	39.2
3a	CH_2		$s_{\alpha\gamma}$[a]	-	ca. 35.2
3b	CH_2		$s_{\alpha\delta}$	ca. 34.7	ca. 34.7
4a	CH_2		$s_{\delta\delta}$	30.0	30.0
4b	CH_2		$s_{\gamma\delta}$[c]	29.8	29.8
5a	CH_2		$s_{\beta\delta}$ - VEEE[a]	25.8	25.8
5b	CH_2		$s_{\beta\delta}$ - VEEV[a]	25.7	25.7
6	CH_2		$s_{\beta\beta}$	-	21.5
7	CH_3		(acetate)	21.0	21.0
B. Carbons due to chain branching[b]					
a	Bu-br	Am-br			38.2	38.2
b			Me-α		37.8	-
c	Bu-α	Am-α		L-α	34.6	34.6?
c		Am-5				
d	Bu-4				34.1	34.1
e			Me-br		33.3	-
f		Am-3			32.8	-
g				L-3	32.3	-
h	Bu-3				30.0	30.0
i	Bu-β	Am-β		L-β	27.5	27.3
j		Am-4	Me-β		26.8	-
k	Bu-2				23.5	23.5
l		Am-2		L-2	22.9	-
m			Me-1		20.0	-
n	Bu-1	Am-1		L-l	14.0	14.1

Table 6.1 Assignments in NMR spectra of ethylene – vinylacetate copolymers

[a] *Assignments made in this work*
[b] *Terminology follows that of low-density polyethylene*
[c] *Possible overlap due to $s_{\alpha\beta}$ (due to inversion of vinyl acetate)*

*Reprinted with permission from H.N. Cheng and G.H. Lee, Polymer Bulletin, 1988, **19**, 1, 89, [67]. Copyright 1988, Springer*

addition, comonomer sequence distribution can be obtained from the LSR-shifted ^{1}H spectrum of ethylene – vinyl acetate copolymer. Other 2-dimensional approaches (e.g., correlation spectroscopy) can also be used in conjunction with lanthanide shift reagents [67].

The assignments of the comonomer sequences in the ^{13}C-NMR generally agree with those of the previous works. A bonus of the 2-dimensional/shift reagent work is that additional features can be noticed. The complete ^{13}C-NMR interpretation of ethylene – vinyl acetate copolymer, including several new assignments, is given in **Table 6.1**. Two copolymers with different compositions have been used. The ^{13}C spectra show distinctive differences; these are due both to the intensity differences in backbone carbons, and to the differences in chain branching, which occurs at low vinyl acetate concentrations.

Other applications of NMR resonance spectroscopy include: styrene – methacrylate [68], propylene – isobutylene [69, 73], ethylene-1-hexane [71], ethylene – vinyl acetate [72], and epoxy styrene [70].

Other applications of PMR include: propylene – styrene [74], α-methyl styrene-*p*-methyl α methyl styrene [75], acrylic-2 substituted 1, 3-diolefins [76], ethylene – ethyl acrylate [77], ethylene acrylate – carbon monoxide [77], ethylene-2-ethyl acrylate-carbon monoxide [77], styrene – MMA [78], α-methyl styrene – butadiene [79, 80], vinyl chloride – trichloroethylene [81], methyl acrylate – acrylonitrile [82], ethylene – vinyl acetate [83], ethylene – vinyl chloride [74], ethylene vinylidene chloride [74], MMA – acrylonitrile [76], methacrylonitrile – isoprene [76], methacrylonitrile – chloroprene [76], bisphenol A – PC [84, 85], chloromethylated PS [86], chloromethylated PS – vinylidine chloride [86], chloromethylated PS – polypropylene oxides [86], vinyl chloride – vinylidine chloride [87, 88, 89], acrylonitrile – styrene [90], acrylonitrile – butadiene [90], methylacrylonitrile – butadiene [90], carboxy terminated adipic acid – ethylene glycol [91], adipic acid – Neopentyl glycol [92], chloroprene – MMA [88], propylene – styrene [87], MMA – styrene [78] and PMMA graft poly(bis(trifluoroethyoxy) phosphazine) [93].

The application of NMR spectroscopy to copolymer characterisation is discussed further in Sections 3.1.3, 3.2.2, 3.4.5, 3.6.2, 3.7.4, 3.9.5, 4.1, 4.2.2 – 4.2.4, 4.4.2 – 4.4.4, 4.4.7, 4.7, 4.9, 4.13 and 4.14.

6.6 Pyrolysis Techniques

Examination of pyrolysis products of copolymers by gas chromatographic and IR spectroscopic techniques are discussed in Sections 3.2.3, 3.4.3, 3.7.2, 3.9.6, 4.1, 4.2.2, 4.3.1, 4.4.4, 4.4.5, 4.8, and 4.13.

6.7 Other Techniques

Another technique which is extremely useful in deducing the microstructure of copolymers, cleavage by acid or fusion with solid alkalies followed by identification and determination of the cleavage products by GC (See Sections 3.7.1, 3.7.6 and 3.13.1).

Thus, in the polyimide:
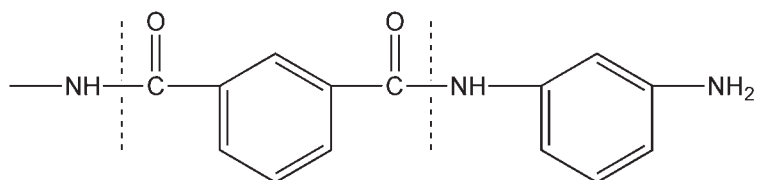
Acid fusion of bonds produces a diamine and alkali fusion of this bond produces:
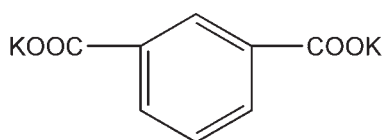
References

1.   M. Johnson-Plaumann, H. Plaumann and S. Keeler, *Rubber Chemistry and Technology*, 1986, **59**, 4, 580.

2.   M.M. Partnov, S.F. Salova, M.G. Matvev and V.S. Shein, *Vysokomolekulyarnye Soedineniya Seriya B*, 1987, **29**, 243.

3.   S.H. Kandil and M.A. El-Gamal, *Journal of Polymer Science, Part A: Polymer Chemistry*, 1986, **24**, 11, 2765.

4.   S.M. Aliev, M.R. Bairomov, A.G. Aziziv, S.A. Aliev and S.T. Akhmedov, *Azerbaidzhanskii Khimicheskii Zhurnal*, 1976, **3**, 70.

5.   J.E. Forrette and A.L. Rozek, *Journal of Applied Polymer Science*, 1974, **18**, 10, 2973.

6.   R. Aslanova, A.A. Yul'chivaev and K.U. Usmanov, *Uzbekskii Khimicheskii Zhurnal*, 1973, **17**, 31.

7.   K.S. Chia, G.M.S. Chen and J. Chin, *Chemistry (Taipei),* 1973, **20**, 241.

8.   F.M. Mirabella, E.M. Barrall and J.F. Johnson, *Polymer,* 1976, **17**, 1, 17.

9.   M.D. Bruch, *Macromolecules*, 1988, **21**, 2, 2707.

10.   J.V. Dawkins and M.J. Hemming, *Journal of Applied Polymer Science,* 1975, **19**, 11, 3107.

11.   W.H. Littke, W. Flebec, R. Schmote and B.W. Kimmer, *Faserforschung und Textiltechnik,* 1975, **26**, 503.

12.   K. Studer, C. Decker, E. Beck and R. Schwalm in *Proceedings of the European Coatings Conference 2004: Polyurethanes for High Performance Coatings III,* Berlin, Germany, 2004.

13.   P. Das, C.N. Saikia and N.N. Dass, *Journal of Applied Polymer Science,* 2004, **92**, 6, 3471.

14.   P. Sivaraman, N.R. Manoj, S. Barman, L. Chandrasekhar, V.S. Mishra, A.B. Samui and B.C. Chakraborty, *Polymer Testing*, 2004, **23**, 6, 645.

15.   D. Cheng, I. Gardner, C. Frederick, A. Dekmezian and H. Wang, *Rubber Chemistry and Technology*, 1990, **63**, 2, 265.

16.   L. Dong and D.J.T. Hill, *Polymer Bulletin*, 1995, **34**, 3, 323.

17.   A. Nagata, K. Ohta and R. Iwamoto, *Macromolecular Chemistry and Physics*, **197**, 6, 1959.

18.   N. Oi, K. Miyazaki, K. Moriguchi and H. Shimada, *Kobunshi Kagaku, English Edition,* 1972, **29**, 388.

19.   R.M. Briber and E.L. Thomas, *Polymer*, 1985, **26**, 1, 8.

20.   T. Doiuchi, H. Yamaguchi and Y. Minoura, *European Polymer Journal*, 1981, **17**, 9, 961.

21.   S. Kawaguchi, T. Kitano and K. Ito, *Macromolecules*, 1991, **24**, 22, 6030.

22.   F. Danusso, M.C. Tanzi, M. Levi and A. Martini, *Polymer*, 1990, **31**, 8, 1577.

23.   G. Schnell, *Berichte Der Bunsen-Gesellschaft*, 1966, **70**, 297.

24.   Y. Yamashita, *Kagaku Zokan*, 1967, **27**, 59.

25. T.N. Bowmer and A.E. Tonelli, *Journal of Polymer Science, Part B: Polymer Physics*, 1986, **24**, 8, 1631.

26. G.H. Olive and S. Olive, *Advances in Polymer Science 32*, Ed., H.J. Cantow, Springer Verlag, Berlin, Germany, p.123.

27. W.R. Krigbaum and N. Tokita, *Journal of Polymer Science,* 1960, **43**, 142, 467.

28. C.R. Bohn, J.R. Schaefgen and W.O. Statton, *Journal of Polymer Science,* 1961, **55**, 162, 531.

29. X-G. Li, M-R. Huang, M-F. Zhu and Y-M. Chen, *Polymer*, 2004, **45**, 2, 385.

30. J. Li, M.F. Lai, J.J. Liu, *Journal of Applied Polymer Science*, 2004, **92**, 4, 2514.

31. H. Ma, T. Uchida, D.M. Collard, D.A. Schiraldi and S. Kumar, *Macromolecules*, 2004, **37**, 20, 7643.

32. S. Tanaka, A. Ogura, T. Kaneko, Y. Murata and M. Akashi, *Macromolecules*, 2004, **37**, 4, 1370.

33. W.P. Li, S.S. Guo, Y.W. Tang, C.L. Sun and X.Z. Zhao, *Journal of Materials Science*, 2004, **39**, 5, 1827.

34. T. Begam, R.S. Tomar, A.K. Nagpal and R. Singhal, *Journal of Applied Polymer Science,* 2004, **94**, 1, 40.

35. X. Wang and X. Luo, *European Polymer Journal*, 2004, **40**, 10, 2391.

36. J. K. Agbenyega, G. Ellis, P. J. Hendra, W. F. Maddams, C. Passingham, H. A. Willis and J. Chalmers, *Spectrochimica Acta Part A*: *Molecular Spectroscopy*, 1990, **46A**, 197.

37. H. G. M. Edwards, A. F. Johnson, I. R. Lewis and J. M. G. Cowie, *Polymer International*, 1993, **31**, 4, 3912.

38. C.R. Shick, Jr., P.A. de Palma and R.K. Marcus, *Analytical Chemistry,* 1996, **68**, 13, 2113.

39. G. Montaudo, E. Scamporrino, C. Puglisi, and D. Vitalini, *Macromolecules*, 1988, 21, 6, 1594.

40. G. Montaudo and S. Daolio, *Rapid Communications in Mass Spectrometry*, 1991, **5**, 3, 95.

41. G. Montaudo, E. Scamporrino and D. Vitalini, *Applied Polymer Analytical Characterisation*, 1992, **2**, 79.

42. M. Simpson, D.R. Anderson, C.W. McLeod and M. Cooke, *Analyst*, 1993, **118**, 4, 449.

43. W.H. McClennen, R.M. Buchanan, N.S. Arnold, J.P. Dworzanski and H.L.C. Meuzelaar, *Analytical Chemistry,* 1993, **65**, 20, 2819.

44. F. Becquart, M. Taha, A. Zerroukhi, J. Kaczun and U. Stebani, *Polymer International*, 2004, **53**, 4, 412.

45. R. Venkatesh, F. Vergouwen and B. Klumperman, *Journal of Polymer Science, Part A: Polymer Chemistry*, 2004, **42**, 13, 3271.

46. A.M. Hawkridge and J.A. Gardella, *Polymer Preprints: Conference Proceedings*, San Francisco, CA, USA, 2000, **41**, 1, 635.

47. M.S. Montaudo, *Polymer News*, 2002, **27**, 4, 115.

48. C.M. Guttman, S.J. Wetzel, W.R. Blair, B.M. Fanconi, J.E. Girard, R.J. Goldschmidt, W.E. Wallace and D.L. van der Hart, *Analytical Chemistry,* 2001, **73**, 6, 1252.

49. B. Lepoittevin, X. Perrot, M. Masure and P. Hemery, 2001, **34**, 3, 425.

50. S. Hunt, G. Cash, H. Liu, G. George and D. Birtwistle, *Journal of Macromolecular Science,* 2002, **A39**, 9, 1007.

51. M. Jayakannan, J.L.J. van Dongen and R.A.J. Janssen, *Macromolecules,* 2001, **34**, 16, 5386.

52. P. Eisenberg, R. Erra-Balsells, Y. Ishikawa, J.C. Lucas, H. Nonami and R.J. Williams, *Macromolecules,* 2002, **35**, 4, 1160.

53. M.S. Montaudo, C. Puglisi, F. Samperi and G. Montaudo, *Polymer Preprints,* 2000, **41**, 1, 686.

54. L.S. Carroccio, C. Puglisi and G. Montaudo, *Polymer Degradation and Stability,* 2003, **80**, 3, 459.

55. R. Murgasova, E.L. Brantley, D.M. Hercules and H. Nefzger, *Macromolecules,* 2002, **35**, 22, 8338.

56. S. Karlsson, *Polymer News*, 2002, **27**, 9, 305.

57. G. Gallet, S. Carroccio, R.J. Rizzarelli and S. Karlsson, *Polymer,* 2002, **43**, 4, 1081.

58. R. Nagahata, J.J. Sugiyama, S. Velmaichie, Y. Nahao, M. Goto and K. Takenchi, *Polymer Journal (Japan)*, 2004, **36**, 483.

59. R. Venkatesh and B. Klumperman, *Macromolecules*, 2004, **37**, 4, 1226.

60. W.M. Leung, D.E. Axelson and J.D. Van Dyke, *Journal of Polymer Science, Part A: Polymer Chemistry*, 1987, **25**, 7, 1825.

61. A. Hashidzume, Y. Kurokawa, A. Harada and M. Kamach, *Designed Monomers and Polymers*, 2004, **7**, 4, 361.

62. W.S. Drummond and S.H. Wang, *Polymer*, 2004, **14**, 74.

63. B.L. Rivas and C.O. Sánchez, *Journal of Applied Polymer Science,* 2004, **92**, 1, 31.

64. X-G. Li, M-R. Huang, Y-M. Hua, M-F. Zhu and Q. Chen, *Polymer*, 2004, **45**, 14, 4693.

65. G.V.S. Shashidhar, K. Ranga Rao, N. Satyanarayana and E.V. Sundaram, *Journal of Polymer Science, Part C: Polymer Letters*, 1990, **28**, 5, 157.

66. E. Kawai, H.C. Lee, Y. Takao, K. Ogino and H. Sato, *Nippon Gomu Kyokaishi,* 2002, **75**, 465.

67. H.N. Cheng and G.H. Lee, *Polymer Bulletin*, 1988, **19**, 1, 89.

68. G.H.J. Van Doremaele, A.L. German, N.K. De Vries and G.P.M. van der Velden, *Macromolecules*, 1990, **23**, 19, 4206.

69. A. Aoki, T. Hayashi and T. Asakura, *Macromolecules*, 1992, **25**, 1, 155.

70. H.N. Cheng, *Macromolecules*, 1991, **24**, 17, 4813.

71. H.N. Cheng, *Polymer Bulletin*, 1991, **26**, 3, 325.

72. A. Viallat, J. P. Cohen-Addad, P. Cassagnau and A. Michel, *Polymer*, 1996, **37**, 4, 555.

73. R.K. Harris, R.R. Yeung, P. Johncock and D.A. Jones, *Polymer*, 1996, **37**, 5, 721.

74. S. Kobayashi, Y. Kato, H. Watanabe and A. Nishioka, *Journal of Polymer Science, Part A-1: Polymer Chemistry*, 1966, **4**, 1, 425.

75. E.M. Banas and O.O. Juveland, *Journal of Polymer Science, Part A-1: Polymer Chemistry*, 1967, **5**, 2, 397.

76. J. Furukawa, E. Kobayashi, Y. Arai, T. Suzuki and Y. Takegami, *Journal of Polymer Science, Part A-1: Polymer Chemistry*, 1976, **14**, 10, 2553.

77. J.E. McGrath and L.M. Robeson, *American Chemical Society Division of Polymer Chemistry*, 1976, **17**, 706.

78. S. Yabumoto, K. Ishii and K. Arita, *Journal of Polymer Science, Part A-1: Polymer Chemistry*, 1970, **8**, 2, 295.

79. K.F. Elgert, G. Seller, G. Puschendorf and H.J. Cantow, *Makromolekulare Chemie*, 1973, **165**, 1, 245.

80. K.F. Elgert, G. Seller, G. Puschendorf and H.J. Cantow, *Makromolekulare Chemie*, 1973, **165**, 1, 261.

81. M.F. Froix, A.O. Goedde and J.M. Pochan, *Makromolecules*, 1977, **10**, 4, 778.

82. K. Udipi, H.J. Harewood, H. Fribolin and H.J. Cantow, *Makromolekulare Chemie*, 1973, **164**, 1, 283.

83. J. Sabottka, G. Keller and K. Wienderlich, *Faserforsch Textiltech*, 1974, **25**, 352.

84. D. Stefan and H.L. Williams, *Journal of Applied Polymer Science*, 1974, **18**, 1279.

85. D. Stefan and H.L. Williams, *Journal of Applied Polymer Science*, 1974, **18**, 1451.

86. I. Cabasso, J. Jagur-Grodzinski and D. Vofsi, *Journal of Applied Polymer Science*, 1974, **18**, 7, 1969.

87. J.L. McClanahan and S.A. Previtera, *Journal of Polymer Science, Part A: General Papers*, 1965, **3**, 11, 3919.

88. K. Okuda, *Journal of Polymer Science: Part A-1*, 1964, **2**, 1, 171.

89. S. Kobayashi, Y. Kato, H. Watanabe and A. Nishioka, *Journal of Polymer Science, Part A-1: Polymer Chemistry*, 1966, **4**, 1, 245.

90. W. Kimmer and R. Schmalke, *Plaste und Kautschuk*, 1973, **20**, 274.

91. R.S. Barshtein, Y.A. Urman, V.G. Gorbunova, T.S. Khramova, A.K. Bulai and I.Y. Sionin, *Doklady Akademii Nauk, Moscow*, 1972, **206**, 1140.

92.   J.R. Ebdon, *Polymer*, 1974, **15**, 12, 782.

93.   H.R. Allcock, E.S. Powell, A.E. Maher and E.B. Berda, *Macromolecules*, 2004, **37**, 15, 5824.

7 X-Ray Photoelectron Spectroscopy

Electron spectroscopy encompasses two main techniques, X-ray photoelectron spectroscopy (XPS; also known as electron spectroscopy for chemical analysis; ESC) and Auger electron spectroscopy (AES). Both techniques identify and quantify elements present and can indicate the chemical state or functionality of elements at the surface. For best results, AES relies upon the sample being electrically conducting and consequently it is very rarely used in polymer analysis [1]. Hence it is not discussed further here.

XPS uses an X-ray beam to cause the emission of electrons from the surface of the sample. The electrons analysed do not have enough energy to escape from a depth of more than ~3-5 nm, so the XPS technique is inherently surface sensitive. The binding energy of the emitted electrons is measured and used to identify the elements present.

XPS is best performed using a monochromatic X-ray source. Monochromatic XPS inflicts the least damage to delicate materials and optimises chemical state sensitivity. A monochromatic X-ray source is an essential requirement to extract the maximum information content from most polymer systems.

The thickness of surface layers and the depth distributions in the extreme surface region can be measured using angle-dependent XPS. By simply changing the angle of the sample to the detector, the effective depth of analysis can be varied in the range 1–10 nm.

XPS is a good technique for elemental analysis of solids and low vapour pressure liquids, with a detection limit to most elements of ~1000 ppm. It can be directly quantified; showing not only what is present, but also how much. This technique can be used to analyse polymers to a surface depth of 1–10 nm.

Swift [1] has discussed the fundamental principles of XPS (and SIMS; secondary ion mass spectrometry) and demonstrates the use of these surface analytical techniques in problem solving. XPS can supply information on factors such as surface coating integrity (e.g., in medical polymer applications, or plastic coating of metals or wire), contamination, molecular diffusion and adsorption phenomena [2], and characterisation of polymer surfaces. Often XPS is used in conjunction with SIMS to solve problems, as discussed in Section 5.4.1.

385

Huang and co-workers [3] used X-ray photoelectron spectroscopy in studies of the underlying hydrogen bonding interactions of blends of a fluorinated polymer containing pyridine, and a non-fluorinated polymer containing methacrylic acid. Although the anchoring effect of hydrogen bonding hindered the migration of the fluorinated component to the surface of the blend, it did not completely eliminate the surface enrichment of the fluorinated component and the surface rearrangement of the fluorinated pendent chain.

Bedekar and co-workers [4] characterised a series of polyaromatic diamines including polymers of *o*-chloroaniline, benzidine, 4,4′ diaminodiphenyl ether and diaminodiphenyl methane using a variety of techniques including X-ray photoelectron spectroscopy, Fourier transform infrared (FTIR) spectroscopy, and elemental analysis. They found that polymers of diamine compounds had an additional S and O in the form of sulfate ions in the polymer matrix.

An attempt was made to elucidate the structure of these polymers and correlate behaviour with structure. A chlorination reaction taking place during synthesis or doping was indicated by the presence of covalent bonded chlorine in the polymers. The difference in structure and less ionically bonded chlorine over covalent chlorine could be the factors that explained the low conductivity of polymers of diamines, compared with that of polyanilines or its derivatives [5].

In addition to polymer characterisation, X-ray photoelectron spectroscopy has been used in a variety of studies, as discussed in the following sections.

7.1 Bulk Polymer Structural Studies

These include studies on reactions between polyacrylic acid and polymethacrylic acid, and polyacrylic acid with poly(4-vinyl pyridine) and poly(2-vinyl pyridene) [6], polybithiophene [7], polyvinyl carbazole sulfonation products [8], β-hydroxybutyrate and β-hydroxyvalerate containing Biopol [9].

7.2 Adhesion Studies

Rattana and co-workers [10] and Leadley and co-workers [11] have studied the adhesion of aluminium and epoxy resins using amine and organosilane primers. Leadley and co-workers [11] give details of coating delamination in a hot, humid environment for a cationic radiation-cured coating of cycloaliphatic epoxy resin. XPS and time-of-flight (ToF) mass spectroscopy of the delaminated surface showed that the phosphorus hexafluoride anion of the photoinitiator segregates to the interface. The durability of the coating was improved by reformulation with a reduced concentration of photoinitiator.

Hoyt and co-workers [12] studied the characteristics of functionalised polysiloxanes and silica coated aluminium nitride filled poly(3-cyanopropylmethyl)siloxane microcomposites, which are considered to be promising thermally conductive adhesives. The interactions between the polysiloxane and filler particles is discussed. It is shown that the polysiloxanes interact strongly with the filler, via interactions between siloxane pendent electron donating groups and the oxide layer on the filler particles. The adhesion and hydrogen bonding capabilities of the polysiloxanes are confirmed by X-ray photoelectron spectroscopy, nuclear magnetic resonance (NMR) and peel strength testing.

Small area XPS has established that electrochemistry is responsible for initial bond degradation in a phosphated, hot-dipped galvanised steel lap joint [13]. A surface analysis investigation of the failure mechanism of adhesively bonded hot dipped galvanised steel exposed to a hostile environment is reported. The failed lap shear joints show areas of apparent interfacial failure, however, these regions are limited to the end of the overlap (and for the purposes of this study are termed initiation zones). These initiation zones seem to be a result of environmental exposure and appear to act as initiation sites for crack propagation on mechanical testing acting as 'notch like' features. These areas of the failed surface are reported, with a view to establishing the role of electrochemical activity at the crevice tip, and its role in the subsequent joint failure.

7.3 Carbon Black Studies

A determination has been carried out of Buckminsterfullerene in carbon black [14].

7.4 Particle Identification

Stickle [15] used XPS, ToF-SIMS, and Auger electron microscopy to carry out particle analysis. It is concluded that XPS has limited utility in this application, but that it can be used as a complementary characterisation tool to ToF-SIMS and AES for particle identification.

7.5 Pyrolysis Studies

XPS has been applied to the study of pyrolysis products of poly(1,4-diphenyl-1-buten-3-yne) [16] and polyphenylsilesquioxane [17, 18].

7.6 Surface Studies

Surface studies have been carried out on polyethylene fibre/polyethylene [19], rubbers [20] and polyamides [21].

7.7 Applications in Which Only XPS is Used

Structural studies of polymer surfaces: materials that have been studied include polymethyl methacrylate (PMMA) [22], PMMA-polypyrrole composites [23], poly(chloromethyl styrene) bound 1,4,8,11 tetrazacrylotetra decane poly(chloromethyl styrene) bound theonyl trifluoroacetone [24], polydimethyl siloxane-polyamide copolymers [25], PS [26], ion-implanted PE [27], monoazido-terminated polyethylene oxide [28], polyurethanes [29], polyaniline [30], fluorinated polymer films [31], poly(*o*-toluidine) [32], polyetherimide and polybenzimidazole [33], polyfullerene palladium [34], imidazole-containing imidazolylethyl maleamic acid – octadecyl vinyl ether copolymer [35], polyphenylene vinylene ether [36], thiphene oligomers [37], fluorinated styrene-isoprene derivative of a methyl methacrylate-hydroxyethyl methacrylate copolymer [38], polythiophene [39], dibromoalkane-hexafluorisopropylidene diphenol and bisphenol A [40], and geopolymers [41].

ToF-SIMS has been used extensively in the characterisation of polymers (see Section 5.4.1). Occasionally, XPS and ToF-SIMS are used in conjunction.

7.8 Applications in Which Both XPS and ToF-SIMS are Used

Some examples of these applications include studies on *p*-hydroxybenzoic acid-6-hydroxy-2-naphthoic acid copolyester-based adhesives [42] and further miscellaneous studies on adhesion [43, 44]. West [45] and Berrand and Wang [46] characterised medical polymers using XPS and ToF-SIMS. These two techniques have also been used to characterise carbon black surfaces [46] and carbon fibres [47]. Other workers have reviewed various aspects of the application of ToF-SIMS to polymer surface studies [48–51].

References

1.   A.J. Swift in *Proceedings of a Rapra Conference on Developments in Polymer Analysis and Characterisation*, Shawbury, UK, 1999, Paper No.3.

2.   R. West in *Proceedings of Rapra Polymers for the Medical Industry - Characterising Medical Polymer Supply Chain by Surface Analysis*

Conference, London, UK, Paper No.18.

3.   H.L. Huang, S.H. Goh, D.M.Y. Lai, A.T.S. Wee and C.H.A. Huan, *Journal of Polymer Science, Part B: Polymer Physics*, 2004, **42**, 7, 1145.

4.   B.A. Bedekar, H.S. Rama and V.K. Kaushik, *Polymer - Plastics Technology and Engineering*, 2001, **40**, 3, 321.

5.   X. Zhou, S.H. Goh, S.Y. Lee and K.L. Tan, *Polymer*, 1998, **39**, 16, 3631.

6.   H. Niino and A. Yabe, *Journal of Polymer Science, Part A: Polymer Chemistry*, 1998, **36**, 14, 2483.

7.   F. Samir, M. Morsti, J.C. Bernede, A. Bonnet and S. Lefrant, *Journal of Applied Polymer Science*, 1997, **66**, 10, 1839.

8.   L-T. Weng, P.C.L. Wong, K. Ho, S. Wang, Z. Zeng and S. Yang, *Analytical Chemistry*, 2000, **72**, 20, 4908.

9.   F-R. Lang, D. Leonard, H. J. Mathieu, E.M. Moser and P. Bertrand, *Macromolecules*, 1998, **31**, 18, 6177.

10.   A. Rattana, J.D. Hermes, M-L. Abel and J.F. Watts, *International Journal of Adhesion and Adhesives*, 2002, **22**, 3, 205.

11.   S.R. Leadley, J.F. Watts, A. Rodriguez and C. Lowe, *International Journal of Adhesion and Adhesives*, 1998, **18**, 3, 193.

12.   J. Hoyt, Y. Kim, J. Riffle and J. McGrath, *Adhesives Age*, 2002, **45**, 19.

13.   M.F. Fitzpatrick, J.F. Watts and J.S.G. Ling, *Proceedings of the ACS Materials Science and Engineering Conference*, New Orleans, USA, Fall Meeting, 1999, Volume 81, 417.

14.   P. Johnson, R.W. Locke, J.B. Donnet, T.K. Wang, C.C. Wang and P. Bertrand, *Proceedings of the 156th ACS Rubber Division Meeting*, Orlando, FL, USA, Fall 1999, Paper No. 179.

15.   W.F. Stickle, *Particles on Surfaces: Detection, Adhesion and Removal, Volume 7*, Ed., K. Mittal, VSP BV, Utrecht, The Netherlands, 2002, p.3.

16.   S.C. Shim, M.C. Suh and D.S. Kim, *Journal of Polymer Science, Part A: Polymer Chemistry*, 1996, **34**, 15, 3131.

17.   J. Ma, L-H. Shi, J-M. Zhang, B-Y. Li, D-Y. Shen and J. Xu, *Chinese Journal*

of Polymer Science, 2002, **20**, 6, 573.

18. J. Ma, L-H. Shi, Y. Shi, S. Luo and J. Xu, *Journal of Applied Polymer Science*, 2002, **85**, 5, 1077.

19. T. Ogawa, H. Mukai and S. Osawa, *Journal of Applied Polymer Science*, 1999, **71**, 2, 243.

20. M. Dimopoulos, N.R. Choudhury, M. Ginic-Markovic, J. Matisons and D.R.G. Williams, *Journal of Adhesion Science and Technology*, 1998, **12**, 12, 1377.

21. C.N. Extrand in *Contact Wettability and Adhesion, Volume 2*, Ed., K.L. Mittal, VSP VB, Utrecht, The Netherlands, 2002, p.289.

22. S. Gross, G. Trimmel, U. Schubert and V. Di Noto, *Polymers for Advanced Technologies*, 2002, **13**, 3, 254.

23. M. Omastova, J. Pavlinec, J. Pionteck, F. Simon and S. Kosina, *Polymer*, 1998, **39**, 25, 6559.

24. Y-R. Wang, Y. Luo, R-M. Wang and L. Yuan, *Journal of Applied Polymer Science*, 1997, **66**, 4, 755.

25. K. Shenshu, T. Furuzona, N. Koshizaki, S. Yamashita, T. Matsumoto, A. Kishida and M. Akashi, *Macromolecules*, 1997, **30**, 15, 4221.

26. Z. Lei, X. Han, Y. Hu, R-M. Wang and Y-R. Wang, *Journal of Applied Polymer Science*, 2000, **75**, 8, 1068.

27. L-S. Tan, K. R. Srinivasan, S.J. Bai and R.J. Spry, *Journal of Polymer Science*, 1998, **36**, 5, 715.

28. X-D. Huang, S.H. Goh and S.Y. Lee, *Macromolecular Chemistry and Physics*, 2000, 201, **18**, 2660.

29. X. Duan, C.M. Griffith, M.A. Dube and H. Sheardown, *Journal of Biomaterials Science, Polymer Edition*, 2002, **13**, 6, 667.

30. L. Zhao, K.G. Neoh and E.T. Kong, *Chemistry of Materials*, 2002, **14**, 3, 1098.

31. V.N. Vasilets, I. Hirata, H. Iwata and Y. Ikada, *Journal of Polymer Science, Part A: Polymer Chemistry*, 1998, **36**, 13, 2215.

32. M. Wan and J. Li, *Polymers for Advanced Technologies*, 2003, **14**, 3–5, 320.

33. T-S. Chung, Z-L. Xu and C-H.A. Huan, *Journal of Polymer Science, Part B: Polymer Physics*, 1999, 37, 14, 1575.

34. K. Winkler, K. Noworyta, A. de Bettencourt-Dias, J.W. Sobczak, C-T. Wu, L-C. Chen, W. Kutner and A.L. Balch, *Journal of Materials Chemistry*, 2003, **13**, 3, 518.

35. H. Jeoung, Y.S. Kwan, B.J. Lee and C.S. Ha, *Molecular Crystals and Liquid Crystals, Section A*, 1997, **294–295**, 443.

36. K. Alimi, P. Molinie, V. Blel, J.L. Fave, J.C. Bernede and M. Ghedira, *Synthetic Metals*, 2002, **126**, 1, 19.

37. J.C. Bernede, Y. Tregouet, E. Gourmelon, F. Martinez and G. Neculqueo, *Polymer Degradation and Stability*, 1997, **55**, 1, 55.

38. A. Böker, T. Herweg and K. Reihs, *Macromolecules*, 2002, **35**, 13, 4929.

39. L. Ugalde, J.C. Bernede, M.A. Del Valle, F.R. Diaz and P. LeRay, *Journal of Applied Polymer Science*, 2002, **84**, 10, 1799.

40. L. Li, C-M. Chan, S. Liu, L. An, K-M. Ng, L-T. Weng and K-C. Ho, *Macromolecules*, 2000, **33**, 21, 8002.

41. H. Xu and J.S.J. Van Deventer, *Industrial and Engineering Chemistry Research*, 2003, **42**, 8, 1698.

42. D. Frich, A. Hall and *J. Economy, Macromolecular Chemistry and Physics*, 1998, **199**, 5, 913.

43. M.C. Biesinger, P-Y. Paepegaey, N.S. Mclntyre, R.R. Harbottle and N.O. Petersen, *Analytical Chemistry*, 2002, **74**, 22, 5711.

44. J.F. Watts and J.E. Castle, *Advanced Composite Materials*, 1999, **19**, 6, 435.

45. R. West in *Proceedings of Polymers for the Medical Industry Conference*, London, UK, Rapra Technology, 1999, Paper No.18.

46. P. Berrand and L.T. Weng in *Proceedings of the 153rd ACS Rubber Division Meeting*, Indianapolis, IN, USA, Spring 1998, Paper No.38.

47. J.F. Watts, P.E. Vickers, A.C. Prickett and P.A. Smith, *Proceedings of the ACS Polymeric Materials Science and Engineering Meeting*, New Orleans, LA, USA, 1999, Volume 81, 380.

48. M. Brenda, R. Döring and U. Schernau, *Progress in Organic Coatings*, 1999, 35, 1–4, 183.

49. D.A. Cole, *Journal of the Adhesive and Sealant Council*, Fall 1996, **1**, 503.

50. R. Michel, R. Luginbuehl, D. Graham and B.D. Ratner, *Polymer Preprints*, 1999, **40**, 2, 591.

51. R.R. Thomas, K.G. Lloyd, K.M. Stika, L.E. Stephans, G.S. Magallanes, V.L. Dimonie, E.D. Sudol and M.S. El-Aasser, *Macromolecules*, 2000, **33**, 23, 8828.

8 Atomic Force Microscopy and Microthermal Analysis

8.1 Atomic Force Microscopy

Scanning probe microscopy initially provided three-dimensional visualisation of surfaces down to the atomic scale using scanning tunnelling and atomic force microscopy (AFM). Today, a range of imaging modes and spectroscopic techniques can be used to determine additional information on physical, chemical, and thermal properties of polymeric materials. Examples of the uses of lateral force microscopy, to determine surface friction and force modulation to elucidate surface stiffness, have been presented. Pulsed force mode now enables both of these properties to be displayed simultaneously. Intermittent contact (tapping force) atomic force microscopy (AFM) combined with phase imaging provides fast imaging of soft polymers, combined with simultaneous materials contrast based on surface viscoelastic properties. Hence, the spatial distribution of multi-component polymers can be determined.

The past decade has witnessed an explosion of techniques used to pattern polymers on the nano- and sub-micrometre scale. This has been driven by the extensive versatility of polymers for diverse applications such as molecular electronics, data storage, and all forms of sensors. Lyuksyutov and co-workers [1] demonstrate a novel lithography technique – electrostatic nanolithography using AFM – that generates features by mass transport of polymers within an initially uniform, planar film, without chemical crosslinking, substantial polymer degradation or ablation.

8.1.1 Polymer Characterisation Studies and Polymer Structure

The application of AFM and other techniques has been discussed in general terms by several workers [2–5]. Other complementary techniques covered in these papers include Fourier transform infrared (FTIR), Raman spectroscopy, nuclear magnetic resonance spectroscopy (NMR) spectroscopy, surface analysis by spectroscopy, gas chromatographyh mass spectroscopy (GC-MS), scanning tunnelling microscopy, electron crystallography, X-ray studies using synchrotron radiation, neutron scattering techniques, mixed crystal infrared spectroscopy, secondary ion mass spectroscopy (SIMS), and X-ray photoelectron spectroscopy (XPS).

Lüpke and co-workers [6] studied the structural changes, at a molecular and super molecular level, of polypropylene (PP), and related this to changes in melting behaviour and mechanical properties. Cast films drawn successively in two perpendicular directions, at temperatures near the melting point, were investigated. Quantitative X-ray texture analysis, small angle X-ray scattering and atomic force microscopy were used to characterise the structure. The first deformation step transforms the initially spherulitic morphology into a shish kebab morphology by partial melting; this is further deformed during transverse drawing into a fibrillar network. The observed structural changes correlated with the melting behaviour and mechanical and thermomechanical properties of the films.

Hu and co-workers [7] studied the solid-state structure of copolyesters based on smectic poly(diethylene glycol 4,4′-bibenzoate)(PDEGBB) and non-liquid crystalline poly(diethylene glycol isophthalate), with isophthalate contents from 10 to 50 mol%. Differential scanning colorimetry (DSC), FTIR spectroscopy, wide-angle X-ray diffraction (WAXD), dynamic mechanical thermal analysis (DMTA) and tapping mode atomic force microscopy were used to characterise the polymers. The combined results indicated that the copolymers could be divided into two classes, depending on isophthalate content. Copolymers with up to 20% isophthalate content possessed some liquid crystalline character. They exhibited a smectic-to-isotropic transition in differential scanning colorimetry DSC smectic layer reflections in WAXD, and lamellar structures in AFM. It appeared that isophthalate groups were excluded from the smectic layers and were, therefore, very effective in disrupting long-range liquid crystalline order. Copolymers with 30% or more isophthalate were amorphous. These materials did not exhibit crystalline or liquid crystalline character after exposure to the thermal histories used in this study. The Fox equation described the dependence of T_g from loss modulus on copolymer composition for non-liquid crystalline glasses and predicted that the T_g of glassy PDEGBB was 14 °C higher than the observed T_g of the liquid crystalline glass.

Kizhakkedathu and co-workers [8] analysed homopolymer brushes of poly(*N*,*N*-dimethylacrylamide) and poly(*N*-isopropylacrylamide) grown on latex particles functionalised with an atom-transfer radical polymerisation (ATRP) initiator. The grafted homopolymer and block copolymer brushes were analysed by gel permeation chromatography/multi-angle laser light scattering, ^{1}H-NMR, particle-size analysis and AFM techniques. In all cases, the measured graft molecular weight increased following the second ATRP reaction, indicating that a second block had been added. Chain growth depended on the nature of the monomer used for block copolymerisation and its concentration. The unimodal distribution of polymer chains in gel permeation chromatography (GPC) with non-overlap of molar mass-elution volume curves, implied an efficient block copolymerisation. This was supported by the increase in hydrodynamic thickness (measured by particle size analysis) equilibrium thickness (observed by AFM), and the composition of the block copolymer layer (as determined by ^{1}H-NMR analysis), both *in situ* and of cleaved chains.

Block copolymer brushes obey the same power-law dependence of hydrodynamic transfer on molecular weight as do homopolymer brushes under solvent conditions. The poly(*N*-isopropylacrylamide)-containing block copolymer brushes were sensitive to changes in the environment, as shown by a decrease in hydrodynamic transfer with increasing temperature of the medium.

Other applications of AFM to the characterisation of polymers include polythiophene [9], nitrile rubbers [10], perfluoro copolymers of cyclic polyisocyanurates of hexamethylene diisocyanate and isophorone diisocyanate [11], perfluorosulfonate [12], vinyl polymers [13], polyhydroxybutyrate [14], polyacrylic acid nanogels [15], acrylic copolymers [16, 17], polyurethanes [18, 19], ethylene methacrylate copolymer [4, 20], polyamides [21], polyvinyl pyrrolidone [22], and polyethyl methacrylate dispersions [23], acryloyl chloride [13], aniline-4-sulfonic acid [24], ethylene propylene 5-ethylidene-2-norbornene terpolymer [25] and butylene adipate – butylene terephthalae [26].

AFM has been used in a variety of other polymer studies as reviewed next.

8.1.2 Morphology

Merrett and co-workers [27] give a brief review of various techniques for analysing surface properties of polymeric biomaterials. Mention is made of scanning electron microscopy, electron microscopy, scanning tunneling microscopy, AFM, confocal scanning microscopy, Auger electron microscopy, XPS, SIMS, FTIR, matrix assisted laser description ionisation time-of-flight (MALDI-ToF) spectroscopy, contact angle and ellipsometry.

The application of AFM to surface morphological studies has been covered in relation to the following polymers: polyesters, polyethylene (PE), polystyrene (PS) [28], polycarbonate, polyimide, polytetrafuoroethylene (PTFE) [29], polyurethane (PU) [30], rubbers [31], polyethylene glycol (PEG) [32], PS and poly(*N*-butyl-methacrylate) [33], PS [34], PP [35, 36], polyethers [37], polyorthoesters [38], poly(*p*-phenylene-vinylene) [39], bisphenol A – 1, 8-dibromooctane copolymer [40], polycatechol [41], polyethylene terephthalate (PET) [42], poly(*p*-dioxanone)-poly(epsilon caprolactone) [43], poly(L-lactide-polyethylene glycol) [44] and polyvinylidene fluoride [45].

8.1.3 Surface Defects

Brogly and co-workers [46] propose a method using AFM for the determination of the persistence length of molecular orientation of thin films adsorbed onto highly reflecting

metals. The approach was based on the fact that molecular orientation persisted only over a given distance from the geometrical interface; this distance being called the 'persistence length of molecular orientation'. It was supposed that the nanofilm adsorbed was stratified, and consisted of an oriented layer (in the near-interface region) plus an isotropic one. The correlation between infrared reflection absorption band intensities and simulated band intensities permitted determination of accurate molecular orientation, and persistence length of orientation, of a considered functional group. This was accomplished using various infrared reflection angles and polarisation state of the incident infrared wave. Film thickness and complex refractive index spectra were only needed to deduce calculated specular reflectance intensities.

8.1.4 Adhesion Studies

AFM has been used in studies of adhesion in the cases of PS/polymethl methacrylate (PMMA) [47], PET/PP [48], and polyurethane- and epoxy-based adhesives [49]. General discussions of the use of this technique in adhesion studies have been reported [50].

8.1.5 Polydispersivity

Janorkor and co-workers [51] used AFM to investigate the surface roughness of PET films.

Zhang and co-workers [52] in their discussion of the polydispersivity of ethylene sequence length in metallocene ethylene-α-olefin copolymers characterised by the thermal fractionation technique, used AFM to study crystal morphology.

8.1.6 Sub-surface Particle Studies

Feng and co-workers [53] used tapping mode AFM in the imaging of sub-surface nanoparticles in poly(*N*-vinyl-2-pyrrolidone) thin films and shear loading in strained semicrystalline polyamide-6-films [54]. Similar studies have been carried out on 2-ethylaniline-2-anisidine and 2-ethylaniline-2-anisidine-5-sulfonic acid copolymers [55].

8.1.7 Size of Nanostructures

The visualisation and size determination of polyacrylate nanostructures has determined by AFM [56]. Lyuksyutov and co-workers [1] have reviewed electrostatic nanolithography in polymers.

8.1.8 Visualisation of Molecular Chains

Individual chains of poly(2-ethynyl-9-substituted carbazoles) have been visualised by AFM [54].

8.1.9 Compositional Mapping

AFM and electric force microscopy are commonly used for compositional mapping of elastomers and multi-component rubber materials. Several aspects of the optimisation of AFM experiments on polymers have been studied [57]. Images reveal changes of ethylene-propylene-diene morphology (EPDM) caused by crosslinking and by loading with fillers (carbon black and silicon particles) and oil. It is shown that the morphology of isotactic polyproplylene (iPP)/EPDM vulcanisates, studied by AFM and electric force microscopy, depends on the ratio of components, degree of cure, and processing conditions. Diffusion of oil from the rubber component to the matrix is evident in the AFM images. Selective distribution of carbon black in the iPP matrix is responsible for the electrical conductivity of the thermoplastic vulcanisate material.

8.1.10 Surface Roughness

Sukhadia and co-workers [58] have used angle light scattering and wide-angle X-ray scattering to investigate the origins of surface roughness and haze in PE blown films.

8.1.11 Microphase Separation

Williamson and Long [59] used AFM in the tapping mode to verify the presence of microphase separation in start shaped polymers comprising poly(1,3-cyclohexadiene-b-isoprene) diblock arms coupled to a divinyl benzene core.

8.1.12 Phase Transition

Li and co-workers [60] used AFM to investigate phase transition and self-assembling behaviour of polyethylene oxide methylether-acrylate-block-PS.

8.1.13 Shrinkage

The shrinkage of chiral polyacrylates end-capped with bornyl groups [61] caused by the photoisomerisation of the composite films was investigated by AFM. A spot

contraction appeared on the surface when it was irradiated with a laser light spot. The contraction was recovered by heat treatment at 80 °C for 10 minutes.

8.2 Microthermal Analysis

This is a technique that combines thermal analysis and AFM. This new technique is discussed in a series of papers published by ASTM in 1999 [62] and other workers [55, 63–67].

Workers at TA Instruments, UK, manufacturer of thermal micro-analysis equipment, have given details of the model TA 2990 system. They give examples of its application to thermal and morphological problems [68].

Microthermal analysis has been used as a heated probe for thermal conductivity imaging. The same probe performs local calorimetric measurements through microthermal mechanical analysis and micro-differential thermal analysis. Application examples include: copolymer identification in food packaging materials; effects of embedded carbon fibres on matrix crosslinking; and transparency films. Alternatively, a sample heating stage can be used to track temperature-dependent morphology, stiffness, and adhesion changes using pulsed force mode.

Microthermal analysis combines the visualisation power of AFM with the characterisation ability of thermal analysis [65]. The AFM head is fitted with an ultra-miniature thermal probe, which provides not only topographic and thermal contrast information, but also information similar to traditional thermal analysis on a sub-micrometre scale.

Microthermal analysis is being developed as a tool for carrying out studies in a number of areas including morphology, topography, glass transitions, depth probing, and phase separation studies.

8.2.1 Morphology

Morphological studies have been conducted on multi-block copolymers [69] and Nylon 6,6/polytetrafluorethylene/silicone blends [70].

8.2.2 Topography

Abad and co-workers [71] used the TA Instruments TA2990 microthermal analyser to carry out topography studies including fabrication failure on biaxially oriented PP film.

8.2.3 Glass Transition

Glass transition studies have been reported on amorphous PS [72], araldite 2011, adhesive-metal bonds [73], thin PS films [74], and PEG entrapped into polylactic acid [75].

8.2.4 Depth Profiling Studies

Grossette and co-workers [76] used microthermal analysis and FTIR spectroscopy to study the physical heterogeneity induced by the photooxidation of PP at a sub-micrometric level.

8.2.5 Phase Separation Studies

Song and co-workers [77] used microthermal analysis to study the phase separation process in a 50:50 (by weight) PS/polyvinylmethylether blend and nitrile rubber. Microthermal analysis will image the composition in the near-surface region or surface region of multi-component materials if the resolution is high enough.

Variable temperature pulsed force mode AFM has been found to be a practical technique [78] for carrying out microthermal analyses of materials. Studies on a PS/PMMA blend showed that the pull-off force of PMMA was relatively insensitive to changes in temperature, whereas PS showed a large step increase above its glass transition temperature. The phase separated morphology could be characterised. However, before the technique can be applied more generally as a characterising tool, further investigation of the force affecting the pull-off force (and its relationship with temperature) is needed. At room temperature, the technique produced high-contrast images, showing the phase separated morphology of three segmented polyurethane elastomers. The results indicated that these materials had a complex structure with phases an order of magnitude larger than the domain size usually obtained using techniques such as small-angle X-ray scattering.

References

1. S.F. Lyuksyutov, R.A. Vaia, P.B. Paramonov, S. Juhl, L. Waterhouse, R.M. Ralich, G. Sigalov and E. Sancaktar, *Nature Materials*, 2003, **2**, 7, 468.

2. M.L. Cerrada, *Revista de Plasticos Modernos*, 2002, **83**, 501.

3.   *Characterisation of Solid Polymers: New Technologies and Developments*, Ed., S.J. Spells, Chapman and Hall, London, UK, 1994.

4.   M. Ezrin, *Plastics Engineering*, 2002, **58**, 40.

5.   J.D. Isner and R.W. Eiden in *Proceedings of Vinyltech 2000 Conference*, Philadelphia, PA, USA, 2000, p.198.

6.   T. Lüpke, S. Dunger, J. Sänze and H-J. Radusch, *Polymer*, 2004, **45**, 20, 6861.

7.   Y.S. Hu, R.Y.F. Liu, D.A. Schiraldi, A. Hiltner and E. Baer, *Macromolecules*, 2004, **37**, 6, 2128.

8.   J.N. Kizhakkedathu, K.R. Kumar, D. Goodman and D.E. Brooks, *Polymer*, 2004, **45**, 22, 7471.

9.   R.C. Advencula, C. Xia, J. Locklin and X. Fan, *Polymer Preprints*, 2002, **43**, 2, 345.

10. T.C. Ward, D.S. Parker and R.E. Jensen in *Proceedings of Adhesion '99*, Cambridge, UK, 1999, p.81.

11. S. Turri, A. Sanguineti, S. Novelli and R. Lecchi, *Macromolecular Materials and Engineering*, 2002, **287**, 5, 319.

12. K. Adachi, W. Hu, H. Matsumoto, K. Ito and A. Tanioka, *Polymer*, 1998, **39**, 11, 2315.

13. E. Bucio, G. Burillo, M. Del Pilar Carreón-Castro and T. Ogawa, *Journal of Applied Polymer Science*, 2004, **93**, 1, 172.

14. M. Nitschke, G. Schmack, A. Janke, F. Simon, D. Pleul and C. Werner, *Journal of Biomedical Materials Research*, 2002, **59**, 4, 632.

15. S. Kadlubowski, J. Grobelny, W. Olejniczak, M. Cichomski and P. Ulanski, *Macromolecules*, 2003, **36**, 7, 2484.

16. R.R. Thomas, K.G. Lloyd, K.M. Stika, L.E. Stephans, G.S. Magallanes, V.L. Dimonie, E.D. Sudol and M.S. El-Aasser, *Macromolecules*, 2000, **33**, 23, 8828.

17. P. Polanowski, J. Ulański, R. Wojciechowski, A. Tracz, J.K. Jeszka, S. Matejcek, E. Dormann, B. Pongs and H.W. Helberg, *Synthetic Metals*, 1999, **102**, 1–3, 993.

18. X. Chen, L. Wu, S. Zhou and B. You, *Polymer International*, 2003, **52**, 6, 993.

19. A. Aneja and G.L. Wilkes, *Polymer*, 2002, **43**, 20, 5551.

20. D.A. Siuzdak, P.R. Start and K.A. Mauritz, *Journal of Polymer Science Part B: Polymer Physics Edition*, 2003, **41**, 1, 11.

21. T. McNally, W.R. Murphy, C.Y. Lew, R.J. Turner and G.P. Brennan, *Polymer*, 2003, **44**, 9, 2761.

22. D.K. Hood, L. Senak, S.L. Kopolow, M.A. Tallon, Y.T. Kwak, D. Patel, J. McKittrick, *Journal of Applied Polymer Science*, 2003, **89**, 3, 734.

23. M.J. Krupers, H.R. Fischer, A.G.A. Schuurman and F.F. Vercauteren, *Polymers for Advanced Technologies*, 2001, **12**, 9, 561.

24. X-G. Li, H-J. Zhou, M-R. Huang, M-F. Zhu and Y-M. Chen, *Journal of Polymer Science Part A: Polymer Chemistry Edition*, 2004, **42**, 13, 3380.

25. S.C. Domenech, J.H. Bortoluzzi, V. Soldi, C.V. Franco, W. Gronski and H-J. Radusch, *Journal of Polymer Science Part B: Polymer Physics Edition*, 2004, **42**, 9, 1767.

26. Z. Gan, K. Kuwabara, M. Yamamoto, H. Abe and Y. Doi, *Polymer Degradation and Stability*, 2004, **83**, 2, 289.

27. K. Merrett, R.M. Cornelius, W.G. McClung, L.D. Unsworth and H. Sheardown, *Journal of Materials Science*, 2002, **13**, 6, 593.

28. R. Ganapathy, S. Manolache, M. Sarmadi, W.J. Simonsick, Jr., and F. Denes, *Journal of Applied Polymer Science*, 2000, **78**, 10, 1783.

29. V. Zaporojtchenko, T. Strunskus, K. Behnke, C. Von Bechtolsheim, M. Kiene and F. Faupel, *Journal of Adhesion Science and Technology*, 2000, **14**, 3, 467.

30. B.D. Kaushiva, S.R. McCartney, G.R. Rossmy and G.L. Wilkes, *Polymer*, 2000, **41**, 1, 285.

31. M. Yerina and S. Magonov in *Proceedings of the 161st ACS Rubber Division Meeting*, Savannah, GA, USA, Spring 2002, Paper No.31.

32. Y.G. Ko, Y.H. Kim, K.D. Park, H.J. Lee, W.K. Lee, H.D. Park, S.H. Kim, G.S. Lee and D.J. Ahn, *Biomaterials*, 2001, **22**, 15, 2115.

33. S. Affrossman, R. Jerome, S.A. O'Neill, T. Schmitt and M. Stamm, *Colloid and Polymer Science*, 2000, **278**, 10, 993.

34. V. Shapovalov, V.S. Zaitsev, Y. Strzhemechny, F. Choudhery, W. Zhao, S.A Schwarz, S.Ge, K. Shin, J. Sokolov and M.H. Rafailovich, *Polymer International*, 2000, **49**, 5, 432.

35. J. Hautojärvi and A. Leijala, *Journal of Applied Polymer Science*, 1999, **74**, 5, 1242.

36. Y. Wang, B. Na, Q. Fu and Y. Men, *Polymer*, 2004, **45**, 1, 207.

37. C-M. Chan, L. Li, K-M. Ng, J. Li and L-T. Weng, *Macromolecular Symposia*, 2000, **159**, 1, 113.

38. S.R. Leadley, K.M. Shakesheff, M.C. Davies, J. Heller, N.M. Franson, A.J. Paul, A.M. Brown and J.F. Watts, *Biomaterials*, 1998, **19**, 15, 1353.

39. W. Wang, Q. He, J. Zhai, J. Yang and F. Bai, *Polymers for Advanced Technologies*, 2003, **14**, 3–5, 341.

40. L. Li, K-M. Ng, C-M. Chan, J-Y. Feng, X-M. Zeng and L-T. Weng, *Macromolecules*, 2000, **33**, 15, 5588.

41. Y. Kong, S.I. Mu and B.W. Mao, *Chinese Journal of Polymer Science*, 2002, **20**, 517.

42. W. Michaeli, S. Göbel and R. Dahlmann, *Journal of Polymer Engineering*, 2004, **24**, 1–3, 107.

43. A.J. Müller, J. Albuerne, L.M. Esteves, L. Marquez, J-M. Raquez, P. Degée, P. Dubois, S. Collins and I.W. Hamley, *Macromolecular Symposia*, 2004, **215**, 1, 369.

44. J. Sun, Z. Hong, L. Yang, Z. Tang, X. Chen and X. Jing, *Polymer*, 2004, **45**, 17, 5969.

45. J. Xu, M. Johnson and G.L. Wilkes, *Polymer*, 2004, **45**, 15, 5327.

46. M. Brogly, S. Bistac and J. Schultz, *Macromolecular Theory and Simulations*, 1998, **7**, 1, 65.

47. H-J. Kim, M.H. Rafailovich and J. Sokolov, *Journal of Adhesion*, 2001, **77**, 1, 81.

48. M.J. Walzak, J.M. Hill, C. Huctwith, M.L. Wagter and D.H. Hunter in *Proceedings of the 20th Annual Anniversary Meeting of the Adhesion Society*, Hilton Head Island, SC, USA, 1997, p.89.

49. W.C. Wang, Y. Zhang, E.T. Kang and K.G. Neoh, *Plasmas and Polymers*, 2002, **7**, 3, 207.

50. A. Hussain, *Adhesive Age*, 2001, **44**, 3, 24.

51. A.V. Janorkar, D.E. Hirt and J.J. Wooster, *Polymer Engineering and Science*, 2004, **44**, 1, 34.

52. F. Zhang, J. Liu, Q. Fu, H. Huang, Z. Hu, S. Yao, X. Cai and T. He, *Journal of Polymer Science Part B: Polymer Physics Edition*, 2002, **40**, 9, 813.

53. J. Feng, L-T. Weng, C-M. Chan, J. Xhie and L. Li, *Polymer*, 2001, **42**, 5, 2259.

54. V. Ferreiro and G. Coulon, *Journal of Polymer Science Part B: Polymer Physics Edition*, 2004, **42**, 4, 687.

55. *Advanced Materials and Processes*, 1998, **153**, 6, 10.

56. Q. Ma and K.L. Wooley, *Journal of Polymer Science Part A: Polymer Chemistry Edition*, 2000, **38**, S1, 4805.

57. V. Percec, M. Obata, J.G. Rudick, B.B. De, M. Glodde, T.K. Bera, S.N. Magonov, V.S.K. Balagurusamy and P.A. Heiney, *Journal of Polymer Science Part A: Polymer Chemistry Edition*, 2002, **40**, 20, 3509.

58. A.M. Sukhadia, D.C. Rohlfing, M.B. Johnson and G.L. Wilkes, *Journal of Applied Polymer Science*, 2002, **85**, 11, 2396.

59. D.T. Williamson and T.E. Long, *Macromolecular Symposia*, 2004, **215**, 1, 95.

60. Y-G. Li, P-J. Shi, Y. Zhou and C-Y. Pan, *Polymer International*, 2004, **53**, 3, 349.

61. J-H. Liu, C-D. Hsieh and H-Y. Wang, *Journal of Polymer Science Part A: Polymer Chemistry Edition*, 2004, **42**, 5, 1075.

62. *Proceedings of the SPE Joint Regional Technical Conference on Thermal and Mechanical Analysis of Plastics in Industry and Research*, Newark, DE, USA, 1999.

63. I.R. Harrison, *Proceedings of the SPE Joint Regional Technical Conference on Thermal and Mechanical Analysis of Plastics in Industry and Research*, Newark, DE, USA, 1999, p.142.

64. D. Price and M. Reading, *Advances in Polymer Technology*, 1999, **18**, 2, 181.

65. H.M. Pollock and A. Hammiche, *Journal of Physics D: Applied Physics*, 2001, **34**, 9, R23.

66. V. Gorbunov, N. Fuchigami, I. Litzinov and V.V. Tsukruk, *Polymer Preprints*, 2000, **41**, 2, 1493.

67. H.M. Pollock, A. Hammiche, L. Bozec, E. Dupas, D.M. Price and M. Reading, *Polymer Preprints*, 2000, **41**, 2, 1421.

68. L' *Industria della Gomma*, 1999, **473**, 45.

69. M. El Fray and V. Altstädt, *Designed Monomers and Polymers*, 2002, **5**, 2–3, 353.

70. A. Gupper, P. Wilhelm, M. Schmied, S.G. Kazarian, K.L.A. Chan and J. Reussner, *Applied Spectroscopy*, 2002, **56**, 12, 1515.

71. M.J. Abad, A. Ares, L. Barral, J. Cano, F.J. Díez, J. López and C. Ramírez, *Journal of Applied Polymer Science*, 2002, **85**, 7, 1553.

72. M.S. Tillman, T. Takatoya, B.S. Hayes and J.C. Seferis, *Journal of Thermal Chemistry and Calorimetry*, 2000, **62**, 3, 599.

73. R. Haessler and H. Kleinert, *Adhasion Kleben und Dichten*, 2000, **44**, 7–8, 36.

74. V.V. Gorbunov, N. Fuchigami and V.V. Tsukruk, *High Performance Polymers*, 2000, **12**, 4, 603.

75. J. Zhang, C.J. Roberts, K.M. Shakesheff, M.C. Davies and S.J.B. Tendler, *Macromolecules*, 2003, **36**, 4, 1215.

76. T. Grossette, L. Gonon and V. Verney, *Polymer Degradation and Stability*, 2002, **78**, 2, 203.

77. M. Song, D.J. Hourston, D.B. Grandy and M. Reading, *Journal of Applied Polymer Science*, 2001, **81**, 9, 2136.

78. D.B. Grandy, D.J. Hourston, D.M. Price, M. Reading, G.G. Silva, M. Song and P.A. Sykes, *Macromolecules*, 2000, **33**, 25, 9348.

9 Multiple Technique Polymer Studies

Frequently, in work carried out to attempt to elucidate the microstructure of polymers and copolymers, it is found necessary to employ not one physical analytical technique, but a range of such techniques. The literature abounds in examples of this need. Judging by the number of papers published, three of the most useful and commonly used techniques are combinations of Fourier transform infrared spectroscopy (FTIR) or infrared (IR) spectroscopy and matrix assisted laser desorption-ionisation time-of-flight (MALDI-TOF) mass spectrometry with nuclear magnetic resonance spectroscopy or photon magnetic resonance spectroscopy.

To an appreciably less extent, other techniques, such as scanning electron microscopy (SEM), x-ray photoelectron spectroscopy (XPS), secondary ion mass spectrometry (SIMS), Raman spectroscopy, and atomic force microscopy (AFM) are used in conjunction with IR or MALDI-TOF techniques.

Below is a brief review of those methods which are most useful for the elucidation of particular types of problems associated with the elucidation of polymer structure. A full review of these methods and their applications is given in **Tables 9.1 to 9.15**.

9.1 FTIR – Nuclear Magnetic Resonance (NMR) Spectroscopy

These techniques are complimentary to each other, with each providing different information on structural details, polymer characterisation, structure and construction of existing and new polymers, measurement of polymer and copolymer composition, effect of catalysts and polymerisation, conditions on structure of polymers, hydrogen bonding in polymers, *cis-trans* measurement, optimum conditions for polymer synthesis, effect of polymer structure on thermal and crystallisation properties, effect of comonomer ratio on polymer structure and properties (for example, thermal and oxidative stability), tensile properties, and studies of competing reactions during polymerisation.

Table 9.1 Multiple technique polymer studies: FTIR – ^{13}C-NMR		
Polymer	**Technique**	**Ref.**
Polyaniline-*co*-acrylonitrile	Characterisation	[1]
Isoprene-*co*-urethane	Molecular structure and morphology	[2]
Trisubstituted ethylene-*co*-styrene	Characterisation	[3]
Acrylic and dienic-4-chloromethyl styrene	Characterisation	[4]
Butadiene-*co*-styrene-*trans*-4-hydroxyl-*R*-proline cyclic esters	Effect of polymerisation conditions on polymer structure	[5]
	Characterisation	[6]
Ethylene, propylene and α-olefin copolymers	Characterisation and effect of comonomer ratio on melting point and crystallinity	[7]
Epoxidised styrene-*co*-butadiene	Determination of 1,4 epoxidised butadiene units	[8]
ABA block copolymers, trimethylmine, carbonate-ε-caprolactone	Effect of structure on tensile properties	[9]
Polybutylene ethers	Characterisation	[10]
Ethylaniline-*co*-anisidine, ethylaniline-*co*-sulfoanisidine	Structure studies	[11]
Thienyl-phenylene-*co*-oligo(ethylene oxide)	Characterisation	[12]
Polystyrene-*co*-vinyl phosphonate	Structure studies	[13]
Oligo(phenylene-vinylene) dimer with fluorine end groups	Characterisation	[14]
Silicon containing polymers	Characterisation	[15]
Polyurethane ethers	Characterisation	[16]
Polyethylene terephthalate-*co*-dibenzoate	Composition of crystalline and amorphous regions	[17]
Polypyridinium salts	Characterisation	[18]
Polyarylene ethers	Characterisation	[10]
Modified epoxy resins	Characterisation, thermal stability studies	[19]
Sulfonated polyarylene ether sulfones	Characterisation, adhesion studies	[20]
Polyamides	Characterisation	[21]
Polyimides	Characterisation, thermal stability studies	[22]

Triethylammonium 2,5-thiophen-dicarboxylato-tri-phenyl stannate	Characterisation	[23]
Isotactic metallocene-Ziegler-Natta polypropylene (PP)	Configurational studies, thermal stability studies	[24]
Polyamide 66	Effect of complexation with Lewis acid on crystallinity	[25]
Polyurethane ureas	Characterisation, thermal properties	[26]
Polyolefins	Crosslinking studies	[27]
Bis(4,4′-hydroxyphenyl sulfide with aliphatic acid dichlorides	Characterisation	[28]
Polypropylene	Effect of catalyst on polymer structure	[29]
Polyamides with *N*,*N*′-di(4-*N*-alkylphenyl) benzodiimide	Characterisation, thermal properties	[30]
Polybutylene sulfide	*Cis-trans* isomerisation	[31]
Poly-*p*-phenylenevinylene containing triphenylamine units and cyano groups	Characterisation	[32]
Ether linked polyamides	Characterisation, tensile properties	[33]
Polysilses quioxanes with maleimide side chains	Characterisation, curing kinetics	[34]
Polydioxolane	Effect of fluorine substitution on polymer structure, study of ring opening	[35]
Polyvanillylidene aryl phosphate esters	Study of hydroxyl groups and photocrosslinking	[36]
Cholesteryl-4-allyl-oxybenzoate-4,4′-bis(10 undecane-1-ylate)	Characterisation	[37]
Carbon dioxide-*co*-cyclohexene oxide	Effect of catalyst on structure kinetic studies	[38]
Polyhydroxyether sulfone-polyethylene oxide blends	Characterisation	[39]
Polyether siloxane	Effect of $LiClO_4$ dopant on microstructure	[40]
Tert-butylmethacrylate-*co*-norbornene	Effect of catalyst on microstructure	[41]
Polyesterimides	Reactions between various glycols and hydroxyl terminated polybutadienes, characterisation of products	[42]
Di(carbazole-3-yl)phenylamine and *N*,*N*′-dicarbazole-3-yl)-*N*,*N*′-diphenyl-1,4-phenylene diamine containing polymers	Characterisation, effect of structure on ionisation potential	[43]

407

Novolak epoxies	Characterisation	[44]
Diepoxy containing sulfonate ester links	Study of crosslinking	[45, 46]
Polyphenylene vinylene dipoxy	Characterisation, light-emitting properties	[47]
(2S, 3S) 2,3 butanediyl, (2S, 4S) 2,4pentanedienyl (2S, 5S)2,5 hexanediyl bis(4-vinylbenzoates)	Study of cyclopolymerisation	[48]
Tris(diphenyliodonium) 9, hydroxypyrene-1,4,6 trisulfonate	Characterisation, photolithographic properties	[49]
Polysulfonated polybenzimidazole	Characterisation, optical properties	[50]
Divinylenediethylhexyl-oxyphenol-*co*-triphenyltriazine	Study of alternating copolymers, photoluminescence properties	[51]
Segmented polyurethanes	Structural analysis of up to 8 methylene units	[52]
Hyperbranched poly(phenylene germolenes)	Characterisation, optical and thermal properties	[53]
Fluorinated polyethers	Study of structure of products (pendent methyl groups) formed by polyaddition of trisphenol AF	[54]
Poly(etheresteramide)-*co*-ε caprolactone, poly(etheresteramide)-co-11-aminoundecanoic acid, Poly(ether-esteramide)-*co*-polyethylene glycol	Characterisation, degradation studies	[55]
Hevacrylated/levaethoxyl cyclophosphazene	Characterisation, flame retardancy	[56]
Phenylformaldehyde-2,4-dihydroxyacetophenone formaldehyde	Characterisation, uptake of metals	[57]
Polyacetylenes with pendent cabazole groups	Characterisation of pendent groups	[58]
Poly(binaphthylene ether)	Characterisation, insulating properties	[59]
Bithiophene-cyclophane (poly(phenyl type))acetylene-fluorene acetylene cyclophane(poly(*p*-phenylene thynylene) type, ethylene-fluorene-ethylene cyclophane(poly(*p*-phenylene-vinylene) type	Characterisation, optical properties	[60]

Poly(heteroarylene methines)	Characterisation, effect of structure on optical properties	[61]
Silicone rubber	Characterisation, thermal properties	[62]
Mixed alkyl and alkoxy substituted poly(phenylene vinylene) hybrid polymers	Characterisation, photoluminescence properties	[63]
Ladder type polysilsesquioxane	Characterisation of ladder type	[64]
Polyolefins	Characterisation	[65]
Poly(*p*-vinylbenzyl chloride)	Effect of catalyst type on structure	[66]
Polyglycidol	Characterisation, mechanism of polymerisation	[67]
N-substituted polyaniline	Characterisation, electrical, thermal properties	[68]
Fluorene-*co*-triphenyl amine	Characterisation,	[69]
Polybenzobisoxazoledivinylene	Characterisation, phytophysical properties	[70]
Poly(acrylloyloxyethylphosphoryl-choline)-*co*-polybutylacrylate	Phtophysical properties	[71]
N-substituted hyper-branched polyureas	Effect of polymerisation conditions on microstructure	[72]
Modified epoxy	Effect of carboxyl and azidocarbonyl groups on structure Characterisation – thermal stabilities	[21]
Polyamides	Characterisation	[73]
Polyether-siloxane organic-inorganic hybrid nanocomposites	Structure, thermal and electrical properties	[74]
Oligo(phenylene vinylene) dimer with biphenyl linkage centre and fluorine end groups	Characterisation, electroluminescent properties	[75]
Poly(D-mannaramide), poly(galactaramide, L-lactic acid-citric acid oligomer	Characterisation, composition	[76, 77]
Chitosan-*co*-isopropyl acrylamide	Physicochemical properties	[78]
Source: Author's own files		

Table 9.2 Multiple technique polymer studies – infrared spectroscopy – ¹³C-NMR spectroscopy

Polymer	Technique	Ref.
Ethylene propylene	Compositional analysis	[79]
Ruthenium(II)(ETA-6-*P*-cymene) complexes of poly(spirophosphazine pyridine)	Characterisation of crosslinking	[80]
Polysilone crown ethers	Characterisation of Cu(II) complexes	[81]
PEG-poly(γ-benzyl-*L*-glutamic acid)	Characterisation of end groups	[82]
Polybutadiene	Microstructure studies	[83]
Polythiophene-poly(-3-methylthiophene)	Structural study	[84]
Various polymers	Review of characterisation	[85]
Source: Author's own files		

Table 9.3 Multiple technique polymer studies – FTIR-electron spin resonance spectroscopy

Polymer	Technique	Ref.
Polybutyl vinyl ether	Microstructure of reaction products with sulfur	[86]
Source: Author's own files		

Table 9.4 Multiple technique polymer studies – FTIR-proton magnetic resonance spectroscopy

Polymer	Technique	Ref.
Poly(-*o*- and *m*-aminobenzyl-amine)-*co*-aniline	Characterisation of complexes with Cu(II)	[87]
Polylactic acid-*co*-β-ethylene glycol	Study of chemical linkages between PEG and PLA segments in block copolymers	[88]
Sulfophenylpolyurethane	Characterisation	[89]
Trihalose vinyl benzyl ether	Characterisation and biodegradability study	[90]
Polyallyl(biguanidine)	Elucidation of structure	[91]
Epoxy resins(aniline-*o*-cresol-formaldehyde type)	Characterisation, thermal properties	[92]
Source: Author's own files		

Table 9.5 Multiple technique polymer studies – infrared spectroscopy – scanning electron microscopy		
Polymer	**Technique**	**Ref.**
Gamma Fe_2O_3 – polystyrene composites	Characterisation, thermal behaviour	[93]
Polycaprolactone – CaO, SiO_2 hybrid	Characterisation, molecular structure – hydrogen bonding	[94]
Source: Author's own files		

Table 9.6 Multiple technique polymer studies – FTIR, microscopy – scanning electron microscopy		
Polymer	**Technique**	**Ref.**
Polyurethane-casein composites	Structure of composites	[95]
Polyurethane	Study of crosslinking reactions with 1,4-butanediol dimethacrylate	[96]
Polyfuran(2-fluoroaniline) composites	Characterisation and study of electrical properties	[97]
Polyethylene	Structure of oxidation products	[98]
Polyaniline	Characterisation, morphology	[99]
Polyurethane-ethylene-propylene-diene melt blends	Characterisation of polymeric network of addition of poly(ethylene-*co*-1-octene) maleic anhydride graft	[100]
Source: Author's own files		

Table 9.7 Multiple technique polymer studies – infrared spectroscopy – x-ray photoelectron microscopy

Polymer	Technique	Ref.
Polyamidoamine grafted onto polyaminomethylstyrene surface	Details of structure	[101]
Polyaniline-gold composites	Examination of chemical properties of polymer with and without gold clusters	[102]
Polyethylene-wood flour composites	Effect of weathering by light exposure on surface oxidation	[103]
Polyimide-arylsilaneimide nanocomposites	Study of structural features	[104]
Fluorinated copolymers of pyridine and non-fluorinated copolymer containing methacrylic acid	Hydrogen bonding interactions	[105]
Source: Author's own files		

Table 9.8 Multiple technique polymer studies – FTIR – atomic force microscopy

Polymer	Technique	Ref.
Polyaniline-sulfonic diphenyl amine	Structure, electrical conductivity	[106]
Ethyl(aniline-*co*-anisidine)	Structure	[107]
Ethylaniline-*co*-sulfanisidine	Structure	[108]
Polyvinylchloride-polyethylene oxide blends	Structure of photoxidation degradation products	[109]
Polyethylene oxide-poly(beta-benzyl-*L*-aspartate) ARA triblock copolymers	Alpha helix/7(2) helix/alpha helix conformation	[110]
Epoxy-aluminium resin	Effect of hydroxy group concentration on durability of adhesive bonds	[111]
Poly(ethylacrylate)-nickel and polyacrylonitrile nickel	Characterisation of chemical bonds	[112]
Source: Author's own files		

Table 9.9 Multiple technique polymer studies – FTIR – Raman spectroscopy		
Polymer	**Technique**	**Ref.**
Polyvinylalcohol Cadmium sulfide composites	Characterisation	[112]
Source: Author's own files		

Table 9.10 Multiple technique polymer studies – X-ray photoelectron spectroscopy - AFS		
Polymer	**Technique**	**Ref.**
Polyethylene	Functional groups	[113]
Butylene adipate-*co*-butylene terephthalate	Solid state microstructure study	[114]
Natural rubber	Characterisation	[115]
Source: Author's own files		

Table 9.11 Multiple technique polymer studies – SIMS-XRPS		
Polymer	**Technique**	**Ref.**
Polyferrocenyl silanes	Characterisation	[116]
Fluorinated acrylic copolymer – hydrocarbon acrylic copolymer blends	Characterisation	[117]
ESR spectroscopy – Raman spectroscopy		
Polystyrene-*o*-*p*-(hexafluoro-2-hydroxy-isopropyl) α methylstyrene(propylene carbonate)	Characterisation of hydrogen bonds	[118]
Source: Author's own files		

Table 9.12 Multiple technique polymer studies – SEM-Raman spectroscopy		
Polymer	**Technique**	**Ref.**
Nylon 6 – ethylene vinyl alcohol blends	Characterisation of hydrogen bonds	[119]
Source: Author's own files		

Table 9.13 Multiple technique polymer studies – MALDI-ToF – MS – IR spectroscopy		
Polymer	**Technique**	**Ref.**
Polyurethane	Oligomers produced on depolymerisation	[120]
Poly-*N*-isopropyl acrylamide	Chain transfer fragmentation	[121]
L-lactide-*co*-polyethyleneglycol	Characterisation of Ge-free multiblock copolymers	[122]
Phenol-resorcinol formaldehyde resins	Structure determination	[123]
Oligo(2,3-dihydroxypropyl-methacrylate acetonides	Characterisation of oligomers prepared by ozonolytic cleavage	[124]
Polyethylene oxides with 1,2,4-triazol-4-yl end groups	Characterisation	[125]
3-Arm star polymers based on 1-phenylethylpolyethylene and 1-phenylethyl dithiobenzoate	Characterisation	[126]
Polycaprolactone	Characterisation	[127]
Methacryloyl macromolecules	Structure determination	[128]
Macrocyclic poly(2-vinyl naphthalene) and poly (9,9-dimethyl-2-vinylfluorene)	Molecular characterisation	[129]
Isorbide-1,8-dimethyloctane	Characterisation	[130]
Dendrimers based on aliphatic polyether type dendritic cores	Characterisation of columnar structure	[131]
Mono and telechelic polystyrenes	Characterisation and polymerisation kinetics	[132]
Poly(ε caprolactone) gamma substituted with benzylidene, 2,2-bis(oxymethyl) propionate	Dendrimer characterisation	[133]
Mono and ditelechelic polyphosphazenes polymethylacrylate	Characterisation	[134]
Poly(γ-benzyl-*L*-glutamate)	Characterisation of diblock copolymers	[135]
Telechelic polyisobutylenes	Characterisation and molecular structure	[136]

Polyethylene terephthalate – ε-caprolactone-*co*-polyesters Aliphatic polyethers	Characterisation and chemical composition	[137]
Amino terminated telechelic polypropylene glycol and polyisobutylene	Characterisation	[138]
Macrocylic(arylene multisulfide) oligomers	Study of ring opening reactions	[139]
N-hexyl-cyclopenta[*c*] pyrrole	Characterisation	[140]
Polyamidoamine dendrimer polyhedral oligosilsesquinoxane nanohybrids	Structure confirmation	[141]
Tadpole polymer topology	Characterisation	[142]
Polyamide dendrons	Structure confirmation	[143]
Polyimides	Characterisation	[144]
2-Stanna-1,3-dioxepone(or 1,3-dioxepone) – dicarboxylic acid chloride condensation products	Characterisation	[145]
Poly ε caprolactones	Characterisation	[146]
Poly(2,3 disubstituted alkyl norborn-2-ene)	Characterisation of molecular structure	[147, 148]
Source: Author's own files		

Table 9.14 Multiple technique polymer studies – PMR spectroscopy – laser assisted desorption adsorption ionisation ToF-MS

Polymer	Technique	Ref.
Heterobifunctional PEG with acryloyl and isocyanate end groups	Determination of acryloyl groups	[149]
Polyimides derived fron 2,2′,3,3′-benzophenone tetra-carbonyl dianahydride	Characterisation of cyclic oligomers	[150]
Vinyl functional cubic silsesquioxane-bis(dimethyl silyl) benzene polyaddition products	Determination of hexenyl groups	[151]
FTIR spectroscopy – Laser assisted desorption, adsorption ionisation ToF-MS		
Polythienobenzothiophenes		[152]
Source: Author's own files		

Table 9.15 Multiple technique polymer studies – Scanning electron microscopy – Laser assisted desorption, adsorption ionisation ToF-MS		
Polymer	Technique	Ref.
Hydroxylated polybutadienes	Microstructural analysis	[153]
Source: Author's own files		

9.2 Other Technique Combinations

The following techniques utilise a range of different combinations for various purposes:

- FTIR-proton magnetic resonance (PMR): as in Section 9.1, plus measurement of segments.

- IR-SEM and FTIR-SEM: morphology studies.

- IR-XPS: characterisation of catalysts, effect of light exposure on structure and hydrogen bonding studies.

- FTIR-AFM: examination of polymer surfaces, morphology, adhesion studies, photooxidative stability, particle size, and helix structure studies.

- FTIR-Raman/IR-Raman: flame retardancy studies, polymer-metal complexes, and polyfibre studies.

- XPS-AFM: polymer roughness and polymer surface studies.

- SIMS-XPS: lithography on ceramics, polymer surfaces and morphology.

- FTIR-MALDI: polymer and dendrimer characterisation and structure isotacticity, cyclo and oligolactides, polymerisation kinetics, molecular weight evaluations, diblock polymers-oligomer studies and *cis-trans* structures.

Schmatloch and Schubert [148] have given an overview of recent developments in analytic equipment for multi-technique polymer research covering the period 1999–2003.

Sections are included on conventional synthesisers, microwave synthesisers, high-throughput FTIR spectroscopy, MALDI-TOF mass spectroscopy, scanning probe microscopy and nanoindentation, X-ray analysis and X-ray photoelectron spectroscopy, and thermal analysis.

References

1. T. Jeevananda, S. Siddaramaiah, S. Seetharamu, S. Saravanan and L. D'Souza, *Synthetic Metals*, 2004, **140**, 2-3, 247.

2. X. Sun and X. Ni, *Journal of Applied Polymer Science*, 2004, **94**, 6, 2286.

3. G.B. Kharas, A.M. Fuerst, E.L. Feitl, M.E. Pepper, F.C. Prillaman, J.R. Pyo, G.M. Rogers, A.Z. Tadros, L.G. Umek and K. Watson, *Journal of Macromolecular Science Part A: Pure and Applied Chemistry*, 2004, **41**, 6, 629.

4. K.D. Sata and M. Babazadeh, *Journal of Macromolecular Science Part A: Pure and Applied Chemistry*, 2004, **40**, 1659.

5. Q. Zhang, X. Ni and Z. Shen, *Journal of Macromolecular Science Part A: Pure and Applied Chemistry*, 2004, **41**, 1, 39.

6. R-S. Lee, T-F. Lin and J-M. Yang, *Polymer*, 2004, **45**, 1, 141.

7. L. Halász, K. Belina, O.C. Vorster and P. Juhász, *Plastics, Rubber and Composites*, 2004, **33**, 5, 205.

8. E. Serrano, M. Larrañaga, P.M. Remiro, I. Mondragon, P.M. Carrasco, J.A. Pomposo and D. Mecerreyes, *Macromolecular Chemistry and Physics*, 2004, **205**, 7, 987.

9. Y.T. Jia, H.Y. Kim, J. Gong, D.R. Lee, B. Ding and N. Bhattarai, *Polymer International*, 2004, **53**, 3, 312.

10. S. Banerjee, N. Sood, V. Kute, A.K. Salunke and D.K. Jaiswal, *Journal of Macromolecular Science Part A: Pure and Applied Chemistry*, 2004, **41**, 10, 1123.

11. X-G. Li, M-R. Huang, W. Feng, M-F. Zhu and Y-M. Chen, *Polymer*, 2004, **45**, 101.

12. A.K. Ghosh and E.M. Woo, *Journal of Materials Chemistry*, 2004, **14**, 20, 3043.

13. Q. Wu and R.A. Weiss, *Journal of Polymer Science Part B: Polymer Physics*, 2004, **42**, 19, 3628.

14. F. He, H. Xia, S. Tang, Y. Duan, M. Zeng, L. Liu, M. Li, H. Zhang, B. Yang, Y. Ma, S. Liu and J. Shen, *Journal of Materials Chemistry*, 2004, **14**, 18, 2735.

15. Y. Kawakami, I. Imae, M. Oishi, M. Seino and Y. Liu, *Molecular Crystals and Liquid Crystals*, 2004, **415**, 1, 75.

16. R.A. Prasath, S. Nanjundan, T. Pakula and M. Klapper, *European Polymer Journal*, 2004, **40**, 8, 1767.

17. H. Ma, T. Uchida, D.M. Collard, D.A. Schiraldi and S. Kumar, *Macromolecules*, 2004, **37**, 20, 7643.

18. P.K. Bhowmik, H. Han, J.J. Cebe, I.K. Nedeltchev, S-W. Kang and S. Kumar, *Macromolecules*, 2004, **37**, 8, 2688.

19. K.Y. Mya, C. He, J. Huang, Y. Xiao, J. Dai and Y-P. Siow, *Journal of Polymer Science Part A: Polymer Chemistry*, 2004, **42**, 14, 3490.

20. I.J. Choi, C.J. Ahn and T.H. Yoon, *Journal of Applied Polymer Science*, 2004, **93**, 3, 1211.

21. X. Cui, D. Yan and D. Xiao, *E-Polymers*, 2004, **68**, 1.

22. S-H. Hsiao and T-L. Huang, *Journal of Polymer Research*, 2004, **11**, 1, 9.

23. C. Ma, J. Sun, L. Qiu and J. Cui, *Journal of Inorganic and Organometallic Polymers*, 2004, **14**, 3, 161.

24. J.M. Gómez-Elvira, P. Tiemblo, M. Elvira, L. Matisova-Rychla and J. Rychly, *Polymer Degradation and Stability*, 2004, **85**, 2, 873.

25. N. Vasanthan, R. Kotek, D-W. Jung, D. Shin, A.E. Tonelli and D.R. Salem, *Polymer*, 2004, **45**, 12, 4077.

26. R. Jayakumar and S. Nanjundan, *Journal of Polymer Science Part A: Polymer Chemistry*, 2004, **42**, 8, 1809.

27. E. Passaglia, S. Coiai, G. Giordani, E. Taburoni, L. Fambri, V. Pagani and M. Penco, *Macromolecular Materials and Engineering*, 2004, **289**, 9, 809.

28. H. Hirano, S. Watase and M. Tanaka, *Journal of Applied Polymer Science*, 2004, **91**, 3, 1865.

29. W. Wiyatno, Z-R. Chen, Y. Liu, R.M. Waymouth, V. Krukonis and K. Brennan, *Macromolecules*, 2004, **37**, 3, 701.

30. K.H. Choi and J.C. Jung, *Macromolecular Materials and Engineering*, 2004, **289**, 8, 737.

31. S. Sundarrajan and K.S.V. Srinivasan, *Macromolecular Rapid Communications*, 2004, **25**, 15, 1406.

32. H. Li, Y. Hu, Y. Zhang, D. Ma, L. Wang, X. Jing and F. Wang, *Journal of Polymer Science Part A: Polymer Chemistry*, 2004, **42**, 16, 3947.

33. S-H. Hsiao and Y-M. Chang, *Journal of Polymer Science Part A: Polymer Chemistry*, 2004, **42**, 16, 4056.

34. P.S.G. Krishnan, C. He and C.T.S. Shang, *Journal of Polymer Science Part A: Polymer Chemistry*, 2004, **42**, 16, 4036.

35. W. Liu, F. Mikes, Y. Guo, Y. Koike and Y. Okamoto, *Journal of Polymer Science Part A: Polymer Chemistry*, 2004, **42**, 20, 5180.

36. P. Sakthivel and P. Kannan, *Journal of Polymer Science Part A: Polymer Chemistry*, 2004, **42**, 20, 5215.

37. J-S. Hu, B-Y. Zhang, Y. Guan and X-Z. He, *Journal of Polymer Science Part A: Polymer Chemistry*, 2004, **42**, 20, 5262.

38. S. Chen, G-R. Qi, Z-J. Hua, and H-Q. Yan, *Journal of Polymer Science Part A: Polymer Chemistry*, 2004, **42**, 20, 5284.

39. H. Lü, S. Zheng and G. Tian, *Polymer*, 2004, **45**, 9, 2897.

40. W-J. Liang and P-L. Kuo, *Polymer*, 2004, **45**, 5, 1617.

41. C-F. Huang, S-K. Wang, S-W. Kuo, W-J. Huang and F-C. Chang, *Journal of Applied Polymer Science*, 2004, **92**, 3, 1824.

42. P. Banu and G. Radhakrishnan, *European Polymer Journal*, 2004, **40**, 8, 1887.

43. A. Balionyte, S. Grigalevicius and J.V. Grazulevicius, *European Polymer Journal*, 2004, **40**, 8, 1645.

44. C. Mustata and I. Bicu, *High Performance Polymers*, 2004, **16**, 3, 419.

45. Y-D. Shin, A. Kawaue, H. Okamura and M. Shirai, *Reactive and Functional Polymers*, 2004, **61**, 2, 293.

46. Y-D. Shin, A. Kawaue, H. Okamura and M. Shirai, *Polymer Degradation and Stability*, 2004, **86**, 1, 153.

47. A.K. Mahler, H. Schlick, R. Saf, F. Stelzer, F. Meghdadi, A. Pogantsch, G. Leising, K-C. Möller and J.O. Besenhard, *Macromolecular Chemistry and Physics*, 2004, **205**, 14, 1840.

48. M. Obata, S. Yano, K. Kamino, K. Yokota and T. Kakuchi, *Journal of Polymer Science Part A: Polymer Chemistry*, 2004, **42**, 18, 4671.

49. N. Tarumoto, N. Miyagawi, S. Takahara and T. Yamaoka, *Polymer Journal (Japan)*, 2004, **36**, 10, 866.

50. H.W. Choi, Y.S. Kim, N.C. Yang and D.H. Suh, *Journal of Applied Polymer Science*, 2004, **91**, 2, 900.

51. J.S. Lee, C.H. Kim, J-W. Yu, J.K. Kim, D.Y. Kim, N.W. Song and C.Y. Kim, *Journal of Polymer Science Part A: Polymer Chemistry*, 2004, **42**, 3, 557.

52. F-J. Huang and T-L. Wang, *Journal of Polymer Science Part A: Polymer Chemistry*, 2004, **42**, 2, 290.

53. C.C.W. Law, J. Chen, J.W.Y. Lam, H. Peng and B.Z. Tang, *Journal of Inorganic and Organometallic Polymers*, 2004, **14**, 1, 39.

54. Y. Konno, H. Suzuki, H. Kudo, A. Kameyama and T. Nishikubo, *Polymer Journal (Japan)*, 2004, **36**, 2, 114.

55. Z.Y. Qian, S. Li, Y. He and X.B. Liu, *Polymer Degradation and Stability*, 2004, **84**, 1, 41.

56. J. Ding and W. Shi, *Polymer Degradation and Stability*, 2004, **84**, 1, 159.

57. A.R. Reddy and K.H. Reddy, *Journal of Applied Polymer Science*, 2004, **92**, 3, 1501.

58. F. Sanda, T. Nakai, N. Kobayashi and T. Masuda, *Macromolecules*, 2004, **37**, 8, 2703.

59. K. Tsuchiya, H. Ishii, Y. Shibasaki, S. Ando and M. Ueda, *Macromolecules*, 2004, **37**, 13, 4794.

60. W. Wang, J. Xu, Y-H. Lai and F. Wang, *Macromolecules*, 2004, **37**, 10, 3546.

61. W. Yi, W. Feng, M. Cao and H. Wu, *Polymers for Advanced Technologies*, 2004, **15**, 7, 431.

62. D.W. Kang, H.G. Yeo and K.S. Lee, *Journal of Inorganic and Organometallic Polymers*, 2004, **14**, 1, 73.

63. D.A.M. Egbe, S. Sell, C. Ulbricht, E. Birckner and U-W. Grummt, *Macromolecular Chemistry and Physics*, 2004, **205**, 15, 2105.

64. H. Li, S.Y. Yu, Z.R. Shen, Z.X. Zhang, Q.H. Duan, J.Q. Jiang, P. Xie and R.B. Zhang, *Chinese Journal of Polymer Science*, 2004, **22**, 445.

65. S. Karlsson, *Advances in Polymer Science*, 2004, **169**, 201.

66. N.I. Pakuro, A.A. Arest-Yakubovich, E.I. Akhmet'eva and E.D. Rogozhkina, *Polymer Science, Series A*, 2004, **46**, 8, 767.

67. A.T. Royappa, M.L. Vogt and V. Sharma, *Journal of Applied Polymer Science*, 2004, **91**, 2, 1344.

68. N. Arsalani, M. Khavei and A.A. Entezami, *Iranian Polymer Journal*, 2003, **12**, 3, 237.

69. Q. Fang and T. Yamamoto, *Macromolecules*, 2004, **37**, 16, 5894.

70. P. Guo, S. Wang, P. Wu and Z. Han, *Polymer*, 2004, **45**, 6, 1885.

71. M.H. Stenzel, C. Barner-Kowollik, T.P. Davis and H.M. Dalton, *Macromolecular Bioscience*, 2004, **4**, 4, 445.

72. A.V. Ambade and A. Kumar, *Journal of Polymer Science Part A: Polymer Chemistry*, 2004, **42**, 20, 5134.

73. T. Seckin, S. Koytepe and E. Çetinkaya, *Journal of Polymer Research*, 2004, **11**, 2, 119.

74. W-J. Liang, C-P. Wu and P-L. Kuo, *Journal of Polymer Science Part B: Polymer Physics*, 2004, **42**, 10, 1928.

75. F. He, H. Xia, S. Tang, Y. Duan, M. Zeng, L. Liu, M. Li, H. Zhang, B. Yang, Y. Ma, S. Liu and J. Shen, *Journal of Materials Chemistry*, 2004, **14**, 18, 2735.

76. M. Mancera, F. Zamora, I. Roffé, M. Bermúdez, A. Alla, S. Muñoz-Guerra and J.A. Galbis, *Macromolecules*, 2004, **37**, 8, 2779.

77. F. Yao, Y. Bai, W. Chen, X. An, K. Yao, P. Sun and H. Lin, *European Polymer Journal*, 2004, **40**, 8, 1895.

78. J.W. Lee, M.C. Jung, H.D. Park, K.D. Park and G.H. Ryu, *Journal of Biomaterials Science: Polymer Edition*, 2004, **15**, 8, 1065.

79. M. Johnson-Plaumann, H. Plaumann and S. Keeler, *Rubber Chemistry and Technology*, 1986, **59**, 4, 580.

80. G.A. Carriedo, F.J.G. Alonso and A. Presa, *Journal of Inorganic and Organometallic Polymers*, 2004, **14**, 1, 29.

81. L. Sacarescu, R. Ardeleanu, G. Sacarescu and M. Simionescu, *European Polymer Journal*, 2004, **40**, 1, 57.

82. S. Zhang, J. Qing, C. Xiong and Y. Peng, *Journal of Polymer Science Part A: Polymer Chemistry*, 2004, **42**, 14, 3527.

83. J.A. Frankland, H.G.M. Edwards, A.F. Johnson, I.R. Lewis and S. Poshyachinda, *Spectrochimica Acta Part A: Molecular Spectroscopy*, 1991, **47**, 11, 1511.

84. J-E. Österholm, P. Sunila and T. Hjertberg, *Synthetic Metals*, 1987, **18**, 1-3, 169.

85. J.A. Konig, *Analytical Chemistry*, 1987, **59**, 19, 1141A.

86. L.V. Morozova, A.I. Mikhaleva, I.V. Tatarinova, G.F. Myachina, T.A. Skotheim, T.V. Mamaseva and B.A. Trofimov, *Polymer Science Series B*, 2004, **46**, 159.

87. B.L. Rivas and C.O. Sánchez, *Journal of Applied Polymer Science*, 2004, **92**, 1, 31.

88. W S Drumond and H-W. Shu, *Polimeros: Ciencia e Tecnologia*, 2004, **14**, 2, 74.

89. Z-H. Wang, Y-Z. Xiao and T-S. Liu, *Polymer Materials Science and Engineering*, 2004, **20**, 4, 69.

90. N. Teramoto and M. Shibata, *Journal of Applied Polymer Science*, 2004, **91**, 1, 46.

91. K. Iio, S. Yamasaki, S. Tasaki, H. Kudoh and M. Matsunaga, *Journal of Polymer Science Part A: Polymer Chemistry*, 2004, **42**, 7, 1707.

92. F. Mustata and I. Bicu, *Journal of Polymer Engineering*, 2004, **24**, 391.

93. B. Govindaraj, N.V. Sastry and A. Venkataraman, *Journal of Applied Polymer Science*, 2004, **93**, 2, 778.

94. M. Catauro, M.G. Raucci, F. de Gaetano, A. Buri, A. Marotta and L. Ambrosio, *Journal of Materials Science, Materials in Medicine*, 2004, **15**, 9, 991.

95. N. Wang, L. Zhang, and Y. Lu, *Industrial and Engineering Chemistry Research*, 2004, **43**, 13, 3336.

96. M. Schnell, J. Borrajo, R.J.J. Williams and B.A. Wolf, *Macromolecular Materials and Engineering*, 2004, **289**, 7, 642.

97. A. Gök, B. Sari and M. Talu, *Journal of Polymer Science Part B: Polymer Physics*, 2004, **42**, 18, 3359.

98. D. Srivastava, P. Kumar and G.N. Mathur, *Advances in Polymer Technology*, 2004, **23**, 1, 59.

99. N. Plesu, A. Kellenberger, N. Vaszilcsin and I. Manoviciu, *Molecular Crystals and Liquid Crystals*, 2004, **416**, 127.

100. X. Wang and X. Luo, *European Polymer Journal,* 2004, **40**, 10, 2391.

101. Z. Guo, H. Feng, H-C. Ma, Q-X. Kang and Z-W. Yang, *Polymers for Advanced Technologies*, 2004, **15**, 1-2, 100.

102. J.M. Kinyanjui, D.W. Hatchett, J.A. Smith and M. Josowicz, *Chemistry of Materials*, 2004, **16**, 17, 3390.

103. N.M. Stark and L.M. Matuana, *Polymer Degradation and Stability*, 2004, **86**, 1, 1.

104. A. Tiwari, K.N. Pandey, G.N. Mathur and S.K. Nema, *Materials Research Innovations*, 2004, **8**, 2, 103.

105. H.L. Huang, S.H. Goh, D.M.Y. Lai, A.T.S. Wee and C.H.A. Huan, *Journal of Polymer Science Part B: Polymer Physics*, 2004, **42**, 7, 1145.

106. X-G. Li, H-J. Zhou, M-R. Huang, M-F. Zhu and Y-M. Chen, *Journal of Polymer Science Part A: Polymer Chemistry*, 2004, **42**, 13, 3380.

107. X-G. Li, M-R. Huang, W. Feng, M-F. Zhu and Y-M. Chen, *Polymer*, 2004, **45**, 1, 101.

108. H. Kaczmarek, J. Kowalonek, Z. Klusek, S. Pierzgalski and S. Datta, *Journal of Polymer Science Part B: Polymer Physics*, 2004, **42**, 4, 585.

109. S. Tanaka, A. Ogura, T. Kaneko, Y. Murata and M. Akashi, *Macromolecules*, 2004, **37**, 4, 1370.

110. A.N. Rider, N. Brack, S. Andres and P.J. Pigram, *Journal of Adhesion Science and Technology*, 2004, **18**, 10, 1123.

111. N. Baute, V.M. Geskin, R. Lazzaroni, J-L. Bredas, X. Arys, A.M. Jonas, R. Legras, C. Poleunis, P. Bertrand, R. Jerome and C. Jerome, *E-Polymers*, 2004, **63**, 1.

112. Y.A. Badr, K.M. Abd El-Kader and R.M. Khafagy, *Journal of Applied Polymer Science*, 2004, **92**, 3, 1984.

113. T. Ogawa, H. Mukai and S. Osawa, *Journal of Applied Polymer Science*, 1999, **71**, 2, 243.

114. Z. Gan, K. Kuwabara, M. Yamamoto, H. Abe and Y. Doi, *Polymer Degradation and Stability*, 2004, **83**, 2, 289.

115. S. Kawahawa, K. Takano, J. Yunyongwattanakorn, Y. Isono, M. Hikosaka, J.T. Sakdapipanich and Y. Tanaka, *Polymer Journal (Japan)*, 2004, **36**, 5, 361.

116. W.Y. Chan, A.Y. Cheng, S.B. Clendenning and I. Manners, *Macromolecular Symposia*, 2004, **209**, 1, 163.

117. R.R. Thomas, K.G. Lloyd, K.M. Stika, L.E. Stephans, G.S. Magallanes, V.L. Dimonie, E.D. Sudol and M.S. El-Aasser, *Macromolecules*, 2000, **33**, 23, 8828.

118. S. Chen, L. Tan, F. Qiu, X. Jiang, M. Wang and H. Zhang, *Polymer*, 2004, **45**, 9, 3045.

119. N. Artzi, B.B. Khatua, R. Tchoudakov, M. Narkis, A. Berner, A. Siegmann and J. M. Lagaron, *Journal of Macromolecular Science Part B: Applied Physics*, 2004, **43**, 3, 605.

120. S.D. Kamau and P. Hodge, *Reactive and Functional Polymers*, 2004, **60**, 55.

121. B. Ray, Y. Isobe, K. Matsumoto, S. Habaue, Y. Okamoto, M. Kamigaito and M. Sawamoto, *Macromolecules*, 2004, **37**, 5, 1702.

122. H.R. Kricheldorf and S. Rost, *Macromolecular Chemistry and Physics*, 2004, **205**, 8, 1031.

123. A. Pizzi, H. Pasch, C. Simon and K. Rode, *Journal of Applied Polymer Science*, 2004, **92**, 4, 2665.

124. Z. Liu, J. Ebdon and S. Rimmer, *Reactive and Functional Polymers*, 2004, **58**, 3, 213.

125. R. Saf, G. Schwarzenbacher, C. Mirtl, G. Hayn, J. Hobisch and K. Gatterer, *Macromolecular Rapid Communications*, 2004, **25**, 9, 911.

126. Y. Kwak, A. Goto, K. Komatsu, Y. Sugiura and T. Fukuda, *Macromolecules*, 2004, **37**, 12, 4434.

127. P.V. Persson, J. Schröder, K. Wickholm, E. Hedenström and T. Iversen, *Macromolecules*, 2004, **37**, 16, 5889.

128. G. Deng and Y. Chen, *Journal of Polymer Science Part A: Polymer Chemistry*, 2004, **42**, 15, 3887.

129. R. Chen, G.G. Nossarev and T.E. Hogen-Esch, *Macromolecular Symposia*, 2004, **215**, 1, 67.

130. S. Chatti, M. Bortolussi, D. Bogdal, J.C. Blais and A. Loupy, *European Polymer Journal*, 2004, **40**, 3, 561.

131. B-K. Cho, A. Jain, J. Nieberle, S. Mahajan, U. Wiesner, S.M. Gruner, S. Türk and H.J. Räder, *Macromolecules*, 2004, **37**, 11, 4227.

132. B.G.G. Lohmeijer and U.S. Schubert, *Journal of Polymer Science Part A: Polymer Chemistry*, 2004, **42**, 16, 4016.

133. C.C. Lee, S.M. Grayson and J.M.J. Fréchet, *Journal of Polymer Science Part A: Polymer Chemistry*, 2004, **42**, 14, 3563.

134. H.R. Allcock, E.S. Powell, A.E. Maher, R.L. Prange and C.R. de Denus, *Macromolecules*, 2004, **37**, 10, 3635.

135. K.R. Brzezinska and T.J. Deming, *Macromolecular Bioscience*, 2004, **4**, 6, 566.

136. W.H. Binder, M.J. Kunz, C. Kluger, G. Hayn and R. Saf, *Macromolecules*, 2004, **37**, 5, 1749.

137. D. Tillier, H. Lefebvre, M. Tessier, J-C. Blais and A. Fradet, *Macromolecular Chemistry and Physics*, 2004, **205**, 5, 581.

138. S. Kéki, M. Nagy, G. Deák, P. Herczegh and M. Zsuga, *Journal of Polymer Science Part A: Polymer Chemistry*, 2004, **42**, 3, 587

139. K. Chen, Y.Z. Meng, S.C. Tjong and A.S. Hay, *Journal of Applied Polymer Science*, 2004, **91**, 2, 735.

140. G. Zotti, S. Zecchin, G. Schiavon, B. Vercelli, A. Berlin and S. Grimoldi, *Macromolecular Chemistry and Physics*, 2004, **205**, 15, 2026.

141. P.R. Dvornic, C. Hartmann-Thompson, S.E. Keinath and E.J. Hill, *Macromolecules*, 2004, **37**, 20, 7818.

142. H. Oike, A. Uchibori, A. Tsuchitani, H-K. Kim and Y. Tezuka, *Macromolecules*, 2004, **37**, 20, 7595.

143. T. Koukets, M-A. Karimoto, M. Jikei and S.Y. Kim, *Polymer Journal (Japan)*, 2004, **36**, 7, 513.

144. X. Fang, Z. Yang, S. Zhang, L. Gao and M. Ding, *Polymer*, 2004, **45**, 8, 2539.

145. H.R. Kricheldorf, S. Chatti and G. Schwarz, *Macromolecular Symposia*, 2004, **210**, 1, 93.

146. C. Iojoiu, T. Hamaide, V. Harabagiu and B.C. Simionescu, *Journal of Polymer Science Part A: Polymer Chemistry*, 2004, **42**, 3, 689.

147. M.F. Ilker, H. Schule and E.B. Coughlin, *Macromolecules*, 2004, **37**, 3, 694.

148. S. Schmatloch and U.S. Schubert, *Macromolecular Rapid Communications*, 2004, **25**, 1, 69.

149. C-Y. Won, *Polymer Bulletin*, 2004, **52**, 2, 109.

150. X-Z. Fang, Q-X. Li, Z. Wang, Z-H. Yang, L-X. Gao and M-X. Ding, *Journal of Polymer Science Part A: Polymer Chemistry*, 2004, **42**, 9, 2130.

151. M. Seino and Y. Kawakami, *Polymer Journal (Japan)*, 2004, **36**, 5, 422.

152. I. Fouad, Z. Mechbal, K.I. Chane-Ching, A. Adenier, F. Maurel, J-J. Aaron, P. Vodicka, K. Cernovska, V. Kozmik and J. Svoboda, *Journal of Materials Chemistry*, 2004, **14**, 11, 1711.

153. L. La Tourte, J.C. Blass, R.B. Cole, G. Bolbeck, R. Escoffier and J.C. Tabet in *Proceedings of the 45th ASMS Conference on Mass Spectrometry and Allied Topics*, Palm Springs, CA, USA, 1997, p.536.

10 Scanning Electron Microscopy and Energy Dispersive Analysis Using X-rays

The earliest paper identified on this technique was published in 1996, in which energy dispersive analysis using X-rays (EDAX) was used for elemental analysis in order to map the non-crystalline regions in semicrystalline polyethylene terephthalate (PET) [1].

Applications of scanning electron microscopy (SEM) to polymer characterisation and microstructure include studies on the zwitterions-type polymer, poly(3-diethyl methylmethacryloyl ethyl) ammonium persulfonate grafted on to a silica surface by treatment of poly(2-dimethyl amino) ethyl methacrylate [2], polyaniline coated glass fibre fillers with different polyaniline contents [3], and also studies on ultra high molecular weight blends [4] and high-density polyethylene (HDPE)-gamma ferric oxide composite films [5].

Stuart and Mauritz [6] used environmental SEM-EDAX, and also AFM and transmission electron microscopy, to study the formation of organic-inorganic nanocomposites within Surlyn (polyethylene-*co*-methacrylate cation forms) random copolymers. SEM-EDAX has also been used to study thin films of Prussian blue and *N*-substituted polypyrrols [7] and epoxy resins [8].

Duan and Mukherjee [9] characterised Si-CNO nanowires [9] functionalised polyureasilazane followed by heat treatment. SEM, together with ^{13}C-nuclear magnetic resonance energy dispersive x-ray analysis and x-ray diffraction between them, enabled the mechanism of the reaction to be determined.

SEM and EDAX have been used in the examination of the structural detail of polymer surfaces. Thus, Dilsiz and co-workers [10] used SEM and EDAX to examine silver coatings of spindle- and filament-type particles for conductive adhesive properties. The same technique was used by Lambert and co-workers [11] to examine the silicate structure deep in PET comonomer/silicate hybrid materials.

Other surface studies include the surface modification of jute films with maleic anhydride grafted polypropylene [12] and the surface characterisation of conductive polymethylmethacrylate/polypyrrole composites [13]. Tavakoli and Riches [14] treated surfaces of HDPE, low-density polyethylene and polypropylene and glass-

reinforced polypropylene with xenon chloride, arsenic fluroide and krypton fluoride eximer to enhance adhesion. SEM studies revealed little or no physical effect on the surfaces.

SEM has been used extensively in morphological studies on polymers. Polymers studied include: epoxy resin-polyaniline composites [3], polyoxyethylene [15], polypropylene-polycaprolactone blends [16], polydimethylsiloxane-*co*-ethylene oxide [17], PET fibres [18], polyurethane/polybutylmethacrylate polymer networks [19], methylacrylate-*co*-cellulose [20], styrene-butadiene copoylmer [21], Nylon 6-ethylene vinyl alcohol [22] and propylene-calcium carbonate or talc composites [23].

References

1.   M. Sundararajan, H-L. Lee, P.Schwartz and S.K. Obendorf in *Proceedings of the ACS Polymeric Materials Science and Engineering Meeting*, Orlando, FL, USA, Fall 1996, Volume 75, p.295.

2.   H. Arasawa, C. Odawara, R. Yokoyama, H. Saitoh, T. Yamauchi and N. Tsubokawa*, Reactive and Functional Polymers*, 2004, **61**, 2, 153.

3.   W. Jia, R. Tchoudakov, E. Segal, M. Narkis and A. Siegmann, *Journal of Applied Polymer Chemistry*, 2004, **91**, 2, 1329.

4.   G. Liu, Y. Chen and H. Li, *Journal of Applied Polymer Chemistry*, 2004, **92**, 6, 3894.

5.   B. Govindaraj, N.V. Sastry and A. Venkataraman, *Journal of Applied Polymer Chemistry*, 2004, **92**, 3, 1527.

6.   P.R. Stuart and K.A. Mauritz, *Polymer Preprints*, 2001, **42**, 2, 75.

7.   R. Koncki and O.S. Wolfbeis, *Analytical Chemistry*, 1998, **70**, 13, 2544.

8.   P.R. Lewis in *Proceedings of the SPE ANTEC 2000 Conference*, Orlando, FL, USA, Paper No.607.

9.   R-G. Duan and A.K. Mukherjee, *Advanced Materials*, 2004, **16**, 13, 1106.

10. N. Dilsiz, R. Partch, E. Matijevic and E. Sancaktar, *Journal of Adhesive Science and Technology*, 1997, **11**, 8, 1105.

11. A.A. Lambert III, K.A. Mauritz and D.A. Schiraldi, *Journal of Applied Polymer Chemistry*, 2002, **84**, 9, 1749.

12. S. Mohanty, S.K. Nayak, S.K. Verma and S.S. Tripathy, *Journal of Reinforced Plastics and Composites*, 2004, **23**, 4, 625.

13. M. Omastová and F. Simon, *Journal of Materials Science*, 2000, **35**, 7, 1743.

14. S.M. Tavakoli and S.T. Riches in *Proceedings of SPE ANTEC 1996 Conference*, Indianapolis, IN, USA, 1996, Volume 1, p.1219.

15. M.A.S.A. Samir, F. Alloin, J-Y. Sanchez and A. Dufresne, *Polymer*, 2004, **45**, 12, 4149.

16. T. Semba, K. Kitagawa, S. Endo, K. Maeda and H. Hamada, *Journal of Applied Polymer Chemistry*, 2004, **91**, 2, 833.

17. P.A. Tamirisa, K.C. Liddell, P.D. Pedrow and M.A. Osman, *Journal of Applied Polymer Chemistry*, 2004, **93**, 3, 1230.

18. A. Hou, K. Xie and J. Dai, *Journal of Applied Polymer Chemistry*, 2004, **92**, 3, 2008.

19. M. Begum and Siddaramaiah, *Journal of Materials Science*, 2004, **39**, 14, 4615.

20. Y. Liu, L. Yang, Z. Shi and J. Li, *Polymer International*, 2004, **53**, 10, 1561.

21. M. Tasdemir and H. Yildirim, *Journal of Applied Polymer Chemistry*, 2002, **83**, 14, 2967.

22. N. Artzi, B.B. Khatua, R. Tchoudakov, M. Narkis, A. Berner, A. Siegmann and J.M. Lagaron, *Journal of Macromolecular Science B*, 2004, **43**, 3, 605.

23. B. Pukánszky and J. Móczó, *Macromolecular Symposia*, 2004, **214**, 1, 115.

Appendix 1. Instument Suppliers

Type of Analysis	Supplier
Carbon, hydrogen, nitrogen	Perkin Elmer Corp.
Chemiluminescence analysis	New Brunswick Scientific Amersham Biosciences
Electrophoresis	Beckman Coulter, Inc. Cole-Parmer Instrument Co.
Energy dispersive and total reflection X-ray fluorescence spectroscopy	Link Analytical Ltd. Oxford Systems Philips Electronic Instruments Richard Seifert & Co. Traor Europa BV
Flame and graphite furnace atomic absorption spectrometry	Thermoelectron Ltd. Perkin Elmer Corp. Varian Instruments GBC Scientific Pty Ltd. Shimadzu Corp. PS Analytical Ltd.
Fourier transform infrared spectroscopy, near infrared Fourier and transform Raman spectroscopy	Mattson Instruments Ltd. Perkin Elmer Corp. Varian Instruments Philips Electronic Instruments Foss Electronic JEOL Ltd. Applied Photophysics EDT Research
Gas chromatography	Thermo Electron Perkin Elmer Corp. Shimadzu Corp. Dyson Instruments Hnu-Nordion Instruments Co. Siemens AG Varian Instruments

Gas chromatography – mass spectrometry and mass spectrometry	Thermo Electron Perkin Elmer Corp. Shimadzu Corp. Dyson Instruments Ltd. Varian Instruments HBI Haakon Buchler
Gas chromatography – Fourier transform infrared spectroscopy	Perkin Elmer Corp. Philips Analytical Shimadzu Europe Varian Instruments
Gel permeation chromatography, size exclusion chromatography	Perkin Elmer Corp. Polymer Laboratories Ltd.
Halogen, sulfur, nitrogen	Sartec Ltd.
Headspace samplers	Perkin Elmer Corp. Shimadzu Corp. Siemens AG Eden Scientific Ltd. Hewlett Packard Inc.
High-performance liquid chromatography	Varian Instruments Perkin Elmer Corp. Kontron Instruments Dionex Corp. Amersham Biosciences Shimadzu Corp. Dyson Instruments Hewlett Packard Kratos Analytical Instruments Cecil Instruments Varian AG GV Analytical Ltd.
High-performance liquid chromatography – mass spectrometry	Hewlett Packard
Inductively coupled plasma mass spectroscopy	VG Isotopes Ltd. Perkin Elmer Corp. Labtam Ltd.
Inductively coupled plasma optical emission spectrometers	Spectro Inc. Philips Analytical Philips Electronic Instruments

Nitrogen	Foss Tecator AB Thermo Electron Mitsubishi Corp. Buchi Labortechnik AG
Nitrogen, carbon and sulfur	Thermo Electron
Nuclear magnetic resonance spectroscopy	Varian Instruments Perkin Elmer Corp. Oxford Systems
Luminescence and spectrofluorimetry	Perkin Elmer Corp. Hamilton Co. Hamilton Bonaduz AG
Mass spectrometry	Oxford Analytical Ltd. Perkin Elmer Corp. Varian Instruments Thermo Electron Hewlett Packard JOEL Shimadzu Corp. GV Instruments Ltd.
Polarography, voltammetry	Metrohm Ltd. EDT Analytical Chemtronics Ltd.
Pyrolysis – gas chromatography	CDS Instruments Perkin Elmer Corp. Philips Analytical Varian Instruments Foxborough Co.
Spectrofluorimetry	Shimadzu Spectrovision Inc.
Sulfur	Mitsubishi Chemicals Industries
Sulfur, chlorine	EDT Analytical Ltd.
Supercritical fluid chromatography	Lee Scientific Inc. Dionex UK Ltd. Pierce Chemical Company
Thin layer chromatography	JT Baker Ltd. Camag Merck Shimadzu Europa Whatman Ltd.

Total elements	Dohrman Instruments (now Emerson Process Management)
Visible, ultraviolet and infrared spectrometers	Philips Electronic Instruments Cecil Instruments Kontron Instruments Perkin Elmer Corp. Gilson International Varian Instruments Foss Electronic
Zeeman atomic absorption spectrometry	Perkin Elmer Corp. Varian Instruments

Appendix 2. Suppliers of Flammability Properties Instruments

Type of Analysis	Supplier
Energy dispersive analysis using X-rays	EDAX International Ltd.
Electron microprobe microscopy	Philips Analytical Japanese Electron Optics Ltd. (JEOL) GV Instruments Co.
Electron scanning microscopy	International Equipment Trading Ltd. Philips Analytical
Electron transmission microscopy	International Equipment Trading Ltd.
Infrared microscopy	Varian Instruments Cambridge Instruments Co. Gallankamp Co. Southern Microinstruments Carl Zeiss Perkin Elmer Corporation Mattson Instruments Ltd.
Laser spectrometry	Shimadzu Corp. GV Instruments Co.
Nuclear magnetic resonance microimaging spectrometry	Varian Instruments
Photoacoustic spectrometry	Perkin Elmer Corp.
Secondary ion mass spectrometry	Cameca Perkin Elmer Corp. Shimadzu Scientific Instrument Co.
X-ray photoelectron spectrometry	Shimadzu Scientific Instrument Co. Tracor Europa BV GV Instruments Co. Perkin Elmer Corp.

X-ray analysers and diffusion equipment	Link Analytical Philips Analytical Tracor Europa BV Spectratech Inc.
X-ray microprobe	Hilgenberg GmbH Perkin Elmer Corp. Whatman Scientific Co.

Appendix 3. Address of Suppliers

Alpine American Corporation	5 Michigan Drive Natick MA 01760 USA
Amersham Biosciences www.amershambiosciences.com	Amersham Biosciences Europe GmbH Filial Sverige Bjorkgaten 30 75125 Uppsala Sweden Pollards Wood Nightengales Lane Chalfont St. Giles Buckinghamshire HP8 4 SP UK
Applied Chromatography Systems	The Arsenal Heapy Street Macclesfield Cheshire SK1 7JB UK
Applied Photophysics Ltd. www.photophysics.com	203/205 Kingston Road Leatherhead Surrey KT22 7PB UK
ATS FAAR www.atsfaar.it	Via Camporiccolserdio 20060 Vignate Italy (UK Agents: Martin Instrument Co. Ltd.)

Beckman Coulter, Inc. www.beckmancoulter.com	4300 N. Habor Boulevard PO Box 3100 Fullerton CA 92834-3100 USA Oakley Court Kingsmead Business Park London Road High Wycombe HP11 1JU UK
Boekel Scientific www.boekelsi.com	855 Pennsylvania Boulevard Feasterville PA 19053 USA
Brinkmann Instruments Inc. www.brinkmann.com	1 Cantiague Road PO Box 1019 Westbury NY 11590 USA
Brookfield Engineering Laboratories Inc. www.brookfieldengineering.com	11 Commerce Boulevard Middleboro MA 02346 USA
Bruker-Biospin www.bruker-biopsin.com	Bruker-Biospin Corporation 15 Fortune Drive Manning Park Billerica MA 01821-3991 USA
Buchi Labortechnik AG www.buchi.com	Meierseggstr 40 CH-9230 Flawil 1 Switzerland
Cahn Instruments (part of THASS) www.thass.net	THASS, Thermal Analysis and Surface Solutions GmbH Pfingstweide 21 61169 Friedberg Germany
Camag www.camag.ch	Sonnenmattstrasse 11 CH-4132 Muttenz Switzerland

Cambridge Instruments www.home.btconnect.com/camsci	12–15 Sedgeway Business Park Witchford Ely CB6 2HY UK
Cambridge Instruments GmbH (now Leica Microsystems) www.hbu.de	Postfach 1120 Heidebergerstrasse, 17-19 D-6907 Nussloch Germany
Cambridge Mass Spectrometry Ltd. (now Kratos Analytical Inc., part of the Shimadzu group) www.kratos.com	Wharfside Trafford Wharf Manchester Road M17 1GP UK
Cameca www.cameca.fr	103 Boulevard Saint Denis BP 6 92403 Courbevoie Cedex France
Carl Zeiss Inc. www.zeiss.com	1 Zeiss Drive Thornwood NY 10594 USA
Carlo Erba Strumentazione SpA now ThermoElectron www.ceinstruments.com	Strada Rivoltana 20090 Rodano Milan Italy
CDS Analytical, Inc. www.cdsanalytical.com	PO Box 277 465 Limestone Road Oxford PA 19363-0277 USA
Cecil Instruments Ltd. www.cecilinstruments.com	Milton Technical Centre Cambridge CB4 4AZ UK
Cole Parmer Instrument Co. www.coleparmer.com	625 East Bunker Court Vernon Hills Illinois 60061-1844 USA

Contraves Space AG www.contraves.com	Schaffhauser Strass 580 CH-8052 Zurich Switzerland
Cypress Systems Inc. www.cypresssystems.com	2300 W 31st Street Lawrence KS 66046 USA
Dionex Corp. www.dionex.com	4 Albany Court Camberley Surrey GU16 7QL UK PO Box 3063 1228 Titan Way Sunnyvale CA 94088-3603 USA
Dohrmann Instruments (now Emerson Process Management) www.emersonprocess.com	Rosemount Analytical Division 1201 North Main Street Orville OH 44667 USA
Dyson Instruments Ltd.	Hetton Lyons Industrial Estate Hetton Houghton le Spring Tyne and Wear DH5 0RH UK
EDAX International Inc. www.edax.com	915 McKee Drive Mahwah NJ 07430 USA
EDT Research Ltd. www.edt.bham.ac.uk	Department of Electronic, Electrical and Computing Engineering University Birmingham Edgbaston Birmingham B15 2TT UK

EI DuPont de Nemours Inc. www.dupont.com	Concord Plaza Wilmington Delaware 19898 USA
Fire Testing Technology Ltd. www.fire-testing.com	Fire Testing Technology Ltd. Charlwoods Road East Grinstead West Sussex RH19 2HL UK
Fisher Scientific UK Ltd. www.fisher.co.uk	Whitbrook Way Stakehill Industrial Park Middleton Manchester M24 2RH UK
Foss Electronic www.foss.dk	NIR Systems Ltd. 7703 Montpellier Road Laurel MD 723 USA
Foss Tecator AB www.foss.tecator.se	Box 70 S263-21 Honagas Sweden
Fritsch GmbH www.fritsche.de	Industriestrasse 8 D-55743 Idar Oberstein Germany (UK Agent: Fisher Scientific UK Ltd.)
Gallenkamp Ltd. www.gallenkamp.co.uk	Units 37–38 The Technology Centre Epinel Way Loughborough LE11 3GE UK
GBC Scientific Pty Ltd www.gbcsci.com	Monterey Road Dandenong Victoria Australia 3175

Gibitre Srl www.gibitre.it	Via Mercii I 24035 Curro (BG) Italy
Gilson International www.gilson.com	Box 27 3000 W. Beltine Highway PO Box 620027 Middleton Wisconsin 53562-0027 USA
Gilson SAS www.gilson.com	19 Avenue de Entrepreneurs Villiers-le-Bel BP 45 F-95400 France
GV Instruments www.gvinstruments.co.uk	Crewe Road Wythenshawe Manchester M23 9BE UK
Hamilton Bonadzu AG www.hamilton.ch	Via Crush 8 PO Box 26 CH-7402 Bonadzu Switzerland
Hamilton Company www.hamiltoncompany.com	PO Box 10030 Reno Nevada 89520-0012 USA
Hewlett Packard www.hpl.hp.com	1501 Page Mill Road Palo Alto CA 94303-0890 USA 150 Route du Nant-d'Avril CH-1217 Meyrin 2 Geneva Switzerland Hewlett-Packardstrasse Post 1180 D-7517 Waldbron Germany

Hilgenberg GmbH www.hilgenberg-gmbh.de	Struachgraben 2 PO Box 9 D-34323 Malsfeld Germany
Hnu-Nordion Ltd Oy www.hnunordion.fi	Atomitie 5 A 3 PO Box 1 SF 00370 Helsinki Finland
Horiba Jobin Yvan, Inc. www.jobinyvon.com	3880 Park Avenue Edison NJ 08820-3021 USA 2 Dalston Gardens Stanmore Middlesex HA7 1 BQ UK
HPLC Technology Ltd. www.hplc.co.uk	3 Little Mundells Mundells Industrial Centre Welwyn Garden City AL7 1EW UK
International Equipment Trading Ltd. www.ietild.com	960 Woodlands Parkway Vernon Hills IL 60061 USA
Japanese Electron Optics Ltd. (JEOL) www.jeol.com	1-2 Musashino 3-chome Aikshima Tokyo 196-8558 Japan
JT Baker Inc. Division of Mallinckrodt Baker www.imaging.mallinckrodt.com	222 Red School Lane Philipsburg New Jersey 08865 USA
Kratos Analytical Inc. www.Kratos.com	100 Red Schoolhouse Road Building A Chesnut Ridge NY 10977 USA

Labtam Ltd. www.labtam.com.au	33 Malcomb Road Braeside Victoria Australia 3195
Martin Instruments Co. Ltd.	6 Windsor Drive Market Drayton Shropshire TF9 1HX UK
Merck K GaA www.merck.de	Frankfurterstrasse 250 Postfach 4119 D-64293 Darmstadt Germany
Metrohm AG www.metrohm.com	68 Obersdorf Strasse CH-9101 Herisau AR Switzerland
Mettler Electronics Corp. www.mettlerelectronics.com	1333 S Claudina Street Anaheim CA 92805 USA
Mettler-Toledo Ltd. www.mt.com	64 Boston Road Beaumont Leicestershire LE4 1AW UK
Mitsubishi Chemical Industries Ltd. www.mitsubishi.com	Instruments Department Mitsubishi Building 5-2 Marunouchi-2-Chrome Chiyoda-ku Tokyo 100 Japan
New Brunswick Scientific (UK) Ltd. www.nbsc.com	17 Alban Park Hatfield Road Hertfordshire AL 4 0JJ UK
Oxford Scientific Instruments Ltd. www.oxisci.com	Culham Innovation Centre D5 Culham Science Centre Abingdon Oxon OX14 3DB UK

Paul N. Gardner Co. Inc. www.gardco.com	316 Northeast First Street Pompano Beach FL 33060 USA
Perkin Elmer Corp. www.perkinelmer.com www.de.instruments.perkinelmer.com www.las.perkinelmer.co.uk	Chalfont Road Seer Green Beaconsfield Buckinghamshire HP9 2FX UK
Life and Analytical Sciences	549 Albany Street Boston MA 02118-2512 USA
Perkin Elmer (LAS) GmbH	Ferdinand Porsche Ring 17 D-63110 Rodgau Germany
Philips Electronic Instruments www.analytical.philips.com	PANalytical EMEA Office Twentepoort Oost 26 7609 RG ALMELO The Netherlands York Street Cambridge CB1 2QU UK PANalytical Inc. 12 Michigan Drive Natick MA 01760 USA
Pierce Chemical Company www.piercenet.com	PO Box 117 Rockford IL 61105 USA
PL Thermal Sciences	Surrey Business Park Kiln Lane Epsom Surrey KT1 7JF UK

	300 Washington Boulevard Mundelein IL 60060 USA
	Polymer Laboratories Kurfuersten Anlage 9 6900 Heidelberg Germany
Polymer Laboratories www.polymerlabs.com	Essex Road Church Stretton Shropshire SY6 6AX UK
	Amherst Fields Research Park 160 Old Farm Road Amherst MA 01002 USA
	Polymer Laboratories BV Sourethweg 1 6422 PC Heerlen The Netherlands
	Polymer Laboratories GmbH PEKA Park T5 (001) Otto-Hesse Straße 19 D-64293 Darmstadt Germany
	Polymer Laboratories SARL GVIO Parc de Marseille Sud Impasse du Paradou Bâtiment D5 BP 159 13276 Marseille Cedex 09 France
PS Analytical Ltd. www.psanalytical.com	Arthur House Crayfields Industrial Estate Main Road Orpington Kent BR5 3HP UK

Sartec Ltd. www.sartec.co.uk	Century Farm Reading Street Tenterden TN30 7HS UK
Shimadzu Deutschland GmbH www.eu.schmadzu.de	Albert-Hahn Strasse, 6-10 D-47269 Duisburg Germany
Shimadzu UK www.shimadzu.com	Unit 1A Mill Court Featherstone Road Wolverton Mill South Milton Keynes MK12 5RD International Marketing Division Shinjuku Mitsui Buildings 1-1 Nishi Shinjuku 2 Chrome Shinjuku ku Tokyo 163 Japan
Siemens AG www.siemens.com	Siemens AG Wittelsbacherplatz 2 80312 Munich Germany
Siemens plc	Siemens House Oldbury Bracknell RG12 8FZ UK
Southern Instruments www.southernmicro.com	Southern Micro Instruments, Inc. 1700 Enterprise Way Suite 112 Marietta GA 30067-9219 USA
Spectratech Inc.	652 Glenbrook Road Stamford Connecticut CT 06906 USA

Spectro Analytical UK Ltd. www.spectro.com	Fountain House Great Cornbow Halesowen West Midlands B63 3BL UK
Spectro Anaylytical Instruments, Inc. www.spectro-ai.com	450 Donald Lynch Boulevard Marlborough MA 01752 USA
TA Instruments www.tainstruments.com	109 Luckens Drive New Castle Delaware 19720 USA
Teledyne Isco Inc. www.isco.com	4700 Superior Street Lincoln NE 68504 USA
Thermo Electron Corp. www.thermo.com	1 Saint George's Court Hanover Business Park Altrincham WA14 5TP UK 1601 Cherry Street Suite 1200 Philadelphia PA 19102 USA
Thermo Electron Ltd.	830 Birchwood Boulevard Birchwood Warrington Cheshire WA3 7QT UK 590 Lincoln Street Waltham MA 02254 USA

Tracor Europe BV www.tracor-europe.tripod.com	PO Box 333 3720 311 Bilthoven The Netherlands
Valco Instruments www.vici.com	Parkstrasse 2 CH-6214 Schenkon Switzerland 7806 Bobbitt Houston TX 77055 USA
Varian AG www.varianinc.com	Steinhauserstrasse CH-6300 Zug Switzerland
Varian Instruments www.varianinc.com	Varian Limited 6 Mead Road Oxford Industrial Park Yarnton Oxford OX5 1QU UK Varian, Inc., Corporate Headquarters 3120 Hansen Way Palo Alto CA 94304-1030 USA
Varian Techtron Pty Ltd.	679 Springvale Road Mulgrove Victoria Australia 3170
Wallace Instruments www.hwwallace.co.uk	Unit 4, St Georges Industrial Estate Richmond Road Kingston KT2 5BQ UK
Whatman Inc. www.whatman.com	200 Park Avenue Suite 210 Florham Park NJ 07932 USA

| Whatman International Ltd.
www.whatman.com | Springfield Mill
James Whatman Way
Maidstone
Kent
ME14 2LE
UK |

Abbreviations

AAS	atomic absorption spectrometry
ABE	allyl butyl ether
ABS	acrylonitrile-butadiene-styrene terpolymer
AFS	atomic force microscopy
AIBN	azobisisobutyronitrile
AES	auger electron spectroscopy
AFM	atomic force microscopy
AFS	atomic fluorescence spectrometry
AR	analar reagent
ATR	attenuated total reflection
ATRP	atom-transfer radical polymerisation
CI	chemical ionisation
COSY	correlation spectroscopy
DC	direct current
DEPT	distortionless enhancement by polarisation transfer
DGEBA	diglycidyl ethers of bisphenol A-based resin
DIRLD	dynamic infrared linear dichroism
DMTA	dynamic mechanical thermal analysis
DSIMS	dynamic secondary ion mass spectroscopy
DSC	differential scanning calorimetry
EDAX	energy dispersive analysis using X-rays
EDXRF	energy dispersive X-ray fluorescence
EI	electron impact
EPDM	ethylene-propylene-diene morphology
ESCA	electron spectroscopy for chemical analysis (see also XPS)
ESI	electrospray ionisation
FAB	fast atom bombardment

FD	field desorption
FI	field ionisation
FID	free induction decays
FTIR	Fourier transform infrared spectroscopy
GC	gas chromatography
GFAAS	graphite furnace atomic absorption spectrometry
GMA	glycidyl methacrylate
GPC	gel permeation chromatography
HDPE	high-density polyethylene
HPLC	high-performance liquid chromatography
ICP	inductively coupled plasma
ICP-AES	inductively coupled plasma atomic emission spectrometry
ICP-OES	inductively coupled plasma optical emission spectrometer
iPP	isotactic polypropylene
IRE	internal reflection element
LC	liquid chromatography
LPLC	low-performance liquid chromatography
LSR	lanthanide shift reagents
MALDI	matrix-assisted laser desorption/ionisation
MALDI-CID	matrix-assisted laser desorption/ionisation collision induced dissociation
MALDI-TOF	matrix-assisted laser desorption/ionisation time-of-flight
MAR	micro analytical reagent
MAS	magic angle spinning
MMA	methyl methacrylate
MS	mass spectrometry
NAA	neutron activation analysis
NMR	nuclear magnetic resonance
NOE	nuclear Overhauser enhancement
OA	orthogonal acceleration
PAR	pyridyl azoresorcinol
PC	polycarbonate
PDEGBB	poly(diethylene glycol 4,4′-bibenzoate)
PDMS	polydimethylsiloxane

PE   polyethylene
PEG   polyethylene glycol
PET   polyethylene terephthalate
PGC   pyrolysis gas chromatography
PMAN   polymethacrylonitrile
PMMA   polymethyl methacrylate
PMR   proton magnetic resonance
PP   polypropylene
PS   polystyrene
PTFE   polytetrafluoroethylene
PU   polyurethane
PVC   polyvinyl chloride
PVOH   polyvinyl alcohol
Py-GC   pyrolysis gas chromatography
RF   radio frequency
SCOT   solid capillary open tubular
SEC   size exclusion chromatography
SEM   scanning electron microscopy
SG   specific gravity
SiOH   silanol
SiH   silane hydrogen
SIMS   secondary ion mass spectroscopy
SMA   styrene – maleic anhydride
SMS   styrene – methyl methacrylate – stryrene
SMAN   styrene – methacrylonitrile
SQW   square wave
SSIMS   static secondary ion mass spectrometry
SSM   styrene – styrene – methyl methacrylate
TCD   thermal conductivity detector
TOC   total organic carbon
ToF-SIMS   time-of-flight secondary ion mass spectrometry
TRXRF   total reflection X-ray fluorescence
TTL   transistor-transistor logic
UV   ultraviolet

WAXD	wide-angle X-ray diffraction
WDXRF	wavelength dispersive X-ray fluorescence
WLF	Williams-Landel-Ferry equation
XPS	X-ray photoelectron spectroscopy
XRF	X-ray fluorescence
XRFS	X-ray fluorescence spectrometry
ZAAS	Zeeman atomic absorption spectrometry

Subject Index

D

E

F

G

H

I

T

U

This book is the first part of a two volume compendium of the types of
methodology that have evolved for the determination of the chemical
composition of polymers.

Volume 1 covers the methodology used for the determination of metals, non-
metals and organic functional groups in polymers, and for the determination
of the ratio in which different monomer units occur in copolymers.

The techniques available for composition determination of homopolymers
and copolymers and other recent modern techniques such as X-ray
photoelectron spectroscopy, atomic force microscopy, microthermal analysis
and scanning electron microscopy and energy dispersive analysis using X-rays
are also included.